Declaration of Authenticity and Author's Rights

‘This thesis is the result of the author’s original research. It has been composed by the author and has not been previously submitted for examination which has led to the award of a degree.’

Signed:

Date:

University of Strathclyde

Bioengineering Department

The design of a prosthetic foot unit for use in developing countries

Philip Andrew Connolly

This thesis is presented in fulfilment of the requirements for the degree of Doctor of Engineering in Medical Devices.

2016

ACKNOWLEDGEMENTS

Firstly, I would like to thank my supervisors, Dr. Arjan Buis of the National Centre for Prosthetics and Orthotics and Mr. Stephan Solomonidis of the Bioengineering department for their ongoing support and insight into the project.

Of the staff within the Bioengineering department, Stephen Murray has always been excellent in producing the materiel for testing with insightful advice on production and use. Dave Smith was very helpful in the initial material testing phases, particularly in showing me how to operate the Instron system, and also in helping prepare the safety requirements for gait testing. While not staff John Burns' help with the Vicon system was extremely gratefully received.

Thanks to the EPSRC for the funding and sponsorship using which this project was carried out.

Thanks to Mr. David Mathews for providing the image of the All-Terrain foot.

My deepest thanks go to my wife, Alex, without whom I could never have made it through my doubts and fears; you have always been there for me when I needed you most. Cian has given me an eye to the future putting things into perspective.

Both of our families have supported me throughout this time and for that I am truly grateful. Their constant belief in me has kept me going throughout this long process.

ABSTRACT

“The design of a prosthetic foot unit for use in low-income countries”

The majority of prosthetic feet used in low-income countries suffer from a limited lifespan and limited durability. The aim of this project is to design a prosthetic foot suited to use in low-income countries that incorporates both durability and a high level of function.

A review of the literature was carried out which included examining the form and function of the anatomical human foot and the existing prosthetic systems used in low-income countries as well as their limitations and successes. Also reviewed were methods of assessment of a prosthetic foot.

A Product Design Specification (PDS) was created to outline the requirements of a prosthetic foot for use in a low-income country based on the information detailed in the literature review. An existing design of Strathclyde foot was tested statically according to the ISO 10328 standard.

The design was modified to improve performance in identified areas followed by an evaluation of layered manufacturing processes. Having identified a potential manufacturing method for prototypes testing of materials was carried out to determine the suitability of these materials for testing. Samples of the new design were tested statically according to ISO 10328.

The foot design was then further modified based on the test results, confirmed by the use of FEA at which point new prototypes were made and static testing was again carried out. A comparison of the Strathclyde foot to other feet used in low-

income countries took place. The second redesign of the Strathclyde foot was assessed via force plate trials by a non-amputee subject wearing prosthetic stilts.

Finally, conclusions were drawn with respect to achieving the PDS and further work was recommended to improve upon the existing design and reach the requirements of the PDS.

Appendix A gives details of the roll-over shape testing carried out on a range of prosthetic feet while Appendix B details the FEA work carried out to support design modification.

CONTENTS

FIGURES

TABLES

ABBREVIATIONS

ASTM - American Society for Testing and Materials

BMVSS - Bhagwan Mahaveer Viklang Sahayata Samiti

BW – Body Weight

C- - Prefix indicating sample is copolymer polypropylene

CES – Cambridge Engineering Selection

COP – Centre of pressure

DER – Dynamic Energy Return

ESAR – Energy storage and return

EX- - Prefix indicating sample is Duraform EX

FDM – Fused Deposition Modelling

FEA – Finite Element Analysis

F_x – Force acting in x direction (also F_y for y direction and F_z for z direction)

HCMC foot – Ho Chi Minh City foot

H- - Prefix indicating sample is homopolymer polypropylene

HDPE – High density polyethylene

HI – Handicap International

ICRC – International Committee of the Red Cross

ID – Inkjet Deposition

ISO – International Standards Organisation

LOM – Laminated Object Manufacture

PA- - Prefix indicating sample is Duraform PA

PCI – Physiological Cost Index

PDS – Product Design Specification

PFLA – Prosthetic foot loading apparatus

PP – Polypropylene

PVC – Polyvinyl chloride

R1 – First redesign of Strathclyde foot

R2 – Second redesign of Strathclyde foot

SACH – Soft Ankle, Cushioned Heel

SAFE – Solid Ankle, Flexible Endoskeletal *alt.* Stationary Attachment Flexible Endoskeletal

SD – Standard Deviation

SF – Strathclyde Foot

SGC – Solid Ground Curing

SLA – Stereolithography

SLS – Selective Laser Sintering

USAID – United States Agency for International Development

UTS – Ultimate Tensile Strength

UV – Ultra-violet

VC – Vacuum Casting

VI – Veterans International

VVAF – Vietnam Veterans of America Foundation

CHAPTER 1 – Introduction

With approximately 25.5 million people in Asia, Latin America and Africa requiring or having had an amputation(World Health Organization, 2005) there is a real need for available prostheses. The industrialised world has benefitted from its relatively high spending on healthcare and a range of prosthetic feet has been developed to help amputees return to their normal lives whether as a minimally active person or highly active individuals (Cochrane, Orsi, & Reilly, 2001). These benefits have, for the most, not been matched in low-income countries (Jensen & Sexton, 2010). The cause of amputations in low-income countries is more often due to traumatic incident than vascular disease (Bisseriex et al., 2011) and so the individuals concerned could potentially return to a higher functioning level than the average Western amputee (Bisseriex et al., 2011). The prostheses currently available in low-income countries are lower functioning than those used in industrialised countries (Jensen & Sexton, 2010) whether it is for example a lack of energy return or limited endurance resulting in premature failure.

Work was previously carried out on the “Strathclyde foot” in developing a prosthetic foot with similar aims by Leona Morton as part of her EngD research (L. E. Morton, Spence, Buis, & Simpson, 2009). A prototype was produced and tested to the A60 level of the ISO 10328 standard, where it was considered to pass static loading conditions, and also worn by an amputee to gather force plate data and subjective opinion. The A60 level is the lightest of three levels and indicates the foot is suitable to be worn by a person of only 60kg or less, making it unusable by many. Post-manufacture the foot required drilling for placement of energy storing rods to be inserted which was targeted for improvement. It was further required that a

specific alignment device and shank be used which could hinder the acceptance and use of the foot.

As such the aim of this project was to build on the design of the Strathclyde foot to develop a design for a durable, cost effective prosthetic foot unit suited to the developing world but with an improved balance of functionality and durability than is currently seen in prostheses available in developing countries. More universal interface with existing lower limb prosthetic systems was desired as was reduced processing of the prosthesis following manufacture. Given the use of expensive and relatively delicate technology in Western prostheses it is not possible to offer the same level of functionality in developing countries while also providing the durability required and maintaining a low production cost. This was the major compromise in this project and so some function was traded for durability and maintaining a low cost.

Several rounds of physical testing, Finite Element Analysis and design were carried out to improve the performance of the keel. Selective laser sintered prototypes were built and tested in an effort to keep cost down while testing iterations of design. While the performance of the intended material (injected polypropylene) and the prototype material (Selective Laser Sintered Nylon) differed and a reduced performance was seen in the prototype samples it was determined to be adequate for design comparison.

ISO 10328 was used as a standard test of strength and durability to ensure a safe design prior to use. This has not been a focus for many of the prosthetic feet designed for use in developing countries and the work of Jensen and Treichl (Jensen & Treichl, 2007) showed the majority of design would not be considered to pass the standards of ISO 10328. This does raise the question of the ethics involved in providing prosthetic limbs to developing countries: Is it acceptable to provide a

prosthesis that does not meet international standards for safety but does allow amputees to improve their quality of life with a risk of prosthetic failure? For this work it was not seen as acceptable to develop a prosthetic foot without taking this standard into account and meeting it.

This thesis has been organised as follows:

Chapter 2 provides a literature review of structure and function of the natural limb considered in different circumstances; be it walking, standing or other functions. Following this is a review of the existing prosthetic feet used in low-income countries and the measures commonly used to evaluate prosthetic foot function, both in clinical and lab tests.

Chapter 3 begins with the generation of a Product Design Specification (PDS). The existing design of Strathclyde foot was tested to ISO 10328 standards up to P5 static proof level successfully at the toe in unreinforced samples. The reinforced toe failed during P3 testing and the heel was determined to have failed at the P4 level due to excessive deformation.

Chapter 4 provides an overview of design changes made with reference to FEA carried out to evaluate the predicted behaviour resulting from said changes. The design was intended to be produced in polypropylene via injection moulding, as the existing design was, however due to cost limitations an alternative method for producing samples had to be determined. A number of rapid prototyping methods were evaluated to determine an appropriate method for sample production. Two materials were experimentally examined to verify material properties. Having determined the properties of Duraform EX as suitable, prototypes were produced and tested. The heel section was determined not to pass to any level of ultimate static testing due to excessive deformation, while the unreinforced toes failed during

P3 testing. The reinforced toes showed mixed results with one sample failing during P3 testing while the other successfully passed to the P5 level.

Chapter 5 begins with the elements of redesign required after the testing in the previous. The new design was produced in prototype form and tested as previously. Heel testing provided one failure during P3 testing and one during P4 testing. Both unreinforced toe samples failed during P3 testing while the reinforced toe sample failed during P4 testing. A comparison of the Strathclyde foot performance to other feet as tested by Jensen & Treichl (Jensen & Treichl, 2007) follows. Finally, a single subject force plate trial was conducted on the Strathclyde foot.

Chapter 6 completes the thesis with a conclusion based on meeting the aims of the Product Design Specification (PDS). Recommendations are then made for further work in order to progress towards the goals outlined in the PDS.

Appendix A provides details of rollover shape testing carried out on the Strathclyde, Iraq, ICRC, Dynamic and Atlas feet.

Appendix B details the FEA carried out to support design modification of the Strathclyde foot to redesign 1 (R1) and redesign 2 (R2).

CHAPTER 2 – Literature review

In order to form a knowledge base from which to proceed this chapter examines existing literature related to the form and function of the human foot, designs of prosthetic feet for use in developing countries and methods of measuring prosthetic foot function.

2.1 The natural human foot

When designing a prosthetic foot, it is important to consider the foot it is to replace. The human foot is unique amongst nature; there is no other animal on the planet that walks on two legs in a plantigrade manner as their main mode of transport (Inman, 1966). The human foot and propulsion method developed over millions of years of evolution, it has even been argued that the development of upright locomotion is one of the key points in human evolution (Lovejoy, 1988).

The foot cannot be considered purely in isolation and therefore a discussion of the whole body, as it relates to the function of the foot, will be involved. The major functions of the foot are to follow along with some of the more important minor functions.

2.2 Standing

2.2.1 Load bearing

A number of adaptations in the human form are visible which make upright walking more efficient and comfortable. Beginning at the connection of the spine to the skull, it is visible that in humans the connection is in such a way that the skull is upright. The spine itself has a double curve that causes the centre of mass of the

head, arms and torso to act directly above the hip joint centre. The pelvis is aligned at a slight forward angle from the coronal plane that causes the knee to be straightened. As such the weight of the body passes through the hip joint and then through the knee joint leading to a stable upright position. The loads of the upright human all pass directly through a line which goes from skull to hip centre, knee centre and then the ground forward of the ankle as shown in Figure 1. In the alignment of the human form, joint moments are eliminated and so a very small energy cost is required to maintain the upright position.

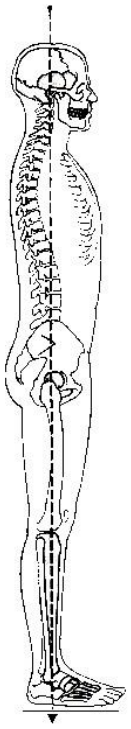

Figure 1 – Proper alignment of the human body demonstrating line of load application(Kendall & McCreary, 1983)

These adaptations whilst useful would not be enough to allow the human being to stand upright comfortably. The foot is the base of this entire structure and without an adequate base the structure could not remain upright.

The foot is made of arched sets of bones, two arches span from the heel to the ball of the foot and one across the metatarsal heads (pictured in Figure 2). These arched structures are rigid and resist flattening even when muscular activity is removed, such as in anaesthetised individuals. This suggests that they rely on the ligaments to maintain their form. These shapes, variably resistant to deformation depending on the extent of pronation or supination of the foot during stance phase, serve to distribute the load from the body across the foot in set ratios which Morton, 1935(D. J. Morton, 1935), found to be 3:1:2 for calcaneus: metatarsal I: metatarsals II, III, IV and V. This distribution of load allows for stability at the base of the human form. The skin on the sole of the foot is specially adapted to allow weight bearing/load transfer to occur without breakdown and is even toughened by repeated activity and frictional contact. The fatty pad under the calcaneus spreads the load across the whole under surface of the bone, which prevents point loading and contributes to comfort during load bearing.

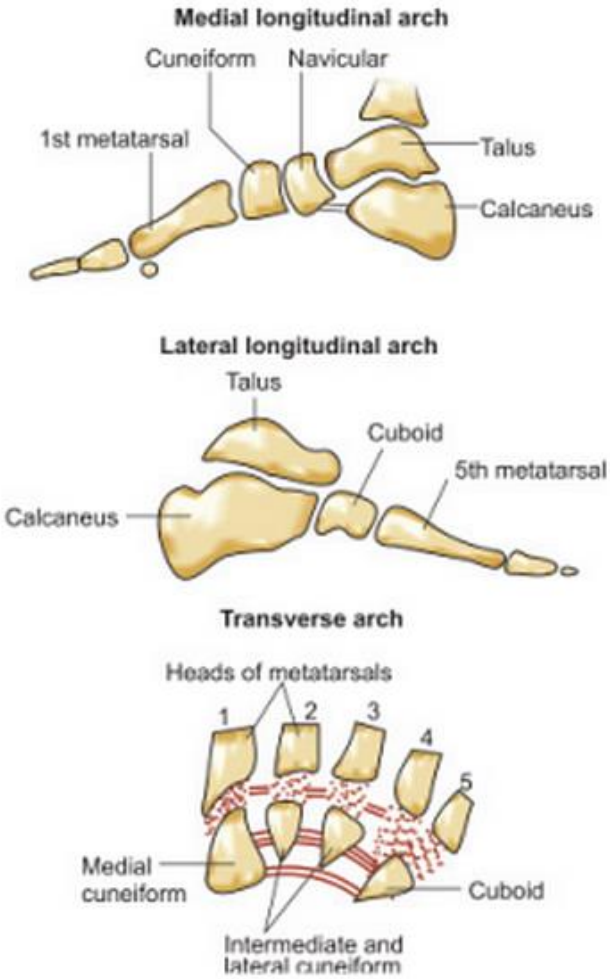

Figure 2 - This image presents the arches of the foot, an important feature of load bearing and stability of the foot (Ashalatha & Deepa, 2011)

The structure of bone is not uniform, a hard outer is supported by a core of sponge-like structure made of rods of tissue called trabeculae. Each bone in the foot displays individual adaptations to load bearing visible in the pattern of the trabeculae within the bone. These trabeculae conform to the lines of stress, both tensile and compressive, applied to the bone and will be digested (by osteoclasts) and reformed (by osteoblasts and osteocytes) to match the new stresses if these stresses change. This was first proposed by Julius Wolff in 1892 (Wolff, 1892) following the work of Culmann and Von Meyer (Meyer, 1867) who noted that the lines of the trabeculae in the femoral head were aligned with the principal stresses occurring there. The lines

of the trabeculae are consistent across bones although separated by the gaps between the bones. This displays the way in which the elements act together in order to form a suitable structural base for the rest of the body. This may be observed in Figure 3, an x-ray image of the rear of a foot.

Figure 3 - An x-ray image of the rear of the foot. The trabeculae are visible as thin white lines. It should be noted that the trabeculae of different bones continue to follow the principal stress lines across the gaps between the segments (University Hospitals of Geneva, 2012)

The tibia is a long bone of the lower leg (the other being the fibula) that must bear the weight of the body during standing and walking. It is particularly adapted to this thanks to its own structure, consisting of a collagen fibre reinforcement set within a hydroxyapatite ($Ca_{10}(PO_4)_6(OH)_2$) matrix. The hydroxyapatite is very hard and so can withstand large loads but is brittle and so prone to failure from impacts, bending or twisting actions. Collagen fibres are strong in tension but buckle under compression. The combination of the two elements gives bone the strength required

to carry the loads but also a resistance to impact, bending and twisting in much the same way as modern composite materials. (Martini & Nath, 2009)

2.2.2 Stability

The load bearing adaptations of the human body permit upright stance however, these do not necessarily provide stability. The arches of the feet do contribute to stability as the load of the body is distributed across the foot rather than concentrated at the heel. The fact that there are two feet, separated and slightly turned out during normal stance, adds to the stability of the overall structure. The muscles of the leg work in combination with the proprioception of the sole and synaptic balance feedback of the inner ear to provide active stability at a small cost of energy. In anteroposterior stability the muscles of the anterior compartment (tibialis anterior, extensor digitorum longus, extensor hallucis longus and peroneus tertius), lateral compartment (peroneus longus and peroneus brevis), posterior compartment (gastrocnemius, soleus and plantaris) and deep posterior compartment (tibialis posterior, flexor digitorum longus and flexor hallucis longus) all contribute in stabilising the lower leg. Stabilisation is not exclusively carried out by the muscles of the lower leg; moving the position of the body over the feet will also aid stability and may be effected by muscles higher in the body such as the abdominals for example. Mediolateral stability is largely maintained through the hip adductors (adductor brevis, adductor longus, adductor magnus, adductor minimus, gluteus maximus via connection to the gluteal tuberosity, quadratus femoris, obturator externus, semitendinosus, pectineus and gracilis) and abductors (gluteus medius, tensor fascia latae, gluteus maximus via connection at fascia latae, gluteus minimus, performs and obturator interns) as the everters (peroneus longus, peroneus brevis and peroneus tertius) and inverters (tibialis anterior, tibialis

posterior, extensor digitorum longus and hallucis longus) also act in plantarflexion and dorsiflexion as described above. (Martini & Nath, 2009)(Wheeless, 2011)

2.3 Walking

2.3.1 Gait cycle

As can be seen in Table 1, a complex interaction of muscle actions is required during gait. Beginning at heel strike the gluteus maximus, gluteus medius, hamstrings, quadriceps and pre-tibial muscles all contract eccentrically, that is they resist loading while lengthening. These actions are carried out in order to maintain the correct position of the leg for initial contact and to decelerate it.

Following the initial contact, the gluteus maximus no longer continues to contract eccentrically but becomes inactive. The remaining muscles continue to function eccentrically as the leg responds to loading.

At midstance the hamstrings, quadriceps and pretibial muscles become inactive while the gluteus medius continues to act eccentrically and the calf muscles become engaged eccentrically. The calf muscles in this case prevent the ankle rotation through midstance occurring too quickly.

As terminal stance is entered the leg begins to move towards propulsion, the calf muscle begin to contract concentrically in order to provide drive prior to swing. The iliopsoas also become active, contracting concentrically in order to flex the hip in order to rotate the thigh forwards and upwards. The gluteus medius maintains eccentric contraction throughout this phase.

In pre-swing, the calf muscles continue to contract concentrically in order to provide push off while the iliopsoas also contract to begin raising the leg out of contact with the ground. The quadriceps contract eccentrically during this phase while the gluteus medius has become inactive as it is no longer useful in maintaining body position or decelerating movement.

During initial swing the pretibial muscles (tibialis anterior, extensor digitorum longus and extensor hallucis longus) contract concentrically in order to raise the toe and prevent collision of the foot with the ground, which could lead to stumbling or falling. The iliopsoas concentric contraction continues to further flex the hip and raise the leg. The hamstrings and the quadriceps act eccentrically to control the movement of the lower leg.

As gait progresses to mid swing the iliopsoas and pretibial muscles continue to contract concentrically, flexing the hip and foot respectively. The hamstrings continue to contract eccentrically but the quadriceps no longer provides any resistance.

Finally, at terminal swing only the hamstring acts eccentrically and the pretibial muscles act concentrically. The hamstrings decelerate the swing through of the leg and the pretibial muscles maintain the raised toe position of the foot. As terminal swing is completed the gait cycle repeats itself once again.

This cycle is carried out by both legs in turn and should results in an even gait pattern if the cycle is well balanced across both legs. In being even the gait is more efficient so reducing energy costs to the walker but more than this, it has been shown to be an indicator of an individual's attractiveness (i.e. generally symmetric motion was evaluated as more attractive than asymmetric motion) (Johnson & Tassinary, 2007)(Giese, Arend, Roether, Kramer, & Ward, 2009) or their current emotional state (Roether, Omlor, Christensen, & Giese, 2009).

Table 1 - Muscle activation during normal gait (Uustal & Baerga, 2004)

Classic gait terminology	Heel strike	Foot flat	Midstance	Heel off	Toe off	Acceleration	Midswing	Deceleration
Rancho Los Amigos Terms	INITIAL CONTACT	LOADING RESPONSE	MID STANCE	TERMINAL STANCE	PRE-SWING	INITIAL SWING	MID SWING	TERMINAL SWING
	STANCE PHASE 60%					SWING PHASE 40%		
% of total phase	0-2%	0-10%	10-30%	30-50%	50-60%	60-73%	73-87%	87-100%
Iliopsoas	Inactive	Inactive	Inactive	Concentric	Concentric	Concentric	Concentric	Inactive
Gluteus maximus	Eccentric	Inactive	Inactive	Inactive	Inactive	Inactive	Inactive	Inactive
Gluteus medius	Eccentric	Eccentric	Eccentric	Eccentric	Inactive	Inactive	Inactive	Inactive
Hamstrings	Eccentric	Eccentric	Inactive	Inactive	Inactive	Eccentric	Eccentric	Eccentric
Quadriceps	Eccentric	Eccentric	Inactive	Inactive	Eccentric	Eccentric	Inactive	Inactive
Pretibial muscles	Eccentric	Eccentric	Inactive	Inactive	Inactive	Concentric	Concentric	Concentric
Calf muscles	Inactive	Inactive	Eccentric	Concentric	Concentric	Inactive	Inactive	Inactive
Key:	Inactive			Concentric			Eccentric	

At heel strike the foot is held either neutrally or slightly plantar flexed, the heel comes into contact with the ground and the fatty pad deforms, taking the impact out of the strike. Initially the sub-talar joint is flexible. The foot will begin to plantar-flex from heel strike on. As the foot comes fully into contact with the ground at foot flat the foot will tend to supinate, i.e. roll out, which causes the sub-talar joint to lock. This locking of the sub-talar joint effectively makes the foot a stiff lever that is then used to carry the weight of the body to the metatarsal heads. The joint remains stiff and is utilised to facilitate push off as a lever arm with the plantar-flexors now contributing to propelling the body forwards (Uustal & Baerga, 2004).

2.3.2 Energy storage, return and input

The structure of the lower leg has developed not only to be load bearing but also to allow the storage and return of energy during propulsion. Energy input is also made possible through various structures of the foot and lower leg, particularly the action of the muscles on the bones via the tendons.

The lower leg passively stores energy as elastic potential through elongation of tendons, particularly the calcaneal (Achilles) tendon. Some of the stored energy is returned during gait to reduce the overall energy cost of walking. Energy is also actively put into each step through the contraction of various muscles of the leg (Martini & Nath, 2009).

2.3.3 Active stability

The human body is covered in skin, which provides a huge sensory input to the brain in terms of temperature, pain and touch sensations. The skin on the legs is no different and this feedback is lost along with the limb in an amputee. Within the leg there are a range of sensory mechanisms that provide the brain with the information relevant for determining the position of the limb in comparison to the rest of the body. These take the form of muscle spindles, which monitor muscle length and

enact stretch reflexes, Golgi tendon organs, which monitor tension developed in tendons as a result of muscle contraction and finally receptors in joint capsules that determine the pressure, movement and tension in a joint. Such mechanisms allow the intact human to adjust to changing conditions such as uneven or sloping surfaces or having caught the toe on a low-lying object. These proprioceptive mechanisms are lost in the amputated limb meaning that the amputee has no sensation of where their prosthesis is. Currently no prosthetic limb can provide similar information to the amputee and is a major limiting factor in prostheses, as the limb must be seen to know where it is or else estimated with practice. The lack of feedback, particularly proprioception is arguably a major factor in stumbling in lower limb amputees and reduced functionality in upper limb amputees. Microprocessor controlled knees are available that can predict the action of the lower limb and respond accordingly to reduce stumbling (Kaufman, Anderson, Schneider, & Walsh, 2009) however, these respond automatically and do not inform the wearer in any way.

2.4 Other functions

Running involves a different mechanical use of the lower limb than walking and has a higher energy cost but is much faster. In running a very different gait pattern is observed. Double stance is eliminated and two double float periods are found when both feet are in the air, one at the start of swing and one at the end (Novacheck, 1998). Toe off occurs prior to 50% of gait cycle, much earlier than the approximately 60% observed in walking, and can be as early as 22% in world-class sprinters (Mann & Hagy, 1980). The pattern of muscle activation is very different from walking (see Figure 4 compared to Table 1) with most activity occurring around initial contact and none at toe off.

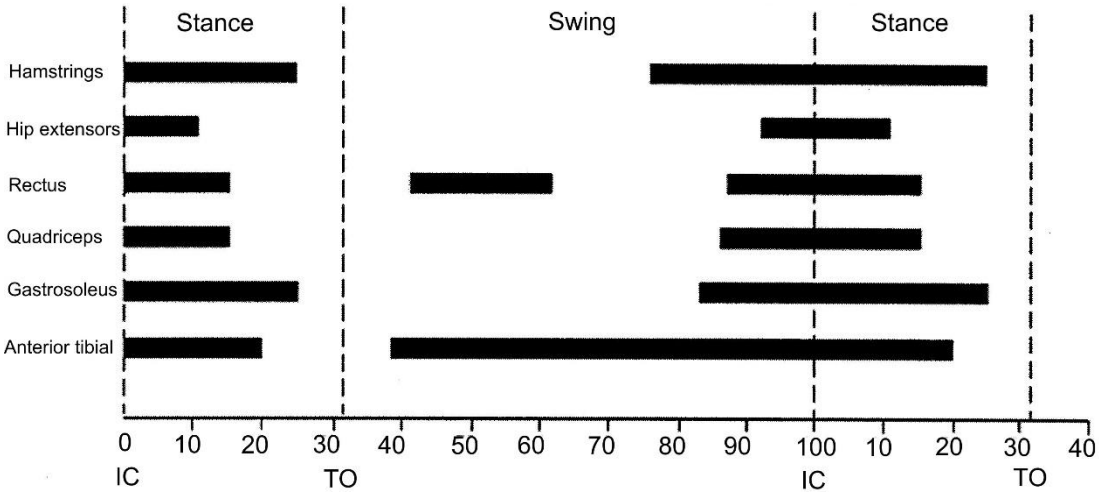

Figure 4 - Activation of muscles during running (Novacheck, 1998)

The contact or footprint observed in running is different to that of walking with heel contact occurring laterally before quickly passing medially. At higher velocities heel contact may be avoided all together in preference for contact at the ball of the foot (Novacheck, 1998).

Another significant difference between walking and running is in the kinetic and potential energy profiles. The potential energy is related to the height of the body while the kinetic energy is related to the velocity of the body. In walking the two energy types are entirely out of phase with kinetic energy peaking when potential energy is at a minimum (i.e. the body is moving fastest at the lowest elevation) however, in running the two energy types peak at the same time (i.e. the body is fastest at the peak elevation)(Novacheck, 1998).

The lower limb is also used in striking for example kicking a ball or as part of a martial art in which case it acts as a rigid club in order to transmit force to the target.

Aside from being used as a rigid club the foot may also be used for finer control, such as in using a pedal in a car or operating a sewing machine. These are not typically considered in design of a prosthetic foot where mobility is the main concern

however, during their lifetime a prosthetic foot will no doubt be used to carry out some such actions.

2.5 Prosthetic feet

The prosthetic feet most people are aware of nowadays are of the high-tech variety, often due to news coverage given to new developments but, typically because of military amputees using them. The vast majority of the world's amputees do not have access to such artificial limbs and instead rely on simpler and somewhat less effective alternatives. A sample of some of the feet available to those in low-income countries is given below with an overview of each foot.

2.5.1 Peg leg

The peg leg was the traditional replacement for a lost leg and is still used in more or less its original form in some areas of the world. Some updates have been made as in the case of Muller (Muller, 1957), where a cosmesis was added to improve the look of the peg leg without contributing to its function. Alternatively, Mathews et al. (Mathews, Burgess, & Boone, 1993), reported on the 'all-terrain foot' which was designed in response to the difficulties found by many users of foot shaped prostheses. The foot shaped prostheses were apparently prone to become caught or tangled on undergrowth and were difficult to use in wet or muddy conditions where they could get stuck. The all-terrain foot is a peg leg with a large, circular rubber pad at the end. The rubber is shaped as a tapered cylinder with a convexly curved bottom surface. A hole in the base allows for a bolt to be used in attaching the foot to the leg, which the authors acknowledge, may fill with mud or snow unless otherwise plugged. The smaller footprint and simpler shape would prevent catching on undergrowth and the durability would make it suitable for use in wet and muddy conditions (see Figure 5).

Figure 5 - The all-terrain foot, displaying the simple and rugged design (Mathews, 2017)

Werner (Werner, 1999), described a number of different versions of trans-tibial peg legs that may be manufactured relatively easily in low-income countries. The first type was to be used with a bent knee and was not recommended for extended use as it could cause knee contracture. It was basically a support for the leg below the knee and could include a long pole extending to head height, which then functioned as a combined crutch and limb (see Figure 6).

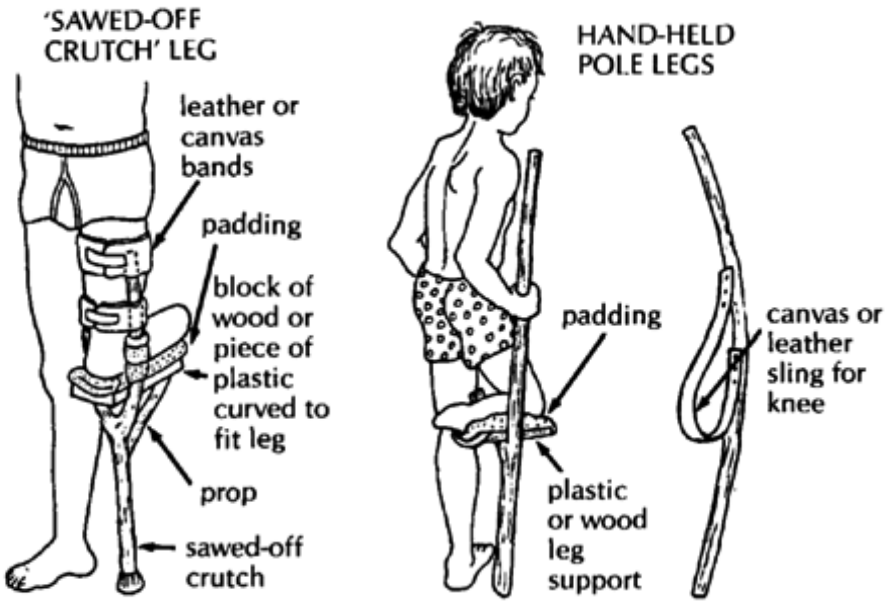

Figure 6 – Peg legs for use with a bent knee (Werner, 1999)

The unbent knee varieties of the peg leg included making a socket from plaster and then using either bamboo or PVC pipe to form the peg with a rubber end to contact the ground (see Figure 7). Instructions were included as to how to lengthen the PVC type to fit as a child grows and how to make a suspension belt. Werner also suggests the addition of a foot to prosthetics legs for improved aesthetics and to prevent sinking in soft ground and included a design for use (see Figure 8). The foot design was similar to that of Muller in that little was added functionally to the foot.

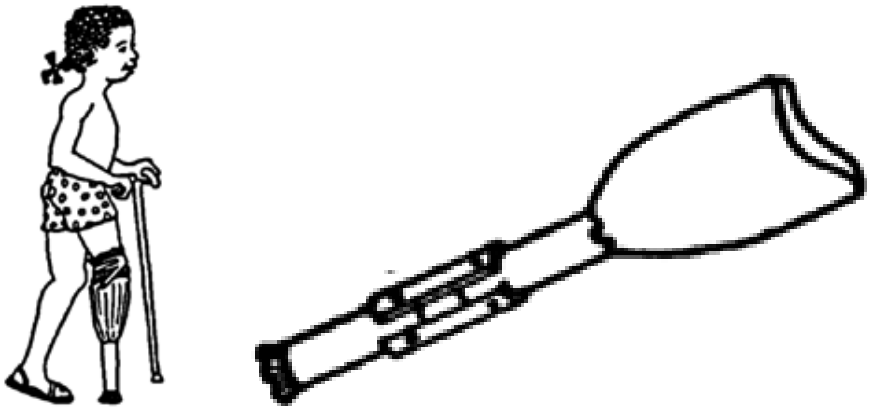

Figure 7 – These images demonstrate a bamboo peg (left) and a PVC peg (right) with added section for growth (Werner, 1999)

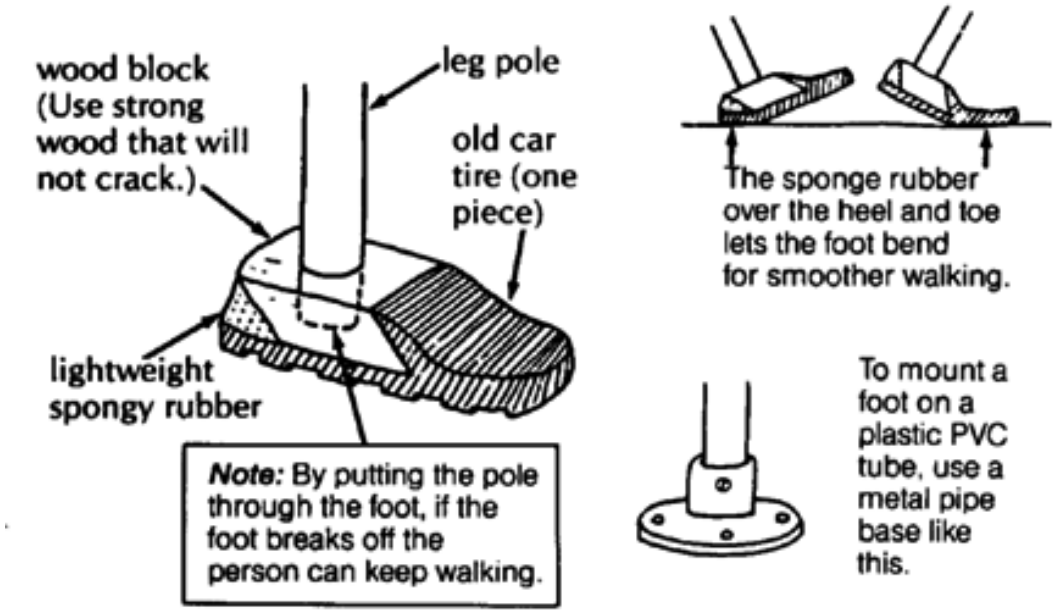

Figure 8 – The foot design recommended by Werner (Werner, 1999).

2.5.2 ICRC foot

The ICRC (International Committee of the Red Cross) foot is a SACH (Solid Ankle, Cushion Heel) foot variant produced by CRÉquipements SA (Coppet, Switzerland)(International Committee of the Red Cross, 2006b). Between 1979 and 2011 the ICRC provided 374,575 prostheses (International Committee of the Red

Cross, 2011). Not all of the prostheses provided would have used the ICRC foot (which was not produced by CRÉquipements SA until 1992 and also due to a proportion of prostheses being for upper limbs for example) however, it would be expected to be a large proportion given the ICRC's particular emphasis on aiding victims of landmines. The ICRC foot costs approximately €45 (CRÉquipements SA, 2013) and is provided through the ICRC overseas programmes although, it is manufactured in Switzerland. By being manufactured in Switzerland it provides a certain control over quality that may be lost in local production.

The foot itself contains a "fenestrated dog tail" (a short, curved and indented shape, see figure 9) keel made of polypropylene surrounded by polyurethane foam that forms the bulk of the foot including the outer surface. The sole is made of polyurethane (Jensen & Treichl, 2007).

Figure 9 – Diagram of a sectioned ICRC foot (Turcot et al., 2013)

The ICRC foot has been extensively tested in both the laboratory and field conditions. Jensen & Treichl (Jensen & Treichl, 2007) partially tested several feet to ISO 10328 standard, including the ICRC foot. Some of the prostheses were exposed to the equivalent of 365 days of 8 hours of sunlight over the course of 20 weeks in a specially built chamber while others were exposed to 98-100% humidity at 38°C for 20 weeks. The groups of prostheses exposed to either UV light or humidity were only tested under static loading as specified in ISO 10328. A further

group of prostheses was not exposed to either of these conditions and was subsequently tested under cyclic loading conditions as well as static loading. Exposure to either humidity or UV light caused the maximum deformation, creep and permanent deformation of the heel to increase. In forefoot loading exposure to UV light caused an increase to maximum deformation and creep but a reduction in permanent deformation. It is possible that the UV light exposure provided a curing effect on the polyurethane, extending the elastic region of deformation. Exposure to humidity caused a decrease in deformations in all areas suggesting that exposure to moisture increases the stiffness of the polyurethane. Jensen and Treichl (Jensen & Treichl, 2007), did not consider the ICRC foot to meet the standard for complete lower limb prosthesis of ISO 10328 (<5mm permanent deformation) however, it does meet the standard described under section 17.2 “Separate tests on ankle-foot devices and foot units” within ISO 10328 and may be considered to pass as such.

Sam et al. (Sam, Hansen, & Childress, 2004), reported that a size 25 ICRC foot weighed 567.6g during their testing. It was found that the ICRC foot had little toe support shown in the shortness of the roll-over shape (see Figure 10) and that its shape varied only slightly from a typical SACH foot in that the transition between flat section and upward break was smoother. It was acknowledged in this study that as only one new foot of each kind was tested the results were limited. In addition, it was noted that a prosthetic foot is required to perform other functions not related to the roll over shape to function well such as shock absorption at heel strike or durability. Eaton et al. (Eaton, Ayers, & Gonzalez, 2006), in testing roll-over shape found the ICRC to have a longer arc length than the natural foot tested but with the same radius. Both studies note the drop off performance in the toe section of the ICRC foot due to the lack of support.

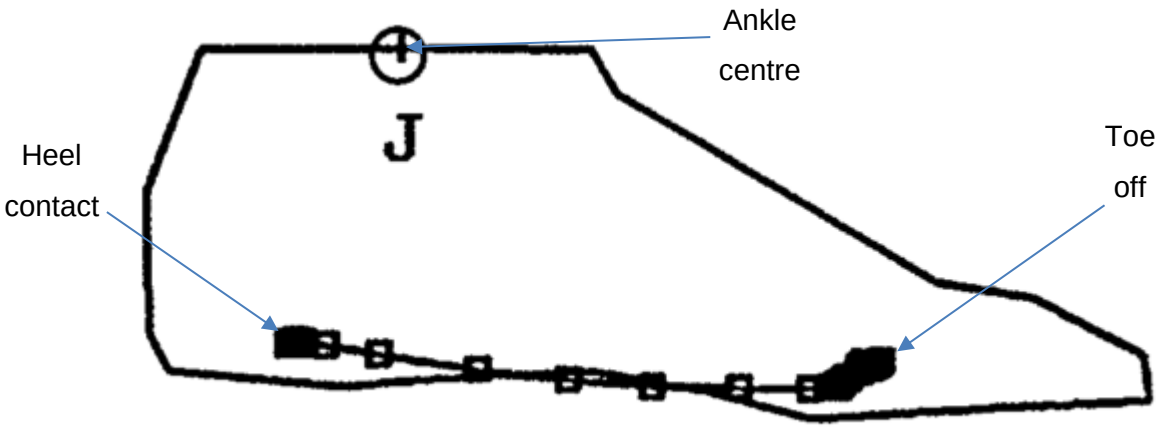

Figure 10 – Roll-over shape of the ICRC Geneva foot in comparison to external boundary of the prosthesis (Sam et al., 2004)

Field testing of the ICRC foot has shown a number of weaknesses in design with failure of the foot cover due to wear or disintegration highlighted by Jensen & Raab (Jensen & Raab, 2004). Jensen et al. (Jensen, Nilsen, Thanh, Saldana, & Hartz, 2006) identified failure of the foot cover or wear of the sole as accounting for 83% of failures (36 of 43 cases of failure) in trans-tibial amputees while in trans-femoral amputees (Jensen & Raab, 2004) three out of four cases of sole wear and cover failure required replacement, accounting for 11.4% of all failures in this group. It was noted that this type of failure was particularly pronounced when the prostheses were used barefoot. For trans-tibial amputees, prosthesis survival rates at 6, 12, 18 and 24 months were found to be 95%, 56%, 31% and 0% respectively. It was subsequently concluded that polyurethane feet could not be recommended for use in tropical areas. It was also observed by Jensen et al. (Jensen, Nilsen, Thanh, et al., 2006) that six of the feet had worn keels and one of the feet failed at the bolt attachment. Jensen, Nilsen, & Zeffer (Jensen et al., 2005) report a quality benchmark for trans-tibial prostheses in low-income countries requiring “walking >1km at 90±10%, non-users at 5±5%, discomfort at 10±10%, pain at 10±10%, and patient satisfaction at 90±10%. The technical performance demands were set for

good socket fit at 60±10%, misalignment at 15±10%, insufficient craftsmanship at 10±10%, and requirements for socket change at 10±10%". Based on these standards the ICRC foot as reported on by Jensen et al (Jensen, Nilsen, Thanh, et al., 2006) satisfied patient requirements in all areas but suffered from unacceptable misalignment rates and requiring new sockets in terms of technical performance.

2.5.3 Handicap International (HI) foot

The Handicap International foot is a SACH foot largely used in Cambodia, but also in Mozambique (Sam et al., 2004), Vietnam, Laos and Thailand (Simon, 1996). It is made in Cambodia by Handicap International and between 1992 and 1996 10,000 pairs of feet were manufactured and distributed from there (Simon, 1996). The foot itself is a polypropylene keel with a foam rubber forefoot and heel, a tyre rubber sole and a rubber cover (Jensen & Treichl, 2007). It was designed with the climate of Cambodia in mind, particularly the heat and humidity, and the need of users in Cambodia to squat (Day, 1996). From the 1996 consensus conference on appropriate prosthetic technology in low-income countries (Day, 1996) it was reported that a trans-tibial system including the HI foot would have cost approximately $25-37 to produce however, as parts were provided free of charge it was estimated a more realistic cost would be $230 per prosthesis. Simon (Simon, 1996) reported that the foot was produced in three sizes, 17cm, 23cm and 25cm, weighing 320g, 600g and 800g respectively and was made of recycled polypropylene and rubber from the local province.

The HI foot has been tested on both clinical field trials and in the laboratory. Sam et al., 2004, used an HI foot produced in Maputo, Mozambique by HI in testing the rollover shape. They reported the length as 26cm, the mass as 854.6g (the heaviest in the study) and that it could be used on either side. While the HI foot appears to have a shorter arc length than the other feet tested but a similar radius,

Sam et al. considered it to have “a functional roll-over shape” that was “similar to that of a typical SACH foot”.

Jensen & Treichl (Jensen & Treichl, 2007) tested the HI foot to the standards of ISO 10328 by the methods described above in the section on the ICRC foot (page 21) and found that humidity exposure increased creep and permanent deformation in both heel and forefoot loading but increased maximum deformation in forefoot loading while decreasing maximum deformation in heel loading. Exposure to UV light decreased maximum deformation, creep and permanent deformation in forefoot loading but decreased deformation in heel loading while the creep and permanent deformation both increased. In cyclic testing, the rubber was found to have permanently deformed under the keel, but the samples passed two million cycles as required by the standard. It was ultimately determined that the HI foot would not pass the standards for an entire lower limb prosthesis (permanent deformation <5mm) however, given the allowance in the standard for separate ankle-foot prostheses testing it would be considered a pass.

Jensen & Heim (Jensen & Heim, 1999) conducted a field trial of the HI foot in Vietnam where it was used by ten amputees who were followed up after 10 or 19 months. Four of the feet were determined to have failed at an average of 12 months (range 8-18 months) while of the six remaining feet only three were used for more than 500m walking a day. Of the failing feet two had failed because of the sole, one because of the keel and one because of the bolt. There is no mention of whether the feet were used barefoot or shod during the trial, the only reference to the conditions of use are body mass, hours worn, daily distance covered (<500m, 500-2000m, >2000m) and wet or dry rural. The four failing feet were used for >2km a day while only one of the unfailing samples was within this distance bracket.

Jensen et al. (Jensen, Nilsen, Zeffer, Fisk, & Hartz, 2006) conducted a study using 30 HI feet which included far more detailed background information than that of Jensen & Heim (Jensen & Heim, 1999). Family, environment, socio-economic background, build, cause of amputation, stump length and condition as well as skin disorders were all included. Recorded in compliance was whether the foot was used barefoot (13 users, 43%), daily distance walked (>1km 100% of users) and hours of use per day (average 14 hours, range 12-16 hours). The amputees were also asked if they experienced pain or discomfort (none reported any), how they felt about the weight (light – 3 users, heavy – 0 users) and if they were satisfied with it (28 satisfied, 2 dissatisfied). The fit was recorded (good in 14 cases, wide in 16 cases) along with any misalignment (5 cases including 3 of the prosthesis, 3 of the foot and 1 of uneven length). Six failures were recorded resulting in replacements although eight failures were recorded in total; three resulting from wear of the sole, four from wear of the keel and one from failure of the bolt attachment. The average time to failure was 10 months (range 7-17 months). Of the failed feet, the average daily use was 14 hours (range 14-15 months) with all feet being used to cover greater than 1km a day with five used barefoot. The fit of the prosthesis was good in six cases and but found to be wide (loose) in two with a further two cases of misalignment reported and one of inadequate craftsmanship. The patient satisfaction was 100% among those with a failed prosthesis. As the authors admitted few feet (four total) were followed up for longer than 12 months however, the 20% replacement rate at the 12-month point was deemed acceptable and was not found to be different in a statistically significant to the failure seen in the PP-Rubber foot in the same study.

2.5.4 Veterans International (VI) feet

The Veterans International group was founded by the Vietnam Veterans of America Foundation (VVAF) in 1992 with funding from USAID's War Victim Fund

(Veterans International Cambodia, 2013). They have built at least three varieties of prosthetic foot with the needs of the local populace and the local environmental conditions in mind (Day, 1996). The VI-Solid was described as a polypropylene big tooth keel with anchor holes, wrapped in rubber bands with a rubber sole, heel and cover and a rubber reinforced forefoot (Jensen & Treichl, 2007) (see Figure 11 for an image). The VI-Cavity is the same with the difference that at the heel a steel ball was included during vulcanizing in order to create a cavity which may provide shock absorption in place of the rubber at the heel (Jensen, Nilsen, Zeffer, et al., 2006) see Figure 12 for an image). No description of the VI multiaxis foot was available.

Figure 11 – A cross section of the VI-Solid foot showing the internal makeup (Jensen, Nilsen, Zeffer, et al., 2006)

Figure 12 – A cross section of the VI-Cavity foot, note the cavity and the steel ball (Jensen, Nilsen, Zeffer, et al., 2006)

Only one laboratory test appears to have been carried out on any of these feet, the VI-Solid foot (Jensen & Treichl, 2007). The feet were treated as described previously in the ICRC foot section (page 21). It was found that exposure to UV light resulted in an increase in maximum deformation, creep and permanent deformation at the forefoot and a decrease in maximum deformation, creep and permanent deformation at the heel. Exposure to humidity resulted in an increase in maximum deformation, permanent deformation and creep measured in the forefoot and increases in maximum deformation and creep at the heel while reducing the permanent deformation there. The VI-Solid foot was unusual in testing in that the heel deformed by around the same amount as the forefoot rather than less as observed in the other feet tested. On completion of the cyclic testing the VI-Solid foot rubber covering was found to have compressed under the forefoot and/or heel. Jensen and Treichl (Jensen & Treichl, 2007) determined that the foot would not

have stood up to the lower limb prosthesis criteria of ISO 10328 however, given the allowance for separate ankle-foot prostheses would be considered a pass.

One of the three foot designs, the VI multiaxis foot was only used in relation to a study on the “quality benchmark for trans-tibial prostheses in developing countries” and not mentioned specifically in terms of performance but rather only as to the quality of provision and craftsmanship (Jensen et al., 2005). No further mention of the VI multiaxis foot was found in the literature however, the VI-Solid was mentioned twice, Jensen & Heim (Jensen & Heim, 1999) and Jensen et al. (Jensen, Nilsen, Zeffer, et al., 2006), with the VI-Cavity also studied in (Jensen, Nilsen, Zeffer, et al., 2006). In Jensen & Heim (Jensen & Heim, 1999) ten amputees were fitted with the VI-Solid foot and followed up over 19 months. The amputees were largely intensive users (8 users out of 10 total) with 2 covering less than 500m a day, 3 covering 500-2000m daily and 5 covering over 2000m per day. The weight of the amputees, hours of daily use and living conditions (wet/dry rural) were similar to those of the other groups tested at the time. One foot was followed up at 10 months and had not failed, the other 9 were followed up at 19 months and had not failed, which was significantly better than the other feet tested at the time (Ba Vi, HCMC and HI feet) and showed that the foot could stand up to intensive use for 19 months.

In Jensen et al (Jensen, Nilsen, Zeffer, et al., 2006), 31 amputees were fitted with the VI-Solid foot. At the 12-month follow up one foot had failed and had to be replaced due to a worn foot sole. The amputee was not recorded as using the prosthesis barefoot but did use it for greater than 1km walking and 14 hours a day. Despite the failure the amputee was recorded as being satisfied with the prosthesis. At the 18-month and 24-month follow ups no further prostheses had failed. 12 (39%) of amputees found the VI-Solid foot to be heavy but only 5 (16%) stated that they were not satisfied with the prosthesis despite the fact that 6 (19%) were recorded as

non-users. In the conclusion the authors state that they considered Cummings (Cummings, 1996) call for a low cost, durable and locally manufactured prosthetic foot fulfilled.

Jensen et al (Jensen, Nilsen, Zeffer, et al., 2006) also followed 35 amputees who had been provided with the VI-Cavity foot. A high percentage (68.6%) of amputees lived in a 'wet' environment compared to the users of the VI-Solid foot (3.2%). All users of the VI-Cavity foot were recorded as walking more than 1km each day and wearing the prosthesis for 10-15 hours each day. 13 of the amputees (37%) were recorded as using the prosthesis barefoot. 60% of users considered the prosthesis light however, 100% reported that they were satisfied with it. The survival rate of the VI-Cavity foot at 6, 12, 18 and 24 months was 100%, 97%, 89% and 86% respectively with 14 prostheses failing in total, all of which required replacement. Of these 14 all were used for over 1km walking a day and worn for between 12 and 15 hours daily with 8 (57%) of the failed prostheses used barefoot. In 13 cases, the failure occurred due to the foot sole being worn and in 1 case due to the keel being worn (see Figure 13 and Figure 14 for images of failures).

Figure 13 – Fracture of the sole of a VI-Cavity foot (Jensen, Nilsen, Zeffer, et al., 2006)

Figure 14 – Penetration of the keel of the VI-Cavity foot (Jensen, Nilsen, Zeffer, et al., 2006)

12 of the amputees (86%) expressed satisfaction despite the failure, with the other 2 (14%) not expressing an opinion. The average time to failure was given as 27 months (range of 7-32 months) however, the authors noted that few of the feet were seen before 26 months and as the amputees would have had other prostheses available to them that they were unlikely to attend a clinic upon failure of the VI-Cavity foot but wait until recalled. In a comparison of the two tested VI feet Jensen et al (Jensen, Nilsen, Zeffer, et al., 2006) found that the VI-Solid was the better performer ($p<0.0002$).

2.5.5 Jaipur foot

The Jaipur foot was developed in the 1970s in Jaipur, India, by P.K. Sethi with local craftsmen and was designed with the local conditions and requirements of local people in mind. Sethi et al,(Sethi et al., 1978) stated the following as the goals of design:

1. It should not require a shoe, and consequently, should have a certain degree of cosmetic acceptance by the amputee.
2. The exterior should be made of a water- proof, durable material.
3. It should allow enough dorsiflexion to permit an amputee to squat, at least for short periods.
4. It should permit a certain amount of transverse rotation of the foot on the leg to facilitate the act of walking as well as to allow cross-legged sitting.
5. It should have a sufficient range of inversion and eversion to allow the foot to adapt itself while walking on uneven surfaces.
6. It should be inexpensive.
7. It should be made of materials that are readily available.

(Sethi et al., 1978)

It could be argued that the Jaipur foot has been largely successful in achieving these goals although perhaps not all of Sethi et al.'s claims for the foot can be upheld so easily. The same paper described the evolution of the Jaipur foot and some of the early mistakes, particularly related to the contact of the foam rubber and wooden block as well as the enclosing of the foam rubber in solid rubber. The Jaipur foot as described by Sethi et al. (Sethi et al., 1978) was ultimately made up of sponge rubber in the toes, with the great toe separated from the others to facilitate the wearing of sandals, a wooden block in the midfoot, a laminar sponge rubber block wrapped in hard rubber at the heel and a laminated wooden block superior to the heel to house the carriage bolt (The design has changed since the 1978 paper and the midfoot wooden block is now made using microcellular rubber instead, see Figure 15 and Figure 16 for comparison). These components were then enclosed in a 2mm layer of vulcanised hard rubber. This layer was made of rubber cushion compound on most of the foot except the sole where tyre tread compound was used to improve the wear capabilities of the sole. This rubber could then be coloured to a shade similar enough to the user's skin tone that it achieved cosmetic acceptance. Due to the large amount of rubber involved in the manufacture of a Jaipur foot the mass was relatively high; in Sam et al's study of 11 different prostheses the average mass was found to be 526.5g while the Jaipur foot measured in at 822g (only the HI foot was heavier at 854.6g)(Sam et al., 2004). The cost of the foot was given as $30 for a trans-tibial amputee (Day, 1996) (~$48 when adjusted for inflation to 2017). It should be noted that the low costs were partly due to the use of local materials and partly due to the low cost of locally trained limb makers rather than trained prosthetists.

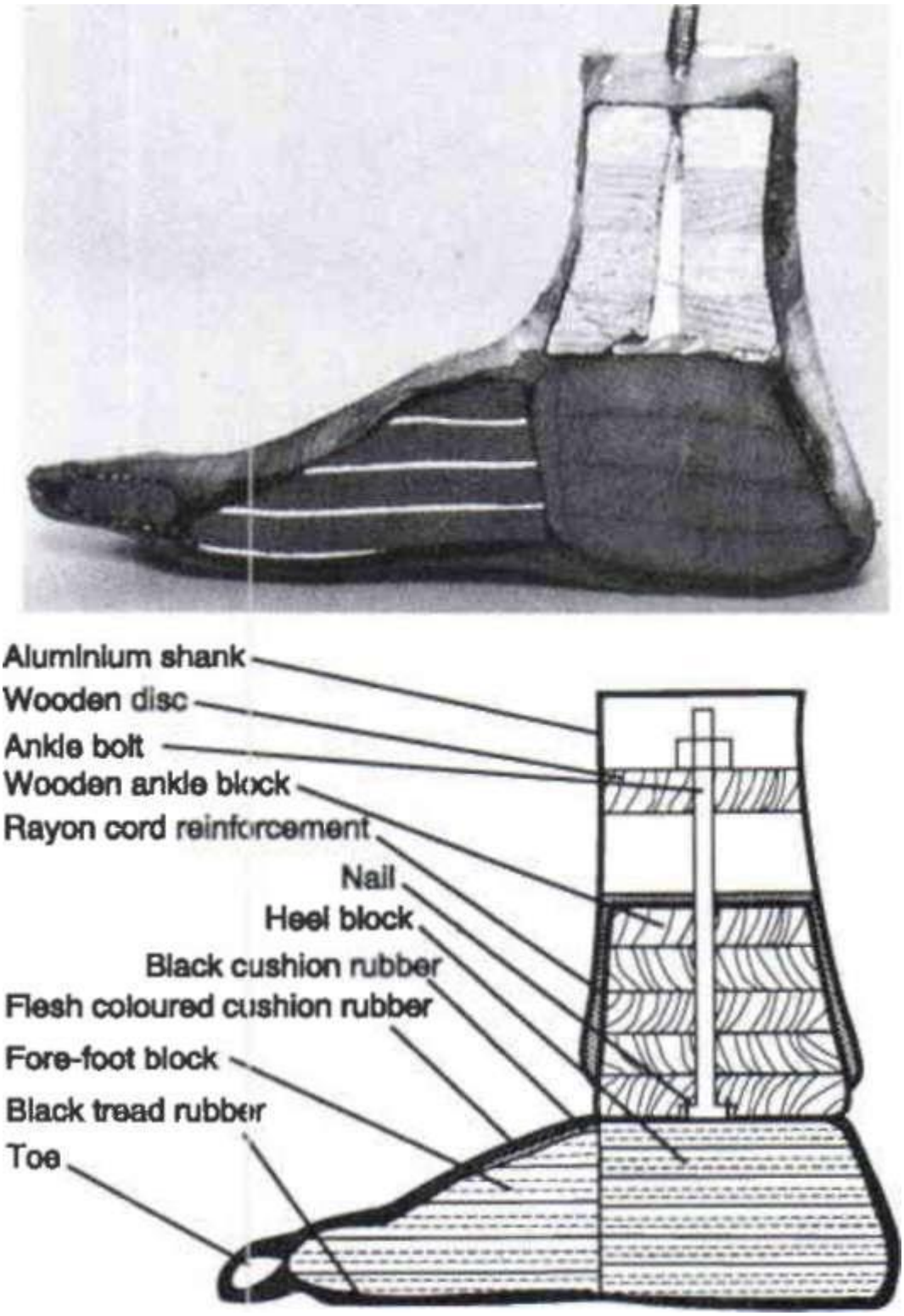

Figure 15 – Sethi et al.'s Jaipur foot in section (Arya, Lees, Nirula, & Klenerman, 1995)

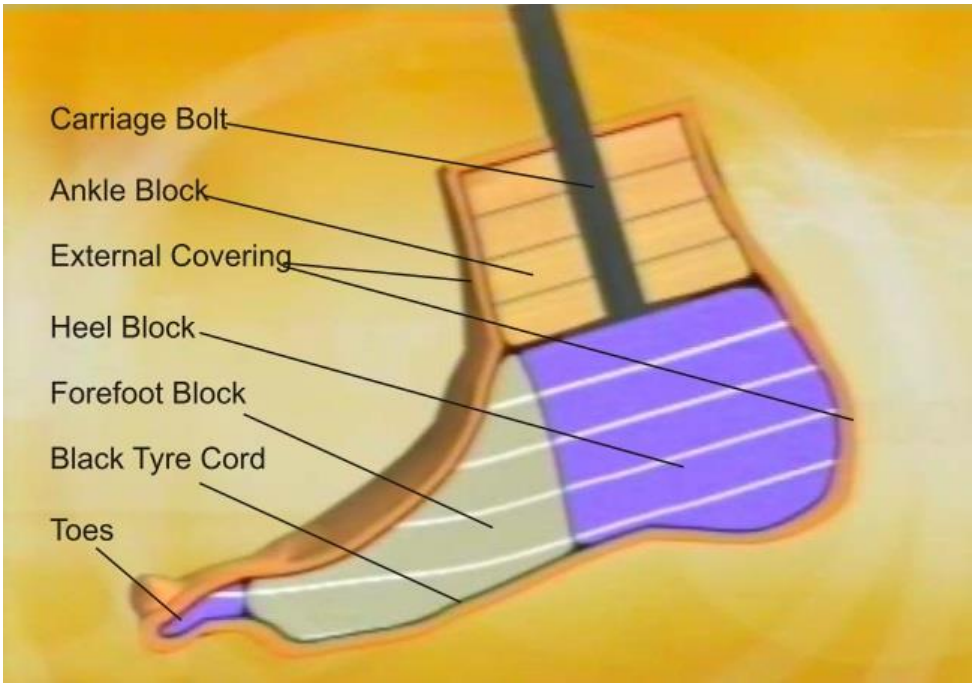

Figure 16 – The Jaipur foot as described in the Jaipur foot manual. The forefoot block is made of microcellular rubber, the heel block is made of laminar sponge rubber and the ankle block is made of wood (Mobility India, 2004)

The development of the foot by Sethi et al. could be described as trial and error or an 'iterative' method and while it may have not been the most efficient development of a design it did ultimately result in a highly resilient prosthesis with certain features culturally important to the users. There have been attempts since to improve the design such as the use of microcellular polyurethane foams in place of the rubber and wooden blocks in the traditional Jaipur foot by Karunakaran (Karunakaran, 2006), or the use of cadaveric human bone endoskeleton by Kabra & Narayanan(Kabra & Narayanan, 1991a). Part of the reason for the work of Karunakaran in producing a PU based foot was so that it may be mass produced at reduced cost, lighter weight and also at more consistent quality, something which has plagued the Jaipur foot due to its production by many different craftsmen and groups (Arya & Klenerman, 2008).

The Jaipur foot has been extensively tested both in the laboratory and in the field however, the field tests for durability and performance did not come until relatively late in the life of the Jaipur foot (Arya & Klenerman, 2008). Sam et al (Sam et al., 2004) included a Jaipur foot in their study on roll-over shape and found that the shape was quite different from the other feet tested in that it diverged the most from a 'standard' SACH roll-over shape. The Jaipur foot was observed to have a smoother progression during roll-over however, lacked toe support. It was also found that the Jaipur foot had a relatively high profile which Sam et al. suggested may limit its use on amputees with a long stump although Sethi et al (Sethi et al., 1978) did describe a modified design suitable for a Syme's amputation so presumably modifications could be made to permit use with a longer stump. Sam et al. suggested that the short roll-over shape with lack of toe support was no surprise given the relative solidity of the rear to mid foot but weak toe structure of the Jaipur foot however, the radius of the roll-over shape was shorter than desired for walking. The shorter radius was noted as giving greater apparent dorsiflexion which in turn aided in actions such as squatting or tree climbing for which the Jaipur foot is so well touted. In Eaton et al (Eaton et al., 2006) the finding of the short radius was confirmed with the value of 150mm compared to 300-740mm of the other feet tested. The arc length was also the smallest measured (129mm compared to 156-224mm). When taken together these seem to rule that Sethi et al.'s claim of the greater lever length provided by the Jaipur foot compared to SACH feet is invalid given the lack of toe support and short arc length however, it must be noted that in sacrificing some of the functionality of walking it provides a wider range of functions (squatting, tree climbing, etc.) that mean the foot is culturally more acceptable and useful to the individual.

In Kabra & Narayanan (Kabra & Narayanan, 1991a) standard Jaipur feet were deflection tested without cyclic testing alongside the bony endoskeleton variant (see Section 2.5.6 Bone endoskeleton Jaipur foot) however, only averaged deflections were made available for the Jaipur feet with the respective standard deviations. The feet were separated into left and right, all being size 7 for analysis with 4 right feet and 11 left feet being tested. In toe loading a general progression was seen with deflection increasing at each 10kg increase in load on the foot however, the standard deviation was relatively large compared to the mean throughout in both left and right feet (ranging from 5% to 32%) suggesting a large variation between individuals in the group. This would be expected given the variations generated in manufacturing; the weights were also noted to vary by as much as 7% (895g + 60g, 11 samples of left feet) and 3.5% (864g + 30g, 4 samples of right feet). The deflections were given in degrees, measured from a custom set up designed by the authors and described in more depth in Kabra & Narayanan (Kabra & Narayanan, 1991b). Table 1 includes the dorsiflexion results from (Kabra & Narayanan, 1991a) as well as the increase in deflection caused by additional loading at each step.

Force (kg)	Right feet		Left feet	
	Deflection (degrees)	Difference (degrees)	Deflection (degrees)	Difference (degrees)
10	5.75 (0.96)		2.75 (0.89)	
20	9.75 (0.50)	4.00	6.35 (1.15)	3.60
30	14.15 (1.75)	4.40	10.29 (1.59)	3.94
40	21.00 (5.15)	6.85	14.90 (2.13)	4.61
50	26.75 (6.02)	5.75	19.90 (3.21)	5.00
60	31.75 (6.02)	5.00	25.90 (4.05)	6.00
70	36.75 (6.40)	5.00	30.00 (4.87)	4.10

Table 2 – Results of deflection testing from Kabra & Narayanan(Kabra & Narayanan, 1991a). Results are averages with SD shown in brackets. Loads were increased stepwise, the difference shown is the increase in average deflection from the previous loading level.

Even between the two groups of feet (left and right) the behaviour was not consistent with quite different deflections visible under the same load and the effect of each 10kg increment had a different effect on the deflection, for example the 40kg mark showed a 6.85° increase in the right feet while it only caused a 4.61° increase in deflection of the left feet. At this point the totals were also very different: 21° for the right feet while only 14.90° for the left feet. This was potentially due to the

inconsistencies of manufacture for the Jaipur foot or alternately in the accuracy of measurements made.

Arya et al (Arya et al., 1995) compared the ground reaction forces and other associated properties of the SACH foot, Seattle foot and Jaipur foot in both walking and jogging to compare performances. The parameters examined were the F_z impact force peak and loading rate, F_z propulsive force peak, F_z support impulse, F_y braking impulse and the F_y propulsive impulse with the Z axis defined as vertical and the Y axis being in the direction of travel. Forces were normalised to values of N/kg body mass, loading rate to N/s.kg and impulses to N.s/kg. Only three subjects were used with one declining to take part in the jogging trials. In the walking trials, the Jaipur foot was shown to have a significantly higher impact force (2.25N/kg compared to 1.29N/kg and 1.62N.kg) and impact load rate (190.3N/s.kg versus 96.8N/s.kg and 136.8N/s.kg) than the other feet ($p<0.001$, both cases) in mean values across all subjects and trials. There was no significant difference found between the feet in terms of propulsive force peak, support impulse or propulsive impulse however, the Jaipur foot did have a significantly higher braking force than the other feet (0.317N.s/kg compared to 0.288N.s/kg and 0.283N.s/kg, $p<0.001$). Arya et al. considered this to indicate that the subjects had greater confidence in the Jaipur foot and therefore carried more of their weight on it and infer that the Jaipur foot then behaved more like the natural foot than the SACH or Seattle feet did. In jogging the feet did not behave significantly differently except that the Jaipur foot had a significantly lower propulsive impulse than the other feet (0.043N.s/kg versus 0.134N.s/kg and 0.111N.s/kg, $p<0.001$). The Jaipur foot is probably better suited to walking rather than jogging given its lack of propulsive force and its higher mass. The sample size was very small which would limit the use of this study in terms of

recommending one foot over the other however, the greater loading by the subjects on the Jaipur foot may suggest its use for less confident users.

Lenka & Kumar (Lenka & Kumar, 2010) conducted a study analysing many different parameters of gait of seven young, male, trans tibial amputees while using six different prosthetic feet, including the Jaipur, SACH, Dynamic, Ranger, Regal and Greissinger feet. Velocity, cadence, stride length, gait cycle duration, double support, single support, stance duration, step duration of prosthetic side, step duration of normal side, swing duration of prosthetic side, swing duration of normal side, symmetry of stance, symmetry step duration, symmetry double support and symmetry swing were reportedly calculated by the authors. However, only mean values for velocity, stride length and cadence were actually reported based on their statistically significant results and the step length symmetry is mentioned for only three of the feet. The subjects, when wearing the Jaipur foot were found to have a velocity of 54.83 ± 14.10 m/minute which was the fourth fastest of the six feet used while the stride length was 1.13 ± 0.24 m (fourth longest) and the cadence was 91.87 ± 10.07 steps/minute (fourth largest). Step length symmetry was given for the Jaipur foot as 87.93% compared to 88.47% for the SACH foot and 94.982% for the Greissinger foot. Force sensor data was also gathered however, what was actually reported was very limited. The load during initial stance phase was compared to that of the sound limb and in the case of the Jaipur foot it would appear that the subjects loaded the prosthesis more heavily than the intact limb. The push off action of the Jaipur foot was found to be the worst of the feet tested which would agree with the poor propulsive force recorded by Arya et al (Arya et al., 1995). Electromyography was reportedly used to record data from the vastus lateralis, vastus medialis and rectus femoris on both the sound and prosthetic sides although only the data for the vastus lateralis was presented for either side. The data was normalised and while

significant differences were found between the amplitudes on the prosthetic side (p=0.011) no explanation was given as to the significance of this. It was noted that the behaviour of both limbs was similar to the unamputated case when using the Greissinger limb and presumably therefore when using the Jaipur limb is not. The Physiological Cost Index (PCI = $\frac{walking\ heart\ rate - resting\ heart\ rate}{gait\ speed}$, measured in beats/metre) was used as a measure of gait efficiency (more efficient gaits require less energy and give a lower PCI value) and was found to be the highest in the Jaipur foot of all the feet tested.

Jensen & Treichl (Jensen & Treichl, 2007) included four Jaipur feet from different manufacturers, the BMVSS, NISHA, MUKTI and OM. There were no significant differences in the manufacture of these feet; all are made of the same basic materials although the individual sources are not described. The feet were exposed to humidity or UV light and then tested as described previously in the section on the ICRC foot. In static proof testing the untreated samples of the four varieties of Jaipur foot showed toe deformation of between 47.34mm and 59.74mm. In the samples exposed to UV this range was 41.32mm to 49.71mm, all feet showed a decrease in maximum deformation. The creep observed was also less in all cases however, the permanent deformation observed was less in three cases and slightly greater in one, the BMVSS model. In heel loading the untreated feet had a range of deformation of 15.58mm to 17.57mm while range of the UV treated feet was 13.41mm to 18.82mm. The maximum deformation was less in the UV treated samples except for the NISHA foot in which the deformation was larger. The creep was less in all cases while the permanent deformation was greater in all cases except that of the BMVSS foot where it was less.

In static strength testing the effect of exposure to UV light or humidity was to reduce the maximum and permanent deformation (except for permanent

deformation of the MUKTI and OM heels where no record was given). All the untreated heels maximum deformation was to a similar level however, the forefoot loading gave much larger deformation in the MUKTI (79.64mm), the OM (73.46mm) and the NISHA (62.30mm) than in the BMVSS (42.83mm). The effect of UV light and humidity on the maximum and permanent deformation of the MUKTI and OM feet was much more pronounced than on either of the other feet. This may suggest that the rubbers used for the shell were quite different and some were more affected by environmental conditions than others which could have implications related to performance of a prosthetic foot over the course of its lifetime however, only one foot of each Jaipur type was tested without exposure to UV or humidity, so the results may have been non-representative. The Jaipur feet showed significantly higher maximum deformation than the non-Jaipur rubber feet ($p<5E^{-08}$), significantly higher permanent deformation of the forefoot ($p<0.00003$) and significantly higher permanent deformation of the heel cushion ($p<0.05$).

All Jaipur varieties passed the two million cycle mark required in cyclic testing however, on sectioning they were all found to have succumbed to delamination of the foam rubber layers. According to the strictest interpretation of ISO 10328 none of the Jaipur feet would have passed however, given the section on single component testing all the feet may be considered to have passed.

The Jaipur foot has also been thoroughly field tested particularly in studies led by Jensen (Jensen, Craig, Mtalo, & Zelaya, 2004a, 2004b; Jensen & Raab, 2006), which will be discussed shortly. It is worth noting that the Jaipur foot, which has been made available since the 1970s, was not clinically field-tested until the early 2000s. Jensen et al (Jensen et al., 2004a) described a study following up trans-femoral amputees given the HDPE Jaipur limb which included a Jaipur foot. 72 subjects were followed up with 25 being non-users, one of whom had a foot that

failed. Of the 47 users 22 sustained foot failures with 6 requiring a new foot. In one case the toes were cut, in five cases the foot screws failed and in the remaining sixteen cases the foot sole/keel was the issue. 8% of the total limbs used required replacement on account of a failed foot.

In the same year Jensen et al. also published a study following up on trans-tibial amputees using the HDPE Jaipur limb including the Jaipur foot (Jensen et al., 2004b). 172 subjects were followed up with 10 being non-users, 35 having non-system related failures, 13 having no complaints. The remaining 122 subjects were users who experienced a system-related failure. Of these 12 of the prostheses suffered from cut toes, 6 from failure of the cover, 10 from failure of the screws and 77 from failure of the sole or keel. Foot failures occurred in 57% of the users but the authors found this was 'significantly influenced by young age ($p<0.002$), hours of daily use ($p<0.0002$), bare-foot walking ($p<0.01$) and of user intensity ($p<0.00000001$)'. The 18-month survival was found to be 82% (73-89%) while the 36-month survival was 53% (42-63%). It was noted that among the subjects from rural Uganda and India with failed feet 50% of them use the prosthesis barefoot while in the non-failing group only 20% used the prosthesis barefoot.

Jensen & Raab (Jensen & Raab, 2006) followed 81 amputees in Vietnam given Jaipur feet. 41 of the subjects were given a MUKTI made Jaipur foot and 40 subjects were given a NISHA made Jaipur foot. The two groups of subjects were quite similar except for that the MUKTI group was 90% urban while the NISHA group was 73% rural. 42 of the feet failed during the study with 20 of those being because of a worn keel. 14 of the MUKTI feet had issues with the screw attachment at the top of the foot resulting in a polypropylene ring being added. The authors stressed that this was a failure in terms of choice of attachment method and not the foot itself. 5 of the failures were attributed to sole failure, 2 failures were due to the

bolt attachment, 1 because of the foot cover and 1 because of an ankle fracture. The survival of the feet was 89% at 12 months and 73% at 16 months. There were a greater number of failures in the first 12 months of the NISHA foot however, after 16 months there was no difference between the feet. 98% satisfaction was reported among subjects whose prostheses failed however, 10% of subjects complained of discomfort and/or pain. All users were walking greater than 1km daily and were wearing their prosthesis for an average of 14 hours daily. Overall it was found that the Jaipur feet tested here performed worse than in Jensen et al (Jensen & Raab, 2006) but that the failures were of a similar nature. In terms of the failure at the heel block Jensen & Raab (Jensen & Raab, 2006) suggested that the problem was in manufacturing technique and that the advantage in the separate layers of sponge as praised by Sethi et al (Sethi et al., 1978) was not valid.

Jensen & Raab (Jensen & Raab, 2006) did find that 99% of the subjects followed were able to squat using a Jaipur foot. In Jensen et al (Jensen et al., 2004a) of the 23 trans-femoral subjects asked only 4 could squat using the limb and only 3 could sit cross legged however, as the trans-tibial amputees were nearly universally able to squat the difference for trans-femoral amputees was likely to be in the prosthetic system rather than the foot specifically. Not all of the claims made by Sethi et al (Sethi et al., 1978) can be upheld however, there is no doubt that the Jaipur foot has made a significant contribution to amputees worldwide at least partially thanks to the design not being patented by Dr. Sethi.

2.5.6 Bone endoskeleton Jaipur foot

Kabra & Narayanan (Kabra & Narayanan, 1991a) took a very different approach in that rather than trying to replicate the function of the natural foot by using three blocks as in other Jaipur feet they rather would use the remains of the natural foot if possible. Initially an otherwise intact and healthy (e.g. not osteomyelitic) cadaveric

foot had the muscles and fat removed leaving only the bone structure and joint capsules fixed with ligaments. This structure was then treated in formalin. The tibia and fibula were fixed to a wooden block that housed a carriage bolt and the foot and block structure was covered in black cushion compound. At this point the process came to strongly mirror the usual Jaipur foot, the foot was wrapped in tire cord, a sole made of tread compound was applied and red cushion compound applied elsewhere prior to vulcanisation (see Figure 17). Three feet were made in this method and were tested alongside 15 standard Jaipur feet (4 left, 11 right, only averaged results were available for these groups) in forced deflection at 10kg increments up to a maximum of 70kg. The 'bone endoskeleton' prostheses were also subjected to cyclic loading at 1Hz to 3cm deflection (reported to be approximately equivalent to 60kg) to 5000 cycles and 100000 cycles with one prosthesis tested to 3 million cycles. After each milestone in cyclic testing the prostheses were radiographed and again subjected to the forced deflection tests. The results of the radiograph did not show the internal structure to have been displaced or any of the bones or trabeculae to have fractured, even following the 3 million cycle test. The toe deflection after cyclic testing was not different after 5000 cycles but did increase after more cycles however, the increase occurred in the first 10kg loading and each added 10kg load only produced a similar deflection before and after testing. Heel deflection was not affected by cyclic testing. When compared to the typical Jaipur foot the toe deflection in the bone endoskeleton foot was greater initially but levelled off whereas the Jaipur foot did not. The heel deflection was similar with the Jaipur foot deflecting slightly more. The authors considered that as the foot lasted to 3 million cycles it satisfied the survival conditions of a foot since no change occurred during the 3 million cycles. They noted that the cyclic test does not take into account aging effects, but that dehydration and autolysis were unlikely to

occur as the endoskeletal structure was formalin fixed and sealed in rubber. One particular advantage postulated was that the articulations would be in the correct locations rather than an approximation as in the Jaipur foot. Unfortunately, no further work has been reported on this development however, as the authors suggested there was a lack of fresh cadaveric feet for this use it may be that this limited their research or else made it unfeasible as a long-term solution.

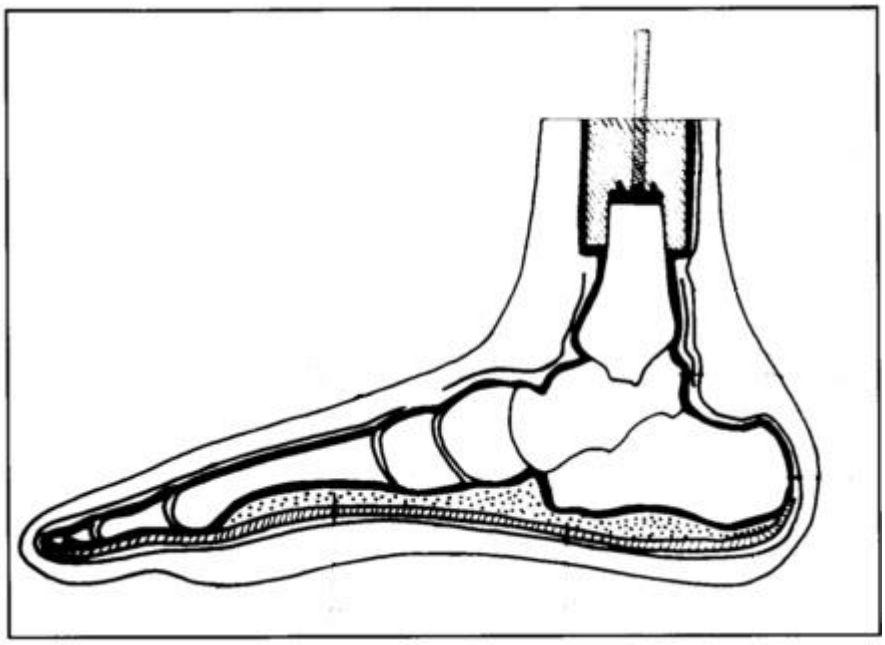

Figure 17 – The bone endoskeleton variety of the Jaipur foot (Kabra & Narayanan, 1991a)

2.5.7 Niagara foot

The design for the Niagara foot was patented in 2001 by Robert Gabourie of Ontario, Canada as ‘a prosthetic foot including an integral spring portion providing motion in the foot, particularly a unitary foot structure providing a selectable degree of plantar flexion, dorsiflexion and a stiff structure for toe off’ (Gabourie, 2001) (see Figure 18).

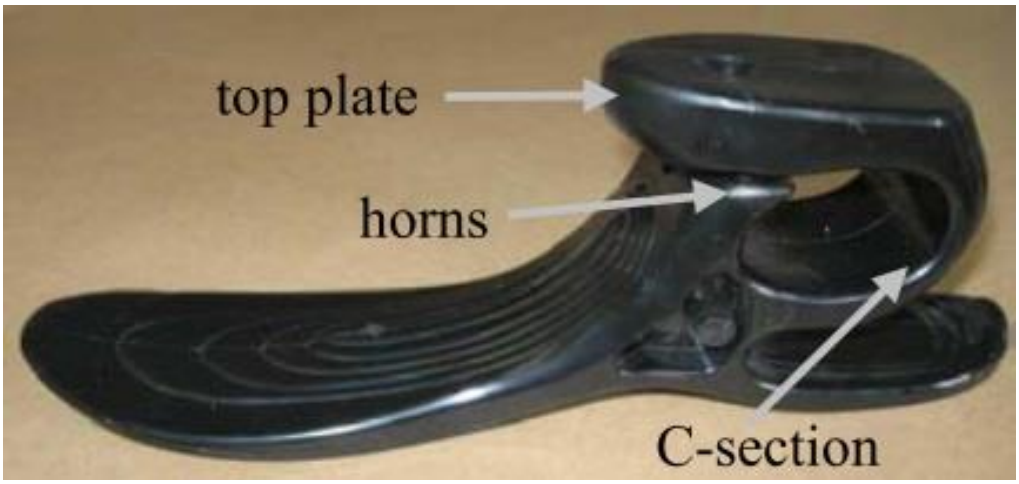

Figure 18 – A Niagara foot showing its “unitary”, or single part, design (Haberman, 2008)

The Niagara foot was designed with active amputees in low-income countries in mind, and more particularly those in areas affected by landmines (Beshai & Bryant, 2003). One of the main points in the design was the separation of cosmesis from the keel as is fairly typical of Western prostheses. The failure of cosmeses is well recorded in literature (Jensen et al., 2004b)(Jensen, Nilsen, Thanh, et al., 2006) so the idea that a cosmesis could be replaced as needed is attractive compared with a new prosthesis solely due to cosmesis wear. Andrysek (Andrysek, 2010) however, stated that as many amputees were unable to make the trip required to a prosthetist for a replacement cosmesis focus should be applied to making a more durable cosmesis. Beshai & Bryant (Beshai & Bryant, 2003) suggested amputees could replace the cosmesis by themselves ‘simply and cheaply’.

The more significant aspect of the design is that which is described in the patent, the integral spring motion with plantar flexion, dorsiflexion and a stiff structure for toe off. This was achieved through the structure of the keel as imaged above (Figure 18). On heel strike the lower C-section deflects upwards causing the toe to deflect downwards. As weight is transferred forwards the lower C-section springs back aiding in roll-over. As the toe is loaded the upper C-section is ‘wound’

storing energy in preparation for toe off. As toe off is achieved the upper C-section can spring back providing energy return at an appropriate time (Beshai & Bryant, 2003). This winding gives the impression of a 'soft' toe as reported by subjects during a field trial in Thailand (T. Ziolo & Bryant, 2001). In the trial 15 subjects were given a choice of two Niagara feet to use, one being stiffer than the other and so suited for greater weight or activity, and then asked to fill out a questionnaire to gauge their opinion in comparison to their original prosthesis. The only area to show a significant difference in opinion between original and Niagara feet was ease of use ($p<0.001$). 7 of the subjects were given the feet for two days after which they were given the same questionnaire again. The only significant finding in these subjects was that the effort required on the opposite side was reduced using the Niagara foot after initially reporting it required more effort. Ziolo & Bryant (T. Ziolo & Bryant, 2001) explain this as an effect of the energy return of the Niagara foot causing less effort to be required in order to achieve toe clearance. The subjects did however, complain that the prosthesis was unable to fit into their shoes while Ziolo & Bryant noted that the foot was designed with barefoot or sandal use in mind and that the subjects in fact used athletic shoes in their daily activities.

Initially the design was tested virtually by Finite Element Analysis and optimised prior to physical testing to the A60 (now P3) level of ISO 10328 in both static and cyclical tests. No failures or significant wear were observed over 3 million cycles and only a minor permanent upward deformation of the toe was seen (Beshai & Bryant, 2003). In laboratory testing by Haberman (Haberman, 2008) it was found that the Niagara foot had the highest displacement but also the greatest stiffness when compared to Otto Bock Axtion (106kg), Axtion (124kg) and SACH 0176 feet. The stiffness was found to increase as the displacement increased and was said to account for the softness reported by subjects in clinical trials. Haberman found that

a SACH foot has a soft heel and a stiff toe while the Axtion foot (representative of Dynamic Energy Return (DER) feet) had a stiff heel and a soft toe. When the Niagara foot was compared to these two it was decided that it represented an intermediary between SACH and DER as it possessed a stiff heel and a toe with stiffness initially similar to the Axtion foot but growing increasingly stiffer as it was further displaced.

Eaton et al (Eaton et al., 2006) in their comparison of roll-over shapes found the Niagara foot to have the second longest arc length of the feet tested (204mm versus 224mm of the Shape and Roll foot) and a short radius (300mm versus 390mm mean of all feet). This was a longer arc length than the natural foot tested (156mm) and a shorter radius (420mm). There was no mention of the foot feeling long or unusual reported by subjects in Ziolo & Bryant (T. Ziolo & Bryant, 2001) so it is possibly not different enough to matter.

Despite the initial design of the Niagara foot being geared towards low-income countries an updated version has been released as the Rhythm foot which appears to be distinctly marketed towards Western users (Rhythm Foot, 2013).

2.5.8 Shape and Roll foot

The Shape and Roll foot was designed within Northwestern University, Chicago, based on work by Knox in his thesis at the same university (Childress, Sam, Hansen, Meier, & Knox, 2004). The work of Hansen through his thesis and a number of papers resulting from it (A. H. Hansen, Childress, & Knox, 2000; A.H. Hansen, 2002; A.H. Hansen & Childress, 2004, 2005; Andrew H Hansen, Childress, & Knox, 2004; Andrew H Hansen, Childress, & Miff, 2004; Andrew H Hansen, Childress, Miff, Gard, & Mesplay, 2004), solidified the concept of a roll-over shape by which the action of a prosthetic foot could be defined. The idea of a roll-over shape is that the natural foot adapts to external influences and in doing so produces

a smooth transition of load along the foot, measurable as the position of centre of pressure relative to the ankle joint, through ground contact period. The shape and roll foot was designed to provide support in the pattern of an intact limb and so give the user a more natural gait. The basic design of a shape and roll foot was a moulded blank with the base shaped as the sole of a shoe and a prism on top, which may be cut at varying intervals to give the desired flexural pattern and so roll-over shape (M. Meier, Steer, Hansen, Sam, & Childress, 2006) (see Figure 19 for the design of the foot and Figure 20 for the comparative roll-over shape of a natural foot and the shape and roll foot).

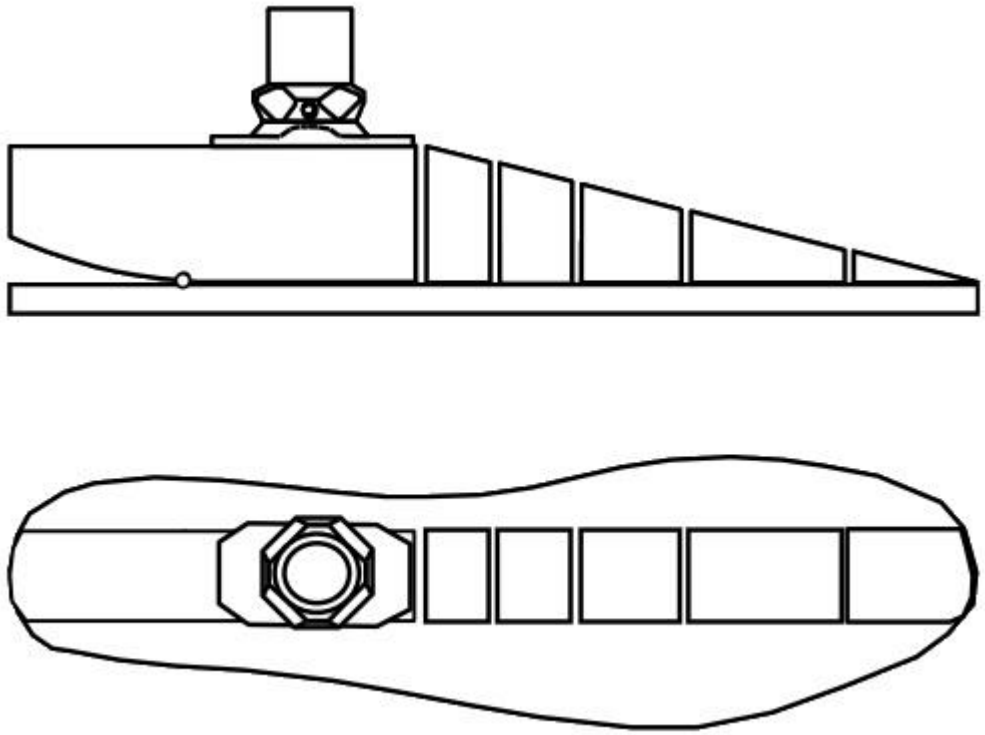

Figure 19 – A side and top view of a shape and roll foot (M. Meier et al., 2006)

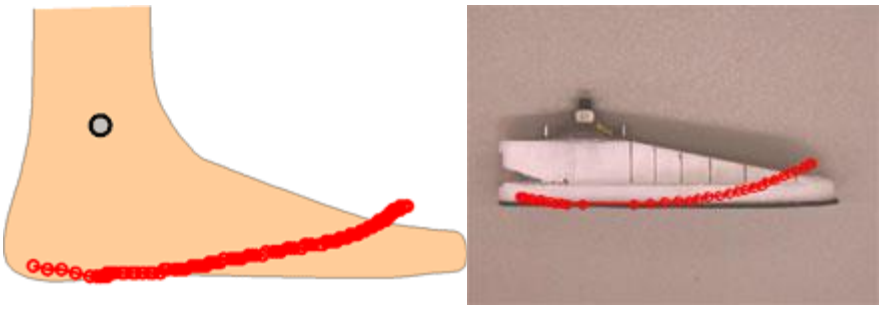

Figure 20 – Roll-over shape of a natural foot and a shape and roll foot ((Childress, Hansen, Meier, & Steer, 2005)

The depth of the sole may be adjusted to compensate for weight or activity level while the position of the cuts along the wedge section adjusts the effective radius of the foot and so tailors the foot for users of different heights (M. Meier et al., 2006) as was originally envisioned for the design (Childress et al., 2005). A comprehensive instruction manual had been written (M. Meier et al., 2006), including instructions for making the manufacturing equipment required, so that the foot may be reproduced elsewhere, despite the patent held for the design.

Cyclic testing was carried out at Northwestern University with the results of 3 feet reported at reaching 3.8, 2.8 and 2.2 million cycles without failing, which was greater than the 2 million cycles required by ISO 10328 (M. R. Meier, Sam, Hansen, Childress, & Casanova, 2004a). Subsequently a small (n=10) clinical test was made in the USA where subjects were questioned on their opinion of their normal prosthesis and the shape and roll foot following three weeks of use. M. R. Meier et al. (M. R. Meier et al., 2004a) report that no significant differences were shown in the subject when using their normal prosthesis or the shape and roll foot. A further clinical trial was carried out in El Salvador with the same questionnaire asked of the subjects of their normal prosthesis and then the shape and roll foot after three weeks of use. In the El Salvador trial the shape and roll foot was found to give a significant increase in distances walked by subjects while improvements were also

seen in the ability to walk quickly and to walk along with non-amputees (M. R. Meier, Sam, Hansen, Childress, & Casanova, 2004b).

Eaton et al (Eaton et al., 2006) calculated the roll-over shape of a shape and roll foot in comparison to certain other prosthetic feet and found the shape and roll foot to have an arc length of 224mm and a radius of 360mm compared to the natural foot measuring an arc length of 156mm and a radius of 420mm. The arc length is anecdotally linked to stability (Eaton et al., 2006) as it effectively gives the length of contact between the foot and floor while the radius indicates how easy it is to move over the foot with smaller radii being easier. Shape and roll feet are customised to the individual's dimensions (e.g. radius of curvature is approximately 0.44 of leg length (M. Meier et al., 2006)) and activity level however, there was no mention as to the configuration of the shape and roll foot in this case i.e. if it was intended to match the natural foot tested or if it was simply treated as a standard example of the foot. As the shape and roll foot was designed to have a customisable roll-over shape this is a significant point as it was not, as with most other feet, a standard component with little variation.

The shape and roll foot has been used in other studies related to more general behaviour of prosthetic feet, particularly two papers by Klodd et al. (Klodd, Hansen, Fatone, & Edwards, 2010a, 2010b). In Klodd et al (Klodd et al., 2010b) the effect of forefoot flexibility on oxygen cost and subject preference was recorded by using sets of shape and roll feet cut to different degrees of stiffness. While the authors had expected that the lowest oxygen cost would be observed with the foot most closely set up to mimic the natural foot the data did not support this with no significant differences found in oxygen consumption regardless of foot used. The subjects in testing did show a preference for the middle or slightly stiffer feet of the five tested, eschewing the most flexible feet. In Klodd et al (Klodd et al., 2010a) it was observed

that the more flexible forefeet led to a limp in subjects. It was suggested that this was as a result of the ground reaction force not being able to progress far enough forward due to the high flexibility, effectively making the foot length shorter which was undesirable.

2.5.9 Blatchford Atlas

The Atlas system was created at Blatchford by J. Shorter and A. Evans and patented in the USA in 2000 (patent no. 6,083,265). It consisted of a combined foot and shin covered in a polyurethane foam cosmesis (see Figure 21). The shin was in the form of an I-beam that could be cut to the required length.

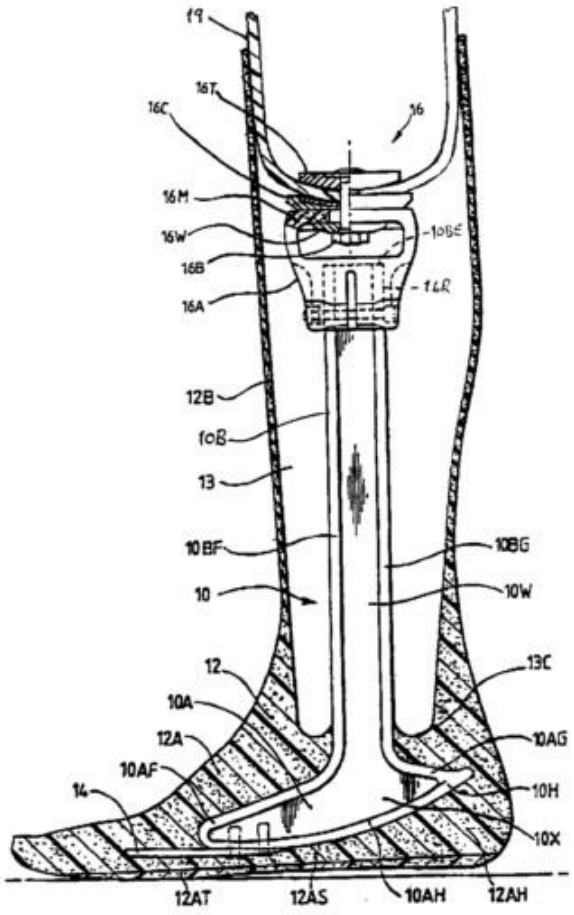

Figure 21 – The Atlas system showing the combined heel and shin (Shorter & Evans, 2000)

Jensen & Raab (Jensen & Raab, 2002) conducted a field trial of the Atlas system for trans-tibial amputees in Cambodia and El Salvador. It was found that of the 87 subjects followed 15 were non-users (17.2%) and 41 had failed prostheses (47.1%). Among the non-users' reasons for giving up use included non-fit, cracking, looseness and noise from the prosthesis. The noise, described as a "shrieking", came from the shank or foot and was believed to be caused by movement between the chassis (for attachment of the socket and I beam) and the I beam. Attempts were made to tighten the screws and resin was added in two cases however, on sectioning of the prostheses later there was found to be movement between the foot plate and the keel as well as the heel padding and the cushion. The failures included shank fracture in 24 cases (58.5% of failures, 36.4% of all users) as well as tightening of the I beam chassis interface required (11 cases, 7 going on to break later), 5 cases of cosmetic cover failure and 9 cases of the sole being badly worn. In either of the two groups the survival rate was 40% or lower by 24 months. It was noted that wear of the foot required replacement of the foot and shin which is costly and as 22% of the feet had been observed to be badly worn in between 5 and 31 months the rate of replacement would be high. Jensen & Raab (Jensen & Raab, 2002) concluded that the Atlas system was unacceptable for use and that it did not perform better than the SACH feet already available in the area. A later study by Jensen & Raab (Jensen & Raab, 2003) looked at the use of the Atlas system in trans-femoral amputees. It found that the knee joint in this case was the weak point (55 failures in 66 subjects) but in two cases fracture of the shank/ankle was recorded. Jensen and Raab (Jensen & Raab, 2003) concluded that the Atlas system for trans-femoral amputees should be abandoned from use and stressed the importance of independent clinical field studies prior to market launch. The Atlas system should be considered a cautionary tale in prosthetic limb design.

2.5.10 EB foot

The EB-1 foot was a development of the Prosthetics Outreach Foundation consisting of a wooden wedge keel, stacked rubber plates for a heel, cotton rubber sole and a rubber cover (Jensen, Nilsen, Zeffer, et al., 2006)(see Figure 22 for a cross section). Due to the extensive use of rubber in the design the EB foot was relatively heavy, weighing 809.8g according to Sam et al (Sam et al., 2004) compared to the study mean of 526.5g.

Figure 22 – A cross section of the EB foot (Jensen & Treichl, 2007)

The EB foot was included in the work of Sam et al (M. Meier et al., 2006) where it was found to show a roll-over shape similar to other SACH feet including the sharp drop off of toe support. Jensen & Treichl (Jensen & Treichl, 2007) tested the EB foot in both its virgin condition as well as after exposure to UV light and humidity (as described in the section on the ICRC foot) to the standards of ISO 10328. Humidity was found to cause a decrease in maximum deformation of the forefoot but an increase in creep and permanent deformation while an increase in all areas was seen in the behaviour of the heel under static proof conditions. UV light exposure

caused an increase to maximum deformation and permanent deformation but a reduced creep of the forefoot while the heel was observed to have a reduced maximum deformation and creep but an increased permanent deformation. When tested to static strength conditions humidity was found to decrease permanent and maximum deformation of the forefoot while increasing both in the heel. UV light caused a decrease in maximum and permanent deformation of both the forefoot and heel. After cyclic testing deformation of the rubber under the keel was observed in common with a number of the other feet tested. Jensen & Treichl (Jensen & Treichl, 2007) note that the foot would have met the standards of ISO 10328.

The results of two clinical field tests of the EB foot were available, that of Jensen et al (Jensen, Nilsen, Zeffer, et al., 2006) and Jensen et al (Jensen et al., 2005). Jensen et al. (Jensen et al., 2005), followed 41 subjects provided with the EB foot after 20 months (20-22 months). 5 subjects were non-users (14%) while the users wore their prosthesis for 12 hours a day (3-14 hours) with 29 (81%) walking greater than 1km each day. 25 users were in a dry rural area and the other 11 were urban dwelling. 21 failures were recorded although it is not mentioned if any of the failures occurred within the same prosthesis. 8 of these failures required a new foot and 3 required a new prosthesis. Subjects reported 83% (30 subjects) satisfaction with the EB foot.

Jensen et al (Jensen, Nilsen, Zeffer, et al., 2006) followed 33 subjects, 3 of whom were non-users (9%) after 20 months (20-22 months). The 12-month survival rate was 100% and at 18 months only 1 prosthesis had failed (97% survival). At 20-21 months (the end of testing) the survival rate was 67% (22/33). 28 of the 30 users walked more than 1km daily (93.3%) with none of the prostheses used barefoot. 45% found the foot heavy but 91% satisfaction was reported despite 11 new feet being required (36.7% of users). 13 failures were reported, 1 was due to the foot

cover, 4 were due to a worn sole and 8 were due to a worn keel. The failure of the wooden keel was reportedly due to rot (see Figure 23). With improvement to the protection of the wooden keel the EB foot could be an effective foot for low-income countries.

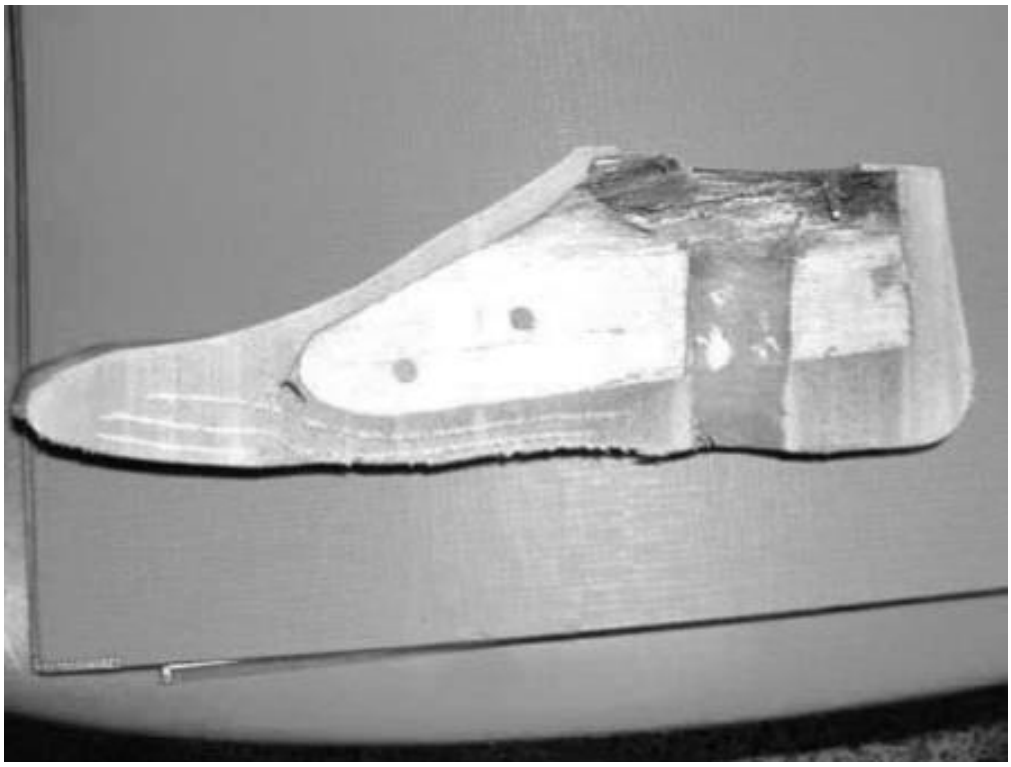

Figure 23 – The EB foot showing rot of the keel at the top (Jensen, Nilsen, Zeffer, et al., 2006)

2.5.11 Kingsley Strider

The Kingsley Strider is a type of SACH foot produced by Kingsley Manufacturing Company (Costa Mesa, California, USA) consisting a wooden dog tail-shaped keel with a flat belt drive for toe support and a polyurethane heel, sole and cover (see Figure 24)(Jensen & Treichl, 2007).

Figure 24 – A cross section of the Kingsley Strider (Jensen & Treichl, 2007)

Jensen & Treichl (Jensen & Treichl, 2007) tested a set of Kingsley Strider feet to ISO 10328 standards, some of which had been exposed to humidity or UV light as described previously. During testing to the static proof level, the effect of UV light was to reduce maximum deformation, permanent deformation and creep in the forefoot but to increase all of them in heel loading. Humidity was observed to increase all measures in forefoot loading while in heel loading the maximum and permanent deformations increased while the creep was reduced. When loaded to static strength levels the effect of UV and humidity on the forefoot was to reduce maximum and permanent deformation. UV light exposure affected the heel by causing increased maximum and permanent deformation while humidity caused the maximum deformation to increase while the permanent deformation decreased. After cyclic testing permanent deformation of the polyurethane foam under the keel was observed. Jensen & Treichl state that the Strider would not pass the most

stringent interpretation of ISO 10328 but given the allowance for separate foot ankle unit testing then the Kingsley Strider may be considered to meet the standard.

In Jensen et al.'s study (Jensen, Nilsen, Thanh, et al., 2006) 33 subjects in El Salvador were provided with Kingsley Strider feet and followed up to generate data on survival and types of failure of the foot amongst other information. 16 of the subjects lived in dry rural conditions with 12 recorded as living in an urban environment, leaving 5 subjects unspecified. 26 of the group (79%) claimed to use the prosthesis for over 1km of walking each day with the average number of hours use daily recorded as 15 (3-16 hours). 26 of the subjects (79%) were satisfied with the prosthesis with only 2 (6%) stating their dissatisfaction. The foot survival at 6, 12, 18 and 24 months were 94%, 73%, 45% and 39% respectively. In the 29 cases of failure 20 were due to the foot sole being worn (see Figure 25) and the other 9 were due to the keel being worn. Of these 29 cases, the foot was replaced in 26 instances (90%). The performance in this test was level with that of the HI-foot from Handicap International.

Figure 25 – Fracture of the forefoot of the Strider (Jensen, Nilsen, Thanh, et al., 2006)

2.5.12 Ho Chi Minh City (HCMC) foot

The HCMC foot was developed jointly by the ICRC and the Army Factory in Ho Chi Minh City and was intended to be used either barefoot or with slippers. Verhoeff et al (Verhoeff et al., 1999) described the HCMC foot as having a keel made from polypropylene pellets oven heated and pressed into a mould, a sole of rubber similar to a tyre tread, a rubber cover on the dorsal side in the inside filled with a foam rubber (see Figure 26). The entire structure was then vulcanized.

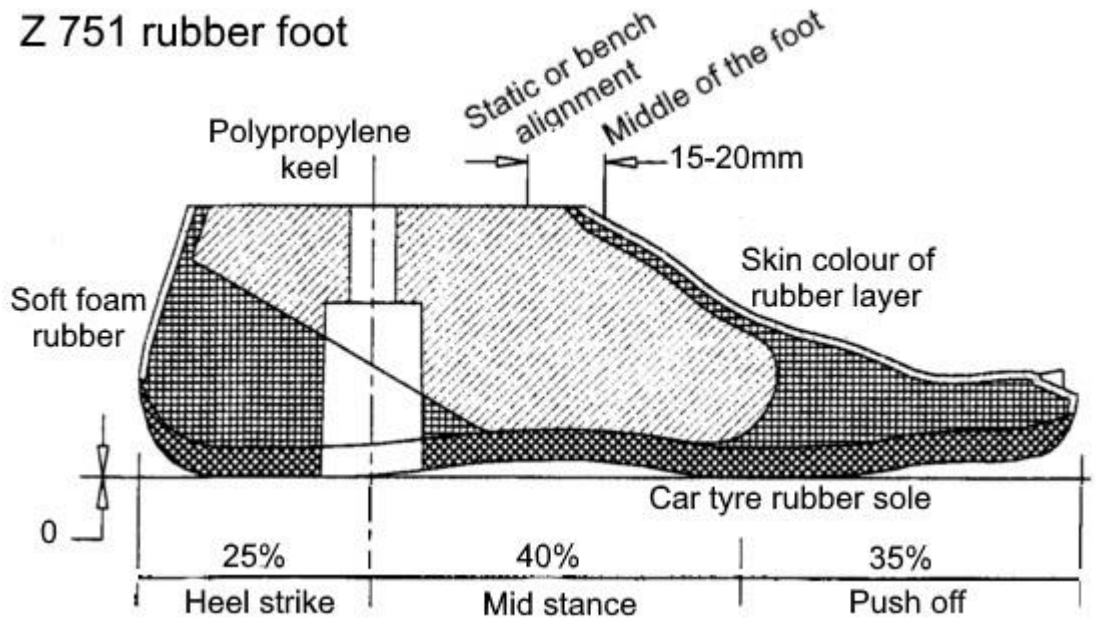

Figure 26 – The HCMC foot in section (Verhoeff et al., 1999)

The subjects in Verhoeff et al (Verhoeff et al., 1999) had both their load levels and hours of use recorded for use in analysis of failure rates. It was found that the hours of daily use were more related to failure than the load level. For the 43 subjects followed a total of 40 replacement feet were provided with 3 subjects receiving 3 replacements each and a further 3 subjects receiving 2 replacements each. These 6 subjects were using their feet for an average of 12.7 hours a day at a high or very high load level. Of all feet, the average life span was 8.9 months however, in the group using the feet for between 12-16 hours per day the average life span was only 6.8 months. The specific causes of foot failure were not given however, as they appeared to be more related to hours of use rather than level of use environmental conditions may have been a significant factor in the breakdown of the feet.

Jensen & Heim (Jensen & Heim, 1999) tested a number of polypropylene SACH feet in Vietnam including the HCMC foot. 9 subjects were given the HCMC foot out of a total of 34 in this fairly small trial. The subjects were recorded as using

the prosthesis on average 14 hours a day (12-15 hours), 5 covering more than 2km a day, 3 between 500m and 2km and 1 covering less than 500m a day. 8 lived in a dry rural setting and one in a wet rural setting. 7 of the feet failed during the study, the first at only 3 months and a further 3 failing at 5 months. By 9 months into the study the survival of the HCMC foot was only 45%. 9 failures were recorded in the 7 failing feet including 2 cases of a dorsiflexed foot, 4 failed keels and 3 failed soles. Jensen & Heim do note that the HCMC foot was under a design overhaul at this time.

By 2007 when Jensen & Treichl reported the results of their series of tests to ISO 10328 level (Jensen & Treichl, 2007) the HCMC foot did have a different design involving an ebonite keel with a foam rubber flat belt drive support in the forefoot, a foam rubber cushion heel and a rubber sole and cover (see Figure 27).

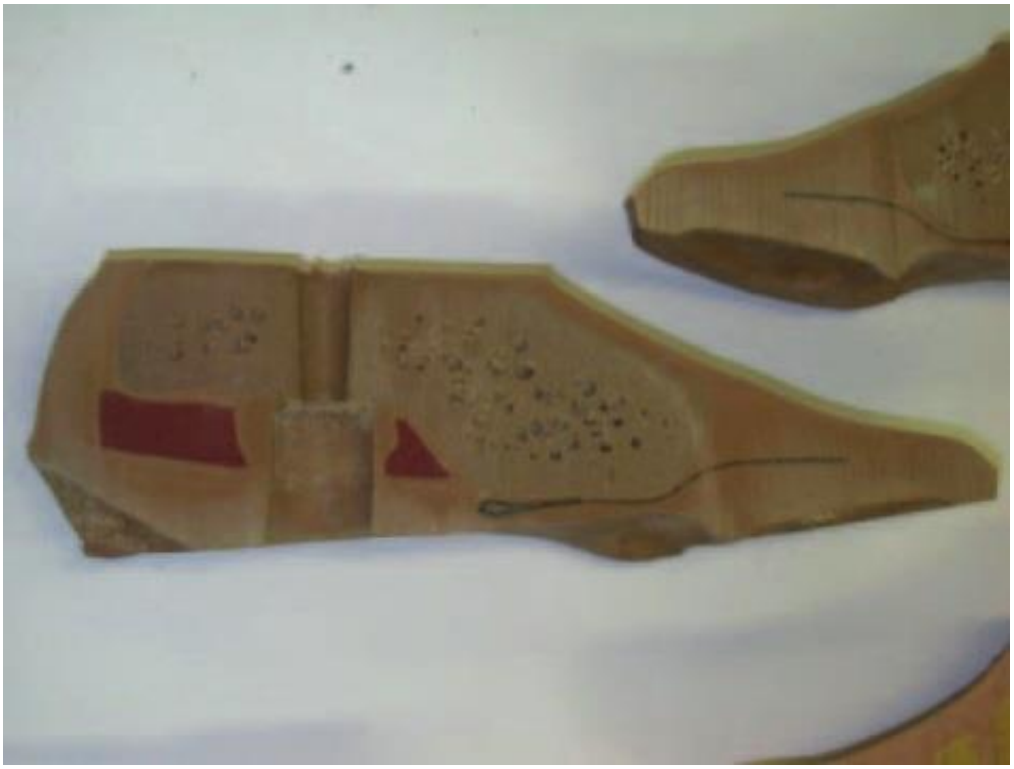

Figure 27 – The HCMC foot as it appeared in 2007 (Jensen & Treichl, 2007)

The feet were tested in virgin form, after exposure to humidity and UV light as described previously. In static proof testing exposure to humidity caused a slight decrease in permanent deformation and creep in both heel and forefoot while a slight increase in maximum deformation was observed in either loading condition. Exposure to UV light caused a decrease in all measurements in the forefoot while at heel loading an increase in maximum deformation as observed while the creep and permanent deformation decreased. When loaded to static strength conditions either exposure caused the maximum and permanent deformations at the forefoot to decrease. At the heel either exposure caused reduced permanent deformation but increased maximum deformation. The HCMC foot was the only foot considered by Jensen & Treichl (Jensen & Treichl, 2007) to have passed ISO 10328 to the most stringent level having a permanent deformation of less than 5mm under static proof loading. After cyclic loading was completed compression of the foam under the keel was observed as in a number of the other feet.

2.5.13 Seattle foot

The Seattle foot was developed over a number of years with many individuals involved (Hittenberger, 1986) and was released in 1981 as the first 'energy storing' prosthetic foot (Hafner, Sanders, Czerniecki, & Fergason, 2002b). It consisted of a shaped keel made of Delrin® (an acetal homopolymer), a reinforced toe plate (of Kevlar®) and a polyurethane foam covering (see Figure 28). By maintaining a simple design, the manufacturing costs were kept low. The function of the foot was of greater interest to the designers though with two of the designers listing the following criteria for the foot:

1. Be capable of deflecting 1-¾ inches at the metatarsal area under a vertical load of 435 pounds. To do this reliably would require the longest possible spring.
2. Feel natural and stable in all phases of gait. This would require adequate dampening during the storage and release of energy at heel-strike and push-off.
3. Have a useful life of at least three years. This would require a durable material for the spring, to make it endure 50,000 cycles at 2.8 x body weight loading or 1,000,000 cycles at 1.4 x body weight, with a permanent set of less than .06 inches.
4. Have the lowest possible weight.
5. Have the lowest possible production cost. This implied a monolithic mouldable keel rather than a composite one.
6. Have a natural cosmetic appearance.
7. Be compatible with existing prosthetic components and techniques.
8. Have a centre of rotation as close to the natural ankle centre as possible.

(Hittenberger, 1986)

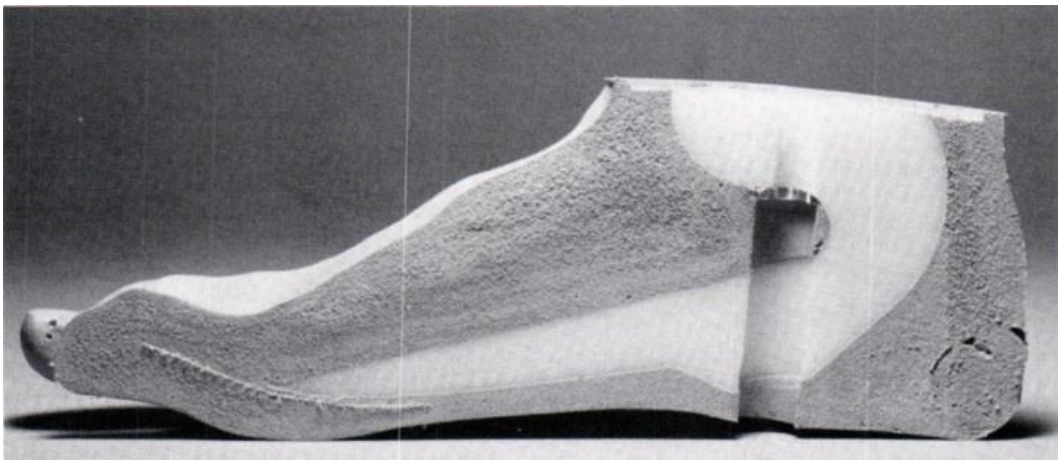

Figure 28 – Cross section of the Seattle foot showing the three components (shaped keel, toe plate and foam cover) (Hittenberger, 1986)

Hittenberger (Hittenberger, 1986) stated that failure of the foam was an issue, particularly when used barefoot. Huston et al (Huston et al., 1998) noted that the Seattle foot was too wide to comfortably fit into narrow shoes and that this was one of the factors leading to the design of the Seattle Lightfoot (see the following section, page 67).

Following the study of Torburn et al (Torburn et al., 1990) all patients chose energy storage and return (ESAR) feet rather than return to a SACH foot (4 out of 5 cases; the other patient had an ESAR foot prior to the study). The Seattle and Carbon Copy II foot were chosen but not the Flex foot, something which Hafner et al. (Hafner, Sanders, Czerniecki, & Fergason, 2002a) claim was partially due to cosmetic appearance but largely due to the perception of faster walking speed and increased stability although Torburn et al. (Torburn et al., 1990) mentioned that for some of the subjects the appearance was important but that all subjects chose the foot that gave them the greatest velocity during free walking regardless. Torburn et al. found no statistically significant differences among the feet they tested (Seattle SACH, Carbon Copy II, Flex foot and STEN) in terms of velocity, stride length or cadence nor in measures of vertical ground reaction force (maximum loading, minimum midstance and maximum terminal stance). In a 20-minute oxygen consumption test there were no differences found between the feet in terms of oxygen consumption or distance walked. Ultimately Torburn et al. acknowledged that further testing was required, particularly including a greater number of subjects. In a test of 10 amputees Perry & Shanfield (Perry & Shanfield, 1993) found that there was no significant difference in loading of the Seattle foot compared to the SACH, Carbon Copy II and Quantum feet however, the Flex foot produced a significantly lower peak load. During testing it was also found that there were no significant differences in the energy expenditure or velocity of the subjects when

wearing the different feet which agreed with the findings of Torburn et al. (Torburn et al., 1990). Arya et al. (Arya et al., 1995) compared the SACH, Seattle and Jaipur feet in results stemming from ground reaction forces in three subjects. They found that the Seattle foot did not absorb shock as well as a SACH foot and that there were no significant differences in gait style between the three feet. The Jaipur foot was found to have a more natural performance than the other feet based on the anteroposterior braking force observed being larger than the other feet and closer to the natural foot despite not showing any other significant differences to the SACH or Seattle foot.

Murray et al (Murray et al., 1988) asked for the opinion of users to gauge the performance of the Seattle foot. In responses from 31 users of the Seattle foot, all of whom had the foot fitted in the two years prior to the study start, Murray et al. found that user opinion of the Seattle foot was largely positive. The heel was felt to be of acceptable stiffness in 80% of responses, range of ankle movement was felt to be good in 81% and 55% felt that shock stress at knee and hip was reduced while a further 39% reported no difference. 87% felt that the Seattle foot improved their gait (13% reported no change) and 87% were aware of the toe off action that was most noticeable when carrying out more strenuous actions (running, climbing up or down, etc.). 48% would have preferred a greater toe off action while 52% were satisfied (it is not mentioned if this includes those who were unaware of it or not). Stair use, hiking, jogging and dancing were found to be easier by over 50% of respondents although there was no breakdown on the previously used prostheses for comparison. As part of Wirta et al's gait study (Wirta et al., 1991) patients were asked to use each prosthesis for a week before the gait trial and were asked to rate the foot on a 5 point scale (poor, fair, good, excellent, superior) and comment on the foot. The Seattle foot scored 1 poor score, 2 fair scores, 4 good scores, 9 excellent

scores and 3 superior scores (the greatest number of excellent and superior scores and equal lowest poor scores) and received comments praising its comfort and ability on slopes. Older subjects however, complained that they were being thrust forward and had balance and control issues. Noting trends in response Wirta et al. suggested that the Seattle foot was preferred by “young, lightweight, medium length residual limb and average stride length” users. In the rest of testing the Seattle foot was shown to have a lower angular acceleration at 8% of gait cycle, representing shock, than the Otto Bock single axis foot or the Greissinger multi axis foot however, it was slightly larger than those of the SACH or SAFE foot. The shock in the Seattle foot was calculated for level walking, up slope, down slope, lateral decline and lateral incline walking and was typically one of the higher values at lower velocities however, the shock did not increase with increasing velocity as much as in some of the other feet. This suggested that using the Seattle foot at greater velocities will bring less shock than say a SACH foot however, the inverse is true for lower velocities so normal walking speed would potentially determine comfort for the user.

The Seattle foot was an improvement on existing prosthetic feet when it was introduced however, it was more properly an improvement for the active amputee who was able to walk quicker or jog or dance, etc., with greater ease. There were improvements to be made and some of these were addressed with the introduction of the Seattle Lightfoot.

2.5.14 Seattle Lightfoot

The Seattle Lightfoot improved upon certain issues present in the Seattle foot; it was for example lighter and slimmer while maintaining a similar performance to the Seattle foot. The Lightfoot included a hollow area and a different keel shape but was otherwise the same (see Figure 29 for a comparison of the two feet).

Figure 29 – A comparison of the Seattle foot (top) to the Seattle Lightfoot (bottom) (Huston et al., 1998)

A number of studies carried out have included stride length, velocity and cadence as a measure of the prosthesis with figures approaching normal being considered indicative of good prosthetic limb function. Snyder et al (Snyder et al., 1995) recorded a mean velocity of 65 m/min (average for all feet tested was 66.5 m/min), a stride length of 1.25m (all feet average was 1.28m) and a cadence of 103.1 steps/min (all feet average was 103.5 steps/min) from 7 below-knee vascular amputees using the Lightfoot. The other feet tested were a Kingsley SACH foot, a Flex foot, a Quantum foot and a Carbon Copy II. During the same testing, the maximum terminal stance ankle dorsiflexion on the amputated side was found to be 16.1° for the Lightfoot which was significantly less than for the Quantum or Flex feet ($p<0.05$) and the knee flexion on loading of the sound side was 20.9° which was not significantly different to the other feet. The peak vertical ground reaction force of the Lightfoot was found to be 106.7% bodyweight compared to 123.2% on the sound side. This pattern of greater load on the sound limb was echoed in the other feet with the exception of the Flex foot, which showed greater loading on the prosthetic side.

Perry et al (Perry et al., 1997) carried out tests on 10 trans-tibial vascular amputees while using single axis, Seattle Lightfoot and Flex feet. The mean velocity when using the Lightfoot was 68.5% normal, the stride length was 75.7% normal and the cadence was 93.1% normal. Unfortunately, no clear values are provided for normal, so the results cannot be converted to absolute terms for comparison with other studies. The time to foot flat as a percentage of gait cycle was recorded and found to be 21.0% in the Lightfoot, which was significantly later than normal ($p<0.05$). The time to contralateral toe off was recorded in the same way and found to be at 16.3%, which is significantly later than normal ($p<0.01$) but was opposite the normal pattern in that it occurred before foot flat. The peak knee flexion was less than normal (12.2° versus 18.2°) but not significantly so, it did however, occur significantly later (20.0% gait cycle versus 13.4% ($p<0.01$)). The peak dorsiflexion, plantar flexion and knee flexion angular velocities were all significantly slower than normal ($p<0.01$) although there was no significant difference in timing. The compliance of knee and ankle joints when wearing a Lightfoot was not significantly different from normal. Perry et al. found these results to suggest that the Lightfoot had a relatively stiff construction and with the low compliance at the ankle this lead to a prolonged heel only support shown by the greater than normal time to foot flat.

Rao et al (Rao et al., 1998) also included velocity, stride length and cadence among their measurements. Among the 9 trans-tibial vascular amputees the mean velocity when using the Lightfoot was 64.2 m/min, which was significantly slower than the non-amputee controls' velocity of 78.5 m/min ($p<0.05$). The stride length was 1.23m, significantly lower than the 1.41m of the control group ($p<0.01$) although the cadence was not significantly different it was lower at 104.2 steps/min compared to 111.4 steps/min. It was found that knee flexion and the end of ankle plantar flexion were significantly later in gait ($p<0.05$ and $p<0.01$ respectively) when

compared to the control group. Rao et al. (Rao et al., 1998) also found the delayed foot flat seen by Perry et al. (Perry et al., 1997) and further go on to relate that this forced the user to take actions against knee flexion resulting in an increase of intensity and duration of quadriceps and hamstring activity.

Following a study of 6 amputees (3 traumatic, 3 vascular) Barth et al. (Barth et al., 1992) felt able to recommend the Lightfoot for 'average-activity-level amputees with no specific gait abnormalities or considerations'. Measured factors included step length, late stance dorsiflexion, change in dorsiflexion and weight acceptance forces, which were compared, sound side to prosthetic side. No significant differences were found in any of these factors for the Lightfoot. Energy cost was also calculated in terms of ml of oxygen uptake per kg per metre travelled but the difference between prosthetic feet tested (SACH, SAFE II, Lightfoot, Quantum, Carbon Copy II and Flex foot) was not significant. There were no significant differences in self-selected walking speed however, there was a significant difference between energy cost of the traumatic and vascular amputees ($p<0.05$).

Torburn et al. (Torburn et al., 1995) conducted a study involving 16 subjects (9 traumatic, 7 vascular) and measured variables including velocity, stride length, cadence, energy cost and energy cost per distance travelled. All results are divided into traumatic and vascular groups and while no values were provided the patterns may be observed on the charts provided. The velocity of users with the Seattle foot was lower than normal, the stride length of traumatic amputees was longer but of vascular amputees was shorter and the cadence of traumatic amputees was higher than normal but for vascular amputees was lower than normal. The energy consumption was greater than normal for both groups but was the higher for the traumatic amputees at 17.08 ml O_2/kg-min. Vascular amputee energy consumption was 13.10 ml O_2/kg-min and normal was 13.0 ml O_2/kg-min. When energy cost was

calculated for each metre travelled the cost is more similar between traumatic (0.215 ml O_2/kg-m) and vascular amputees (0.211 ml O_2/kg-m) however, it remained greater than in the normal case (0.16 ml O_2/kg-m).

2.5.15 Comparison of feet

The prosthetic feet described in section 2.5 Prosthetic feet are summarised in Table 3. Of the feet examined, eight of fifteen were SACH feet, with dynamic response accounting for three, Jaipur feet for two and the Shape and Roll foot and peg leg being the only examples of their type.

Costs were not well reported with only the ICRC (€45 - $48.30 at the time), HI ($25-37 (estimated approximately $230 with labour)), Jaipur ($30) and Niagara ($7.50) available. Of these the ICRC foot was produced in Switzerland, the HI foot in Thailand, the Jaipur foot in India and the Niagara foot in the USA. The Niagara foot cost is only for the keel and does not represent a complete foot as the others do. The HI foot included a cost estimate with labour and overheads included, the only to do so – approximately increasing the price by $200. The cost of the other feet does not specify if labour and overheads are included but, particularly in the case of the Niagara foot, this seems unlikely. These costs do not include the costs associated with having a prosthetist fit the prosthetic.

A range of materials were used in forming the keel of the feet with polypropylene being the most common (six), followed by wood and Delrin (three each) while ‘fibre-reinforced thermoplastic’ (Atlas), cadaveric foot (bone endoskeleton Jaipur foot), microcellular rubber (Jaipur) and ‘various’ (Peg leg) were each observed only once.

	Type	Cost	Materials	Survival at X time	Available sizes	Mass	Typical failures	Roll over characteristics	Adaptation to patient	Other advantages	Other disadvantages
Peg leg	Peg leg	Reportedly cheap, but no figures available	Locally available. Not specified but wood, steel, bamboo and PVC piping have been used	Not recorded, variation likely too great	Made to measure	Unknown, likely to range greatly depending on exact build	Unknown	Not recorded but expected to have short radius and short arc length	Individually customised	Cheap, simple, can be made from a range of available materials	Unsuitable for use on soft ground due to small contact area to disperse weight
ICRC	SACH	~€45 (CRÉquipements SA, 2013)	Polypropylene keel with polyurethane outer and sole (Jensen & Treichl, 2007)	95% at 6 months, 56% at 12 months, 31% at 18 months (Jensen, Nilsen, Thanh, et al., 2006)	14-21cm (child) 22-28cm (adult) (International Committee of the Red Cross, 2006a)	567.6g (size 25) (Sam et al., 2004), 506g (size 25) 314g (size 19) (International Committee of the Red Cross, 2006a)	Worn sole, worn keel, worn cover (Jensen, Nilsen, Thanh, et al., 2006)	178mm arc length 420mm radius (foot size not given) (Eaton et al., 2006)	None	Centralised production in Switzerland so quality control is high. Part of a complete trans-tibial system	Centralised production means that final product must be transported as required
Handicap International	SACH	$25-37 for materials, including labour estimated to be closer to $230 (Day, 1996)	Polypropylene keel, foam rubber forefoot and heel, tyre rubber sole and a rubber cover (Jensen & Treichl, 2007)	80% at 12 months (Jensen, Nilsen, Zeffer, et al., 2006)	17cm, 23cm and 25cm (Simon, 1996)	320g, 600g and 800g respectively (Simon, 1996), 854.6g (26cm) (Sam et al., 2004)	Worn sole, worn keel, bolt attachment failure (Jensen, Nilsen, Zeffer, et al., 2006)	Arc length and radius not provided but "similar to SACH foot" (Sam et al., 2004)	None	None	None

	Type	Cost	Materials	Survival at X time	Available sizes	Mass	Typical failures	Roll over characteristics	Adaptation to patient	Other advantages	Other disadvantages
Veterans International Solid	SACH	Unknown	Polypropylene keel, tyre rubber sole and exterior, rubber foam heel, textile reinforcement of heel, mid-foot and dorsum (Jensen, Nilsen, Zeffer, et al., 2006)	100% at 6 months, 97% at 12 months, 97% at 18 months, 97% at 24 months (Jensen, Nilsen, Zeffer, et al., 2006)	Unknown	Unknown	Worn sole (Jensen, Nilsen, Zeffer, et al., 2006)	Unknown	None	None	None
Veterans International Cavity	SACH	Unknown	Polypropylene keel, tyre rubber sole and exterior, textile reinforcement of heel, mid-foot and dorsum (Jensen, Nilsen, Zeffer, et al., 2006)	100% at 6 months, 97% at 12 months, 89% at 18 months and 86% at 24 months (Jensen, Nilsen, Zeffer, et al., 2006)	Unknown	Unknown	Worn sole, worn keel (Jensen, Nilsen, Zeffer, et al., 2006)	Unknown	None	None	None

	Type	Cost	Materials	Survival at X time	Available sizes	Mass	Typical failures	Roll over characteristics	Adaptation to patient	Other advantages	Other disadvantages
Jaipur	Jaipur	$30 (Day, 1996)	Sponge rubber toes, laminar sponge rubber wrapped in hard rubber heel, wooden/ microcellular rubber midfoot block, laminated wooden ankle block, all enclosed in vulcanised rubber with a tyre rubber sole (Mobility India, 2004; Sethi et al., 1978)	82% at 18 months, 53% at 36 months (Jensen et al., 2004b) 89% at 12 months, 73% at 16 months (Jensen & Raab, 2006)	Unknown but a range (Mobility India, 2004; Sethi et al., 1978)	822.0g (23cm)	Worn sole, worn keel, screw attachment failure (Jensen & Raab, 2006)	129mm arc length 151mm radius (foot size not given) (Eaton et al., 2006)	None	Produced locally by local craftsmen, users can squat, climb trees and other activities requiring flexible toes (Sethi et al., 1978). Designed for barefoot use (Arya et al., 1995). User requires little gait training (Arya & Klenerman, 2008)	Variable quality depending on materials and craftsmen used

	Type	Cost	Materials	Survival at X time	Available sizes	Mass	Typical failures	Roll over characteristics	Adaptation to patient	Other advantages	Other disadvantages
Bone endoskeleton Jaipur foot	Jaipur	Unknown	Otherwise healthy cadaveric foot (preferably from intended user) wrapped in hard rubber and enclosed in vulcanised rubber with a tyre rubber sole (Kabra & Narayanan, 1991a)	No known real-world testing carried out	Unlimited – dependent on source foot	850g, 900g and 920g (Kabra & Narayanan, 1991a)	Unknown	Not tested	Joints articulated at dimensions of source foot. No discussion of further modifications of dimensions.	If source foot is intended user's original foot, then foot segment lengths match the user's original lengths	Difficulty in sourcing fresh, healthy cadaveric feet of the correct size as required
Niagara	Dynamic response	$7.50 (Tara Ziolo, Zdero, & Bryant, 2001)	Dupont™ Delrin®(T. Ziolo & Bryant, 2001)/ Hytrel® (Haberman, 2008) keel, unknown cosmesis material	100% at 12 months	Unknown	Unknown	Unknown	204mm arc length, 300mm radius (foot size not given) (Eaton et al., 2006)	None	None	None

	Type	Cost	Materials	Survival at X time	Available sizes	Mass	Typical failures	Roll over characteristics	Adaptation to patient	Other advantages	Other disadvantages
Shape and roll (S&R)	Shape and roll	Unknown	Polypropylene/ polyethylene keel (M. Meier et al., 2006), unknown cover.	Unknown	22-29cm (Childress et al., 2005)	Unknown	Unknown	224mm arc length, 360mm radius (foot details not given – the S&R foot is designed to vary foot to foot to suit the user)	Customised to the height, weight and foot length of user (Childress et al., 2005)	Can be highly customised to the user	No energy return function
Atlas	SACH	Unknown	Polyester polyurethane foam cosmesis, polystyrene bead filler, fibre-reinforced thermoplastic keel and shank (Shorter & Evans, 2000)	60% at 18 months (Jensen & Raab, 2002)	23-26cm (Jensen & Raab, 2002)	Varies depending on user due to integrated shaft	Shank fracture, worn keel, looseness of IH beam (Jensen & Raab, 2002)	Unknown	Shank cut to suit user stump length (Jensen & Raab, 2002)	None	"Shrieking" of prosthesis during normal walking (Jensen & Raab, 2002)
EB-1	SACH	Unknown	Wooden keel, rubber plate heel, cotton rubber sole, rubber cover (Jensen, Nilsen, Zeffer, et al., 2006; Jensen & Treichl, 2007)	100% at 6 months, 100% at 12 months, 97% at 18 months, 67% at 24 months (Jensen, Nilsen, Zeffer, et al., 2006)	Unknown	809.8g (25cm) (Sam et al., 2004)	Worn sole, worn keel (due to wood rot) (Jensen, Nilsen, Zeffer, et al., 2006)	Approximates the shape of the wooden keel (Sam et al., 2004)	None	None	None

	Type	Cost	Materials	Survival at X time	Available sizes	Mass	Typical failures	Roll over characteristics	Adaptation to patient	Other advantages	Other disadvantages
Strider	SACH	Unknown	Wooden keel, textile belt drive forefoot reinforcement, moulded polyurethane foam cover (Jensen, Nilsen, Thanh, et al., 2006)	94% at 6 months, 73% at 12 months, 45% at 18 months, 39% at 24 months (Jensen, Nilsen, Thanh, et al., 2006)	Unknown	Unknown	Worn sole, worn keel (Jensen, Nilsen, Thanh, et al., 2006)	Unknown	None	None	None
HCMC	SACH	Unknown	Polypropylene/ ebonite (Jensen & Heim, 1999; Jensen & Treichl, 2007) keel, rubber foam forefoot, rubber foam heel and exterior, reinforced tyre compound sole (Jensen & Heim, 1999)	56% at 6 months, 44% at 12 months, 33% at 18 months (Jensen & Heim, 1999)	Unknown	Unknown	Failed keel, failed sole (Jensen & Heim, 1999)	Unknown	None	Passed static proof test of ISO 10328 (Jensen & Treichl, 2007)	None
Seattle	Dynamic response	Unknown	Delrin® (polyoxymethy-lene) keel, rubber bumper, Kevlar® toe reinforcement, polyurethane foam cover (Hittenberger, 1986)	Unknown	6-12 inches (men), 5-8 inches (women) (Hittenberger , 1986)	Unknown	Worn cover on sole (Hittenberger , 1986)	Unknown	Additional configurati ons for weight/ activity level (Hittenberg er, 1986)	None	Not recommended for barefoot use due to cover failure (Hittenberger, 1986)

	Type	Cost	Materials	Survival at X time	Available sizes	Mass	Typical failures	Roll over characteristics	Adaptation to patient	Other advantages	Other disadvantages
Seattle Lightfoot	Dynamic response	Unknown	Delrin® (polyoxymethy-lene) keel, rubber bumper, Kevlar® toe reinforcement, polyurethane foam cover (Huston, Dillingham, & Esquenazi, 1998)	Unknown	Unknown	Unknown	Unknown	Unknown	Unknown	None	None

Table 3 – Comparison of the feet discussed in chapter 2

Fewer materials were used for cosmesis, only polyurethane (five) and rubber (seven) were recorded with three feet not specifying cosmesis material but it seems likely either polyurethane or rubber was used in these cases.

Some of the feet required extra support at the toe, this was achieved with either Kevlar (two) or ‘textile’ (three) reinforcement. This extra support was found in feet with a relatively short keel (VI Solid, VI Cavity, Strider, Seattle and Seattle Lightfoot) with the reinforcement increasing the stiffness of the toe section without direct support of the keel.

Rubber foam (VI Solid) and a rubber plate (EB-1) were specifically called out as heel materials in two cases while the rest of the feet used a combination of keel and cosmesis to provide heel support. The VI feet also made use of textile reinforcement of the heel.

Sizes available were poorly reported with only the ICRC foot (children 14-21cm, adult 22-28cm) and the Seattle foot (men’s sizes (6-12 inches/15-30cm) and women’s sizes (5-8 inches/12.5cm to 20cm)) detailed in full range. The HI foot is available in at least three sizes (17cm, 23cm and 25cm). The bone endoskeleton Jaipur foot would be available in a range of sizes, depending on the cadaveric foot provided for the prosthesis but this is not specifically mentioned, nor is any potentially size-limiting process condition (e.g. available mould sizes). The Shape and Roll foot is available in 22-29cm sizes, similar in range to the Atlas foot (23-26cm). Single sizes were reported of the Jaipur foot (23cm) and the EB-1 foot (25cm)

Like size, mass was a poorly reported quality of prosthetic feet. Three samples of the bone endoskeleton Jaipur foot massed between 850-920g, the heaviest reported. A 25cm EB-1 foot was recorded as 809g while a 25cm HI foot massed 800g and two 25cm ICRC feet massed 568g and 506g. A 23cm Jaipur foot massed

822g compared to a 600g 23cm HI foot. The smallest feet, a 19cm ICRC foot (314g) and a 17cm HI foot (320g), were the lightest reported.

Causes of failure reported were overwhelmingly related to sole and keel wear (nine and eight reports respectively) and occurred in feet with either polyurethane or rubber keels. One count of each of the following was reported: failure of bolt attachment (HI), worn cover (ICRC, specifically separate to sole wear), screw attachment failure (Jaipur), shank fracture (Atlas) and beam looseness (Atlas).

In terms of customisability to user; many of the feet seem to offer a range of sizes to accommodate users (typically relating to weight or activity level) however some of the feet are individually customisable to the user. The bone endoskeleton Jaipur foot recommends using the user's own cadaveric foot as possible in order to preserve segment lengths of the foot so that articulation will match the opposite foot wherever possible. The Atlas foot included an integrated shank which would be cut to length as required by the user, but this was the limit of the customisation of the prosthesis. The Shape and Roll foot is customised to the user based on their height, weight and foot size with notches cut into a blank to create a rollover shape appropriate to the user based on those criteria.

Based on the results gathered above it might be suggested that the typical prosthetic foot found in developing countries:

- Is a SACH foot
- Costs between $25 and $50 (excluding labour and overheads)
- Has a polypropylene or wood keel
- Has a rubber or polyurethane cover
- Masses 320-810g, depending on size and type
- Will most likely fail due to sole or keel wear
- Will not be customisable to the user.

2.6 Measures relating to prosthetic foot performance

A number of different measures have been used to determine the performance of prosthetic feet; some rely on subject opinions, some on measured properties of gait and others on performance of the foot under specific lab conditions (e.g. machine loading). The following attempts to catalogue as many of these as possible but is not exhaustive. Most are described by Hafner et al. in their paper ‘Energy storage and return prostheses: does patient perception correlate with biomechanical analysis?’ (Hafner et al., 2002a)

2.6.1 Subject opinion

Some measures are related to subject perception and are usually found through the use of questionnaires. They may include descriptive dialogue where the subject may describe how the foot feels to them, which may reveal things such as a feeling of instability in stance, which may not be apparent from test data alone (Haberman, 2008). In tests involving multiple prosthetic feet, subjects are often asked for their preference among the choices (Hafner, Sanders, Czerniecki, & Fergason, 2002a; Jensen & Heim, 2000; Torburn, Perry, Ayyappa, & Shanfield, 1990; Wirta, Mason, Calvo, & Golbranson, 1991). The subject may feel that a particular prosthesis is better than another despite there being no significant difference measurable by the investigator as happened in Torburn et al., 1990, where each subject preferred the prosthesis that gave them the highest velocity despite the differences in velocity not being statistically significant. Other insights may be gained from subject opinion for example the appearance of the cosmesis of the prosthesis (Hafner et al., 2002a), which could be a major factor in acceptance.

The subject may also be asked on the function of the prosthesis for example "Is walking uphill easier with the test prosthesis or your currently used prosthesis?" (T. Ziolo & Bryant, 2001) The reply may be worse, same or better and when a group is

questioned it may highlight weak and strong areas of performance however, this does not provide evidence of the performance, only subjective opinions. Alternatively, a numerical scale may be used which allows the data to be analysed statistically and so can highlight the significant differences of the opinions of the subjects (Bryant & Bryant, 2002).

2.6.2 Measured gait properties

A great range of properties of gait have been measured and analysed to quantify the performance of prosthetic feet. Some are directly measurable while others must be derived from other recorded data. Commonly used are the relatively straightforward stride length, cadence and self-selected walking speed (Bryant & Bryant, 2002; Perry & Shanfield, 1993; Postema, Hermens, de Vries, Koopman, & Eisma, 1997; Rietman, Postema, & Geertzen, 2002), which indicate both the comfort of the subject in using the prosthesis and the capability of the prosthesis in walking. The symmetry of gait can be measured and indicates whether the prosthetic side behaves in a similar manner to the natural foot and therefore well (Au, Herr, Youcef-Toumi, & Anand, 2007; A. H. Hansen, Childress, & Knox, 2000; van der Linde et al., 2004). The timing of different phases of gait may also be recorded with the aim again being as close as possible to natural gait (Coleman, Boone, Smith, & Czerniecki, 2001; O'Keefe, 1998; Perry & Shanfield, 1993; Snyder, Powers, Fontaine, & Perry, 1995).

Force plates are frequently used and can expose much more information about the behaviour of the foot including the vertical ground reaction forces, the braking and propulsive forces and the path of the centre of pressure (Arya & Klenerman, 2008; Coleman et al., 2001; Perry & Shanfield, 1993; Seelen, Anemaat, Janssen, & JHM, 2003). The forces recorded can be measured on both the prosthetic and the sound side to indicate if symmetric gait is achieved. The shock absorption of a

prosthetic foot can be determined using the initial loading peak to calculate the rate of loading (Arya, Lees, Nirula, & Klenerman, 1995; Murray, Hartvikson, & Anton, 1988). Accelerometry may also be used to determine the shock absorption of a foot as energy loss can be determined in relation to the rate of deceleration of a prosthesis from initial impact with the ground (Hafner et al., 2002a; Van Jaarsveld, Grootenboer, & De Vries, 1990).

Muscle activation may be recorded which would be an indication of the effort required in using the prosthesis, either in the prosthetic or sound sides, and may include the duration of the activity and the timing for comparison to normal gait (Au et al., 2007; Hafner et al., 2002a) Energy cost can be used and is typically calculated using oxygen intake which requires specialised equipment to analyse the composition of exhaled air as well as the rate of air intake (Buckley, Jones, & Birch, 2002; Houdijk, Pollmann, Groenewold, Wiggerts, & Polomski, 2009; Klodd, Hansen, Fatone, & Edwards, 2010b; Schmalz, Blumentritt, & Jarasch, 2002). As the energy cost of walking is higher in amputees than in normal gait the least increase is clearly the most desirable.

2.6.3 Lab tests

Certain testing may be carried out to assess prostheses separately from subjects. These include the rollover shape as described by Hansen in his PhD thesis and several other papers (A. H. Hansen et al., 2000; A.H. Hansen, 2002; A.H. Hansen & Childress, 2004, 2005; Andrew H Hansen, Childress, & Knox, 2004; Andrew H Hansen, Childress, & Miff, 2004). Essentially the rollover shape is a description of the centre of pressure when viewed relative to ankle joint centre. This provides a rocker shape which through various tests Hansen et al. have shown is consistent in non-amputees across changing conditions of heel height, weight carried, surface inclination and declination, etc. The roll-over shape may be found

through one of three methods, one of which does not involve any subject and two that may be found using an amputee or non-amputee using prosthetic stilts. The simplest method is the third, the dynamic roll-over method, where the subject walks across a force plate while the ankle is defined by motion capture. This allows a transformation of the COP data to the ankle frame of reference as the foot rolls over. The quasi-static method involves a similar setup however, this time the foot is placed heel first onto the force plate and the foot is then rolled across the plate without being part of normal walking. Finally, the quasi-static PFLA (prosthetic foot loading apparatus) method involves a specialised piece of equipment (the PFLA itself) to load the foot to 800N at different angles with the deflection at each angle being measured. The three methods Hansen et al. (A. H. Hansen et al., 2000) used were found to give similar results however, the dynamic method and the quasi-static PFLA method did differ towards toe off which Hansen et al. believed was an effect of using the stilts and thus giving a longer leg length and meaning that the 60° angle used in the PFLA method was not achieved in dynamic testing.

ISO 10328 and ISO 22675 both relate to the testing of lower limb prostheses (specifically ankle-foot devices and foot units in the case of ISO 22675) within a lab environment. ISO 10328 grew out of the consensus reached in a series of meetings held by the ISPO, culminating in Philadelphia in 1977. From 1979 onwards, the work was continued by ISO Technical committee 168 leading to the creation of ISO 10328:1996, although it is noted that as the standard is based on the consensus of the ISPO meetings that the test procedures may not be applicable to prosthetics of different mechanical characteristics to those used in the consensus. ISO 10328 includes testing in static and cyclic loading conditions. The static tests were intended to represent the worst loads generated in any activity whereas the cyclic tests related to normal walking activities with regular loading each step (Comité Européen

de Normalisation, 2006a). ISO 10328 included testing for fatigue however, it was acknowledged that the testing was not sufficient to predict service life of the prosthesis and that the standard did not include testing for function, wear and tear, new material developments, environmental influences or user activities. ISO 22675 was first published in 2006 in a bid to better address weaknesses in ISO 10328 related to lines of application of forces, the unrealistic course and magnitude of loading during cyclic testing and the periodic simultaneous loading of heel and forefoot in cyclic testing. ISO 22675 did not supersede ISO 10328 in application to ankle-foot devices and both test methods remain valid for ankle-foot devices and foot units (Comité Européen de Normalisation, 2006b). It should also be noted that ISO 22675 does not include testing in the areas mentioned previously which were not included in ISO 10328. Test samples were to be taken from normal production with a minimum of two tests required and the potential for a single replacement in all but the separate test in torsion, cyclic testing of separate ankle-foot devices and foot units, and separate static ultimate strength test in maximum knee flexion on knee joints and associated parts. Jensen & Treichl examined a large variety of prosthetic feet used in low-income countries according to ISO 10328 static proof and cyclic test conditions and concluded that such testing was useful prior to release of a prosthetic lower limb (Jensen & Treichl, 2007). Jensen & Treichl also suggested that invasive inspection following cyclic testing may help in identifying mechanisms of failure although in doing so would prevent the piece from being tested to destruction.

2.7 Summary

This chapter described the aim of the project, namely to design a highly functional prosthetic foot unit suited to the developing world but with a greater level of functionality such as seen in Western prostheses. Following this was an overview

of the structure, including internal structure such as trabeculae, of the human lower limb related to supporting the body and facilitating locomotion. An overview of the prosthetic feet currently used in low-income countries followed which included the Blatchford Atlas, EB, HI Cambodia, Ho Chi Minh City, ICRC, Jaipur, Kingsley Strider, Niagara, Seattle, Shape and Roll, VI foot as well as peg legs. The various leg systems had different strengths and weaknesses however, the most prevalent weakness of design was the lack of durability, particularly of the cover and keel. The limited number of materials used across all feet examined was particularly pronounced in the cover where only polyurethane and rubber were recorded in use. There was also a general lack of function observed with the majority of feet taking the form of SACH feet which can provide a good walking base but do not offer any energy return as the dynamic feet do, or other function like the ability to squat as the Jaipur foot does. The feet that attempted energy return performance tended to have the least durability. The Jaipur foot was notable for its great durability and its apparent function although it provided little in the way of energy return to users and was among the heaviest of the feet examined, while the Seattle foot was praised for the energy return provided but lacked durability. These findings were useful in defining the available solutions as well as their strengths and weaknesses in order to inform the design process for the Strathclyde foot.

A summary of methods used to evaluate prosthetic foot performance was included which contained subject opinion, measured gait properties and lab tests. Each of these different areas potentially offers insight into the function of the foot that may be of value to the designer in evaluating design performance to provide the balance of function and durability sought.

CHAPTER 3 - Design considerations on proposed foot and existing design testing

This chapter begins with the formation of a Product Design Specification, based on the information presented in chapter 2, before static loading tests were carried out to the P3, P4 and P5 requirements of ISO 10328 on both the toe and heel of the Strathclyde foot, including samples with and without fibreglass rods included for energy return.

3.1 Introduction

A product design specification was drawn up to define the requirements of the project using the guidelines provided in Total Design (Pugh, 1990). Not all of the suggested criteria were used but rather the most relevant were chosen with the goals for each defined based upon the feet described in the literature review of chapter 2. The existing design was then tested to the static loading conditions of ISO 10328 to assess its performance under those conditions.

3.2 Product Design Specification

Total Design is a method developed by Stuart Pugh at the University of Strathclyde in the 1980s. It is a process through which as many aspects as possible in the ultimate success of a design may be considered early on to maximise the product's success. Pugh's 1990 book "Total Design: Integrated methods for

successful product engineering" (Pugh, 1990) was used as a guide during this process. Not all of the suggested headings were used but only those that the author felt the most relevant to this particular project e.g. political considerations were not used. The information gathered regarding the existing prosthetic feet used in developing countries was used to define the requirements of this Product Design Specification.

3.2.1 Performance

The prosthesis will be required to meet ISO 10328 standards to the P5 level. This standard includes the requirement to meet static test conditions, representing extreme single loading of the prosthesis, and cyclic testing conditions that represents the ongoing use of the prosthesis, but is not enough to predict the lifespan due to limited loading conditions not reflective of real world conditions. The static conditions of ISO 10328 relate to worse case loading of the prosthesis during normal gait. This was not a condition met by the majority of the prosthetic feet examined by Jensen & Treichl, 2007, with them only considering the HCMC foot to have passed the standard. The prosthesis should allow for an even and comfortable gait to be assessed via force plate trials and, if possible, user feedback.

The return of energy stored in deformation of the prosthesis should be comparable to the natural human function and so should provide a large portion of 14J return at approximately 65% of gait cycle (Das, Burman, & Mohapatra, 2009) as the human foot (the human foot also inputs energy which will account for a larger difference between the two). Only the dynamic return feet (Niagara, Seattle and Seattle Lightfoot) provide any energy return to the user which was generally well received by users although the extent of energy return has not been reported hence the use of anatomical foot energy return has been used as the target energy return.

The human foot has up to 10° dorsiflexion in walking up to 8km/h and a range of 19.2° inversion and 15.6° eversion (Das et al., 2009). The values of dorsiflexion should be considered with regards to the requirement to allow normal gait however, the inversion and eversion values might need to be sacrificed for overall stability. Dorsiflexion of 36.75° was recorded in the bone endoskeleton Jaipur foot under 70kg load which is much greater than that of the natural foot however it is this dorsiflexion that allows the user of Jaipur feet to squat. The Seattle Lightfoot recorded a peak dorsiflexion of 16.1° during terminal stance phase which is greater than the anatomical foot but much less than that of the bone endoskeleton Jaipur foot. None of the feet examined had reported values of inversion or eversion.

The human heel can provide shock absorption of up to 50% of load applied (based on isolated cadaveric heel pads (P Aerts, Ker, De Clercq, Ilsley, & Alexander, 1995)) and so shock absorption of a similar level should be shown in the prosthetic foot using a modified version of Aerts et al.'s method to account for the use of a prosthetic foot. This is clearly limited in that it is carried out in a laboratory environment and would not account for different surfaces met in daily life. Arya, Lees, Nirula, & Klenerman, 1995, used a force plate to compare the SACH, Seattle and Jaipur feet and reported their findings in N/kg body mass with a lower heel strike peak force representing better shock absorption (of the feet tested the SACH foot was determined to have the best shock absorption). This method could provide a way of showing the shock absorption under normal walking conditions.

The prosthesis should be customisable to the user through changing of the energy return feature and shock absorption feature of the heel. This would provide better performance for the individual as the prosthesis could be modified to suit their mass and activity level. This type of customisability is not found in the prosthetic feet examined. The Shape and Roll foot does offer customisation based on user height,

weight and foot size, which allow for a roll-over shape more closely matching the user's intact foot, however it offers no energy return.

3.2.2 Environment

The prosthesis should be able to deal with a wide range of temperatures and humidity levels. The Least Developed Countries, as defined by the UN, span a wide range of climates and environments including for example, Haiti, Nepal, Yemen, Cambodia and Chad (UN-OHRLLS, 2014). The extreme temperatures of human habitation (100 days plus continuous exposure) were identified by the Rand corporation for NASA in 1958 as 30°F – 120°F (-1°C – 49°C) with the upper limit depending on relative humidity (Buchheim et al., 1958). Humidity was evaluated as relative humidity rather than absolute humidity and a complete range (from 0-100%) across temperatures should be used in assessing materials. Allowance should be made for contact with solvents to include petrol, water and weak acids and bases. Measures should be taken to prevent ingress of dust or particulate matter to prevent wear within the prosthesis.

3.2.3 Life in service

The prosthesis would ideally meet a standard of surviving for three years of daily use. Testing would be through clinical field trial, most likely in a method similar to that carried out by Jensen et al. (Jensen, Nilsen, Zeffer, et al., 2006). While ISO 10328 specifically states that the 3 million loading cycles in the cyclic test is not sufficient to predict actual service life it should be used as a base standard prior to clinical field trial. Limited information was available for the life of prosthetic feet examined in Chapter 2 with only the Jaipur foot having any results recorded at 36 months of use (53% survival). At 24 months survival rates were recorded for the VI solid foot (97%), the VI cavity foot (86%), the EB-1 foot (67%) and the Kingsley Strider (39%). These results show that high survival rates at times of two to three

years are possible but are likely to be challenging, the HCMC foot showed only 56% survival at 6 months (despite passing 2 million loading cycles of ISO 10328 testing (Jensen & Treichl, 2007).

3.2.4 Maintenance

No maintenance of the internal structure should be required for the prosthesis. If maintenance were required, it would be by a prosthetist and as access is often limited in developing countries to qualified prosthetists this would increase the burden on those prosthetists and likely mean that the prosthetic foot would go without maintenance in many cases. It is therefore considered that if the prosthesis may be developed in a maintenance free fashion it will be of most use to user and reduced burden to the local prosthetists. Repair to the cosmesis should be possible by the user if so required to maintain the protection of the internal components and prolong prosthesis life. None of the prosthetic feet examined in Chapter 2 has maintenance per se reported however on visits to prosthetists replacement of the cosmesis occurred or replacement of the entire prosthesis. For the Niagara foot Beshai & Bryant, 2003, suggest that the user could take responsibility for cosmesis replacement.

3.2.5 Target product cost

The production cost should be as low as possible without compromising quality. The total cost should include the purchase of materials, the cost of labour and the cost of machine time/amortisement if possible and should be based on production of not more than five thousand units per year. It is undecided as to the nature of the project is to result in a charitable or business endeavour so the cost and method of delivery to the user is undetermined until such a decision is made. It is expected that at minimum the keel will be produced centrally and either distributed with energy absorption and energy return components to be applied dependant on the intended

user by the fitting prosthetist or else plans and requirements for such components to be provided for the prosthetist to source locally. The cost would be determined based on the chosen distribution method. The range of approximately $25-50 seen in existing prosthetic feet does not account for equipment and overheads so the true cost of manufacturing a prosthesis will likely be significantly higher than this. If the prosthesis is to be provided as part of a charitable organisation, then it may be provided at cost as the ICRC and HI foot are.

3.2.6 Quantity

The design of the prosthesis should allow for production of thousands of units per year in an economical and effective manner.

3.2.7 Size

As a prosthetic foot unit, the prosthesis must remain within or at least very close to the anatomical bounds of the human foot. A variety of sizes should be available to allow for people of different sizes. The foot should allow shoes to be worn over it (unlike the Niagara foot, which was designed for barefoot use).

3.2.8 Mass

An entire trans-tibial system should mass less than 1kg, so the foot unit alone would be required to mass much less than this although it should be noted that outside of smaller people and those with vascular dysfunction increased mass is not necessarily a penalty. The heaviest prosthesis found in the literature review was a bone endoskeleton Jaipur foot of unknown size, massing 920g. This would be considered heavy with a 25cm ICRC foot massing only 567.6g.

3.2.9 Aesthetics, appearance and finish

A somewhat lifelike appearance is required; however, the function is to be considered more important than the aesthetics. A range of skin tones befitting the individuals to use the prosthesis should be included.

3.2.10 Materials

The materials to be used must meet the required physical, chemical and environmental resistance requirements. The materials should be recyclable or minimum waste and must not be toxic. Costs will limit material availability. Depending on production model to be used a need for locally sourced materials with good recyclability and suitable production techniques may be required however, the performance of the components is the driving factor, not the material choice. A range of materials are currently in use in existing prostheses and may be considered as a jumping off point, but not a limiting group.

3.2.11 Standards and specifications

The prosthesis must meet both the static and cyclic requirements as defined in the ISO 10328 standard.

3.2.12 Ergonomics

A range of sizes should be available to suit different sized users. Assuming an otherwise healthy user, the user should be able to doff and don the prosthesis by themselves. The prosthesis must be comfortable when worn and used. There should be some ability to adjust the prosthetic foot to the individual user. The Shape and Roll foot offers the only example of a prosthetic foot that can be modified to better suit the individual user by accounting for user height, weight and foot size.

3.2.13 Quality and reliability

The prosthesis should have a 95% survival rate at three years. There is no current method for determining the survival rate in everyday use outside of a clinical field trial and so this cannot be accounted for until such a trial is carried out. This is a very aggressive goal as the Jaipur foot (the only one followed up at 36 months use in the literature) had only a 53% survival rate. The VI solid and VI cavity feet were able to achieve 97% and 86% survival rates at 24 months respectively and so should be examined for factors contributing to their success. Aside from in extremis the prosthesis should continue to function when broken during normal use albeit at a much-reduced level. This should allow the user to seek replacement in reasonable time. The prosthesis will be assessed on aesthetic appearance on production before being passed for distribution with a mechanical test regimen to be determined based on production scales.

3.2.14 Safety

The safety standards required by the ISO 10328 standard and tested for according to the methods prescribed should provide suitable safety levels.

3.2.15 Legal

With the requirements of ISO 10328 met and documentation, in the form of a manual provided in the local language to highlight the limits of the prosthesis, the legal liabilities should be minimised by highlighting all improper use. The prosthesis itself should have built in safety margins (as required by ISO 10328) to negate all but the grossest misuse of the prosthesis. A guarantee may be included to offer free replacement of failure depending on the business model used.

3.2.16 Installation

A trained prosthetist would be required to fit the prosthesis and to carry out any alignment and adjustment of the fit of the prosthesis. This is standard across all prosthetic feet examined in Chapter 2.

3.2.17 Documentation

Fitting documentation should be provided to the prosthetists fitting the prostheses along with any maintenance documents. A user's guide should be included in the local language to highlight the limits of the prosthesis and the proper use as well as information relating to damage and replacement. The terms of any guarantee should be provided in the local language.

3.3 Strathclyde foot testing

Previous work carried out within Strathclyde University led to the development of the "Strathclyde foot", a polypropylene keel with a cosmetic cover. Following appraisal of the PDS (section 3.2 Product Design Specification) and evaluation of the prior work (L. E. Morton, Spence, Buis, & Simpson, 2009) it was deemed that the Strathclyde foot had the potential to meet the performance and financial requirements of the project. Further development of the design to address the existing shortcomings, particularly in the keel, was decided to be appropriate.

Based on the requirements of the PDS the current design of the Strathclyde foot was evaluated to form a baseline. A great number of samples had been produced previously (RPWorld, Beijing, China) which could be tested. These samples were initially injection moulded in polypropylene (no further information was available on the specific material properties for this particular variety of polypropylene) in 2007 and were stored in an internal loft space within the Bioengineering department at the University of Strathclyde. As such they were

exposed to typical range of room temperatures and humidities for approximately 3 years. The static standards of ISO 10328 were to be used in evaluating the current design. Cyclic testing would take a number of weeks running continually and it was decided that at this stage it was unnecessary.

The feet would be tested at P3 level, then depending on performance to higher levels.

3.3.1 ISO 10328 testing

3.3.1.1 Specimens

The samples were already available having been previously manufactured by RPWorld (Beijing, China) however they required some modification to take them to a testing condition. These modifications were carried out in the fashion indicated by (L. E. Morton et al., 2009). Pultruded glass fibre rods were among a number of rod types sampled in the aforementioned thesis and showed good performance for their cost and so were used in this test. Four samples were chosen from those available and were individually marked with the numbers 1-4. The following modifications were carried out:

- A hole was drilled to accommodate a steel threaded bush in the top of the feet for attaching a pyramid adapter
- Holes were drilled through the middle of keels 3 and 4 to allow for insertion of rods
- Glass fibre rods (Free Flight Supplies Norwich, UK) were cut to length then inserted, and remained otherwise unfixed

A rubber ball (It's my party, Hixon, UK) was inserted into the heel of each keel. These balls were of the same outward appearance and had no obvious defects. These were balls of a mass-produced variety with no material properties available.

A custom designed adapter was manufactured to the author's design (see Figure 30) to allow the feet to be mounted within the Instron universal testing machine within the Bioengineering department at the prescribed 15° (heel) and 20° (toe).

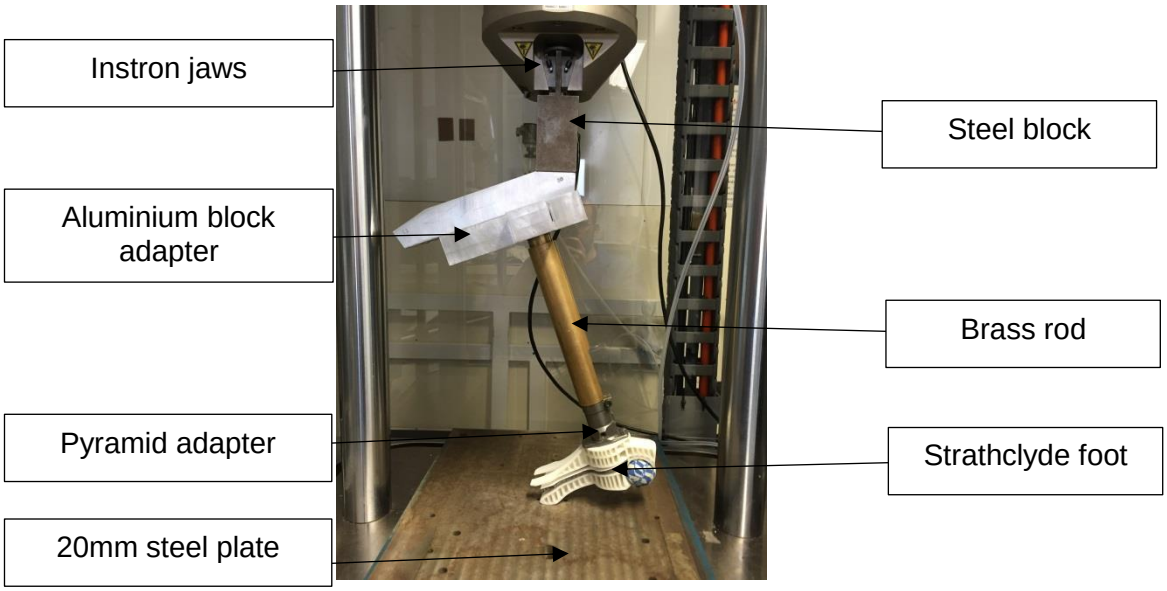

Figure 30 – The custom adapter design demonstrating toe loading setup.

The custom adapter allowed for the loads to be applied at the required angles while approximately maintaining the linear loading of the Instron machine as the load cell in the machine has a very limited capacity for moments. The various parts of the adapter were made from brass, steel and aluminium in order to transfer the load without deformation of the adapter itself.

A 20mm thick steel plate was placed on the base of the Instron universal loading machine to give an even and nearly unbroken surface for the foot samples to contact.

3.3.1.2 Method

The adapter was set up for the required loading condition (heel or toe), which would give the loading angle required (20° for toe loading, 15° for heel loading). The adapter was then mounted into the Instron machine with the grip being closed on

the topmost part. That the alignment was correct was determined using a goniometer. A pyramid was attached to the foot and a pyramid adapter mounted on the bottom of the brass rod to allow for connection. The crosshead of the Instron was then lowered until the foot barely contacted the baseplate at which point the crosshead would be locked. The load was increased at a rate of 175N/s (between the 150N/s – 250N/s rate required in ISO 10328) until the ultimate static test force upper limit was met (see Table 4). The ultimate static test load was maintained for 30s to allow for creep measurement, per ISO 10328 static loading protocol, at which point the load was reduced at a rate of 175N/s until 0N load was recorded. The test was to be stopped prior to completion if the sample was observed to fail or the setup became unsafe in any way.

Test procedure and test load			**Unit**	**Test loading level (Px) and test loading condition (F_{1x}; F_{2x})**					
				P5		**P4**		**P3**	
				Heel loading, F_{1x}	**Forefoot loading, F_{2x}**	**Heel loading, F_{1x}**	**Forefoot loading, F_{2x}**	**Heel loading, F_{1x}**	**Forefoot loading, F_{2x}**
Static test procedure	**Proof test force**	**F_{1sp}, F_{2sp}**	N	2240	2240	2065	2065	1610	1610
	Ultimate static test force	**F_{1su} lower level, F_{2su} lower level**	N	3360	3360	3098	3098	2415	2415
		F_{1su} upper level, F_{2su} upper level	N	4480	4480	4130	4130	3220	3220

Table 4 – Test load levels for static P3, P4 and P5 tests (taken from ISO 10328, table 11)

3.3.2 P3 testing – toe

3.3.2.1 Specimens

Samples 1 and 2 were tested initially. A further two samples were then tested, samples 3 and 4, which included pultruded glass fibre rods (Free Flight Supplies Norwich, UK) inserted into the toes, see Figure 31. All keel samples were randomly selected from a batch of injection moulded polypropylene pieces (no further specific material information provided). Each sample had a rubber ball (It's my party, Hixon, UK) inserted into the heel cavity.

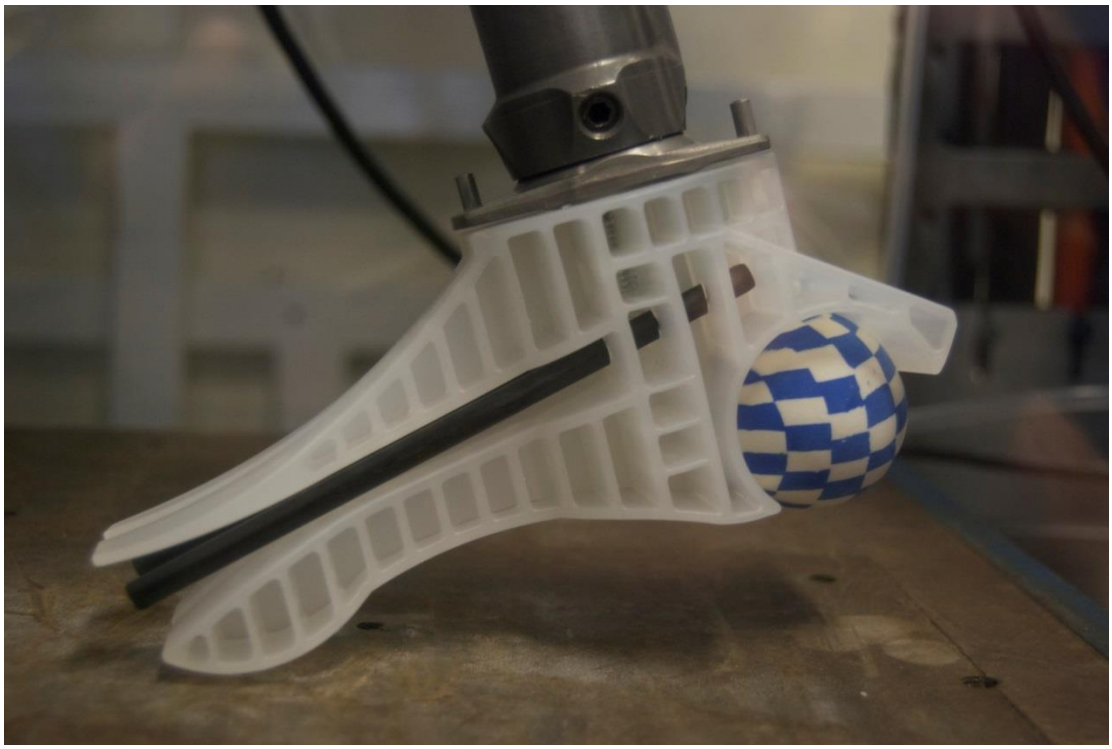

Figure 31 – Image showing the rod setup included in samples 3 and 4 of the Strathclyde foot

3.3.2.2 Method

The adapter was set so that the toe would contact the baseplate at 20° with the load increasing at 175N/s until the upper load of 3220N was reached. This load was

to be held for 30 seconds before being reduced at a rate of 175N/s until zero loading was achieved.

3.3.2.3 Results

The ultimate static test force for the P3 level was applied in each case. Samples 1 and 2 were observed to slip on the steel baseplate however, the foot settled and loading continued. The lower section of the foot was observed to deflect into the upper toe sections as loading progressed. The deflection continued until the ball at the rear of the foot and subsequently the rear of the keel itself contacted the baseplate (see Figure 32). As a result, there were two changes of gradient visible in Figure 33 and Figure 34 during loading which correspond to the two stages of contact.

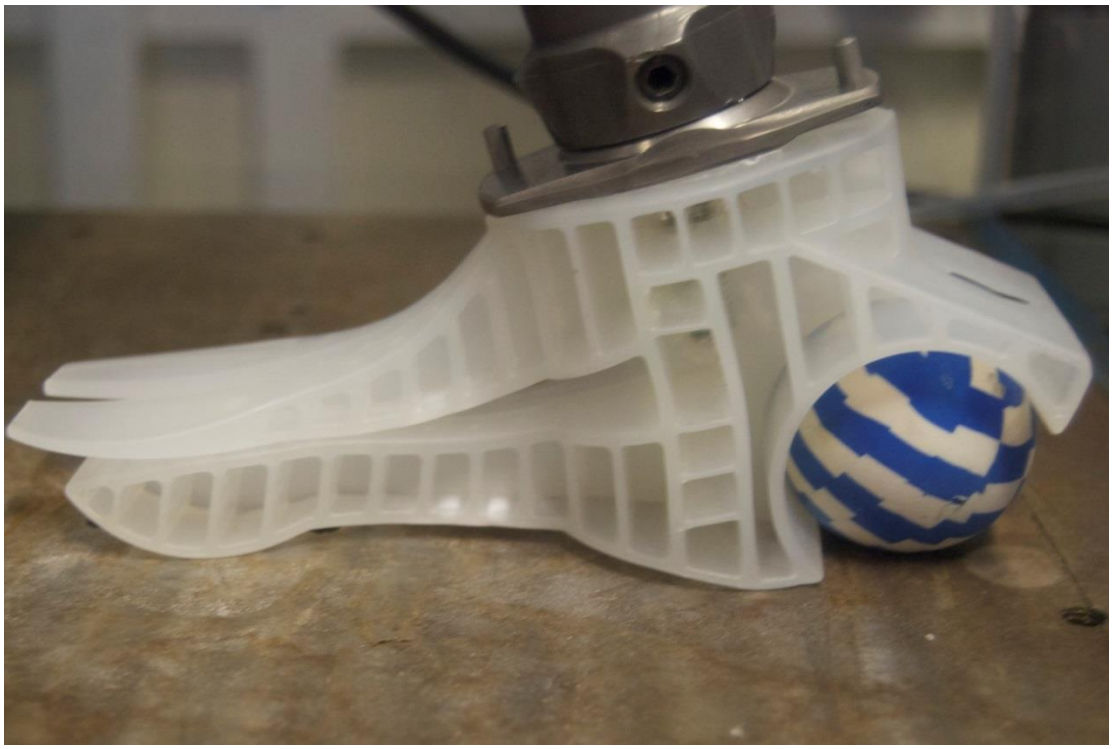

Figure 32 – Sample 1 of the Strathclyde foot at maximum P3 toe load demonstrating contact at front and rear

The first change of gradient was subtle however in unloading these two stages were much clearer. The slipping may be observed in Figure 33 or Figure 34 at 5-13mm compression on loading and at approximately 20 mm compression on unloading. The slipping was due to friction at the contact between the toe and the baseplate being overcome and could have been prevented with a low friction surface. Following the slip there will have been a change in magnitude and realignment of the stresses within the keel due to the relative change in alignment of force application. As the slip was able to occur at relatively low loading it was determined that the overall effect would be relatively minor and that the results were still valid.

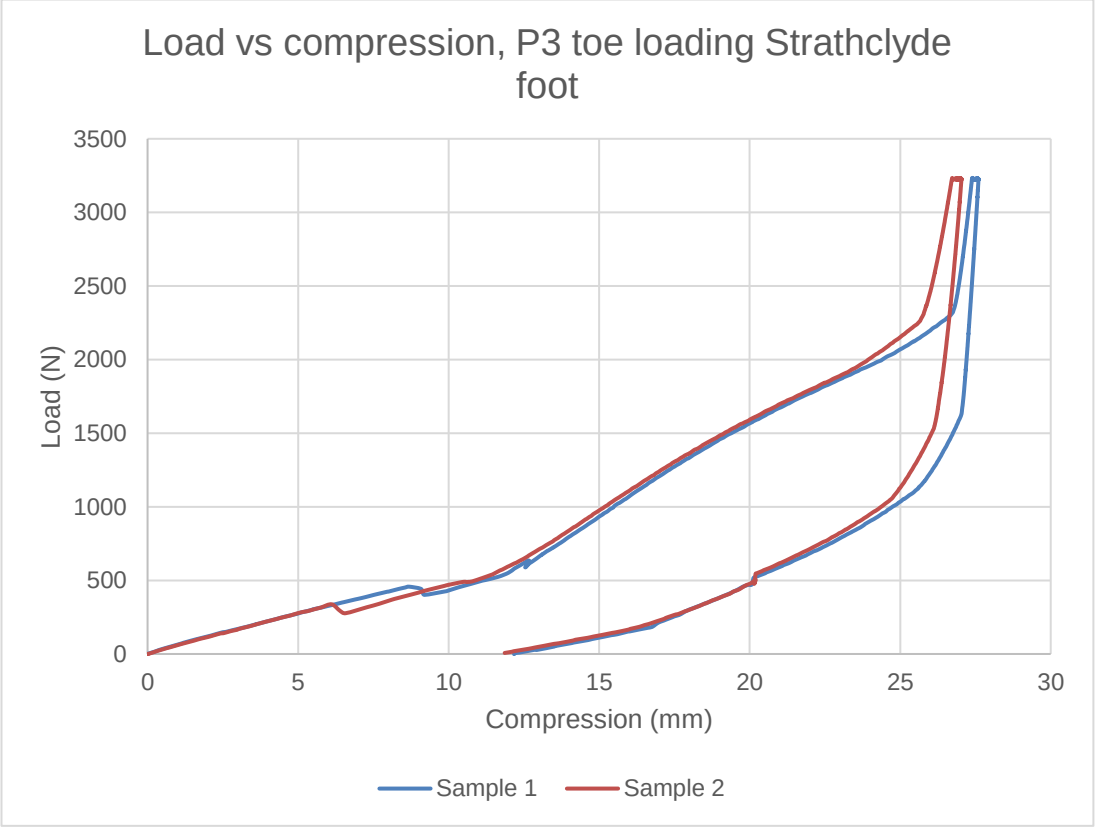

Figure 33 – A graph showing load vs. compression of samples 1 and 2 of the Strathclyde foot under P3 toe loading conditions

The energy input and return were determined using the following areas as defined: that loading concluded at the end of the hold phase with unloading began at

the first step following that and concluded when the load reached zero (see Figure 33). By applying the mid-ordinate rule to the values as defined some approximate values for energy input and return could be gained. This was done by taking the difference of two consecutive x values then multiplying by the mean of the corresponding y values to give the area of a rectangle approximating the area under the line. For example, taking two consecutive points during loading in sample 1, (1.154, 68.890) and (1.189,71.856) would give a difference of 0.035s for time and a mean of 70.373N for the force giving approximately 0.00246J of energy input. In this case for sample 1 there was a total input of 27.35J and a total return of 9.06J giving a loss of 18.29J. For sample 2 a total input of 26.79J was calculated and a total return of 8.96J giving a loss of 17.82J.

The samples were not checked for lasting deformation after being unloaded however at the completion of unloading there remained 12.2mm and 11.8mm of compression in samples 1 and 2 respectively.

Samples 3 and 4 included glass fibre rods to act as energy storage and return. The rod design was inherited from (L. E. Morton et al., 2009) but no reason was given for why a rod was used rather than another shape although it was mentioned that different rods could be used depending on the user so customisability appears to have been a factor. As two rods were to be used that would act independently this may also have been a consideration in choosing a rod based design. They were tested in an identical fashion to samples 1 and 2. Both samples were observed to deflect with the lower toe section coming into contact with the rods. The lower section and the rods then deflected together until contact was made with the upper section after which the sample broke. Failure occurred at approximately 2900N for sample 3 and 2800N for sample 4. The rods fractured and in the case of sample 1 the upper toe section also broke off. The test was automatically stopped at this

point. Figure 34 and Figure 35 below show the data captured up to fracture. Figure 36 shows sample 4 post-testing with the remains of the fractured rods in place within the keel while Figure 37 shows the broken toe section and rods in sample 3.

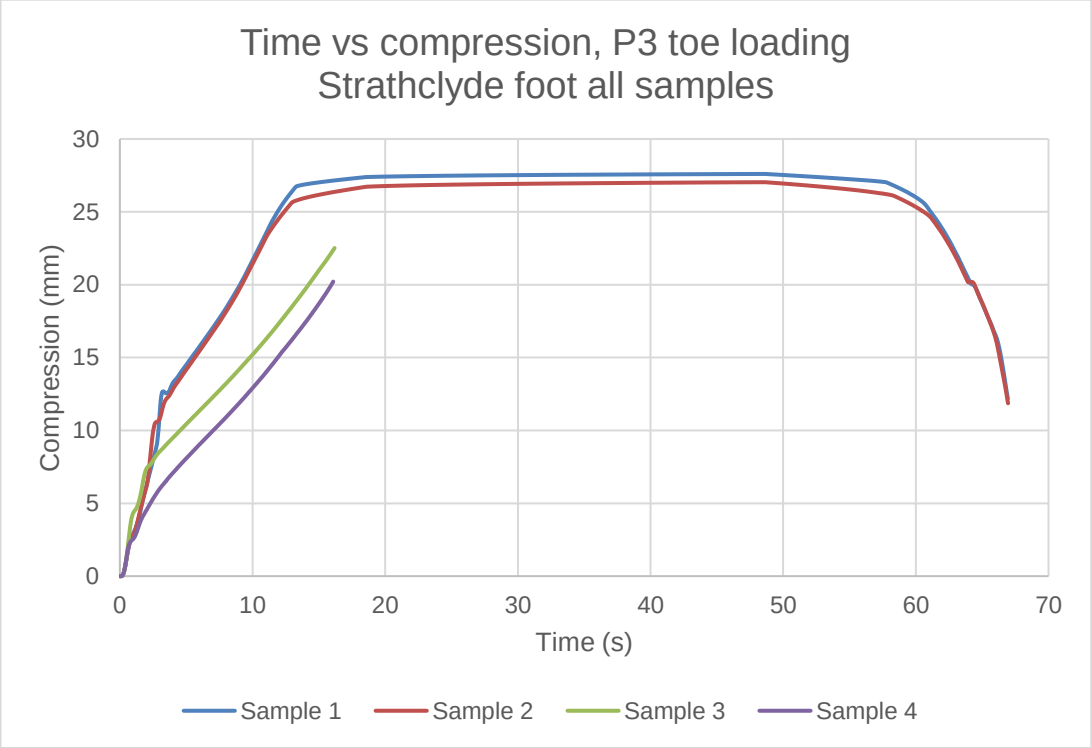

Figure 34 – A graph showing time vs. compression of all samples of the Strathclyde foot under P3 toe loading conditions

Figure 34 shows all samples of the Strathclyde foot having undergone P3 static load testing per ISO 10328. Samples 1 and 2 successfully completed testing but samples 3 and 4 failed at approximately 16.1s in each case. The change in gradient seen in samples 1 and 2 corresponded with the contact of the lower toe section to the upper toe section while in samples 3 and 4 the earlier change in gradient corresponded to the contact of the lower toe section to the glass fibre rods. In both cases the stiffness was increased however, once samples 3 and 4 reached approximately 16.1s both rods fractured, as did one section of the upper toe in sample 4 while samples 1 and 2 were able to continue the test to completion.

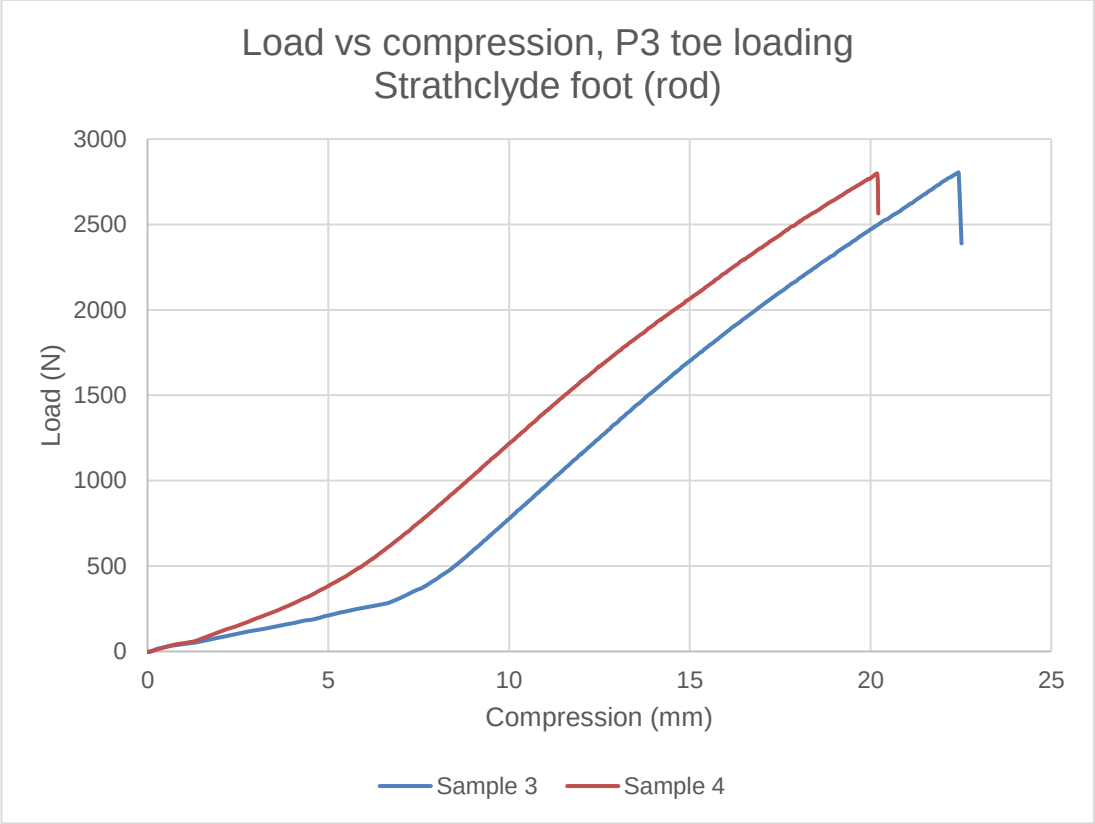

Figure 35 – A graph showing load vs. compression of samples 3 and 4 of the Strathclyde foot under P3 toe loading conditions prior to fracture

Figure 35 shows the loading of samples 3 and 4 until the rods fractured and the test was concluded. For the first millimetre of compression the samples showed a similar response however, sample 4 then became stiffer, sooner than sample 3 (at approximately 7mm). This change in stiffness corresponded to contact being made between the deformed lower toe sections and the glass fibre rods. The difference in deformation before contact was likely due to the production method as holes were manually drilled into the keel to accommodate the rods which introduced variation in manufacture. Within a single keel this can lead to rods contacting at different times which may explain why the change in stiffness observed in sample 3 (rods contacting separately) is less rapid than that of sample 4 (rods contacting together).

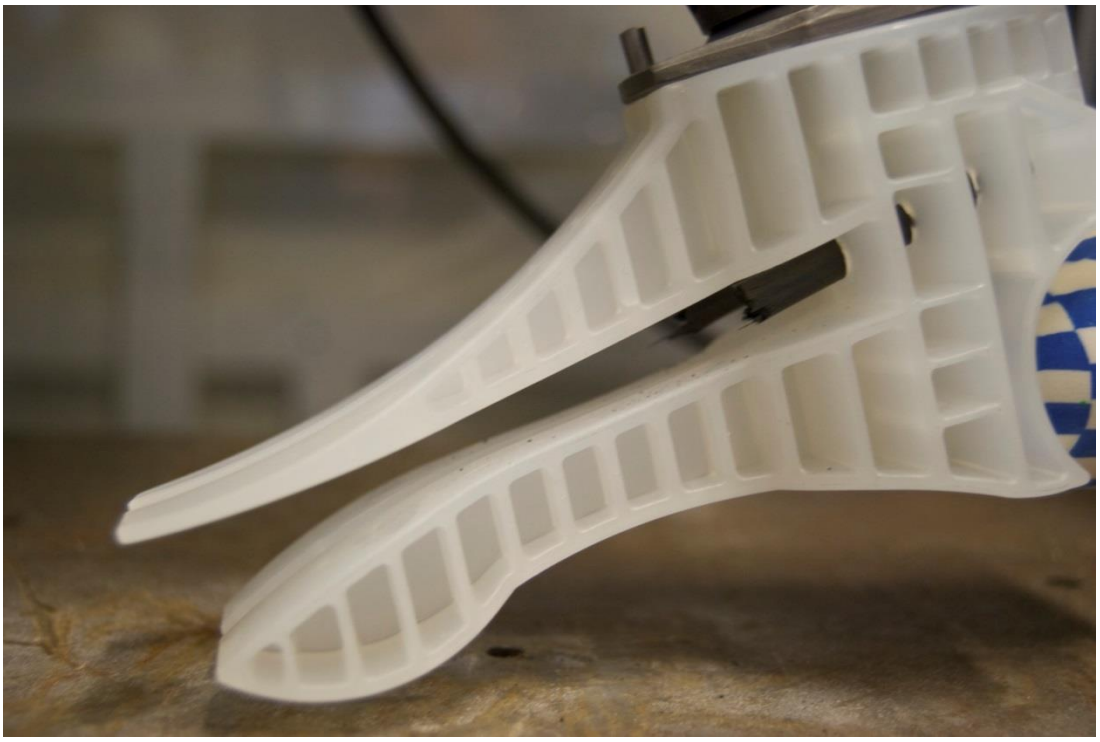

Figure 36 – An image of sample 4 following testing showing the fractured glass fibre rods

The rods in both samples broke in similar positions (see Figure 36 and Figure 37), being closer to the insertion contact point than the toe section contact. The failure itself showed more fibres extending from the underside of the rod which suggests a failure in tension on this part. Once a crack was formed it would rapidly propagate across the rod leading to failure.

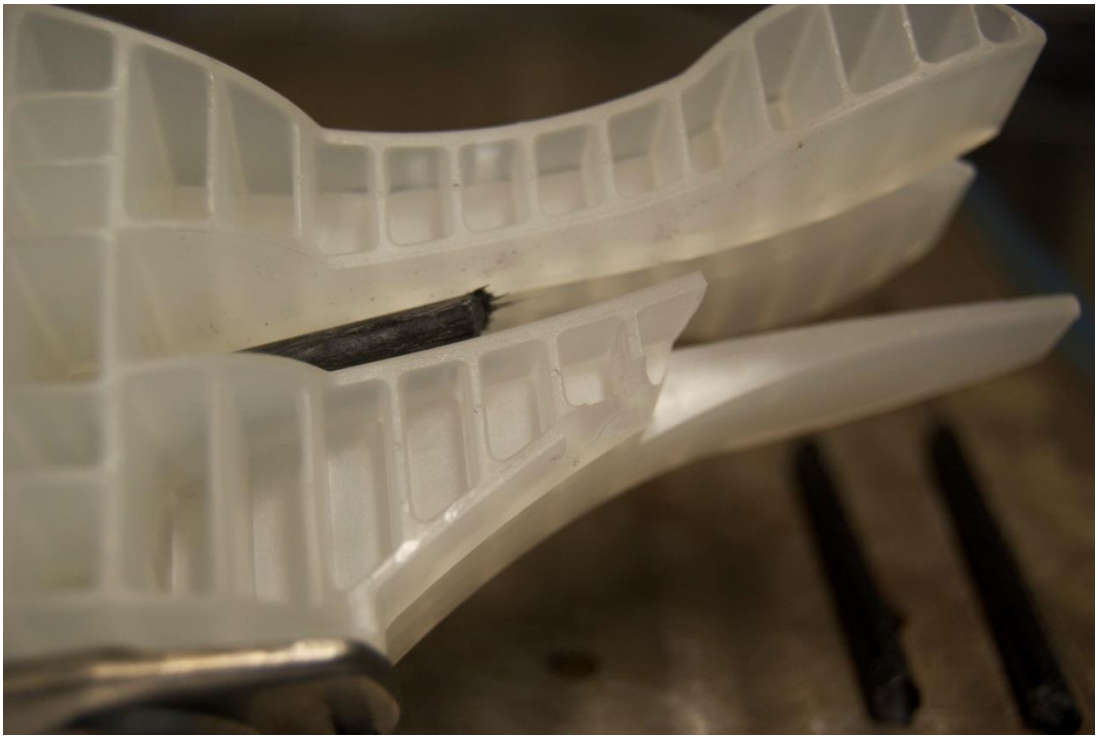

Figure 37 – An image of sample 3 showing the broken toe section and rods following P3 testing

The upper toe section of sample 3 failed approximately halfway along the toe section with part of the fracture extending posteriorly to the lateral side of the toe. The toe section fractured distally to the rod fracture site. As it was the only toe section of four to have failed during this testing it is possible that a weakness existed within the section from manufacture. Small air bubbles had been observed in some of the samples although nothing was specifically noted at this location.

3.3.2.4 Discussion

The hysteresis between loading and unloading in Figure 33 represented energy dissipated. This energy loss was due to internal friction and friction between sections (lower and upper toe on contact) which caused energy to be dissipated as heat, and deformation and creep occurring in the keel. In maintaining the maximum load for 30 seconds, per ISO 10328, there is creep in the keel which would have reduced the spring back of the material giving a reduced energy return. The 30

second hold would not be expected in normal gait, but could occur in daily use. Repeated longer holds on the toe section are possible in daily use and could potentially lead to creep occurring although the loads expected in normal daily use would be relatively low compared to the yield strength of the polypropylene which Vas & Bakonyi, 2012, show to have a smaller effect on material failure compared to higher loads. Testing at the P3 level, as occurred here, is intended to determine suitability of a prosthesis for use by a normal user (rather than highly active or sedentary) 60kg individual so to reach a maintained load of 3220N they would have to maintain an additional load of more than 2600N for an extended time. This occurrence would be considered unlikely and outside of normal use so cautioned against in user literature. Eftekhari & Fatemi, 2016, have shown that fatigue life of polypropylene samples was improved under loading between 0.1 – 2 Hz so with human walking gait occurring at just under 2Hz (David A Winter, 1984; David A Winter, Patla, Frank, & Walt, 1990) then it may have a positive effect on fatigue life of the keel.

The deformation within the keel is evidenced by the discolouration which occurred as shown in Figure 38. This discolouration is caused by the formation of micro voids or micro crazes within the material affecting the optical properties of the materials. The presence of such micro features, which can reach the surface and cause brittle failure, would lead to an expectation of reduced durability and potentially a reduced performance in further testing compared to an untested specimen. The micro crazes and voids will act as stress concentrators within the keel and could lead to greater deformation at lower loads than those observed during this test. The load at which the discolouration occurred is unknown, particularly due to the area not being readily visible during testing but may be worth attempting to identify in further testing.

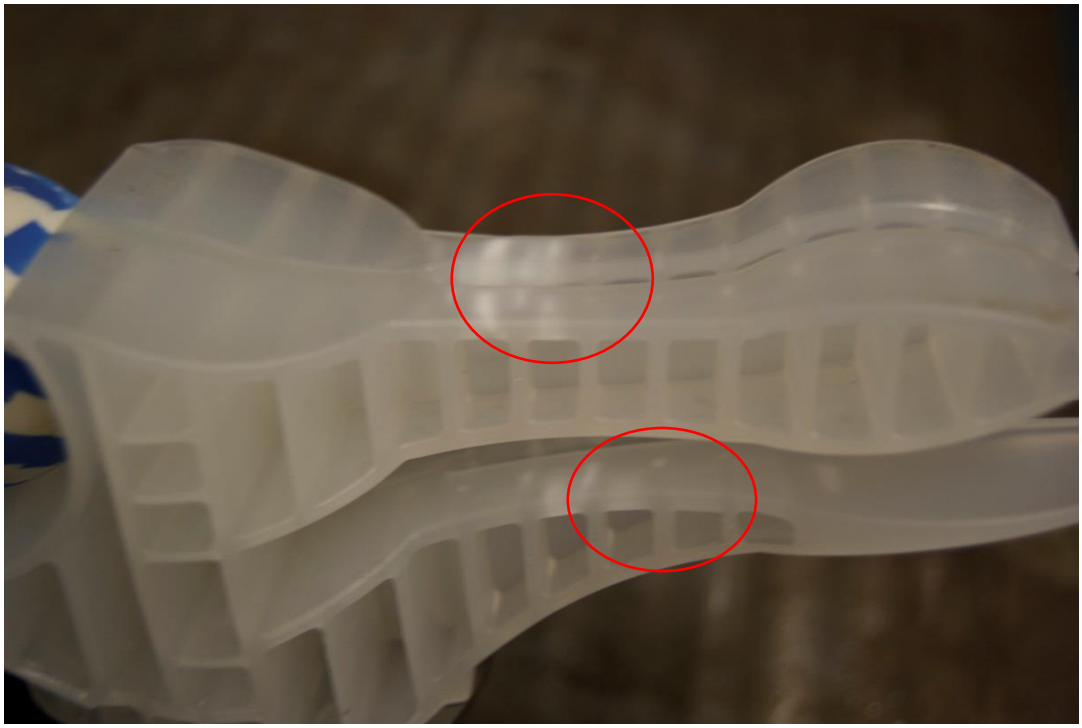

Figure 38 – An image showing the discolouration present on the underside of the toe sections (within red circles) in sample 1 following P3 testing

The approximate energy return for samples 1 and 2 was 34%. The maximum load was held for 30 seconds during which time the compression of the sample increased. This led to a greater difference between the compression observed during loading and unloading. Were the unloading to have happened sooner after the loading was completed, as in walking, a smaller energy loss may be expected to be observed. Due to the nature of this test the time the load is maintained cannot be reduced but it is significant, and recommended, for future testing as to the efficiency of energy return of the foot.

Samples 1 and 2 both survived with no damage observed excluding the discolouration seen on the underside of the lower toe section as in Figure 38. Given time the feet were deemed to have returned to their original shape although this was not measured.

Samples 3 and 4 included glass fibre rods which were to improve the energy storage and return properties of the foot however the glass fibre rods snapped and in the case of sample 3 also broke off the top section of the toes. The glass fibre rods were held in place through a series of holes drilled into the keel. If the rod were to have been fixed over a shorter length (while maintaining its total length) the effective flexible length would have been greater and would have led to a reduced stress within the rod over the same displacement and reduced the likelihood of failure at this point. The requirement to drill holes in the keel was also an undesirable additional manufacturing step. This was considered a flaw in the design and was addressed in later design work.

The P3 level of ISO 10328 required a minimum load of 2415N be reached to be considered a pass which samples 3 and 4 met, failing at 2804N and 2822N respectively. This was approximately 87% of the P3 ultimate static upper load level. To satisfy the P4 static proof load level the feet would be required to reach a minimum of 3098N (they reached approximately 91% of this value) and for the P5 static proof load level, 3360N (they reached approximately (84% of this value). The catastrophic nature of the failure is inappropriate for a prosthetic limb as during normal use such a failure could lead to injury to the wearer whereas in a plastic failure there is a better opportunity for the user to respond to prevent further damage to the prosthesis and injury to themselves.

The specimens tested outperformed the expectations of the FEA modelling (detailed in Appendix B – Finite Element Analysis of foot designs). FEA predicted failure at several different areas prior to the proof load of 805N being met however samples 1 and 2 survived to 3220N. In either case stress whitening occurred at an area identified during FEA as areas 3 and 5 (see section B2.3 Results). This would

suggest that the properties used in the FEA were not adequate to represent the polypropylene used.

3.3.2.5 Conclusion

The Strathclyde foot passed the P3 ultimate static loading requirements for the toe condition. In static loading, there was no requirement that the heel not contact a support as there is in cyclic testing. Testing continued to the P3 level for the heel. Further design was required to ensure proper integration of energy storage and return features to the foot system.

3.3.3 P3 testing – heel

3.3.3.1 Specimens

The feet used in the P3 toe testing were examined for signs of damage or permanent deformation and were observed to have suffered some deformation as evidenced by whitening of the material on the underside of the toe sections. The toes were not expected to contact the baseplate during this test and so further deformation of the toes was not expected. As such it was decided that P3 heel testing could be pursued using the same samples used in P3 toe testing.

3.3.3.2 Method

The adapter was set so that the heel would contact the baseplate at 15° with the load increasing at 175N/s until the upper load of 2240N was reached. This load was to be held for 30 seconds before being reduced at a rate of 175N/s until zero loading was achieved.

3.3.3.3 Results

The samples were loaded at the prescribed 175N/s with no signs of breakage or slippage. In both cases the ball was observed to deform under loading until the

keel came in contact with the steel base plate as seen in Figure 39. The contact occurred at around 11.8mm compression in either sample and may be observed in Figure 40 or Figure 41 by the sharp change in gradient as the system becomes stiffer and a significant reduction in deformation is seen afterwards. The static load was maintained for 30 seconds during which 0.2mm of creep occurred in sample 1 and 0.24mm of creep occurred in sample 2 as shown in Figure 40. During unloading the removal of contact from the keels was seen by the change in gradient at 12mm compression, although this was less clear in sample 2.

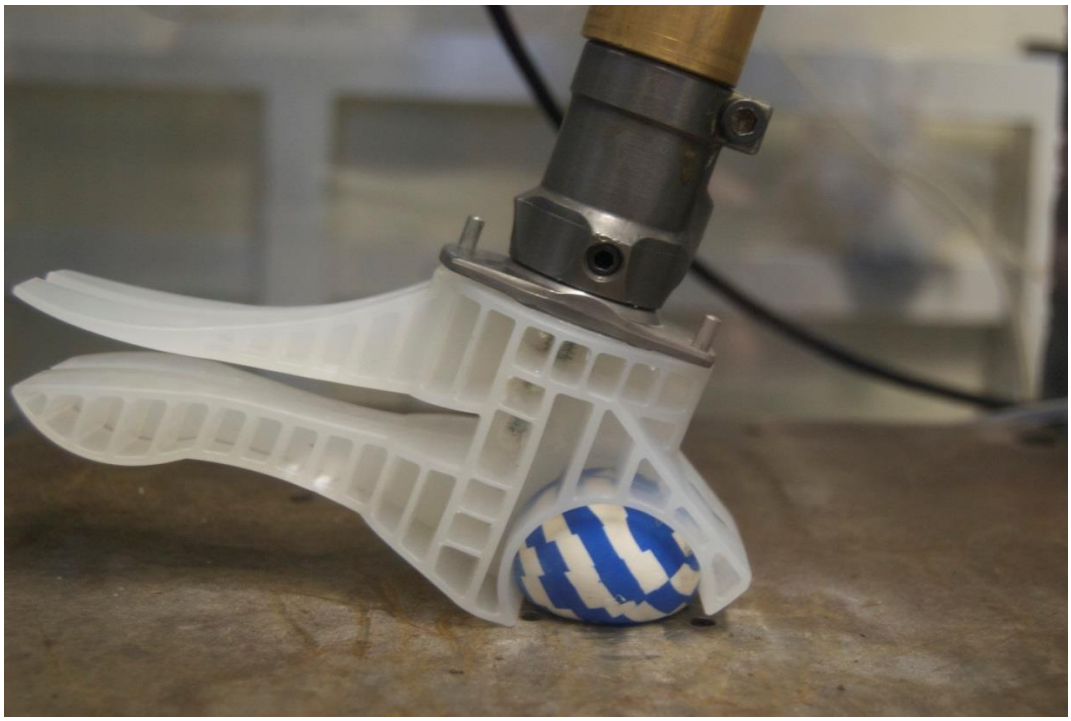

Figure 39 – An image showing sample 2 under maximum P3 heel loading showing contact of keel and baseplate

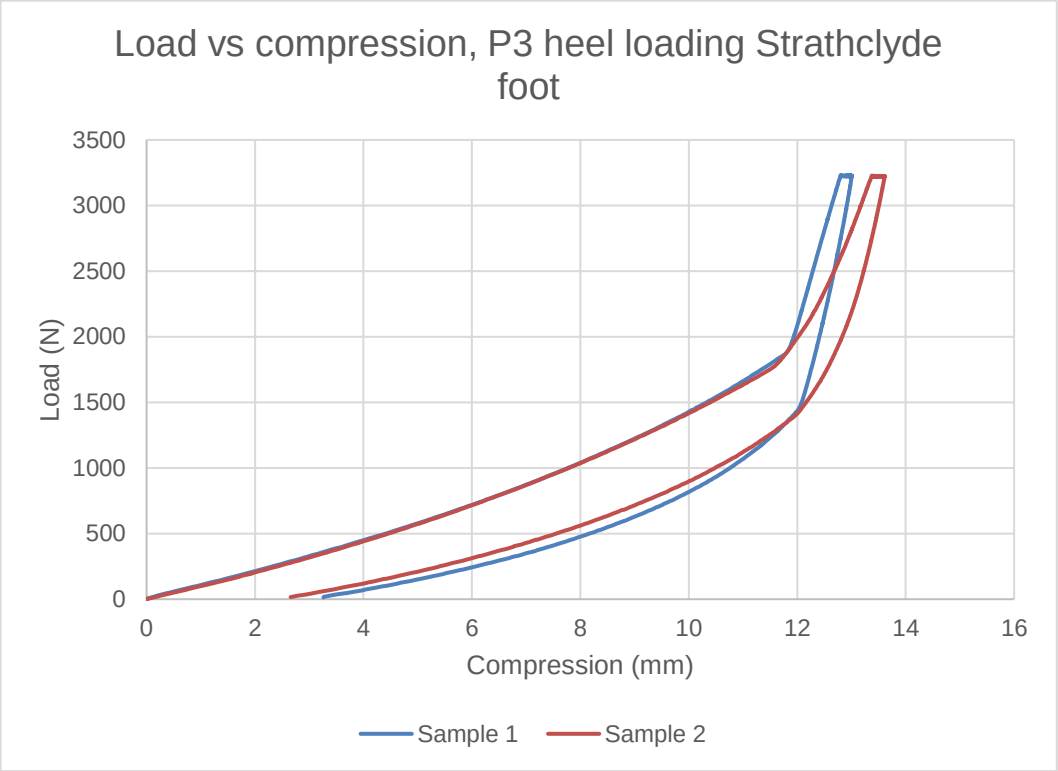

Figure 40 – Load vs. compression results of Strathclyde foot under P3 heel testing

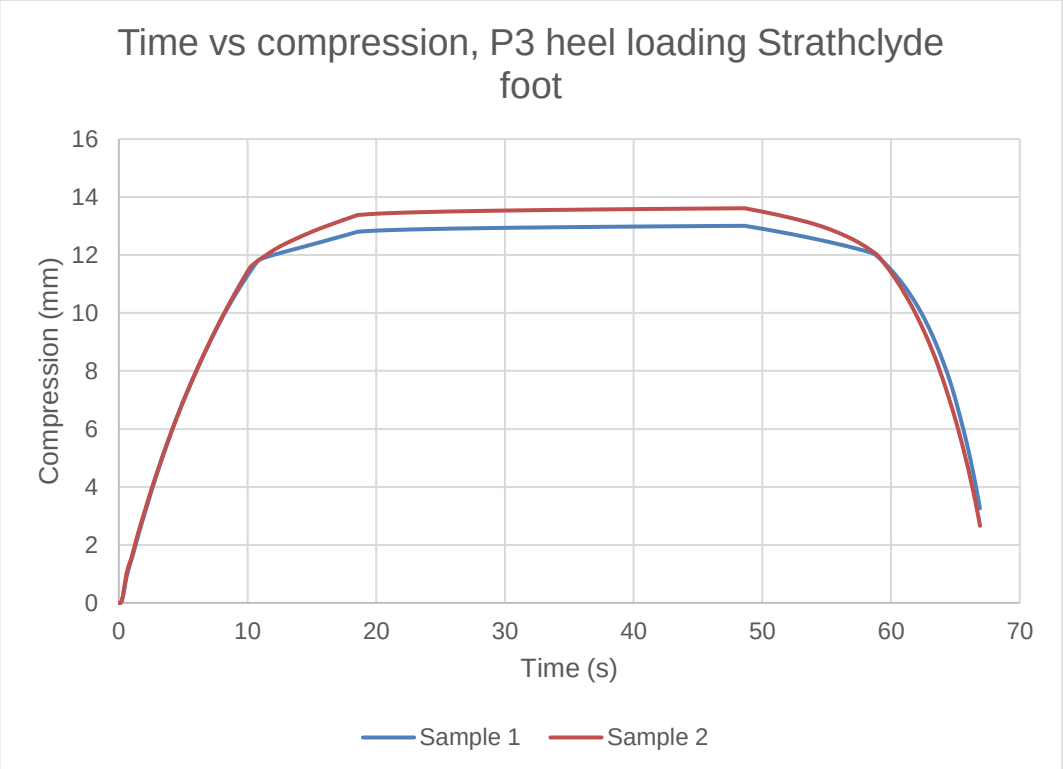

Figure 41 – Time vs. compression graph of Strathclyde foot under P3 heel testing

Hysteresis was observed in Figure 40 in both samples due to some heat dissipation and creep occurring during testing. This creep was not observed for recovery post testing and the extent of recovery was unknown but is recommended for investigation in further testing. By using the mid-ordinate rule, as previously described, approximate values for the energy put into and returned from the system can be calculated. The lower limit for the loading phase was taken from the final compression of the unloading phase; the upper limit was the last value prior to unloading. The unloading phase was taken from the first value after the end of loading and continued until the load had reduced to zero. Sample 1 had an energy input of 12.31J and an output of 6.66J giving a loss of 5.65J while sample 2 had an input of 13.71J and an output of 8.43J giving a loss of 5.28J.

3.3.3.4 Discussion

The two feet both survived with no further damage or obvious permanent deformation, although the final deflection during testing, approximately 3mm in either case, was not re-examined post testing and may have persisted. During testing the balls both deformed to the point where the keel was directly in contact with the baseplate however this contact occurred at different loads despite the balls being visually identical (approximately 1890N for sample 1 and 1790N for sample 2). This is potentially due to differences internally produced during manufacture. The consistency of the balls should have been checked, but was not. The nature of balls used in testing is considered to be an important point of investigation in further work. For manufacture a more consistent ball for use in the prosthesis would be required, possibly a polyurethane elastomer and this should be checked as a part of internal quality control however, the existing stock of balls was used for all further testing.

The energy dissipation was beneficial in the heel section of the foot as the intention of the rubber ball in the heel was to provide shock absorption through

energy dissipation and to provide a softer feel during rollover. The loading conditions were not representative of walking and cannot be used to characterise the behaviour of the foot under real world conditions however, shock loading tests would be recommended to characterise this performance. There is no consideration for shock loading in ISO 10328, but it is noted that other tests should be carried out to assess the suitability of a prosthesis for use. The fairly high level of energy return after the 30 second hold (54% for sample 1, 62% for sample 2) is positive as the combination of the ball, which would have a high energy return ratio, and the keel still gives a high return under these conditions. The difference in energy input to the feet was likely to represent the stiffness of the system with greater energy being required in the stiffer system, in this case sample 1.

3.3.3.5 Conclusion

The Strathclyde foot samples tested passed the P3 ultimate static loading requirements for the heel condition. As the P3 ultimate static loading level was met for both the heel and the toe of the foot, in samples without reinforcing rods, further testing was to occur to the P4 level. No further testing was to be carried out on samples with reinforcing rods present.

3.3.4 P4 testing – toe

3.3.4.1 Specimens

The feet previously used in the P3 testing were examined for signs of damage or permanent deformation and were observed to have suffered some stress whitening on the underside of the toe sections, indicating that permanent deformation had occurred. ISO 10328 allows for test samples to be reused if they have passed the prior testing (except for use in cyclic testing if they have previously been subjected to static ultimate strength tests). These samples were deemed to

have passed both toe testing and heel testing at the P3 level and as such it was decided that P4 toe testing could be pursued using the same samples. As samples 3 and 4, which had included glass fibre rods, failed they were not included in any further testing.

3.3.4.2 Method

The method was as described for P3 toe testing (3.3.2.2 Method) however the upper load was increased to 4130N in line with P4 requirements.

3.3.4.3 Results

The ultimate static test force for the P4 level was applied in each case. Slipping was again observed in both samples however, as the foot settled loading continued. The slipping on loading may be observed between 4 and 9mm compression in Figure 42. The lower section of the foot was then observed to deflect into the upper toe sections and then the heel contacted the baseplate in the two contact stages as previously observed (see Figure 43). The first change of gradient is visible at 9mm compression for both samples with the second change of gradient occurring at 22mm compression for sample 1 and 21mm compression for sample 2. On unloading a single change of gradient is clear but a second change was not easily discernible. Slipping during unload was seen between 16 and 11mm compression in Figure 42 or Figure 44.

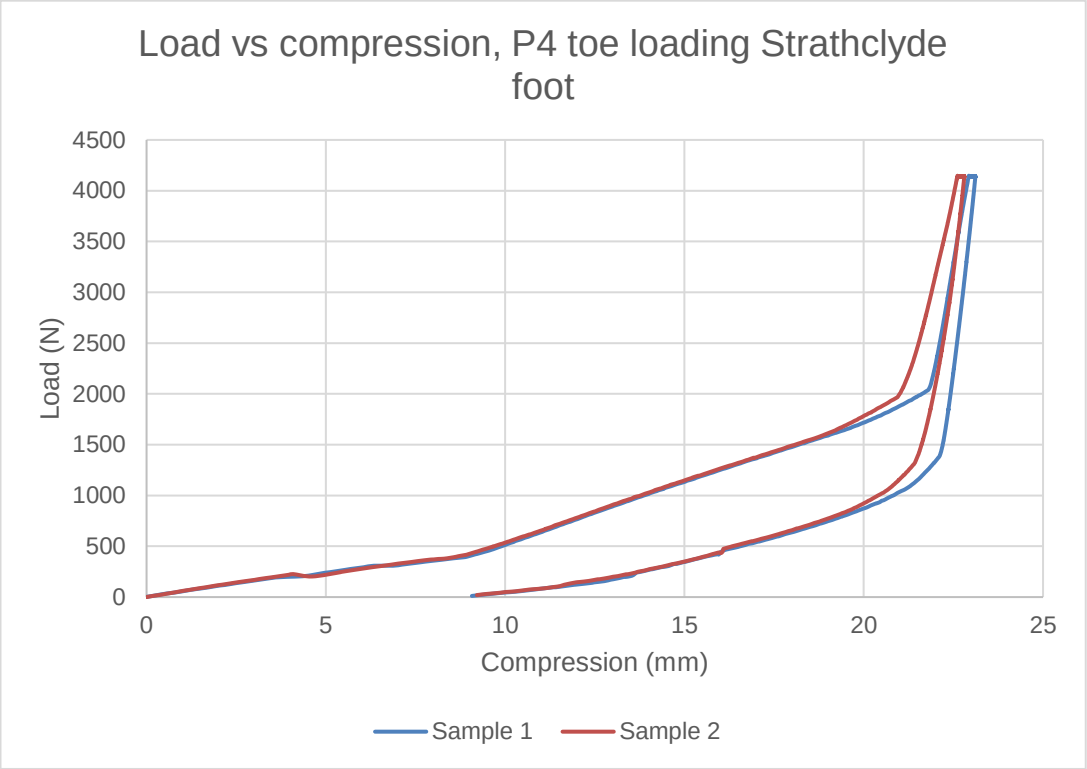

Figure 42 – A graph showing load vs. compression of samples 1 and 2 of the Strathclyde foot under P4 toe loading conditions

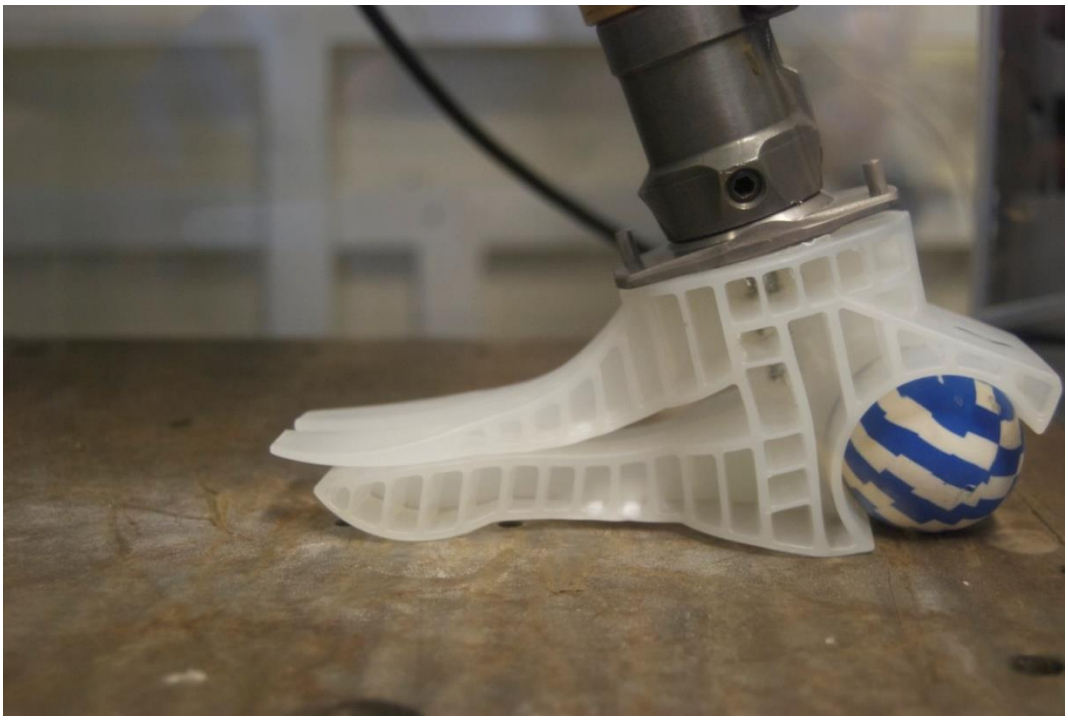

Figure 43 – An image showing sample 1 of the Strathclyde foot under maximum P4 toe loading

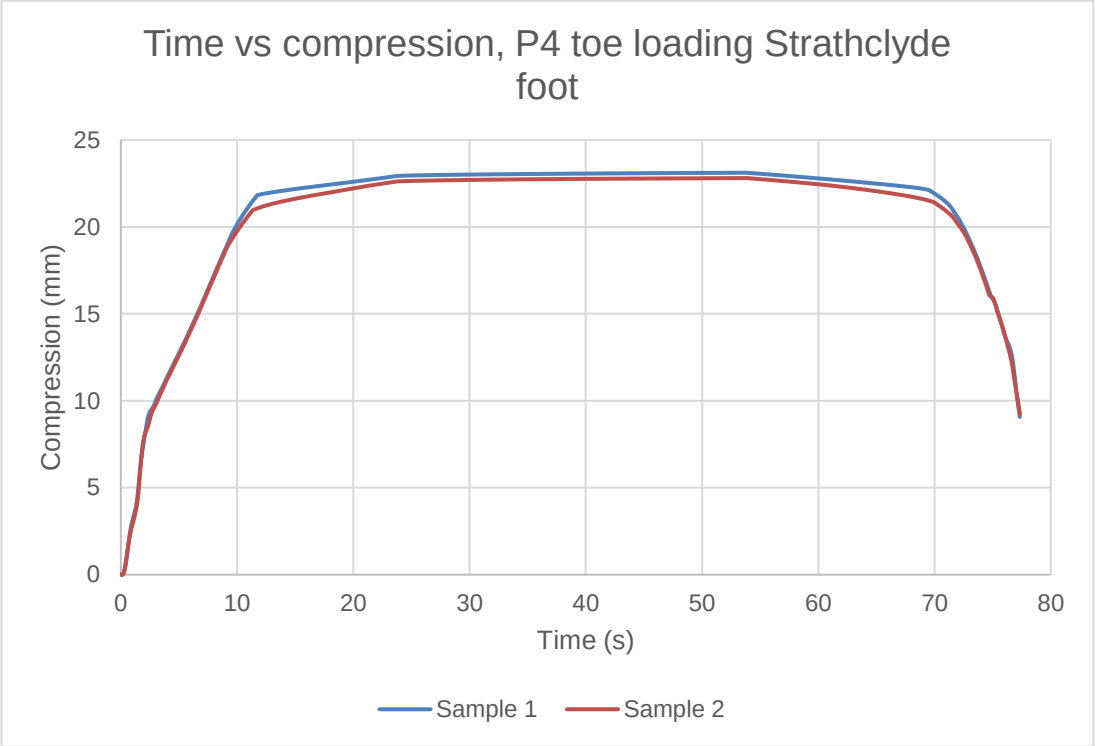

Figure 44 – A graph showing time vs. compression of samples 1 and 2 of the Strathclyde foot under P4 toe loading conditions

Creep was observed at maximum load of 0.18mm in sample 1 and 0.19mm in sample 2. Deformation was present at the end of testing, 9.1mm and 9.2mm respectively in samples 1 and 2.

By applying the mid-ordinate rule to the values as defined some approximate values for energy input and return were gained. In this case for sample 1 the input was 21.04J and a return of 8.61J giving a loss of 12.43J. For sample 2 an input of 21.15J was found and a return of 8.83J giving a loss of 12.32J.

3.3.4.4 Discussion

The approximate energy return for samples 1 and 2 was 41% and 42% respectively. When compared to the P3 results a lower energy input into the system was seen, 27.07J average at the P3 level but only 21.09J at the P4 level. A similar absolute energy return is observed, 9.01J at the P3 level and 8.72J at the P4 level.

As a result, the energy return was a larger percentage of input at P4 than at P3 (33% in each sample at P3). The system appeared stiffer, likely because of P3 testing causing lasting deformation. Compared to the results of P3 testing the samples were observed to have reached heel contact at approximately 21.8mm (sample 1) and 21.0mm (sample 2) which was 4.9mm and 4.7mm sooner, respectively, than in P3 testing of the same samples. This suggested that deformation persisted in the samples after testing however, this was not as large as the values at the end of P3 testing, 12.2mm and 11.8mm respectively, which indicated partial recovery between tests. Given the 9.1mm and 9.2mm deformation at the end of testing in samples 1 and 2 there was expected to be further permanent deformation within the keels although the amount was undetermined.

In Figure 43 it was seen at the rear of the pyramid adapter and foot interface that there was a gap. This suggested rotation had occurred about the contact point and will have added to the deformation recorded. On conclusion of testing no deformation of the threaded rod was observed nor damage from the rod to the keel. Some damage was observed on the front of top surface of the keel where it contacted the pyramid adapter. Two tracks had been pressed into the top surface leading to some of the rotation and deformation observed.

Samples 1 and 2 both survived with increased discolouration visible on the underside of the lower toe section and the damage to the top surface. The samples had likely retained deformation from this testing as they did from P3 testing, even given time to rest between tests.

3.3.4.5 Conclusion

ISO 10328 does not specify what constitutes failure of a sample. The permanent deformation may be considered to qualify as failure however, as the keels remained functional it was decided to continue testing using these samples.

The samples had previously undergone permanent deformation from the P3 level and were able to sustain the maximum loading of the P4 level under toe conditions. Testing continued to the P4 level for the heel condition and if successfully completed then could proceed to testing at the P5 level.

3.3.5 P4 testing – heel

3.3.5.1 Specimens

Samples 1 and 2 from P3 testing and P4 toe testing were inspected for damage or deformation and found to have whitening on the toe sections demonstrating some permanent deformation. The toe section of the keel was unlikely to contact the baseplate during and as such they were used again in heel testing at the P4 level.

3.3.5.2 Method

The sample was prepared and treated in the same manner as described in section 3.3.3.2 Method with the upper load being increased to 4130N to reflect the P4 loading requirement.

3.3.5.3 Results

The samples were loaded at the prescribed 175N/s with no signs of breakage or slippage by the upper limit of 4130N. In both case the ball was observed to deform under loading until the keel contacted the steel base plate (Figure 45). The contact occurred at around 12.1mm compression in sample 1 and 10.3mm compression in sample 2, observable in Figure 46 or Figure 47 by the sharp change in gradient as the system becomes stiffer. The static load was maintained for 30 seconds during which the Instron recorded 0.39mm of creep in sample 1 and 0.43mm of creep in sample 2 as shown in Figure 46. During unloading the removal of contact from the keels may be seen by the change in gradient at 12.6mm

compression for sample 1 and 10.8mm compression in sample 2, although this was less clear in sample 2.

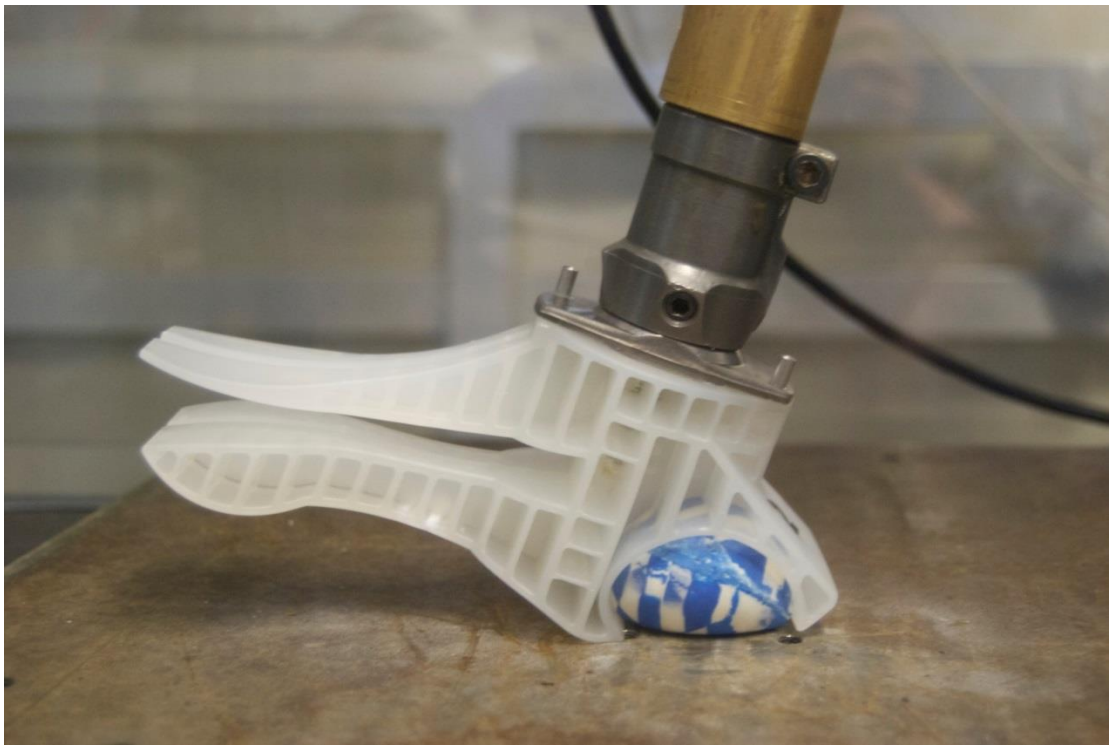

Figure 45 – An image showing sample 2 of the Strathclyde foot under maximum P4 heel loading

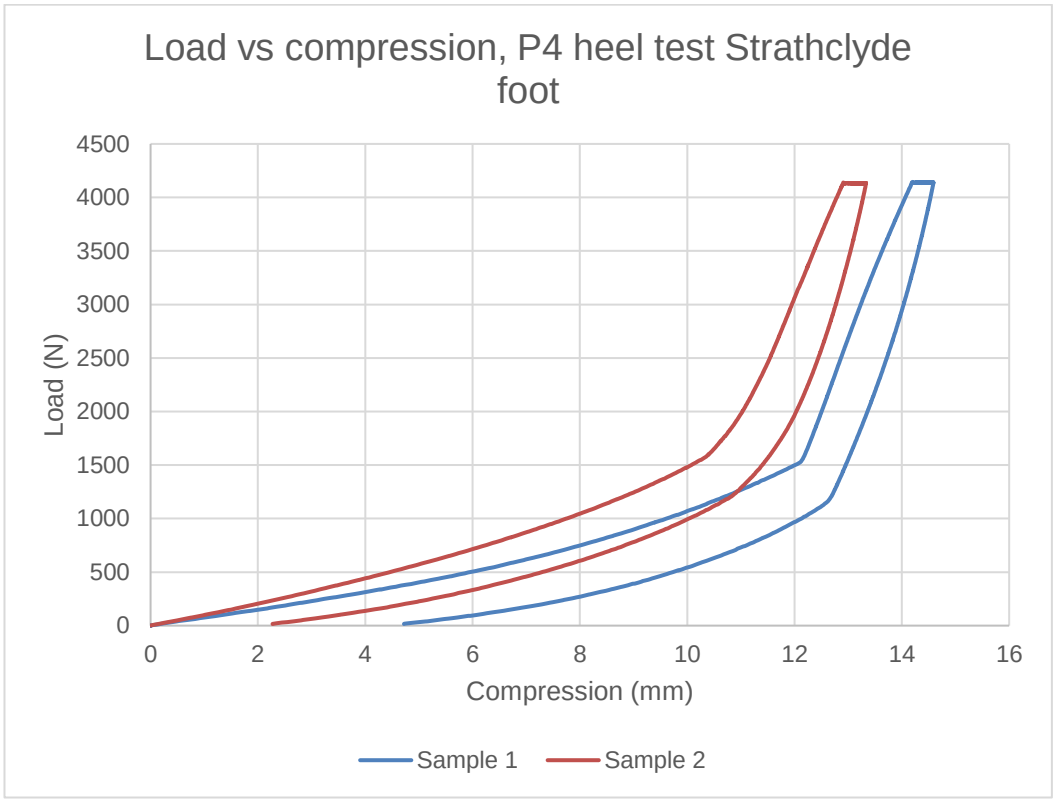

Figure 46 – Load vs. compression results of Strathclyde foot under P4 heel testing

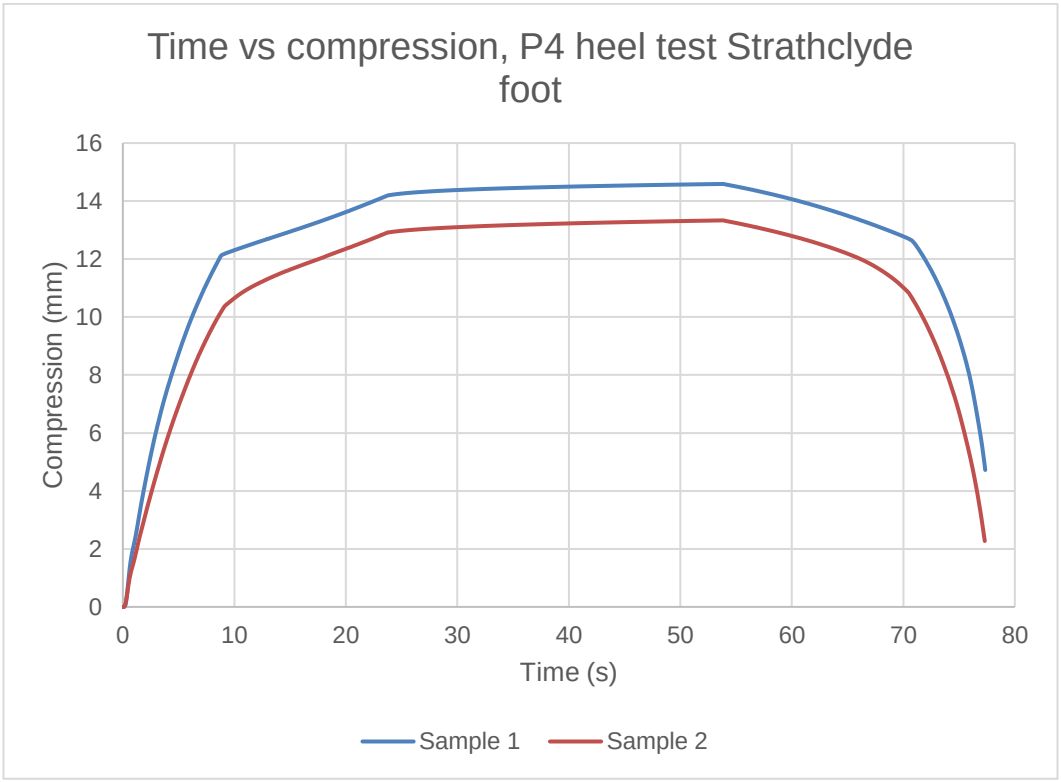

Figure 47 – Time vs. compression graph of Strathclyde foot under P4 heel testing

Using the same method as described previously in section 3.3.2.3 Results, energy in the system was calculated. Sample 1 had an energy input of 14.77J and an output of 8.13J giving a loss of 6.64J while sample 2 had an input of 15.42J and an output of 9.66J giving a loss of 5.77J.

3.3.5.4 Discussion

During testing the balls both deformed to the point where the keel was directly in contact with the baseplate however this contact occurred at different loads for each sample, approximately 1570N for sample 1 and 1530N for sample 2. The same balls were used as in testing to the P3 level. The loads required here for contact were lower than in P3 testing (by 320N and 260N respectively – see Figure 48) which indicated that the balls were less stiff during P4 testing. The compression at keel contact for sample 1 during P4 testing was greater than during P3 testing (12.04mm compared to 11.81mm) but in sample 2 the compression in P4 was less than during P3 testing (10.26mm compared to 11.64mm). When combined with the reduced loads to keel contact this gave two different explanations for the samples' performances. The ball in sample 1 appeared to be less stiff during this test and the distance to keel contact increased, perhaps due to deformation remaining in the keel or the ball from P3 testing. In sample 2 however, keel contact occured at a slightly higher force but a reduced compression potentially indicating a stiffer but deformed ball after P3 testing.

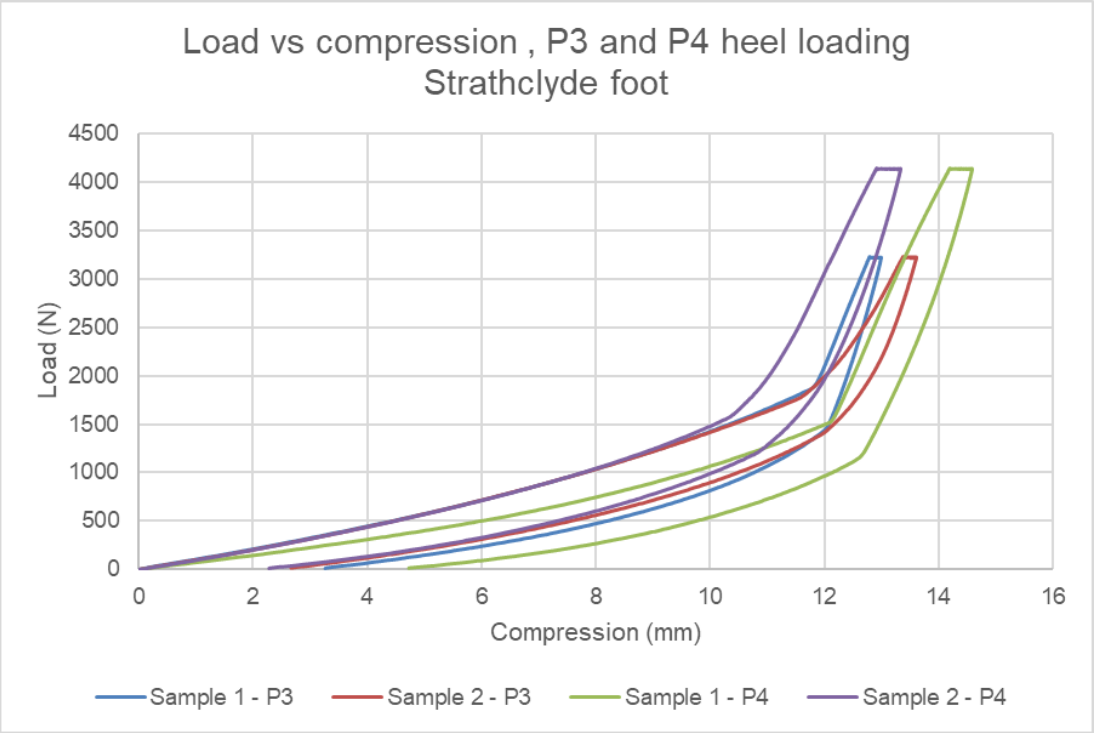

Figure 48 - Comparison of samples 1 and 2 under P3 and P4 ultimate static heel loading

While increased temperature of a rubber can cause a reduction in modulus of elasticity the fact that the balls were kept together between tests and performed so differently ruled out an environmental effect causing the change in properties.

With the same caveat regarding the sustained upper load affecting the energy return, the energy return of the feet was 55% for sample 1 and 63% for sample 2. This was very similar to the results from the P3 level (54% and 62% respectively).

The two feet both survived without observable damage to the keel or ball although given the results observed there was the possibility of lasting deformation from P3 testing. Further deformation due to P4 testing may not be ruled out although not observed directly.

3.3.5.5 Conclusion

The Strathclyde foot was considered to have passed the ultimate static loading condition in the heel condition of the P4 level. As the toe condition of P4 level has already been passed testing should continue to the P5 level.

3.3.6 P5 testing – toe

3.3.6.1 Specimens

The feet previously used in the P3 and P4 testing were examined for signs of damage or permanent deformation and were observed to have stress whitening on the underside of each toe section. 9.1mm and 9.2mm of deformation remained in samples 1 and 2 respectively at the conclusion of P4 testing however, the remaining permanent deformation was expected to be much lower. As such it was decided that P5 toe testing could be pursued using the same samples as even failure would have provided insight into the performance of the setup following previous high loading.

3.3.6.2 Method

The method was as described for P3 toe testing (3.3.2.2 Method) however, the load was increased to 4480N in line with P5 requirements.

3.3.6.3 Results

The ultimate static test force for the P5 level was applied in each case. Slipping was observed in both samples however, as the foot settled loading continued. The slipping on loading may be observed between 1.5 and 9mm compression in Figure 49. The lower section of the foot was then observed to deflect into the upper toe sections in the two contact stages as previously observed. The foot then continued to deflect until the ball at the rear of the foot and subsequently the keel at the rear of the foot contacted the baseplate (Figure 50). The first change of gradient was visible at 9mm compression for both samples with the second change of gradient

representing heel contact occurring at 22mm compression for sample 1 and 21mm compression for sample 2. On unloading a single change of gradient was visible at approximately 2.05mm compression in either sample but a second change was not easily discernible. Slipping during unload was seen between 16 and 11mm compression as in Figure 49 or Figure 51.

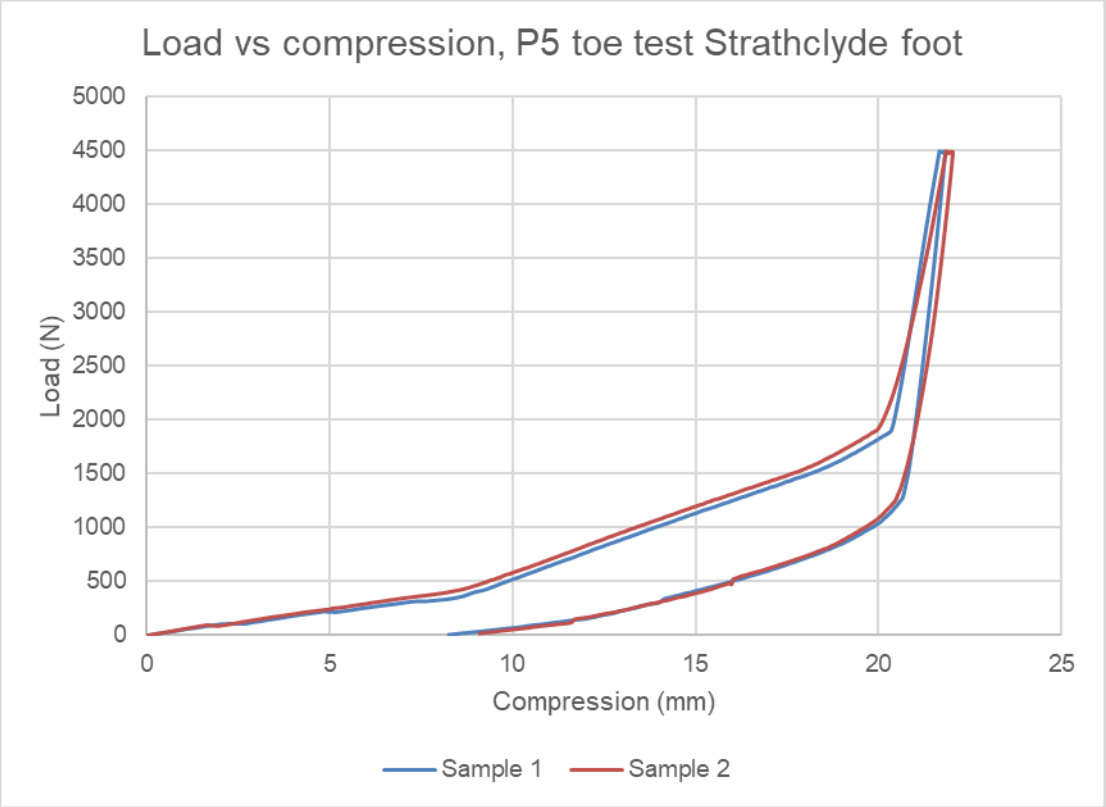

Figure 49 – A graph showing load vs. compression of samples 1 and 2 of the Strathclyde foot under P5 toe loading conditions

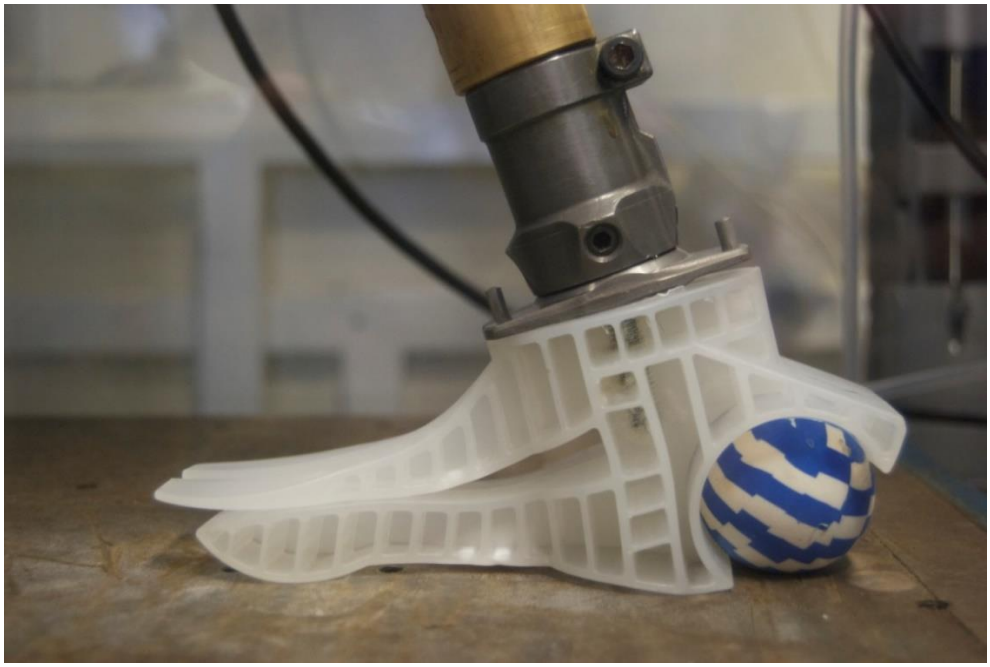

Figure 50 – An image showing sample 1 of the Strathclyde foot under maximum P5 toe loading

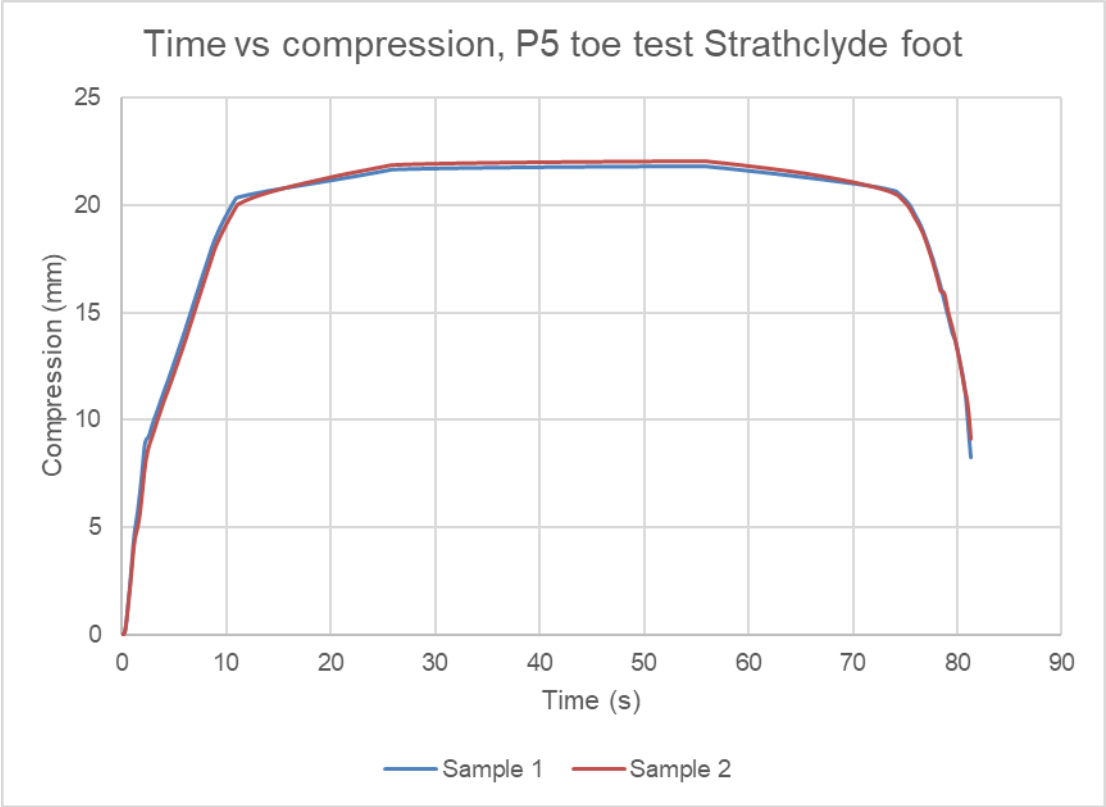

Figure 51 – A graph showing time vs. compression of samples 1 and 2 of the Strathclyde foot under P5 toe loading conditions

By applying the mid-ordinate rule to the values as defined some approximate values for energy input and return could be calculated. In this case for sample 1 the input was 9.48J and a return of 4.25J giving a loss of 5.23J. For sample 2 an input of 10.37J was found and a return of 4.54J giving a loss of 5.83J.

3.3.6.4 Discussion

The approximate energy return for samples 1 and 2 was 44% and 43% respectively. This was greater than both P3 testing (33% in each) and P4 testing (41% and 42% respectively). This increased energy return was likely to be as a result of the increased stiffness causing a slightly smaller final compression to occur in P5 testing compared to P4 testing (1.28mm and 0.77mm less for sample 1 and sample 2 respectively). The increased stiffness may be an effect of permanent deformation remaining in the system, reducing the deformation required before the heel section of the keel contacts the baseplate. The majority of increased resistance from the heel is as a result of the keel contacting the baseplate. The extent of permanent deformation in the heel section of the keel caused during heel testing was unknown as the keel may not return as readily as the ball and so the final deformation cannot provide an effective measure of keel deformation.

Both samples showed reduced compression at each increased level of loading with the greater decrease occurring between P3 and P4 testing (4.49mm and 4.23mm respectively, see Figure 52 and Figure 53) rather than between P4 and P5 testing (1.28mm and 0.77mm respectively).

Contact between the lower toe section and the upper toe section occurred at approximately 8.5mm at the P4 and P5 level of testing on sample 1 and 8.8mm for sample 2. In P3 testing both samples slipped slightly, at 8.7mm in sample 1 and 6.1mm in sample 2 but contact between lower and upper toe sections occurred at 11.1mm and 10.6mm respectively. This suggested a permanent deformation of the

lower toe section of approximately 2.6mm in sample 1 and 1.9mm in sample 2 in the loading axis. This permanent deformation appeared to change by less than 0.5mm between P4 and P5 loading in either sample which suggested the effect of heel contact prevents, or greatly reduces, further deformation of the toe section. This was a good design feature as under extreme loading the load would be distributed away from the toe section and may prevent failure of the toe section.

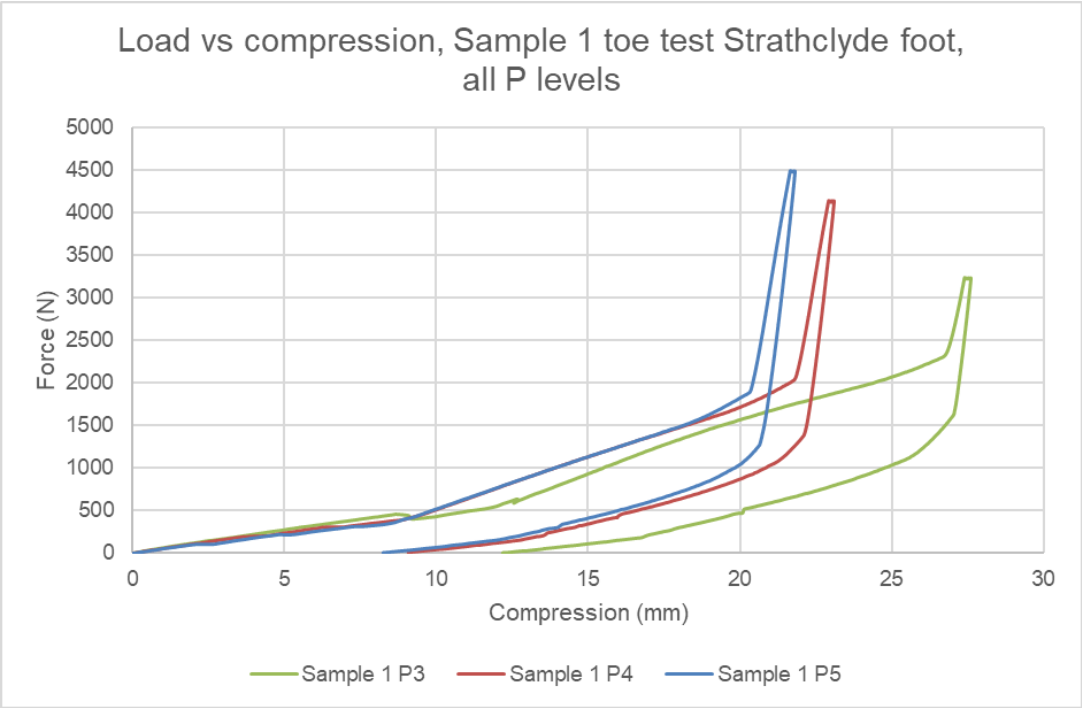

Figure 52 – Load vs. compression at all P testing levels of Strathclyde foot sample 1

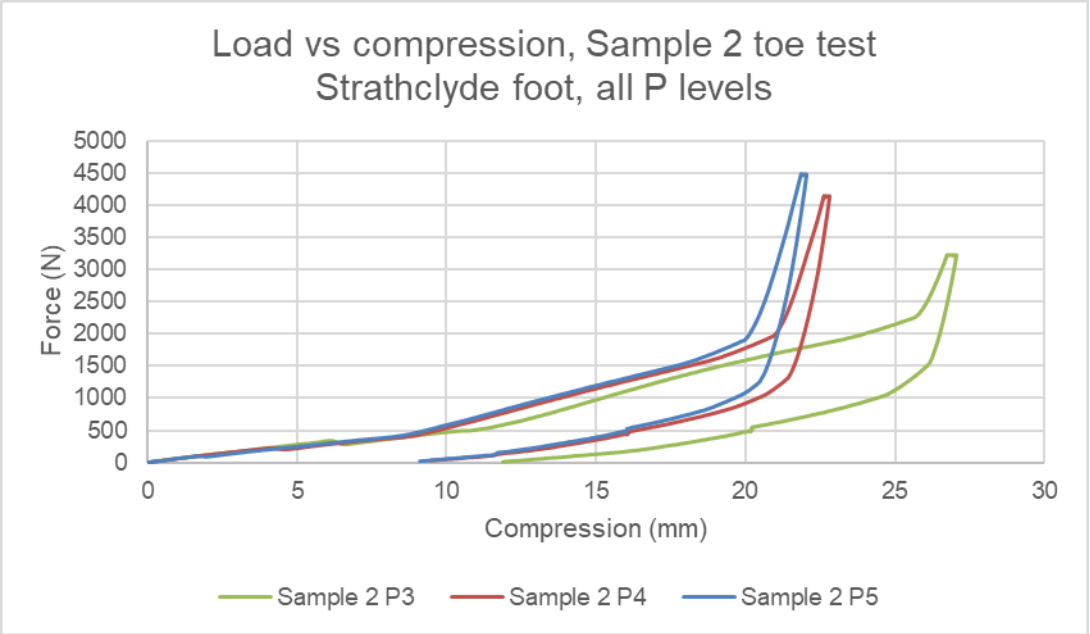

Figure 53 – Load vs. compression at all P testing levels of Strathclyde foot sample 2

Samples 1 and 2 both survived with increased discolouration on the underside of the toe sections and likely an increased permanent deformation. A final deformation of 8.25mm remained in sample 1 at the conclusion of testing (see Figure 52) while sample 2 had 9.09mm deformation remaining (see Figure 53). These values would be expected to decrease given time to recover however some permanent deformation would remain in the samples.

3.3.6.5 Conclusion

The Strathclyde foot passed the P5 ultimate static loading requirements for the toe condition. While there was permanent deformation remaining in the keel it is not of a high level and would not preclude use of a foot under normal loading levels and patterns for a short time until a replacement could be made. There appeared to have been a large permanent deformation remaining in the heel section as a result of P4 heel testing (approximately 7.24mm in sample 1 and 8.71mm in sample 2). The result of heel testing at the P4 level then should not be considered a pass as there was significant, lasting deformation. Testing was to be carried out for the heel

condition to the P5 level to observe performance following this deformation, but it would not be appropriate to consider further testing as validation to the P5 level.

3.3.7 P5 testing – heel

3.3.7.1 Specimens

Samples 1 and 2 from P3 and P4 testing and P5 toe testing were found to have permanent deformation on the forward edge of the heel area of the keel. This deformation meant that they were not considered to have passed the P4 level however they were used again in heel testing at the P5 level to inform on behaviour following failed condition.

3.3.7.2 Method

The sample was prepared and treated in the same manner as described in section 3.3.3.2 Method with the upper load being increased to 4480N to reflect the P5 loading requirement.

3.3.7.3 Results

The samples were loaded at the prescribed 175N/s with no signs of breakage or slippage by the upper limit of 4480N in the case of sample 2. In sample 1 the ball was observed to split after the keel had contacted the baseplate (Figure 54). The contact occurred at around 9.9mm compression in sample 1 and 9.8mm compression in sample 2, observable in Figure 55 or Figure 56 by the sharp change in gradient as the system becomes stiffer. Figure 55 shows that 0.42mm of creep occurred in sample 1 and 0.41mm of creep in sample 2 at maximum loading. During unloading the removal of contact from the keels was seen by the change in gradient at 10.3mm compression for sample 1 however there was no clear point highlighting the removal of contact from sample 2.

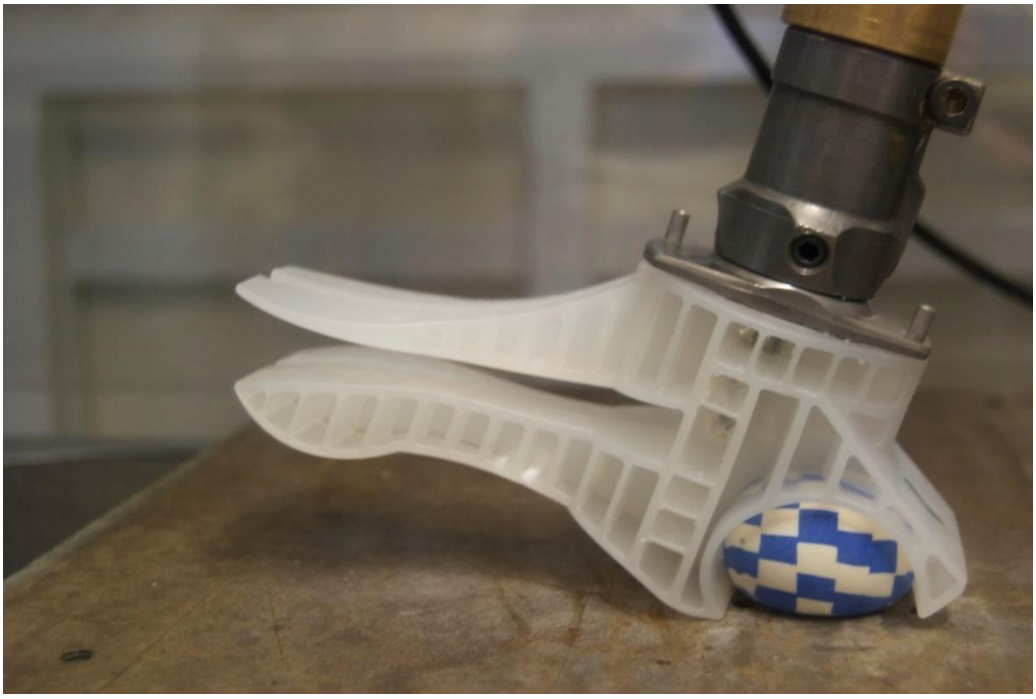

Figure 54 - An image showing sample 1 of the Strathclyde foot at maximum P5 heel loading

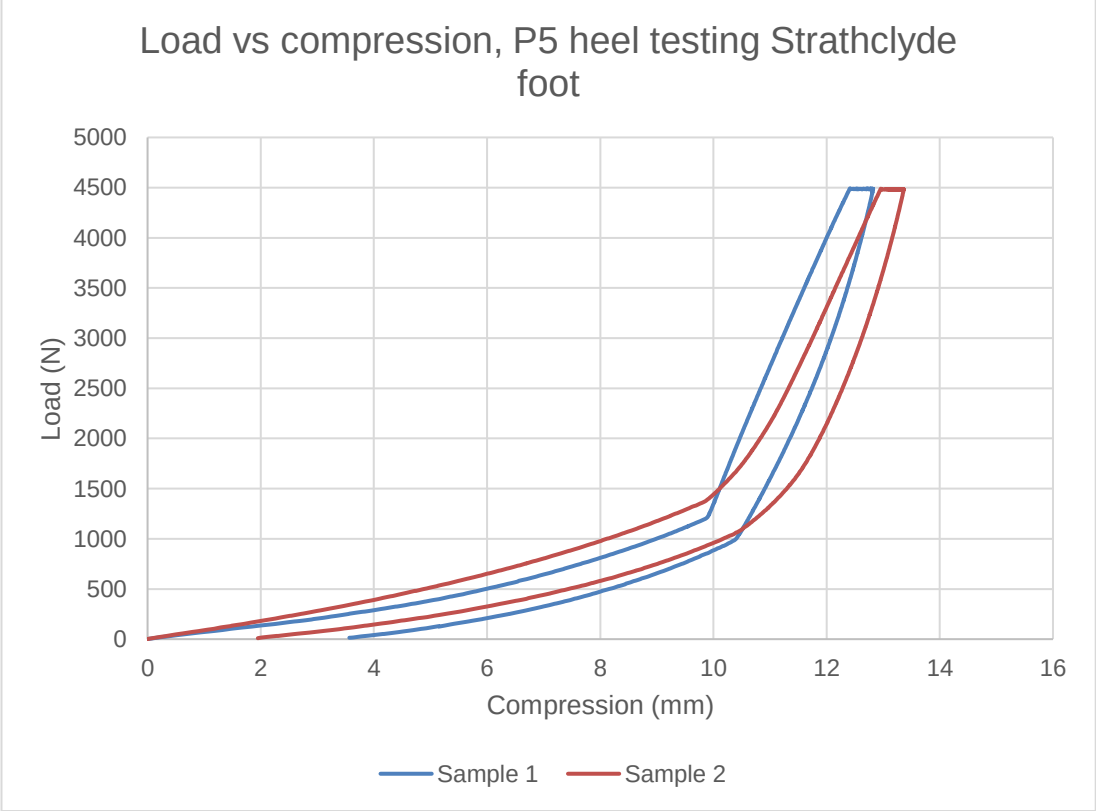

Figure 55 – Load vs. compression results of Strathclyde foot under P5 heel testing

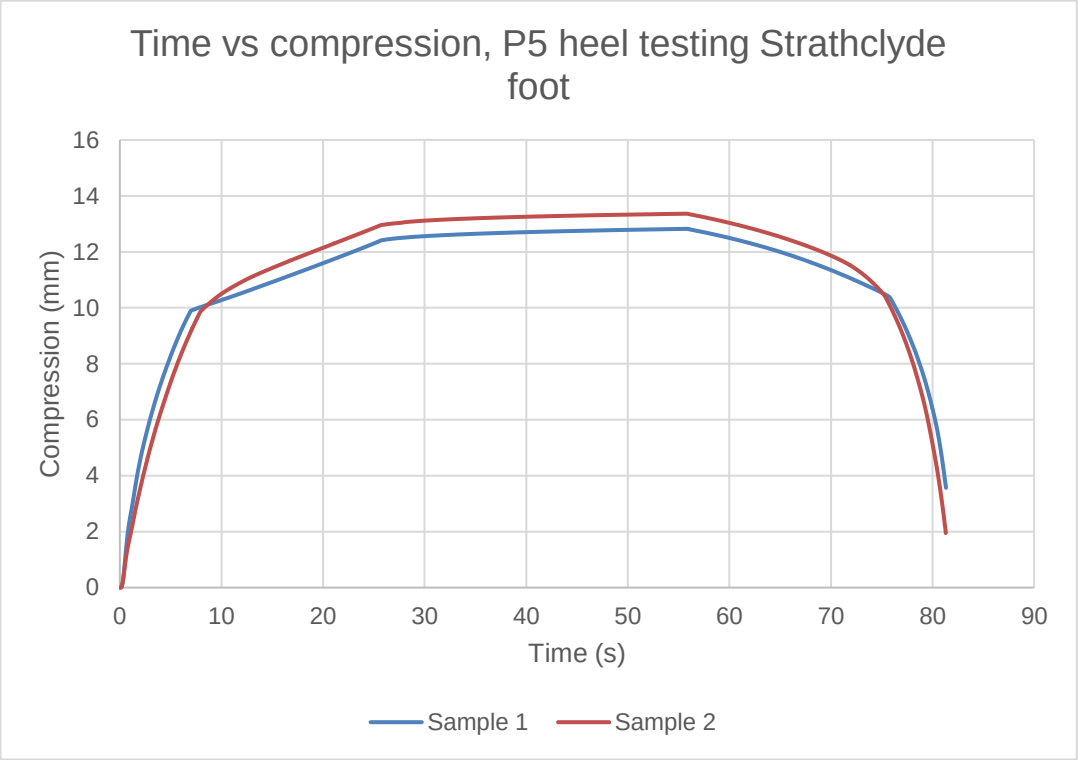

Figure 56 – Time vs. compression graph of Strathclyde foot under P5 heel testing

Using the same method as described previously in section 3.3.2.3 Results energy in the system was calculated. Sample 1 had an energy input of 13.64J and an output of 8.59J giving a loss of 5.05J while sample 2 had an input of 15.79J and an output of 10.12J giving a loss of 5.67J.

3.3.7.4 Discussion

The ball in Sample 1 split after the keel had contacted the baseplate. As the performance of sample 1 was similar after this point in both P4 and P5 testing it may be assumed that the effect of the ball at this stage of testing was much smaller than the effect of the keel on overall performance. During testing the balls both deformed to the point where the keel was directly in contact with the baseplate however this contact occurred at different loads for each sample, approximately 1215N for sample 1 and 1370N for sample 2. The same balls were used as in testing to the P3 and P4 level. The loads required here for contact were again lower than in P4

testing, by 355N and 160N respectively, and a total of 675N lower for sample 1 and 370N lower than in the P3 loading condition (see Figure 57 and Figure 58).

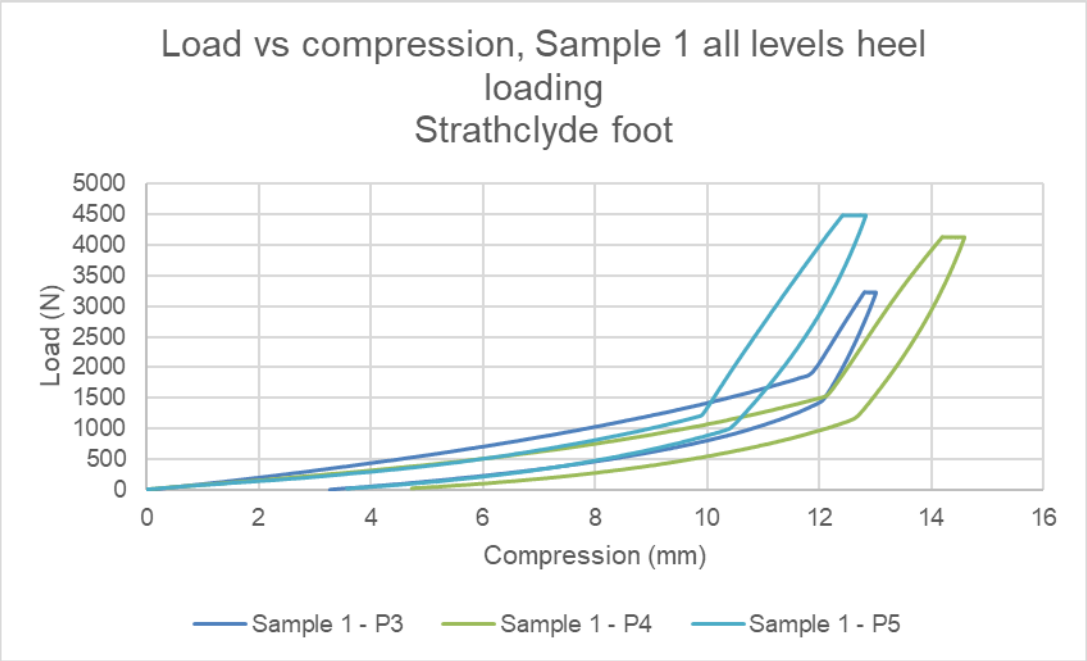

Figure 57 – Load vs. compression at all P testing levels of Strathclyde foot sample 1

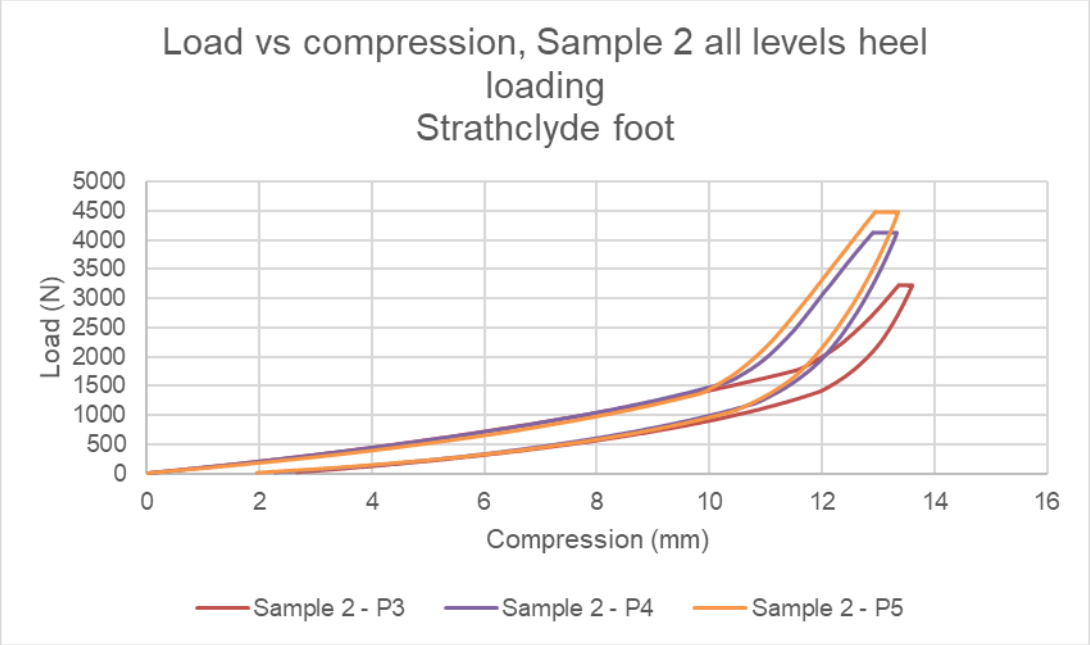

Figure 58 – Load vs. compression at all P testing levels of Strathclyde foot sample 2

With the same caveat regarding the sustained upper load affecting the energy return, the energy return of the feet was 63% for sample 1 and 64% for sample 2. In

either P5 case the keel contact point occurred at a lower compression than in the P4 case. This strongly indicated that deformation had remained within the ball between tests. After this contact the performance was similar to that observed at the P4 test level. This did not rule out the possibility of deformation remaining in the keel between tests (as indicated by the results of toe testing at the P5 level) but the similarity in performance indicates that, aside from localised deformation, the keel had not been compromised in testing.

In comparing the performance across different levels sample 2 showed similar initial load-compression behaviour with the keel contacting the baseplate at progressively lower compressions and thereafter a similar load-compression behaviour, although with increasing maximum loads only resulting in similar maximum compressions (13.61mm, 13.33mm and 13.36mm at P3, P4 and P5 test levels). In contrast sample 1 showed an increased compression before the keel contacted the baseplate (by 0.33mm) during P4 testing compared to P3 testing and a reduction at the P5 level. The load-compression behaviour prior to the keel contacting the baseplate at the P4 and P5 level was similar however in either case it was less stiff than during P3 testing. The reduced stiffness was likely to be as a result of damage to the ball. As the P4 level showed an increase of 0.33mm in compression until contact with the baseplate this may have been a result of lasting deformation in the ball following P3 testing coupled with an alignment change after the ball was removed for inspection. In P5 testing a reduction in compression at keel-baseplate contact was observed, in line with the performance of sample 2. The P4 testing may then have caused further deformation to the ball however with a similar alignment to P4 testing a reduction rather than an increase in compression was observed at keel-baseplate contact.

3.3.7.5 Conclusion

The Strathclyde foot was not considered for verification to the ultimate static loading condition in the heel condition of the P5 level. The permanent deformation and declining performance of the ball in sample 1 between P3 and P4 tests indicated damage in the ball, which while not preventing use of the foot would certainly impair function however, the lasting permanent deformation of the keel following P4 heel testing was considered to be a failing condition at the P4 level. During P5 heel testing the ball split which would have counted as a failure even without the keel deformation. The keel itself did withstand the full force of loading without breaking which might be considered a qualified success, however given the permanent deformation resulting from P4 testing this increased loading will have resulted in even greater permanent deformation.

3.3.8 Discussion

The Strathclyde foot was tested up to the P5 level in heel and toe conditions. The keel with a ball in the heel was found to pass to all levels in toe loading. With the addition of the glass fibre rods (intended to provide energy storage and return) catastrophic failures occurred in both samples at the P3 level. The method for rod inclusion at the time, as specified by (L. E. Morton et al., 2009), was to drill through three walls within the keel and slide the rods into the holes made. Aside from being a highly inconsistent method and weakening the structure, it introduced an additional manufacturing step. This method of energy storage and attachment to the keel was to be changed for these reasons.

The energy storage and return of the toe section ranged from 43-62% which is positive in that a significant portion of the energy was returned. With adjustment to ensure the function and safety of an energy storage and return system the

percentage of energy return could be much higher which in turn could contribute to the function of the prosthesis.

The heel tests were passed to the P3 level by both samples however at the P4 level both samples were determined to have suffered significant permanent deformation of the keel resulting in failure being recorded. Energy return at the heel was calculated at 54% in P3 testing. This was higher than was potentially necessary as part of the function of the heel was energy dissipation at heel strike. It should be noted that the loading conditions used in testing were not representative of normal gait and as such performance of the prosthesis in gait is likely to be different, with higher energy returns likely due to shorter contact times, reducing creep as well as lower maximum loads.

3.3.9 Conclusion

The Strathclyde foot may be deemed to have met the ultimate static toe loading condition of the P5 level of ISO 10328. The model used in FEA was inadequate to predict the survival of the samples under toe loading to the P5 level.

The Strathclyde foot did not technically meet the ultimate static heel loading to the P4 level of ISO 10328 due to significant permanent deformation of the keel. The Strathclyde foot did pass both test conditions to the P3 level.

Based on prior work (L. E. Morton et al., 2009), the expected working condition of the Strathclyde foot was to be with composite rods inserted into the keel. When tested using this setup the feet were seen to fail catastrophically prior to successful completion of the P3 level ultimate static toe loading and as such this method of energy storage was deemed unacceptable and to be replaced.

The keel design required improvement to accommodate the energy storage and return function. The next step was to address these issues prior to further testing.

3.4 Summary

A Product Design Specification was drawn up to define the project outcomes. The existing design of the Strathclyde foot was then to be tested to form a baseline for design improvements. The Strathclyde foot was tested sequentially at the P3, P4 and P5 levels for the ultimate static loading conditions. In toe loading the Strathclyde foot was found to pass at each level up to P5. The heel loading achieved the P3 condition successfully but did not meet the P4 condition due to significant permanent deformation of the keel. P5 level heel testing was carried out to view performance of a compromised keel and while the keel suffered further permanent deformation it did not fracture although the ball in sample 1 did split in testing. When a pair of glass-fibre rods was included in the setup for heel testing catastrophic failure was observed prior to completion of the P3 loading condition. In both sample 3 and 4 the glass fibre rods snapped and in sample 3 one of the top toe sections broke off. The next step was to improve the design prior to retesting, particularly the energy storage and return method.

CHAPTER 4 – Design improvement and testing

The Strathclyde foot design was to be developed based on the results of the physical tests carried out on the existing design and with specific points from the Product Design Specification. Methods of prototype manufacture were to be examined and evaluated for a suitable method and material with which to produce physical prototypes for testing. These prototypes were then to be tested with results being compared to the results from the existing Strathclyde foot design and FEA results for the revised design.

4.1 Design development

Following evaluation of the current Strathclyde foot design (see Figure 59) the following areas were identified for further development:

- The method of foot to shank attachment
- The heel of the foot was wide at the rear, unlike the heel of the anatomical foot
- Thermal distortion effects in manufacture caused by design
- The rods used for energy storage and return were found to fail in testing
- No specific location for attachment of energy storage elements

In order to advance the design, each of these issues required dealing with in turn.

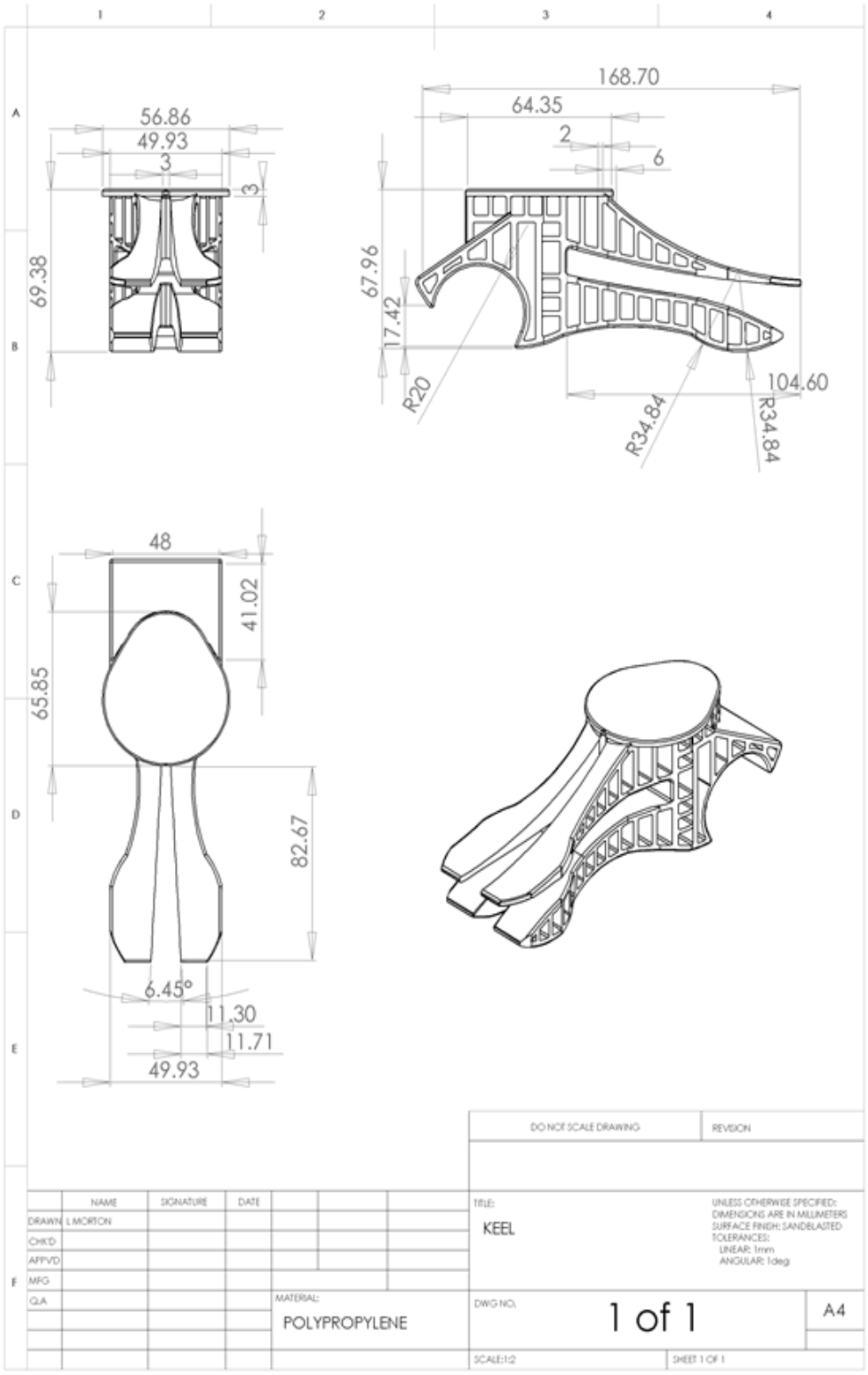

Figure 59 - The Strathclyde foot keel design at the beginning of the current project (L. E. Morton et al., 2009)

4.1.1 Foot to shank attachment

The existing design of the Strathclyde foot suggested welding the foot to a specific, polypropylene shank (L. E. Morton, Spence, Buis, & Simpson, 2009). As the selected material for the design was copolymer polypropylene, it was decided to continue with this material in concept. Welding is potentially of use as a method of connection for the foot to shafts or sockets however this would reduce the applicability of the foot where existing systems are already in use as it would not guarantee interface.

Even though the Strathclyde foot was designed with the intention of welding to a shank, in Morton et al.'s previous testing (L. E. Morton et al., 2009) a hole was drilled through the top surface and a threaded fastener inserted (see Figure 60).

Figure 60 – Strathclyde foot showing the inserted threaded fastener used in previous testing (L. E. Morton et al., 2009)

Pyramid adapters are commonly used to provide a connection between foot unit and shank whilst also allowing for alignment to be carried out (see Figure 61). Inclusion of a pyramid adapter would allow the foot unit to be more widely.

Figure 61 – A typical pyramid adapter with bolt and washer for attachment.

The previously used method of drilling into an injection moulded keel was unacceptable and not to be continued. A feature should be included in the keel design to allow the insertion of a bolt for the pyramid adapter without additional modification. This feature would increase the complexity of the injection moulding process however would allow the foot to be more widely used. To accommodate such a feature, the design was to be altered with the heel moved backwards to allow clearance for a through hole to be created in the foot without hindering the strength of the heel section.

To prevent impact during walking, which could cause a severe jar to the user, the bolthole was to be countersunk from the underside.

Figure 62 below shows the outline of the hole feature including the countersunk part at the bottom. The shaft appears very wide in Figure 62 due to it including the thickness of the injection moulded material and thus representing the outside dimensions. It may also be observed that the heel now juts out further than before to accommodate the hole. Figure 63 better shows the internal dimensions.

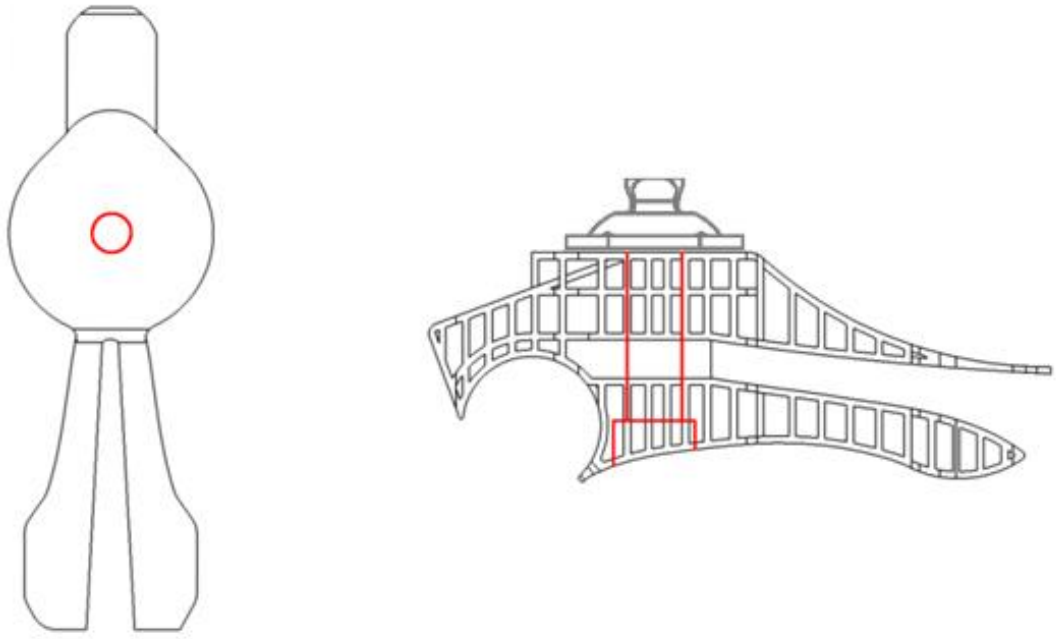

Figure 62 - The new design with the bolthole location highlighted in red and pyramid adapter for reference

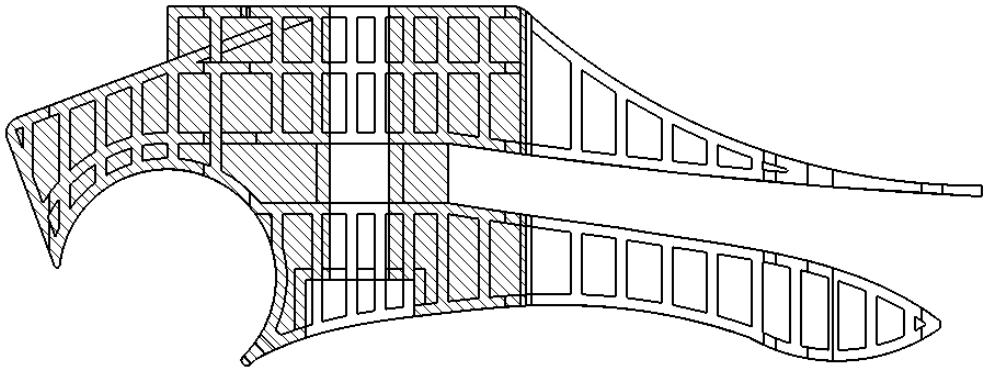

Figure 63 - Cross section through the centreline of the keel superimposed on complete keel to display the through hole feature within it

FEA was used to determine the strength of the main ankle block of the keel was not compromised vertically by including a hollow central column to accommodate the bolt (see section B3.3 Heel modification). It was determined that the introduction of the bolthole did not compromise the keel design with respect to heel loading however a reduced load to yield was seen with respect to vertical loading of the

underside of the ankle block, although this was more likely related to changes to allow the energy return feature (discussed in 4.1.4 Energy return feature).

4.1.2 Heel width

As the heel of the new Strathclyde foot design was far wider than that of the anatomical foot it was decided that it should be narrowed as closed shoes would be impossible to use with the current keel design. The heel area of the keel was used to retain a ball in place that acts as a shock absorber on heel impact. There was also the potential of using a cylinder cut to length, but the same requirements would be made of the keel. As the heel section did not provide any lateral constraint on the ball/cylinder it did not need to be as wide as the initial design and so should not have provided any issues in reducing the width in this respect. A requirement of the cosmesis was then to constrain the ball, or cylinder, within the heel cavity. The existing width was compared to a tapered heel design and a more narrow, constant width design (see section B3.2 Heel width). The heel was loaded in a worst-case scenario and it was found that the variant design had lower load to yield in either case than the original heel design so further development was carried out and modelled in B3.3 Heel modification, where satisfactory performance was reached by increasing the heel section height and altering the rib pattern. In reducing the width of this section of the heel the stability should not have been impacted as the contact at heel strike remained on the ball as before and with the retention offered by the cosmesis the ball would have been unable to shift. Figure 64 below shows the initial design of the heel from above compared to the updated version.

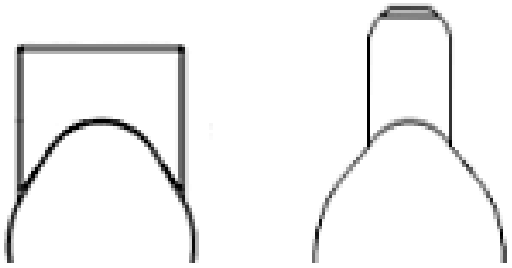

Figure 64 - The initial Strathclyde design, left, and the updated design, right. The designs are shown approximately to the same scale.

The reduced width is clear to see from Figure 64 but also the increased length of the heel due to the inclusion of a bolthole in the design.

4.1.3 Thermal distortion effects

The existing design was injection moulded previously but all samples showed a dip along the medial line of the top surface of the keel (see Figure 65). This appeared to be a result of the cooling after the injection moulding leading to thermal shrink. It would have been preferable, particularly if the keel were to be welded to a shaft, to have had a flat surface.

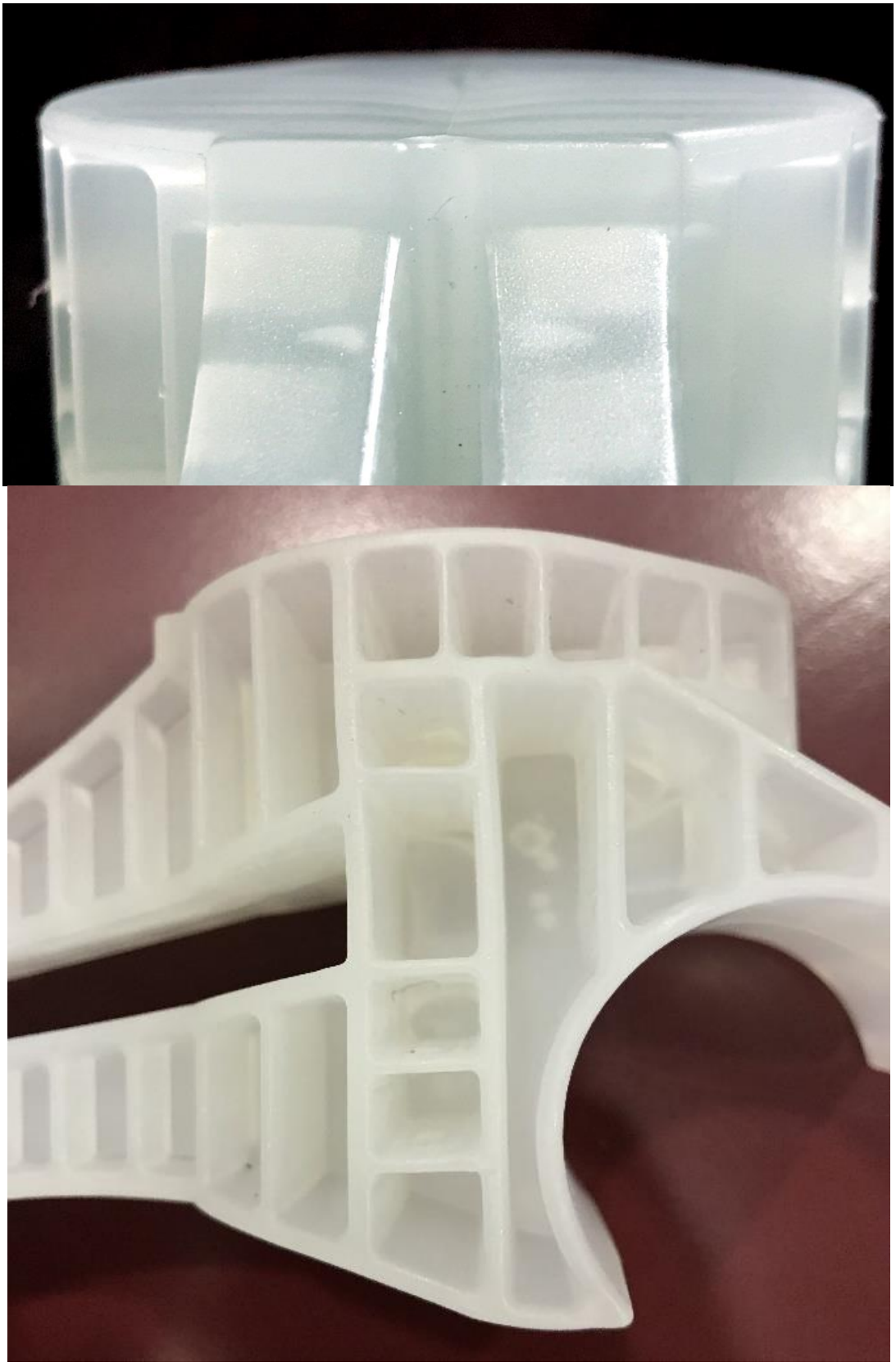

Figure 65 – Image showing thermal distortion of Strathclyde foot (top) and void formation (bottom)

While (L. E. Morton et al., 2009) included FEA related to mould design, it did not take into account cooling effects on the finished item. RPWorld (Beijing, China) were the company who produced the injection moulded samples however there was no record of discussion with them regarding thermal distortion of the finished product. The material within the keel running along the medial line of the foot is approximately 7mm thick compared to the 2.5mm and 1.4mm thicknesses found elsewhere. By reducing the thickness of this central rib and standardising the size of the ribs, the shrinkage visible on top of the keel should be reduced. The voids observed within the existing design are likely to have been caused due to the large wall thickness of the medial section meaning that the outside skin cooled more quickly than the inside and so pulled outward, forming a void. By reducing this thickness, a more even cooling will be possible reducing the likelihood of void formation and shrinkage on the top surface. FEA was carried out to determine the effect of varying the wall thickness from 7mm to 5.3mm, 3.7mm and 2mm on the strength of the ankle structure (see section B3.1 Distortion due to manufacturing effects). It was determined that reducing the wall thickness to 2mm did not detrimentally affect the strength of the ankle structure and so this change was applied. Upon determining the final shape of the keel, all ribs were also adjusted to 2mm for consistent wall thickness throughout the keel.

4.1.4 Energy return feature

The initial design of the Strathclyde foot had no built-in allowance for an energy return feature. The concept that rods could be used to store energy during deflection of the toe section was applied previously (L. E. Morton et al., 2009). Rods of various materials had been inserted into the foot between the upper and lower toe sections, these rods would then flex as the lower toe section contacted them and return to their original form as the toe was unloaded, returning stored strain energy. This

method required holes to be drilled into the keel after manufacture, through several sections of the plastic keel (see Figure 66 below). One of the concepts in the foot design was that it could be easily customised in situ for the user. As such drilling holes to insert rods was unacceptable and not to be implemented.

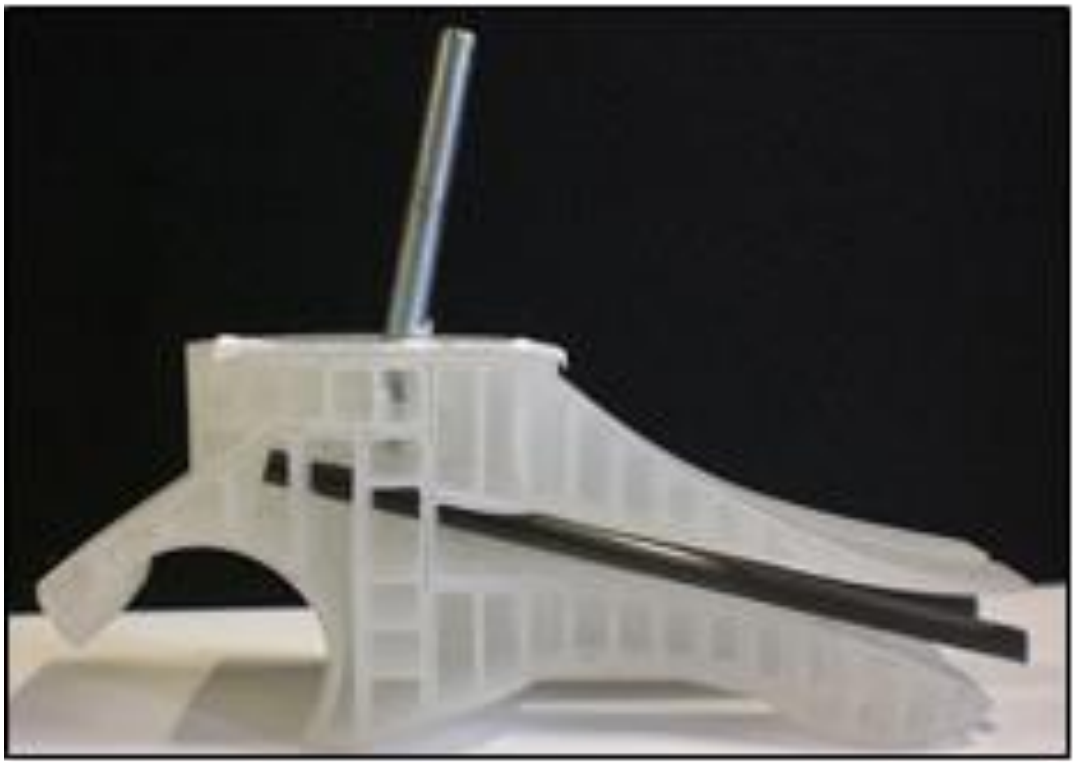

Figure 66 - This image demonstrates the energy return rod system between the upper and lower toe sections used previously, note the three layers of plastic in the keel that were drilled through (L. E. Morton et al., 2009)

Strain energy stored in a flexed beam is defined as:

$$U = \frac{M^2 L}{2EI}$$

Where M is moment, L is beam length, E is Young's modulus of the material and I is the moment of inertia of the beam cross-section.

Assuming a constant M, L and E then I is desired to be as small as possible so that U will remain large however the competing interest of maintaining a low bending stress requires I to be large:

$$\sigma_{bending} = \frac{My}{I}$$

An alternative way to reduce the bending stress would be to reduce the y value. As the beam is expected to be in tension on the underside when flexed a shape with the neutral axis towards the underside will reduce the tensile stress.

For example, a rectangular shape with equal I value to a circle but with a total height equal to the radius of the circle would have a bending stress on the most extreme edge of half that of the equivalent location on the circular section. A beam with a cross-section that tapered towards the top would offer a further way to reduce y while maintaining I.

For simplicity in producing samples a rectangular cross section formed the basis for the energy return feature to be used. This “blade” was to be cut from sheets of material to simplify production.

In using a blade then a method of attachment had to be considered. The concept that the blade could be shaped in a way to provide an interference fit with the keel was applied but requires further testing to ensure friction would not damage either keel or blade and cause the connection to become loose. The keel had to be modified to create a clear space where such a blade could be inserted without further modification of the keel post manufacture, the evaluation of which is detailed in sections B3.3 Heel modification through B3.6 Whole design evaluation. Although the modification did reduce the load to yield of the keel in various conditions it was unclear if these would be unacceptable, so it was determined that prototypes should be formed to test. With the idea of user customisation, the use of a blade with different flexibility on either side could make a symmetric foot become either a left or right foot. To allow this, it was conceived that a blade be customised then slotted into the keel. Stock blades could be produced and then reinforced to increase resistance as required by the user’s weight or physical activity level.

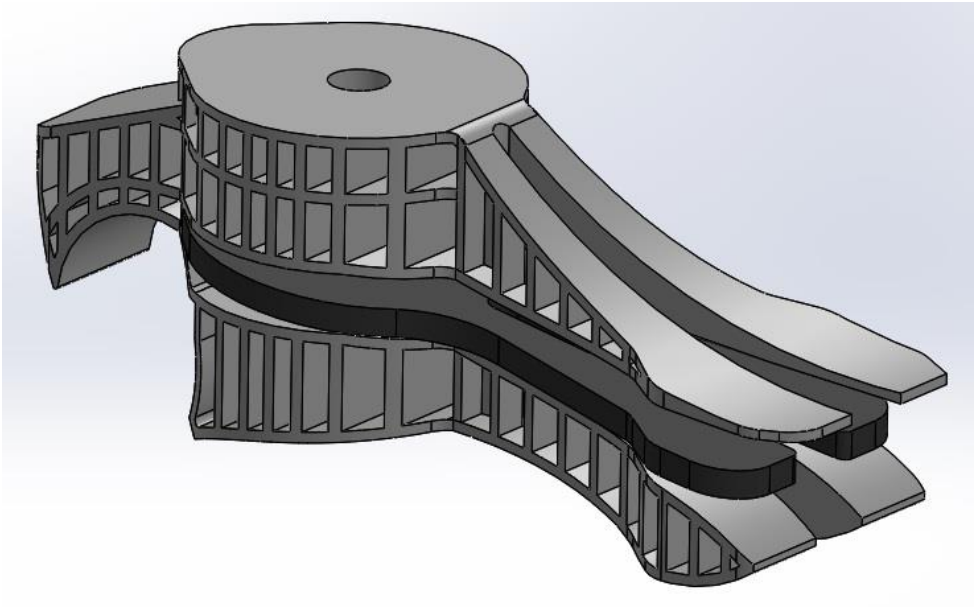

Figure 67 - The foot displaying the concept of using a blade insert

The blades were to initially be made of fibreglass based on the results of testing by Morton, Spence, Buis, & Simpson, 2009 however, a thorough evaluation of materials is recommended with emphasis on energy return and fatigue properties in determining a final material selection. Modification of the shape was to come later when tuning the performance with particular attention to tapering along the length of the beam and of the section. The blade was to be required to be tested in both static and cyclic testing with particular attention to the fatigue occurring during cyclic testing.

4.1.5 Design conclusion

With the updated design in place, testing was required to determine its performance. The FEA described in section B3.7 Duraform EX models predicted a load at yield in toe loading of 296.2N on a half foot model (492.4N full foot) however physical samples were required.

Injection moulding in polypropylene was the desired production method however with a small batch size the costs become very high per unit because of

tooling costs. Due to the elapsed time from the previous order the mould from the existing design had not been retained by the manufacturer and so was unavailable for modification. As such alternative methods were sought to provide more cost-effective prototypes for testing. The process should be able to produce small batches and should be cheap enough to produce batches of different designs within the budget of the project. The turnaround time was important given the time scale of the project.

The methods detailed below do not bond materials in the same way as injection moulding and will not adequately represent the material properties of polypropylene. The samples produced were to be used to determine the effects of design changes rather than as tests for compliance to standards, although testing was modelled on standards. The testing of physical samples was also to act to provide verification to the FEA model. As a result of the criteria imposed layered manufacturing techniques were determined to be potentially suitable and investigated, with the details examined below.

4.2 Layered manufacture

Layered manufacture is the term given to a number of manufacturing methods which work by employing CAD to produce scale 3D models of designs through additive means, i.e. the model is built up rather than carved out of existing material (such as milling would do, for example). These methods allow net shape manufacture, where a product is manufactured to its final form without the need for additional manufacturing processes to be carried out. Some of the methods to be discussed allow for mixture of materials to tailor the properties for the specific use required. Included in this definition are Stereolithography (SLA), Laminated Object Manufacture (LOM), Selective Laser Sintering (SLS), Fused Deposition Modelling

(FDM), Inkjet Deposition (ID), Solid Ground Curing (SGC) and Vacuum Casting. Other techniques exist but only those mentioned above will be covered in some detail as the more commonly available methods.

4.2.1 Stereolithography

Stereolithography is a photopolymer based technique; an ultraviolet laser is passed over an ultra violet light curable resin layer by layer. The design is constructed from the base up with fresh resin being applied over each cured layer and then cured in turn to form the next layer. Supports are required where the shape may deflect, either due to gravity or the resin applicator as it makes each pass. These supports must be removed by hand once the process is completed. Post curing is also required to ensure material properties. Other methods exist such as ascending suspension, ascending surface or masked-lamp descending platform as well as the descending platform method described above.

A range of materials is available for use that may approximate plastics such as ABS, polypropylene or nylons. These materials may be mixed in multi head powder feeds giving differing material properties throughout the product, tailoring for specific function. Products may suffer from poor adhesion between material layers if the parameters are not carefully controlled as layers cool before the addition of following layers. Stereolithography involves high initial start up and running costs due to machinery and materials handling and so the cost per unit is relatively high compared to other layered manufacturing methods. Stereolithography was judged to be a good potential prototyping process.

4.2.2 Laminated Object Manufacture

Laminated Object Manufacture is carried out by gluing layers of plastic, paper or metal together and cutting at each layer to the desired shape. It is most commonly used with paper and can have long-term dimensional stability issues,

mainly to do with water absorption, although this may be avoided by sealing. There is a large amount of waste produced in the off cuts.

This was not a viable prototyping method and was discarded since the material strength of LOM produced models is low.

4.2.3 Selective Laser Sintering

SLS uses lasers to fuse small particles of plastic, metal, wax, glass or ceramics to form a 3D shape. A 2D shape is scanned on a flat bed of the powdered material resulting in the particles melting and fusing. More powder is added to cover the first level and the process is repeated until the full 3D shape has been formed. Supports are not required to be built into the design as the unused powder serves this function. SLS can produce complex geometries and is beginning to be used in production for working products of limited production size rather than just for prototyping. The use of multiple powder heads allows for the mixture of materials and so properties and performance of the product.

SLS can make use of a variety of materials, notably polymers, and has a good dimensional accuracy as well as providing good material properties but it should be noted that it can suffer from stepping in the machine's vertical axis and poor surface finish.

4.2.4 Fused Deposition Modelling

Fused Deposition Modelling works by laying down material through an extrusion nozzle. The nozzle heats the material, which then cools on departing the nozzle. The nozzle moves to cover the desired shape and builds the structure up in layers. Plastic or metal wires can be used and there is also a disposable material that is used to provide support when required. The material costs involved in FDM are relatively high, presumably due to the requirement for a coiled filament of the materials, which also limits the material choices available.

Based on the higher costs and complex geometry likely to be involved as well as potential poor layer to layer adhesion this was discarded as a process choice.

4.2.5 Inkjet Deposition

Inkjet deposition comes from the printing industry however in the case of layered manufacture it is a fast curing compound, adhesive or molten material which is used rather than ink. In the case of fast curing or molten materials the shape is printed directly onto a work surface and built up in successive layers, each printed directly on top of the last. Supports may be required where a structure is not sufficiently strong until its completion. Where an adhesive material is used a powder is required which the adhesive will bind thus forming the solid shape, the powder filling the workspace at each layer provides support in this case. Once again, the 3D shape is built up in layers.

This process is more usually used to produce investment casting patterns and not functional parts and so was discarded.

4.2.6 Solid Ground Curing

Solid ground curing is another photopolymer based process. A photosensitive resin is exposed to light through a mask (formed on glass through an electrostatic process, similar to photocopying), which represents a layer of the model being produced. Once a layer has been exposed to light the excess resin is removed and replaced with wax that acts as a support for the structure during manufacture. The surface is milled, partly to ensure dimensional accuracy but also partly to ensure a good bonding surface between layers. The next layer of resin is put on top and again exposed to light through a mask for the next layer and the process is repeated until a complete product is formed. The support wax may then be removed, and any finishing required carried out. The disadvantages of the process lie in the fact that

there are few materials available for use and that over exposure of the resins during the process can cause unused material to be unrecyclable.

Solid Ground Curing is not a process available in the UK and thus was discarded.

4.2.7 Vacuum casting

Vacuum casting is not technically a layered manufacturing technique; it does however possess the advantages of being relatively fast, accurate and has a similar process to injection moulding. It is suitable for producing small batches and has many material options available, some of which are similar in properties to polypropylene.

Vacuum casting works by creating a mould in degassed silicon, based around an original pattern, either formed for this purpose or an existing piece. The mould is separated along a dividing line to remove the pattern and to allow for removal of moulded parts. The mould is placed in a vacuum while the resin is added at which point the pressure is reintroduced effectively forcing the resin fully into the mould. After being allowed to cure the mould can be separated and the part removed. The mould may be reused several times and is thus useful for producing batches of products.

4.2.8 Comparison of manufacturing methods

The comparison of manufacturing methods presented here in Table 5 is to determine which method may be used to produce a small batch of prototypes that can be used in mechanical testing. Certain of the methods listed were easily removed from consideration; laminated object manufacturing for the low material strength of materials available for fabrication, fused deposition modelling for the weakness of layer to layer bonding, inkjet deposition for the lack of a functional part produced and solid ground curing for not being available in the UK at the time of

research. The remaining methods, stereolithography, selective laser sintering and vacuum casting were determined to be worthy of further investigation.

	Method of operation	Strengths	Weaknesses
Stereolithography	Ultraviolet light cured resin built in layers	Speed Large print envelope Supports required	Relatively expensive materials Post curing required
Laminated Object Manufacture	Laminate formed from base material and adhesive, sample cut to shape	Low cost	Lower dimensional accuracy Long term stability issues
Selective Laser Sintering	Lasers used to fuse powdered material in layers	No supports required High strength and stiffness products Speed	Porosity Delamination Visible stepping Surface finish
Fused Deposition Modelling	Material is extruded in a pattern, built in layers	Speed Relatively high cost	Limited material choice Limited geometric complexity of product
Inkjet Deposition	Layers are built of rapidly-solidifying liquid material	Efficient material use Potential to tailor material properties	Limited material choice
Solid Ground Curing	Photosensitive material is selectively exposed to light to produce ascending layers	No support required High accuracy	High waste Limited material choice Unavailable in the UK
Vacuum Casting	A silicon mould is depressurised prior to introduction of a resin under pressure	Single mould for small batch production Good accuracy Good mechanical properties	High costs Thin wall sections not recommended

Table 5 – Comparison of described manufacturing methods in section 4.2 Layered manufacture

4.2.9 Evaluation of remaining manufacturing methods

The remaining potential processes for manufacture to be used were Vacuum Casting, Stereolithography and Selective Laser Sintering.

ARRK Europe is a large manufacturing company with particular experience in rapid prototyping (including layered manufacture). As VC, SLS and SLA were available from them it was decided that they be contacted. The SLS process coupled with the material 'Duraform EX' was recommended for this application and datasheets for the materials available for use in VC, SLS and SLA were provided. Upon examination of said datasheets it was noted that the materials used in SLA were relatively brittle and would not be suitable for the mechanical tests planned of the prototypes. As a result, SLA was discarded as a prototyping method.

When provided with quotes for the respective methods the costs involved in vacuum casting were significantly higher than that of SLS (£1,336 compared to £696 for 8 samples) as a prototype would be produced through SLA in order to form the mould and then the production of the samples would be carried out. It was noted that the design provided would require modification to be cast using the VC method. Similar changes to the design would likely be required to make the design suitable for injection moulding and these were to be borne in mind for future design changes. As the models were to be produced in small batches the high cost of vacuum casting would quickly exhaust the budget for the project, leading to a preference for SLS methods.

The material properties of an injection moulded polypropylene design are not accurately reproducible outside of that method due to the nature of flow characteristics, mould and material conditions contributing to the final properties of the product. As the prototypes could not serve to claim compliance with ISO 10328 and were only to serve as validation of design concepts prior to investing in mould

tooling for injection moulding the cost is a more significant factor than achieving very similar material properties to polypropylene. After an examination of the data sheets, samples were requested of two of the SLS materials, Duraform EX and Duraform PA, for examination in order to determine suitability for testing.

The datasheet provided by ARRK Europe contained the following relevant claims about the nature of the sample materials, Duraform EX and Duraform PA, displayed in Table 6.

	Duraform PA (ARRK Europe, 2010)	Duraform EX (ARRK Europe, 2010)	Polypropylene, Copolymer (Overview) (MatWeb, 2017b)	Total PPH 3480Z Polypropylene, Extrusion grade (MatWeb, 2017c)
Specific gravity (g/cm^3) *	1.00	1.01	0.952	0.905
Tensile Strength, Yield (MPa)	N/A	37	26.6	-
Tensile Strength, Ultimate (MPa)	43	48	28.6	35.6
Elongation at Yield	N/A	5%	17.9%	10%
Elongation at Break	14%	47%	178%	>100%
Tensile (Young's) modulus (MPa)	1586	1517	1390	1515
Flexural Strength, Yield (MPa)	N/A	42	50.7	-
Flexural Strength, Ultimate (MPa)	48	46	-	-
Flexural Modulus (MPa)	1387	1310	1410	1380
Moisture absorption – 24 hours	0.07%	0.48%	0.0472%	-
Impact strength (notched Izod 23°C) (J/m)	32	74	139	26.5
Impact strength (unnotched Izod 23°C) (J/m)	336	1486	385	1270
Heat deflection temperature @ 0.45 MPa (°C)	180	188	95.6	107
Heat deflection temperature @ 1.82 MPa (°C)	95	48	67.6	-

Table 6 - This table displays the relevant material properties from the datasheets provided by ARRK Europe. * The data has been represented here as presented on the datasheet.

Upon inspection of the samples provided it was decided that they would be too thin to provide meaningful data when subjected to a three-point bending test. To purchase thicker samples for testing would have cost several hundred pounds and with the limited budget in mind it was decided that tensile testing would be carried out on the samples and compared to the stated tensile values. Should the experimental tensile properties be similar to the quoted tensile properties then it would be reasonable to assume the accuracy of all values provided by ARRK Europe.

It may be assumed that the material properties quoted by ARRK Europe are based on ideal specimens, i.e. the layer orientation is normal to loading to reduce likelihood of delamination during testing. The samples provided for tensile testing appeared to have been manufactured in this way with the layers built normal to test orientation, across the thinnest section in order to reduce the number of layers (see Figure 68), and as such a similar result should be achievable. If other samples were produced with the layering occurring in different orientations then the laminar binding would become a factor and lower tensile strengths would likely be observed, but it is recommended this be determined experimentally.

4.3 Material testing

4.3.1 Specimens

ARRK Europe (Gloucester, UK) provided four samples, two of Duraform EX (EX I and EX II) and two of Duraform PA (PA I and PA II), both materials used in the SLS process. The measurements of samples are recorded in Table 7 with Figure 68 identifying where measurements were taken, the overall length of all samples was 16mm. Sample layers were built in the “d” direction, although for further testing it is recommended that samples be obtained with varying build orientations, particularly

in “l” and “d” directions. A further two samples each of copolymer polypropylene (CA and CB) and homopolymer polypropylene (HA and HB) were cut from sheets (North Sea Plastics, Glasgow, UK), however, samples were made to a different size and measurements were not recorded to the same precision. It was thought at the time that testing would be used only to determine Young’s modulus, so the initial dimension of the test sample would not be relevant however, it is recommended that in any further testing samples be made to the same size and measurements be made to the same precision. Homopolymer polypropylene is produced using only propylene monomers while copolymer propylene has additional monomers added, often ethylene, to form the polymer. The addition of these monomers means that copolymer polypropylene was more flexible but also more durable than homopolymer polypropylene.

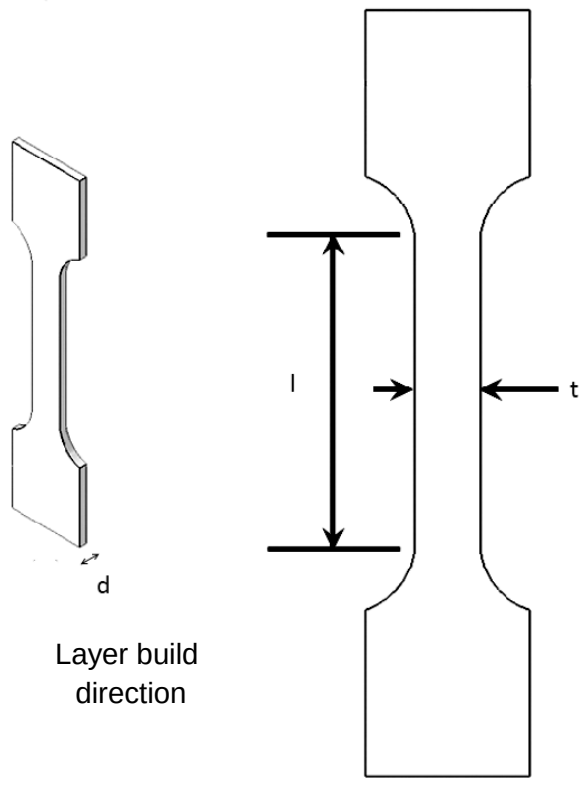

Figure 68 – The reported dimensions of tensile testing samples, in SLS made samples the layers were built across the ‘d’ dimension.

Sample	d (mm)	l (mm)	t (mm)
EX I	1.30	65	12.74
EX II	1.30	65	12.68
PA I	1.33	65	12.75
PA II	1.35	65	12.78
CA	6	60	13
CB	6	60	13
HA	5	60	13
HB	5	60	13

Table 7 – Recorded measurements of compared samples (see Figure 68 for reference locations)

4.3.2 Method

The samples were loaded in the Instron and auto balance was applied to give zero load initially. Samples had pure tension applied at a rate of 500mm/min until failure. This was an arbitrary loading rate and it is recommended that any further testing be carried out according to a standardised method, such as that of ISO 527.

The Young's modulus of each sample was determined from the gradient of the initial elastic region in each case up to 0.01 strain. Yield point was determined at the intersection of a line with the Young's modulus as the gradient and 0.2% offset and the recorded data from testing.

4.3.3 Results

The following graphs show the load-extension curves formed by the samples.

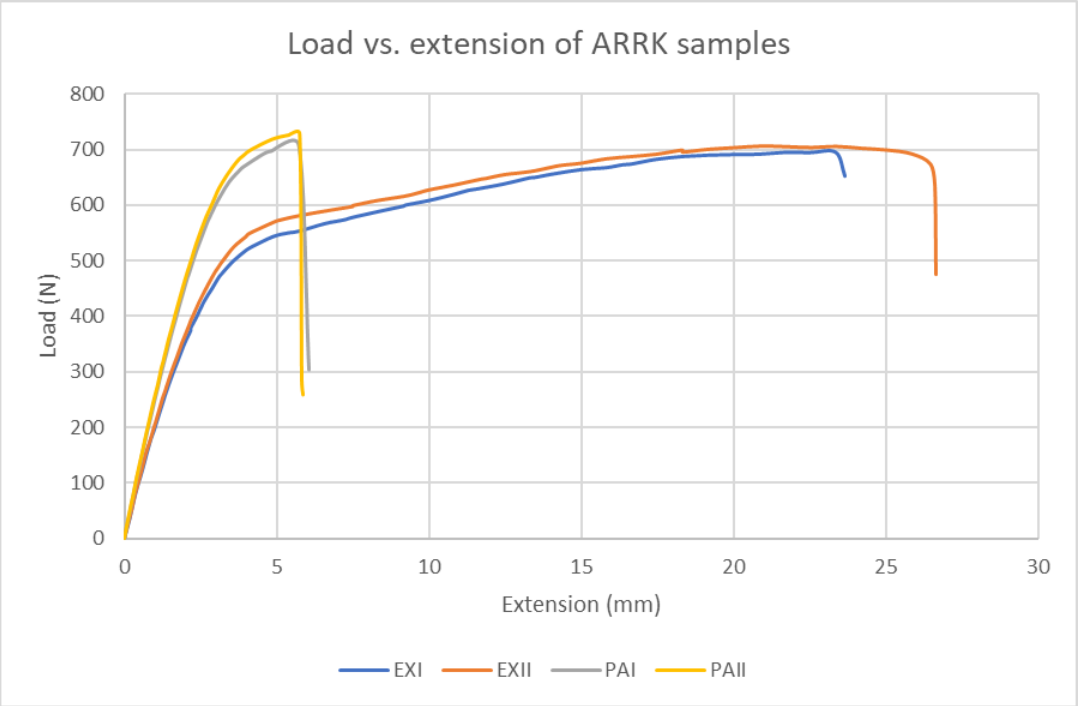

Figure 69 - Load vs. extension of ARRK samples (Duraform EX and PA)

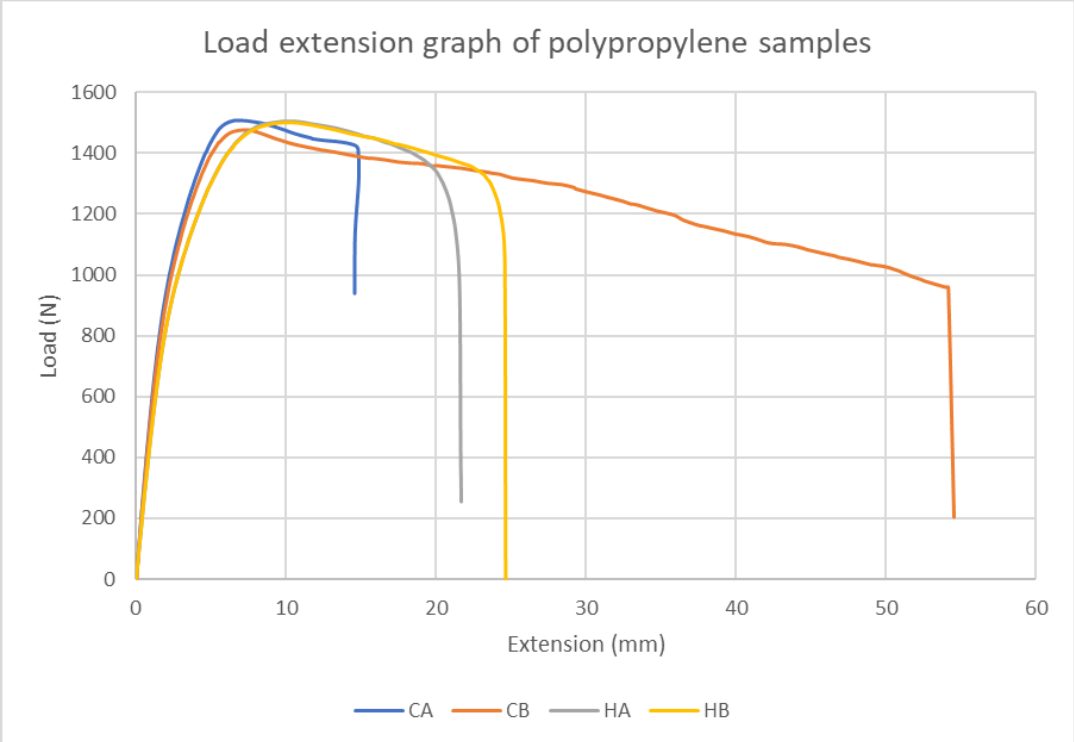

Figure 70 – Load vs. extension of polypropylene samples (copolymer and homopolymer)

A limit was tripped prior to the failure of EXI however the sample had undergone significant plastic deformation and so could not be retested. The result was included to this point to demonstrate its similarity with that of EXII prior to that point.

4.3.4 Discussion

The EX samples were seen to behave in a similar manner, with EXI becoming more flexible than EXII upon exiting the elastic region. Similarly, with the PA samples PAI became more flexible than PAII upon exiting the elastic region prior to failing at a load approximately 23N lower than that of PAII (707.3N compared to 729.9N). In comparing the different types of Duraform it was observed that the EX samples were more flexible (maximum extension of EXII was 26.6mm compared to 6.1mm for PAI and 5.9mm for PAII) however, the failure of EXII occurred at a similar maximum load (706.4N) to the failure of the PA samples. The PA samples were observed to behave more stiffly than the EX samples through all stages prior to failure.

The polypropylene samples showed some variation between samples of the same material. The copolymer samples behaved in a similar manner initially with CA reaching a higher maximum load than CB (1508.8N vs. 1477.3N) before both samples began extending further under decreasing loads. CA then failed at 14.9mm extension compared to 54.2mm in CB. The homopolymer samples showed very similar behaviour through maximum load (1504.7N in HA vs. 1499.0N in HB) and initially during extension under decreasing load however, HA then failed at approximately 21.6mm extension compared to 24.7mm in HB. Comparing the types of polypropylene is difficult as CB showed much greater elongation at failure than both HA and HB however, CA failed with a lower elongation than either of the homopolymer samples. All four samples reached a similar maximum load (range:

1477.3N – 1508.8N) with the copolymer samples performing more stiffly than the homopolymer samples until reaching this point and then becoming less stiff than the homopolymer samples.

Direct comparison of the polypropylene results to those of the Duraform samples cannot be done due to the very different dimensions of the polypropylene and ARRK samples, the polypropylene samples were approximately 60mm in length, 13mm wide and 5mm thick (homopolymer) or 6mm thick (copolymer). In order to allow a comparison, the results were converted to a stress-strain format. This was achieved by dividing the load by the initial cross-sectional area of the sample to give stress and the extension divided by the original length to give strain. The original length used was that of the narrowed test section. This means that any extension of the wider, unclamped sections was not accounted for and could lead to errors in the presented data, although this was likely to be small enough to be inconsequential.

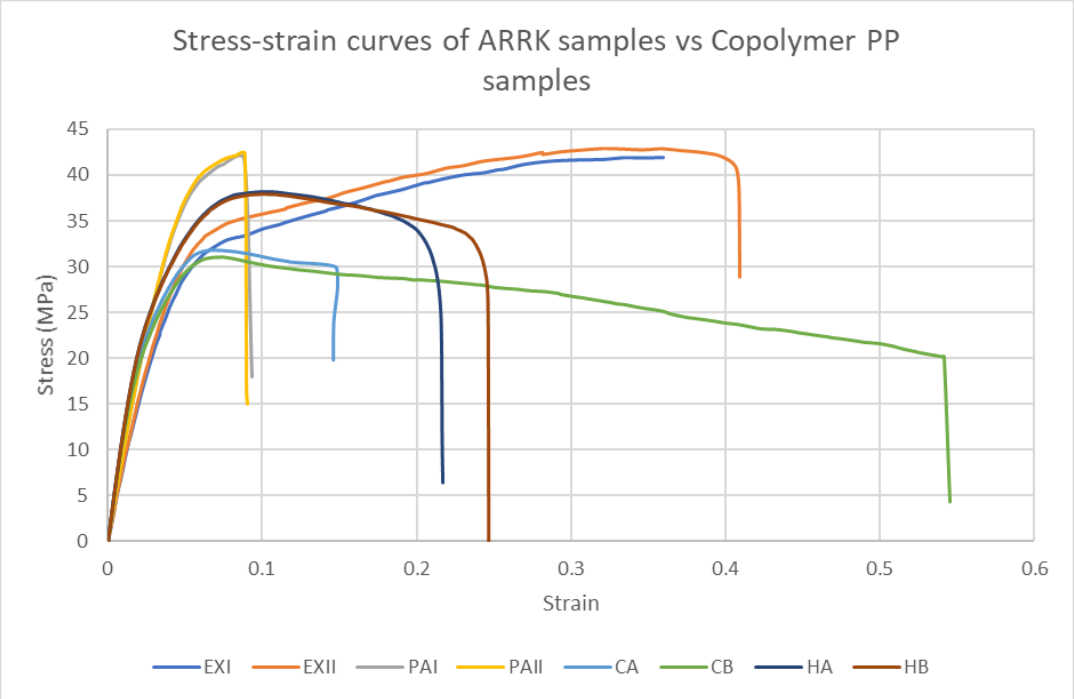

Figure 71 - Stress-strain curve of ARRK samples compared to PP samples

Figure 71 shows both Duraform PA and EX from ARRK compared to copolymer and homopolymer polypropylene. The samples began to diverge in performance beyond a certain point, so they will be looked at in more detail prior to and around that point.

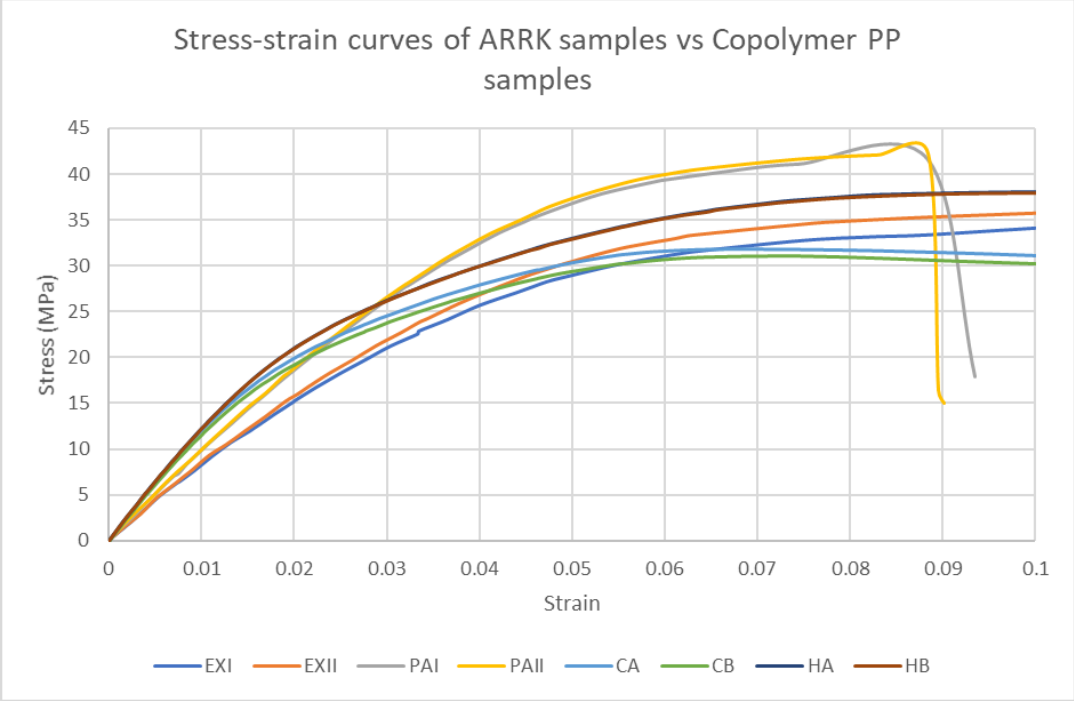

Figure 72 - Stress-strain curve of Duraform EX and PA samples vs. copolymer and homopolymer polypropylene samples, displayed to 0.1 strain

It can be seen in Figure 72 that there was an area of similar performance initially between the copolymer and homopolymer polypropylene samples however the Duraform PA samples were less stiff and the Duraform EX samples were less stiff again. Notably the stress continued to increase in the EX samples while decreasing in the copolymer samples. It took approximately 0.04 strain to reach a difference in stress of 5MPa. The PA samples were initially a closer match for the PP however past approximately 20MPa stress the PA samples began to diverge from the PP quite significantly, reaching a difference in stress of about 8MPa over the course of 0.02 strain. In comparison to the homopolymer samples the PA samples again showed a better match initially than the EX samples however the PA

samples went on to demonstrate much higher stresses at the same levels of strain before failing at around 42MPa slightly before 0.09 strain was reached. The EX samples had greater strain at particular stresses when compared to the homopolymer samples however from around 25MPa on the EX samples did display a similar gradient, albeit at lower stress and strain values.

From Figure 72 the Ultimate Tensile Strength (UTS) and elongation at break of each of the materials may be determined as below in Table 8. The Young's modulus was calculated using the values under 0.01 stress and was then used as the gradient of a line using a 0.2% offset to calculate the tensile yield strength and elongation at yield.

Sample	UTS (MPa)	Elongation at break (%)	Tensile Yield strength (MPa)	Elongation at Yield (%)	Young's modulus (MPa)
EXI	N/A	N/A	17.1	2.3	813
EXII	42.8	40.9	16.5	2.1	862
ARRK EX properties	48	47	37	5	1517
PAI	41.7	8.9	N/A	N/A	940
PAII	42.3	8.9	N/A	N/A	944
ARRK PA properties	43	14	N/A	N/A	1586
CA	31.8	14.6	18.0	1.7	1204
CB	31.1	54.2	17.4	1.7	1160
HA	38.1	21.2	19.7	1.8	1226
HB	38.0	24.4	19.8	1.8	1216

Table 8 - Properties of Duraforms EX and PA and homopolymer and copolymer polypropylenes. (EXI has incomplete properties due to not failing during the test)

The UTS value for EXII was approximately 10.8% lower than that quoted by ARRK on their materials datasheet while the elongation at break recorded was 13.0% lower. The tensile yield strength, elongation at yield and Young's modulus recorded were only approximately 45% of the values quoted by ARRK. Although EXI had only limited properties in the above table a similar behaviour was observed to EXII beyond the yield point but at lower stresses. The Duraform PA samples had very similar performance to one another, with the recorded UTS within 2.4% of the 43MPa quoted by ARRK, however the elongation at break was quite different at 8.9% experimentally compared to 14% quoted by ARRK. Simply looking at the values above it became clear that Duraform PA was very brittle compared to the other materials having experienced only a very small elongation at break and not having a tensile yield strength. The relative brittleness of Duraform PA was confirmed by the notched Izod impact strength, 32J/m compared to 74J/m for Duraform EX, and unnotched Izod impact strength, 336J/m to Duraform EX's 1486J/m. The Young's modulus was calculated based on the gradient of the curve in the initial elastic region, as per ASTM D638, using values up to 0.01 strain. The values for the Duraform samples were much lower than those given in the data sheet (942MPa compared to 1586MPa), EX was quoted at 1517MPa while achieving only 862MPa (EXII) and 813MPa (EXI) in testing and PA was quoted at 1586MPa while only reaching 940MPa and 944MPa.

4.3.5 Conclusion

Due to the large discrepancy in Young's modulus calculated and that reported by ARRK it was decided to use another method to calculate Young's modulus. Based on the brittleness observed in Duraform PA it was discounted as a possible prototype material.

4.4 Extensometer testing

An extensometer was employed to more accurately determine the Young's modulus of the Duraform EX samples, using ISO 527 methods.

4.4.1 Method

Samples were mounted in the Instron universal testing machine. An Instron 2620-603 mechanical, dynamic extensometer (accuracy ±0.15%) of gauge length 10mm was used, giving a limit of 1mm extension. The extensometer was attached to the sample in the test region using two elastic bands as supplied and per the operating instructions as shown in Figure 73. Per ISO 527, extension was applied at 1mm/min to the 1mm limit. The load at each data point was then divided by the cross-sectional area (d × t) to give the stress at each instant. Data was recorded through the Instron Bluehill software and processed in Microsoft Excel and MATLAB.

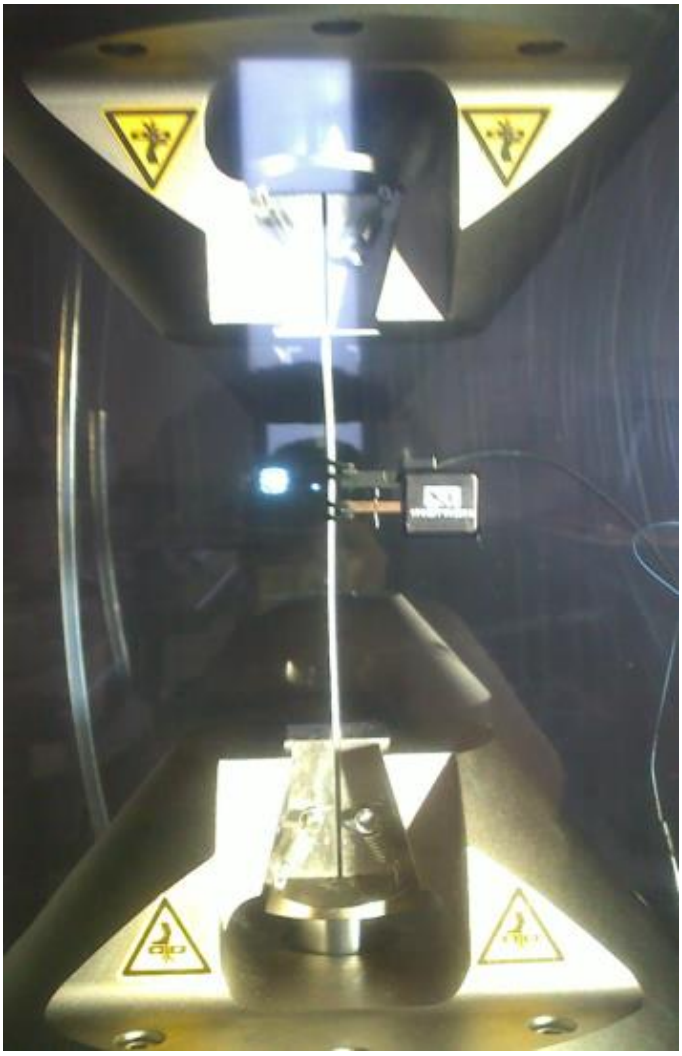

Figure 73 - A sample of Duraform EX mounted in the Instron with the extensometer visible on the right hand side of the sample

4.4.2 Specimens

Six SLS formed dumbbell shape samples of Duraform EX were purchased from ARRK Europe. Each sample was labelled from A to F and measured (dimensions identified, Figure 68, and included below, Table 9). Three measurements were taken for d and t of each sample and averaged to give a final value. All measurements were taken with a set of Vernier callipers. It was noted that sample E felt notably grainier than the other samples and that this was also visible although without any clear alignment and was not believed to be related to layer build up. Layers were built across the ‘d’ dimension (see Figure 68) and so were perpendicular to the

loading direction. These samples did not conform to the size criteria of ISO 527, being too thin, and is recommended that if further testing were to be done on these materials then standardised samples should be produced to the requirements of ISO 527.

Duraform EX	l (mm)	d (mm)	t (mm)
A	68	1.27	12.61
B	68	1.24	12.70
C	68	1.27	12.64
D	68	1.26	12.70
E	68	1.30	12.66
F	68	1.26	12.65

Homopolymer	l (mm)	d (mm)	t (mm)
A	100	4.06	10.24
B	100	4.00	10.20
C	100	4.01	10.41
D	100	4.12	10.06

Copolymer	l (mm)	d (mm)	t (mm)
A	100	4.74	10.28
B	100	4.77	10.08
C	100	4.78	10.09
D	100	4.78	10.17

Table 9 - Dimensions recorded from samples

A set of samples was produced, four of homopolymer (North Sea Plastics, Glasgow, UK) and four of copolymer polypropylene (North Sea Plastics, Glasgow,

UK), to the required dumbbell test shape by milling from standard sheet. The samples were not notably rough on the edges. In future testing these samples should be made to standard sizes as recommended for the SLS samples. The polypropylene samples were measured the same way as the Duraform EX samples.

4.4.3 Results

Each sample of Duraform EX was recorded without incident. The samples showed a small initial curve followed by a nearly linear region in each case.

Per ISO 527 Young's modulus was calculated using $E_t = \frac{\sigma_2 - \sigma_1}{\varepsilon_2 - \varepsilon_1}$, with values of ϵ_2 = 0.0025 and ϵ_1 = 0.0005 and corresponding stresses to those strain values. The values calculated for Young's modulus of Duraform EX samples were within 93MPa of each other (max 1.484GPa, min 1.391GPa) with a mean value of 1.439GPa.

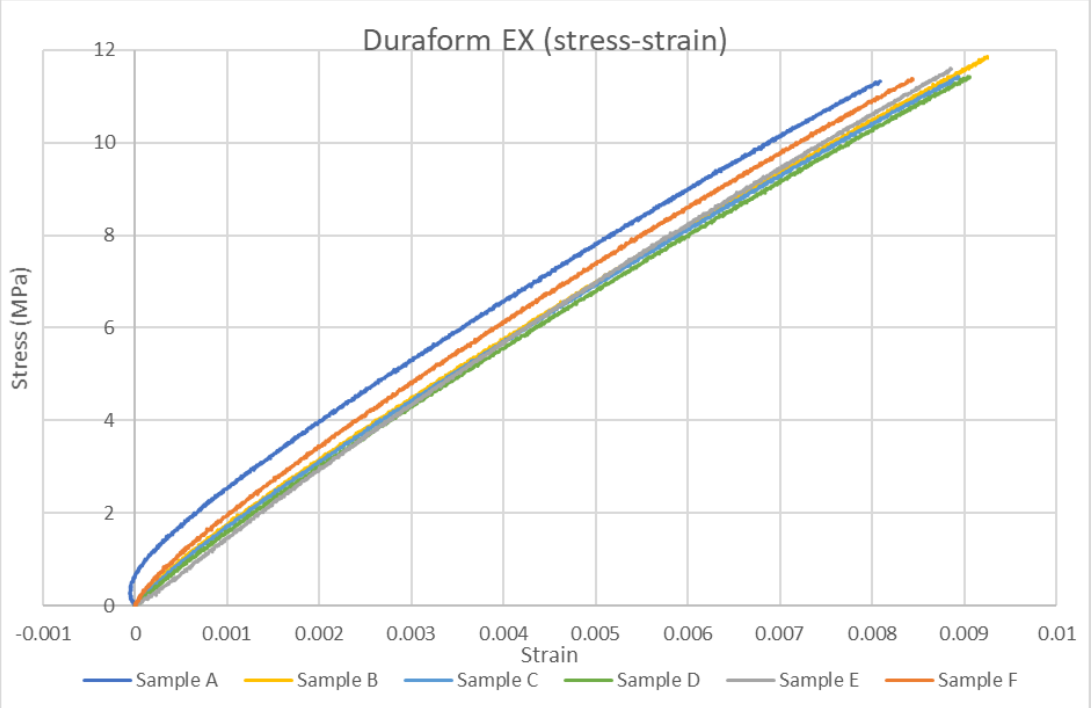

Figure 74 - Stress-strain graphs displaying ARRK samples A to F

The same method was used for the homopolymer samples with the range of values calculated as 131MPa (minimum 1.752GPa, maximum 1.621GPa). The mean value was 1.680GPa

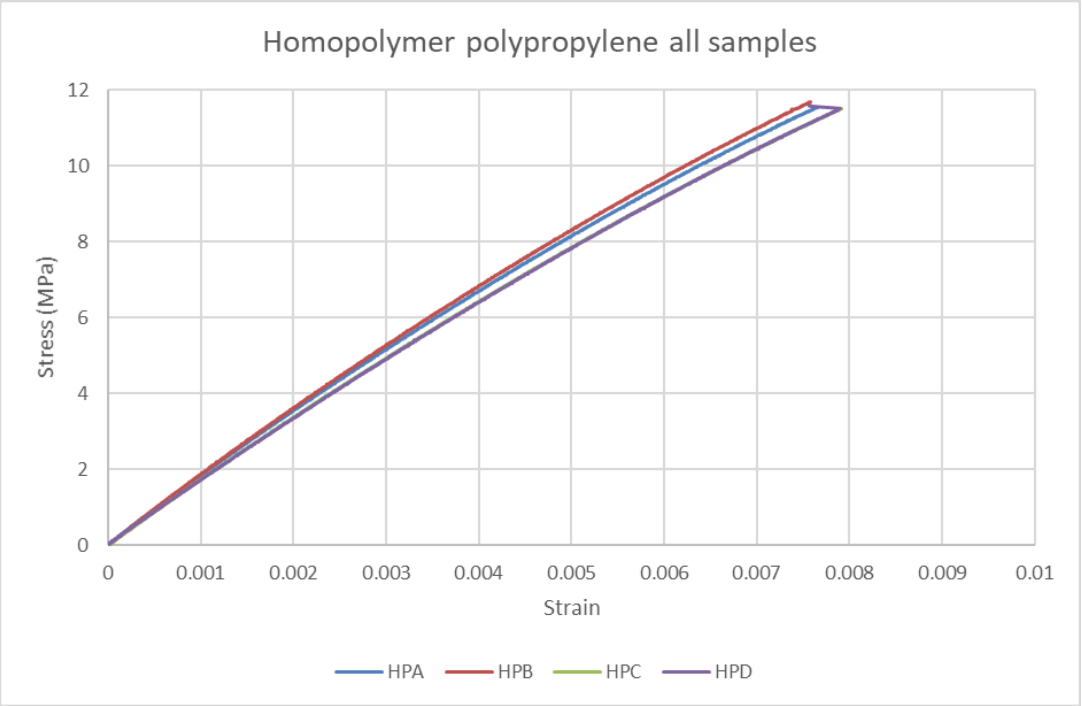

Figure 75 - This graph displays the stress strain results of the extensometer testing carried out on homopolymer polypropylene samples.

It was observed that in homopolymer sample D a sharp decrease in strain occurred although the cause of this is unknown.

During testing of the first of the copolymer samples noises were heard during testing. On plotting the results two significant anomalies were seen on the graph, shown in Figure 76, at points that corresponded to sounds heard at the time. It was determined that this was the result of the wedge grips (see Figure 73) slipping slightly due to the pressure being too low. The pressure was duly adjusted, and the sample retested, and the other samples tested. The sample was not considered to have failed and was retested and those results included in analysis.

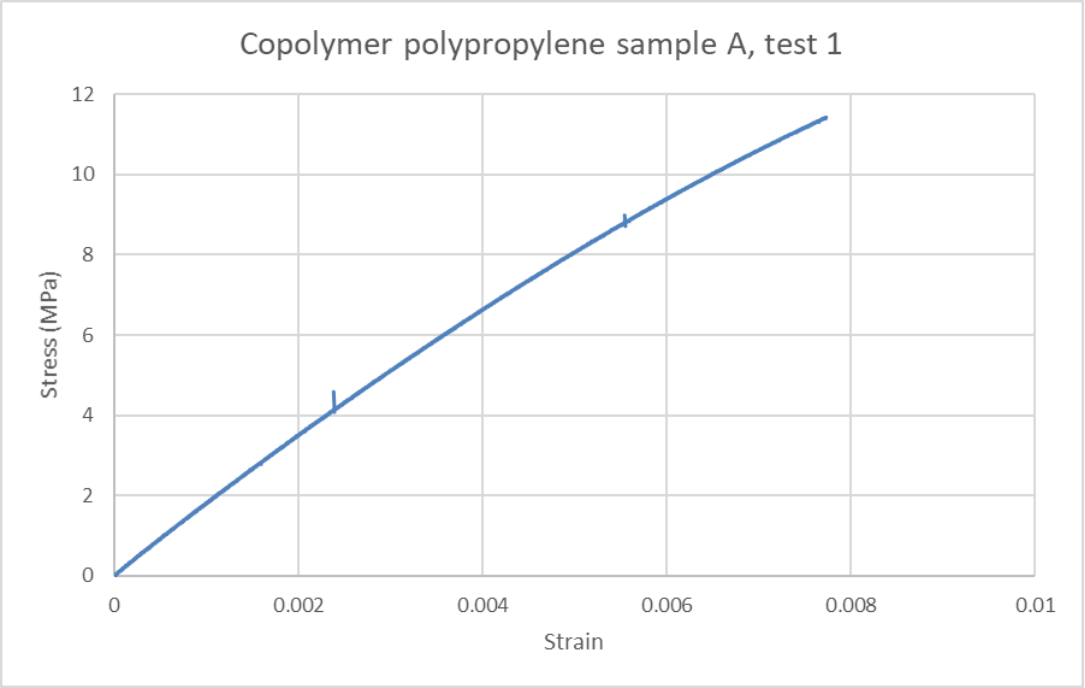

Figure 76 - Graph showing the anomalies on the extensometer testing of copolymer sample A during the first test.

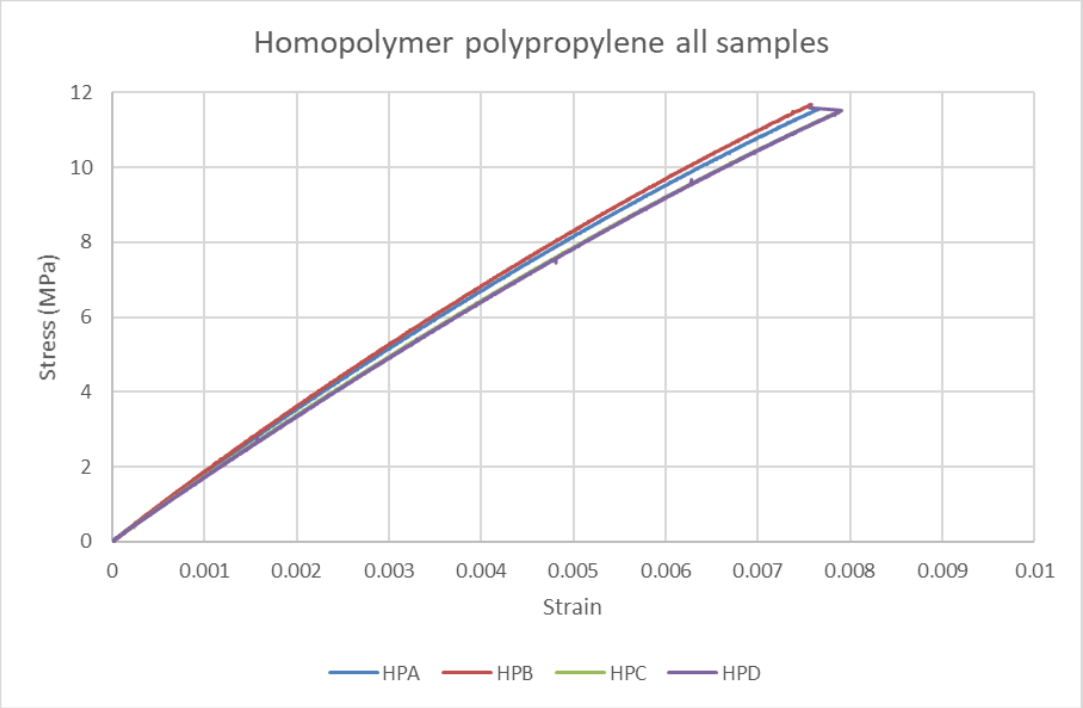

Figure 77 - Graph showing the stress strain results of the extensometer testing carried out on copolymer polypropylene samples.

The copolymer samples had a range of Young's modulus of 12MPa (minimum 1.660GPa, maximum 1.673GPa) with a mean of 1.665GPa.

4.4.4 Discussion

During data processing, small peaks became visible apparently indicating sudden increases in stress (see sample HPD in Figure 75 for examples of several of these). As these peaks only lasted for a single sample point (0.001s) they were determined to be unlikely to have been caused by slipping of grips or extensometer and were likely caused by noise in the system.

The Young's modulus of the Duraform EX was much lower than that of the polypropylenes however this was to be expected from the previous tensile testing. The mean value of the EX samples was 1.439Pa compared to 1.680GPa for homopolymer and 1.665GPa for the copolymer. The Young's modulus for Duraform EX is 85.7% of that of the homopolymer and 86.4% of that of the copolymer.

4.4.5 Conclusion

In terms of comparing the quoted values of Duraform EX to those determined experimentally the Young's modulus appears to be 94.9% of what was quoted. If a similar percentage was assumed for the flexural yield strength, then it would have been around 39.9MPa and the ultimate flexural strength would be 43.7MPa. These results were deemed to be adequate to confirm those quoted by ARRK.

The behaviour of Duraform EX was found to be significantly different to both copolymer and homopolymer polypropylene and cannot be considered to be an adequate analogue to either, having a lower Young's modulus, greater elongation at yield and comparable UTS and tensile yield strength in ideal testing conditions. In any prototype model, the sample will be tested along and across build layers included as part of the SLS process rather than simply along build layers as in these tests. Further testing should be carried out to test the properties of Duraform EX

when pulled across the build layers however the performance is likely to be substantially reduced unless full bonding occurs across layers.

While these results suggested the values provided by ARRK Europe may be trusted, these values did not describe the performance of the material after any moisture absorption occurs, for example (Jia, Fraenkel, & Kagan, 2004) showed that even 1% increase in mass by water absorption can lead to a reduction in yield stress of nylon (which Duraform EX is largely made of) by as much as 30MPa. It is recommended that prior to any longer-term testing, tests be carried out to determine material properties after equilibrium for moisture absorption is achieved under testing conditions.

It was deemed that samples could be produced using Duraform EX in an SLS process in order to test design changes and validate FEA data however ultimately any design would need to be verified in the final material produced using the intended process, in this case likely copolymer polypropylene through injection moulding.

4.5 P3 toe tests

4.5.1 Specimens

Two prototypes were produced by ARRK Europe from Duraform EX via SLS and were labelled 1 and 2 respectively. These each had a 56mm diameter rubber ball (It's my party, Hixon, UK) inserted into the heel space. It was acknowledged that failure of the balls was seen at the P5 level of heel loading however to eliminate the balls at this point based on two results was deemed premature. Two more samples were produced and labelled 3 and 4. Samples 3 and 4 included a rubber ball but also a fibreglass blade, Figure 78, as shown in Figure 79. The blade profile was develop based on the outline of the keel when viewed from above. This was not an

optimised solution for energy return but did offer some protection to the blade by keeping the outer dimensions matched to that of the keel. Optimisation of the blade is recommended for further work, both in terms of profile and with respect to applying reinforcement to the initial shape to tune the response based on the intended mass and activity level of the user. This blade profile was only to serve as a first step in determining the effect on the keel of insertion of a flexible member and to indicate the changed stress distribution on the keel this caused. The blades were cut from 4mm fibreglass (polyester gelcoat and resin, 3 layers of 600g chopped strand matting – East Coat Fibreglass Supplies, South Shields, UK). The blades were pushed into place, anchoring in the corner while the 2mm thick central cut out held snugly to the centre of the keel. This arrangement was likely to be adequate for static load testing however with the load/unload cycle of cyclic testing this was likely to lead to wear occurring between the blade and the keel. As such it is recommended that a method for fixing the blade in position be developed, potentially through the cosmesis or alternatively an epoxy resin to provide bonding and location to the blade.

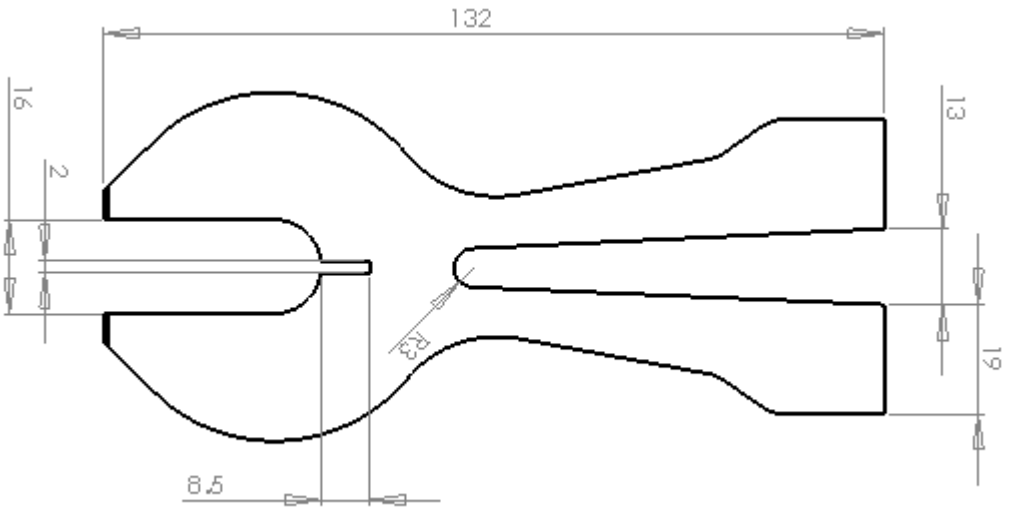

Figure 78 – The design used for the blades for samples 3 and 4. All dimensions in mm

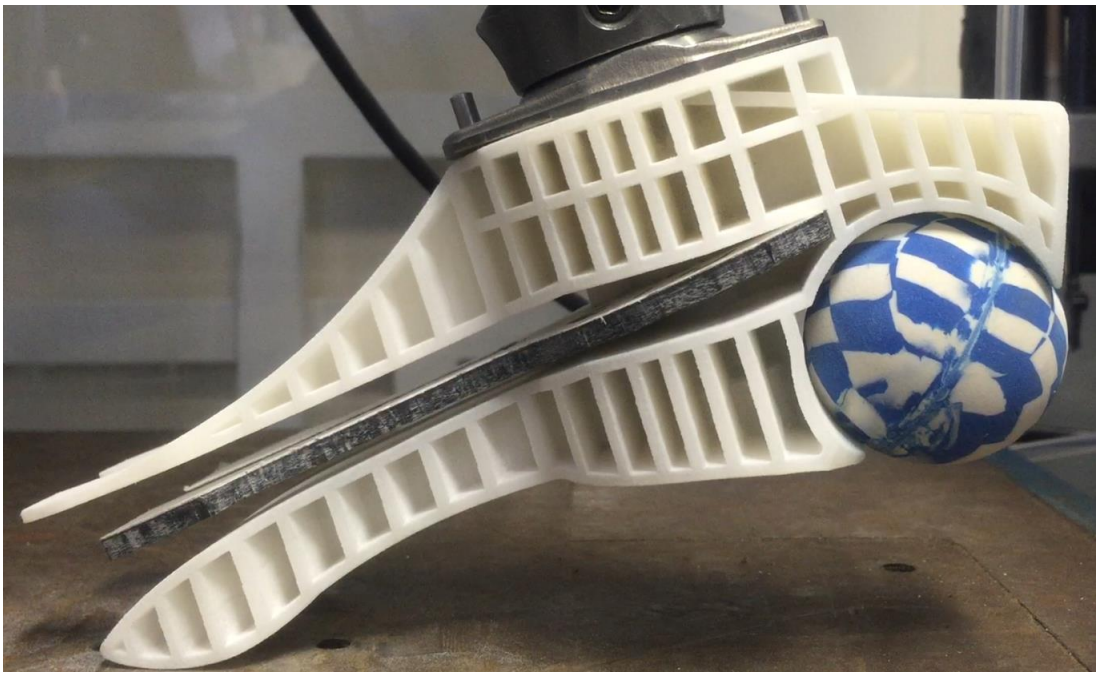

Figure 79 – Sample 3 including inserted blade prior to testing

4.5.2 Method

The same method as had been used on the original Strathclyde foot was used, namely:

The adapter was set up for the required loading condition (heel or toe), which gave the loading angle required (20° for toe loading, 15° for heel loading). The adapter was then mounted into the Instron machine with the grip closed on the topmost part. That the alignment was correct was determined using a goniometer. The foot was then attached via a pyramid attached to the foot and a pyramid adapter mounted on the bottom of the brass rod. The crosshead of the Instron was then lowered until the foot barely contacted the baseplate at which point the crosshead was locked. The load was increased at a rate of 175N/s until the ultimate static test force upper limit, 3220N, was met (see Table 4), for loads for all P-levels). The ultimate static test load was maintained for 30s at which point the load was reduced at a rate of 175N/s until 0N load was recorded. The test was to be stopped prior to completion if the sample was observed to fail or the setup became unsafe in any way.

4.5.3 Results

Samples 1 and 2 broke before reaching the P3 ultimate static load. Sample 1 broke prior to reaching 100N however the crosshead continued to move into further contact before the limit was tripped leading to a large spike in the results as seen in Figure 80.

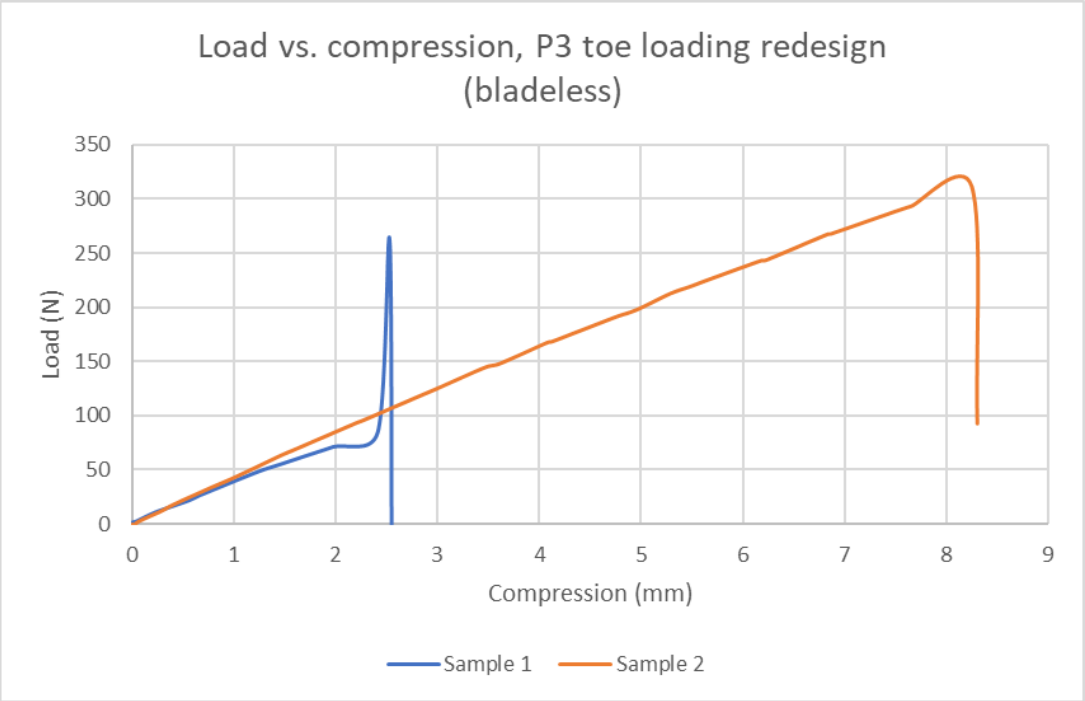

Figure 80 – Load vs. compression of Strathclyde redesign samples 1 and 2 tested to the P3 toe loading condition

The lower toe sections snapped but remained attached to the keel while the upper toe sections broke off entirely (see Figure 81). A puff of dust was seen from the underside of the break in the lower toe section. Sample 2 fared better reaching approximately 310N before the bottom toe sections separated entirely from the keel (see Figure 82).

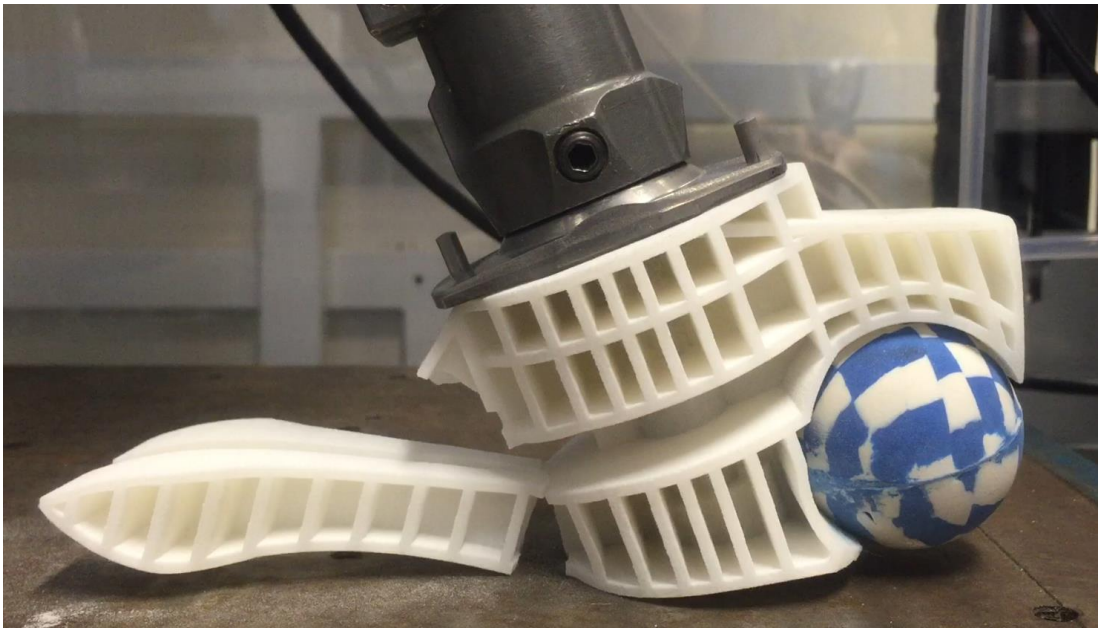

Figure 81 – Sample 1 of the Strathclyde foot redesign immediately after failure

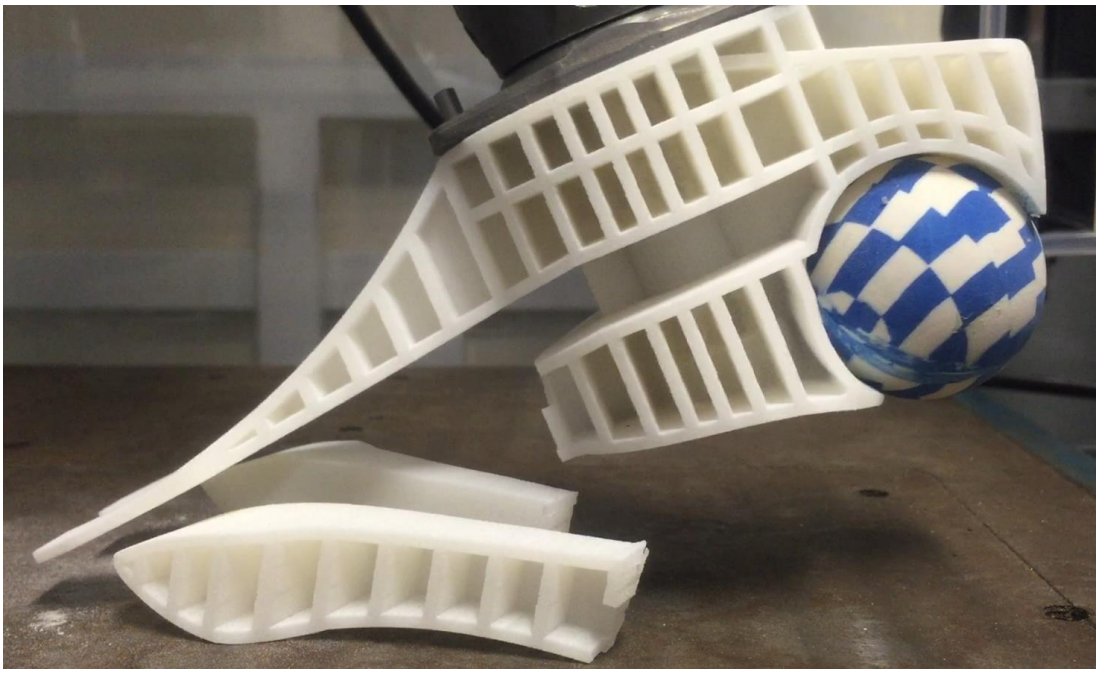

Figure 82 – Sample 2 of the Strathclyde foot redesign immediately after failure

Sample 3 reached 540N at failure (see Figure 83) but failed in a similar location to samples 1 and 2. Figure 84 shows sample 3 immediately after failure demonstrating the break. A fine dust was observed coming from the sample as it

failed. When the surfaces were examined it was seen that there was little deformation of the surfaces suggesting a brittle failure. The layers of the keel were built in the vertical direction with the toe and heel in contact with the base layer. The failure did not occur along the layers however, the step between layers may have acted as a stress concentrator allowing the crack to propagate. In sample 2 it may be seen that failure crossed the vertical support (see Figure 82). This section of the failure did occur between build layers and as such may indicate that incomplete bonding is present between layers in the sample however, the overall cause of failure was not delamination of layers in this case.

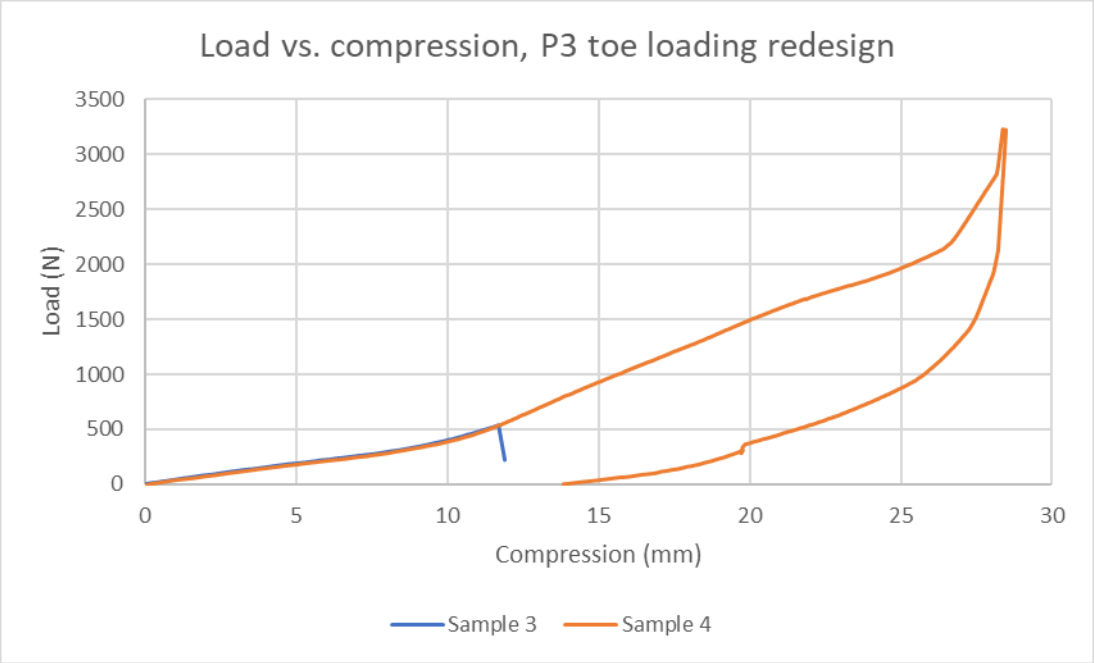

Figure 83 - Load vs. compression of Strathclyde redesign samples 3 and 4 tested to the P3 toe loading condition

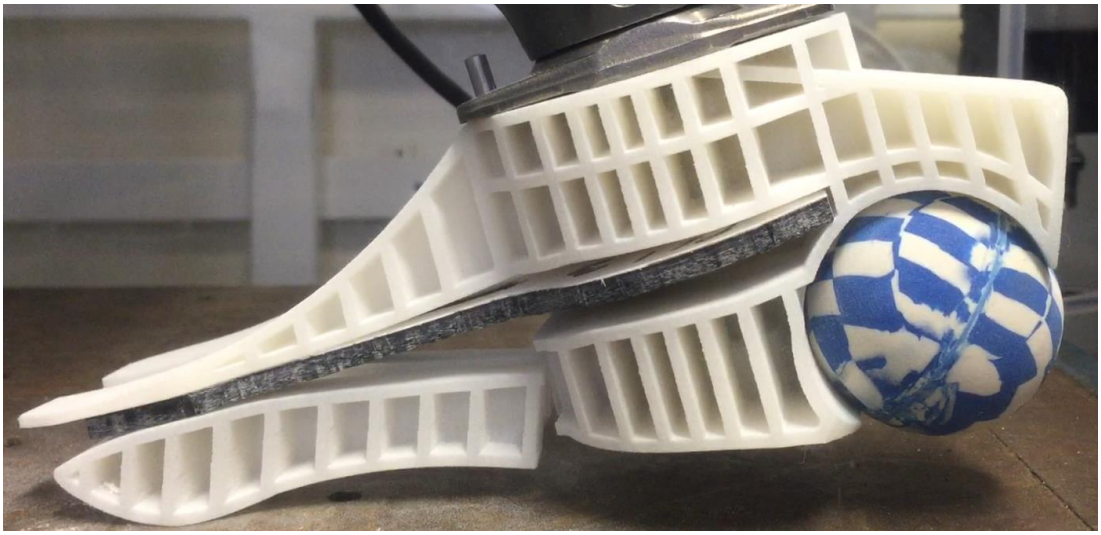

Figure 84 – Sample 3 of the Strathclyde foot redesign immediately after failure

Sample 4 achieved the maximum load for the P3 toe loading condition and returned to zero load with no sign of damage or lasting deformation (see Figure 83). The lower toe section, blade and upper blade section were observed to slide over one another as the load was applied. On unloading the blade was seen to have moved forward from its initial position by approximately 2mm.

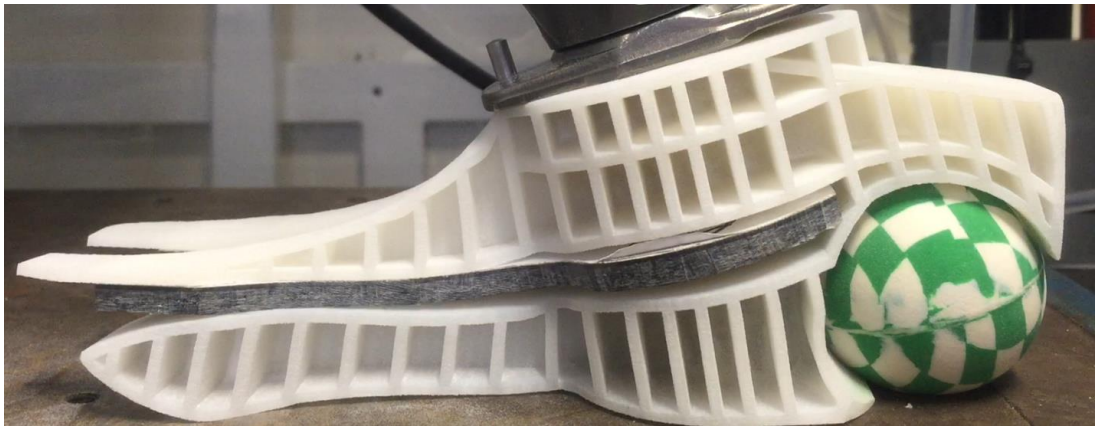

Figure 85 – Sample 4 at maximum ultimate static load for P3 toe loading

The energy input and output were calculated for sample 4 in the same manner as for the original Strathclyde foot. The input energy was calculated as 27.87J and

the output as 8.62J giving a 19.25J energy loss, corresponding to a 31% energy return.

4.5.4 Discussion

The failure of samples 1,2 and 3 was indicative of a design issue as each failed in approximately the same area however, the puff of white dust observed in sample 1 suggested the manufacture of the samples was partially responsible. The Selective Laser Sintering (SLS) process is based on a fine plastic dust being fused using a laser (see section 4.2.3 Selective Laser Sintering for more detail). If the plastic was not adequately heated then incomplete fusion may have occurred which would have led to weaker material properties than expected and, in the case of sample 1, some of the improperly bonded material being released in a violent failure. The nature of SLS construction tends to build in layers to the product which can lead to more rapid failure due to incomplete fusion between layers. Based on the FEA modelling of the keel the bladeless samples would have been expected to reach a load of 592.4N before yield at the central vertical rib of the main block however samples 1 and 2 failed at 84.7N and 311.7N respectively, apparently at the underside of the lower toe section (point 3 in section B3.6 Whole design evaluation, predicted to reach yield at 669.8N load). The bladed samples were predicted to reach yield at 592.4N, on the top surface of the lower toe section however sample 3 failed at 540N on the underside of the lower toe section (point 3 in section B3.7 Duraform EX models, predicted to fail at 850.1N).

In terms of energy storage and return the return was slightly lower than what was returned by the original Strathclyde foot, without rods, at the P3 testing level (30% in redesign sample 4 vs. 33% in samples 1 and 2 of the original Strathclyde foot). This was likely due to a difference in the materials used, with the original

polypropylene likely having a greater elongation at yield with a similar Young's modulus leading to better energy return performance.

A thorough failure analysis is recommended after any further testing.

4.6 P3 heel tests

4.6.1 Specimens

Sample 1 and 2 had both suffered damage during the toe loading condition of testing however based on the observed pattern of loading during testing of the original Strathclyde foot it was deemed that this damage would not affect the load carrying capacity of the rear of the foot. As such samples 1 and 2 were to be reused.

4.6.2 Method

The adapter was set so that the heel would contact the baseplate at 15° with the load increasing at 175N/s until the upper load of 2240N was reached. This load was to be held for 30 seconds before being reduced at a rate of 175N/s until zero loading was achieved.

4.6.3 Results

Sample 1 was observed to fail during testing. The ball deformed until the keel made contact after which loading continued to increase. A cracking sound was heard however the test continued. A break was observed in the keel in front of the ball as seen in Figure 86. Sample 2 was able to successfully complete the test without permanent damage or deformation. As such sample 3 from toe testing was included in heel testing. Sample 3 was able to successfully complete the test without permanent deformation or damage but did slip on the plate at approximately 3080N.

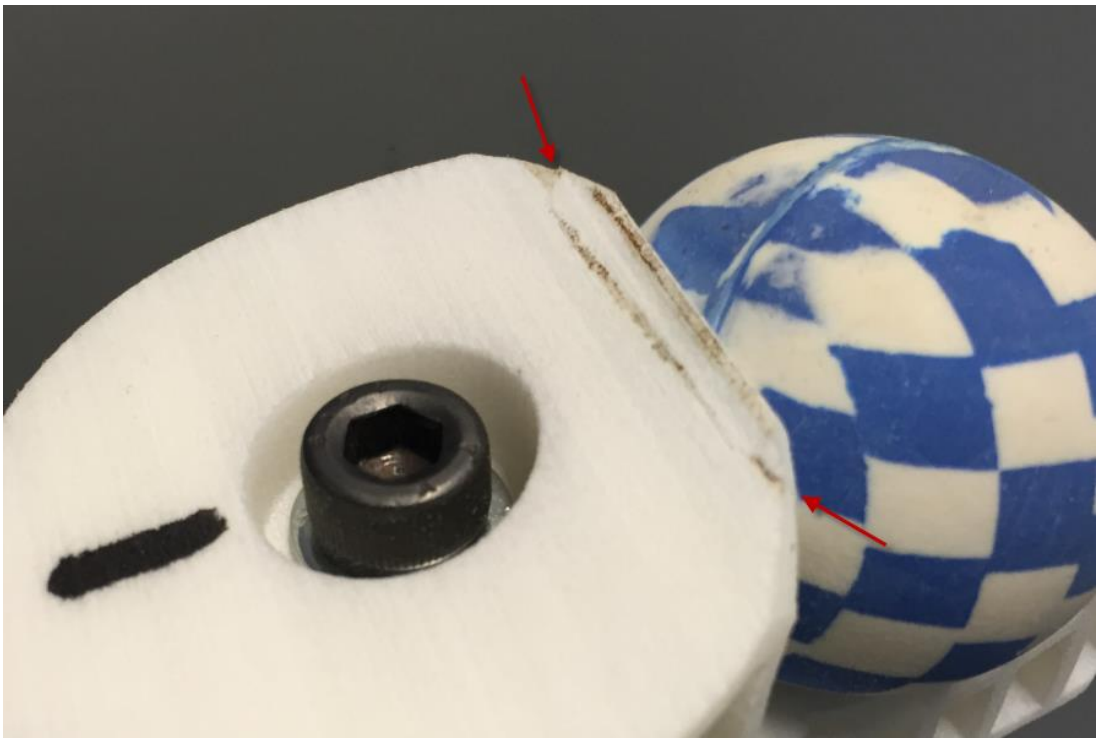

Figure 86 – An image showing the fracture in sample 1 from P3 heel testing. Arrows indicate the edges of the dark line highlighting the break

The load vs. compression profiles of the three samples were quite different from one another with the keel contacting the baseplate at approximately 8.1mm compression for sample 1, 7.6mm compression for sample 2 and 10.9mm for sample 3 as seen in Figure 87. Sample 2 showed a maximum compression of 13.8mm while sample 3 reached 14.1mm compression (see Figure 88). Despite the break sample 1 was the stiffest overall, only reaching a maximum of 13.0mm compression.

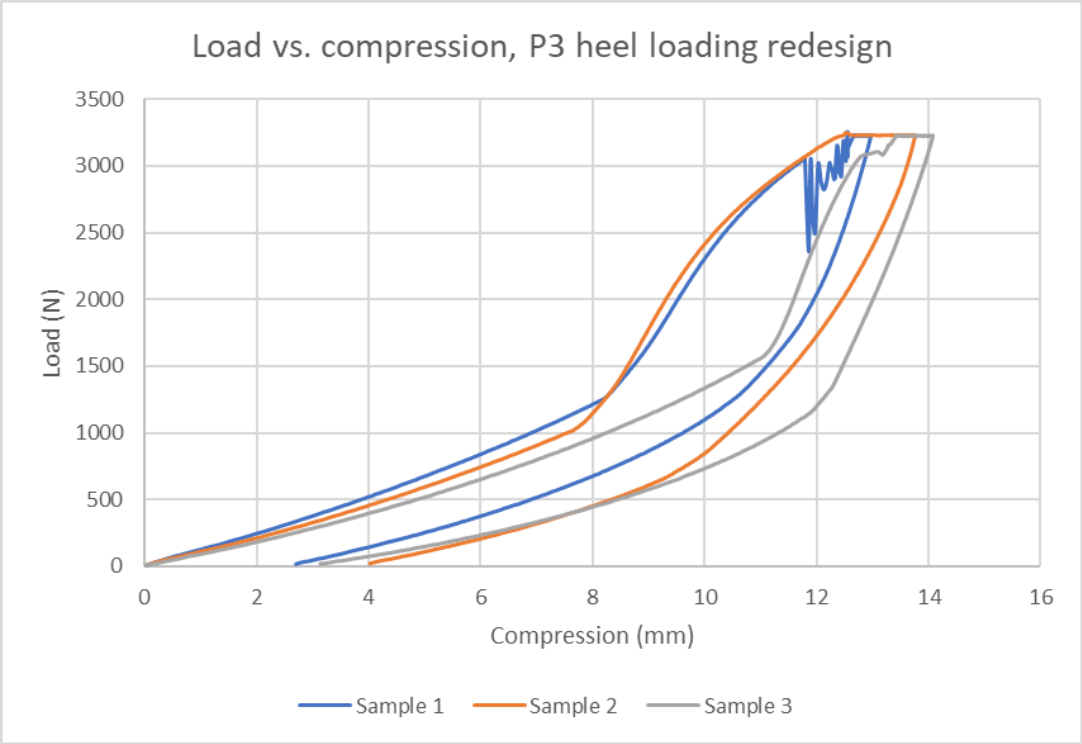

Figure 87 - Load vs. compression results for Strathclyde redesign under P3 heel testing

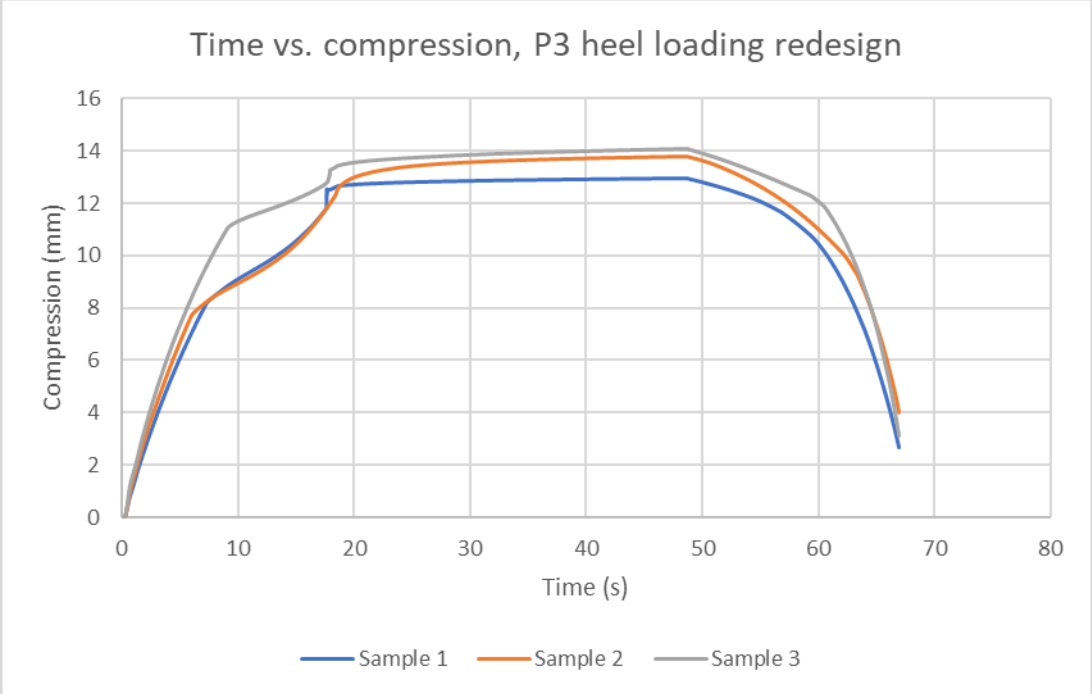

Figure 88 - Time vs. compression results for Strathclyde redesign under P3 heel testing

The energy input and output were again calculated for samples 2 and 3; sample 1 was excluded due to failure. Using the same method described earlier the energy input was calculated for sample 2 at 18.64J with an output of 8.68J showing a 9.96J loss. Sample 3 required less energy input at 15.29J with and output of 8.31J giving an energy loss of 6.98J.

4.6.4 Discussion

Sample 1 suffered from a fracture during testing and so was not considered a pass for the purposes of this test. Sample 2 did pass with no visible damage or permanent deformation. With one pass and one fail a third sample was introduced and was found to pass. This means that overall a pass could be declared according to ISO 10328 which required a minimum of two passes with a single replacement permitted in case of a failing sample. The reason for the failure of sample 1 was not clear, the loading condition for all three feet was the same and samples 2 and 3 both survived. The manufacturing process could have introduced a weakness either through inclusion or through incomplete fusion of the base material.

ISO 10328 is not intended to serve as an ongoing test of performance during production and is limited in testing to two samples per test condition with a single substitution permitted in case of failure. Surviving samples may be used in other tests however this does not increase the number of substitutions permitted. A permissible failure rate of one in three samples would be very high when scaled into production quantities and so the standard would not be adequate as a control in production and an alternative, preferably non-destructive, test would be required internally following successful meeting of the ISO 10328 standard.

The properties of the surviving samples were quite different with approximately 540N difference in force required to make the keel contact the baseplate (1017N for sample 2, 1556N for sample 3) while the difference in compression was

approximately 3.3mm (7.7mm for sample 2, 11.0mm for sample 3). The difference in compression and load required of the balls may have been due to the way they were inserted into the keels. Each ball had to be squeezed through a narrow gap between two sections of the keel. It is possible that the ball in sample 3 could have been protruding slightly which would have given additional compression length if the ball were pushed into place during testing. This could also account for the reduced stiffness of the system compared to sample 2 as in sample 3 the ball would initially deform then move under loading giving a greater apparent compression for the same load as sample 2. The effect would have to have been gradual as there are no sudden changes of gradients that would indicate a sudden movement of the ball into the keel. Alternatively, geometric and material inconsistencies between the balls could have accounted for the difference in performance observed.

Sample 3 had a lower energy input than sample 2 (15.29J compared to 18.64J) but returned a greater percentage of it overall (54.4% for sample 3, 46.6% for sample 2). There was little difference in the absolute value of energy returned by either foot with 8.68J calculated from sample 2 and 8.31J from sample 3. Sample 2 was observed to have undergone 1.34mm of creep as the maximum load was held compared to only 0.66mm for sample 3 which would have an adverse effect on energy return observed.

4.6.5 Conclusion

The Strathclyde redesign may be said to have passed the P3 level of the ultimate static loading test for the heel condition. Testing should continue to the P4 level.

4.7 P4 Toe test

4.7.1 Specimens

Samples 1, 2 and 3 all failed during P3 testing. Only sample 4 remains without deformation or damage and so will be the only sample tested.

4.7.2 Method

The foot was to be set up the same way as described in section 4.5.2 Method, with the exception that the upper load limit was raised to 4130N.

4.7.3 Results

Sample 4 was able to complete the test successfully, without showing any damage or permanent deformation. The sample was observed to slip slightly during initial loading and again when unloading. The foot followed the pattern observed in loading during the P3 toe tests where the lower toe section deflected into the blade which then deflected into the upper toe sections. The blade could be seen to slide forward slightly as the lower toe section pressed against it. Subsequently the rear of the foot contacted the baseplate with the ball contacting initially before the keel then contacted (see

Figure 89). This was observed in reverse during unloading. The slip in loading may be seen at 1.3 seconds in Figure 90. At approximately 2 seconds a subtle change in gradient was observed, indicating the contact between the lower toe sections and the blade. At 14.4 seconds, the keel contacted the baseplate resulting in a sudden gradient change due to the reduced compression of the system. At 67 seconds, a change in gradient was observed, corresponding to the keel being removed from contact. Further contact changes are less clear but the slip during unloading was observable at 76.5 seconds.

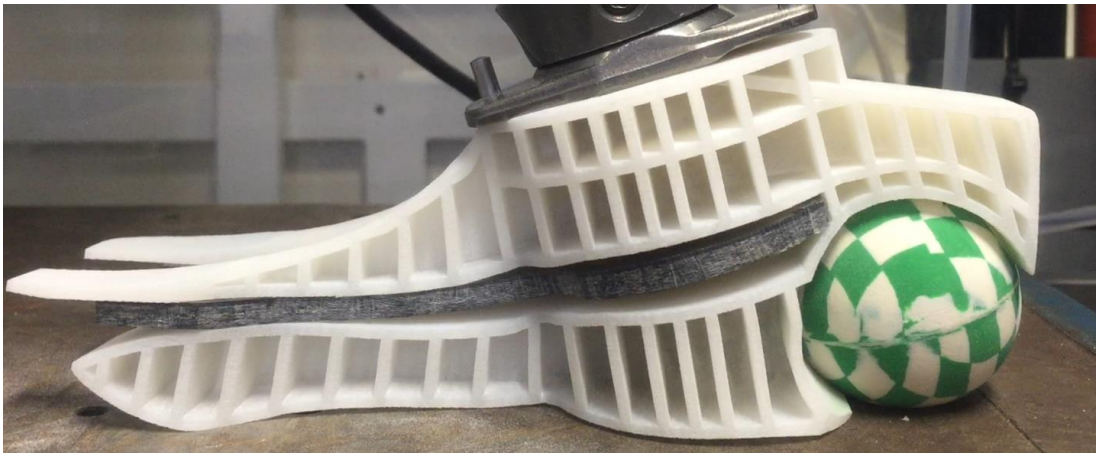

Figure 89 – Sample 4 under maximum P4 ultimate static testing toe load

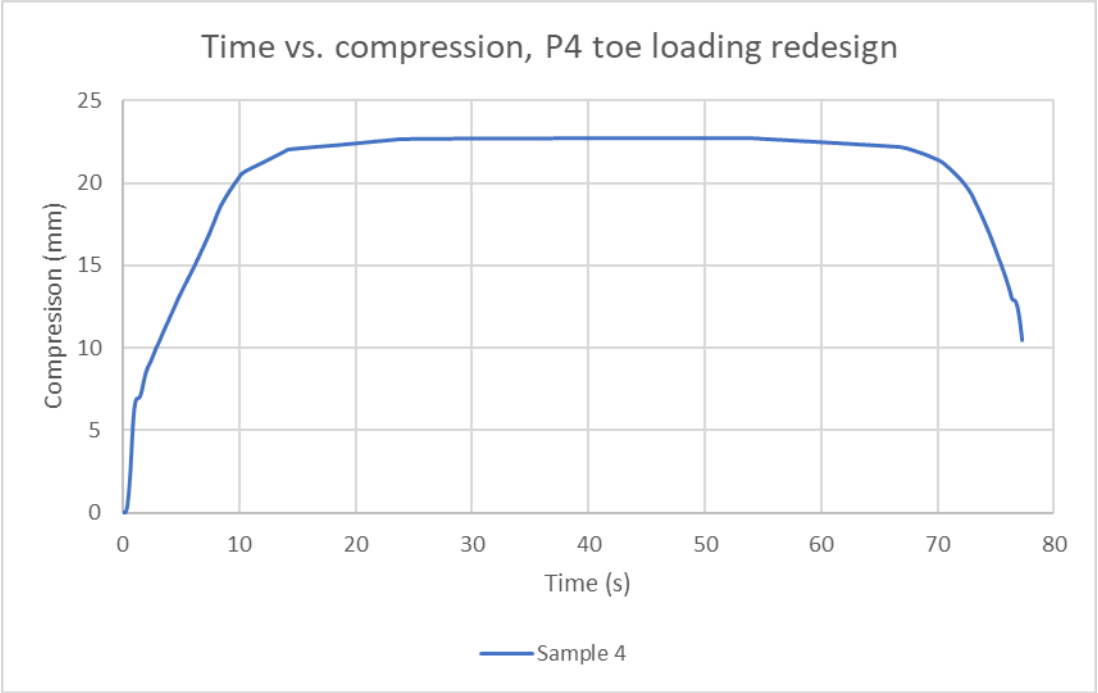

Figure 90 – Time vs. compression results for sample 4 of Strathclyde redesign under P4 toe testing

Many of the same features seen in Figure 90 may also be seen in Figure 91 however in this case the gradient was representative of stiffness. The sample was clearly stiffest once the keel had contacted the baseplate at the rear. 0.07mm of creep was observed while the maximum load was held.

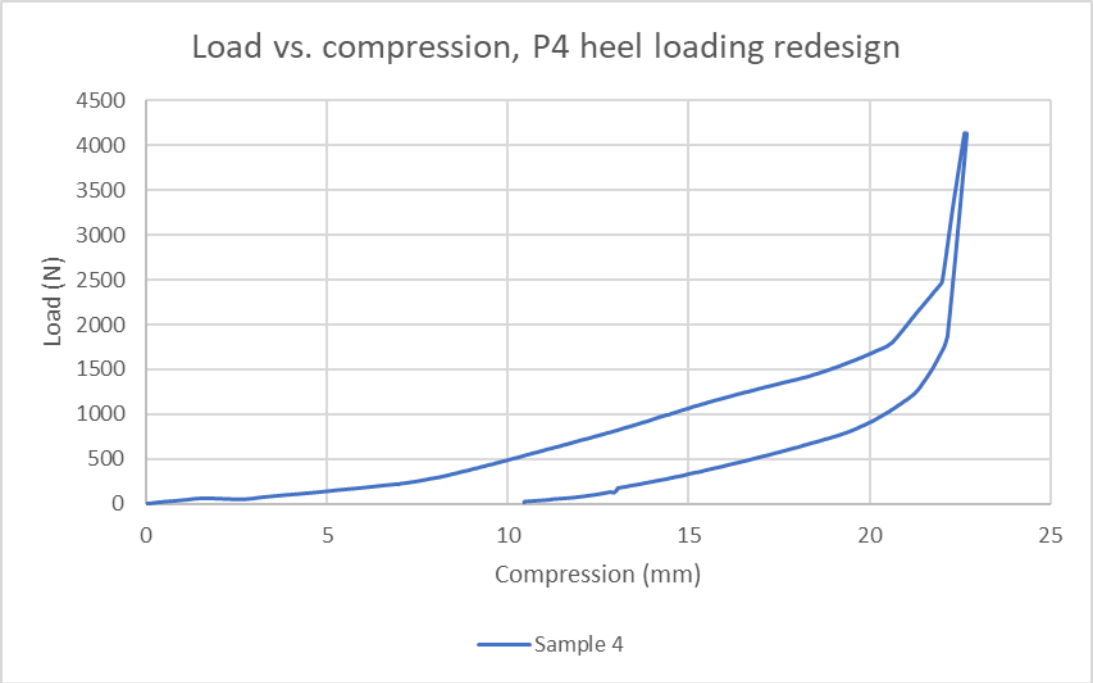

Figure 91 - Load vs. compression results for sample 4 of Strathclyde redesign under P4 toe testing

As before the energy input and output was calculated for the sample with the regions used defined using the same method as previously. The energy input was found to be 18.55J with a return of 7.83J giving a total energy loss of 10.72J.

4.7.4 Discussion

The energy return in sample 4 at the P4 level was 42% which is higher than under P3 testing (30%). There is a 5.8mm decrease between maximum deflections observed between the P3 and P4 level, see Figure 92; this would be expected if some deformation had remained from the previous round of testing. It is recommended that measurements be taken before and after further testing to determine whether this is occurring. This remaining deformation led to a reduced overall compression before the rear of the foot contacted the baseplate and a higher apparent stiffness. This higher stiffness in turn contributed to the higher percentage energy return as the material underwent a lower strain and did not extend as far into

the plastic deformation zone, permitting the material to better spring back to the initial loading condition. Due to the reduced overall deformation at the P4 level a lower absolute energy was returned (7.83J) compared to that at the P3 level (8.62J).

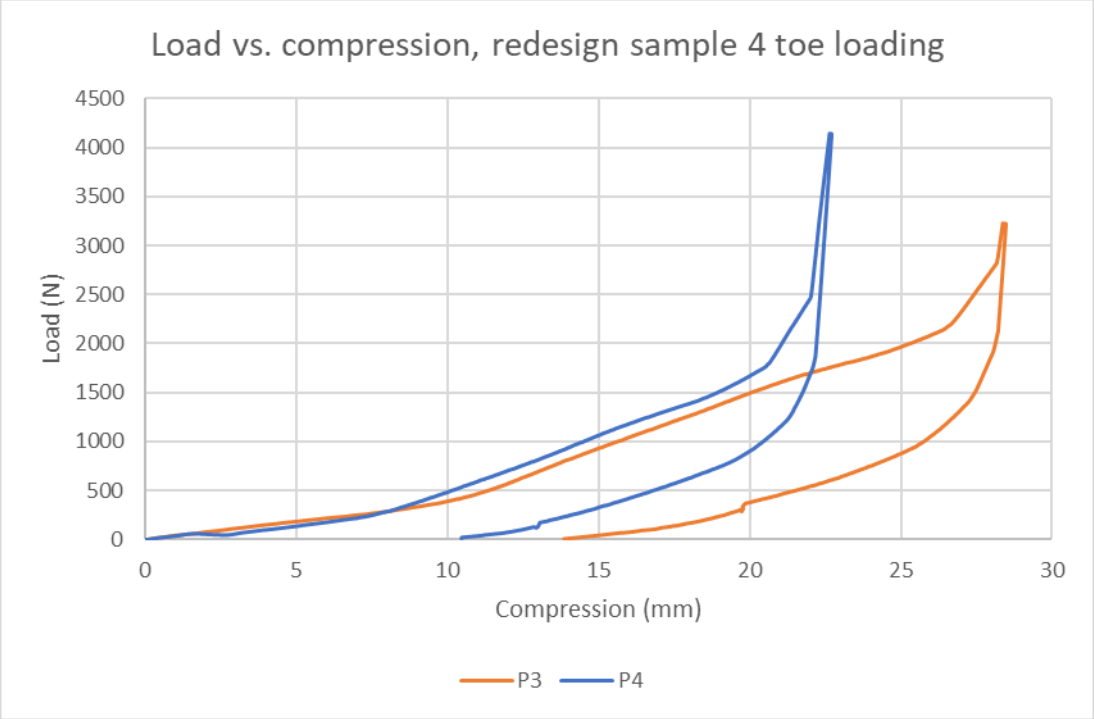

Figure 92 – Comparison of load vs. compression of Strathclyde redesign sample 4 at P3 and P4 ultimate static loading tests

The foot was observed to have returned to its original form post testing although as it appears to have remained deformed by 5.8mm after P3 testing it is possible that deformation has remained and is not apparent. It is recommended that key dimensions be recorded before and after each further test.

4.7.5 Conclusion

The sample did not meet the standard required for the ultimate static test to the P3 level, having suffered significant permanent deformation, and should not be considered in terms of passing to the P4 level subsequently. Deformation itself is not a disqualifying factor in ISO 10328 ultimate static testing however given the amount

of deformation remaining from P3 testing (5.8mm) and the likelihood of further deformation having occurred during P4 testing it was not reasonable to consider the sample passing. This sample was to be tested at the P5 level to determine further behaviour. Samples were first to be tested to the P4 level of ultimate static loading in the heel condition.

4.8 P4 Heel test

4.8.1 Specimens

Sample 1 failed during P3 toe and heel testing and was excluded from any further testing. Having passed testing to the P3 level, samples 2 and 3 were to be reused. There was the possibility of remaining deformation from the P3 test as indicated in the toe section after P4 testing.

4.8.2 Method

The foot was to be set up the same way as described in section 4.6.2 Method, with the exception that the upper load limit was raised to 4130N.

4.8.3 Results

Sample 2 was deemed to have successfully completed testing, however the ball in sample 3 split during testing as shown in Figure 93, so was not considered to have passed. During loading the ball was observed to deform until the keel came into contact with the baseplate. There was a slip in sample 2 at 12mm compression and in sample 3 at 13mm compression (see Figure 94) however as each foot settled loading continued.

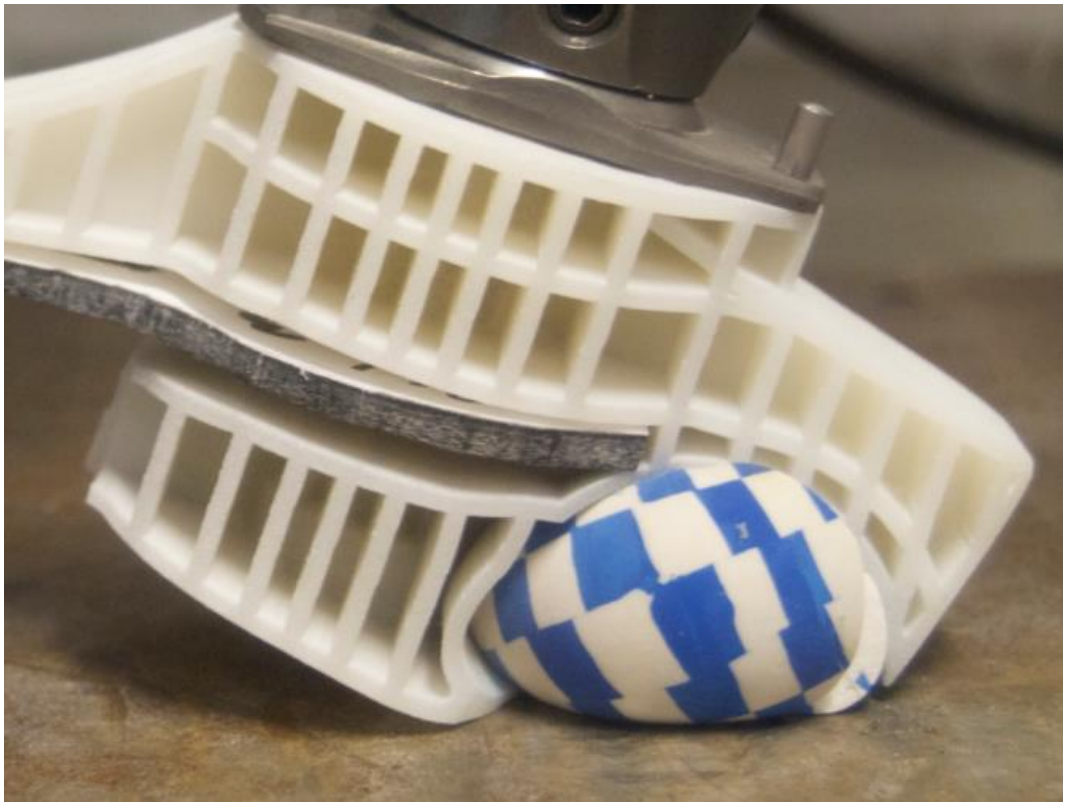

Figure 93 – Sample 3 showing the split ball under maximum P4 ultimate static load

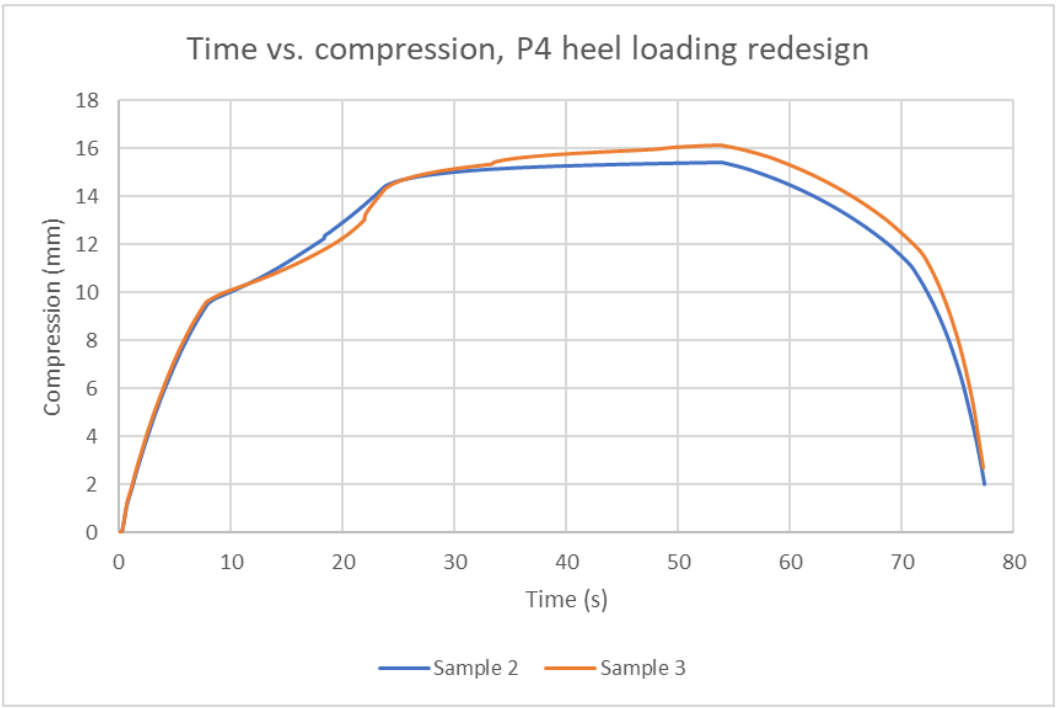

Figure 94 - Time vs. compression results of Strathclyde redesign under P4 heel testing

After this point no further deformation was obvious although Figure 95 shows that 1.01mm of compression occurred during load holding in sample 2 and 1.86mm in sample 3. Both keels contacted the baseplate at approximately 9.6mm compression as visible by the sharp change in gradient observed in Figure 95 at that point. In unloading the removal of contact between keel and baseplate was not clearly defined.

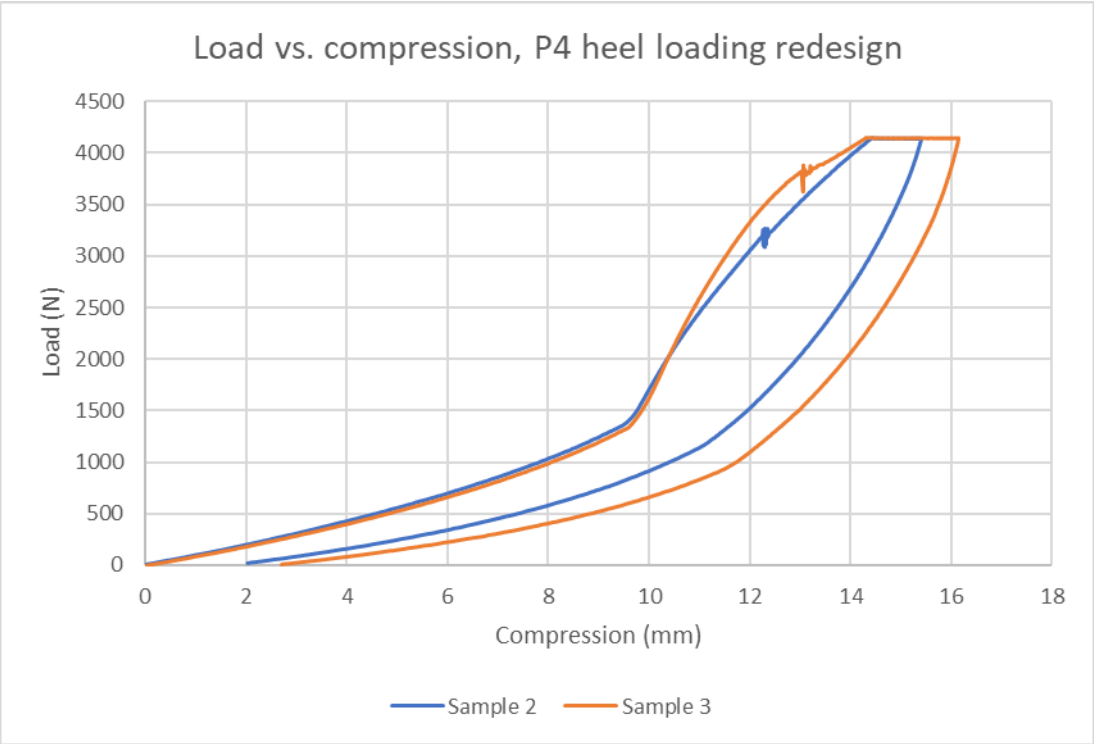

Figure 95 – Load vs. compression results of Strathclyde redesign under P4 heel testing

Energy calculations were carried out as discussed previously. Sample 2 was calculated to have an energy input of 23.79J and an energy output of 14.10J giving a 9.69J loss. Sample 3 was found to have a 27.34J energy input and 13.04J energy output giving a 14.30J loss.

4.8.4 Discussion

Both keels survived testing however, the ball in sample 3 split open. The same balls were used as in P3 testing of these samples however in this case the compression was greater before the keel contacted the baseplate (see Figure 96). On review, this was likely caused by deformation of the heel section of the keel leading to the difference observed. While this deformation was not observed after testing it was apparent when comparing images from before and after testing at the P3 level as in Figure 97. The extent of this deformation is approximately 1.4mm for sample 2 and 1.8mm for sample 3.

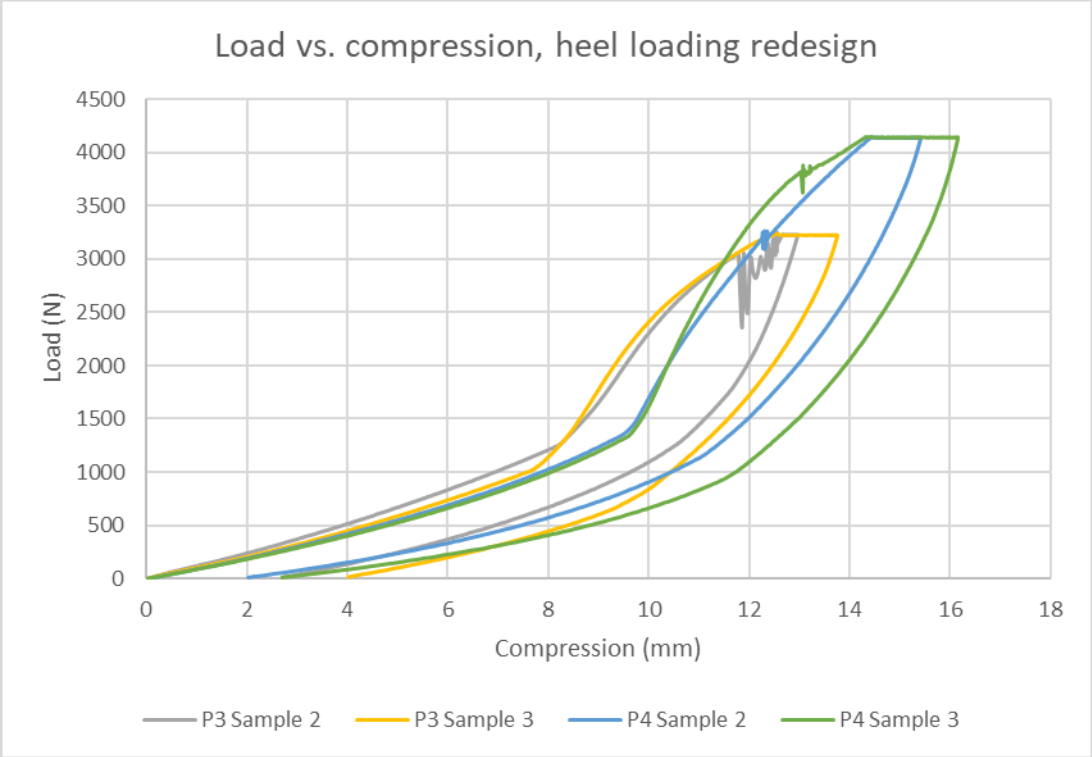

Figure 96 – Load vs. compression results for Strathclyde redesign at P3 and P4 levels

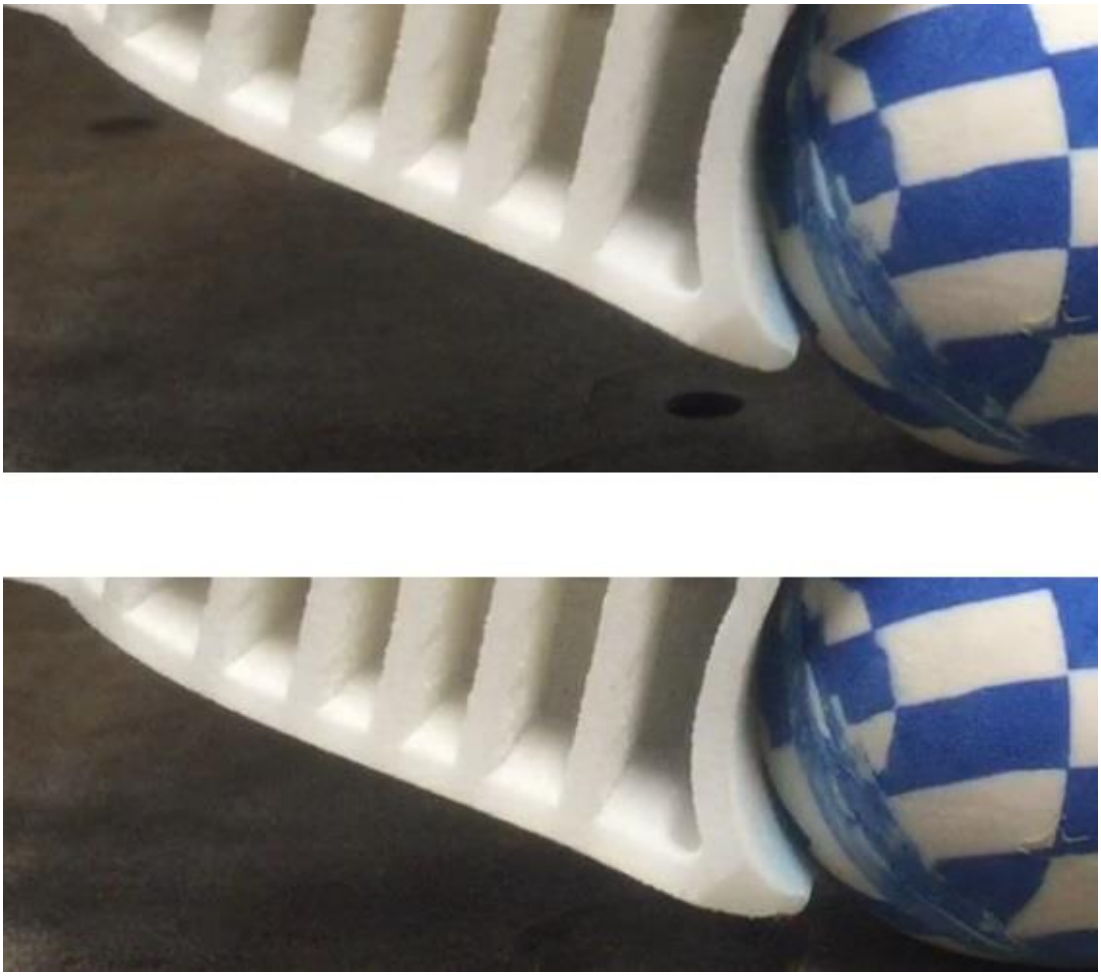

Figure 97 – Comparison of sample 2 pre- and post- P3 heel testing showing the deformation of the keel section

The energy returned in sample 2 was 59.2% which was a greater percentage than the return at the P3 level (46.6%). This was due to the increased load, the majority of the increase of which loads the keel which is stiffer than the ball thus leading to greater energy input and return.

In sample 3 47.7% of energy was returned in P4 testing which was lower than the 54.4% return achieved in P3 testing. This was not unexpected as the ball would have been expected to return a portion of the energy stored however its failure meant that this energy was lost instead.

The greater creep seen in sample 3 may have been as a result of the ball failing causing a greater load to pass through the lower part of the keel directly leading to greater deformation.

4.8.5 Conclusion

ISO 10328 required two surviving samples to declare compliance however the failure of the ball in sample 3 is to be considered a clear sample failure. The Strathclyde redesign was not considered to have met the P4 ultimate static loading condition at the heel because of this. Upon inspection both samples would not have been considered to have passed the P3 heel test due to the presence of deformation in the keel and this is also true for the P4 level. Testing was to continue to the P5 level using the same samples, with a replacement ball to be included in sample 3, however it was only to examine behaviour of the samples as they had already failed to meet ISO 10328 at any level.

4.9 P5 Toe test

4.9.1 Specimens

Sample 4 was the only sample used in this test.

4.9.2 Method

The method used was the same as in previous toe tests (see 4.5.2 Method) however the maximum load was increased to 4480N in line with the requirements of ISO 10328.

4.9.3 Results

Sample 4 was successfully loaded to the upper limit of the P5 ultimate static loading test and then unloaded with no apparent damage. The same stages of

deflection were noted as previously with the lower toe sections deflecting into the blade and subsequently the blade deflecting into the top toe section. The ball then came into contact with the baseplate, followed by the keel. The arch of the toe continued to flatten with part of the back of the toe section contacting the baseplate also. Figure 98 shows sample 4 under maximum loading.

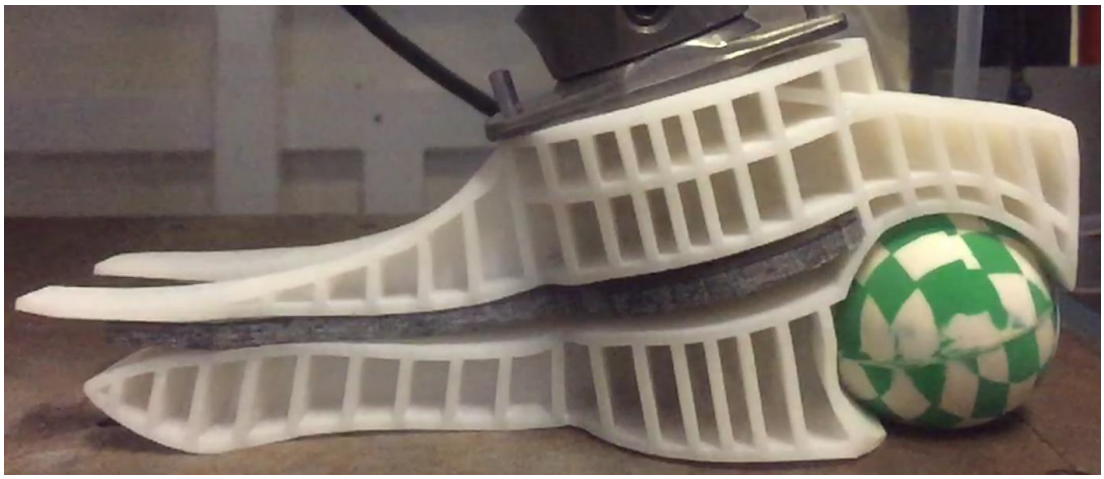

Figure 98 – Sample 4 at maximum load during P5 toe testing

During loading sample 4 showed ball contact at 19.3mm and keel contact at 20.8mm as visible in Figure 99. During unloading the keel was removed from contact at 20.9mm while the ball left contact at 20.1mm. There was a slight slip during unloading, visible at 12.2mm compression.

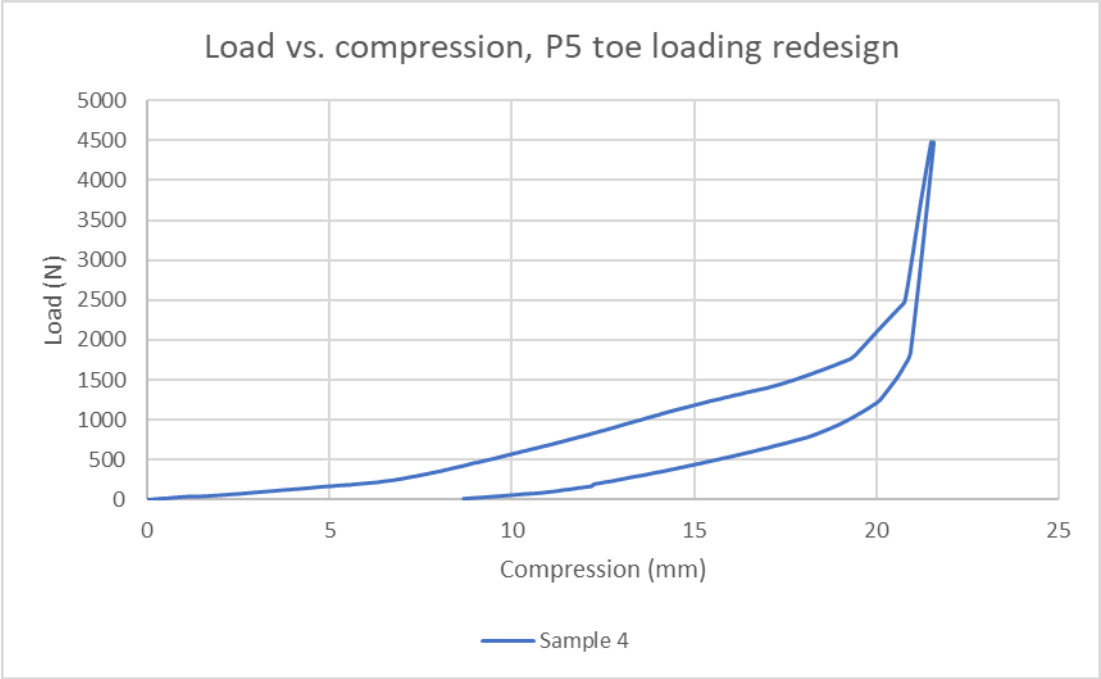

Figure 99 – Load vs. compression results of Strathclyde redesign under P5 toe testing

Energy values were calculated as described previously in section 3.3.2.3 Results. Energy input was calculated to be 18.62J with energy output being 8.25J giving an energy loss of 10.37J.

4.9.4 Discussion

The energy return of the foot when tested to the P5 level was 44.3% which is slightly higher than 42.2% of the P4 level and much higher than the 30.9% of P3 level. This was likely to be partly due to some permanent deformation from previous tests. As seen in Figure 100 the maximum compression during the P5 test was lower than during P4 testing and also less than occurred during the P3 test, which suggested residual deformation of the sample.

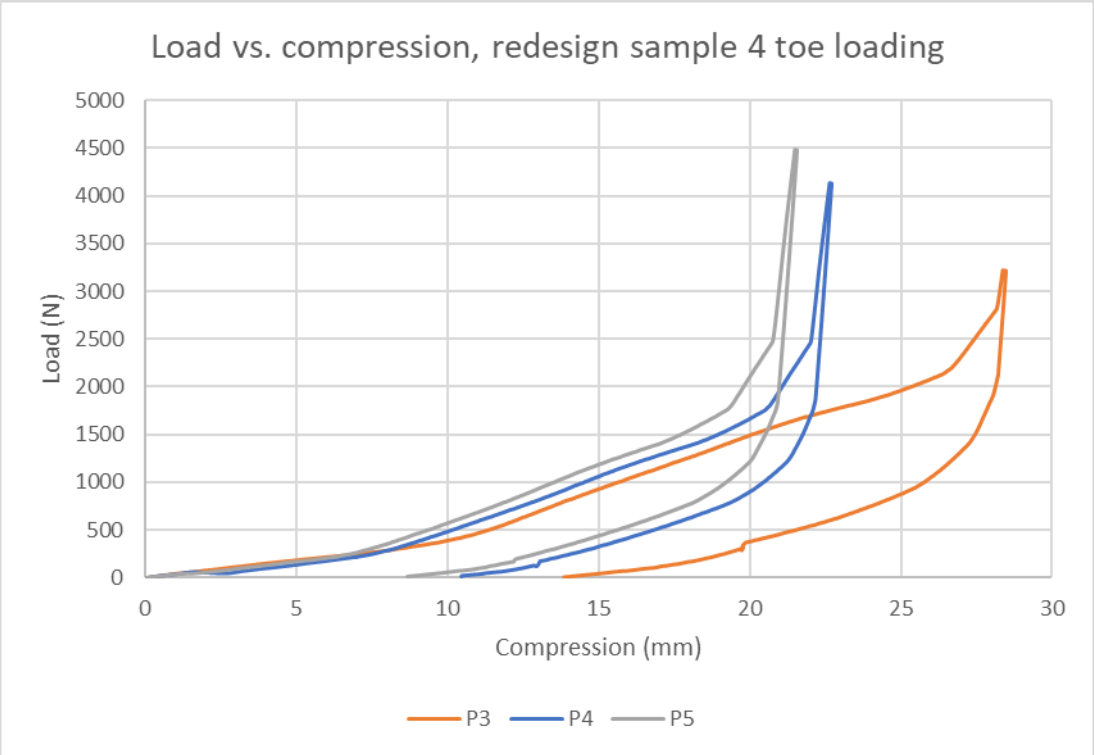

Figure 100 - Comparison of load vs. compression of Strathclyde redesign sample 4 at P3, P4 and P5 ultimate static loading tests

The percentage energy return increased with the loading level however the absolute energy input dropped from the P3 to the P4 level (27.87J vs. 18.55J) and remained similar between P4 and P5 tests (18.55J vs. 18.62J). With increased permanent deformation of the sample at each level the system would be stiffer overall leading to a reduced total deformation despite increased loading. This would have led to lower energy values than might have been expected at increased loads than if the deformation were not present.

Residual deformation increased by approximately 1.1mm following P4 testing which reduced the maximum compression that the sample underwent during P5 testing. This was less than the residual deformation resulting from P3 testing (5.8mm). The increase in residual deformation remaining from P4 testing was smaller than that remaining after P3 testing and would indicate a stiffer system, most

likely the effect of the heel contacting the baseplate sooner. This meant that permanent deformation would need to occur simultaneously in heel and toe, increasing the loading required to create permanent deformation.

Sample 4 required greater force to reach a similar level of compression as in previous tests. This was a result of deformation remaining from previous loading conditions. This was a similar pattern as was observed during the testing of the original Strathclyde foot although in the single redesign sample there was a decrease in compression at contact between the lower and upper toes sections between P4 and P5 testing (0.7mm, see Figure 100). This increased compression at the P5 level was in contrast to the unchanged compression between P4 and P5 loading in the original Strathclyde foot and may have been as a result of the changed material. As the material that moved was from the very edges of the section closest to the baseplate the effect is likely to have been small, which would have indicated that this difference was largely a result of the changed material. The FEA results for toe loading in polypropylene and Duraform EX predicted a higher load to yield in the Duraform EX samples (see section B3.6 and B3.7), suggesting that polypropylene would reach a lower load at yield in prototype testing. This did not take into account the manufacturing of the parts themselves, particularly the apparent weaknesses, caused by the SLS procedure, between layers of material.

4.9.5 Conclusion

This may not be considered towards passing the P5 criteria of ISO 10328, having already been ruled out following P3 testing. The design showed some similar patterns under toe loading as the original Strathclyde foot

4.10 P5 Heel test

4.10.1 Specimens

Samples 2 and 3 are to be reused despite the presence of permanent deformation to the rear of the foot as a result of testing to P3 or P4 ultimate static load conditions. A replacement ball of the same type as previously used was placed in sample 3.

4.10.2 Method

The foot was to be set up the same way as described in section 4.6.2 Method, with the exception that the upper load limit was raised to 4480N.

4.10.3 Results

In both samples, the balls were observed to split after the keel contacted the baseplate (Figure 101). The keels however did survive without damage but did show some deformation of the keel in front of the ball.

Figure 101 – Sample 2 (left) and sample 3 (right) showing the split balls at maximum load

At maximum load creep was seen in sample 2 of 0.41mm and in sample 3 of 1.01mm (Figure 102). Contact of the keel was observed at different compressions and loads in the samples. The keel of sample 2 made contact at 9.3mm

compression and 1315N while the keel of sample 3 made contact at 11.4mm and 1870N. In unloading the removal of contact is not clearly visible in the data.

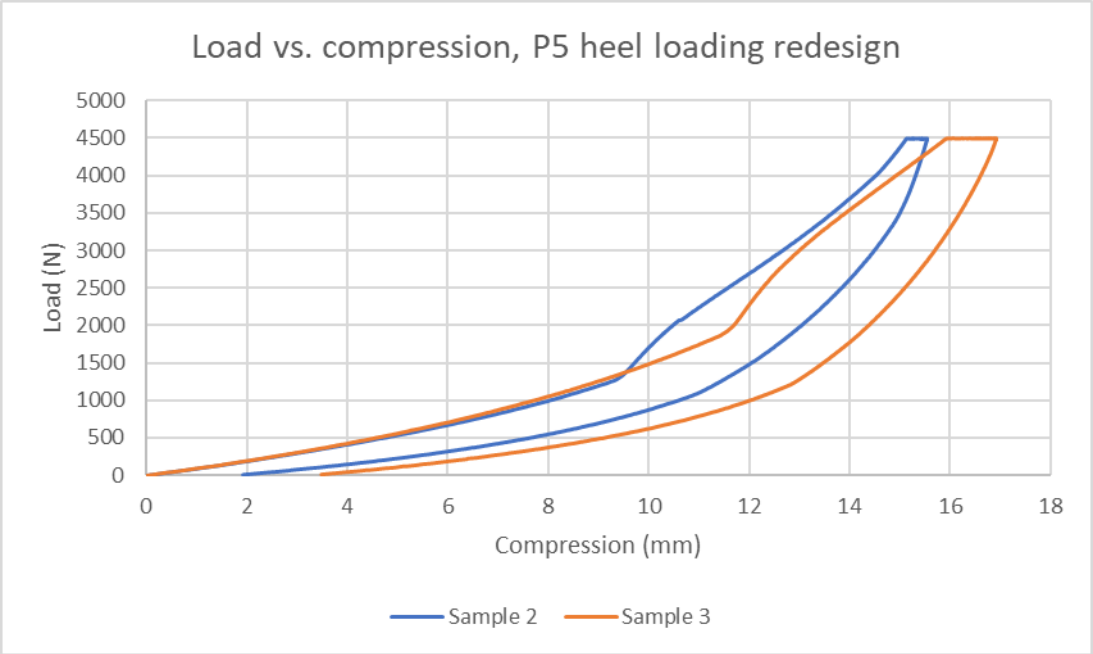

Figure 102 - Load vs. compression results of Strathclyde redesign under P5 heel testing

The energy values were calculated through the same method described in section 3.3.2.3 Results with sample 2 found to have an energy input of 23.22J, an energy output of 14.27J and an energy loss of 8.95J while sample 3 had an energy input of 27.88J, an energy output of 14.45J and an energy loss of 13.42J.

4.10.4 Discussion

The energy return percentages for samples 2 and 3 were 61.4% and 51.8% respectively which was higher than the P4 level (59.2% and 47.7%) and the P3 level (46.6% and 53.4%) In terms of absolute energy sample 2 showed a lower energy input at P5 (23.22J) than P4 (23.79J) but a higher energy output (14.27J vs. 14.10J) while sample 3 showed a higher energy input (27.88J vs. 27.34J) and output (14.45J vs. 13.04J).

During P5 testing sample 2 required less deflection than sample 3 before the keel came into contact with the baseplate due to existing greater deformation from previous testing. This in turn meant that less energy could be stored in the system despite the higher load.

When compared to previous test results sample 2 showed almost the same unloading curve in P5 testing as P4 testing (see Figure 103). This would suggest that the sample had reached a maximum stiffness during P4 testing however the loading patterns are quite different after keel contact has been made. The exact time of the ball failure was not known however if it happened shortly after keel contact it would have caused the system to be less stiff than when it was intact and account for the divergence in loading pattern observed while still giving a similar unload pattern. As the ball in sample 3 had been replaced since P4 testing it is possible that it was slightly larger giving the approximately 2mm difference in compression between the keel contact in P4 and P5 testing. The new ball did split as part of the testing which could explain the similarity in the end of the unloading curve between the P4 and P5 tests.

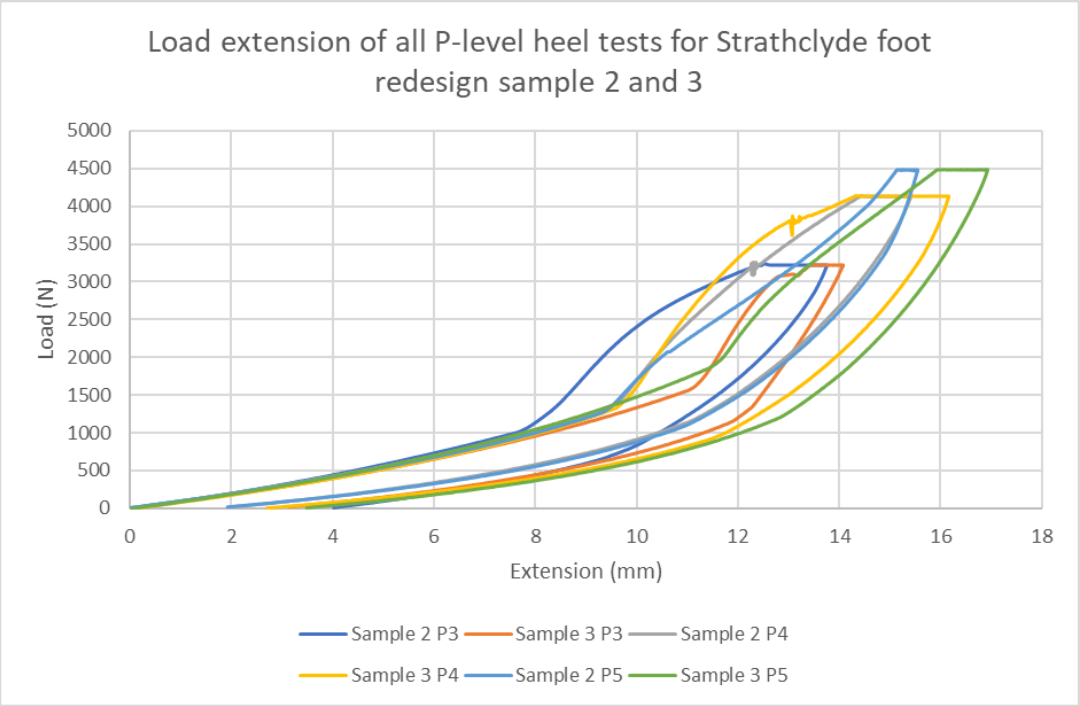

Figure 103 - Comparison of load vs. compression of Strathclyde foot redesign at all P-levels of ultimate static heel loading tests

The performance observed on increasing load levels was different to that observed for the original Strathclyde foot in that increased load led to increased compression at each level of testing (in the original Strathclyde foot decreased compression was observed with increased loading in sample 2 while sample 1 had increased compression at the P4 level and then reduced compression at the P5 load level – see section 3.3.6.4 Discussion for more details). As both the design and material changed from the original Strathclyde foot it was likely that both had an impact on performance however, the individual effect of each was not determined. As permanent deformation was observed from the P3 level in the redesigned samples the increased compression is in addition to, and greater than, deformation at previous levels. The original Strathclyde foot did show increased compression at the higher load levels but the increase due to P4 loading was less than the increase due to P3 loading.

4.10.5 Conclusion

The Strathclyde foot redesign was not considered for verification to the ultimate static loading condition in the heel condition of the P5 level. The effect of changing design and material will have both impacted the performance of the redesign however the extent of each is difficult to determine based only on these tests. FEA was carried out on the existing design and this redesign however it suggested that the existing polypropylene Strathclyde design would reach yield at a load of 354.2N while the Duraform EX redesign would reach yield at 592.4N. This disparity in results between the FEA models and the prototype testing meant that the FEA models were unsuitable for accurately predicting real-world performance but may still be used to compare designs virtually for design improvements.

Overall the testing of the Strathclyde foot redesign highlighted areas for improvement, particularly after the poor results achieved by three out of the four samples under toe loading conditions. The heel of the keel appeared to undergo permanent deformation as early as during P3 testing and the extent of deformation increased with increased test level. The failure of the ball was an issue to be addressed having confirmed the performance observed during the testing of the original Strathclyde foot design.

4.11 Summary

Initially several methods of layered manufacture were described including Stereolithography, Laminated Object Manufacture, Selective Laser Sintering, Fused Deposition Modelling, Inkjet Deposition and Solid Ground Curing as well as the non-layered manufacturing process, Vacuum Casting. SLS was selected and two materials were put forward for potential use. These materials Duraform EX and Duraform PA were tested in tension both to destruction and non-destructively to

determine the ultimate tensile strength, elongation at break, tensile yield strength, elongation at yield and Young's modulus, which were in turn compared to polypropylene, both homopolymer and copolymer. Duraform EX was determined to be a suitable material to produce sample models to test concepts but that these were not adequate to predict the performance of polypropylene parts due to differences in properties and manufacture method. Prototypes made of Duraform EX were tested to the ultimate static loading procedure specified in ISO 10328. Testing revealed that the performance of the toe section was inconsistent as one sample survived through to the P5 level of testing (with excessive deformation to be considered a pass at any level) while three samples (two without reinforcing blades) did not survive P3 testing. In heel testing permanent deformation of the keel was found at the P3 level with increased deformation following P4 and P5 testing as well as balls being observed to fail at the P4 and P5 level. The design did not meet any level of ISO 10328 ultimate static testing however, the performance is partially due to the material and manufacturing method.

CHAPTER 5 – Further redesign, testing and evaluation

This chapter begins with the elements of redesign required after the testing in the previous. Toe and heel loading was carried out to the ultimate static loading levels. Each design of the Strathclyde foot was compared across P-levels. A comparison of P5 Strathclyde foot performances to other prosthetic feet as tested by Jensen & Treichl, 2007, follows. Finally, a single subject force plate trial was conducted on the Strathclyde foot.

5.1 Introduction

Certain shortcomings in the design were visible following testing:

- The failure of the toe sections under test conditions, both lower and upper
- Excessive deformation of the surviving keel in toe loading
- The engagement of the blade with the keel
- Failure of the ball at the heel

To address these shortcomings the following changes were made:

- The gap between the upper and lower sections was reduced
- The toe section width was increased where it met the ankle block
- The upper face of the lower toe section was made flat

The gap between the upper and lower toe sections was reduced to 5mm to allow for a 3mm blade to be included while also retaining room for potential

modification of the blade (e.g. a stiffer blade may better suit a heavier or more active user) by a method to be determined at a later stage (see Figure 104). The gap was reduced by increasing the height of the lower toe section. The height increase led to a predicted increase in moment of inertia from $1.97x10^{-9}m^4$ to $4.33x10^{-9}m^4$ (calculated as in for the C channel in section B2.4 Model Validation) at the section of the lower toe where the high stress points 2 and 3 were observed to form in section B3.6 Whole design evaluation. This increased moment of inertia reflected an increased stiffness of the toe section, which was desired to reduce the deformation from that observed in the surviving keel of first redesign.

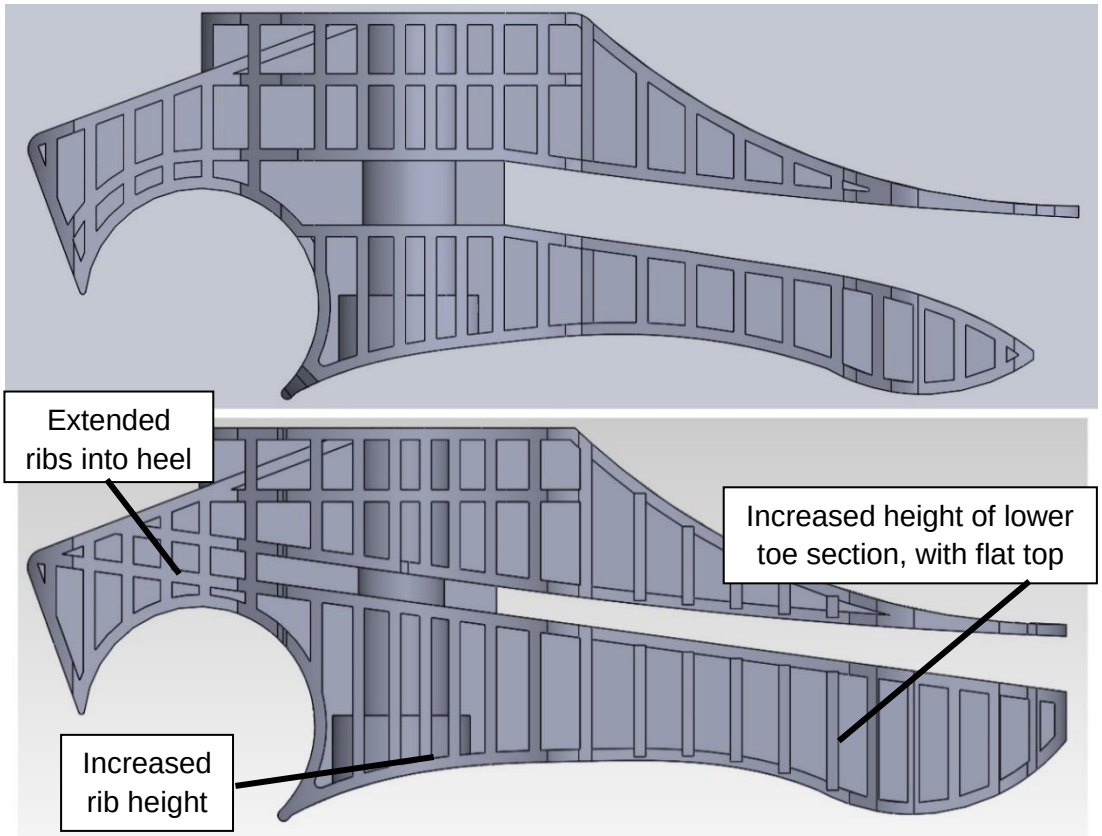

Figure 104 – First redesign (top) compared to second redesign (bottom)

The width of the toe sections was increased where they met the ankle block by reducing the taper back towards the ankle block (see Figure 105), which increased

the width and so further increased the predicted moment of inertia at the point previously mentioned to $6.01x10^{-9}m^4$.

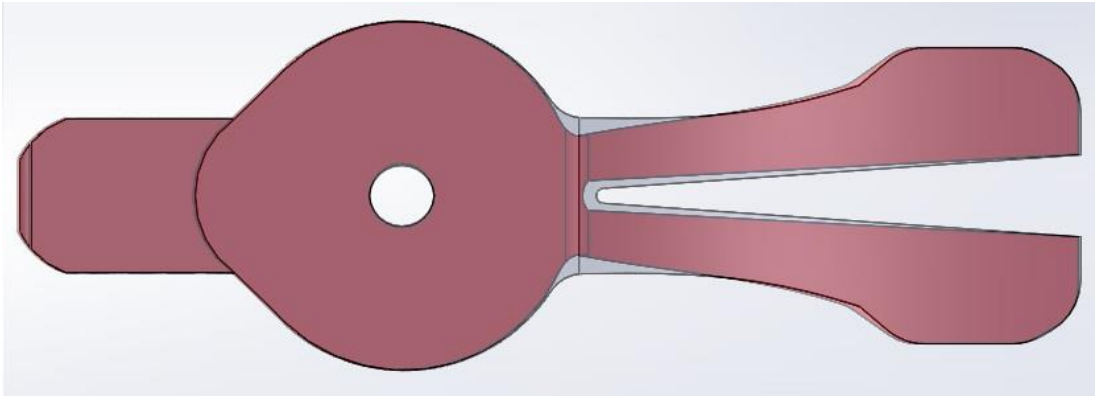

Figure 105 – Both redesigns of the Strathclyde foot viewed from above, first redesign (red), second redesign (grey) showing increased width at rear of toe

The reduced gap between the lower and upper toes sections combined with the flat surface applied to the upper surface of the lower toe section meant that the lower toe section would contact the blade at a reduced deformation to the first redesign. The blade would then come into contact with the upper toe section sooner than previously. This would lead to the load being shared across multiple sections and so contribute to preventing an early failure of the lower toe section. The flat top surface of the lower toe section would also reduce friction between the lower toe section and the blade allowing each section to flex separately and the point of contact between the lower toe section and blade to travel backwards as the deformation increased, helping reduce the stress on the sections.

The changes made to reduce the gap between sections led to an adjusted rib pattern in the ankle block, in terms of rib height, the top of the lower section and the bottom of the upper section, which also continued into the heel (see Figure 104).

An additional minor change was made to the design at this stage; the outside of the end of the toe sections as viewed from above had a single, larger fillet applied

as opposed to two smaller fillets connected with a short straight section (see Figure 105).

The failure of the ball was not addressed in this redesign process in order to keep the conditions at the heel constant between the redesigns to allow comparison however, it is considered an area of attention for further work.

The changes made were validated using the FEA described in section B4 Second design revision. The keel design was broken down into sections; lower toe, upper toe, heel and ankle block where the second redesign was compared to the first redesign. The lower toe was found to have lower stresses and deformation in the second redesign than the first at a given load. The upper toes were deemed similar and so analysis of the whole system would be sufficient. The heels were examined in section B4.3 Heel FEA, and the second redesign was expected to show higher load to yield and reduced deformation when compared to the heel section of the first redesign. The ankle blocks were loaded from the bottom faces, with the load applied vertically upwards, and appeared to perform in a similar manner (see section B4.4 Ankle block FEA). Another FEA model was run on the ankle blocks with loading being applied only on the bottom corner of one side of the keel where it was found that the second redesign was generally stiffer, undergoing less deflection, and had higher load to yield at all high stress points identified in redesign 1 (see section B4.5 Edge loaded ankle block FEA). A new high stress point was apparent in redesign 2 that was not present in redesign 1 however the load at yield was more than double all points in redesign 1. A further model based on that in section B4.5 Edge loaded ankle block FEA was run, this time including the blades for the respective keels (section B4.6 Modified edge loaded ankle block FEA) during which the redesign 2 setup was found to show less deflection while the stresses generated were not considered to be representative of real world conditions.

The second redesign was tested to ISO 10328 toe loading conditions in FEA, both without (see section B4.7 Full foot bladeless polypropylene) and with a blade (see section B4.8 Duraform EX models). The bladeless model was found to reach a higher load at yield, or not yield before maximum load, at each high stress point when compared to redesign 1 with the exception of point 1, in the centre of the keel on the vertical support. This was found to be acceptable as the difference was slight and this area was not observed to fail in the prototype testing of 4.5 P3 toe tests.

The bladed model was run with the keel using the properties of Duraform EX, rather than the polypropylene used in other models so that a direct comparison could be made between the FEA models and prototype tests. The results of FEA testing suggested that failure would be reached on the vertical support (point 2 in B4.8.5 Results, equivalent to point 1 in the bladeless model in B4.8.2 Results) at 392.8N. Failure has not been observed in previous prototypes at this point so the second point to failure, point 1 in B4.8.5 Results (equivalent to point 1 in the bladeless model), was predicted to fail at 1333N load. Due to the differences observed between previous FEA and prototype tests a further round of prototype tests was required.

5.2 P3 Toe test

5.2.1 Specimens

Three samples were produced by ARRK Europe by SLS using Duraform EX and were labelled 1, 2 and 3. Each had a 56mm rubber ball (It's my party, Hixon, UK) inserted into the heel. Samples 2 and 3 each had a blade made from 4mm fibreglass (polyester gelcoat and resin, 3 layers of 600g chopped strand matting – East Coat Fibreglass Supplies, South Shields, UK) inserted into the toe section (see Figure 106). The blade was pushed into place with the 2mm wide cut out holding the blade within the keel.

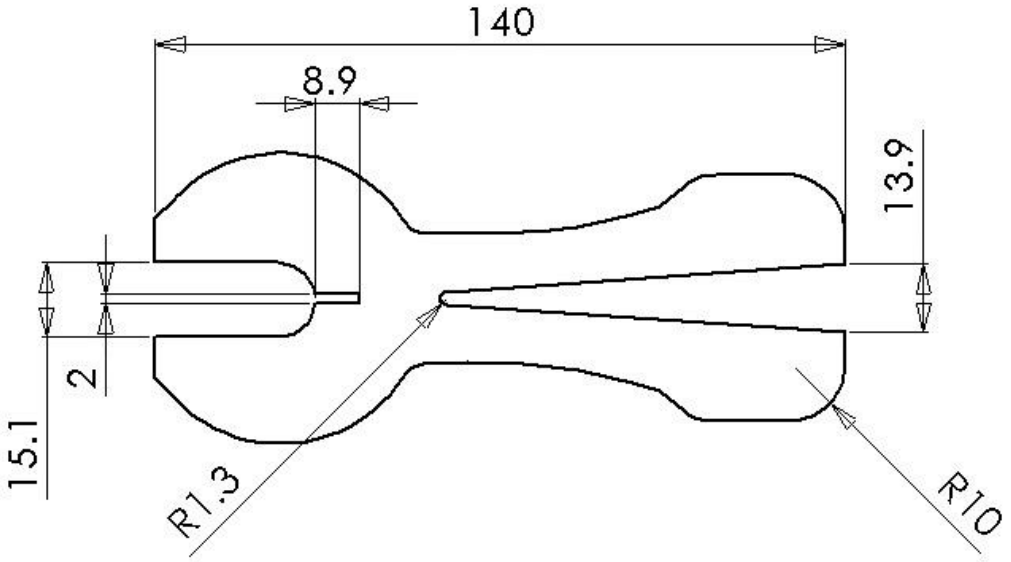

Figure 106 – The design used for the blade in the Strathclyde foot second redesign

5.2.2 Method

The same method as had been used on the original Strathclyde foot and the first redesign was used, namely:

The adapter was set up for the required loading condition (heel or toe), which gave the loading angle required (20° for toe loading, 15° for heel loading). The adapter was then mounted into the Instron machine with the grip being closed on the topmost part. That the alignment was correct was determined using a goniometer. The foot was then attached via a pyramid attached to the foot and a pyramid adapter mounted on the bottom of the brass rod. The crosshead of the Instron was then lowered until the foot barely contacted the baseplate at which point the crosshead was locked. The load was increased at a rate of 175N/s until the ultimate static test force upper limit, 3220N, was met (see Table 4 for loads for all P-levels). The ultimate static test load was maintained for 30s at which point the load was reduced at a rate of 175N/s until 0N load was recorded. The test was to be

stopped prior to completion if the sample was observed to fail or the setup became unsafe in any way.

5.2.3 Results

Samples 1 and 3 were able to reach the maximum load and were unloaded without catastrophic failure however; sample 1 was observed to have suffered from severe deformation on the top section of the toes (see Figure 107) and was ruled out of further toe testing. Sample 2 reached maximum load but was automatically stopped by machine controls at approximately 15.8s into the hold phase (see Figure 109). A crackling noise was heard during loading. Upon observation after unloading sample 2 was observed to have suffered a similar severe deformation on the top section of the toes as sample 1 (see Figure 108) and was discounted from further toe testing. Sample 3 was loaded to the maximum load but had a highly irregular loading pattern (see Figure 110). The same crackling sound was heard during testing as with sample 2. Following the test, the blade in sample 3 was observed to have moved laterally, away from the initially loaded side of the foot (blade shifted right) as seen in Figure 111.

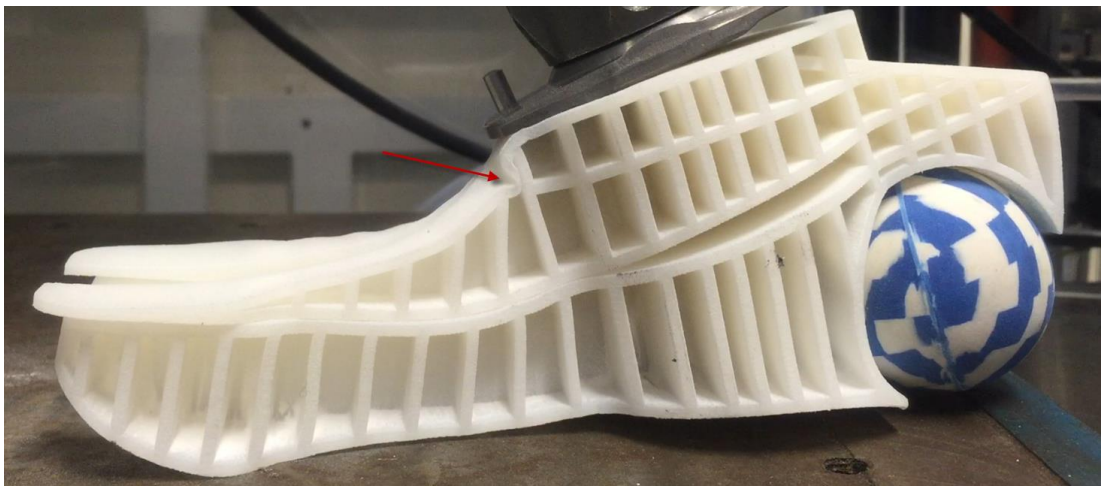

Figure 107 – Sample 1 at maximum load, an arrow indicates the deformation on the toe section

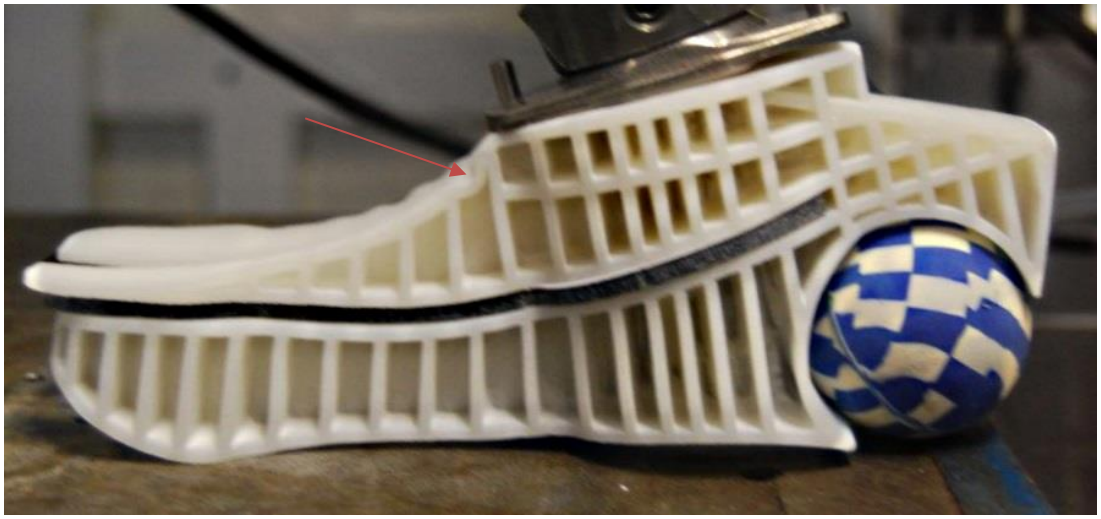

Figure 108 – Sample 2 of redesign 2 showing failure of top side of upper toe section

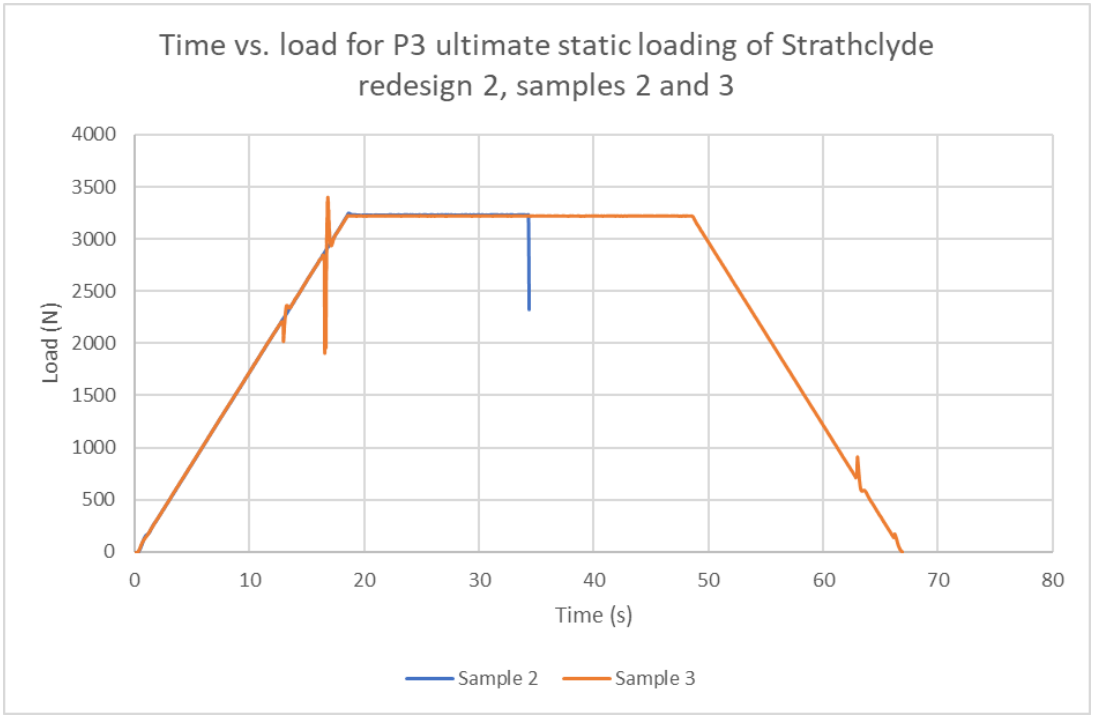

Figure 109 – Time vs. load of samples 2 and 3 of Strathclyde redesign 2 tested to the P3 toe loading ultimate static load condition

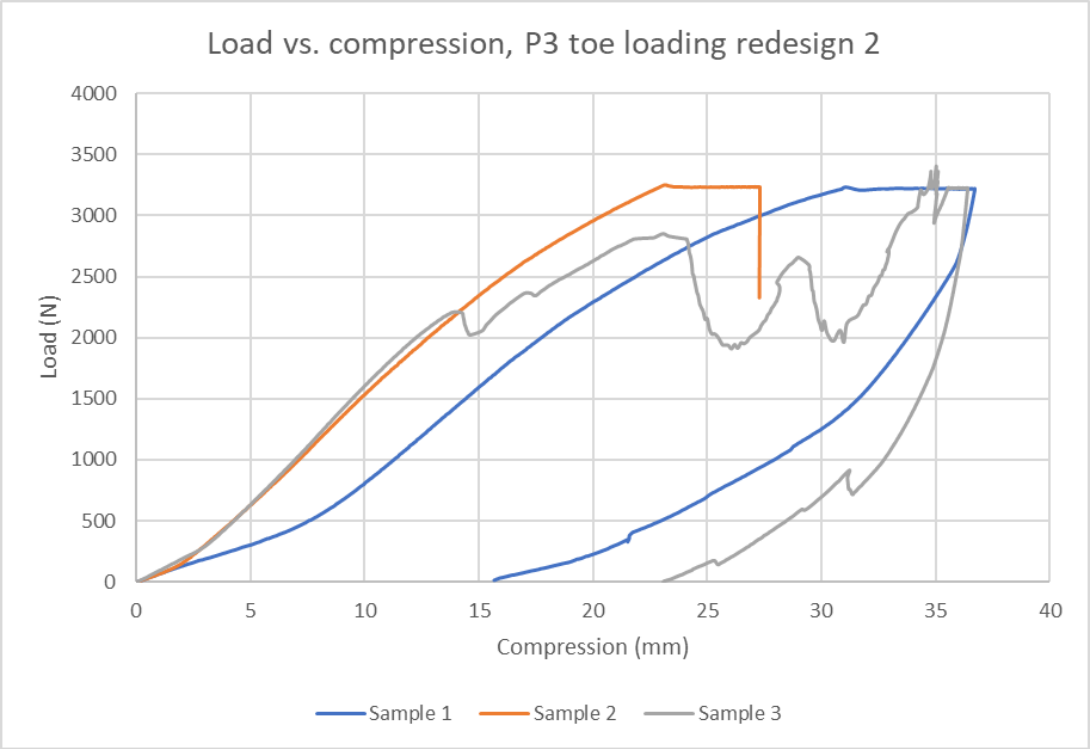

Figure 110 – Load vs. compression of all samples of Strathclyde redesign 2 tested to the P3 toe loading ultimate static load condition

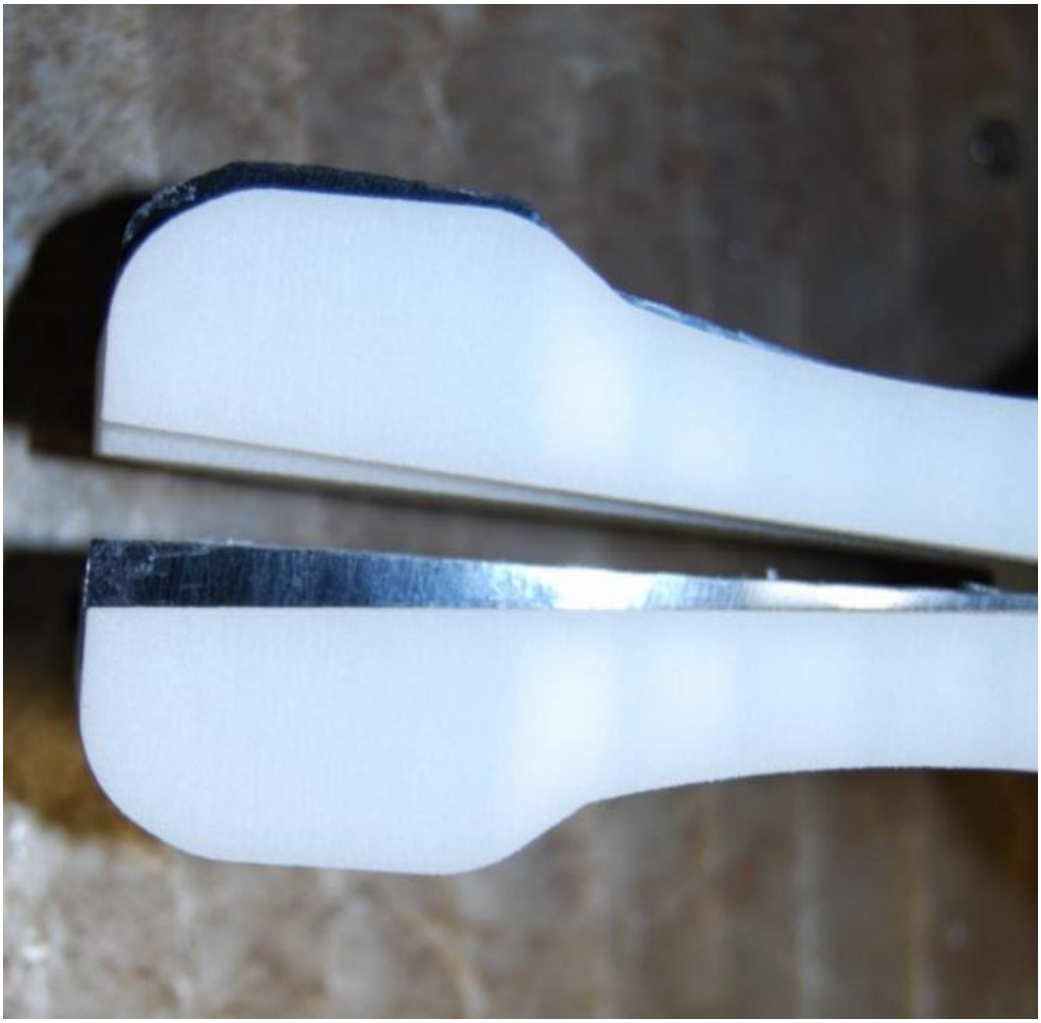

Figure 111 – The blade slipped to the right side during the P3 toe loading test

5.2.4 Discussion

Sample 1 was initially less stiff than samples 2 and 3 however at approximately 400N load the sample became stiffer before gradually becoming less stiff again at higher loads. This lesser stiffness was not a surprise as sample 1 had no blade while sample 2 and 3 did. The severe deformation in this case disqualified it from being considered to have passed the P3 level of ultimate static loading.

Sample 2 briefly exceeded the maximum load at this level by 30N. The results showed no sudden increase in load or deformation however the Instron machine's safety was triggered and the test halted. Upon unloading the top of the toe section was observed to have been deformed in a manner similar to sample 1 and so was

excluded from further to testing. The cracking heard during testing may have been a number of small fractures occurring within the material, or perhaps separation of layers, however when observed no external signs of such fractures could be found. There was no clear effect on the load vs. compression results due to any such fracture.

Sample 3 was loaded erratically (Figure 110) although the only obvious sign of this at the time was a single large increase in compression, also visible in Figure 112. The same crackling was heard as during sample 2 but if the erratic loading were somehow a cause of the crackling then a similar effect would be expected in sample 2 where it was not observed.

The three samples were nominally produced the same, having been ordered together from ARRK Europe while the program used in the Instron machine for loading pattern in each case was the same. The behaviour of sample 1 seemed reasonable, as did the performance of sample 2 prior to failure. Sample 3 initially had a similar load compression curve to sample 2 however at approximately 2210N the load reduced to 2020N before increasing again. During this unloading period the compression increased. When the time vs. load chart (Figure 109) was examined this rapid load drop off and increase was viewed on the chart at approximately 13 seconds. A further two similar areas of rapid load/unload were seen at 16-17 seconds and 63 seconds. Cross referencing these times to Figure 112 shows rapid compression during the 13 second and 16-17 second time points as well as an area of held compression at approximately 63 seconds. The changes seen may have been caused by the resistance of the test piece changing rapidly, potentially by the blade slipping within the keel, although this was not observed at the time, and the system attempting to maintain the load control on the piece, causing oscillation about the intended load which when coupled with any lag in the actuation of the

machine may have caused the extended time over which the load was deviated. The blade slipping could have caused a rapid decrease in load until a new position was settled upon where loading could increase again. The test was not videoed which could have provided insight into the cause of this rapid compression and load variation and as such is highly recommended for further tests.

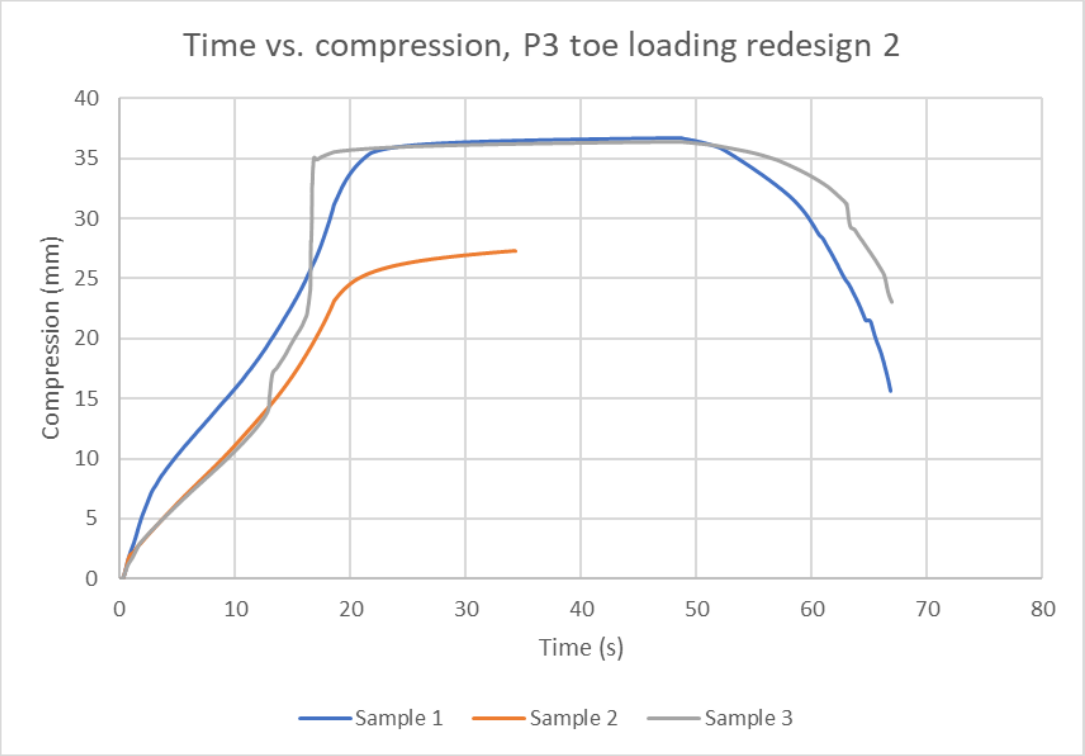

Figure 112 - Time vs. compression of all samples of Strathclyde redesign 2 tested to the P3 toe loading ultimate static load condition

5.2.5. Conclusion

The second redesign of the Strathclyde foot is not considered to have met the ultimate static loading standard for toe loading although sample 3 may be argued to have met the standard. Samples 1 and 2 were ruled out of further toe testing but not in heel testing. As such samples 1 and 2 were to be used in heel testing while sample 3 was reserved to be retested in toe loading.

5.3 P3 Heel test

5.3.1 Specimens

Samples 1 and 2 were judged to be fit for use in heel testing after failing in the toe loading condition at the P3 level.

5.3.2 Method

The adapter was set to 15° for heel loading, the samples mounted in turn and aligned at 7° toe out. The samples were lowered to make contact with the baseplate before loading was applied at 175N/s until 3220N was met. The load was held for 30s then unloaded at 175N/s until zero load was applied.

5.3.3 Results

The balls of the samples were observed to deform until the keel contacted the baseplate. This slowed the deflection however in sample 1 the ball was observed to split (see Figure 113) while in sample 2 the ball tore open entirely (see Figure 114). In both cases at maximum load the front wall of the heel arch was observed to deform. On unloading sample 1 was deemed to have returned to approximately preloading condition while sample 2 remained deformed.

Figure 113 – Sample 1 under maximum P3 heel loading condition displaying the split in the ball

Figure 114 – Sample 2 under maximum P3 heel loading condition displaying the ruptured ball

Sample 1 was stiffer than sample 2 throughout loading but did show a sudden change in stiffness at around 2500N, as seen in Figure 115, which corresponded to the ball splitting. In sample 2 the stiffness of the system was reduced from approximately 500N onwards indicating early damage of the ball. After 2000N load was applied the stiffness increased as the ball had collapsed to the point where the keel was exclusively carrying the load. Sample 2 deformed by approximately 3.5mm more than sample 1 (18.1mm vs. 14.6mm) at maximum loading.

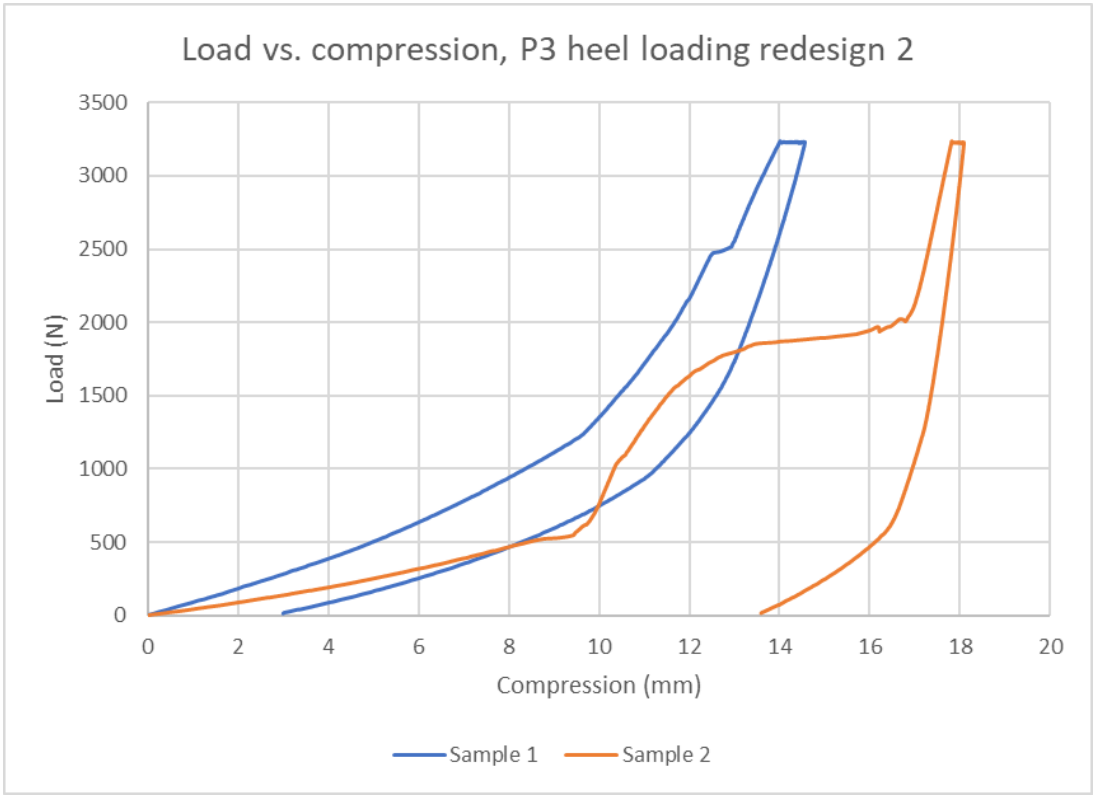

Figure 115 – Load vs. compression results for Strathclyde redesign 2 tested to the P3 toe loading ultimate static load condition

5.3.4 Discussion

The Strathclyde redesign 2 did not pass the P3 heel loading standard as two successful samples were required. Sample 1 did reach the maximum load without considerable damage to the keel however the ball was damaged beyond further use. In sample 2 the ball failed completely and it is proposed that the additional

loading on the keel caused lasting deformation to the heel arch, which could not be considered a pass. Sample 2 was initially less stiff than sample 1 which was believed to be due to a difference in the balls used as they were the only initial contacts. The continually changing gradient of the load-compression line in sample 2 after 500N may have been due to the failure of the ball leading to changing system stiffness as the ball continued to degrade under loading. In sample 1 the sudden increase of compression at approximately 2500N may have been caused by the split occurring in the ball however the keel would then have taken the majority of the load and a similar gradient was observed afterwards. No energy return figures were calculated for sample 2 due to the failure of the ball. Sample 1 was calculated to have an energy input of 8.03J, an output of 4.78J giving a loss of 3.25J or a 59.5% energy return. The values were calculated as described in 3.3.2.3 Results.

While this was only a single sample it did show an improvement on the first Strathclyde redesign in terms of energy return (59.5% vs. 47.2% and 55.2% for the first redesign).

5.3.5 Conclusion

The Strathclyde foot redesign 2 was not considered to have met the P3 ultimate static loading condition for the heel. Sample 1 suffered from a split ball while sample 2 suffered from a ruptured ball and permanent damage to the front wall of the heel arch and so is considered a failure. The same type of ball was used in these tests as in the heel tests carried out in Chapter 4 and similar failures were seen. The same type of ball was used so that the effect of loading on the heel could be directly compared however, the early failure of the ball changes the loading pattern experienced by the keel. A new ball type is required for future tests. Sample 1 was to be used in further testing to the P4 level for the heel but required a replacement ball. Sample 2 was excluded from further testing.

5.4 P4 Toe test

5.4.1 Specimens

Sample 3 was to be tested having successfully passed at the P3 level of ultimate static loading in the toe condition.

5.4.2 Method

The same method was used as described in section 5.2.2 Method with the exception that the maximum load for the P4 level, 4130N, was to be used.

5.4.3 Results

During testing sample 3 deflected until the ball of the heel almost contacted the baseplate. The Instron machine automatically halted the test at approximately 3805N, 325N short of maximum load (see Figure 116). Sample 3 showed some deformation in the same area on top of the toe section as samples 1 and 2 however after resting it was found to not be permanent and the sample was remounted to run the test again. During the second attempt at the P4 ultimate static loading test the Instron halted the test again at the lower load of 3662N. When sample 3 was inspected again the deformation on top of the toe was greater and after resting was found not to return to its original shape. At this point testing was concluded with sample 3 unable to meet the ultimate static toe loading condition at the P4 level.

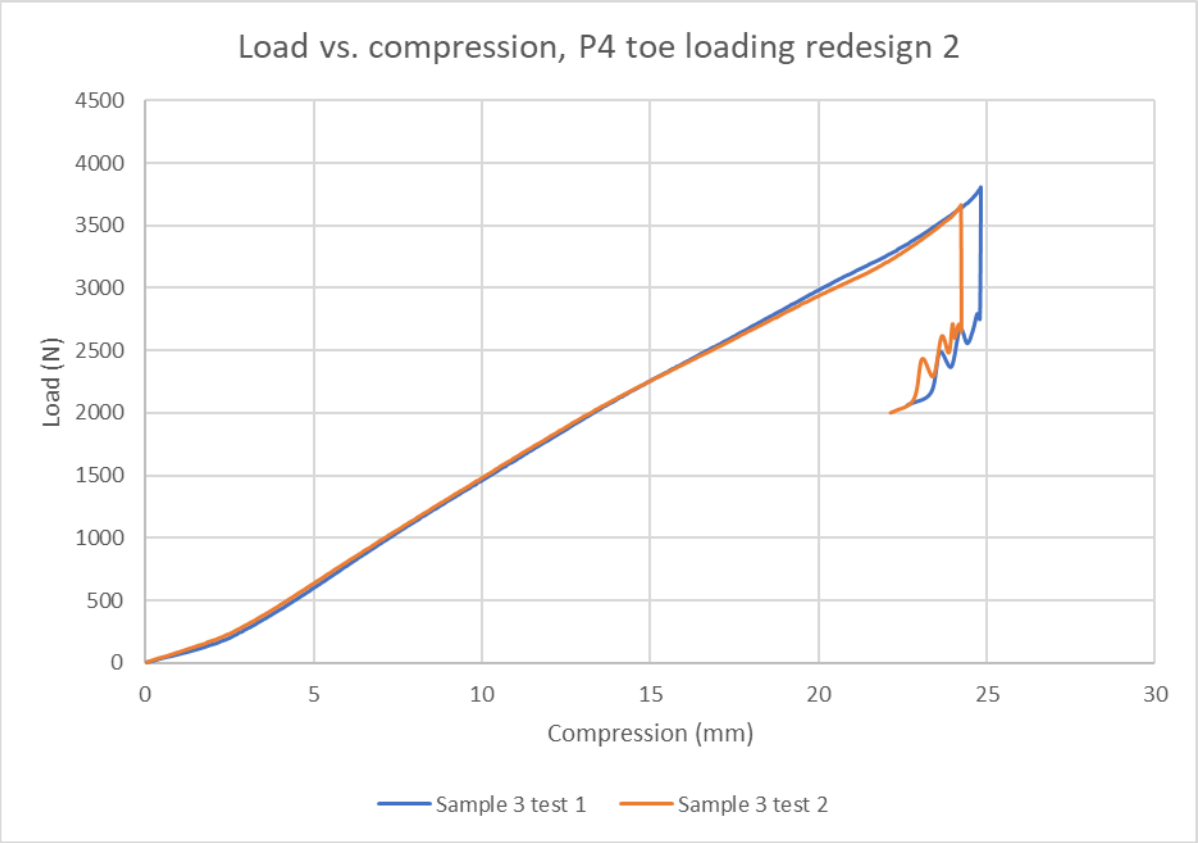

Figure 116 – Load vs. compression of Strathclyde redesign 2 sample 3 tested to the P4 toe loading ultimate static load condition

5.4.4 Discussion

The reasons for the stops in the testing of sample 3 are unknown. The sample showed no sudden failure nor was the Instron at the limit of its extension. The loading pattern of the sample was similar in both cases despite the permanent deformation observed at the conclusion of the second test. The deformation having become permanent after the second test precludes the sample from any further testing.

5.4.5 Conclusion

The sample and the design may not be said to have met the P4 level for ultimate static loading in the toe condition. With no undamaged samples remaining toe testing has concluded.

5.5 P4 Heel test

5.5.1 Specimens

Sample 1 was to be used having successfully completed the P3 ultimate static heel loading condition. During the heel testing carried out in Chapter 4 one of the balls was observed to not fail during P4 level testing and as no other balls were available the test was carried out using a ball from the same stock as previously. An improved ball or other shock absorption feature at the heel is required for further work.

5.5.2 Method

The same method was applied as in section 5.3.2 Method with the exception that the maximum load was increased to the upper limit of the P4 condition, 4130N.

5.5.3 Results

The heel was loaded as prescribed with the ball deforming before the keel came into contact with the baseplate. Prior to maximum load being reached the ball ruptured (see Figure 117). This ruptured occurred at 3830N and caused an increased compression in the sample as shown in Figure 118. At maximum load the sample was observed to have creep of 0.5mm while on unloading a compression of 9.0mm remained in the sample. The sample was observed to have undergone significant deformation of the front wall of the heel arch, which, when rested was observed to be permanent (see Figure 119).

Figure 117 – Image showing the ruptured heel ball during P4 ultimate static loading heel testing

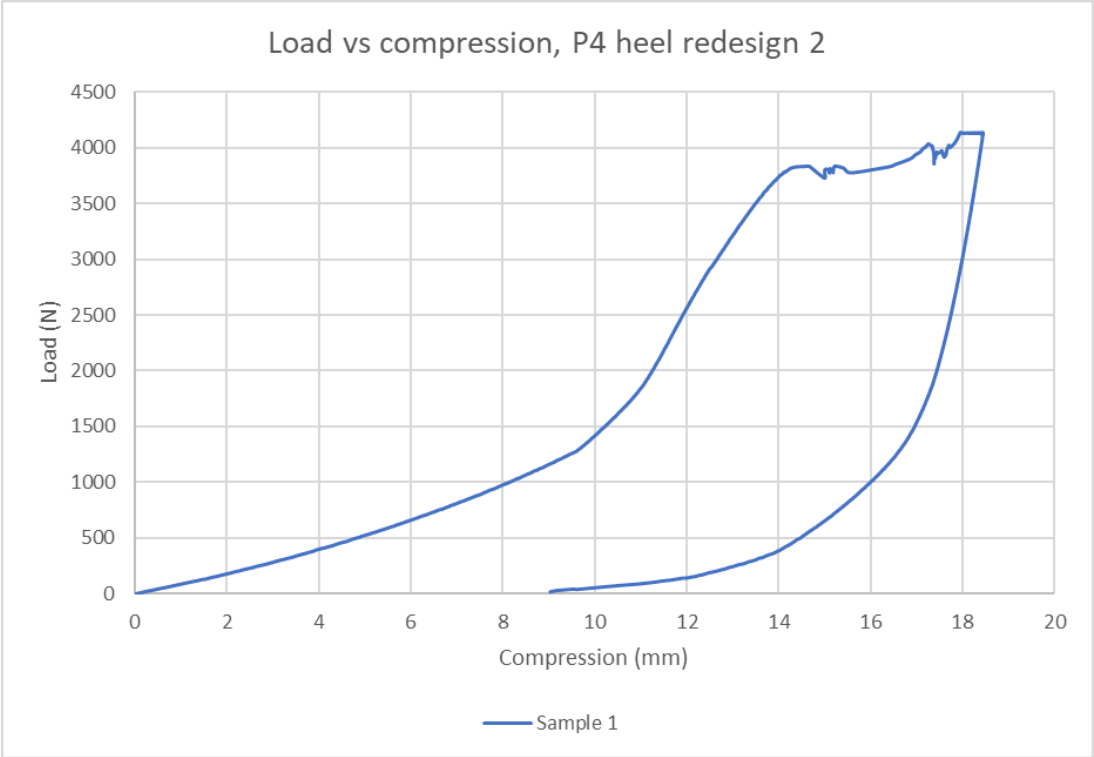

Figure 118 - Load vs. compression of Strathclyde redesign 2 sample 1 tested to the P4 heel loading ultimate static load condition

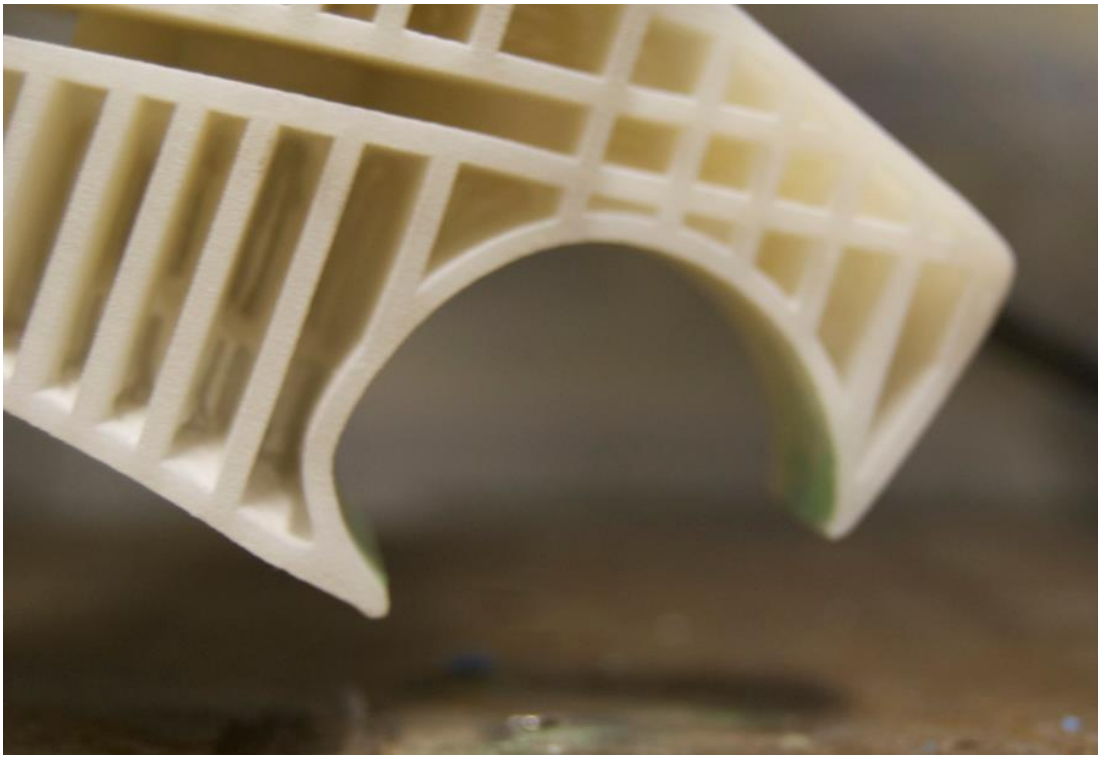

Figure 119 – Sample 1 showing permanent deformation of heel arch following P4 ultimate static loading in the heel condition

5.5.4 Discussion

The failure of the ball led to the failure of the keel as previously observed in the first redesign of the Strathclyde foot. The keel did not fail catastrophically which was a positive outcome however it was put beyond use as a result of the testing and was considered a fail per the standards of ISO 10328. A substitute for the ball was required in future testing to eliminate such failures and to improve the consistency of the ball itself.

5.5.5 Conclusion

The Strathclyde redesign 2 did not meet the standard required of the heel under the testing to ultimate static loading. The ball in the heel proved to be a weak point and requires further research and development in order to address this shortcoming.

5.6 Comparison of Strathclyde foot designs

A comparison of the three designs of Strathclyde foot was carried out to track the design development.

5.6.1 Toe tests

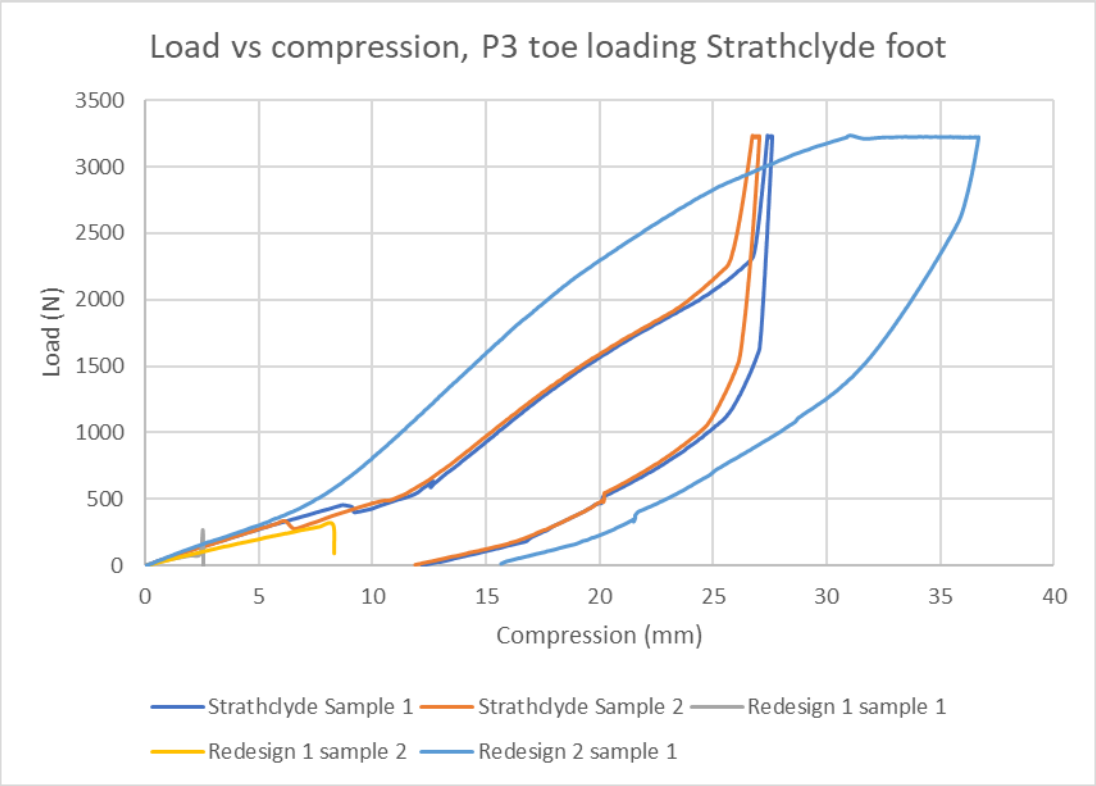

Figure 120 – Comparison of all designs of the Strathclyde foot tested to the P3 ultimate static load for toes without reinforcement

The initial design of the Strathclyde foot was able to meet the P3 level for ultimate static loading in the toe condition with no supporting rods (see Figure 120). The first redesign did not meet the standard with both samples failing catastrophically at low loads (85N and 311N for samples 1 and 2 respectively). For the second redesign only one sample was tested but it did complete the test procedure although the deformation experienced was considered too great to merit a pass. The survival of the keel for redesign 2 may be considered an improvement, although the sample size was too small to make this claim with certainty, however

the failure to achieve the P3 level of loading due to excessive deformation gave the second redesign the same status as the first. The original design of the Strathclyde foot was able to pass at the P4 and P5 levels however the material performance was a larger factor in this than the design itself, as shown in Appendix B – Finite Element Analysis of foot designs, with the R2 design performing better under toe loading conditions than the existing Strathclyde foot when using the same material properties.

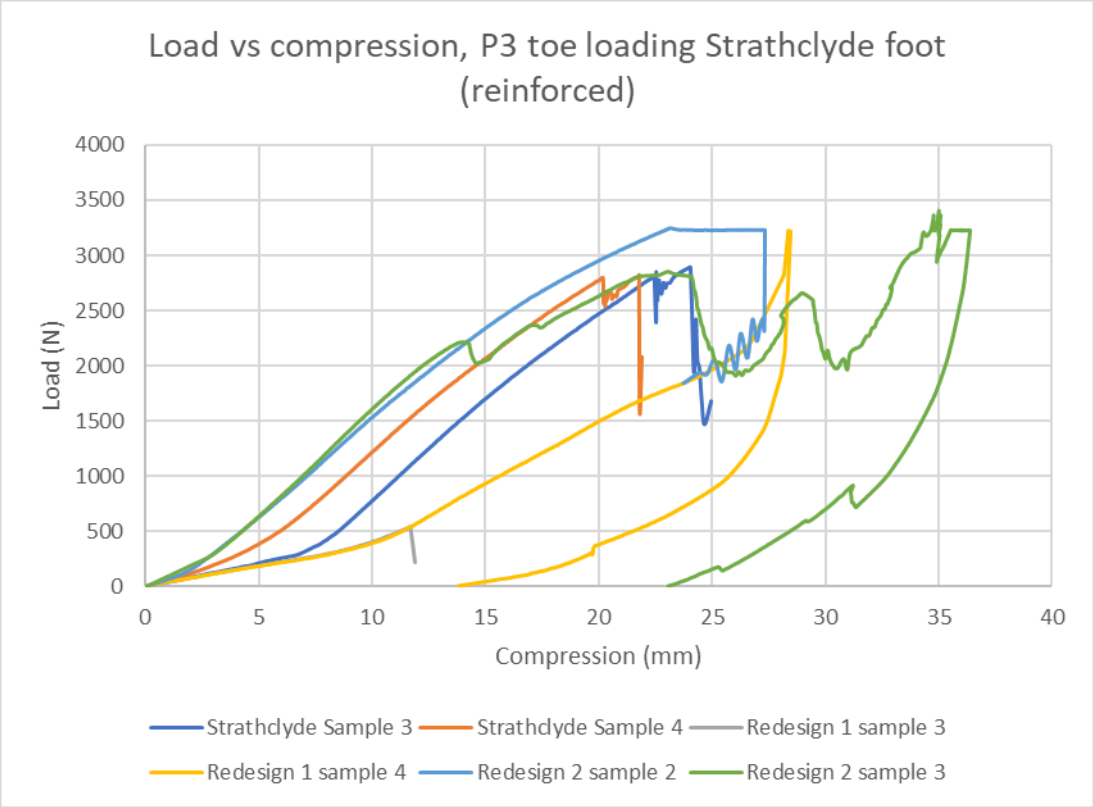

Figure 121 - Comparison of all designs of the Strathclyde foot tested to the P3 ultimate static load for toes with reinforcement

When reinforcements were included (rods for the original design and blades for the subsequent redesigns) the behaviour observed was quite different (see Figure 121). The original design of the Strathclyde foot failed catastrophically with the rods failing in both cases and one of the upper toe sections in sample 3 breaking off. The maximum loads achieved were 2890N for sample 3 and 2825N for sample 4. The

first redesign had a catastrophic failure (both lower toe sections broke off) at 540N of sample 3 while sample 4 was able to safely reach the maximum load and unload without damage. Both samples of the second redesign were able to reach the maximum load of the P3 ultimate static however sample 2 stopped suddenly and upon examination was found to have deformed significantly and so considered a fail. The compression at maximum load was greater (4.4mm) than that observed in either sample 4 of the first redesign (0.1mm) or sample 3 of the second redesign (0.9mm) and probably the cause for the test stopping. Sample 3 showed unusual load-compression behaviour, with loads increasing and decreasing across compression rather than at 175N/s as programmed. This was not observed during testing and the maximum load was met and held for 30s with sample 3 showing no excessive deformation post-testing. As such sample 3 was declared a pass. Each of the feet showed a significant change in gradient early on which corresponds to the engagement of the reinforcement with the lower toe section adding additional resistance to loading, and so system stiffness. The second redesign was the earliest to engage followed by the original design and later, but less distinctly, the first redesign. It was considered that the replacement of the rod feature with a blade was an improvement as one sample of either redesign was able to complete the loading cycle without failing however, redesign 1 sample 3 failed at a load well below that of the original Strathclyde feet and redesign 2 sample 2 did fail, although not catastrophically and at the maximum load of this test, unlike the existing Strathclyde feet. Redesign 1 sample 4 did continue to survive being loaded to the maximum conditions of P4 and P5 toe loading conditions without failure however it was not considered to pass at any level due to deformation sustained during P3 loading. With such a small sample size, excessive deformation in samples and the differences in manufacture and material the redesigns could not be declared

improvements over the existing Strathclyde foot, although the FEA, carried out in Appendix B – Finite Element Analysis of foot designs, predicted improved performance of the R2 design when compared to the existing design using the same material properties.

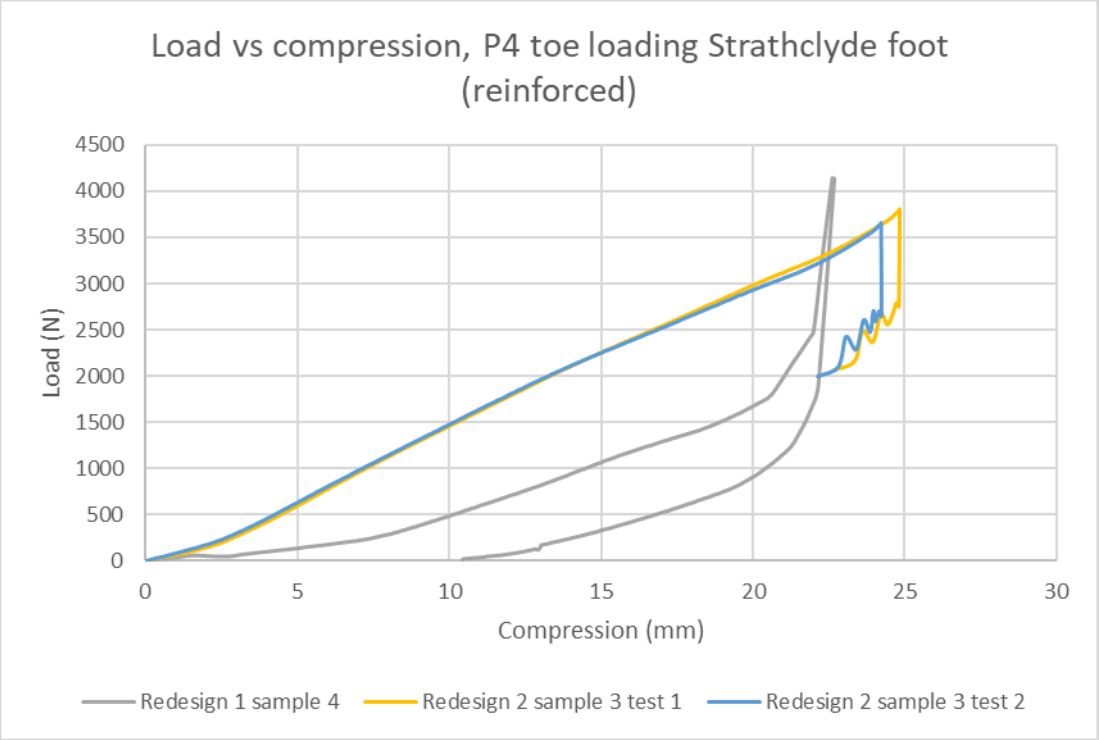

Figure 122 - Comparison of all designs of the Strathclyde foot tested to the P4 ultimate static load for toes with reinforcement

Sample 4 of the first redesign and sample 3 of redesign 2 passed the P3 ultimate static loading condition and were tested to the P4 ultimate static loading condition (Figure 122). Redesign 2 sample 3 was tested twice at this level as during the initial test the Instron machine automatically stopped the test with no apparent cause. No permanent deformation or damage was observed so the sample was retested however the test again unexpectedly stopped and permanent damage was observed this time precluding the sample from further tests. Redesign 1 sample 4 was able to reach and maintain the maximum load and unload with no permanent

deformation or damage. This sample also went on to successfully meet the P5 ultimate static loading level. Comparing the two samples directly shows the difference in initial stiffness highlighted in P3 testing due to the point of engagement of the blade with the keel with redesign 2 being initially stiffer. As loading increased redesign 1 sample 2 became stiffer reaching a maximum compression of 22.7mm at 4130N while redesign 2 sample 3 reached a maximum compression of 24.8mm at 3805N (the point at which testing stopped).

The performance of the redesign samples with blades included was a clear improvement on the original design, which failed in both samples prior to 3000N. The first redesign had mixed results with sample 4 successfully completing testing to the P5 ultimate static loading level (maximum load 4480N) while sample 3 failed catastrophically at 540N during the P3 test. The second redesign had one sample fail at the maximum load during P3 testing (3220N) and one sample fail at approximately 3600N during P4 testing. The consistency of the manufacture of the samples must be questioned given the wide range of performances observed although the area of failure was consistent within each model. Redesign 1 failed under tension at the underside of the bottom toe section, in the three cases where it failed, where redesign 2 failed in compression on the top surface of the upper toe (see Figure 107) in all cases. The failure at the heels was initially due to the ball failing in all cases however, deformation was also observed in the keel itself at the bottom of the heel section.

In redesign 2 the toe section was strengthened by increasing the width as well as the depth of the lower toe section and lead to the failure occurring elsewhere, namely on top of the upper toe section.

5.6.2 Heel tests

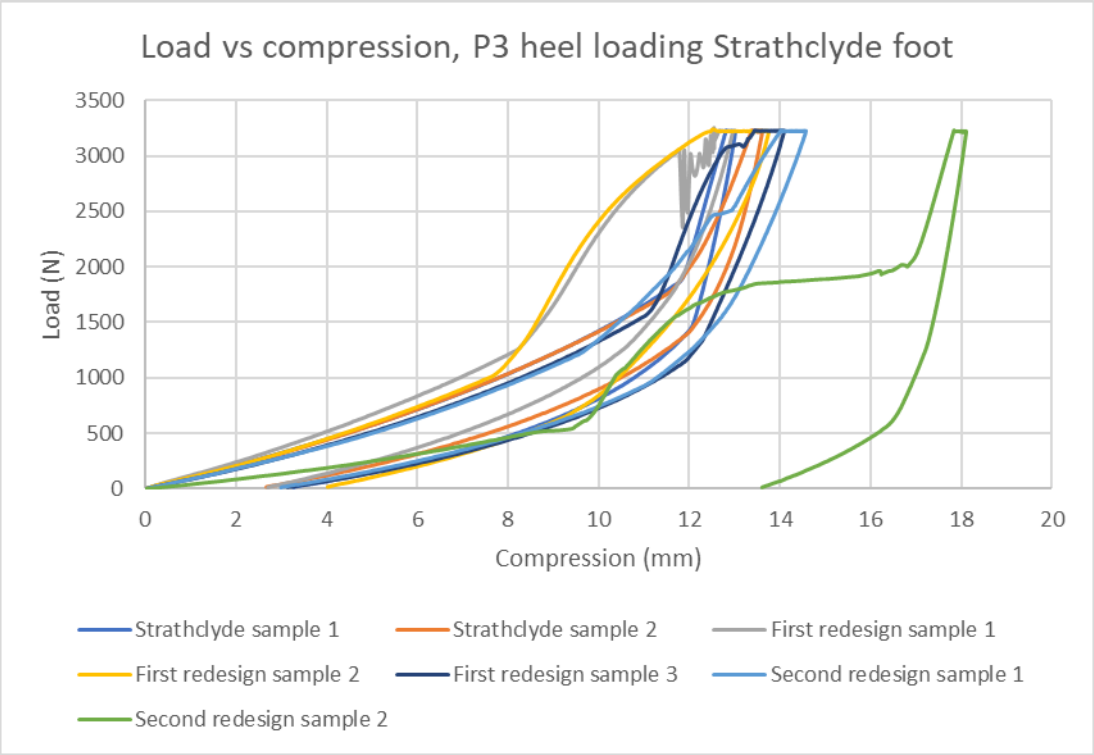

Figure 123 - Comparison of all designs of the Strathclyde foot tested to the P3 ultimate static load for heels

The original Strathclyde foot was able to meet the P3 ultimate loading condition for the heel for both cases. The first redesign had one failure in sample 1 due to fracture of the keel followed by two successes with samples 2 and 3. The second redesign passed with sample 1 however sample 2 failed with excessive deformation of the keel and failure of the ball. The second sample of the second redesign showed a very different behaviour to all of the other samples from the outset which suggests the ball may have had different properties to the others. The failure of this ball is what likely caused the keel to deform so much more than the other samples, although redesign 2 sample 1 did deform the most of the surviving samples. All surviving samples of both redesigns showed a greater degree of creep at maximum load than the original design (see Table 10). Creep was measured by subtracting the compression of the sample at the first load point at or above maximum load from

the final compression of the sample at or above maximum load prior to unloading. This creep was likely a result of material properties of the samples as the samples made of Duraform EX (all redesigns) showed creep at greater than twice the rate of the polypropylene samples (Strathclyde samples). Creep may occur in polymers at stresses that are below yield, as appears to have happened in these cases. Creep in polymers is caused by untangling of polymer chains as yielding is not possible (Jansen, 2015). The greater creep in the Duraform EX samples suggests that such untangling is more easily achieved than in the polypropylene samples, which is consistent with the differences in manufacturing methods between samples. In SLS small areas are melted together and cooled over a short time period compared to the extended time the injection moulded polypropylene is maintained at a higher temperature, allowing longer chains to form. The lack of extended chains and bonding in the Duraform EX is likely a cause of the poorer performance observed when compared to the polypropylene samples despite the predicted improved performance of the FEA carried out in Appendix B – Finite Element Analysis of foot designs. It is recommended that samples of the existing Strathclyde foot be produced in Duraform EX by SLS to allow for a fair comparison of designs or preferably a method better representing the final injection moulding of samples is found for future prototypes. The deformation during creep is potentially largely elastic and may be mostly recovered from after loading has been removed however, this did not appear to have been the case in these samples as remaining deformation was observed when the samples were loaded again as described in 4.8 P4 Heel test and 5.5 P4 Heel test.

Sample	Creep at maximum load (mm)
Strathclyde sample 1	0.22
Strathclyde sample 2	0.24
First redesign sample 2	1.34
First redesign sample 3	0.66
Second redesign sample 1	0.56

Table 10 – Creep at maximum load of surviving samples following P3 ultimate static loading of the heel

All three samples of the first redesign may be seen to become stiffer sooner than the original Strathclyde foot (see Figure 123) however in all three cases the stiffness decreased as the load continued to increase while in the Strathclyde foot the stiffness was maintained until maximum load. The initial increase in stiffness of the redesigned feet was due to contact between the keel and ground being made sooner than in the existing design, which would reduce the feeling of a ‘soft’ heel when in use, although potentially causing a pivot point and forcing the user forward prematurely. It is recommended that a gait trial be carried out to determine if this effect is present and potential redesign be carried out to amend this if it is the case.

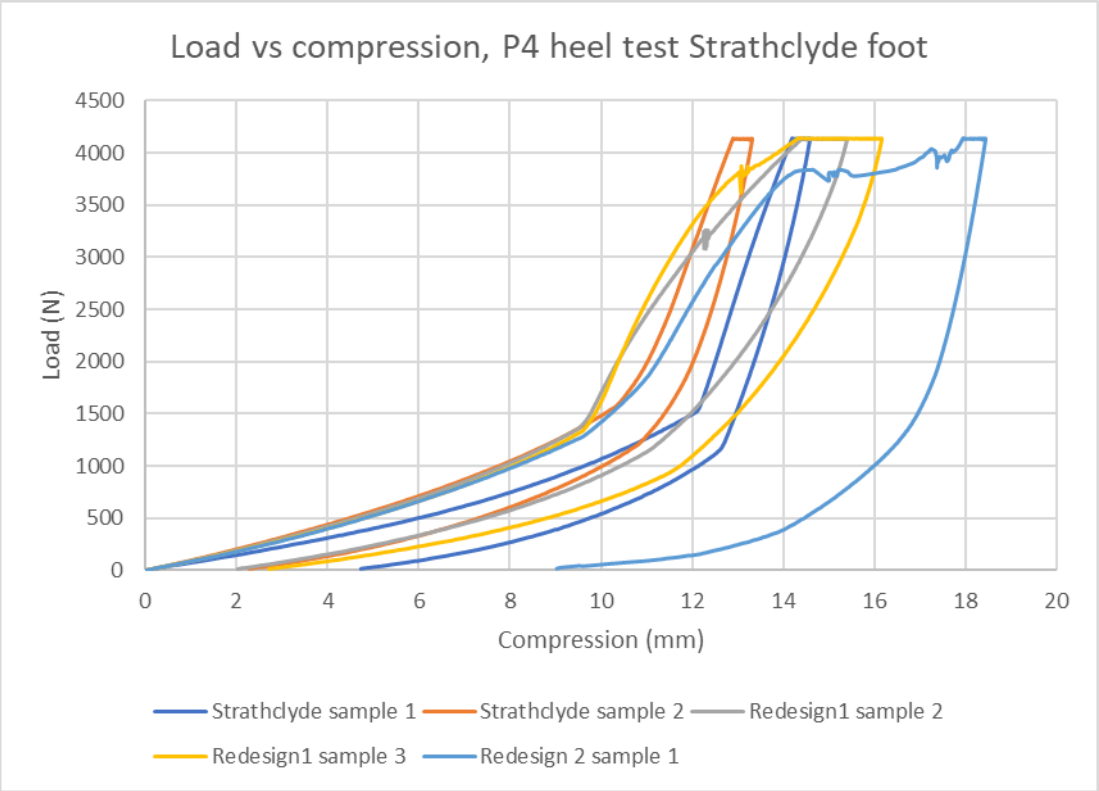

Figure 124 - Comparison of all designs of the Strathclyde foot tested to the P4 ultimate static load for heels

The surviving samples were tested to the P4 ultimate static loading level with both samples of the original Strathclyde foot and the first redesign surviving the process without permanent deformation or damage. Redesign 2 sample 1 failed during testing with the ball breaking and permanent deformation of the keel occurring. The first design was observed to become stiffer at a lower load than the original Strathclyde foot however the decreasing stiffness at increasing load was once again observed. Creep was measured by subtracting the deformation at the first load value at, or exceeding the target load, from the final deformation at or exceeding the target load. The creep at maximum load was once again larger than that of the original Strathclyde foot (see Table 11) by more than double, again probably related to the manufacturing method and material rather than the design however, the design may require modification to increase the stiffness of the keel at

the lower side of the heel or to prevent a pivot point occurring and forcing the user forward prematurely.

Sample	Creep at maximum load (mm)
Strathclyde sample 1	0.41
Strathclyde sample 2	0.42
First redesign sample 2	1.01
First redesign sample 3	1.86

Table 11 – Creep at maximum load of surviving samples following P4 ultimate static loading of the heel

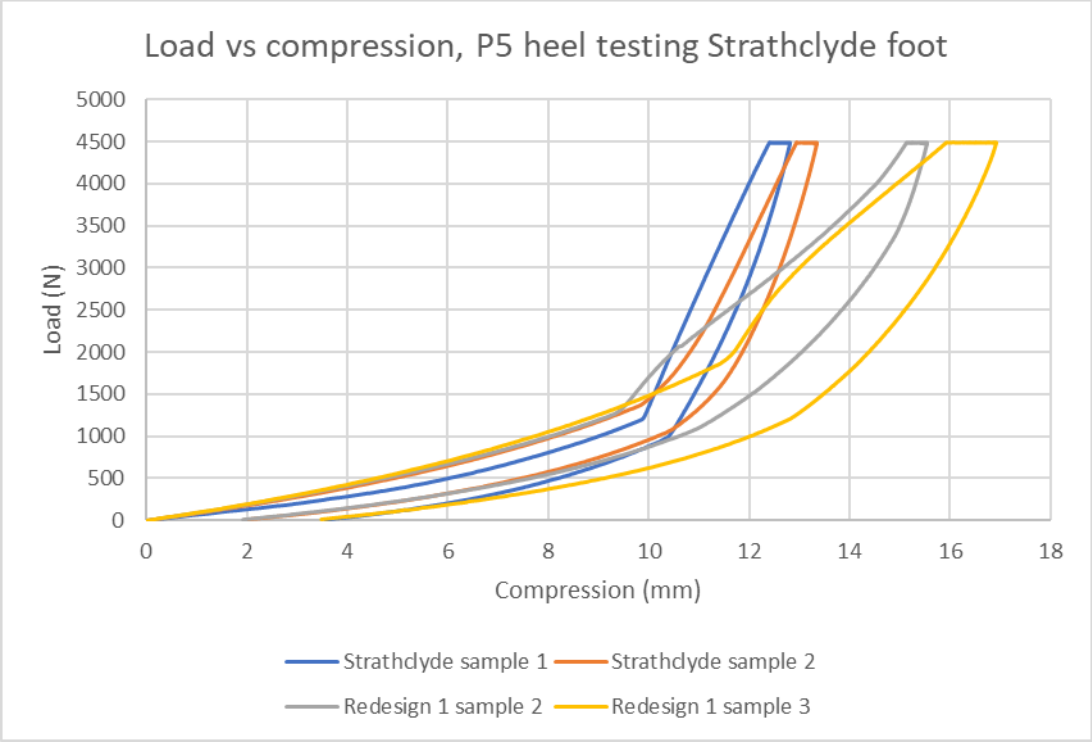

Figure 125 - Comparison of all designs of the Strathclyde foot tested to the P5 ultimate static load for heels

The balls in all samples tested to the P5 ultimate static loading level for the heel failed and permanent deformation was seen in the keels. The balls are a major area of concern and are recommended to be further investigated in terms of both shape and material (see section 6.2.1 Performance). The behaviour of the two redesign

samples were more different to one another than previously observed with sample 3 requiring approximately 500N more load before the increase in stiffness due to keel contact was observed. This was due to the change of ball between P4 and P5 testing with the replacement ball not having been compressed by previous testing. Creep was measured by subtracting the deformation at the first load value at, or exceeding the target load, from the final deformation at a load equal to or exceeding the target load. The creep observed in redesign 1 sample 2 during this testing was similar to that of the original Strathclyde foot samples while in redesign 1 sample 3 the creep was again more than twice that of either original Strathclyde sample although less than that observed during the P4 testing (see Table 12). This creep had possibly reduced due to the effect of permanent deformation remaining in the sample from prior loading conditions causing a larger area of the foot to contact the baseplate and resist greater deformation.

Sample	**Creep at maximum load (mm)**
Strathclyde sample 1	0.42
Strathclyde sample 2	0.41
First redesign sample 2	0.41
First redesign sample 3	1.01

Table 12 - Creep at maximum load of surviving samples following P5 ultimate static loading of the heel

The original Strathclyde foot and the first redesign cannot be claimed to have met the P5 level of the ultimate static loading at the heel due to failure of the rubber balls however both samples did pass at the P4 level. Redesign 2 cannot claim to have met any loading level as only sample 1 was able to pass the P3 loading level and did not successfully complete the P4 loading level. The second redesign showed a worse performance than the first redesign with the keel permanently

deforming during P3 testing for sample 2 and P4 testing for sample 1. The change in design between the first and second redesigns partially increased the stiffness of the keel at the heel. This increased stiffness led to increased deformation of the front wall of the heel arch which was not strengthened in the redesign. This increased deformation may have contributed to the failure of the balls as they would then experience a greater compression, conversely, if the balls used in redesign happened to be weaker than those used in other samples the early failure of the balls could have contributed to the deformation of the keels. The most significant point to address in further work regarding the heel would be to find a more consistent and better suited solution to the heel cushion than the rubber balls used in these tests however, the stiffness of the heel arch from redesign 2 would need to be remedied. Such a ball, once included, may lead to other effects, such as increased deformation of the heel section or additional stress points and failures becoming apparent.

5.7 Comparison to other feet

A comparison to other feet from literature was carried out to compare the performance of the Strathclyde foot second redesign to systems currently in use around the world. Using the performances of the existing feet as a comparison to the Strathclyde feet would give an indication of areas which require improvement and potential features which could contribute to such improvement. Jensen & Treichl, 2007, tested many prosthetic feet used in low-income countries to the ISO 10328 standard so it makes sense to compare the results from the testing here where possible. Jensen & Treichl tested virgin feet and feet exposed to UV light or humidity however the Strathclyde feet were not exposed to any environmental conditions so only the virgin feet will be used for comparison. Only the P5 level was applied by Jensen & Treichl with loads of 2240N applied at toe and heel in static

proof testing and 4480N in ultimate static strength testing. It should be noted that the Strathclyde feet were loaded to each of the P-levels sequentially in testing but were not subjected to the proof loading. Another factor which would undoubtedly have some bearing is that in each case Jensen & Treichl tested a complete foot unit, that is to say that each foot had a cosmesis, whereas the Strathclyde feet were tested only as the core structure. The cosmesis would be expected to deform more easily than the keel and so would increase the total deformation observed at a given load compared to a sample without a cosmesis. By comparing the Strathclyde keels to existing feet, a target deformation may be decided and so the extent of deformation permissible in the cosmesis. The results for the heels (where multiple samples of each design of the Strathclyde foot were used the mean value is presented) under ultimate static test conditions were:

Heel	Peak load (kN)	Maximum deformation (mm)
HCMC	4.46	17.62
VI	4.44	29.59
EB-1	4.48	17.24
HI	4.47	19.79
Myanmar	4.47	20.42
Mozambique	4.44	20.96
Angola	4.47	32.56
PHN	4.47	35.50
Tatcot	4.48	16.63
Jaipur	4.48	23.09
NISHA	4.71	27.98
Mukti	4.60	24.92
OM	4.57	26.90
Kingsley	4.48	34.39
Bock	4.47	42.81
CR	4.47	27.38
PF-Thai	4.46	23.38
Pro-cir	4.47	25.44
Afghan	4.47	36.67
Alimco	4.47	41.87
ASB	4.48	24.10
Strathclyde original	4.48	13.09
Strathclyde redesign 1	4.48	16.24
Strathclyde redesign 2	4.13	18.45

Table 13 – The peak load and maximum deformation values of the heels tested. The Bavi foot had no normal values supplied and so was not included. Modified from Jensen & Treichl, 2007 (Jensen & Treichl, 2007) tables IV and V.

The original Strathclyde foot and first redesign deformed less than all of the samples tested by Jensen and Treichl, as may be expected given the lack of cosmesis. The second redesign of the Strathclyde foot was included and although it did not reach the P5 level of loading it did show increased deformation compared to the previous iterations of Strathclyde foot bringing it into the lower end of the range of results recorded by Jensen and Treichl. The Tatcot foot was the least deformed of all samples tested by Jensen and Treichl with a maximum deformation of 16.63mm. The Tatcot foot is formed of a wooden keel and rubber heel and exterior as shown in Figure 126. The most deformed foot under heel testing was the Bock foot, a polyurethane keeled foot (no other details provided), at 42.81mm.

Figure 126 – Cross section of a Tatcot foot (from Jensen & Treichl, 2007(Jensen & Treichl, 2007))

If the Strathclyde feet were to be tested with a cosmesis a greater degree of deformation would be expected as the cosmesis would be unlikely to provide as much resistance to loading as the core structure. The amount of deflection has to be balanced in a way that provides adequate cushioning to the user (to prevent jarring

at heel strike) without being so great as to give a feeling of a ‘soft’ heel and the impression of walking uphill. The balls in the heel of the Strathclyde samples failed, leading to greater compression, so with a sturdier replacement in future designs the compression may not be greatly increased by the addition of a cosmesis. A ball of similar stiffness is recommended so it may be appropriate to apply a softer cosmesis to provide some initial damping upon heel loading and prevent a jarring sensation or alternatively to modify the design of the heel to allow increased flexion, particularly around the lower part of the heel where the keel first contacts the baseplate. The prostheses with rubber cosmesis tended to have less deformation than the prostheses with polyurethane or polyurethane foam cosmeses. Given the apparent stiffness of the Strathclyde feet it may be that a polyurethane cosmesis may provide balance to the stiffness of the system. A rubber cosmesis may be pursued if it were to replace the ball in the design and so provide the shock absorption function as in the Tatcot, Mozambique and Angola feet, for example.

The results from toe testing were as follows:

Toe	Peak load (kN)	Maximum deformation (mm)
HCMC	4.46	24.54
VI	4.45	28.42
EB-1	4.48	34.61
HI	4.46	27.63
Myanmar	4.47	26.99
Mozambique	4.47	29.93
Angola	4.47	41.07
PHN	4.46	33.75
Tatcot	4.48	28.52
Jaipur	4.47	42.83
NISHA	4.53	62.30
Mukti	4.50	79.64
OM	4.57	73.46
Kingsley	4.47	34.40
Bock	4.48	24.42
CR	4.47	32.49
PF-Thai	4.46	53.94
Pro-cir	4.47	45.80
Afghan	4.47	63.72
Alimco	4.46	58.21
ASB	4.48	57.38
Strathclyde original	4.48	21.94
Strathclyde redesign 1	4.48	21.58
Strathclyde redesign 2	3.22	36.40

Table 14 - The peak load and maximum deformation values of the toes tested. The Strathclyde redesign 1 values are those of sample 4 only. The Bavi foot had no normal values supplied and so was not included. Modified from Jensen & Treichl, 2007 (Jensen & Treichl, 2007) tables IV and V.

The existing Strathclyde design and first redesign feet were again the most stiff however, in toe loading the first redesign deformed by 0.36mm less than the original design. The second redesign deformed excessively at the P3 load level and was included for completeness, but not comparison. The Bock foot (24.42mm) was again the stiffest of the feet tested by Jensen & Treichl with the HCMC foot only deformed by 0.12mm more (24.54mm). The Mukti foot, a Jaipur foot, deformed by the greatest amount, 79.64mm with the OM Jaipur foot deforming the second most at 73.46mm. That such a large deformation at the toe is seen in Jaipur feet is not a surprise as the Jaipur foot has a microcellullar rubber block froming the toe with no other support. The keel of the Strathclyde foot only extends to an equivalent of the ball of the toes and so similarly to the Jaipur feet has no toe support. With a cosmesis the Strathclyde foot would be expected to have toes although with no current design the resistance and deformation they would undergo during P5 ultimate static loading is unknown. Assuming that they only serve a cosmetic function this would efectively increase the deformation observed in samples by approximately 0.34cm for each cm of toe length with no significant additional resistance. If the Strathclyde foot were to be made up to a 24cm configuration this could add aproximately 20.4mm to the compression observed bringing the total deformation to approximately 42mm which would put the Strathclyde foot as the 10th most deformed in the list of samples tested by Jensen & Treichl. This suggests that care must be paid to the design of the cosmesis to involve some resistance (for example the flat belt drive present in the HCMC, Kingsley and Alimco feet or the tyre-rubber sole of the HI foot) or else that the keel should perhaps be increased in length to prevent excessive toe deformation.

5.8 Force plate trials

It was decided to attempt some walking samples of the second redesign of the Strathclyde foot upon a force plate to better understand the behaviour of the foot in terms of centre of pressure, force and Pedotti diagrams.

5.8.1 Specimens

One of the two remaining untouched sample feet was used along with a blue and white rubber ball from the same batch as the others previously used. A fibreglass blade was made by the same method and from the same material as the previous blades. These were assembled and the ball was fixed with masking tape into the heel socket, as there was no prevention of mediolateral slip of the ball otherwise. A pair of prosthetic stilts were sourced from the National Centre for Prosthetics and Orthotics on which were attached a pair of Otto Bock size 24 SACH feet (with toes). The right foot was removed and replaced with the Strathclyde foot sample. Both feet were unshod and adjusted to make the heights as equal as possible

5.8.2 Method

The investigator (male, height 173cm without stilts, weight 85kg) was to walk for a number of minutes on the stilts (see Figure 135, page 306) to grow familiar with them before attempting any tests, with frequent breaks to be taken as required. The investigator would then walk across the force plates (Kistler 9218C model) in as normal a manner as possible with the results being recorded. Results without a clean, single foot hit on a single force plate were to be discarded. Results were recorded by Vicon Nexus at 100Hz and imported into Microsoft Excel for processing later.

5.8.3 Results

Five clean strikes of the Strathclyde foot were recorded during the testing period. Walk 4 was travelling in the opposite direction to the other results and so was adjusted and presented in the same sense as the others. The direction of travel was indicated by increasing X values with Y equals zero at the most lateral point of each step.

The foot contacts varied somewhat in all recorded variables however certain features were clearly displayed in all cases. When the centre of pressure (COP) was plotted x against y (Figure 127), a clear progression was visible laterally as the contact advanced before a sharp change in direction medially prior to contact being broken. The lateral progression varied from between 25.3mm and 36.0mm (mean 29.9mm) while the length of the contact was between 125.4mm and 158.8mm (mean 143.8mm). All contacts were of approximately the same endurance, 0.6s (0.59-0.61s).

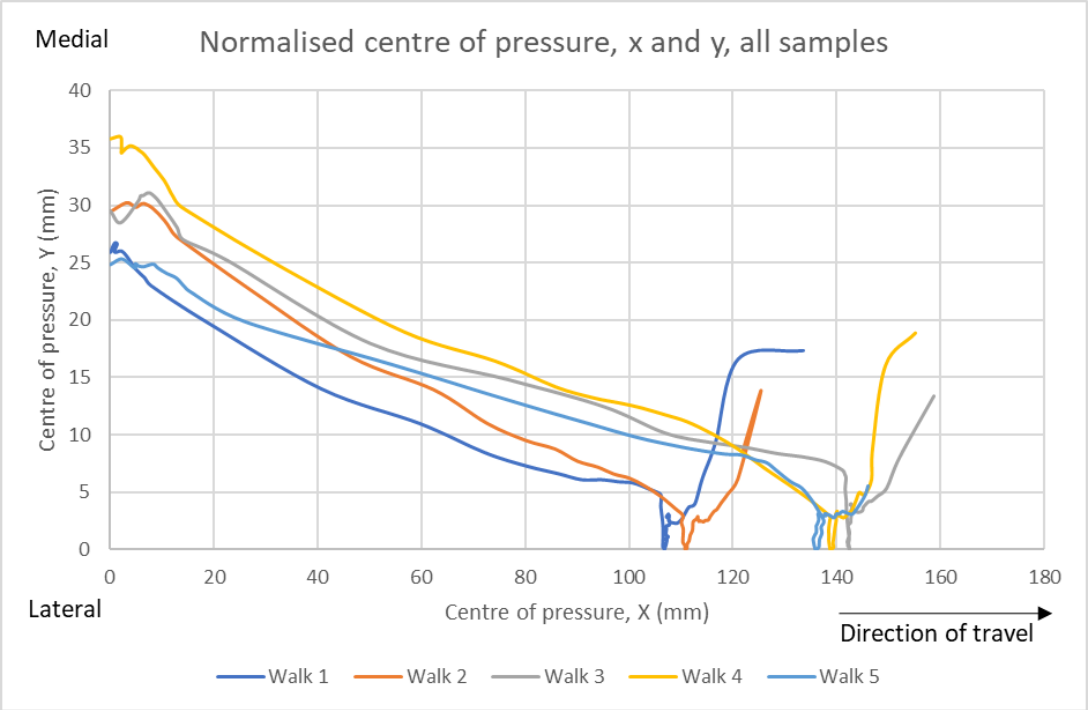

Figure 127 – Normalised centres of pressure for all samples. Contact begins at 0mm on the x axis and the most lateral position reached in the sample is set to 0mm on the y axis.

When looking at the F_x values of all walks (Figure 128) negative force values that would indicate force acting against the direction of motion, or a braking force may be observed. Within these values a double trough was seen in all of the samples. At this point the heel would be the only part of the foot in contact with the ground so it was an effect of the heel that causes the observable troughs. The initial trough was due to the contact of the ball with the ground and the rise was likely due to deformation of the ball prior to it increasing in stiffness leading to the second trough. There was a smooth progression through zero to a single peak of propulsive force in each case. These forces varied from between 167.1N and 227.3N (mean 191.1N).

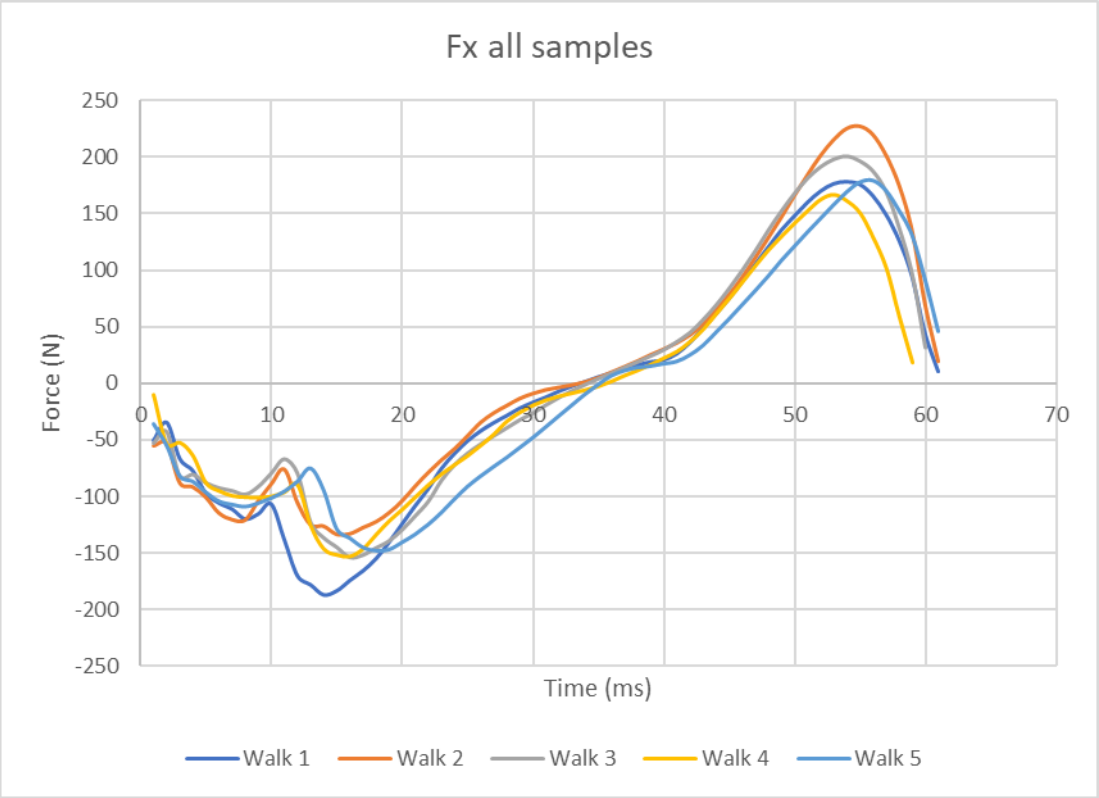

Figure 128 - F_x of all Strathclyde foot walking samples

When looking at the F_z pattern a clear two-peak structure was visible (Figure 129). The trough and second peak were very smooth however there was some disturbance on the rising side of the first peak in each case. This was likely caused by the ball at the heel deforming and then the keel coming into contact with the ground and compensation by the investigator for this. The range between the highest values of the first peak is 159.7N (minimum 915.6N, maximum 1075.3N) and for the second peak was 82.7N (minimum 915.4N, maximum 998.1N) while the range in the values at the nadir of the trough was only 24.5N (minimum 511.0N, maximum 535.5N).

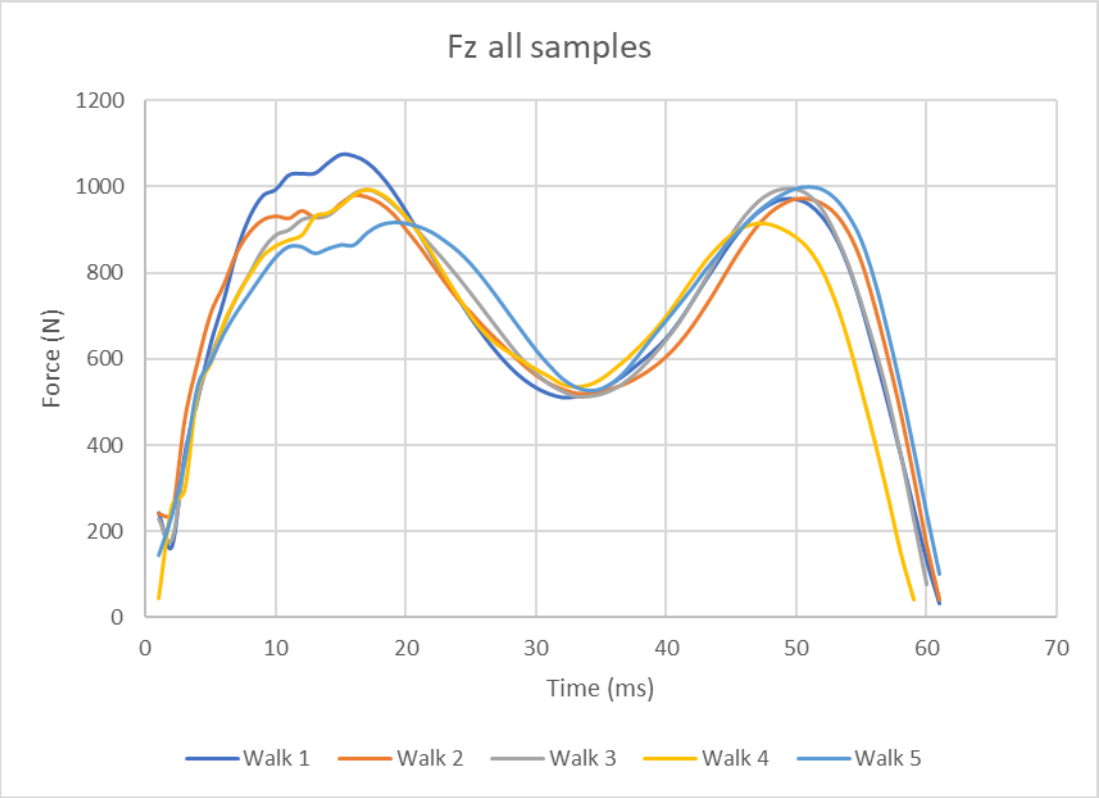

Figure 129 – F_z of all Strathclyde foot walking samples

In Arya, Lees, Nirula, & Klenerman, 1995 (Arya et al., 1995), a number of measures were derived from force plate data which were used to characterise the performance of the feet. These were F_z impact force peak, F_z impact load rate, F_z propulsive force peak, F_z support impulse, F_y braking impulse and F_y propulsive impulse (F_y for Arya et al. corresponds to F_x here). The first two values were determined using the 'impact force peak' which was not visible in the data recorded here, perhaps as a lower sampling rate was used compared to Arya et al. (100Hz compared to 200Hz) and as such could not be calculated for this data. The other measures however could be and were found to be as follows:

	F_z propulsive force peak	F_z support impulse	F_x braking impulse	F_x propulsive impulse
Walk 1	11.43	2.59	0.179	0.141
Walk 2	11.44	2.57	0.151	0.171
Walk 3	11.71	2.54	0.161	0.156
Walk 4	10.77	2.42	0.157	0.118
Walk 5	11.74	2.60	0.180	0.131
Mean	11.42	2.55	0.166	0.143
SACH	9.76	5.85	0.288	0.273
Seattle	9.76	5.93	0.283	0.278
Jaipur	9.67	5.79	0.317	0.274
Normal	11.13	6.57	0.388	0.361

Forces are N/kg and impulses are N.s/kg as in Arya et al., 1995

Table 15 – Peak force and impulses for each walking test on the second redesign Strathclyde foot and the mean values recorded by (Arya, Lees, Nirula, & Klenerman, 1995)

The Fz propulsive force peak of the Strathclyde foot second redesign was greater than the mean values recorded by (Arya et al., 1995) for the SACH (9.76N/kg), Seattle (9.76N/kg), Jaipur (9.67N/kg) and normal foot (11.13N/kg) however in each other measure the Strathclyde foot had lower values (see Table 15).

Pedotti diagrams were generated for each walk; Figure 130 shows a representative sample.

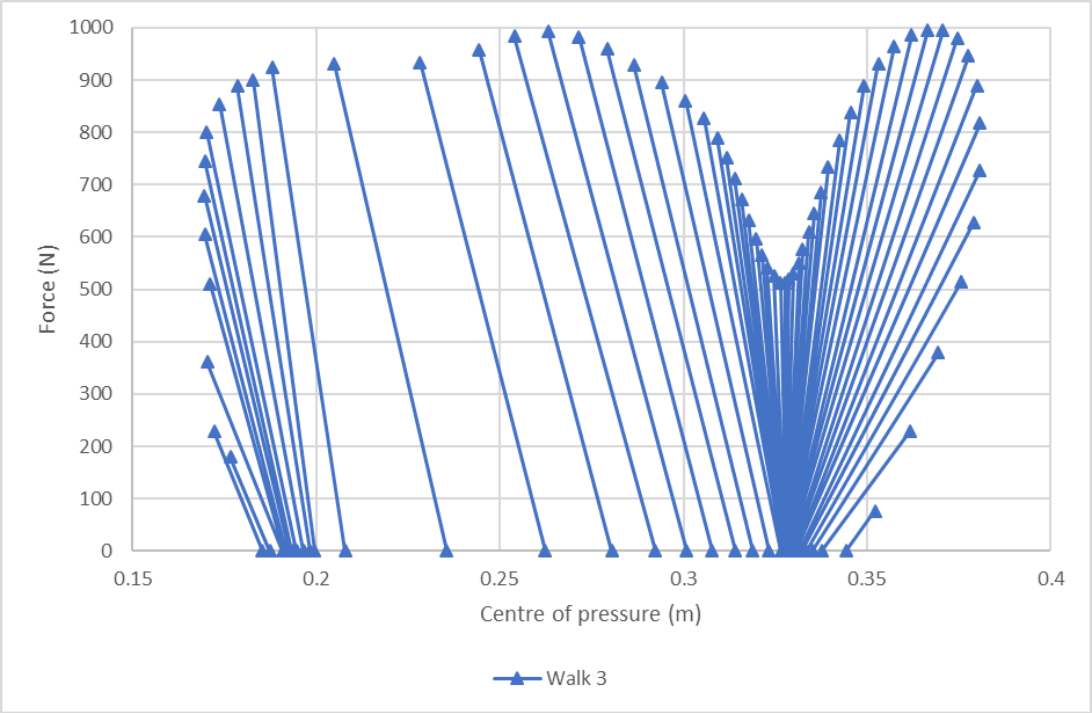

Figure 130 – The Pedotti diagram for walk 3

It was seen that the Pedotti diagram for walk 3 shows a cluster of COP points at the rear and another at the front. The rear cluster was likely to be around the point of the keel where it contacted the floor on compression of the rubber ball at the heel. The front cluster was due to the ball of the foot (the end of the toes effectively for this keel) rotating as the subject moved toward toe off. The transition between these two clusters was sparsely populated which indicated that it occurred relatively quickly. The x direction of forces showed that there was some braking force applied until contact at the ball of the foot where it transitioned to propulsive action. The reduction in force seen beginning in midstance and reaching a minimum during toe contact corresponded with what may be observed in normal gait in response to contact of the opposite foot. When all these points were combined it appeared that little time was spent on the heel of the Strathclyde foot.

5.8.4 Discussion

The foot did not break or show signs of permanent deformation under repeated loading and unloading under working conditions during which several measurements were taken. Clear patterns were observed although there was variation in each case. The differences in behaviours were likely related to variations in the walking of the investigator, as there was no attempt to keep these similar other than the investigator walking at what they felt to be the same speed in each case, which was not recorded and is recommended to be in future testing. This could be controlled through the use of a metronome or similar device in order to ensure a more even pace across samples or as (Arya et al., 1995) did, using a timing gate to exclude readings with excessive speed variation. A controlled walking speed is likely to produce more consistent results in terms of contact duration time and length, although if the pace were set to a value outside of the subjects' typical range it could lead to unusual effects being observed in contact duration and COP progression. The clear double peak visible in F_z (Figure 129) was similar to what would be expected in normal gait. In three of the cases the second peak was lower than the first which is the opposite of normal gait however the other two samples showed a higher peak on the second which was consistent with normal gait (see Figure 131). It would have been beneficial to have the investigator's normal gait without stilts for comparison but this was not recorded. There was likely to be some variation caused by the changed segment lengths and mass by removing the stilts however, it is recommended for future gait studies to include a normal condition for comparison.

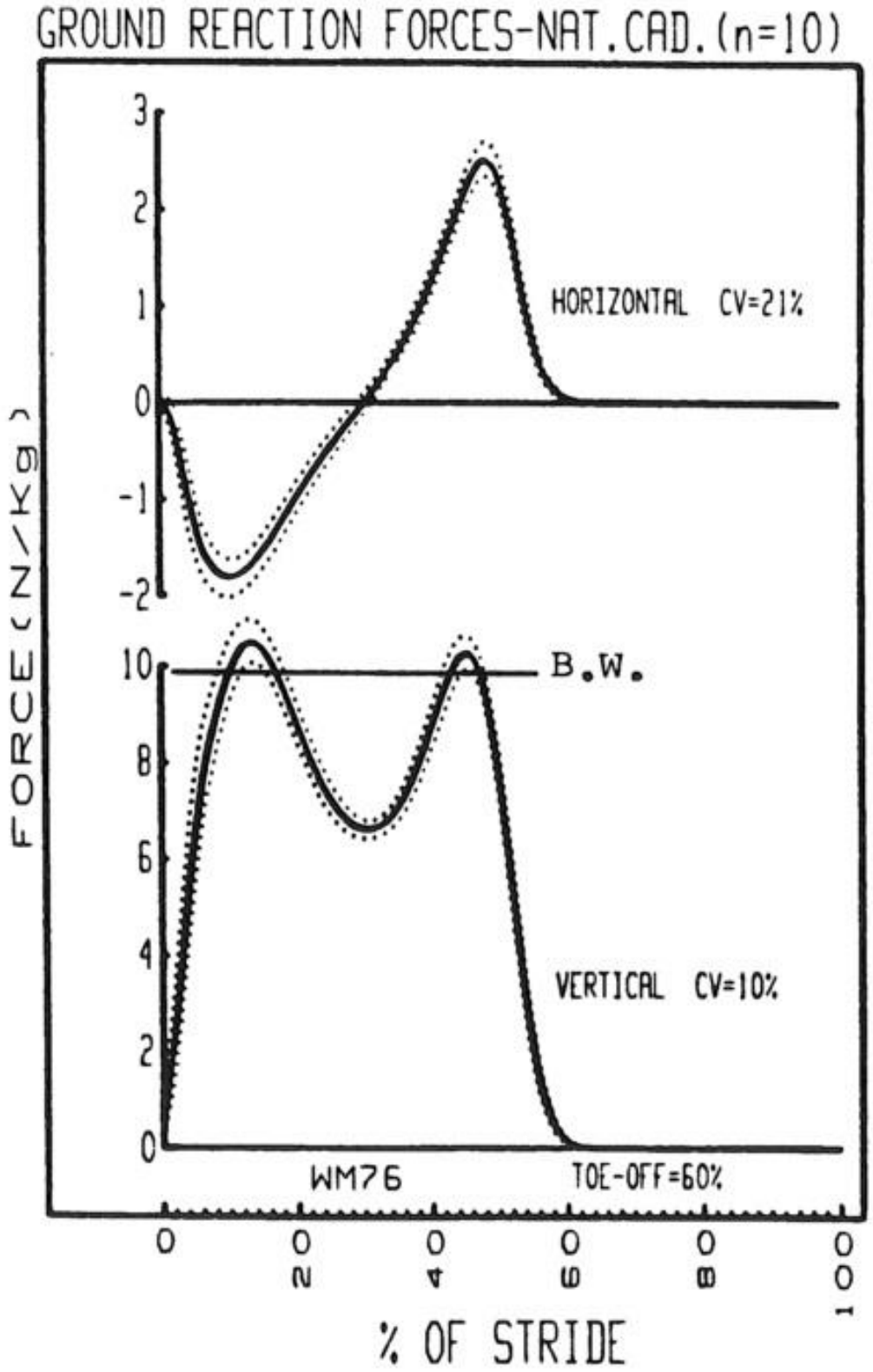

Figure 131 – Normal ground reaction forces in non-amputee walking gait at natural cadence (horizontally, top and vertically, bottom) from (D. A. Winter, 1988)

The double trough of F_x is not a natural pattern in gait (see Figure 131) and could be improved with the inclusion of a stiffer material within the heel socket to more closely resemble the natural pattern. This should serve to give a more constant force through loading and also reduce the likelihood of the ball deforming to the extent that the keel contacts the floor at the heel. This in turn, by providing a more stable base for the subject, could extend the time spent on the heel and prevent any pivoting effect by the keel when in contact with the ground.

The centre of pressure followed a similar pattern to what would be expected in normal human gait initially (allowing for variability across individuals – see Figure 132) however it diverged suddenly at the end when the centre of pressure rapidly moved medially. The keel was relatively short and had no ‘toes’ with the keel coming to a finish at the ball of the foot. As the intention was to include a cosmesis with toes this could allow the centre of pressure to return medially more gradually than viewed in these tests and so provide a more natural pattern for centre of pressure. The investigator did note during testing that the front of the foot seemed short compared to the SACH foot opposite.

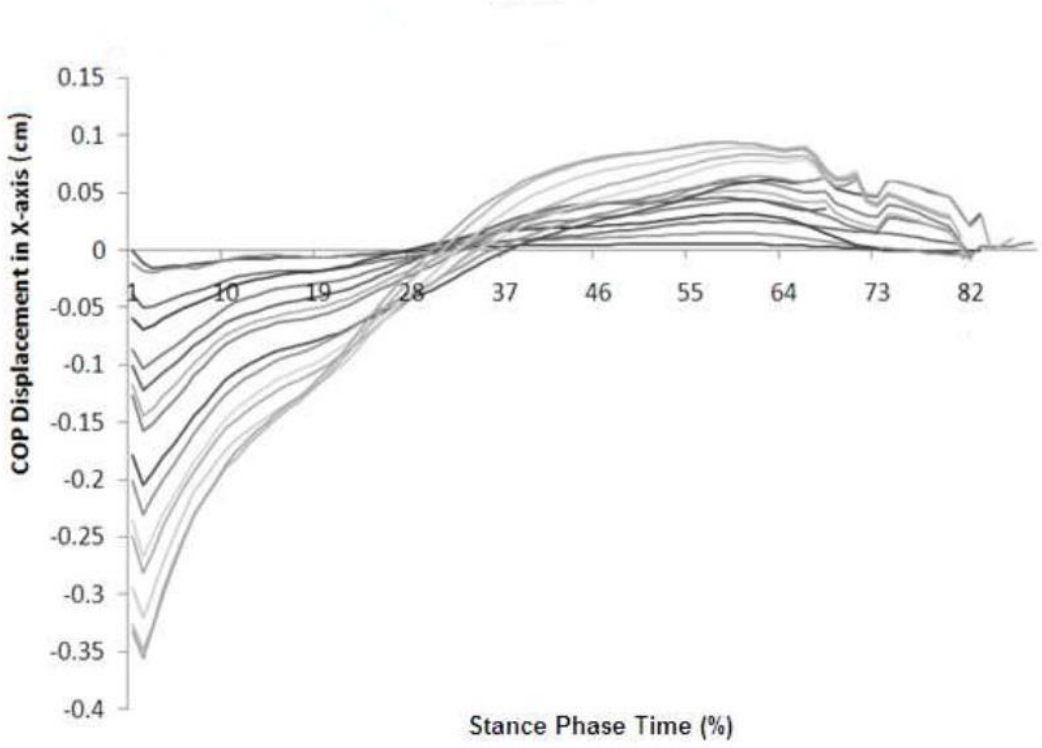

Figure 132 – COP of normal foot in walking (from (Jamshidi et al., 2010)) x is positive laterally

In the Pedotti diagram (Figure 130) each line represents one sample point. The spread of points is an indication of time spent in a particular loading, so the initial cluster at the heel (left) suggested a greater time spent on the heel than at midstance, and a lesser time than that spent at the toe (right). Centre of pressure can be plotted against time to show the time spent on each section of the foot more clearly (see Figure 133). The total contact time during the step was 0.6 seconds, of which more than half of the time was spent with the centre of pressure in the region of the toe. At heel contact the centre of pressure was not fixed with some forward progression (0.01m) seen over the 0.1 seconds however this was relatively slow compared to the subsequent transition to the toe. The transition of centre of pressure from heel to toe was rapid, progressing approximately 0.1m over 0.15 seconds. The short time spent on the heel and midfoot suggests that the foot

encouraged the wearer to progress forward, potentially due to the distance between the centre of rotation of the limb and the heel contact point generating a moment which tended to rotate the foot towards flat. This effect in the human foot would be controlled through eccentric contraction of muscles not available in the prosthetic foot. The relatively large amount of time spent on the toe was suggestive of flexion of the keel causing the heel section to be rotated upwards, out of contact with the ground.

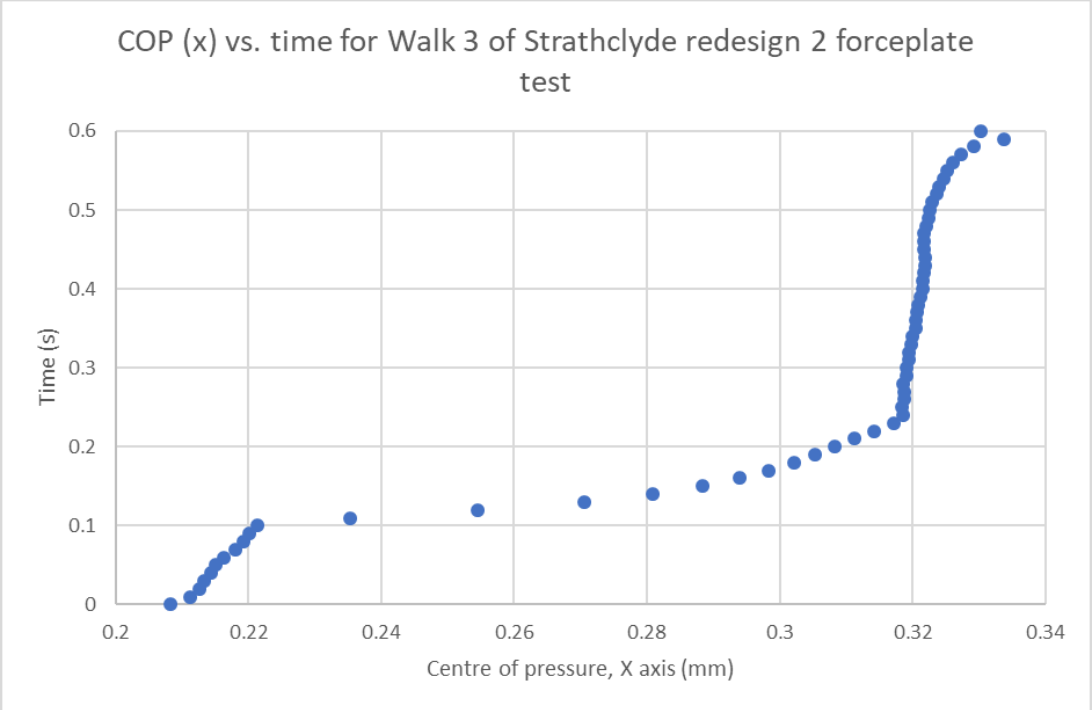

Figure 133 – Centre of pressure in the x-axis against time for Walk 3

The values obtained for F_z propulsive force peak, F_z support impulse, F_x braking impulse and F_x propulsive impulse were compared to the results found by Arya et al. The F_z propulsive force peak was higher than those found for the SACH, Seattle or Jaipur foot at 11.42N/kg compared to 9.76N/kg, 9.76N/kg and 9.67N/kg respectively. It was much closer to that reported for the normal foot 11.13N/kg. The support impulse was very low by comparison however at 2.55N.s/kg as opposed to 5.85N.s/kg, 5.93N.s/kg and 5.79N.s/kg for the prosthetic feet respectively and

6.57N.s/kg for the normal foot. This difference may have been partly due to the fact the subject in this case was not a unilateral amputee (as in Arya et al.) but rather a non-amputee wearing two different prosthetic feet. There is also the possibility that the foot felt unstable causing the subject to place their opposite foot down quicker and so limiting the load carrying of the Strathclyde foot during gait. This could also explain why the F_x braking impulse and F_x propulsive impulse were both similarly low in comparison to the results of Arya et al. as the subject may have been relying on the opposite foot to provide most of the forward movement and only used the Strathclyde foot to pass over onto the opposite foot again. The subject did not report any sensation of this at the time and no trials were recorded for the opposite foot to conduct a comparison between the feet so the reason for this is currently undetermined.

5.8.5 Conclusion

Testing on a forceplate and comparing the results to other works showed that the Strathclyde foot required additional design improvements although certain aspects of performance appeared to be positive. The centre of pressure of the Strathclyde foot was shown to travel laterally as it progressed in the direction of travel before returning sharply medially due to the lack of toe support present in the design, a requirement for further design work, either in the keel or as a feature in the cosmesis. The F_x ground reaction force was similar to that of a normal foot, with the exception of the double trough seen during the initial loading, which was likely due to deformation of the ball, which would be remedied by increasing the stiffness. The lack of stiffness in the ball was also a likely factor in the disturbance visible in the first peak in the F_z response of the foot although the rest of the loading observed was smooth and similar to that typically found in normal feet. A comparison to the results of Arya, Lees, Nirula, & Klenerman, 1995, showed that the Strathclyde foot

had an F_z propulsive force peak similar to that of the normal foot however the values of F_z support impulse, F_x braking impulse and F_x propulsive impulse were all much lower than the normal foot and the other feet tested by Arya et al. It is recommended that force plate testing be repeated in future with multiple subjects, on multiple designs of prosthetic feet as well as in the subjects' normal condition to allow a more complete comparison to be carried out. The walking speed should be controlled, either through a rhythmic device or by exclusion of values outside of a range as Arya et al. did.

The Pedotti diagram highlighted the tendency of the Strathclyde foot to progress forward quickly across the midfoot while still decelerating during toe contact. This was not observed within the natural foot as during midstance the force transfers from decelerating to accelerating the individual. Design work was required to reduce this rapid forward progression to adjust the behaviour of the Strathclyde foot towards the normal foot. The stiffness of the ball was again potentially a cause as an unstable feeling would cause the subject to advance more quickly towards toe contact. There was potentially flexion within the foot leading to the heel coming out of contact sooner than in the natural foot however, this would require identification either through recording a gait test with an uncovered foot sample or through a simulated loading pattern.

The Strathclyde foot second redesign still required design work on the toe section for late stage support and the heel to prevent rapid forward progression and to provide a more natural ground reaction force pattern.

5.9 Summary

This chapter began with the elements of redesign required after the testing in the previous chapter namely increased strength of the toe section and improved interface for the blade and toe sections. The second redesign of the Strathclyde foot

was tested with reinforcement and without to the P3 ultimate static loading condition on the toe with only sample 3 (reinforced) being considered to have passed. Samples 1 and 2 were tested to the ultimate static loading level of P3 on the heel where sample 1 was judged to have passed but sample 2 failed due to ball failure and permanent deformation of the keel. Sample 3 underwent loading to the P4 level of ultimate static loading where it was deemed to have failed due to permanent deformation of the keel. Sample 1 was tested to the P4 level in the heel condition where it was deemed to have failed due to ball failure and permanent deformation of the keel. A comparison of the various Strathclyde foot performances was carried out comparing the feet at respective P-levels for direct comparison. Using the P5 level results for the Strathclyde foot design a comparison was carried out to compare other prosthetic feet as tested by Jensen & Treichl, 2007. Finally, a single subject force plate trial was conducted using the Strathclyde foot to evaluate behaviour in terms of loading and Pedotti diagram where it was found that the foot had a tendency to encourage forward progression of centre of pressure. The F_x pattern observed showed signs of the flexibility of the ball being too great while the F_z pattern was similar to that of normal gait. The Pedotti diagram highlighted the tendency of the foot to progress forward, showing the rapid progression of centre of pressure from the heel towards the toe. It was concluded that the Strathclyde foot required further design work prior to production. The next chapter provides suggestions as to how this may be achieved.

CHAPTER 6 – Conclusions and recommendations for further work

This chapter concludes the project by examining progress towards reaching the requirements of the Product Design Specification (PDS). Recommendations for further work are then included, based on the contribution to reaching the requirements of the PDS before additional recommendations are made regarding design and testing of the prosthesis.

6.1 Conclusions

The aim of the project was stated as 'to develop a highly functional prosthetic foot unit suited to the developing world'. The design work carried out during this project related to the keel only while the PDS was written with a complete prosthesis in mind. The design development was measured against the PDS however gaps were present as a prosthesis entire cannot be evaluated and as such the conditions of the PDS will not be considered met where a full prosthesis is required. The PDS can be carried forward into further design work as components are developed and included and may require modification as new information comes to light. The conclusions to this project are presented below under the headings of the PDS.

6.1.1 Performance

The Strathclyde foot R2 design (second redesign) was tested in toe and heel loading according to the ISO 10328 static loading condition. In each of the redesigns testing without an energy return feature led to failure before achieving the P3 level of loading whereas the existing Strathclyde design was able to continue to complete P4 and P5 loading of the toe without failure. It was found that the inclusion of an

energy return feature in the form of a blade lead to an improved performance of the keel designs when compared to the existing Strathclyde foot design as both samples of the existing Strathclyde design failed catastrophically during P3 level toe loading while the R1 design (first redesign) had one sample fail catastrophically during P3 toe loading and the other sample able to be loaded to the P4 and P5 levels (this was however discounted from claiming successful completion due to excessive deformation during P3 testing). The R2 design was able to reach maximum loading during toe loading at the P3 level however one sample was determined to have failed due to excessive deformation and was not tested further while the other continued to the P4 level where excessive deformation was again encountered. Neither of the redesigns was able to meet the P5 level of static toe loading conditions as required in the PDS.

In heel loading the balls were found to be a major weakness, failing in every test at the P5 level and during some of the P4 heel tests. During P4 testing the R2 design was found to have permanent deformation of the keel, thus failing and ruling it out of further testing. In P5 testing the existing Strathclyde foot and R1 keels were found to have permanent deformation and so were considered to fail the P5 level, although given the failure of one of the balls in sample 3 of R1 then the R1 design may be considered only a partial pass at the P4 level in heel loading. Neither redesign was able to meet the P5 level of static heel loading conditions as required in the PDS.

Energy return was calculated during static loading, which is an underestimate of potential as energy is likely to be dissipated during the 30 second hold specified in ISO 10328, however the value calculated in P3 testing of the surviving samples of R1 with blade (8.62J) is a positive indication on the level of energy return potentially available in the design. This calculation was not carried out for the R2 design due to

the only surviving sample having an erratic loading pattern which would give a misrepresentation of energy return in the design.

No testing was carried out to evaluate the performance of any of the Strathclyde feet to the cyclic testing conditions of ISO 10328 as specified in the PDS and so no conclusion may be drawn to the performance however it is likely that the balls would have failed during cyclic testing given the performance observed in static loading. The nature of the manufacture of the keels (SLS) meant that weaknesses were present between layers and it is therefore considered likely that cyclic testing would lead to failure through the stress cycling between layers in toe loading.

Force plate trials were carried out on a single, able-bodied subject wearing prosthetic stilts. No measure of gait symmetry was carried out and any feedback from the subject was of limited value given the lack of experience in walking on prosthetic feet so the requirements of the PDS are not considered satisfied despite a force plate test having been carried out. The force plate trial did reveal that the R2 design appears to have a similar F_z loading pattern to natural gait, an unusual double trough in F_x loading and to be short, lacking toe support. When compared to the work of (Arya, Lees, Nirula, & Klenerman, 1995) the R2 design appears to have a similar propulsive force peak to the natural foot however this should be confirmed with testing on multiple individuals, with comparisons to a range of other designs. The same test also showed a relatively low F_z support impulse, F_x braking impulse and F_x propulsive impulse compared to the natural foot.

Shock absorption of the heel was not calculated and while the evaluation carried out by (Arya et al., 1995) did include F_z impact force peak and F_z impact load rate this could not be calculated from the force plate trial on the R2 design due to the apparent lack of impact peak, whether due to its absence or the sampling frequency being too low to record the peak. There was no determination of energy

return during gait so the magnitude and point of return during the gait cycle was not determined so this requirement of the PDS is not satisfied. The dorsiflexion, inversion and eversion of the designs were not determined, as required by the PDS.

There has been no design work specifically aimed towards the customisability of the prosthetic setup at the heel or energy return feature to the individual user's requirements or preference per the PDS.

6.1.2 Environment

No work has been carried out to determine the behaviour of the current design in the range of environments specified in the PDS. The intended polypropylene and fibreglass components do have an operating temperature range outside of that specified in the PDS and low moisture absorption rates so should be only affected a small amount by humidity. Polypropylene and polyester reinforced fibreglass are generally resistant to water, petrol and weak acids and bases as required by the PDS however, no work has been carried out on the cosmesis to determine a suitable material or the design in order to prevent ingress of particulate matter.

6.1.3 Life in service

No work has been carried out to determine the potential life in service of the prosthesis so no conclusion may be drawn regarding this.

6.1.4 Maintenance

Currently the keel design requires no maintenance. Although the PDS specifies that no maintenance of the internal structure should be required, given the failure of the balls in the heel (despite the recommendation to change the material) it is considered that replacement of the ball and blade should be possible to remove the requirement to replace the entire foot for the failure of only a single component. Inspection as a part of preventative maintenance should be included as it would

allow for identification of wear and potential failure prior to occurrence and so could increase the overall life of the prosthesis.

6.1.5 Target product cost

Based on the R2 design a per unit cost of £0.833 was quoted for the polypropylene keel when produced at the rate of 2000 units annually (Boddingtons, Tonbridge, UK). At current costs of the fibreglass sheet used combined with labour at minimum wage the cost per blade would be approximately £2.10 (assuming non-industrial prices and a production rate of only four per hour). The final ball material is not as yet determined so no price can be calculated. The total per unit so far is then £2.93 (based on 2000 units annually). This does not include the cost of a cosmesis, which would be heavily determined by both material and production method used. No accounting of overheads or tooling costs is included in this number so the actual cost is likely to be higher however at this stage no more accurate costs could be determined.

6.1.6 Quantity

The design and methods intended to be used at this point were suitable to a production rate of thousands of units per year however there is no cosmesis design as yet nor were the heel ball and blade design finalised so the production rate must be borne in mind when addressing these areas.

6.1.7 Size

The shape of the Strathclyde foot was modified during this process to better reflect the anatomical foot however when compared to the measurements carried out by (Witana, Xiong, Zhao, & Goonetilleke, 2006) the heel is still outside the bounds of the natural human foot while the toe remains short. No version of the

Strathclyde foot can be said to be within the bounds of the anatomical foot. No work has been carried out on creating a variety of sizes to suit a range of user sizes.

6.1.8 Mass

The R2 design keel has a volume of 118537mm^3 which would give a mass of 107.2g when made in copolymer polypropylene (density 0.904 g/cm^3). The blade used had a mass of approximately 22g. The ball and cosmesis are to be determined so no final conclusion may be drawn on whether the prosthesis will remain below the 1kg target described in the PDS.

6.1.9 Aesthetics, appearance and finish

The cosmesis has not been determined so no conclusion may be drawn on the aesthetics, appearance and finish of the prosthesis.

6.1.10 Materials

The intended polypropylene and polyester reinforced fibreglass meet the chemical and environmental resistance requirements of the PDS. The physical performance has not been fully determined as no cyclic testing was carried out however the survival of the original Strathclyde design to the P5 level (when tested without a blade) shows that polypropylene has the potential to meet the static loading physical requirements. Polypropylene is highly recyclable however the polyester fibreglass is less so and requires specialised methods to effectively recycle the material. An alternative material may be sought to replace the fibreglass or else the disposal method should be determined ahead of time in order to minimise waste. The cosmesis and ball materials were not determined so no conclusion may be drawn on their recyclability. It was not determined where manufacture would be located so the availability of materials was not considered.

6.1.11 Standards and specifications

The static requirements of ISO 10328 were tested to but not passed for any design. The redesign samples were not produced in the intended material (copolymer polypropylene) by the intended method (injection moulding) so compliance could not have been claimed regardless. No cyclic testing was carried out so there is no information available regarding the potential performance.

6.1.12 Ergonomics

There was no design of multiple sizes for different sized users. The attachment method of the foot was changed from a welded polypropylene shank to a pyramid adapter. While no testing was carried out relating to user ability to don and doff the prosthesis it should not be more difficult than existing prostheses. No user study was carried out to determine the comfort of the prosthesis while worn and in use. No design work was carried out related to customisability of the prosthesis to the individual user although an allowance was created in the ability to change the blade and ball.

6.1.13 Quality and reliability

A clinical field trial was not carried out so survival rate over time cannot be determined. Deformation of the heel and toe were observed after testing had continued to higher levels. While these tests were not satisfactory to meet the requirements of ISO 10328 they do suggest that the prosthesis may potentially continue to function even after damage has occurred. The materials used were not the intended final material however so this observation may not apply to the prosthesis when produced in polypropylene.

6.1.14 Safety

The redesigns of the Strathclyde foot have not met the required standard of ISO 10328.

6.1.15 Legal

The redesigns of the Strathclyde foot have not met the required standard of ISO 10328.

No work towards creating a manual was carried out, nor has a guarantee of any kind been determined.

6.1.16 Installation

The inclusion of a pyramid adapter will have simplified the job of any prosthetist required to fit one of these prostheses. The removal of the welded shaft component means the Strathclyde foot can now be integrated with other systems and alignment may be carried out as for other prosthetic feet through use of the pyramid adapter system.

6.1.17 Documentation

No documentation has been developed to accompany the Strathclyde foot.

6.2 Recommendations

With the conclusions specific to the PDS laid out the recommendations to improve in those areas may now be addressed.

6.2.1 Performance

It is recommended that further FEA be carried out in order to optimise the shape of the Strathclyde foot, particularly with regards to rib spacing and the shape of the upper and lower toe sections. The failure that occurred in the upper toe

section in the R2 design may be eliminated by changing the geometry of the toe section or potentially the spacing of ribs within the toe. The lower toe section was increased in height to increase the stiffness and reduce the likelihood of failure there however this shape has not been optimised and could be unnecessarily large, wasting material and increasing mass without adding to the function of the prosthesis. The blade itself may be optimised and modified to account for different loading requirements of the user (whether through body mass or activity level) through the use of FEA.

SLS using a nylon based material may be of some use in developing the design however the difference in performance of the alternative material when compared to injection moulded polypropylene is great, due to the lack of crosslinking of molecules and the introduction of laminar faults in the product. It would be preferable if further testing of the keel were to be carried out using injection moulded copolymer polypropylene.

The failure of the ball at the heel is unacceptable and the balls should be replaced with an appropriate alternative, potentially a uniform elastomer. Thorough characterisation of any replacement material should be carried out to allow FEA to provide more accurate results and to inform any further decisions relating to material changes.

The failure of the keel through permanent deformation leads to the recommendation that some design development be focussed here. When this failure is combined with the observation that the heel is outside the boundaries of the anatomical foot it may be suggested that an alternative design be sought in this area. Many of the feet examined in Chapter 2 make use of the cosmesis to provide this shock absorbing feature (e.g. Seattle foot, EB foot) where others embed material within the cosmesis to contribute to shock absorption (e.g. HCMC foot, VI

foot). The Shape and Roll and Niagara feet used a lever as part of the keel to act as a shock absorption feature. Any of these methods may be suitable for the Strathclyde foot in further design development and are provided at this point only as suggestions to potential solutions.

Cyclic testing is a requirement of further development however the material and manufacturing method should be of the intended final production. ISO 10328 requires that the heel and forefoot be loaded alternately for 2 million cycles at a rate in the range of 0.5 - 3Hz, with the load depending on the P-level being tested to, following which final static forces are applied in the same sense as loading during cyclic testing. Two samples from normal production are required to pass with a single substitution of samples possible under specific conditions of the standard and as such it is recommended that a minimum of three samples be tested to each P-level.

It is recommended that ISO 22675 - Testing of ankle-foot devices and foot units, be re-evaluated as an alternative to ISO 10328 - Structural testing of lower-limb prostheses, both of which have been updated since the conclusion of testing for this project. While either of these standards may provide a base testing level there are further important properties of the prosthesis that they do not reveal, such as shock absorption properties or edge loading behaviour, which may be relevant in daily use. It is then recommended that a shock absorption test method be developed to evaluate development of the heel. The method used by Peter Aerts, Ker, De Clercq, & Ilsley, 1996, on cadaveric feet may be used as a starting point in developing a pendulum test to determine shock absorption of the heel. A pendulum method would give a better representation of shock absorption and energy return properties of the heel (or toe) than the calculations carried out during the loading of ISO 10328 as reported in this thesis. Dorsiflexion, eversion and inversion of the

prosthesis should be determined, potentially through loading in an Instron machine with edge loading for eversion and inversion (currently the same given the symmetrical setup of the prosthesis) or offset toe loading for dorsiflexion.

Trials should be carried out with amputees, preferably experienced with a range of prostheses, and so able to give subjective feedback on the Strathclyde foot. A questionnaire should be provided to include, but not limited to questions covering the users' opinions on ease of walking on level, inclined and declined surfaces as well as ascending and descending stairs, comfort, opinion on aesthetics, stability and confidence in the prosthesis. Jogging and running tests would provide useful information as the prosthesis is likely to be used this way by users however other testing does not reflect this particular use. Objective data may be gained through the use of motion capture and force plate trials, allowing a determination of gait symmetry, timing of phases of gait, ground reaction forces, Pedotti diagram and rollover shape. Such trials should be either cadence controlled through the use of a rhythmic beat for the user to walk to (as in (Adamczyk & Kuo, 2009)) or by taking a range of samples and eliminating any that deviate by more than a certain threshold from the mean value of self-selected walking speed (as in (Arya et al., 1995)). Measures of muscle activation and energy consumption may be useful to determine that the Strathclyde foot has a positive effect on the user's energy consumption compared to existing prostheses. All trials should also be carried out under the same conditions using the amputee's preferred prosthesis for the tasks required to provide a base level for comparison.

6.2.2 Environment

A thorough evaluation of any material to be used in the prosthesis should be carried out, initially from the literature but then using samples kept in environmental chambers to simulate exposure to a range of humidities and temperatures. These

temperatures and humidities should reflect the extremes of human habitation highlighted in section 3.2.2 Environment. Testing may be carried out for short term exposure outside of these ranges as individuals may range outside of the continual inhabitation range occasionally. Once satisfactory materials have been identified entire prosthesis samples may be exposed to the various environmental conditions prior to testing to ISO 10328 standards or other any other conditions deemed appropriate to ensure performance and safety requirements are adequately met. It may be necessary to revise the PDS to reflect a reduced range of environments if the current demands are too great.

6.2.3 Life in service

Once the safety and performance standards have been met in laboratory testing (particularly the 3 million cycles of ISO 10328 cyclic testing), a clinical field trial may be initialised with a view to determining the life in service that may be expected. (Jensen, Nilsen, Zeffer, Fisk, & Hartz, 2006) carried out a clinical field trial which may be used as a basis to determine the requirements of such testing. A range of locales may be used to determine the effect on life in service of different environments. Such locales may be guided by the results of environmental chamber testing.

6.2.4 Maintenance

It is recommended that in the design of the cosmesis, as well as the choice of heel (design and material) and blade accommodation be made of periodic inspection and potential replacement of components. This has to be balanced against the prevention of particle ingress and it may be that cosmesis replacement occurs at each inspection, reducing the service life requirement of the cosmesis. The maintenance period should be based on when during cyclic testing the breakdown of components is observed.

6.2.5 Target product cost

The target product cost depends on whether all components will be produced centrally and distributed or whether some components will be sourced locally by prosthetists. As such it is recommended that a business plan be generated in order to identify such requirements with the possibility of a spin out company from the University considered as an option. The business plan should include number of prostheses to be produced each year, how they will be produced (both in terms of method of component manufacture, whether centralised or decentralised along with material sourcing, and assembly process) and the costs associated with production, how the prosthesis is to be distributed (i.e. through prosthetists, through a charitable organisation or direct to the users), shipping methods and costs, testing regimen for production and also the required standards prior to sale (for example gaining CE marking). The number and costs of testing involved into design should also be factored into the plan as part of the development time and total costs. This would then allow the determination of likely costs. If the prosthesis is to be distributed as part of a charitable organisation the supplied cost may be lower than that of the production cost, another important reason for determining a business plan, and in such a case, identifying a partner charitable organisation. As the design becomes more finalised cost estimates on tooling, materials and overheads would be required. These costs should also account for shipping and registration or certification costs, if any.

6.2.6 Quantity

In determining a business plan the annual production quantity will be determined as well as any changes to quantity over time. Further design should be carried out with the understanding that the production goal will be thousands annually although the exact range will be determined by a business plan.

6.2.7 Size

The heel of the Strathclyde foot is in particular need of attention as it extends posteriorly to a greater degree than the anatomical foot. It is recommended that the heel be modified in a way similar to that shown in Figure 134. In doing so the ball in the heel would be eliminated and an alternative shock absorption method would require development. Such a development could also help to alleviate the rapid forward progression present in the foot by removing the pivot point at the underside of the heel.

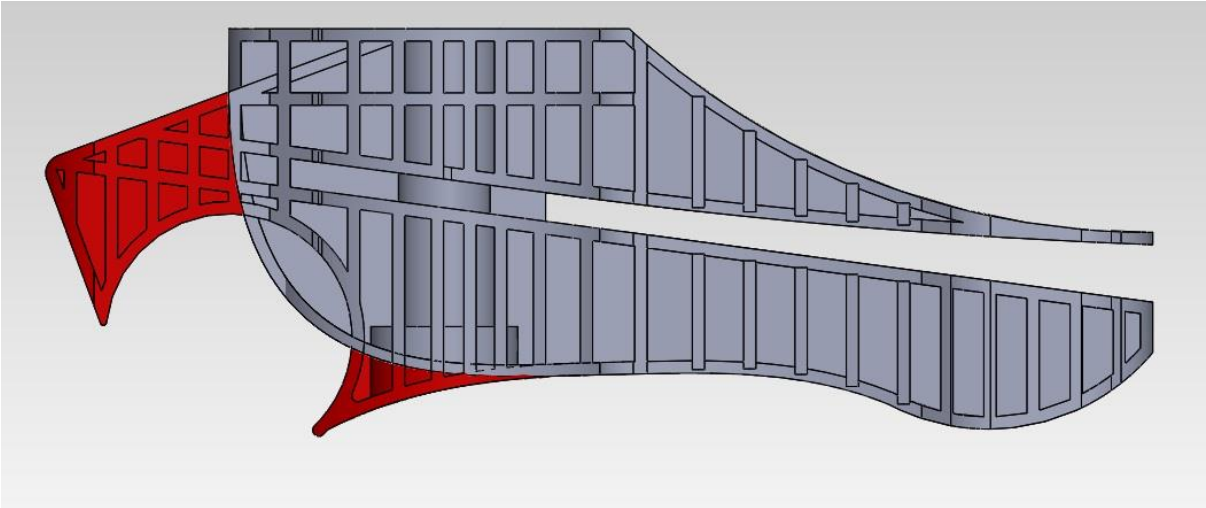

Figure 134 – Suggested modification of the heel of the Strathclyde foot (red shows areas to be eliminated)

The toe of the Strathclyde foot was found to be short in action during forceplate trials. It is recommended that either the toe section of the keel be extended to provide a longer foot, a reinforced feature be included in the cosmesis or a combination of the two features.

It is recommended that other sizes be produced to suit a range of users however this will not be a simple case of scaling the components. FEA could provide initial insight into performance of different sized feet however physical testing of

samples would be required to meet the ISO 10328 standard. Reference should be made to measurements of anatomical feet to ensure that the sizes are appropriate.

6.2.8 Mass

The prosthetic foot complete should not exceed 1kg as determined in the PDS. This must be considered during any further redesign process along with material selection.

6.2.9 Aesthetics, appearance and finish

It is recommended that a cosmesis be developed which takes an outer shape based on the anatomical foot. A material that may be dyed would be beneficial as it would allow a range of skin tones to be produced or potentially even individual customisation depending on the requirements of the business plan.

6.2.10 Materials

Depending on the business plan, alternative materials may be researched for the blade, heel shock absorption feature and cosmesis so that a range of materials may be sourced locally by prosthetists. It is recommended that along with redesign of the heel a cosmesis material be researched that may act as shock absorption feature, as the polyurethane foam cosmesis does in, for example, the Seattle foot. Polyurethane foam is a potential material but given the survival issues, particularly in tropical conditions, highlighted by (Jensen, Nilsen, Thanh, Saldana, & Hartz, 2006) it must be evaluated thoroughly. The end of life considerations must be addressed for any material included in the prosthesis.

6.2.11 Standards and specifications

The latest version of ISO 22675 should be compared to the latest version of ISO 10328 to see which is more appropriate for further evaluation and validation of the prosthetic foot design.

6.2.12 Ergonomics

A range of sizes should be developed for users of different sizes. Amputee trials are required to determine the comfort of the prosthesis when worn and in use. This should be part of the amputee trials as described in section 6.2.1 Performance. A range of blades and shock absorption features at the heel should be developed to better suit the individual user depending on their body mass and activity level.

6.2.13 Quality and reliability

No work has been done to address the longevity and survival of the prosthesis and is required in the form of a clinical field trial following successful laboratory testing and amputee trials. There has been no testing related to function following damage of the Strathclyde foot although during testing of the R1 design permanent deformation occurring during P3 testing was not identified until testing had already been completed at the P4 and P5 level. The material and manufacturing method are different to that intended so it cannot be claimed that the design will function following this type of damage. A test regimen is required to be developed to ensure the quality of the product is guaranteed throughout and across production. This should include sample testing of components, if produced centrally, to standards to be determined. If production is not to be carried out centrally then testing may be suggested for locally sourced components although responsibility for such components would ultimately rest with the prosthetist acquiring them. If CE marking were appropriate it would serve as a mark of quality of the prosthesis however this would likely depend on the production method with certification likely to prove difficult if a range of components were to be sourced locally and so this would depend on the business plan implemented.

An injection moulding specialist should be consulted regarding the design of the foot to determine mould requirements and parameters and any modification required to permit repeatable, fault-free production of specimens.

6.2.14 Safety

The standard of ISO 10328 was not met during testing and should be aimed for using complete foot units, including all components such as blade, ball and cosmesis. All components should all be made of the final materials, using the intended manufacturing method, to effectively be representative of final production. If these conditions are met the standard may be claimed to have been met and the safety requirement of the PDS met.

6.2.15 Legal

The standard of ISO 10328 was not met during testing so the current design may not be used outside of testing. No manual has been produced and should be considered an item to be addressed as design progresses. The business plan will determine whether a guarantee should be made for free replacement of a foot upon failure. It is recommended that CE marking be researched and applied if possible. CE marking would permit sale/provision of the device within Europe possible and would serve as a mark of quality of the prosthesis. As a non-sterile device with only intermittent skin contact (the socket is not provided as a part of this prosthesis so skin contact is limited) the prosthesis would be considered a class I device and only require notification of a Competent Authority and a self-compiled declaration of conformity.

6.2.16 Installation

The prosthesis is to be installed by a qualified prosthetist and as such it is recommended that an installation manual be written and translated as required to

aid the prosthetist. If any requirement falls on the prosthetist to source or manufacture components this should be fully included within the manual.

6.2.17 Documentation

Documentation should be produced in the form of an installation manual for the prosthetist and a user's guide to outline proper and improper use, along with any required maintenance. The prosthetist's guide should include information related to customisation of the prosthesis to suit the user's body mass and activity level. All documents should be translated into local languages as required and appropriate to the distribution locations.

6.2.18 Other recommendations

There are further recommendations that do not directly fall under any of the criteria listed above and so are included here under the relevant subheadings.

6.2.18.1 FEA

The FEA carried out for the project could be improved in further work through the inclusion of radii at the corners to reduce stress concentration in the model. Such stresses are not realistic and may give incorrect information about the location and stage of failure in models. This was particularly an issue in the R1 and R2 designs where high stresses were calculated in locations which were not observed to fail in prototype testing.

The materials used should be fully characterised to provide more accurate performance in future FEA work. The Duraform EX samples were observed to behave very differently during prototype testing compared to FEA models and so with a full characterisation of the material an allowance could be built in to account for the layer properties of the SLS method, if SLS of Duraform EX were to be considered a prototyping method for future work.

The FEA model of edge loading may be improved through the inclusion of a bolt and pyramid adapter to include the effect these have on the system as more flexibility will be present than permitted in the existing model and the impact of this should be determined prior to production.

Prior to injection moulding of samples FEA should be carried out to determine that the flow characteristics of the mould are appropriate, although this is potentially a service provided by moulding companies if the samples were to be produced through a contractor and would then not be required to be carried out by the investigator.

6.2.18.2 Manufacture

Manufacturing methods have continued to develop during the course of this project and re-evaluation of potential methods of prototype development should be carried out to determine if other methods are more appropriate than the SLS process used in prototype production.

SLS should be reviewed to determine if there are other materials, such as polypropylene powders (available from Advanc3d Materials, GmbH, Hamburg, Germany), that may present a prototype better representative of the intended final product. SLS does not currently allow for mixing of materials to create a product with varying material properties throughout (Jing, Hui, Qiong, Hongbo, & Zhanjun, 2017) however, other processes may be able to provide this ability (Vaezi, Chianrabutra, Mellor, & Yang, 2013) and should be researched further. Structural foam is a potential manufacturing method and should be investigated to evaluate feasibility.

The SLS method and Duraform EX material used for samples did not perform as well as was predicted in FEA. This is likely due to the nature of the manufacturing method causing faults between layers as the prototype was built up. The finish of the part was noticeably grainy and the performance of samples varied widely while

the cost was approximately 100 times greater than injection moulded samples (depending on production volume) which had a smooth finish and similar performance across samples. It is recommended that any prototypes be produced in large enough quantity to determine consistency in manufacture through testing multiple samples produced from multiple batches.

The manufacture of prostheses may be carried out either in a central location and distributed or produced at a smaller scale locally to where use will be. Either case brings its own advantages and disadvantages which require examination in more detail but would include at minimum factors such as manufacturing cost, shipping and distribution costs, quality control, and material availability. Central production would require variable components (blades, balls and cosmeses) to be provided in sufficient quantity to meet the required combinations (for user body mass, activity level, skin tone, etc.) to be provided with lack of supplies leading to inappropriate or no prosthesis build for the individual user. Conversely distributed production would require moulds to be available locally, multiplying the cost of a relatively expensive process while reducing the control over the final product but allowing flexibility in the sourcing and creation of the variable components. A mixed model could provide some of the quality control and consolidation of costs (centrally produced keel) while retaining the flexibility of the distributed production in producing variable components. The method chosen will have effects on aspects of the PDS, for example attaining a CE marking for a distributed or mixed production model would be difficult given the increased range of materials and supply present compared to a centralised model however the customisability may suffer in a centralised model.

6.2.18.3 Further design related work

The design work carried out in this project related largely to the keel and so the variable components noted above (blade, cosmesis and ball/heel shock absorption

feature) require further development to meet the requirements of the PDS. As suggested above FEA would provide a useful tool in developing blades optimised to different loading levels, whether relating to the user's body mass or activity level. An integrated cosmesis/heel shock absorption feature could potentially reduce the number of components involved and reduce construction time and cost and could also be explored in FEA with different materials or material conditions (such as density) being explored prior to prototype testing. Any materials to be used should be thoroughly characterised prior to FEA simulation and if possible should be exposed to varying environments (in terms of humidity and temperature mainly) to characterise performances in the environments where the prosthesis may be required to function.

The use of the Cambridge Engineering Selector (CES) and Ashby's plots to determine appropriate materials determined by their properties is highly recommended for all components and a review of the copolymer polypropylene intended for use in the keel may serve to confirm selection or suggest an improved alternative, particularly with end of life considerations for recyclability or disposal in mind.

The blade requires fixation within the keel in the R1 and R2 designs and this remains an area for development, whether the blade is to be held by the design of the keel or if an external substance such as epoxy is required.

The shock absorption method at the heel was not adequately addressed during this project and is recommended to be developed as a priority. It was suggested in section 6.2.7 Size, that the heel be shortened to bring it into line with the anatomical foot. This provides an opportunity to adjust the heel shock absorption method from the ball previously used and into something more aligned with existing prosthetic feet. The shock absorption feature could be combined with the cosmesis (as in

SACH feet, for example) however the material selection requires a thorough analysis of the environmental conditions and performance requirements. The cosmesis would be required to operate in the same environmental conditions identified for the whole prosthesis in section 3.2.2 Environment and provide a wear resistant layer to prevent damage to the foot while also guarding against particle ingress to the interior structure of the prosthesis. It is recommended that the cosmesis incorporate the shock absorption requirements at the heel. The performance requirement of the reinforcement of the toe section of the cosmesis to extend the effective length of the foot has to be determined as does the method of inclusion of the reinforcement into the cosmesis.

The existing Strathclyde feet are not recommended for cyclic testing and at minimum the keel would require producing in copolymer polypropylene by injection moulding, the blade would need a fixation method to be determined and applied, the material of the heel ball would require changed to a more resilient material of a similar stiffness and a fixation method determined, and a cosmesis would need to be designed with an appropriate material and manufacturing method determined. It is recommended that further design development be carried out to address other issues described in this section before cyclic testing is attempted.

The inclusion of end users into the design and development process would provide a valuable source of information and potentially lead to an improved outcome for the prosthesis design.

Scaling of the foot is not considered appropriate given the complex geometry of the keel however the recommendation remains that alternative sizes be developed so that the prosthesis may be worn by users of a variety of sizes as the current design will only serve a small range of all users.

6.2.18.4 Static testing recommendations

Static loading tests should include measurement of key dimensions before and after testing to evaluate the extent of deformation occurring during testing. This should also be couple with periodic measurements following the end of testing to determine the time to recovery and also the extent of recovery following deformation under loading. A longer time to recovery could mean that samples undergoing cyclic testing would not recover from each cycle of loading applied and lead to premature failure.

Testing should be recorded on video to allow comparison of measured results from testing equipment to visible responses of the prosthesis during loading.

Testing should be carried out on samples that have been environmentally conditioned to the extreme conditions of potential use environments (in terms of humidity and temperature) to determine how the performance will be affected and if they remain safe to use in the range of human inhabitation.

Full failure analysis of all failing samples should be carried out to inform further design work.

The extent of dorsiflexion of the foot may be determined from the static loading condition of ISO 10328 by defining a point, or set of points to represent the top surface of the foot and measuring the positions at zero load and maximum load. This will give a larger value than would be expected in normal gait due to the higher load value but would provide an extreme value. Determination of dorsiflexion during gait may be carried out using reflective markers during amputee trials where multiple trials may be recorded across different users to give a typical range.

The complete foot system should be tested together (keel, blade, heel shock absorption feature and cosmesis) to determine the system behaviour rather than some combination of components as was carried out during this project.

6.2.18.5 Cyclic testing recommendations

Cyclic testing should be carried out on complete prosthetic feet assemblies, produced from the final material by the intended manufacturing method, once the static loading conditions have been successfully met. As ISO 10328 permits two samples with one replacement in case of a failure (requiring two successful trials total) to claim compliance, a minimum of three samples should be tested at each P-level. Such testing will be time consuming (2 million cycles at 1Hz taking approximately 23 days to complete per sample) depending on the equipment available to carry out this testing. Cyclic testing of this nature could be used to indicate expected time to failure of various components and so inform the required maintenance schedule for inspection and part replacement.

6.2.18.6 Amputee gait trials

Trials should be carried out with trans-tibial or trans-femoral amputees, preferably experienced with a range of prostheses, and so able to give subjective feedback on the Strathclyde foot. A questionnaire should be provided to include, but not limited to questions covering the users' opinions on ease of walking on level, inclined and declined surfaces as well as ascending and descending stairs, comfort, opinion on aesthetics, stability and confidence in the prosthesis. Jogging and running tests would provide useful information as the prosthesis is likely to be used this way by users however other testing does not reflect this particular use. Objective data may be gained through the use of motion capture and force plate trials, allowing a determination of gait symmetry, timing of phases of gait, ground reaction forces, Pedotti diagram, rollover shape and extent of dorsiflexion, inversion and eversion of the prosthesis during gait. Energy return/input may be determined from forceplate trials and compared across feet tested which may be compared to the amputee's intact limb, assuming it is present. Such trials should be either cadence controlled

through the use of a rhythmic beat for the user to walk to (as in (Adamczyk & Kuo, 2009)) or by taking a range of samples and eliminating any that deviate by more than a certain threshold from the mean value of self-selected walking speed (as in (Arya, Lees, Nirula, & Klenerman, 1995)). Video recording of tests would permit additional examination of gait to occur particularly if synchronised with force plate data. Measures of muscle activation and energy consumption may be useful to determine that the Strathclyde foot has a positive effect on the user's energy consumption compared to existing prostheses. All trials should also be carried out under the same conditions using the amputee's preferred prosthesis for the tasks required to provide a base level for comparison.

6.2.18.7 Additional testing

Shock absorption tests should be carried out on both the heel and toe of the prosthesis. It is recommended that this follow a method similar to that used by (Peter Aerts, Ker, De Clercq, & Ilsley, 1996). The sample would be set up in a horizontal position with a weighted pendulum set to contact the sample at the lowest point of swing as described by (Peter Aerts et al., 1996). The load-deformation loops could be determined and then the energy return and absorption characteristics. This would be an improvement over the values calculated during this project which included a 30 second hold which will have reduced the energy return provided by the prosthesis.

Testing of samples in other loading conditions, such as the edge-loading described in B4.5 Edge loaded ankle block FEA, or an impact of the end of the toe as in kicking, should be considered as the loading conditions specified in ISO 10328 only consider the extreme positions of normal gait and do not account for other typical conditions of everyday activities.

Thorough characterisation of materials used should be carried out and should refer to relevant standards, such as ISO 527 for determination of tensile properties of plastics or ISO 7743 for determination of compression stress-strain properties of rubber, vulcanized or thermoplastic.

6.3 Summary

The R2 design of the Strathclyde foot was found not to meet many of the requirements of the PDS, particularly due to the properties of samples produced in Duraform EX via SLS. It was concluded that this material and manufacturing method is not suitable for testing of designs to the ISO 10328 standard but may have limited use in further development of the design.

The balls used in the heel section of the foot were inadequate for the purposes required and must be replaced or the design altered to render them unnecessary.

The R2 design of the Strathclyde foot was shown to produce a similar Fx loading pattern to natural gait and a similar propulsive force peak to the results of (Arya, Lees, Nirula, & Klenerman, 1995) although this requires further testing to validate the results.

Recommendations were made to develop the design towards meeting the goals of the PDS and to address shortcomings in testing. Potential modifications to the design were suggested to address weaknesses observed during testing, particularly in the weakness of the balls used for shock absorption at the heel and the effective shortness of the toe. Additional tests were suggested outside of the international standards to account for other daily activities not addressed.

REFERENCES

Adamczyk, P. G., & Kuo, A. D. (2009). Redirection of center-of-mass velocity during the step-to-step transition of human walking. *The Journal of Experimental Biology*, *212*(Pt 16), 2668–78. https://doi.org/10.1242/jeb.027581

Aerts, P., Ker, R., De Clercq, D., & Ilsley, D. (1996). The effects of isolation on the mechanics of the human heel pad. *Journal of Anatomy*, *188*(Pt 2), 417.

Aerts, P., Ker, R., De Clercq, D., Ilsley, D., & Alexander, R. (1995). The mechanical properties of the human heel pad: a paradox resolved. *Journal of Biomechanics*, *28*(11), 1299–1308.

Andrysek, J. (2010). Lower-limb prosthetic technologies in the developing world: A review of literature from 1994-2010. *Prosthetics and Orthotics International*, *34*(4), 378–398. https://doi.org/10.3109/03093646.2010.520060

ARRK Europe. (2010). SELECTIVE LASER SINTERING (SLS) MATERIAL RANGE. MATERIAL PROPERTIES. ARRK Europe.

Arya, A. P., & Klenerman, L. (2008). The Jaipur foot. *The Journal of Bone and Joint Surgery. British Volume*, *90*(11), 1414–6. https://doi.org/10.1302/0301-620X.90B11.21131

Arya, A. P., Lees, A., Nirula, H. C., & Klenerman, L. (1995). A biomechanical comparison of the SACH, Seattle and Jaipur feet using ground reaction forces. *Prosthetics and Orthotics International*, *19*(1), 37.

Ashalatha, P. R., & Deepa, G. (2011). Fig. 8.14: Arches of the foot. In R. Saxena (Ed.), *Textbook of Anatomy & Physiology for Nurses* (3rd ed., p. 64). New Delhi: Jaypee Brothers Medical Publishers.

Au, S. K. W., Herr, H., Youcef-Toumi, K., & Anand, L. (2007). *Powered ankle-foot prosthesis for the improvement of amputee walking economy*. *Mechanical Engineering*. Massachusetts Institute of Technology.

Barbero, E. J. (2011). *Introduction to Composite Material Design*.

Barth, D. G., Schumacher, L., & Thomas, S. S. (1992). Gait analysis and energy cost of below-knee amputees wearing six different prosthetic feet. *JPO: Journal of Prosthetics and Orthotics*, *4*(2), 63–75.

Beshai, M., & Bryant, T. (2003). Victim Assistance Efforts: The Niagara Foot. *Journal of Mine Action*, *7*(1).

Bisseriex, H., Rogez, F., Thomas, M., Truffaut, S., Compere, S., Mercier, H., … Thefenne, L. (2011). Amputation in low-income countries: Particularities in epidemiological features and management practices. *Médecine Tropicale*, *71*(6), 565–571.

Bryant, K. P., & Bryant, J. T. (2002). *Niagara Foot Pilot Study in Thailand - Midterm Report: October 18 2002*. Ontario, Canada.

Buchheim, R. W., Bjork, R. L., Cohen, S. T., Crain, C. M., Davis, M. H., Davis, R. A., … Vogel, J. (1958). *Space handbook: Astronautics and its applications Staff report of the select committee on astronautics and space exploration*. (M. J. Horgan, M. A. Palmatier, & J. Vogel, Eds.) (1st ed.). New York, U.S.A.: Random House.

Buckley, J. G., Jones, S. F., & Birch, K. M. (2002). Oxygen consumption during ambulation: comparison of using a prosthesis fitted with and without a tele-torsion device. *Archives of Physical Medicine and Rehabilitation*, *83*(4), 576–581. https://doi.org/10.1053/apmr.2002.30624

Childress, D. S., Hansen, A. H., Meier, M. R., & Steer, S. A. (2005). The Shape &

Roll Prosthetic Foot for Use in Low-Income Countries. Retrieved 7 August 2015, from http://www.nupoc.northwestern.edu/research/projects/lowerlimb/srfoot_lowincome.html

Childress, D. S., Sam, M., Hansen, A. H., Meier, M. R., & Knox, E. H. (2004). Shape and roll prosthetic foot. *US 20040153168 A1*. USA: United States Patent Office.

Cochrane, H., Orsi, K., & Reilly, P. (2001). Lower limb amputation Part 3: Prosthetics-a 10 year literature review. *Prosthetics and Orthotics International*, *25*(1), 21. https://doi.org/10.1080/03093640108726564

Coleman, K., Boone, D., Smith, D., & Czerniecki, J. (2001). Effect of trans-tibial prosthesis pylon flexibility on ground reaction forces during gait. *Prosthetics and Orthotics International*, *25*(3), 195–201.

Comité Européen de Normalisation. (2006a). Prosthetics - Structural testing of lower limb prosthesis - Requirements and test methods BS EN ISO 10328:2006. British Standards.

Comité Européen de Normalisation. (2006b). Prosthetics - Testing of ankle-foot devices and foot units - Requirements and test methods BS EN ISO 22675:2006. British Standards.

CRÉquipements SA. (2013). Adult foot [CRE 590-600]. Retrieved 21 February 2013, from http://www.crequipements.ch/CatalogCRE/product_info.php?currency=EUR&cPath=14&products_id=28

Cummings, D. (1996). Prosthetics in the developing world: a review of the literature. *Prosthetics and Orthotics International*, *20*(1), 51–60.

Das, R., Burman, M., & Mohapatra, S. (2009). Prosthetic Foot Design for Transtibial Prosthesis. *Indian Journal of Biomechanics Special Issue*, (March), 142–146.

Day, H. (1996). A review of the consensus conference on appropriate prosthetic technology in developing countries. *Prosthetics and Orthotics International*, 15–23.

Eaton, D., Ayers, S., & Gonzalez, R. (2006). Comparison of Prosthetic Feet Roll-Over Shapes Used in Developing Nations. In *5th World Congress of Biomechanics*. Munich, Germany: LeTourneau University.

Eftekhari, M., & Fatemi, A. (2016). On the strengthening effect of increasing cycling frequency on fatigue behavior of some polymers and their composites: Experiments and modeling. *International Journal of Fatigue*, *87*, 153–166. https://doi.org/10.1016/j.ijfatigue.2016.01.014

Gabourie, R. (2001). Prosthetic foot providing plantar flexion and controlled dorsiflexion. *US Patent 6,197,066*. USA: United States Patent Office.

Giese, M. A., Arend, I., Roether, C., Kramer, R., & Ward, R. (2009). Relationship between sexual dimorphism and perceived attractiveness in the perception of biological motion. *Journal of Vision*, *9*(8), 607. https://doi.org/10.1167/9.8.607

Haberman, A. (2008). *Mechanical properties of dynamic energy return prosthetic feet*. Queen's University, Kingston, Ontario, Canada.

Hafner, B. J., Sanders, J. E., Czerniecki, J., & Fergason, J. (2002a). Energy storage and return prostheses: does patient perception correlate with biomechanical analysis? *Clinical Biomechanics*, *17*(5), 325–344.

Hafner, B. J., Sanders, J. E., Czerniecki, J. M., & Fergason, J. (2002b). Transtibial energy-storage-and-return prosthetic devices: A review of energy concepts and a proposed nomenclature. *Journal of Rehabilitation Research and*

Development, *39*(1), 1–12.

Hansen, A. H. (2002). *Roll-over characteristics of human walking with applications for artificial limbs*. Northwestern University.

Hansen, A. H., & Childress, D. S. (2004). Effects of shoe heel height on biologic rollover characteristics during walking. *Journal of Rehabilitation Research and Development*, *41*(4), 547–554.

Hansen, A. H., & Childress, D. S. (2005). Effects of adding weight to the torso on roll-over characteristics of walking. *Journal of Rehabilitation Research and Development*, *42*(3), 381. https://doi.org/10.1682/JRRD.2004.04.0048

Hansen, A. H., Childress, D. S., & Knox, E. H. (2000). Prosthetic foot roll-over shapes with implications for alignment of trans-tibial prostheses. *Prosthetics and Orthotics International*, *24*(3), 205–215. https://doi.org/10.1080/03093640008726549

Hansen, A. H., Childress, D. S., & Knox, E. H. (2004). Roll-over shapes of human locomotor systems: effects of walking speed. *Clinical Biomechanics (Bristol, Avon)*, *19*(4), 407–14. https://doi.org/10.1016/j.clinbiomech.2003.12.001

Hansen, A. H., Childress, D. S., & Miff, S. C. (2004). Roll-over characteristics of human walking on inclined surfaces. *Human Movement Science*, *23*(6), 807–21. https://doi.org/10.1016/j.humov.2004.08.023

Hansen, A. H., Childress, D. S., Miff, S. C., Gard, S. a, & Mesplay, K. P. (2004). The human ankle during walking: implications for design of biomimetic ankle prostheses. *Journal of Biomechanics*, *37*(10), 1467–74. https://doi.org/10.1016/j.jbiomech.2004.01.017

Hittenberger, D. (1986). The Seattle foot. *Orthotics and Prosthetics*, *40*(3), 17–23.

Houdijk, H., Pollmann, E., Groenewold, M., Wiggerts, H., & Polomski, W. (2009).

The energy cost for the step-to-step transition in amputee walking. *Gait & Posture*, *30*(1), 35–40. https://doi.org/10.1016/j.gaitpost.2009.02.009

Huston, C., Dillingham, T., & Esquenazi, A. (1998). Rehabilitation of the Lower Limb Amputee. In R. Zajtchuk & R. F. Bellamy (Eds.), *Rehabilitation of the injured combatant - Volume 1* (pp. 79–159). Washington DC, USA: Office of The Surgeon General, Department of the Army, United States of America.

Inman, V. (1966). Human Locomotion. *Canadian Medical Association Journal*, *94*, 1047–1054.

International Committee of the Red Cross. (2006a). *Manufacturing guidelines Physical Rehabilitation Programme*. Geneva, Switzerland.

International Committee of the Red Cross. (2006b). *Polypropylene Technology*. Geneva, Switzerland.

International Committee of the Red Cross. (2011). *PHYSICAL REHABILITATION PROGRAMME: ANNUAL REPORT 2011*.

Jamshidi, N., Rostami, M., Najarian, S., Menhaj, M. B., Saadatnia, M., & Salami, F. (2010). Differences in center of pressure trajectory between normal and steppage gait. *Journal of Research in Medical Sciences*, *15*(1), 33–40. https://doi.org/10.3109/13625181003733178

Jansen, J. A. (2015). Understanding Creep Failure of Plastics. *Plastics Engineering*, (July/August), 39–47.

Jensen, J. S., Craig, J. G., Mtalo, L. B., & Zelaya, C. M. (2004a). Clinical field follow-up of high density polyethylene (HDPE)-Jaipur prosthetic technology for trans-femoral amputees. *Prosthetics and Orthotics International*, *28*(2), 152–166. https://doi.org/10.1080/03093640408726700

Jensen, J. S., Craig, J. G., Mtalo, L. B., & Zelaya, M. (2004b). Clinical field follow-up

of high density polyethylene (HDPE)-Jaipur prosthetic technology for trans-tibial amputees. *Prosthetics and Orthotics International*, 230–244.

Jensen, J. S., & Heim, S. (1999). Preliminary experiences with modified SACH feet manufactured and used in a tropical developing world setting. *Prosthetics and Orthotics International*, *23*(3), 245–248.

Jensen, J. S., & Heim, S. (2000). Evaluation of polypropylene prostheses designed by the International Committee of the Red Cross for transtibial amputees. *Prosthetics and Orthotics International*, *24*(1), 47–54. https://doi.org/10.1080/03093640008726521

Jensen, J. S., Nilsen, R., Thanh, N. H., Saldana, A., & Hartz, C. (2006). Clinical field testing of polyurethane feet for trans-tibial amputees in tropical low-income countries. *Prosthetics and Orthotics International*, *30*(2), 182–94. https://doi.org/10.1080/03093640600794684

Jensen, J. S., Nilsen, R., & Zeffer, J. (2005). Quality benchmark for trans-tibial prostheses in low-income countries. *Prosthetics and Orthotics International*, *29*(1), 53–58. https://doi.org/10.1080/17461550500085147

Jensen, J. S., Nilsen, R., Zeffer, J., Fisk, J., & Hartz, C. (2006). Clinical field testing of vulcanized rubber feet for trans-tibial amputees in tropical low-income countries. *Prosthetics and Orthotics International*, *30*(2), 195–212. https://doi.org/10.1080/03093640600794692

Jensen, J. S., & Raab, W. (2002). Clinical field-testing of ATLAS prosthetic system for trans-tibial amputees. *Prosthetics and Orthotics International*, *26*(2), 86–92. https://doi.org/10.1080/03093640208726630

Jensen, J. S., & Raab, W. (2003). Clinical field-testing of ATLAS prosthetic system for trans-femoral amputees. *Prosthetics and Orthotics International*, 55–62.

Jensen, J. S., & Raab, W. (2004). Clinical field testing of trans-femoral prosthetic technologies: Resin-wood and ICRC-polypropylene. *Prosthetics and Orthotics International*, *28*(2), 141–151. https://doi.org/10.1080/03093640408726699

Jensen, J. S., & Raab, W. (2006). Clinical field testing of vulcanized Jaipur rubber feet for trans-tibial amputees in low-income countries. *Prosthetics and Orthotics International*, *30*(3), 225–36. https://doi.org/10.1080/03093640600867233

Jensen, J. S., & Sexton, S. (2010). *Appropriate Prosthetic and Orthotic Technologies in Low Income Countries (2000-2010)*. Brussels, Belgium.

Jensen, J. S., & Treichl, H. B. (2007). Mechanical testing of prosthetic feet utilized in low-income countries according to ISO-10328 standard. *Prosthetics and Orthotics International*, *31*(2), 177–206. https://doi.org/10.1080/03093640701210986

Jia, N., Fraenkel, H. A., & Kagan, V. A. (2004). Effects of Moisture Conditioning Methods on Mechanical Properties of Injection Molded Nylon 6. *Journal of Reinforced Plastics and Composites*, *23*(7), 729–737. https://doi.org/10.1177/0731684404030730

Jing, W., Hui, C., Qiong, W., Hongbo, L., & Zhanjun, L. (2017). Surface modification of carbon fibers and the selective laser sintering of modified carbon fiber/nylon 12 composite powder. *Materials & Design*, *116*, 253–260. https://doi.org/10.1016/j.matdes.2016.12.037

Johnson, K. L., & Tassinary, L. G. (2007). Compatibility of basic social perceptions determines perceived attractiveness. *Proceedings of the National Academy of Sciences of the United States of America*, *104*(12), 5246–51. https://doi.org/10.1073/pnas.0608181104

Kabra, S. G., & Narayanan, R. (1991a). Ankle-foot prosthesis with articulated human

bone endoskeleton: force-deflection and fatigue study. *Journal of Rehabilitation Research and Development*, *28*(3), 13–22.

Kabra, S. G., & Narayanan, R. (1991b). Equipment and methods for laboratory testing of prostheses as exemplified by the Jaipur foot. *Journal Of Rehabilitation Research And Development*, *28*(3), 23–24. https://doi.org/10.1682/JRRD.1991.07.0023

Karunakaran, V. (2006). Quality assurance and optimization studies of light weight PU prosthetic foot. *Trends in Biomaterials & Artificial Organs*, *19*(2), 63–69.

Kaufman, K., Anderson, T., Schneider, G., & Walsh, K. (2009). Mechanisms of stumble recovery: Non-microprocessor controlled compared to microprocessor-controlled prosthetic knees. In *American Academy of Orthotists and Prosthetists Journal of Proceedings*. Atlanta, Georgia, USA.

Kendall, F. P., & McCreary, E. K. (1983). Ideal Segmental Alignment: Side View. In *Muscles - Testing and Function* (3rd ed., p. 280). Baltimore: Williams & Wilkins.

Klodd, E., Hansen, A., Fatone, S., & Edwards, M. (2010a). Effects of prosthetic foot forefoot flexibility on gait of unilateral transtibial prosthesis users. *The Journal of Rehabilitation Research and Development*, *47*(9), 899. https://doi.org/10.1682/JRRD.2009.10.0166

Klodd, E., Hansen, A., Fatone, S., & Edwards, M. (2010b). Effects of prosthetic foot forefoot flexibility on oxygen cost and subjective preference rankings of unilateral transtibial prosthesis users. *The Journal of Rehabilitation Research and Development*, *47*(6), 543. https://doi.org/10.1682/JRRD.2010.01.0003

Lenka, P., & Kumar, R. (2010). Gait Comparisons of Trans Tibial Amputees with Six Different Prosthetic Feet in Developing Countries. *Indian Journal of Physical Medicine and Rehabilitation*, *21*(1), 8–14.

Lovejoy, C. O. (1988). Evolution of human walking. *Scientific American*, *259*(5), 82–89.

Mann, R., & Hagy, J. (1980). Biomechanics of walking, running, and sprinting. *The American Journal of Sports Medicine*, *8*(5), 345–350.

Martini, F. H., & Nath, J. L. (2009). *Fundamentals of Anatomy & Physiology* (8th ed.). San Francisco, California, USA: Pearson Benjamin Cummings.

Mathews, D. (2017). Personal communication (e-mail - 7th September).

Mathews, D., Burgess, E., & Boone, D. (1993). The all-terrain foot. *JPO: Journal of Prosthetics and Orthotics*.

MatWeb. (2017a). Dow D 114.01 Polypropylene. Retrieved 22 July 2017, from http://www.matweb.com/search/DataSheet.aspx?MatGUID=3fad3d1abcb54ed79df43ee103cb2327&ckck=1

MatWeb. (2017b). Overview of materials for Polypropylene Copolymer. Retrieved 22 July 2017, from http://www.matweb.com/search/DataSheet.aspx?MatGUID=1202140c34e8443bbf273862e24c5f0e

MatWeb. (2017c). Total PPH 3480Z Polypropylene, Extrusion Grade. Retrieved 22 July 2017, from http://www.matweb.com/search/datasheet.aspx?MatGUID=f8ee493f63f8455597dc1e56cc2d3535&ckck=1

Meier, M. R., Sam, M., Hansen, A. H., Childress, D. S., & Casanova, H. R. (2004a). The shape and roll prosthetic foot (Part I): Design and development of appropriate technology for low-income countries. In *11th World Congree of the International Society for Prosthetics and Orthotics*. Hong Kong, China.

Meier, M. R., Sam, M., Hansen, A. H., Childress, D. S., & Casanova, H. R. (2004b).

The shape and roll prosthetic foot (Part II): Field testing in El Salvador. In *11th World Congree of the International Society for Prosthetics and Orthotics*. Hong Kong, China.

Meier, M., Steer, S. A., Hansen, A. H., Sam, M., & Childress, D. S. (2006). *Shape & Roll Prosthetic Foot*. Chicago, Illinois, USA: Northwestern University.

Meyer, G. H. (1867). Die Architectur der Spongiosa. *Reichert Und Du Bois-Reymond's Archiv*, *8*, 615–628.

Mobility India. (2004). *Jaipur foot manual*. Bangalore, India.

Morton, D. J. (1935). *The Human Foot: Its Evolutionary Development, Physiology and Functional Disorders* (1st ed.). New York, USA: Columbia University Press.

Morton, L. E., Spence, W., Buis, A., & Simpson, D. (2009). *The Design and Development of a Trans-tibial Prosthetic System for use in Low Income Countries*. University of Strathclyde.

Muller, G. M. (1957). A simple prosthesis for rural amputees. *Journal of Bone and Joint Surgery-British Volume*, *39–B*(February), 131–132.

Murray, D., Hartvikson, W., & Anton, H. (1988). With a spring in one's step. *Clinical Prosthetics and Orthotics*, *12*(C), 128–135.

Novacheck, T. F. (1998). The biomechanics of running. *Gait & Posture*, *7*(1), 77–95.

O'Keefe, C. (1998). *Muscle Activation Patterns in the Trans Tibial Amputee*. Monash.

Perry, J., Boyd, L. A., Rao, S. S., & Mulroy, S. J. (1997). Prosthetic weight acceptance mechanics in transtibial amputees wearing the Single Axis, Seattle Lite, and Flex Foot. *Rehabilitation Engineering, IEEE Transactions on*, *5*(4), 283–289.

Perry, J., & Shanfield, S. (1993). Efficiency of dynamic elastic response prosthetic feet. *Journal of Rehabilitation Research and Development*, *30*(1), 137–43.

Postema, K., Hermens, H. J., de Vries, J., Koopman, H. F., & Eisma, W. H. (1997). Energy storage and release of prosthetic feet. Part 1: Biomechanical analysis related to user benefits. *Prosthetics and Orthotics International*, *21*(1), 17–27.

Pugh, S. (1990). *Total Design: Integrated Methods for Successful Product Engineering* (1st ed.). London, UK: Pearson Education Limited.

Rao, S. S., Boyd, L. A., Mulroy, S. J., Bontrager, E. L., Gronley, J. K., & Perry, J. (1998). Segment velocities in normal and transtibial amputees: prosthetic design implications. *Rehabilitation Engineering, IEEE Transactions on*, *6*(2), 219–226.

Rhythm Foot. (2013). Rhythm foot - Dynamic performacne every step of the cycle. Retrieved 14 July 2010, from http://www.rhythmfoot.ca/

Rietman, J., Postema, K., & Geertzen, J. (2002). Gait analysis in prosthetics: opinions, ideas and conclusions. *Prosthetics and Orthotics International*, *26*(1), 50–57. https://doi.org/10.1080/03093640208726621

Roether, C. L., Omlor, L., Christensen, A., & Giese, M. A. (2009). Critical features for the perception of emotion from gait. *Journal of Vision*, *9*, 1–32. https://doi.org/10.1167

Sam, M., Hansen, A., & Childress, D. (2004). Characterisation of prosthetic feet used in low-income countries. *Prosthetics and Orthotics International*, *28*, 132–140.

Schmalz, T., Blumentritt, S., & Jarasch, R. (2002). Energy expenditure and biomechanical characteristics of lower limb amputee gait::: The influence of prosthetic alignment and different prosthetic components. *Gait and Posture*, *16*,

255–263.

Seelen, H., Anemaat, S., Janssen, H., & JHM, D. (2003). Effects of prosthesis alignment on pressure distribution at the stump/socket interface in transtibial amputees during unsupported stance and gait. *Clinical Rehabilitation*, *17*, 787–796. https://doi.org/10.1191/0269215503cr678oa

Sethi, P., Udawat, M., Kasliwal, S., & Chandra, R. (1978). Vulcanized rubber foot for lower limb amputees. *Prosthetics and Orthotics International*, *2*, 125–136.

Shorter, J. J., & Evans, A. J. S. (2000). A FOOT AND SHIN COMPONENT FOR A LOWER LIMB PROSTHESIS. USA: United States Patent Office.

Simon, P. (1996). Handicap International. *Prosthetics and Orthotics International*, *20*, 42–44.

Snyder, R. D., Powers, C. M., Fontaine, C., & Perry, J. (1995). The effect of five prosthetic feet on the gait and loading of the sound limb in dysvascular below-knee amputees. *Journal of Rehabilitation Research and Development*, *32*(4), 309–315.

Torburn, L., Perry, J., Ayyappa, E., & Shanfield, S. L. (1990). Below-knee amputee gait with dynamic elastic response prosthetic feet: A pilot study. *The Journal of Rehabilitation Research and Development*, *27*(4), 369. https://doi.org/10.1682/JRRD.1990.10.0369

Torburn, L., Powers, C. M., Guiterrez, R., & Perry, J. (1995). Energy expenditure during ambulation in dysvascular and traumatic below-knee amputees: a comparison of five prosthetic feet. *Journal of Rehabilitation Research and Development*, *32*(2), 111–119.

Turcot, K., Sagawa, Y., Lacraz, A., Lenoir, J., Assal, M., & Armand, S. (2013). Comparison of the International Committee of the Red Cross foot with the solid

ankle cushion heel foot during gait: A randomized double-blind study. *Archives of Physical Medicine and Rehabilitation*, *94*(8), 1490–1497. https://doi.org/10.1016/j.apmr.2013.03.019

UN-OHRLLS. (2014). *State of the Least Developed Countries 2014*. New York, U.S.A.

University Hospitals of Geneva. (2012). Calcaneus. Retrieved 7 August 2015, from http://www.mypacs.net/cases/62591145.html

Uustal, H., & Baerga, E. (2004). *Physical Medicine and Rehabilitation Board Review*. (S. Cuccurullo, Ed.) (3rd ed.). New York, USA: Demos Medical Publishing.

Vaezi, M., Chianrabutra, S., Mellor, B., & Yang, S. (2013). Multiple material additive manufacturing - Part 1: A review: This review paper covers a decade of research on multiple material additive manufacturing technologies which can produce complex geometry parts with different materials. *Virtual and Physical Prototyping*, *8*(1), 19–50. https://doi.org/10.1080/17452759.2013.778175

van der Linde, H., Hofstad, C. J., Geurts, A. C. H., Postema, K., Geertzen, J. H. B., & Van Limbeek, J. (2004). A systematic literature review of the effect of different prosthetic components on human functioning with a lower-limb prosthesis. *Journal of Rehabilitation Research and Development*, *41*(4), 555–570.

Van Jaarsveld, H. W., Grootenboer, H. J., & De Vries, J. (1990). Accelerations due to impact at heel strike using below-knee prosthesis. *Prosthetics and Orthotics International*, *14*(2), 63–6.

Vas, L. M., & Bakonyi, P. (2012). Estimating the creep strain to failure of PP at different load levels based on short term tests and Weibull characterization.

Express Polymer Letters, *6*(12), 987–996. https://doi.org/10.3144/expresspolymlett.2012.104

Vaziri, M., Stott, F., & Spurr, R. (1988). Studies of the friction of polymeric materials. *Wear*, *122*, 313–327.

Verhoeff, T. T., Poetsma, P. A., Gasser, L., & Tung, H. (1999). Evaluation of use and durability of polypropylene trans-tibial prostheses. *Prosthetics and Orthotics International*, *23*, 249–255.

Veterans International Cambodia. (2013). Veterans International Cambodia - History. Retrieved 11 August 2010, from http://www.ic-vic.org/History.html

Werner, D. (1999). Artificial Legs. In *Disabled Village Children - A guide for community health workers, rehabilitation workers, and families* (2nd ed., pp. 625–636). Berkley, CA, USA: Hesperian Foundation.

Wheeless, C. R. (2011). Wheeless' Textbook of Orthopaedics. Retrieved 15 July 2010, from http://www.wheelessonline.com/

Winter, D. A. (1984). KINEMATIC AND KINETIC PATTERNS IN HUMAN GAIT: VARIABILITY AND COMPENSATING EFFECTS. *Human Movement Science*, *3*, 51–76.

Winter, D. A. (1988). *The Biomechanics and Motor Control of Human Gait* (2nd ed.). Waterloo, Ontario, Canada: University of Waterloo Press.

Winter, D. A., Patla, A. E., Frank, J. S., & Walt, S. E. (1990). Biomechanical Walking Pattern Changes in the Fit and Healthy Elderly. *Physical Therapy*, *70*(6), 340–347.

Wirta, R. W., Mason, R., Calvo, K., & Golbranson, F. L. (1991). Effect on gait using various prosthetic ankle-foot devices. *Journal of Rehabilitation Research and Development*, *28*(2), 13–24. https://doi.org/10.1682/JRRD.1991.04.0013

Witana, C. P., Xiong, S., Zhao, J., & Goonetilleke, R. S. (2006). Foot measurements from three-dimensional scans: A comparison and evaluation of different methods. *International Journal of Industrial Ergonomics*, *36*(9), 789–807. https://doi.org/10.1016/j.ergon.2006.06.004

Wolff, J. (1892). *Das Gesetz der Transformation der Knochen* (1st ed.). Berlin: Verlag von August Hirschwald.

World Health Organization. (2005). *Guidelines for training personnel in developing countries for prosthetic and orthotic services*. Geneva, Switzerland: World Health Organization.

Ziolo, T., & Bryant, J. T. (2001). *Technical Report - Niagara Foot Pilot Study in Thailand*. Kingston, Ontario, Canada.

Ziolo, T., Zdero, R., & Bryant, T. (2001). *The NPO Fatigue Tester: The design and development of a new device for testing prosthetic feet*. Kingston, Ontario, Canada.

APPENDIX A – Rollover shape tests

A1 Abstract

This test set out to find the rollover shape of the Strathclyde foot (SF), the Iraq foot, the ICRC foot, the Dynamic foot and the Atlas foot. Initially a number of methods were examined and finally a dynamic test using the Vicon motion capture system was carried out. Pseudo-prosthesis or stilts were worn with the various feet attached underneath in order to allow an able-bodied subject to test the feet. The results showed that the SF had a similar pattern to the other feet tested although the Iraq foot did have a much shallower rollover shape than the other feet. The Iraq foot appeared to have the best shape from the feet tested as this enabled easier rollover. The rods present in the toe section of the SF affected the shape and require development. The results gained were similar to the previous tests carried out by Hansen et al., 2000, over the mid-section of rollover shape however the ends lacked the characteristic hooks present in Hansen et al.'s results. This was particularly true of the Dynamic feet compared to the SACH foot of Hansen et al.'s tests. The testing process has a number of points to be addressed to provide an accurate rollover shape for each foot especially in terms of noise elimination and marker placement and tracking. Two other methods, quasi-static prosthetic foot loading apparatus and quasi-static rollover method were identified but not used and may be beneficial in any future testing.

A2 Introduction

The development of an effective trans-tibial prosthetic system for developing countries is highly important as it is here that the majority of amputations occur and

without the funds for the typically expensive prostheses common in the West many amputees find themselves unable to work and become a drain on their families or governments (Cummings, 1996). Up to the present time the majority of prosthetic development has focused on high end technical improvements, for example intelligent prostheses, and there have not been great improvements seen in prostheses available at the lower end of the economic scale (Day, 1996).

The aim of this mini-project study was to determine the rollover shape of the Strathclyde Foot (SF) being developed within the Department of Bioengineering in collaboration with the NCPO at the University of Strathclyde and to compare it with a number of established feet including the Atlas system from Blatchford, the Iraq foot designed by Emergency - Life Support for Civilian War Victims and the International Committee of the Red Cross (ICRC) foot. The SF was designed with function and cost in mind, particularly aimed at developing countries. The overall aim of this EngD project was to produce a durable, functional prosthesis. The existing, polypropylene, injection moulded foot design is representative of intended final production and has been tested to the ISO 10328 static P3 level (L. E. Morton et al., 2009) and has demonstrated its ability to meet this part of testing but has no functional indicator. The rollover shape can show the ease by which an amputee can walk during stance and so can be used to indicate efficient walking. (A. H. Hansen et al., 2000)

The roll over shape may be considered to simulate the geometry of a solid rocker that would produce the same effect during walking as the original foot. The roll over shape has a significant effect on gait (A. H. Hansen et al., 2000) and altering the shape could provide a more suitable roll over shape. In comparing the

SF to other similar feet, it is possible to determine why differences occur and what improvements may be included in further design work as well as how the shape could be “tuned". It is expected that the roll over shape of the SF will not be in its ideal form yet but that as the heel and toe may be adjusted this may be improved upon in future. It should be noted that the SF should have an energy return component, and this may affect the rollover shape.

Hansen et al., 2000, described three methods for determining the roll over shape of a prosthetic foot. Each of the methods described was considered in terms of direct comparison and with a view to its use. One of these methods was to be selected to provide an overall representative roll over shape which may then be used in future rather than using all three methods. This would facilitate the process of tuning the foot by altering heel and toe components as is currently foreseen. It should be noted however that the rollover shape is only relevant on flat surfaces as inclines or declines affect walking pattern and so also rollover.

A3 Materials and Method

In this experiment three methods were considered. These were all previously detailed by Hansen et al., 2000 (A. H. Hansen et al., 2000) as: quasi-static PFLA (prosthetic foot loading apparatus) method, quasi-static rollover method and dynamic rollover method.

In the case of quasi-static PFLA Hansen et al. used a test rig specifically for this purpose. Given the time frame for this report production of such a rig was deemed impractical. As such another method was investigated using an Instron machine, a standard piece of testing equipment, but this unfortunately proved impractical due to

machine limitations and foot geometry, so this first experimental method had to be abandoned. It is a potentially useful piece of future work as a standard method using readily available equipment could make determining rollover shape much simpler in future and would be of significant benefit in the tuning process.

The quasi-static rollover method was described by Hansen et al. as being carried out using pseudo-prostheses. A pseudo-prosthesis consists of an Aircast leg brace coupled to a socket for a pyramid to be fitted into on the base. This permits non-amputees to experience walking on a prosthetic foot. However, body parameters are affected as the shank becomes much longer (see Figure 135 for an example of pseudo-prostheses in use). The user would wear the system then slowly roll the test foot over a forceplate. Motion capture was carried out using two markers, one on the ankle and one on the Aircast brace. A similar method was planned, using 3 markers on the pylon and a further two points defined on the ankle rather than the two described by Hansen et al. to describe the system in 3D space and allow off angle roll to be considered. The points on the ankle were to be defined by placing a previously calibrated pointer in the screws on either side of the ankle pyramid where available or at a matching height if not. Due to time limits, this was not carried out although the method is prepared and could be done in future.

Figure 135 – An example of pseudo-prostheses in use

Dynamic rollover was achieved through the investigator wearing a pair of pseudo-prosthesis and walking across a force plate. The same marker system was used as for the quasi-static rollover test. The pylon markers were attached via a Velcro strap which could be stretched to fit a variety of pylon sizes and shapes and the further two points were defined using the Vicon system. The recording was done through the Vicon system and was processed through a model formed in Bodybuilder. A coordinate system was designated with its origin at the centre of the two ankle points, X as the direction of progression, Y perpendicular towards the knee and Z perpendicular to the subject's right. Results from Workstation using the Bodybuilder model were exported to Microsoft Excel to form graphs. The investigator is a healthy male of approximately 175cm height and approximately 775N weight. As the investigator was the test subject, there was no requirement for consent to be supplied but a Departmental Safety Committee was convened to

determine the safety of the procedure. Recommendations were made and implemented allowing testing to proceed.

The pseudo prostheses were produced by the National Centre of Prosthetics and Orthotics at the University of Strathclyde, Glasgow, from Aircast FP Walker braces manufactured by DJO Incorporated, Vista, CA, USA. The feet to be tested were originally available from the following sources:

SF - Department of Bioengineering, University of Strathclyde, Glasgow

Atlas foot - Chas A Blatchford Sons Ltd, Basingstoke

ICRC foot - ICRC, Geneva, Switzerland

Iraq foot - Emergency - Life Support for Civilian War Victims, Rome, Italy

A4 Results

In each case the origin is centred around the ankle centre with the X-axis representing the direction of travel and the Y-axis vertically perpendicular to the X axis. The rollover shape is ideally a continuous line progressing from behind ankle (negative X values) to the toe before ground contact is broken and the line terminates at a positive X value. Each set of results is presented with the axes scaled to the same range to allow direct comparison. Data was sampled at 120Hz so the gap between points on the line represents 0.0083 seconds. The data was unfiltered however certain values at the beginning were removed (e.g. in Dynamic foot (left) sample 1 the initial values were large and positive in the Y-direction which was not a possible condition for heel contact). The heel contact is identified where the data was not removed for apparent error. The end of toe contact is marked as the final point in each line. The “ball” of the foot is identified as a region of tightly

clustered points over which the foot spent time in contact with only a slight change in point of contact relative to the ankle centre.

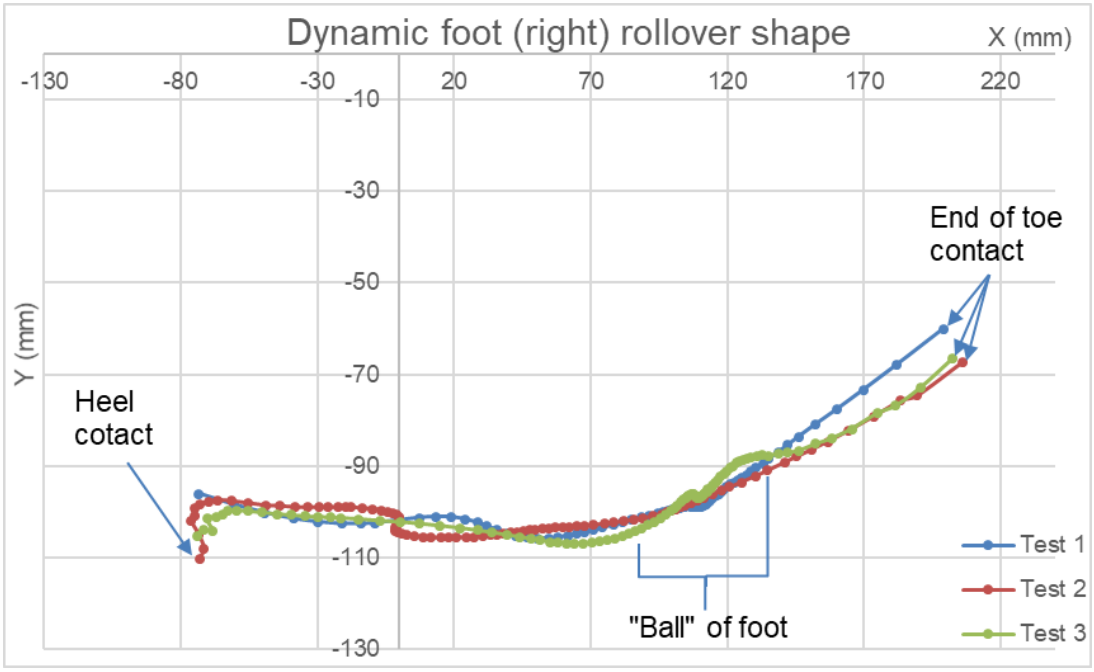

Figure 136 - Dynamic foot (right) rollover shape

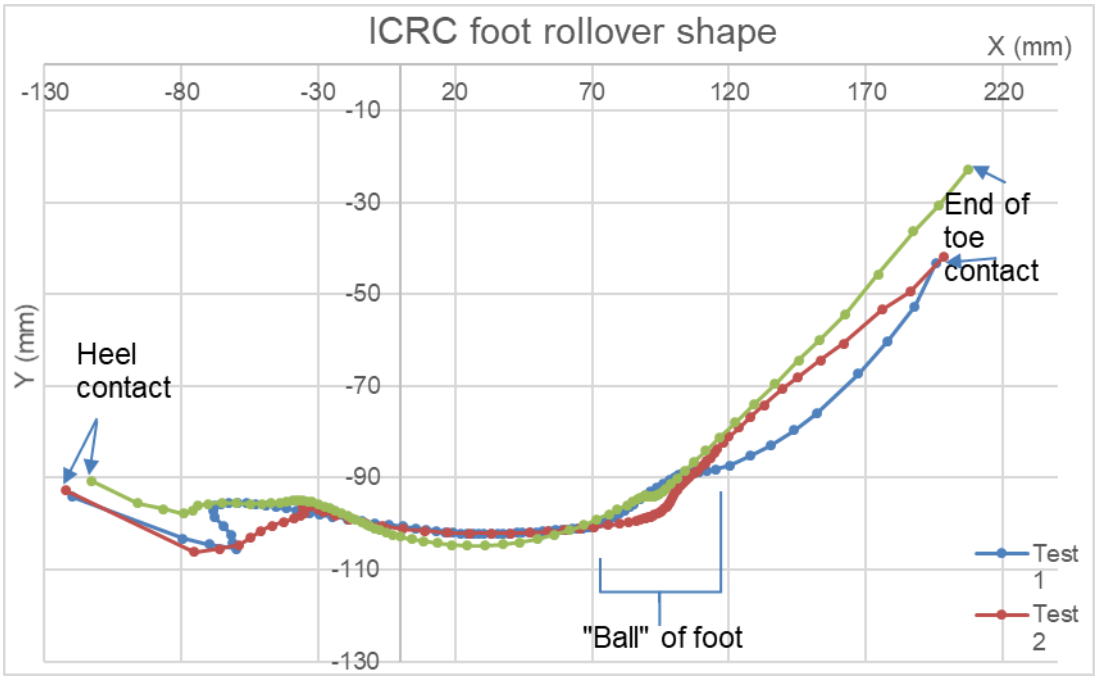

Figure 137 - ICRC foot rollover shape

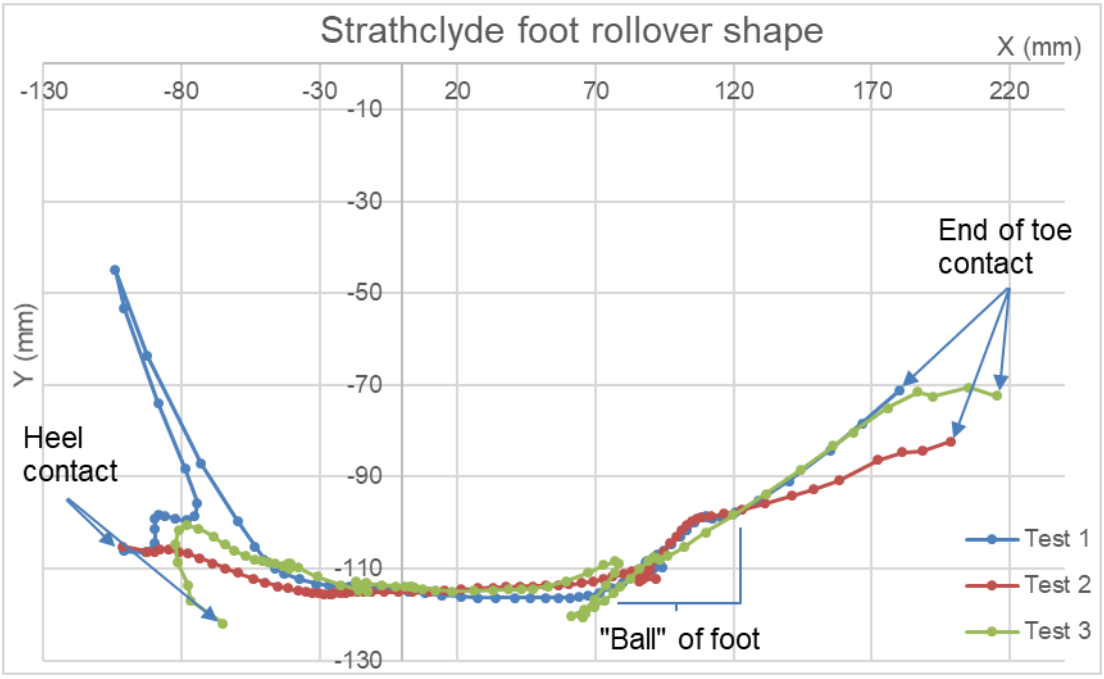

Figure 138 - Strathclyde foot rollover shape

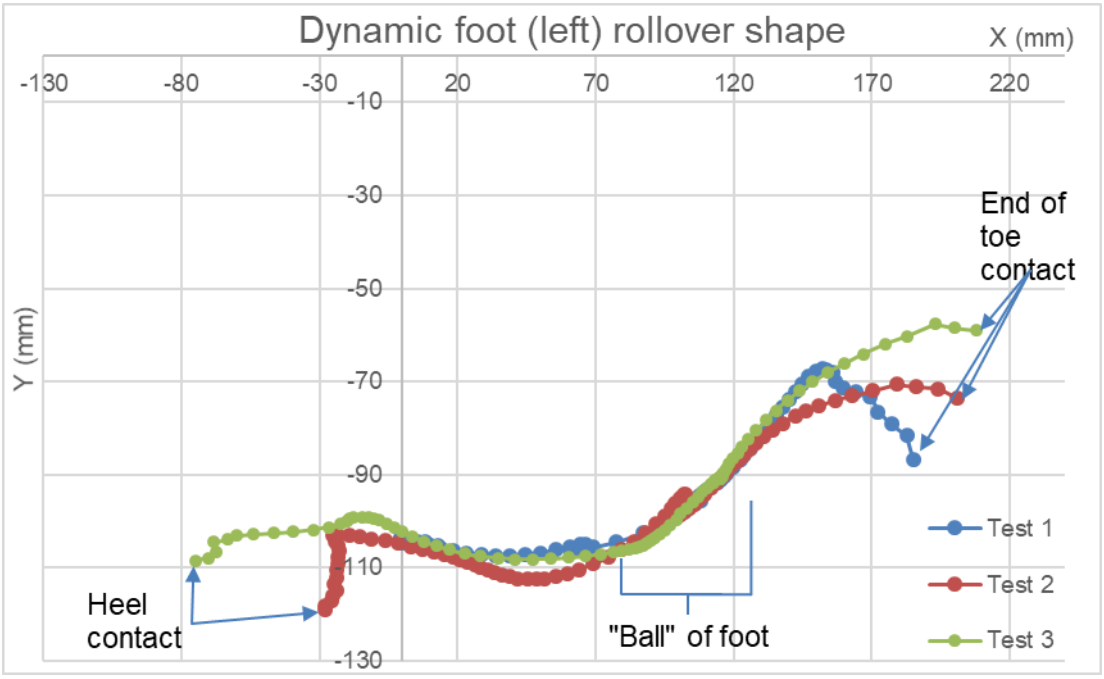

Figure 139 - Dynamic (foot) left rollover shape

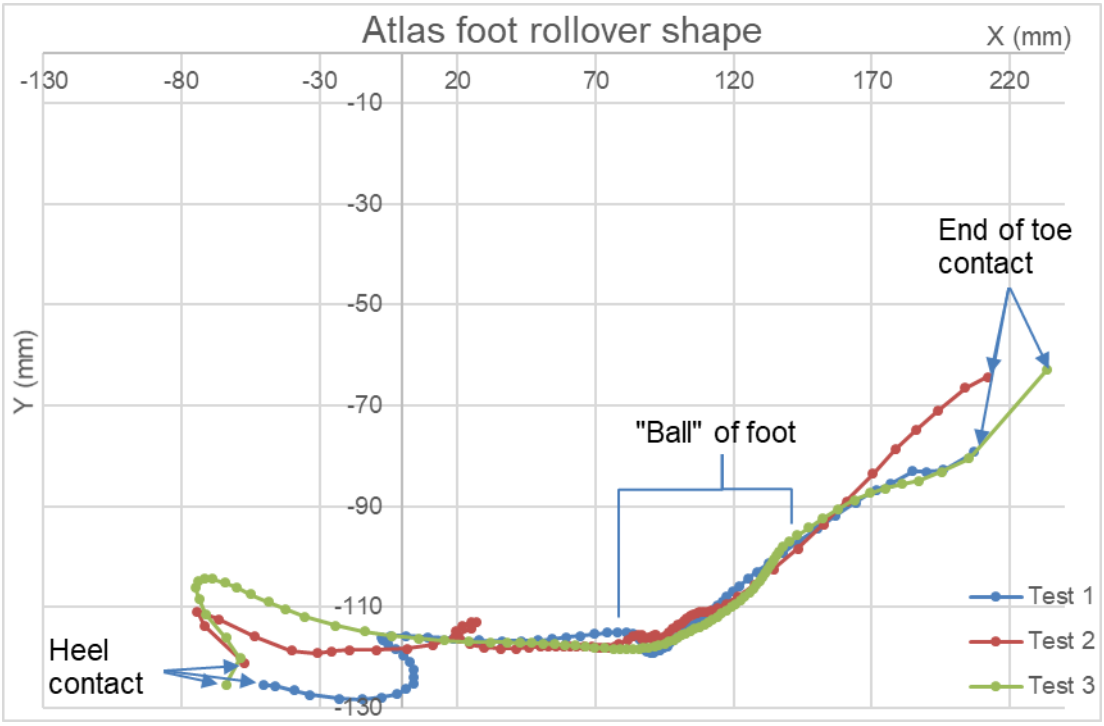

Figure 140 - Atlas foot rollover shape

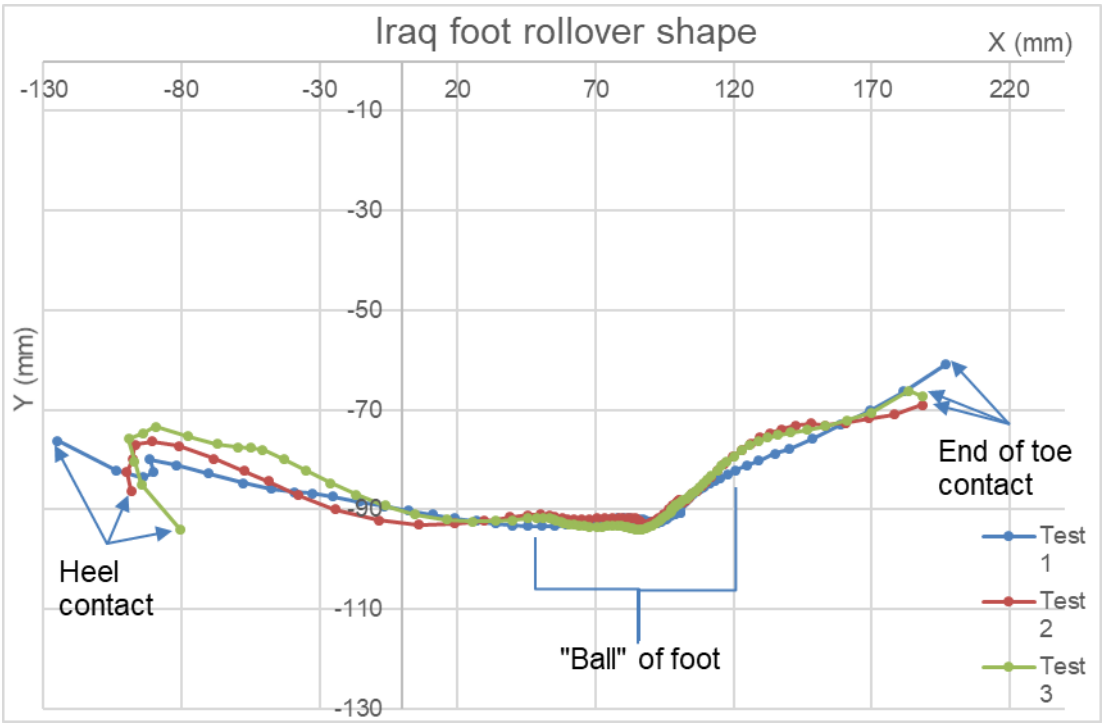

Figure 141 - Iraq foot rollover shape

A5 Discussion

The results displayed in Figure 136 - Figure 141 show the rollover shapes for each of the three tests carried out on each foot. These are displayed as all three tests for each foot on the same sheet for direct comparison. The first test is always displayed in blue, the second red, and the third green. The same scale has been used for all graphs and X and Y are the distance from the origin which was set at the ankle of the feet, as described above. It should be noted that this was a constantly moving frame within the laboratory. Certain results led to problems as erroneous points altered the scale drastically. This was true for the first test in each case of the Dynamic foot, left and right and the SF. These results occurred as a result of noise and marker errors; as such they were removed for displaying results.

The Dynamic right foot did show a fairly consistent pattern with variation in the Y axis between each of the three tests reaching a maximum of approximately 10mm at the toe off end. Through the body of the curve the difference remained under 5mm. Some noise was present in the first result which was removed for clarity of results. This significantly affected the periods of the test where a lower force was acting upon the forceplate, namely heel strike and toe off. Heel strike was effectively removed from the presented results so some of the pattern present in the other two cases was not visible. At the toe off end of the noise had the effect of increasing the apparent force which accounts for the greater difference between results at this end.

The ICRC foot was a right foot and showed a fairly consistent pattern through mid-stance between the three tests. While the stride length was very similar in each case the heel strike appeared to differ. This then accounted for variation seen at the beginning of the rollover shape. At toe off each test followed a similar line but at

different values, there was a Y axis separation of up to 20mm at points between the various tests. These were again likely to be caused by differences in walking pattern.

The SF was a right foot and was the main target of this investigation. In the first test, there was a loss of detection of markers during heel strike and a number of erroneous points formed in the roll over shape. These were included in Figure 138 and were the cause of the large peak visible near the beginning. In the third tests, a drop was seen prior to the incline seen towards toe off. There appeared to have been a slight rocking on the foot and so the progression was not as smooth as it may have been accounting for the drop. During the testing, there was a clicking sound noted as occurring during the latter part of stance phase from the SF. This click was probably caused by the rods present in the foot shifting and can be seen in the first and second test as a small figure of eight shape just after the drop in the third test. There was a pinch within the drop of the third test and it may be that the click had some effect in causing this drop. This click is clearly undesirable aesthetically, but it is worth noting that it also had an effect on the rollover shape of the foot.

As the Iraq and Atlas feet provided for testing were left feet a Dynamic left foot was also tested in case of any significant gait differences between the subject's left and right side. During the mid-stance, a similar pattern was viewed with none of the tests exceeding a 6mm difference from one another in the Y axis. Towards the end however a much larger difference appeared, up to 25mm at the extreme end. The results of the first test unfortunately suffered from an error in marker reading leading to the initial part of the line being erroneous and so removed from the results. There

was no apparent reason for the jink in the results of the second test although this may have been due to the subject slightly altering their balance during stance.

Comparing both Dynamic feet against one another there was generally a good correlation. Through the centre section all results are within 6 mm of each other in the Y axis however towards the end of the shape they had spread to a maximum of approximately 26mm difference however even at this point five of the results lay within 15mm of one another.

The Atlas foot was a left foot and appears to show good correlation through the middle section and most of the way to the end. In the central section, there was approximately 3mm difference between results on the Y axis while towards the end it increased from this to approximately 16mm. There appeared to be some marker movement in the second test which gave the odd loop in the central section as well as the ripple seen later on the same test.

The Iraq foot was a left foot and had probably the best correlation of any of the feet tested. The difference between the three tests never exceeded 8mm in the Y axis and throughout the central section was less than 3mm. Overall the shape was quite consistent except for the start of the first test. This was probably due to the heel strike being slightly different. The Iraq foot also had the shallowest roll over shape of any of the feet tested. This would suggest that it was the easiest to roll over, particularly at the toe.

Throughout all the feet aside from the SF it was seen that the shape got much steeper towards the toe off end. This was due to the end of the keel effectively being

a point for the foot to rotate over. In the SF, however there was initially a steepening followed by a shallower section before again becoming steeper. This was likely to have been caused by the curve present on the bottom of the toe section of the keel. This made the foot easier to roll over prior to rotating about the end of the keel. The subject had noted at the time that the SF felt firmer than the Dynamic foot and this was reflected in the results. Although it might be thought that this was a disadvantage in a foot, as it becomes more difficult to roll over it may in fact be beneficial as the user is offered more stability as they pass over the toe. The roll over shape does not take into account the energy return properties of a foot and it might be that while the roll over shape suffers the overall effect on a patient's gait is improved through the energy return function.

Hansen et al., 2000, carried out a similar experiment in determining the roll over shapes of four feet, the Flexwalk foot, the Quantum foot, the SACH foot and the SAFE foot. As the Dynamic foot is a type of SACH foot it may be compared to the SACH foot tested by Hansen et al. The pattern observed in the Dynamic foot is quite similar to the pattern observed in the SACH foot with a similar Y range being seen as well as a similar curved range through the centre. A notable difference between the feet is however the bump seen towards the right of the SACH foot. This was likely caused by the centre of pressure passing into the toe region of the foot. There was a similar bump seen in the first and third test on the Dynamic foot however it was not so large. The most noteworthy point from Hansen's study is the presence of a hook on either end of the shape where it turned underneath the foot. This was missing in almost all tests carried out for this paper. A reason for this may have been the difference in gait between the two subjects in the different tests.

The results from the testing appeared to vary significantly and a second set of tests which have the noise eliminated and complete marker detection would be better in determining an accurate roll over shape. A greater number of tests would be preferable as well as having all feet of the same side in order to eliminate some effects of gait deviation from the results. Some method of regulating variations in the subject's walking speed would be beneficial as it is possible that some of the differences within a foot's rollover patterns were due to changes in walking speed. This may be potentially remedied with a regular beat for the subject to walk to. The stilts raised the subject's height by approximately 20cm in each case which obviously has serious implications on segment length and potentially affects gait and so reducing this as much as feasible could serve to improve the validity of the test. The Velcro system should be removed to avoid potential bobbing of markers during testing.

Appendix B – Finite Element Analysis of foot designs

This appendix includes an overview of the FEA modelling that was undertaken for this project and the resulting design improvement. Toe and heel tests were simulated on the existing Strathclyde design using experimentally determined material properties while a hand calculation was carried out for the toe test. Sections of the design were evaluated and modified before the redesign complete was evaluated in toe loading in both polypropylene and Duraform EX, with and without a blade. Comparison of sections between the first and second redesign was carried out before the second redesign was evaluated in toe loading in both polypropylene and Duraform EX, with and without a blade.

B1 Introduction

A combination of Finite Element Analysis (FEA) and prototyping was utilised to maintain an efficient design process The FEA would determine whether a given design would survive the conditions required of it, so reducing manufacture of prototypes. With prototyping used to validate the FEA, confidence could be found in the results allowing for further design without additional prototyping.

Injection moulding in polypropylene was the desired production method however with a small batch size the costs became very high per unit because of tooling costs. The developed design could be tested in FEA using polypropylene material values to reduce unnecessary manufacturing costs.

B2 Existing Strathclyde foot design FEA

The existing design was used to form a simulation of the conditions of ISO 10328 static testing using the FEA package, Ansys Workbench 17.1, to allow direct comparison with the physical tests carried out on sample Strathclyde feet. The test of interest is the separate static ultimate strength test, a brief description of which follows.

B2.1 Separate static ultimate strength tests for ankle-foot devices and foot units

To test the heel; the heel loading platform shall be aligned at 15° to the horizontal, to test the toe; the toe loading platform shall be aligned at 20° to the horizontal. In both cases a toe out of 7° of the foot is required. Either the foot or heel may be loaded first and then subsequently the other. The toe platform should support the heel of the foot in case of significant deformation in toe loading (and the reverse is true in heel loading) or in a twin actuator setup the heel platform should not be contacted by the heel. The test load should be applied at a rate between 100N/s and 250N/s to the required load and then held for (30 ± 3) s before being reduced to zero. Depending on the results of this test it should be decided whether to test the opposite end of the foot.

B2.2 Model generation

Using the CAD model designed earlier two assemblies were created, one to represent toe loading and the other heel loading. The foot model was sectioned along the medial plane, as a symmetrical model would be used to reduce required computing power and time to resolve. This meant that the 7° toe out would not be included. A small square plate was inserted and aligned to act as the loading platform in each case. The plate was located under the toe for toe contact and under the ball in heel contact. These files were imported into Ansys Workbench for FEA testing.

Once the model was in Workbench conditions had to be applied to the model to represent the real-world situation as accurately as possible. These include material properties, boundary conditions, solver properties, etc.

B2.2.1 Material properties

Material properties of the polypropylene were required as well as the ball material. Also used was the structural steel properties supplied with Ansys which was used for the load plate so that it would be significantly stiffer than the foot, maintaining the deformation within the foot design.

The properties used for copolymer polypropylene were:

Density	915 kgm^{-3}
Young's Modulus	9×10^8 Pa
Poisson's ratio	0.43
Bulk Modulus*	2.143×10^9 Pa
Shear Modulus*	3.147×10^8 Pa
Tensile Yield Strength	3.5×10^7 Pa
Tensile Ultimate Strength	4.5×10^7 Pa

* Bulk modulus and shear modulus were calculated by Ansys using Young's modulus and Poisson's ratio.

The values for Young's modulus, tensile yield strength and ultimate tensile strength were calculated experimentally (sections 4.3 Material testing and 4.4 Extensometer testing). Density was taken at the middle of the range (0.90-0.93 gcm^{-3}) provided by North Sea plastics, the PP suppliers.

No value of Poisson's ratio was readily available for North Sea Plastic's polypropylene. A similar variety (Dow D 114.01 polypropylene) with a value of 0.43 was found (MatWeb, 2017a) so this value has been used in the FEA.

The rubber for use in the ball was initially given the following properties:

Density	1340 kgm^{-3}
Young's Modulus*	1.2×10^8 Pa
Poisson's ratio	0.49
Bulk Modulus	2.0×10^9 Pa
Shear Modulus*	4.0268×10^7 Pa
Tensile Ultimate Strength	25.0×10^6 Pa

*Bulk modulus and Poisson's ratio were used by Ansys to calculate a value for Young's modulus and shear modulus.

Apart from calculated values all properties were taken from the Polymer Data Handbook, Oxford University Press, 1999. The section used was that on 'poly(isobutylene), butyl rubber, halobutyl rubber'. The tensile ultimate strength was given the mid value of the range given in the handbook.

The given structural steel properties were:

Density	7850 kgm^{-3}
Young's Modulus	2×10^{11} Pa
Poisson's ratio	0.3
Bulk Modulus	1.6667×10^{11} Pa
Shear Modulus	7.6923×10^{10} Pa
Tensile Yield Strength	2.5×10^8 Pa
Compressive Yield Strength	2.5×10^8 Pa
Tensile Ultimate Strength	4.6×10^8 Pa

Alternating stress mean stress and strain-life parameters were also included but these are not relevant to the simple loading case for which the values are to be used. The steel was required to be significantly stiffer than the polypropylene so that deformation would occur in the foot rather than the loading plate.

B2.2.2 Contact conditions

In toe loading two contact conditions were required, that for the interface between the steel plate and the underside of the toe and that for the contact of the two sections of the toe.

Vaziri, Stott, & Spurr, 1988, give the coefficient of friction for polypropylene in flat on flat contact at low speeds to be 0.28. From the same work, the coefficient of friction between PP and steel was found to be approximately 0.57.

In heel loading, there were again two contact regions, the ball/foot and the ball/plate interfaces. The ball was treated as bonded to the foot while the contact between the ball and plate was rough as defined by Workbench.

In the case of the non-bonded contacts the interface treatment was to adjust to touch, normal stiffness and the pinball region were left to the remit of Workbench however no updates were made to the stiffness. The augmented Lagrange method was used in each case.

B2.2.3 Symmetry

The cut surfaces of the model were highlighted as symmetry regions with symmetry normal to the face to account for the fact that the model is halved.

B2.2.4 Boundary conditions

In each case certain boundary conditions were required which were the same in that the foot was to be fixed and the plate should be free to move in the y direction only. Selecting the top surface of the foot and constraining it as fixed achieved this (marked as ‘B’ in Figure 142). The four sides of the plate were given frictionless support status (marked ‘C’ in Figure 142), preventing them from rotating or moving laterally and ensuring that the motion was preserved in the y direction only.

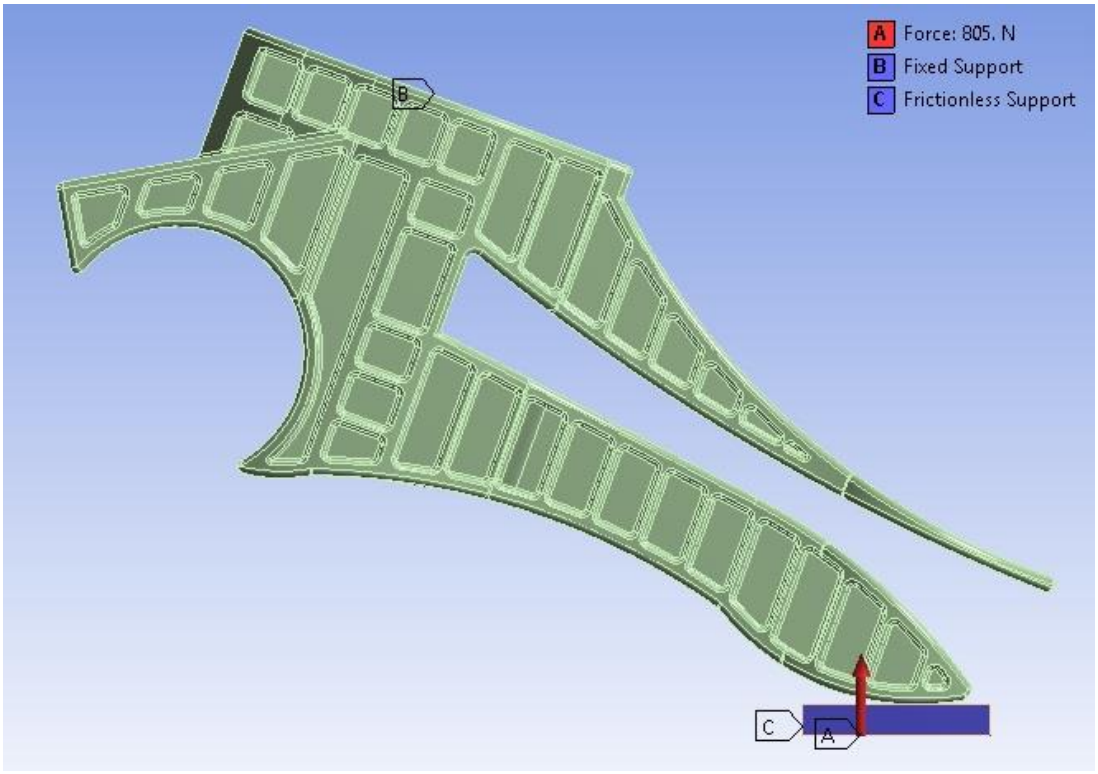

Figure 142 – Boundary conditions of the model

B2.2.5 Mesh

The meshing procedure was the same for both setups. Initially the entire model was meshed using a relevance centre setting of ‘coarse’ with a medium smoothing and fast transition. The contact areas were then further refined by element size, which was set to 0.002m (see Figure 143).

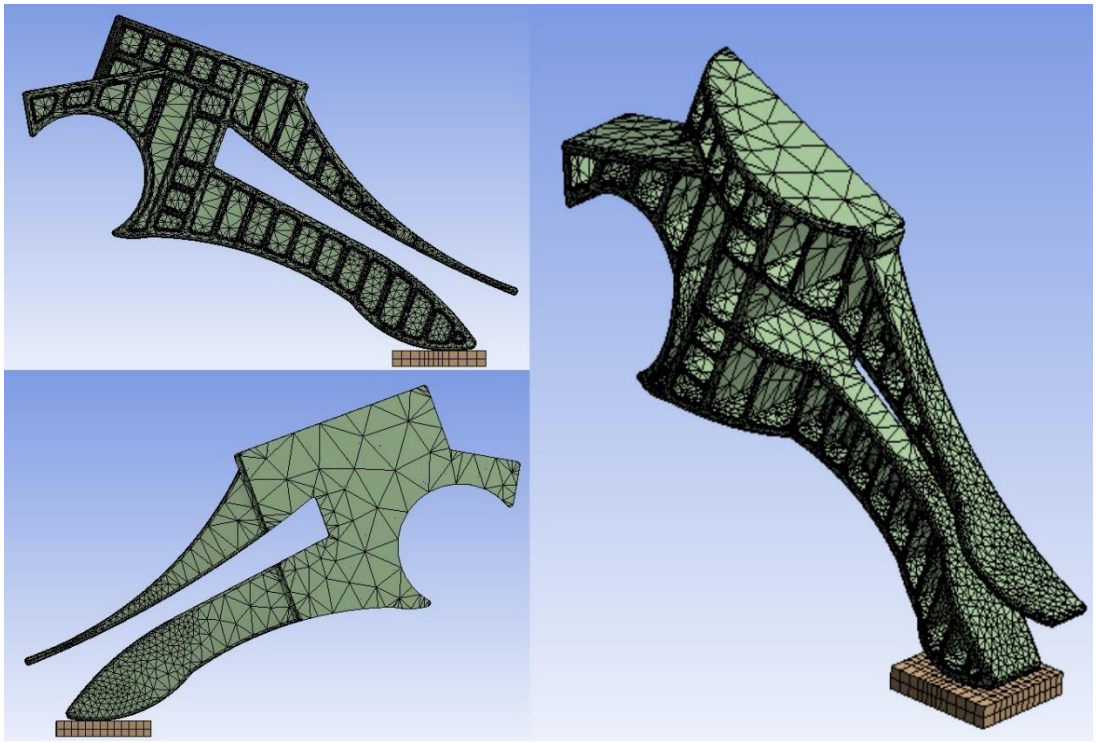

Figure 143 – Mesh of setup used to analyse Strathclyde foot in Ansys

B2.2.6 Loading

A ramped load was applied over the course of 4.6 seconds to a maximum value of 805N (half the static proof load of 1610N for the P3 level as specified in ISO 10328).

B2.2.7 Analysis settings

The model was set to run over 4.6 seconds split into 250 sub steps, this gave a loading rate of 175N/s, which is midway in the range of 100N/s to 250N/s specified in ISO 10328. Weak springs were turned off, large deflection was turned on while inertia relief was off, and the solver type left as program controlled.

B2.2.8 Solution

The required information from the solution was total deformation, directional deformation, equivalent elastic strain and equivalent stress.

B2.3 Results

B2.3.1 Toe loading

The bottom section of the toe was observed to have deformed upwards, meeting the upper section of the toe, which then reduced the rate of deformation. The maximum deformation shown in Workbench was 2.67×10^{-2}m at the tip of the bottom toe section. The maximum deflection on the upper toe section was 1.97×10^{-2}m (see Figure 192).

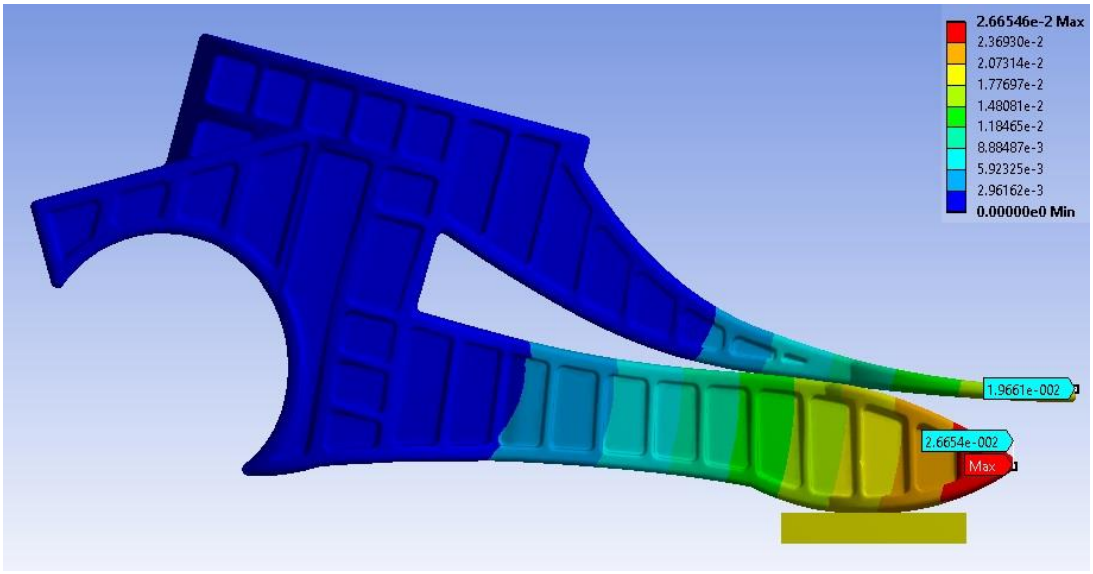

Figure 144 - The deformed condition of the model shown at 805N load. The highest deformations of the upper and lower toe sections are highlighted.

In the analysis five major areas of high stress became apparent and are highlighted in Figure 145. While other high stress areas were visible these were achieved later than the five highlighted areas and as such the foot would be likely to fail due to one of the five highlighted areas before the other areas were able to reach yield stress.

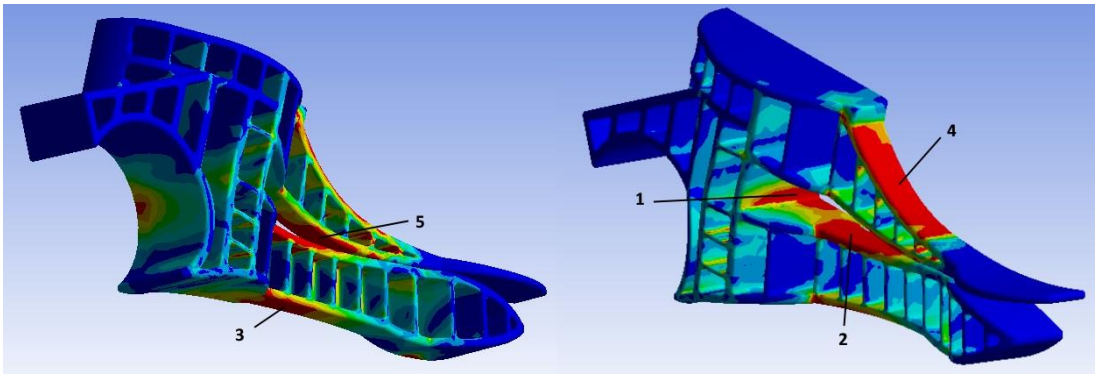

Figure 145 – The high stress areas found in the sample with identifying numbers.

$3.5x10^7$Pa (the yield stress of the polypropylene) was reached at area 1 at a load on the model of 177.1N (354.2N on the full foot). This area appears to effectively be the pivot for the lower toe section.

In area 2 the tensile yield stress of the polypropylene was surpassed at 238.3N loading (476.6N on the full foot).

In area 3 the tensile yield stress was reached at 376.7N (753.5N on the full foot). This section appears to be largely in tension.

In area 4 the tensile yield stress was reached at 615.0N (1230.0N on the full foot).

In area 5 the tensile yield stress was reached at 631.1N (1262.2N on the full foot). This section appears to be largely in tension.

B2.4 Model Validation

As a check for the validity of the FEA model a simple hand calculation was carried out on the toe loading condition, treating the part of the toe section indicated to fail as a simple I-beam with a point load on one end and fixed at the other (see Figure 146 for a section view of the model at this point). In this case area 1 identified in the previous section, being the first to reach yield stress (at approximately 280.1N), would provide the following values to be (see Figure 147 for diagram):

F = 280.1N d = 0.08m y = 0.0123m a = 0.011m

b = 0.054m t_1 = 0.003m t_2 = 0.007m h = 0.019m

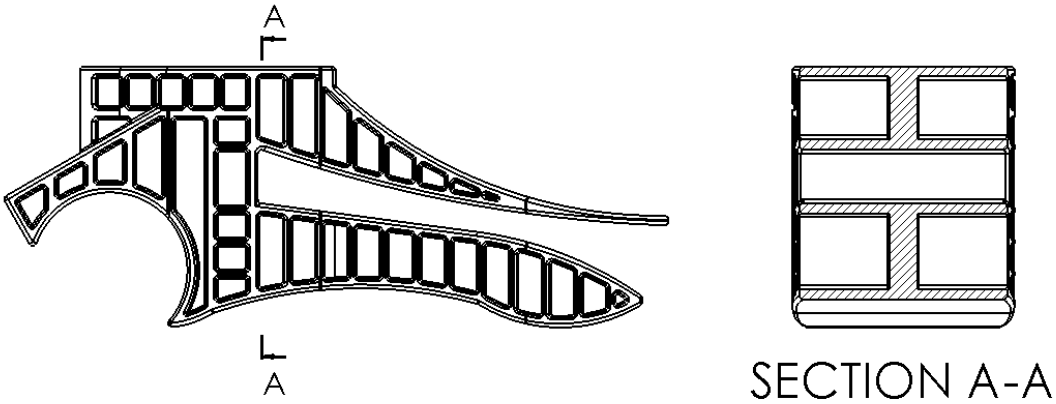

Figure 146 – Section of the foot model through high stress area 1, highlighting the I-section in the lower part of the foot

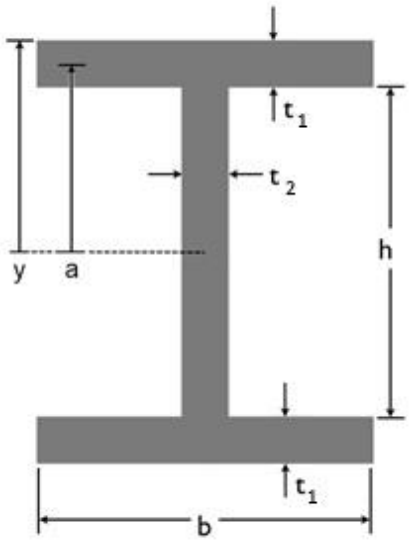

Figure 147 – Image highlighting the dimensions used in beam bending equation

The dimensions were taken directly from the model, as at the section of failure the shape was that of an I-beam.

Using the simple beam bending equation of $\sigma = \frac{My}{I_x}$ where M is moment (Fd), σ is stress and I_x is 2nd moment of area the stress was calculated given the other

values using the parallel axes theorem leading to $I_x = 2\left[{}^1/_{12}\, bt_1{}^3 + bt_1a^2\right] + {}^1/_{12}\, t_2h^3$

Using this equation, the value was determined as follows.

$$I_x = 2\left[{}^1/_{12}\, 0.054 \times (0.003^3) + 0.054 \times 0.003 \times 0.011^2\right] + {}^1/_{12}\, 0.007 \times 0.019^3$$

$$I_x = 2[1.215 \times 10^{-10} + 4.901 \times 10^{-9}] + 4.001 \times 10^{-9}$$

$$I_x = 3.803 \times 10^{-8} + 4.001 \times 10^{-9}$$

$$I_x = 1.405 \times 10^{-8}\text{m}^4$$

Given that y = 0.0123m, M = Fd = 280.1(0.08) = 64.4Nm and I_x = 4.20 x 10^{-8}m^4 the stress in the beam was calculated.

$$\sigma = \frac{My}{I_x}$$

$$\sigma = \frac{22.41 \times 0.0123}{1.405 \times 10^{-8}}$$

$$\sigma = 19.62\text{MPa}$$

Ansys calculated a load of 35MPa at this point under maximum load which was significantly different to the 19.62MPa calculated here. This was likely due to the stress not being purely a result of bending as the toe section showed some lateral motion which would increase the stress at the given location, particularly as it was mirrored on the opposite side.

The stress at area 2 was also calculated as the stress generated here should have been largely a result of only the bending. The beam at this point resembled a C channel (see Figure 148 for a section view of the model at this point), so the stress was calculated, using the value at which Ansys predicted yield stress to be surpassed as follows:

F = 805N	d = 0.065m	b = 0.0116m
t_1 = 0.0027m	t_2 = 0.0025m	h = 0.0149m

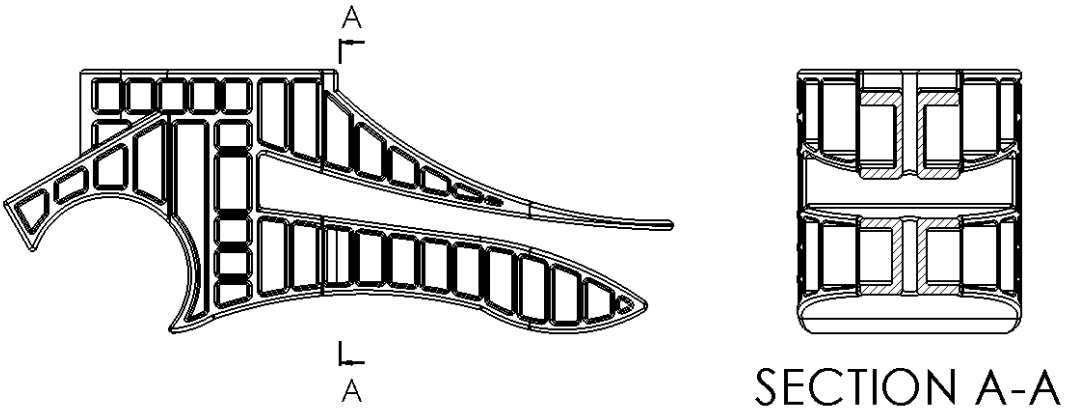

Figure 148 - Section of the foot model through high stress area 2, highlighting the C-section of the lower toe sections

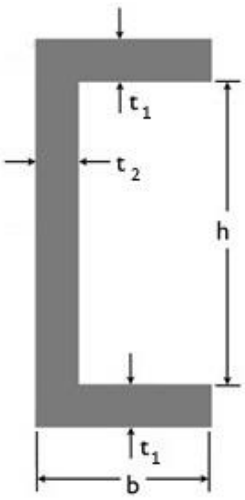

Figure 149 – Image highlighting the dimensions used in beam bending equation

The dimensions given here were taken directly from the model, as at the section of failure the shape was that of a C channel.

Using the simple beam bending equation of $\sigma = \frac{My}{I_x}$ where M is moment (Fd), σ is stress and I_x is 2nd moment of area the stress was calculated given the other values using the parallel axes theorem leading to

$$I_x = {}^1/_{12}\ h^3 t_2 + 2[{}^1/_{12}\, {t_1}^3 b + {}^1/_4\, t_1 b(t_1 + h)^2]$$

Using this equation, the 2nd moment of area may be determined

$$I_x = {}^1\!/_{12}\,(0.0149^3 \times 0.0025) + 2\left[{}^1\!/_{12}\,0.0027^3 \times 0.0116 + {}^1\!/_4\,0.0027 \times 0.0116(0.0027 + 0.0149)^2\right]$$

$$I_x = {}^1\!/_{12}\,(8.270 \times 10^{-9}) + 2\left[{}^1\!/_{12}\,8.013 \times 10^{-9} + {}^1\!/_4\,3.132 \times 10^{-5}(3.098 \times 10^{-4}\right]$$

$$I_x = 6.892 \times 10^{-10} + 2[6.678 \times 10^{-10} + 2.425 \times 10^{-9}]$$

$$I_x = 6.892 \times 10^{-10} + 6.186 \times 10^{-10}$$

$$I_x = 6.876 \times 10^{-9}\text{m}^4$$

Given that y = 0.0102m, M = Fd = 473.3(0.065) = 30.76Nm and I_x = 6.876 x 10^{-9}m^4 the stress in the beam may be calculated.

$$\sigma = \frac{My}{I_x}$$

$$\sigma = \frac{30.76 \times 0.0102}{6.876 \times 10^{-9}}$$

$$\sigma = 45.64\text{MPa}$$

At this point Ansys had calculated a stress of 35MPa, which would indicate that the Ansys model underestimates the stresses in the beam at this point.

As an alternative, the yield strength of polypropylene was used as the stress value to give a value of moment and so load at which the beam would be expected to fail at this point. This took the form of:

$$F = \frac{\sigma I_x}{yd}$$

$$F = \frac{3.5 \times 10^7 \times 6.876 \times 10^{-9}}{0.0102 \times 0.065}$$

$$F = \frac{0.241}{6.63 \times 10^{-4}}$$

$$F = 362.96\text{N}$$

This suggested that the foot would fail at approximately 363N (726N full foot) or approximately 30% lower than the Ansys model suggested. It should be noted that

for either of these equations the load was taken as acting perpendicular to the beam which was not the case for this loading condition as it was initially at 20° offset with this changing as the toe deflects.

B2.5 Heel loading

Some deformation was visible in the ball and the rear of the foot, with the ball deforming more than the foot. The ball itself did not deform as much as would be expected, only 0.36mm at maximum under 402.5N load (See Figure 150).

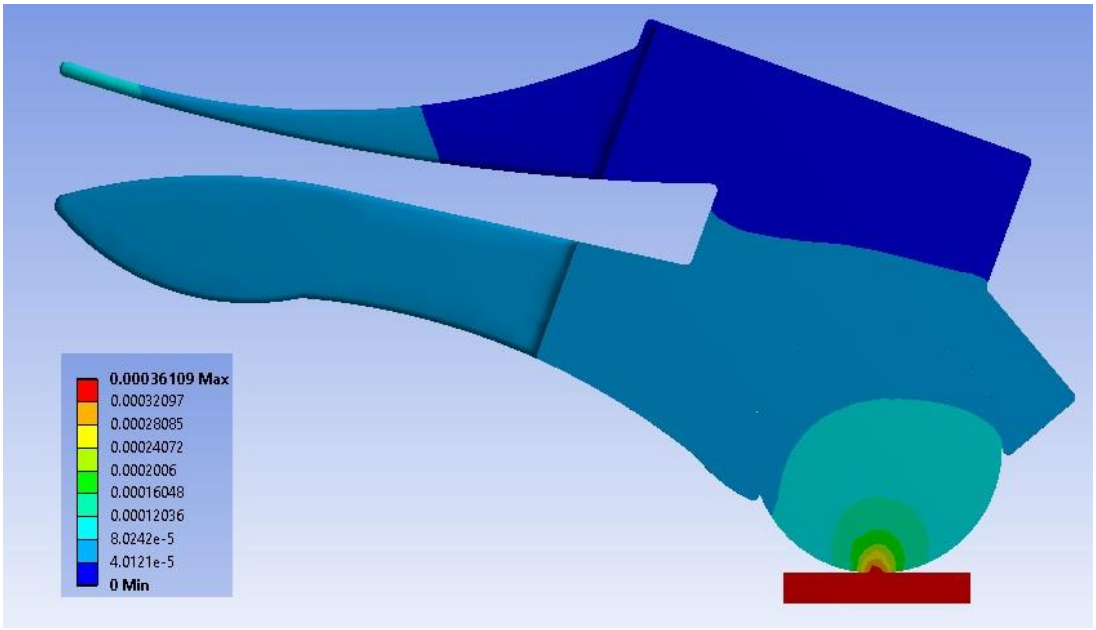

Figure 150 – The deformations observed in heel loading at an applied load of 402.5N

The largest stresses to be found in the heel-loading model were in the plate used for applying the load (see Figure 151). The stresses peaked at 4.73×10^{7}Pa while those found in the ball of the heel were no higher than 3.20×10^{7}Pa. All stresses within the foot were lower than 5.54×10^{6}Pa, approximately 15% of the yield strength of Duraform EX.

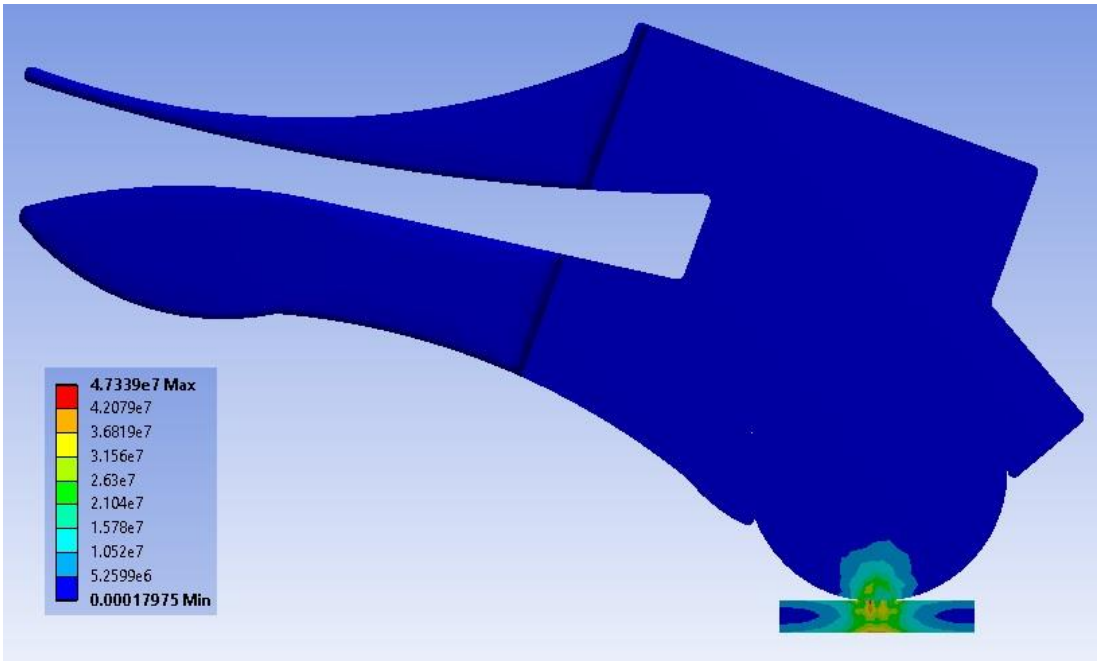

Figure 151 – The stresses observed in heel loading at an applied load of 402.5N

This was not a realistic representation of the behaviour expected of an elastomeric ball, constrained by a polypropylene keel, when loaded by a rigid steel plate. This was due to a limitation in the material properties with the rubber ball instead acting like a rigid solid and resisting the loading placed on it by the steel plate. The ball material was not characterised during the course of research and improved properties to be used in modelling were thus not available. Required for improved characterisation of the material would be uniaxial tensile testing, shear testing, biaxial testing and uniaxial compression. Further modelling of heel loading including a ball was ruled out without improved material properties.

For the purposes of evaluation this was inadequate and should be remedied by a thorough characterisation of the material to be used in the heel using the tests identified above. ISO 37 and ISO 7743 are the standards recommended to guide such testing, otherwise an external laboratory might be contracted to carry out such testing. No such testing was carried out on the balls available but is a vital part of

any further evaluation of materials to be used in the heel section of the foot in further design and is also recommended for materials to be used in the cosmesis.

B3 First design revision

Following the physical testing of the Strathclyde foot, redesign was carried out to improve on the weaknesses observed in the design.

The areas highlighted for attention in Chapter 4 were the reduction of distortion due to manufacturing effects, the width of the heel, the inclusion of a bolthole to allow connection to a pyramid adapter and the allowance for inclusion of an energy return feature.

B3.1 Distortion due to manufacturing effects

With injection moulding the wall thickness was important as uneven cooling can cause distortion of the material leading to voids and warped surfaces. These were both observed in the Strathclyde foot, particularly a clear sink line running along the centre of the top surface of the foot as well as voids within the central wall of the foot (see section 4.1.3 Thermal distortion effects)

This distortion was most likely due to the relative thickness of the central wall (7mm) compared to the top surface (2.5mm) as shown in Figure 152. To reduce the effects of this the central wall should be reduced in thickness while maintaining the strength of the foot. A set of models was created in Ansys Workbench to test the effect of reducing the central wall thickness on the current design.

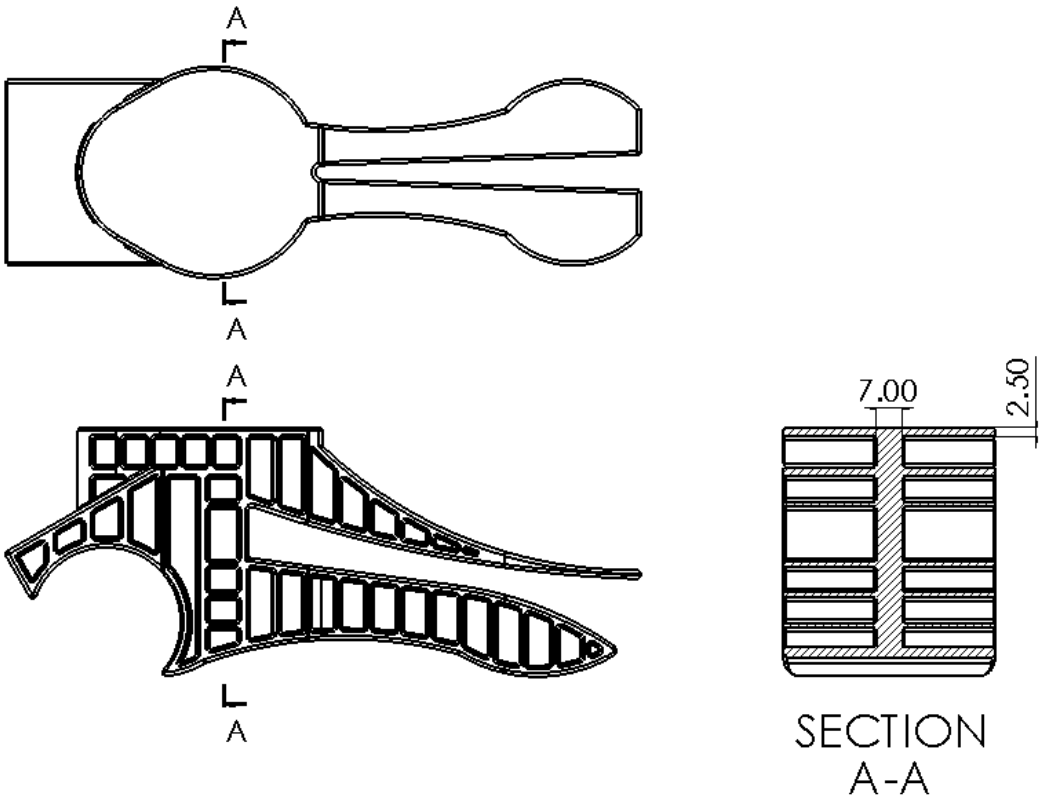

Figure 152 – Section view of the Strathclyde foot displaying the central wall

B3.1.1 Model generation

Four models were created by removing the toe section from the CAD model of the Strathclyde foot. The initial model maintained the 7mm central wall thickness with subsequent models having 5.3mm, 3.7mm and 2mm wall thicknesses.

B3.1.2 Material properties

The same material properties for polypropylene were used for all models.

The properties used for copolymer polypropylene were:

Density	915 kgm^{-3}
Young's Modulus	9 x 10^8 Pa
Poisson's ratio	0.43
Bulk Modulus*	2.143 x 10^9 Pa
Shear Modulus*	3.147 x 10^8 Pa
Tensile Yield Strength	3.5 x 10^7 Pa
Tensile Ultimate Strength	4.5 x 10^7 Pa

Table 16 – Copolymer polypropylene material properties used in FEA

B3.1.3 Boundary conditions

The top surface of each foot was a fixed surface (see Figure 153).

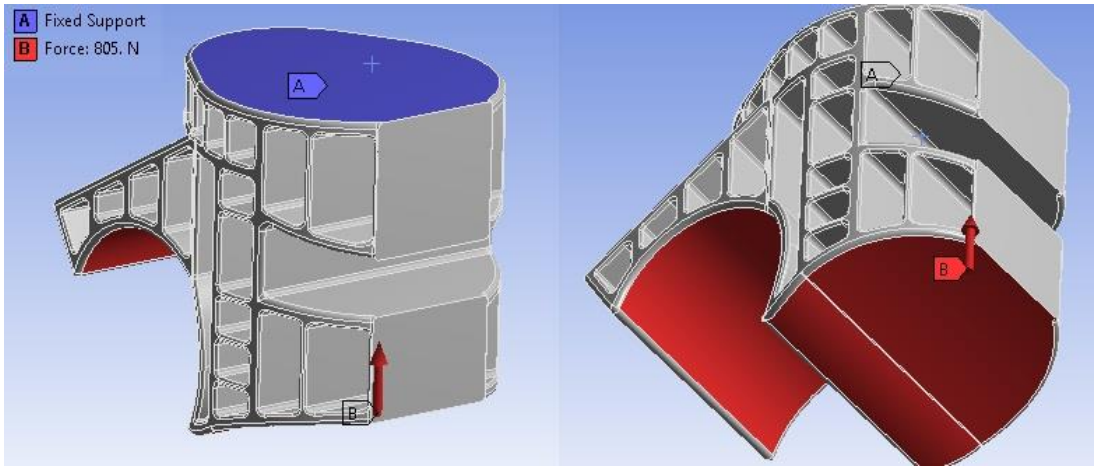

Figure 153 – Boundary conditions of the wall thickness model

B3.1.4 Mesh

The entire model was meshed using a relevance centre setting of 'coarse' with a medium smoothing and fast transition (see Figure 154).

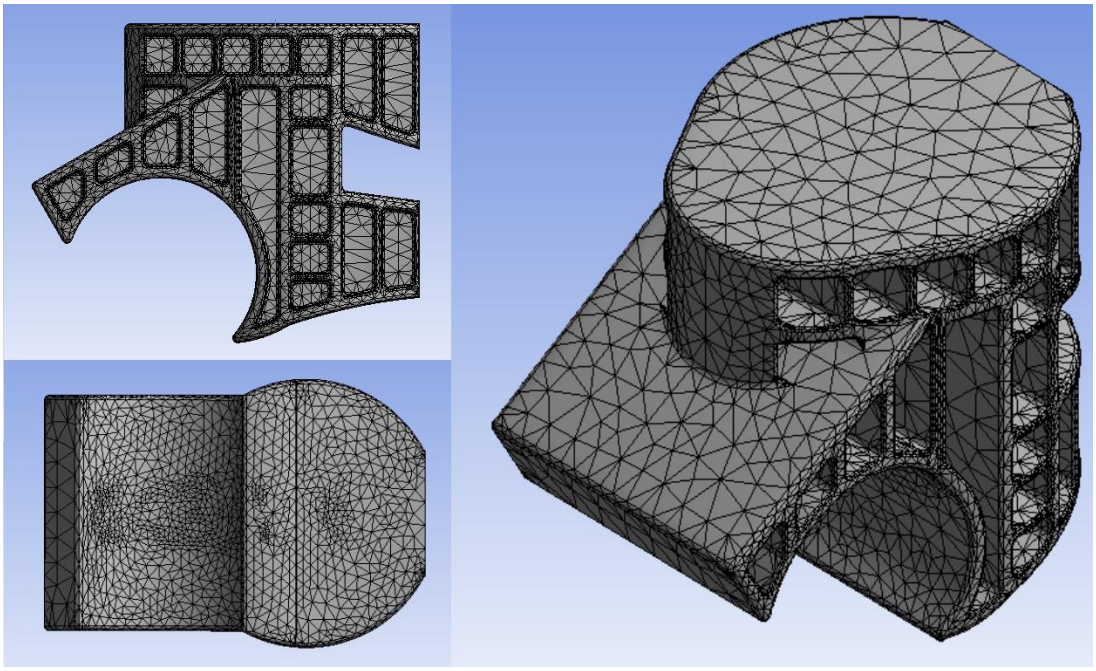

Figure 154 – Mesh of setup used to analyse Strathclyde foot wall thickness in Ansys, side, bottom and isometric (rear, right) views

B3.1.5 Loading

A distributed, ramped load was applied over the course of 9.2 seconds to a maximum value of 1610N (the static proof load for the P3 level as specified in ISO 10328) on the large bottom surfaces of the model, vertically upwards (see Figure 153). While the load was not applied in the direction specified by the standard it was felt to be a useful benchmark.

B3.1.6 Analysis settings

The model was set to run over 9.2 seconds split into 500 sub steps, this would give a loading rate of 175N/s, which is midway in the range of 100N/s to 250N/s specified in ISO 10328. Weak springs were turned off, large deflection was turned on while inertia relief was off, and the solver type left as program controlled.

The required information from the solution was total deformation, directional deformation, equivalent elastic strain and equivalent stress.

B3.1.7 Results

All wall thickness models showed the maximum stress area at either side of the vertical section at the back of the main foot block above the heel (see Figure 155). This is due to the corner present here at the edge of two fillets. In every case the value is below the tensile yield strength of the polypropylene material used ($3.5x10^7$Pa).

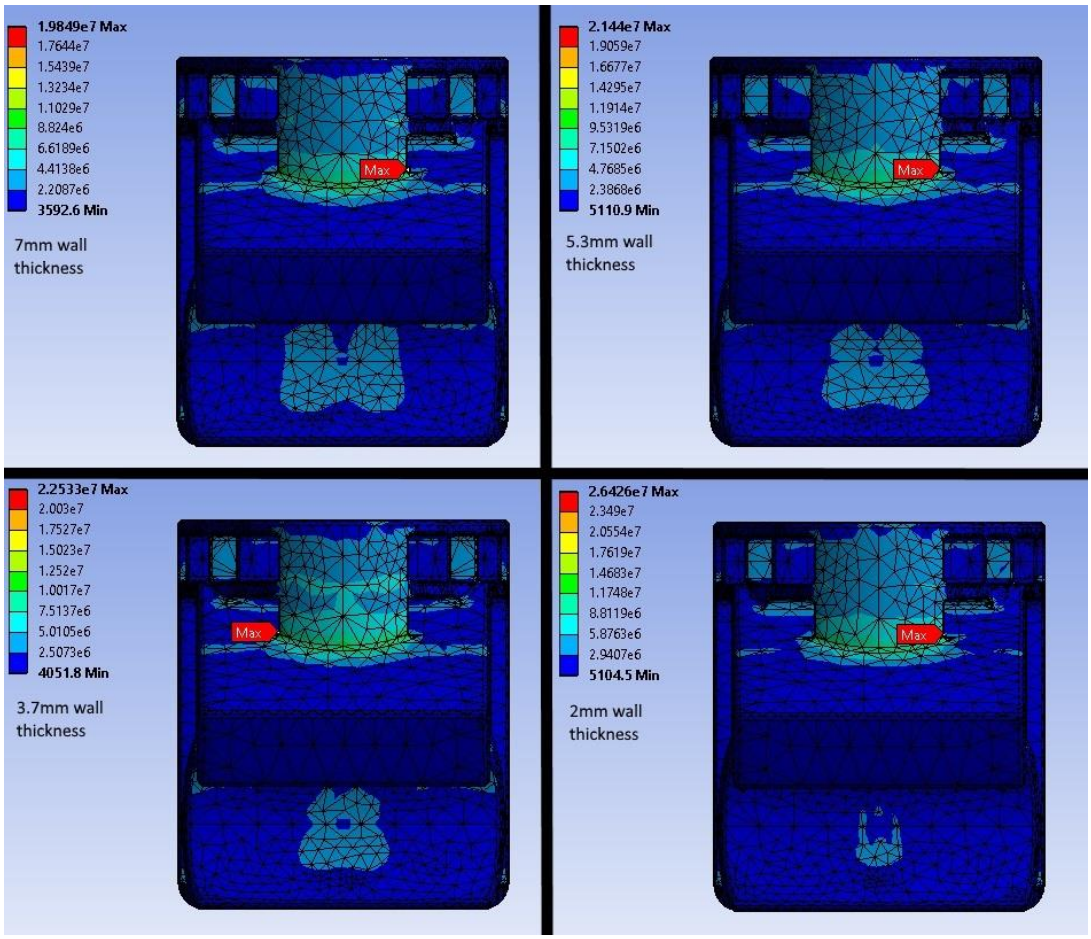

Figure 155 – Maximum stress point in all wall thickness models

The second highest stress area was at the vertical section at the back of the main foot block where it met the angled top of the heel (see Figure 156). The exact location of the highest value varied by model here however the thinner the central wall the greater the area reaching higher stresses. Even in the case of the 2mm wall

thickness model the stress did not exceed 2.64x10^{7}Pa, well below the 3.5x10^{7}Pa tensile yield strength of the material used.

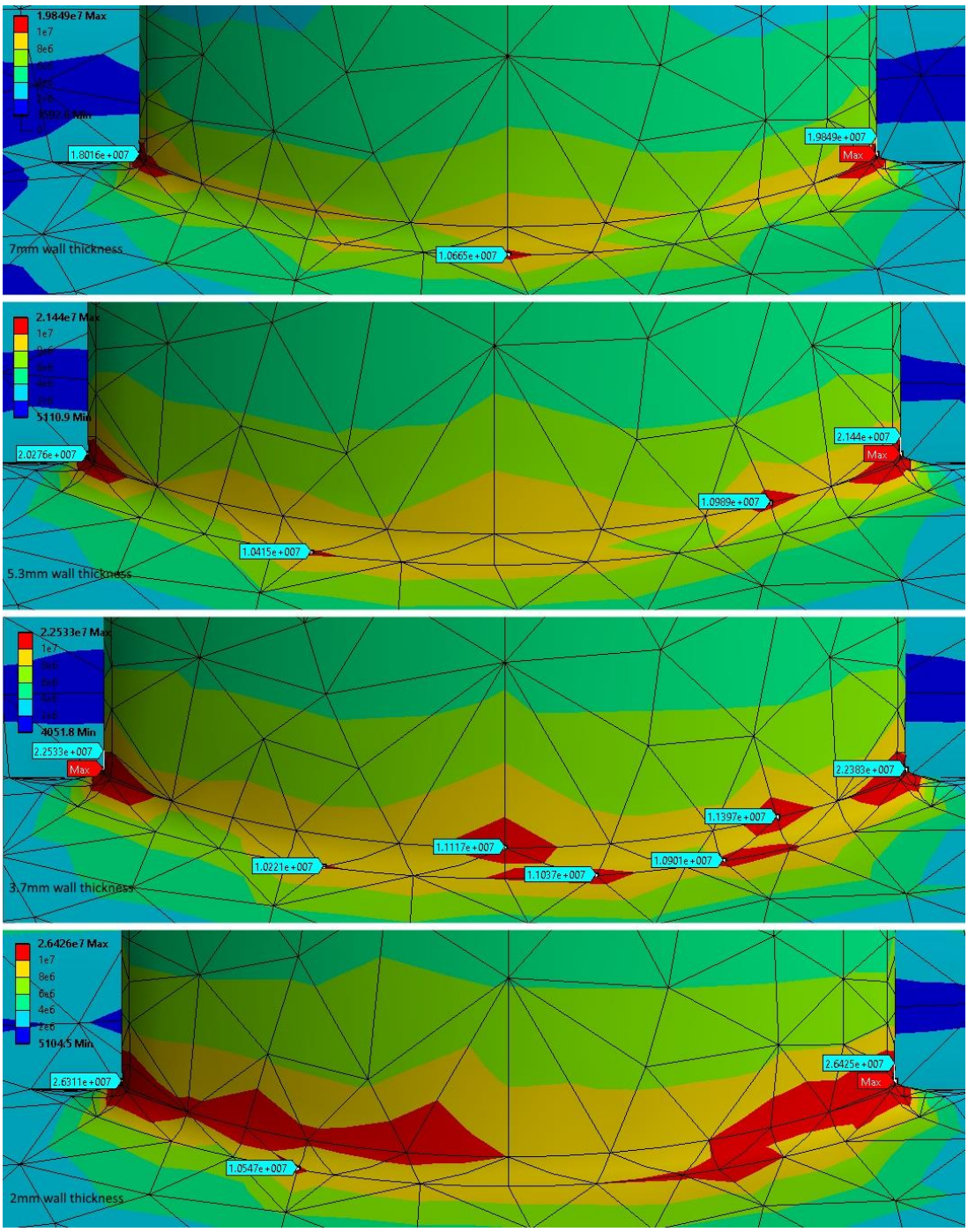

Figure 156 – Rear of vertical section showing high stress values in all models

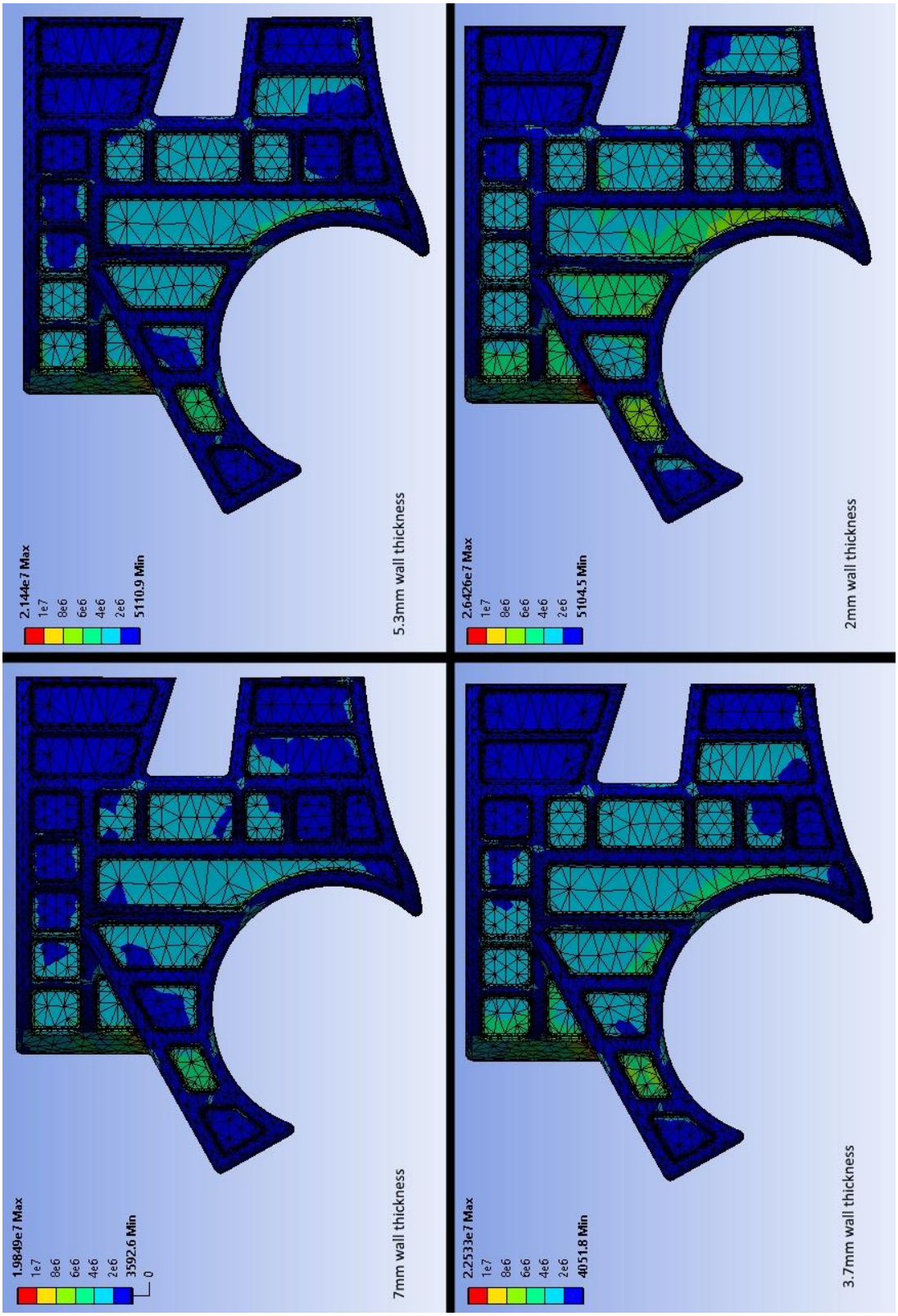

Figure 157 – Stress on central wall in each model

The stress on the central wall showed increased stress with reducing wall thickness however, the stresses are relatively low, with the 2mm wall thickness model not exceeding a maximum stress of $1.0x10^7$Pa at maximum load (see Figure 157).

B3.1.8 Discussion

The stresses in the simulations were below failure however the load applied was only 1610N, below the maximum required load of 3360-4480N at the P5 level of ultimate static loading. The load would not be applied directly to the section as shown and so was no indication of survival when tested to the ISO 10328 standard. In comparing the relative strength of different wall thicknesses, it was clear, and expected, that the thinner the wall thickness the weaker the wall. This was shown through the stress on the central wall increasing in magnitude and spread in Figure 157. The reduction in strength of the central wall caused stress to increase in other areas of the foot, such as the junction of the sloped top of the heel and the vertical section to the rear of the ankle. While the area affected increased in size, the maximum stress in this area only increased by 33.1% when reducing the thickness by 71.4% (from 7mm to 2mm) and remained far below yield stress. The stress observed at the corner at the edge of the heel/ankle junction increased from $1.98x10^7$Pa in the 7mm condition to $2.64x10^7$Pa in the 2mm condition, but again, remained below yield stress.

B3.1.9 Conclusion

The stresses in the 5.3mm, 3.7mm and 2mm wall thickness models were not considered to be too great to prohibit their use in a physical model. The weight and material savings of the 2mm wall thickness made this the preferred option going forward.

B3.2 Heel width

The Strathclyde foot had a wide, square heel, very different in form to the anatomical human foot. This shape prevented use of the Strathclyde foot in closed shoes as it would not fit. To test the effect of reducing the width of the heel three models were created, the first was the Strathclyde foot with its original heel width, the second was a tapered heel, reducing to a width of 26mm, and the third was a heel that was 26mm wide for the entire length (see Figure 158). All models used the 2mm central wall thickness.

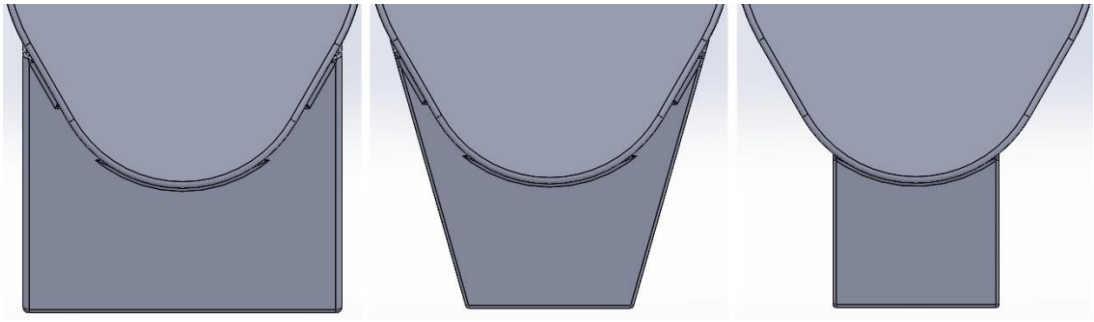

Figure 158 – Comparison of heel widths from above (L-R Original, taper and narrow designs)

B3.2.1 Material properties

The same material properties were used as for the previous models (see B3.1.2 Material properties).

B3.2.2 Boundary conditions

The top surface of each foot was fixed as in Figure 159.

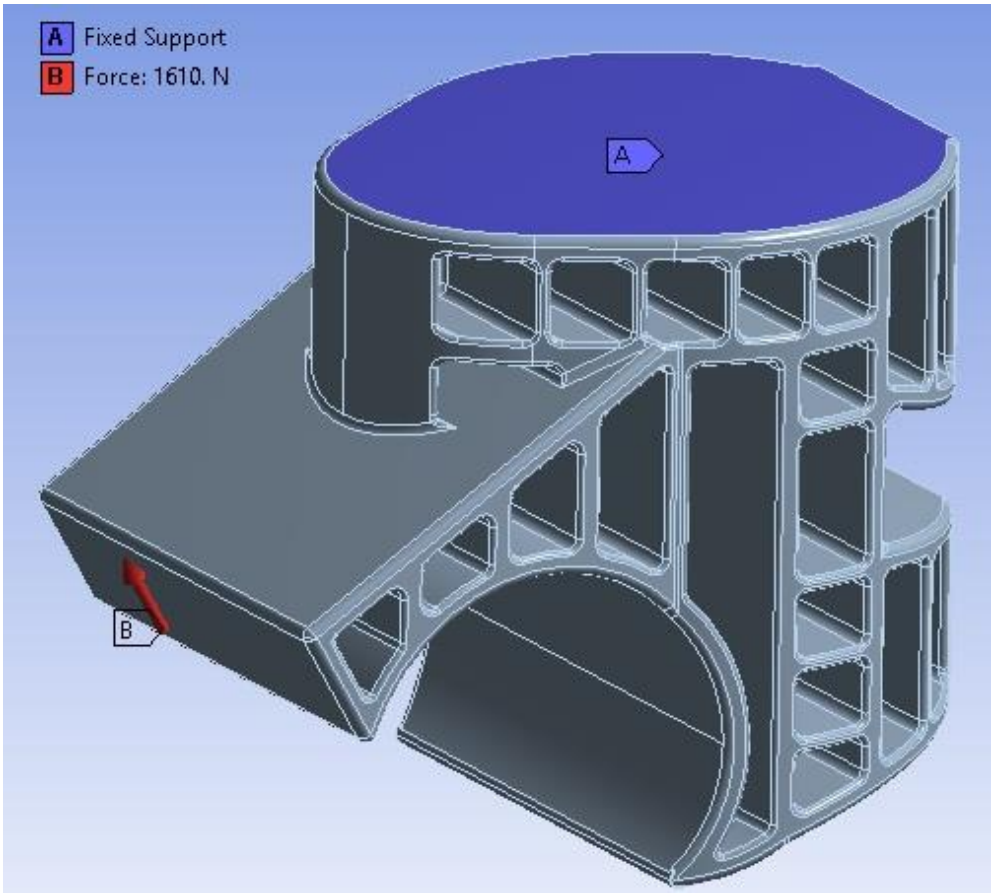

Figure 159 – Boundary conditions used in heel width models

B3.2.3 Mesh

The entire model was meshed using a relevance centre setting of ‘coarse’ with a medium smoothing and fast transition (see Figure 160).

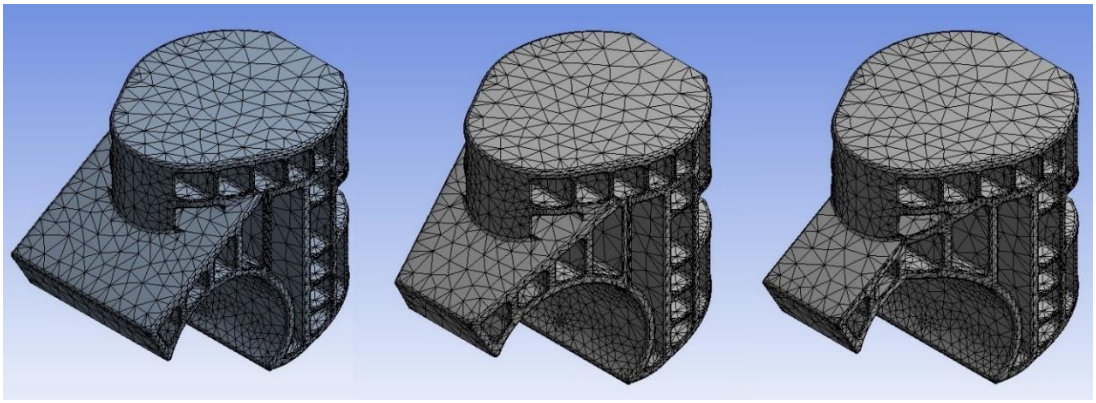

Figure 160 – Mesh of the heel width variation models

B3.2.4 Loading

A load of 1610N (the P3 static load from ISO 10328) was applied to the fillet face on the bottom of the heel section, parallel to the rear face of the heel to give an extreme loading condition for the heel (see Figure 159). This loading condition was not specified or required by ISO 10328 but was felt to be useful as a benchmark.

B3.2.5 Analysis settings

The model was set to run over 9.2 seconds split into 500 sub steps, this would give a loading rate of 175N/s, which was midway in the range of 100N/s to 250N/s specified in ISO 10328. Weak springs were turned off, large deflection was turned on while inertia relief was off, and the solver type left as program controlled.

The required information from the solution was total deformation, directional deformation, equivalent elastic strain and equivalent stress.

B3.2.6 Results

In all models the yield stress was exceeded well before the maximum load was reached. For the original heel this occurred at the top of the heel surface at the point it met the ankle block (see point 1 in Figure 161) at approximately 454N load. The same area was where the thinned model also first exceeded yield strength at 396N. The thinnest model first exceeded yield strength at 332N but at a different location (see Figure 162). Several high stress areas were identified (see Figure 161) and the step at which yield stress at that point was exceeded was noted and converted to Newtons as an indication of load at failure for each point (see Table 17).

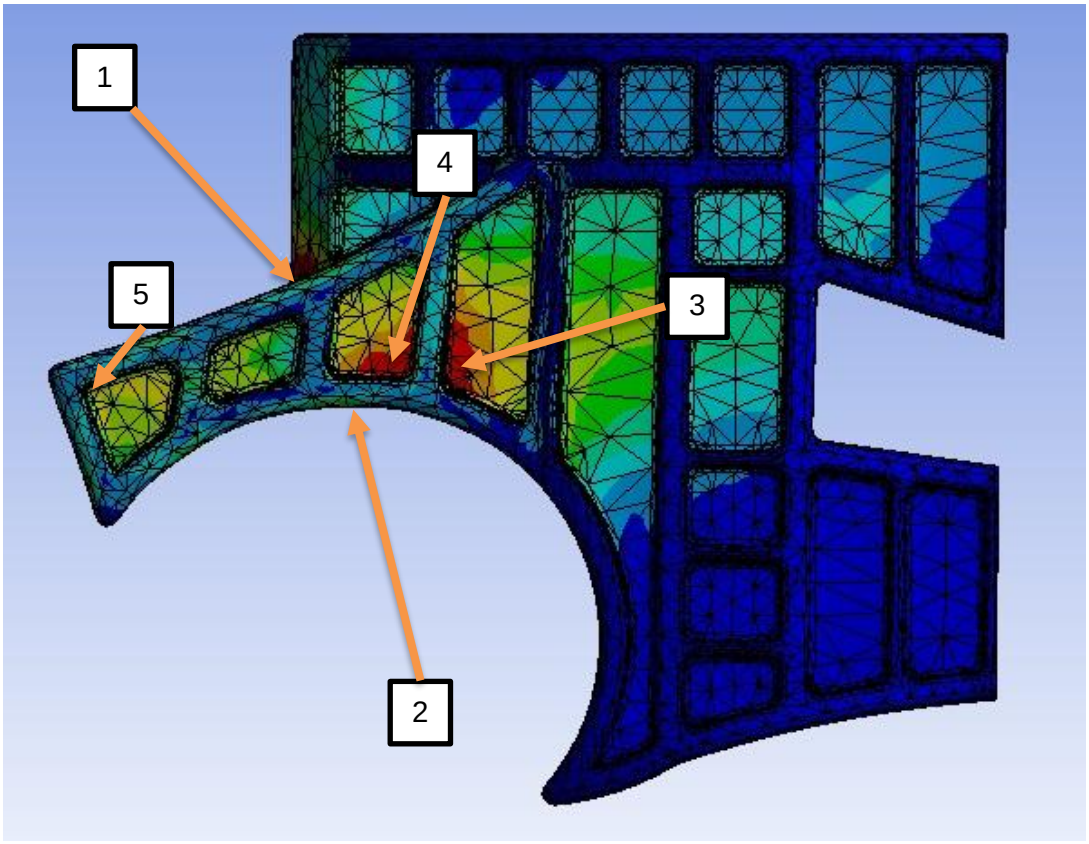

Figure 161 – High stress areas identified in heel width modification models

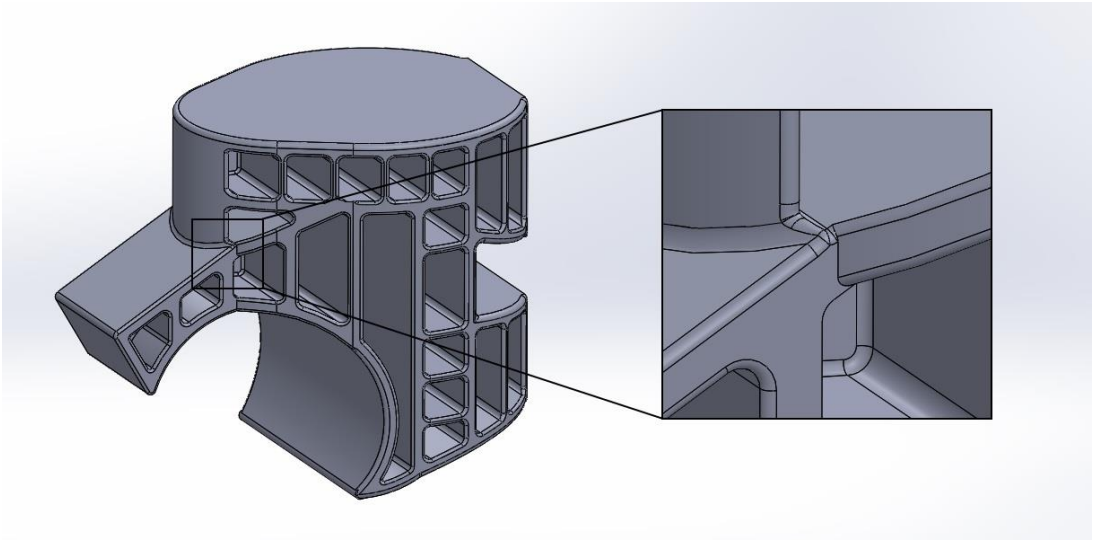

Figure 162 – Detail of the highest stress area in the thinnest heel model (point 6)

	Original heel	Thinned heel	Thinnest heel
Point			
1	454N	396N	348N
2	573N	483N	409N
3	544N	547N	499N
4	622N	580N	512N
5	725N	309N	361N
6	N/A	N/A	332N

Table 17 – The load at failure of points identified in Figure 161 and Figure 162 for each model

B3.2.7 Discussion

It was seen that generally as the width of the heel decreased the load at yield reduced. The major exception to this was that at point 5 the thinned heel had the lowest load at yield stress. This was due to the shape of the rear face of the heel changing from a constant width, as in the other models, to a trapezoid and so concentrating the load applied at the bottom edge to a smaller area towards the top surface. Figure 163 shows the rear face directly, compared to that of the other models. As the bottom edge of the heel was loaded in line with the face shown the force transferred towards the top edge. In the case of the thinned heel the top edge was less wide than the bottom edge so stress concentrated towards the corners of the top edge.

At point 3 the thinned heel showed a slightly higher load at yield than the original heel (547N compared to 544N) but this was such a small difference that it was not considered significant.

Point 6 was only present in the thinnest heel model and this was because of the solid model itself. It may be seen in Figure 162 that a group of fillets meet awkwardly

which led to the mesh forming a re-entrant corner at this point giving the high stress point observed. This was not corrected for the purposes of this model but did highlight a feature to avoid for the further design work that was carried out in this area.

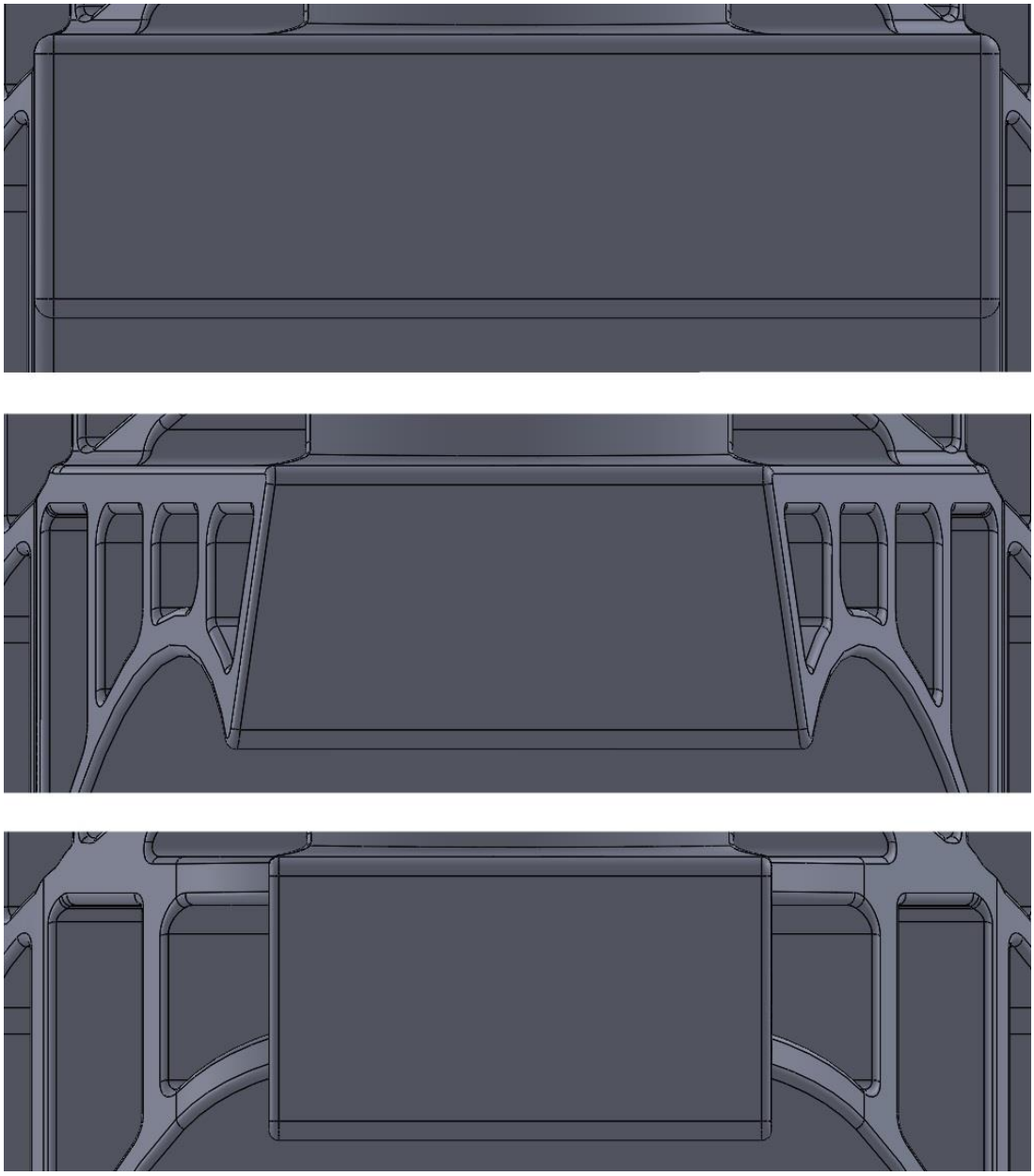

Figure 163 – Comparison of shape of rear face in each model (top – bottom, original heel, thinned heel, thinnest heel)

The stresses at point 5 were not considered to be significant for the design as they are a result of the loading method which was unlikely to occur in actual use and was not a condition of testing per ISO 10328.

The loads observed at yield were low compared to the requirements of ISO 10328 however the method of loading was very different than ISO 10328 in that the load was applied at the furthest point rearwards on the heel rather than on the complete foot rotated to 15° (simulating heel strike). The conditions of ISO 10328 would be more representative of regular use and would cause the load to be distributed through the heel section of the model.

B3.2.8 Conclusion

The low stresses observed did not indicate that the thinned heel designs were unacceptably weak, but it did indicate that they were significantly weaker than the original design in each of the identified areas (apart from point 3 for the thinned heel model, which was similar in load at yield). It was determined that further design should be carried out on the heel with a view to improving the performance of the heel section.

B3.3 Heel modification

Using the thinnest heel width, adjustments were made to the height and internal support of the heel to try and improve the performance while maintaining the narrow width. This model also included changes to the main body of the keel which were included in more detail in section B3.4 . Figure 164 to Figure 166 show the changes made between versions. Figure 164 shows the increased length of the heel due to the inclusion of the bolthole. The height of the heel section was already increased in this revision and an additional rib (initially horizontal before curving down to avoid meeting in the corner) was included in the heel. In Figure 165 the increased height of the heel section is visible in the rear face of the heel. The corners were also

curved which may have led to stress concentration as was seen in the thinned heel model in section B3.2 Heel width.

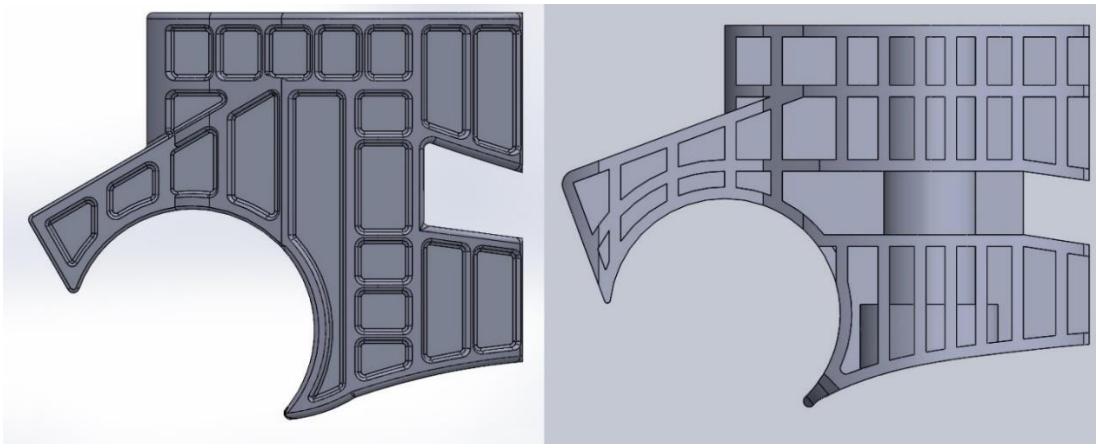

Figure 164 – Side view comparing previous design to first revision

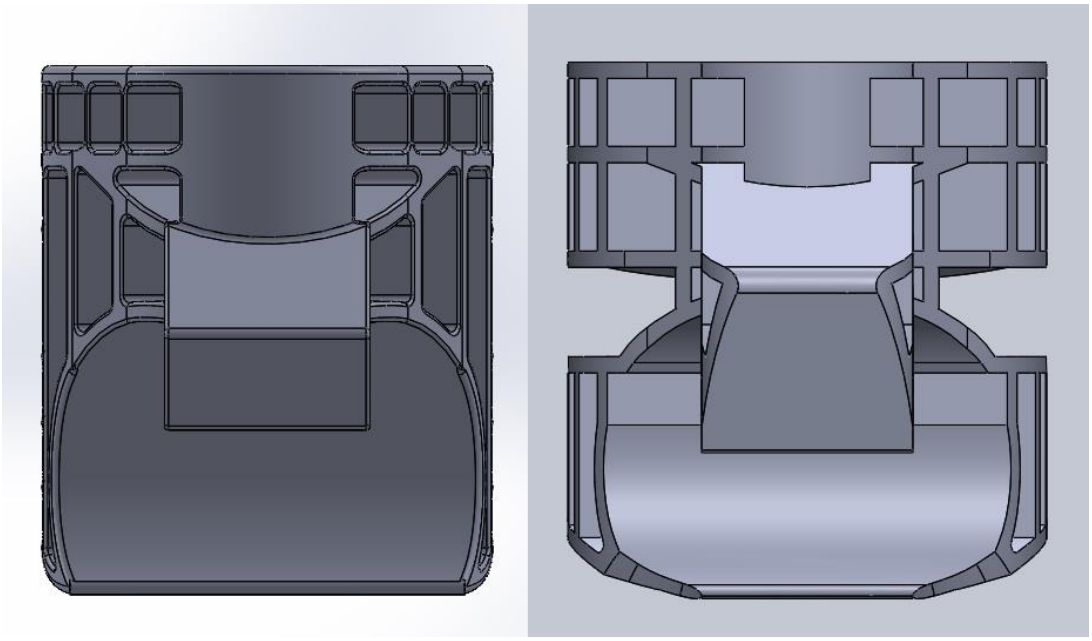

Figure 165 – Rear view comparing previous design to first revision

It may be seen in Figure 165 the omission of certain ribs to accommodate the energy return feature. The lateral stability of the keel was to be investigated as it may have been impacted by these changes and is described in section B3.4 .

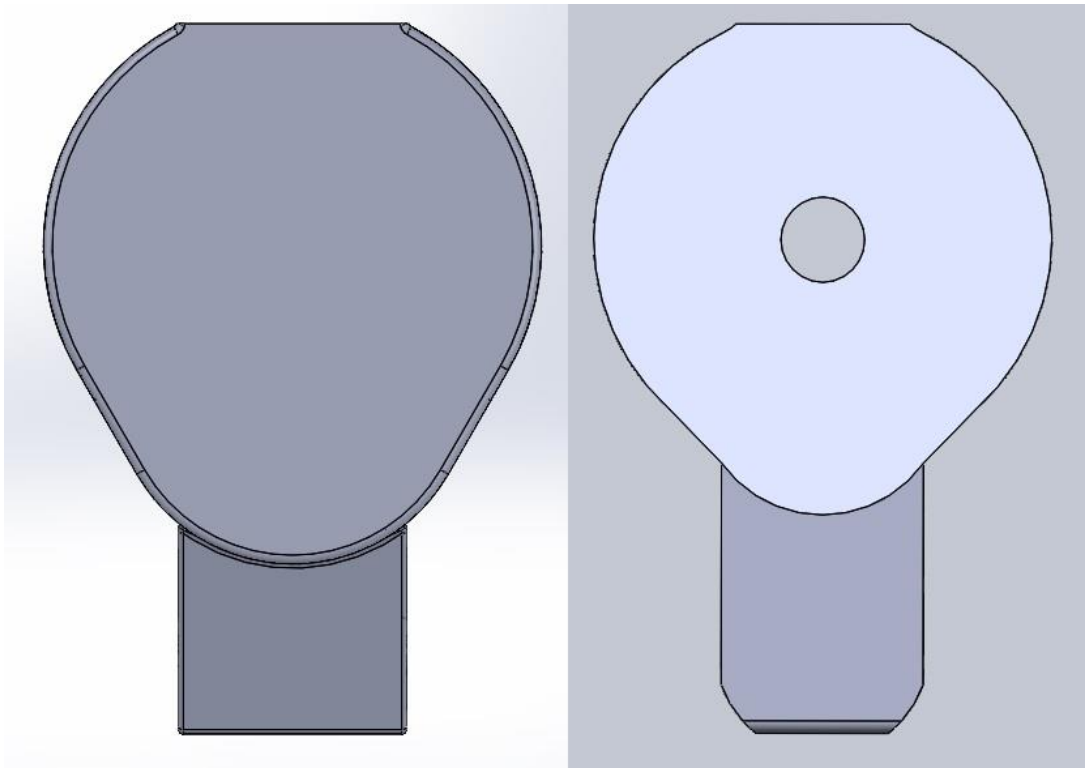

Figure 166 – Top view comparing previous design to first revision

Figure 166 shows the inclusion of the bolthole and the resulting length increase of the heel. The rounded corners at the rear of the keel are also visible. In the first design revision, most corners were not filleted. This may have led to stress concentration in some corners giving unrealistic results. It is recommended that further work could be done to evaluate the effect of filleting corners on stress readings in these models.

Two additional variations of the heel were also modelled and compared to the previous version (Figure 167). These variations include an increased heel height and altered rib support to the heel.

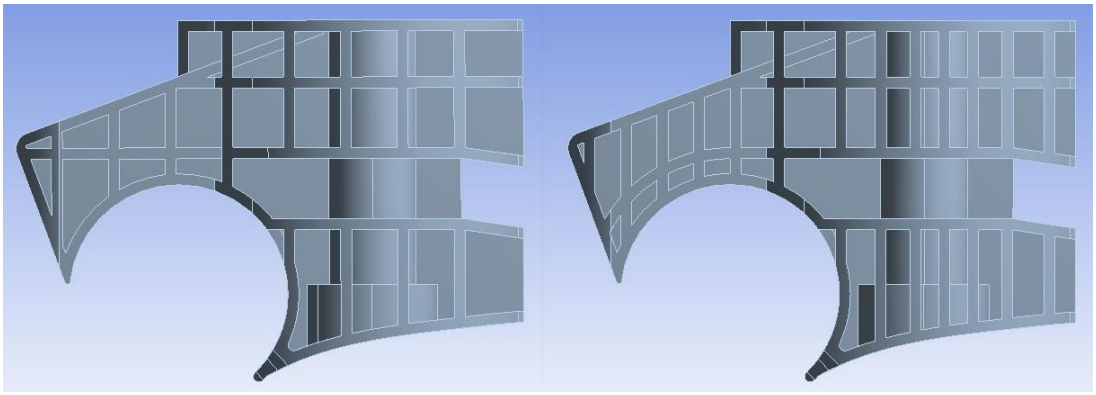

Figure 167 – Tall heel variations tested in first design revision (wide gap and narrow gap)

B3.3.1 Material properties

The same material properties were used as for the previous models (see B3.1.2 Material properties).

B3.3.2 Boundary conditions

The top surface of each foot was fixed as shown in Figure 168. Symmetry was applied to the symmetry regions shown in Figure 169.

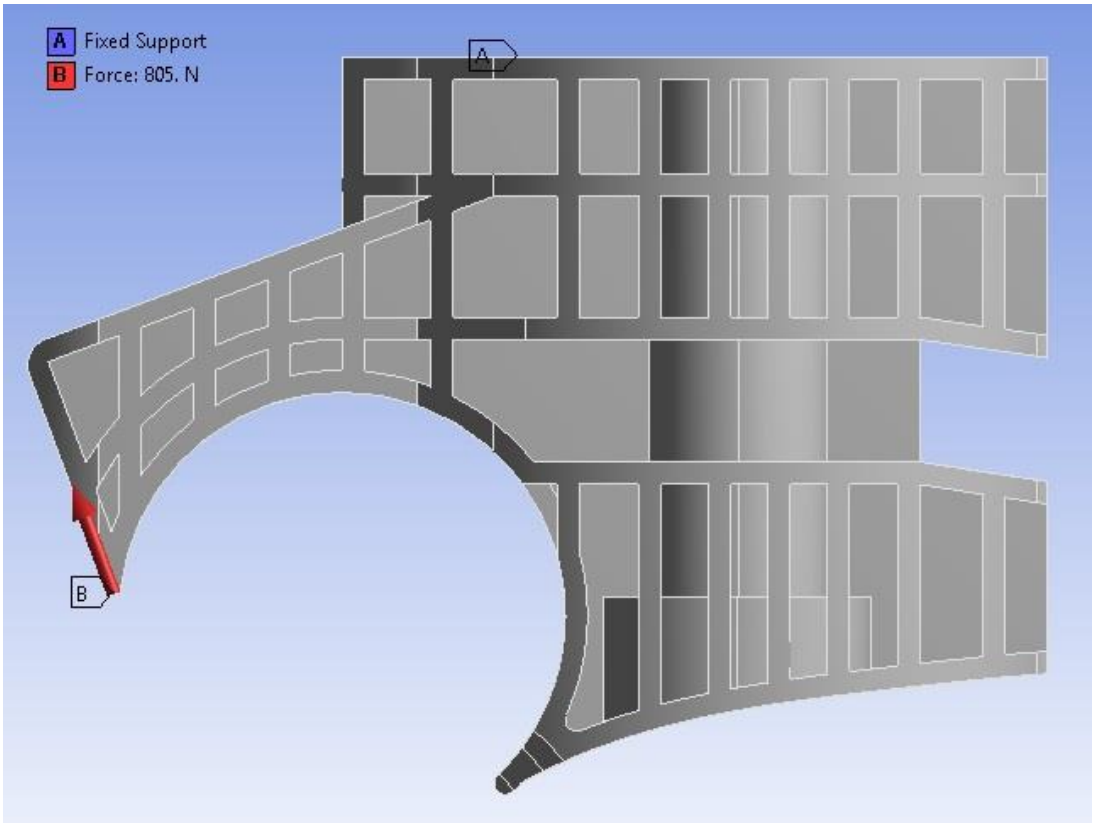

Figure 168 – Boundary conditions used in heel modification models

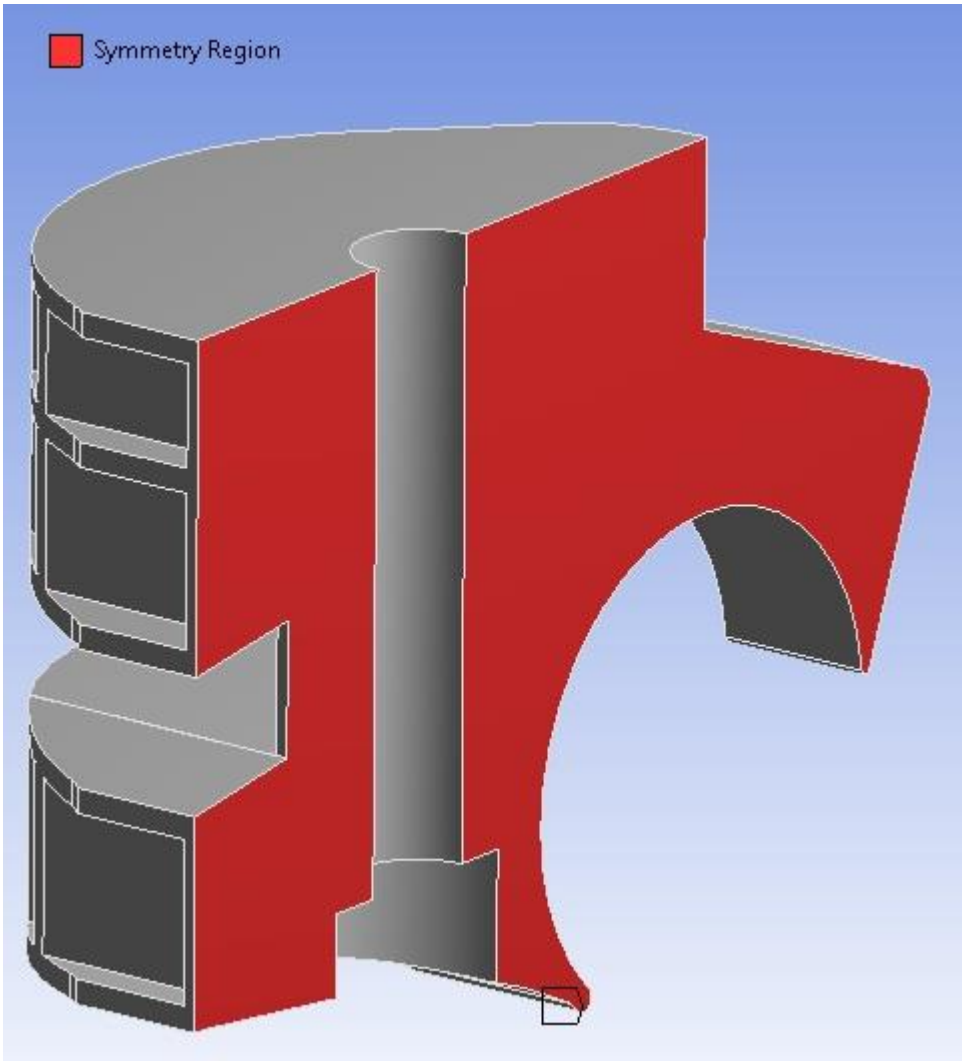

Figure 169 – Symmetry regions used in heel modification models

B3.3.3 Mesh

Each model was meshed using a relevance centre setting of ‘coarse’ with a medium smoothing and fast transition (see Figure 170 for example).

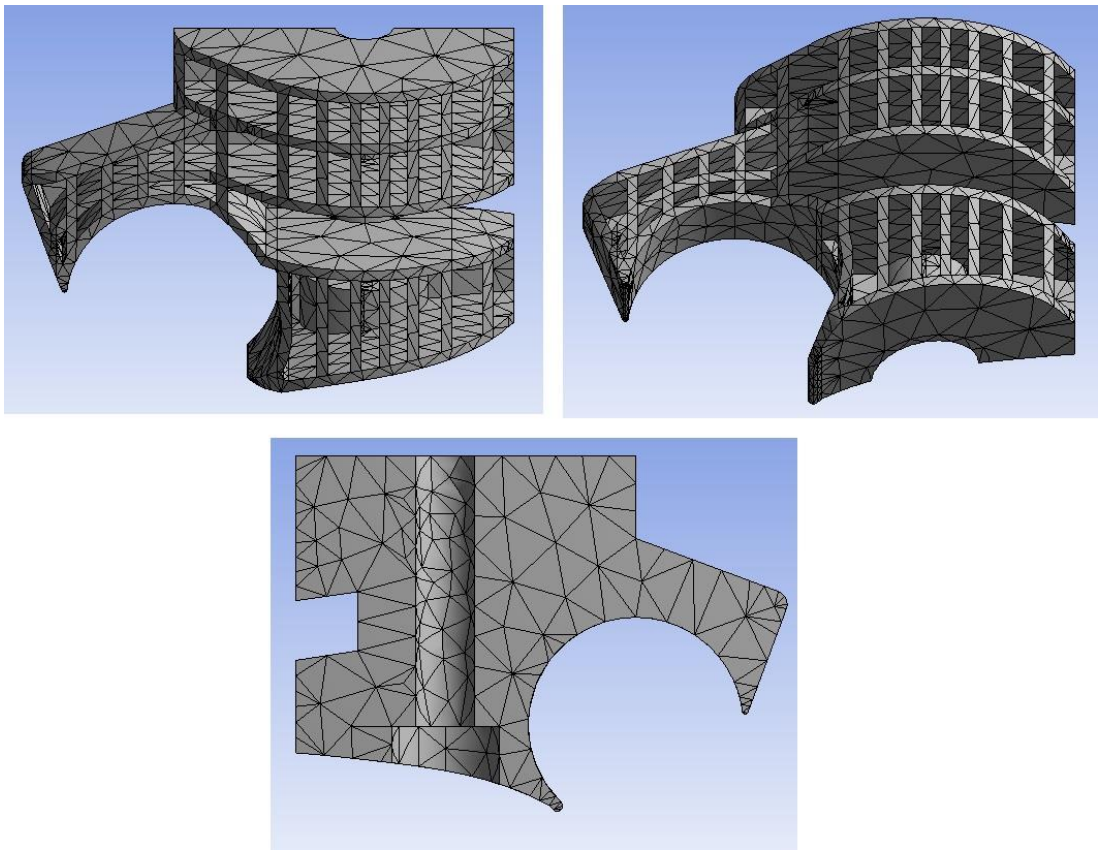

Figure 170 – Mesh of initial heel modification model

B3.3.4 Loading

A load of 805N (half of the P3 static load from ISO 10328) was applied to the fillet face on the bottom of the heel section, parallel to the rear face of the heel to give an extreme loading condition for the heel (see Figure 168). This loading condition was not specified or required by ISO 10328 but was felt to be useful as a benchmark.

B3.3.5 Analysis settings

The model was set to run over 4.6 seconds split into 250 sub steps, this gave a loading rate of 175N/s, which was midway in the range of 100N/s to 250N/s specified in ISO 10328. Weak springs were turned off, large deflection was turned on while inertia relief was off, and the solver type left as program controlled.

The required information from the solution was total deformation, directional deformation, equivalent elastic strain and equivalent stress.

B3.3.6 Results

The load results quoted for these models have been doubled to account for the model having been formed with a symmetry condition and allows direct comparison with the results from B3.2 Heel width. As in B3.2 Heel width, the models all met yield stress at loads below the maximum applied. In each case the yield stress was reached on the rear face of the heel just above where the load was applied (point 3 – see Figure 171). For the initial design this occurred at 451N, for the tall heel, wide gap model it occurred at 489N and for the tall heel, narrow gap model it occurred at 586N. There was not an equivalent point recorded in the models from B3.2 Heel width. Points 1 and were equivalent to points 1 and 2 from B3.2 Heel width and may be directly compared. Point 4 was the highest loaded of points at yield stress for the initial design and tall heel, wide gap however for the tall heel, narrow gap model point 4 was the second to reach yield stress (see Table 18).

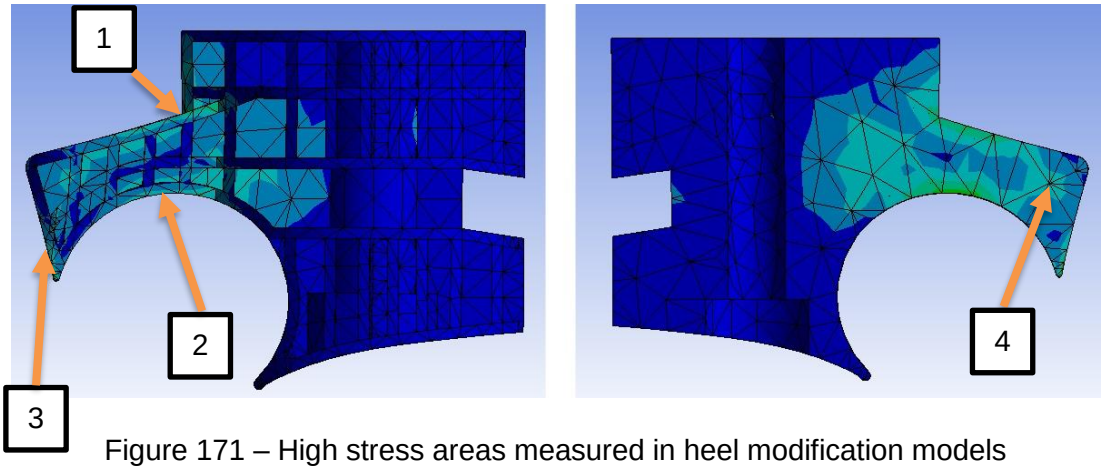

Figure 171 – High stress areas measured in heel modification models

	Thinnest heel (from B3.2 Heel width)	Original heel (from B3.2 Heel width)	Initial redesign	Tall heel, wide gaps	Tall heel, narrow gaps
Point					
1	348N	454N	573N	760N	889N
2	409N	573N	541N	818N	915N
3	N/A	N/A	451N	489N	586N
4	N/A	N/A	773N	844N	811N

Table 18 – The load at failure of points indicated in Figure 171 for select models

All models showed improvement over the thinnest heel model from B3.2 Heel width in the two comparable areas with both increased heel height models requiring more than twice the load of the thinnest heel model to reach yield stress at both points. Both increased heel height models showed greater loading to yield stress at all points than the initial redesign model however at all points except point 4 the tall heel, narrow gap model outperformed the tall heel, wide gap model. When compared to the original heel design from the Strathclyde foot both tall heel designs showed increased load at yield stress at the two comparable points.

B3.3.7 Discussion

The high stresses observed at point 3 were likely a result of loading conditions in the models and were not considered to be important for this analysis. The loading conditions encountered in use would not be expected to be as extreme as those imposed here so the stresses would be unlikely to form.

The two tall heel models performed better than the original heel and thinnest heel examined in section B3.2 Heel width, which was likely to do with the increased height of the section causing an increase in second moment of area and subsequently the stiffness of the heel. This increased stiffness of the heel would

increase the overall stiffness of the heel in use and would increase the emphasis on appropriate material choice for the heel ball to achieve the desired performance.

The tall heel, narrow gap model showed improved performance over the tall heel, wide gap model at points 1, 2 and 3 due to the additional supports present in the heel. The curved support in the heel would resist bending of the heel section better than the horizontal support in the tall heel, wide gap model and the increased number of supports would also have improved the stiffness of the heel, reducing the bending and so reducing the stresses generated. The changed pattern of support in the heel was also likely to be the reason for the wide gap model having a higher load at yield stress at point 4 than the narrow gap model however, the difference was not large and given the improved performance of the narrow gap model it was decided that the narrow gap model was the appropriate design to continue with.

B3.3.8 Conclusion

The tall heel, narrow gap model showed the best results overall from this round of models and a large improvement over even the original design in comparable areas of high stress. The heel modifications were sufficient for this round of design improvement.

B3.4 Vertical loading of keel

The bolthole and allowance for an energy return feature considerably altered the design of the main ankle section of the keel. To evaluate the changes models were run of the existing Strathclyde foot and the redesign.

B3.4.1 Material properties

The same material properties were used as for the previous models (see B3.1.2 Material properties).

B3.4.2 Boundary conditions

See Figure 172 and Figure 173 for the initial boundary conditions of either model.

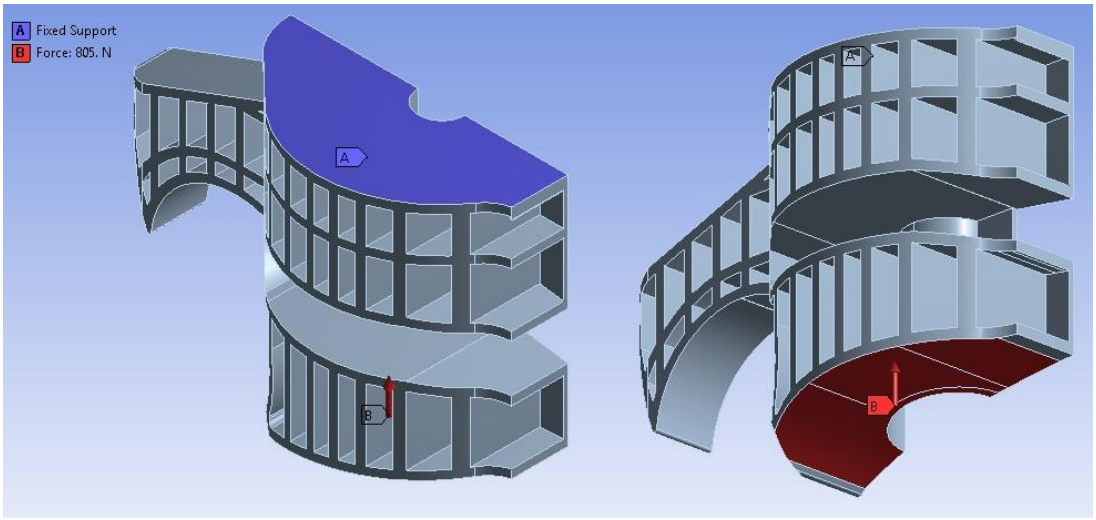

Figure 172 – Boundary conditions of main block loading (revision model)

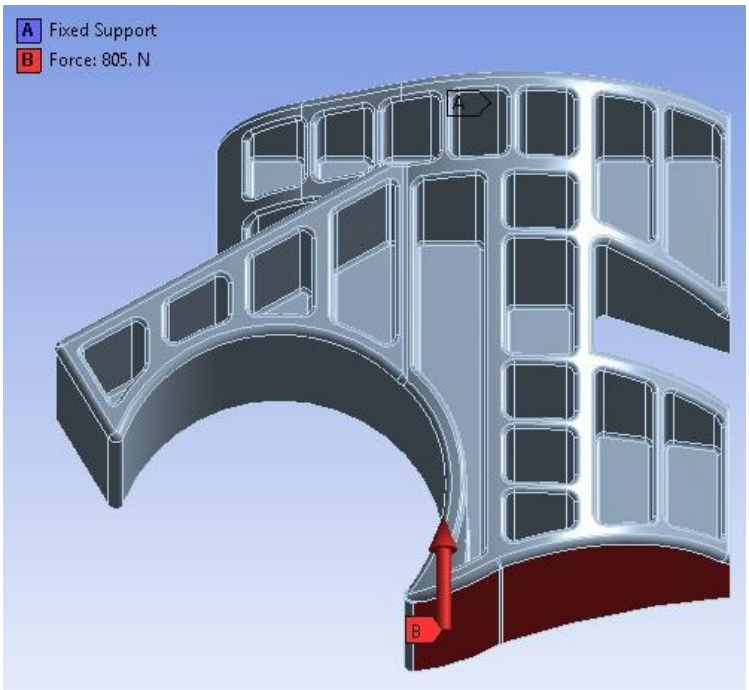

Figure 173 – Boundary conditions of main block loading (existing Strathclyde model)

B3.4.3 Mesh

Each model was meshed using a relevance centre setting of ‘coarse’ with a medium smoothing and fast transition (see Figure 174 and Figure 175).

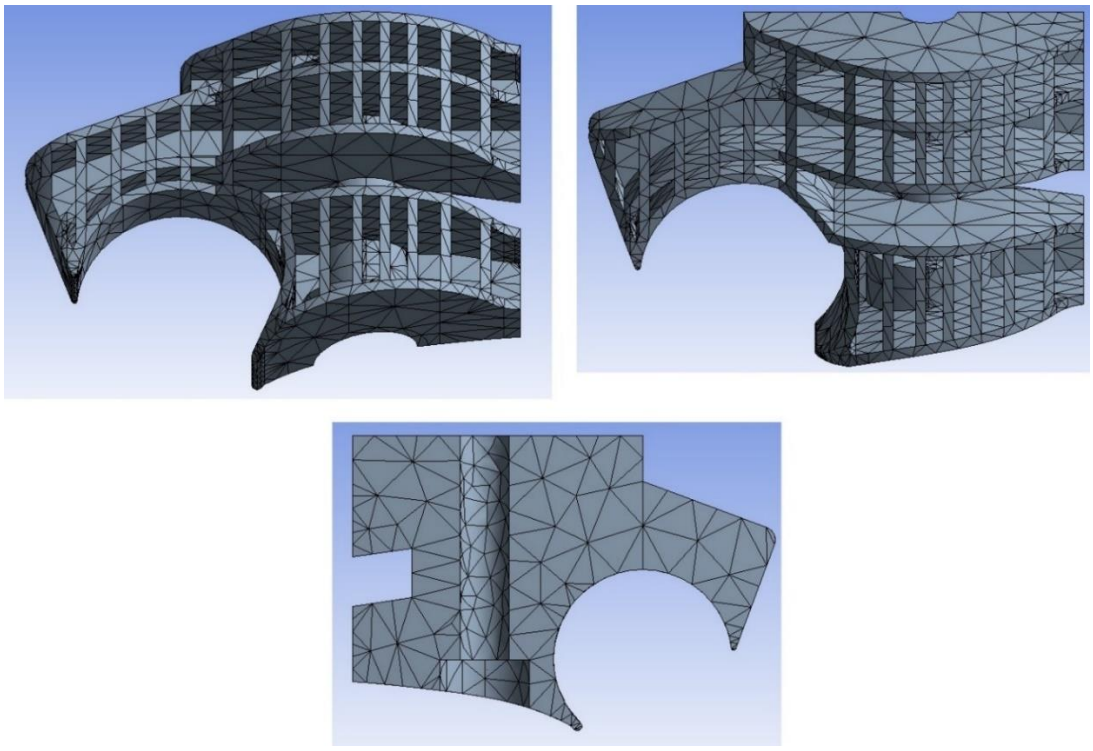

Figure 174 – Mesh used for main block loading (revision model)

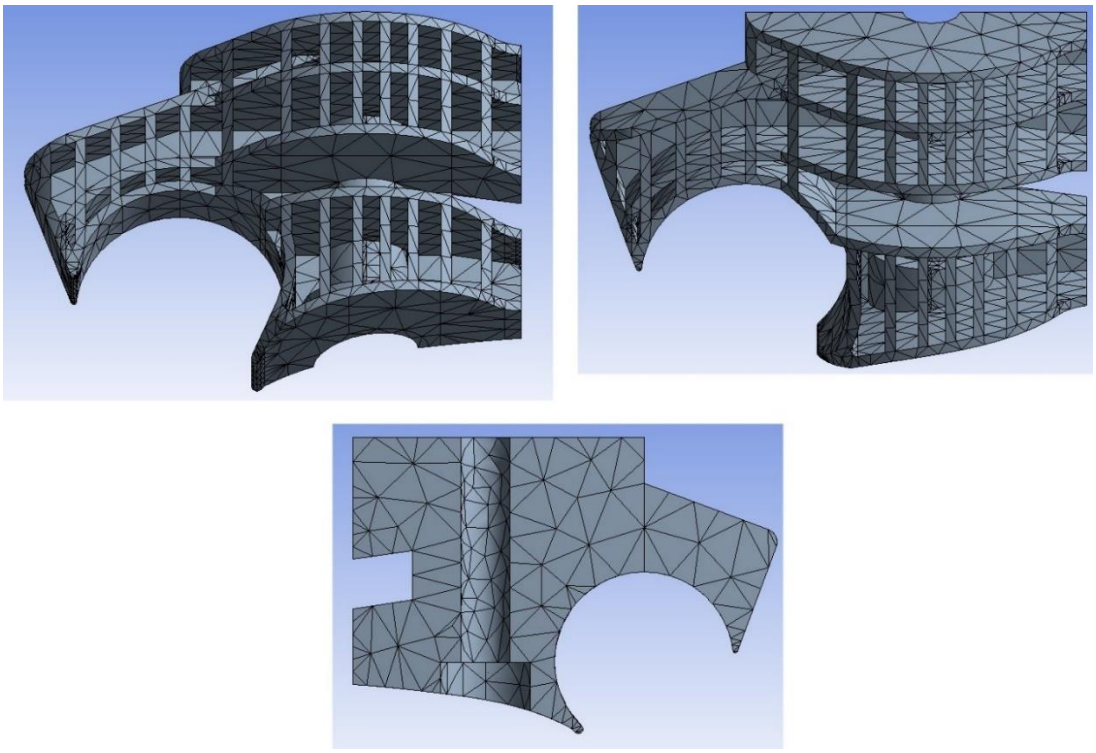

Figure 175 – Mesh used for main block loading (existing Strathclyde model)

B3.4.4 Loading

A load of 805N (half of the P3 static load from ISO 10328) was applied to the faces on the bottom of the mid-section of the keel, vertically upwards (see Figure 172). This loading condition was not specified or required by ISO 10328 but was felt to be useful as a benchmark.

B3.4.5 Analysis settings

The model was set to run over 4.6 seconds split into 250 sub steps, this would give a loading rate of 175N/s, which was midway in the range of 100N/s to 250N/s specified in ISO 10328. Weak springs were turned off, large deflection was turned on while inertia relief was off, and the solver type left as program controlled.

The required information from the solution was total deformation, directional deformation, equivalent elastic strain and equivalent stress.

B3.4.6 Results

The results observed for the two models was very different. In the case of the existing Strathclyde design several points of higher stress were observed although the highest was only $1.23x10^7$Pa at the maximum 1610N load (see Figure 176), which is far below the $3.5x10^7$Pa yield strength of the copolymer polypropylene used.

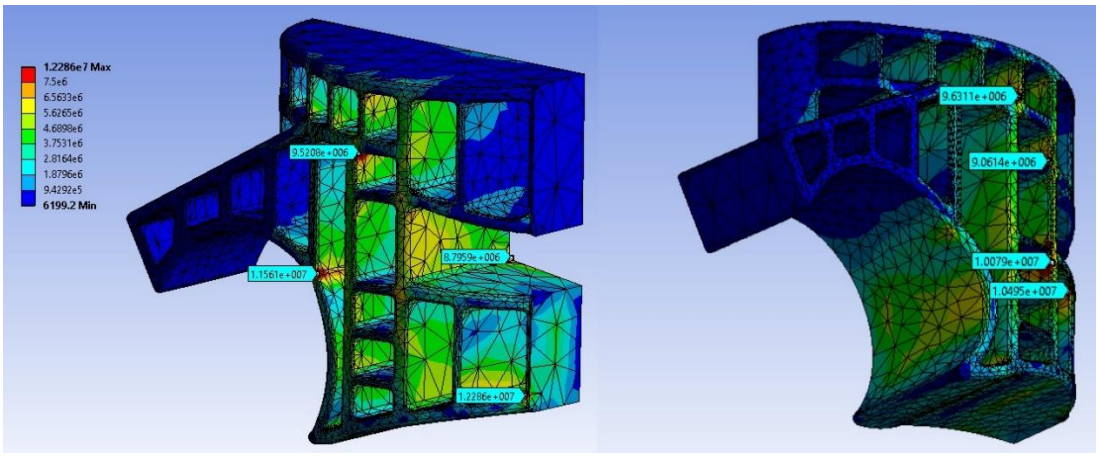

Figure 176 – Result from main block loading of existing Strathclyde model (custom scale for emphasis)

In the case of the revision design a single high stress point was observed, only exceeding the yield stress at 1610N load. This was by far the highest stress point in the model as highlighted in Figure 177 by the custom scale used.

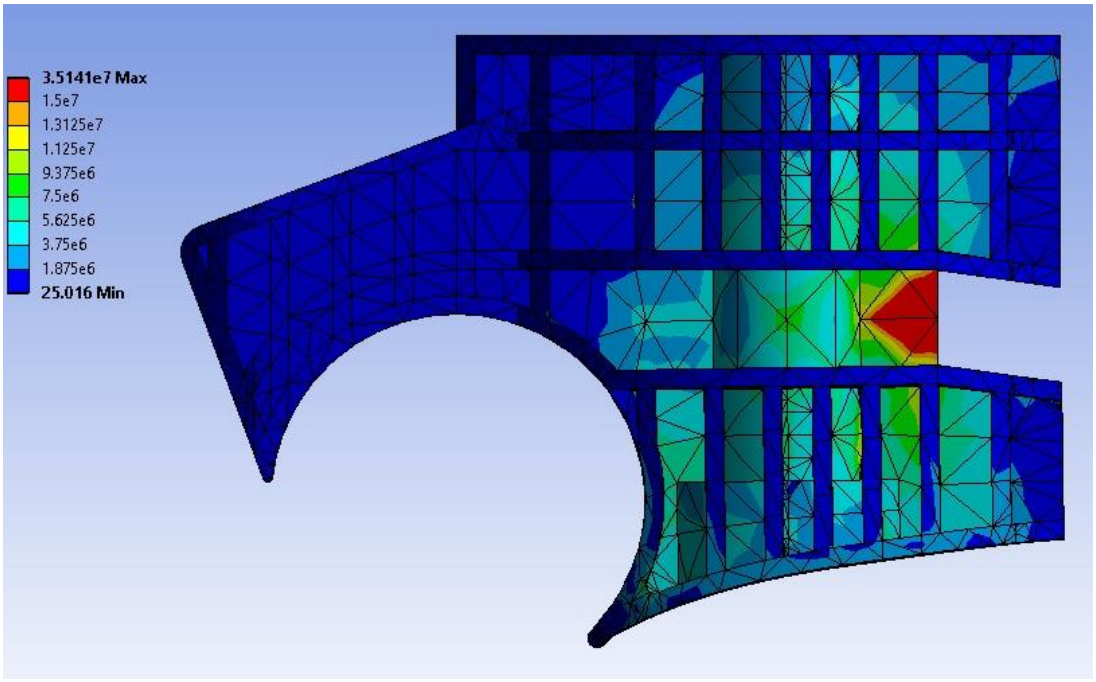

Figure 177 – Result from main block loading of revision design (custom scale for emphasis)

B3.4.7 Discussion

The high stress points observed in the existing Strathclyde model were likely to be a result of the meshing involved with corners causing stress peaks at these points. The results were just above the yield stress however, so in loading a physical model to 1610N failure would be possible.

For the revision model the stress was concentrated at a single area, the foremost vertical support in the centreline of the keel. This was not a surprise as the load was applied across an area that extended in front of the forward edge of the support and the forward edge of the model did deform to a greater extent than the rear, leading to bending of the model and the high stresses observed (see Figure 178).

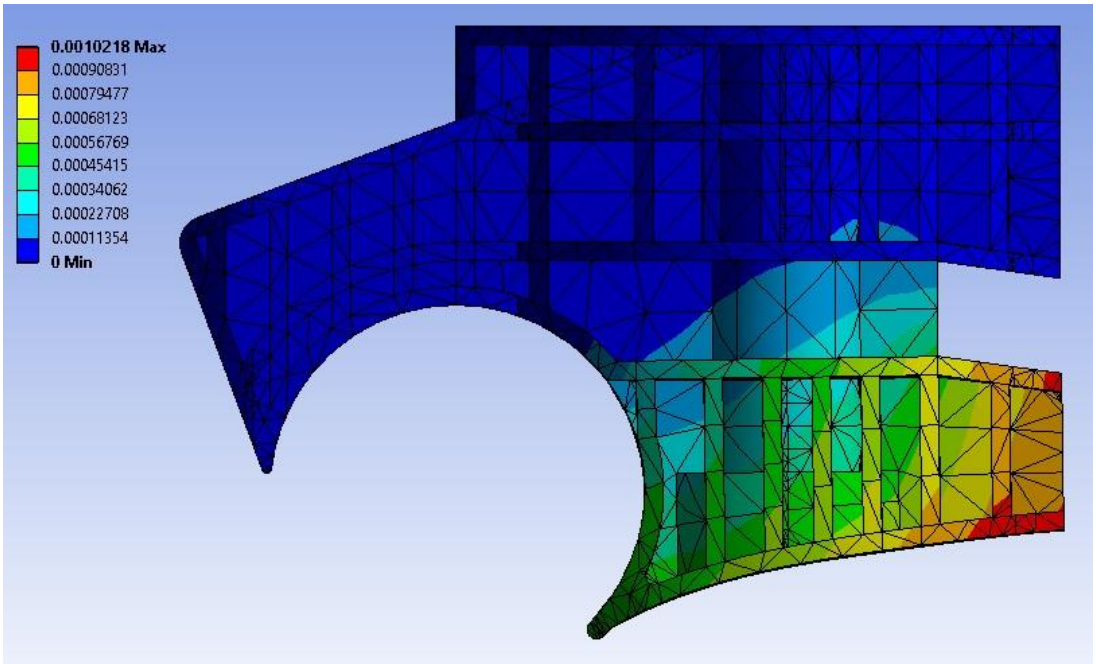

Figure 178 – Deformation of revision model at maximum load (values in m)

B3.4.8 Conclusion

The differences between the two models did show that the revision block had been significantly weakened by the removal of the material in the middle section to allow the inclusion of an energy return feature. Further development of this area was required in the next revision of the design however, further FEA modelling was carried out on this section to determine the effect on lateral strength.

B3.5 Vertical edge loading of keel

The gap in the midsection of the redesign would have increased susceptibility to rolling laterally so edge loading was used to determine the extent with reference to the existing Strathclyde foot.

B3.5.1 Material properties

The same material properties were used as for the previous models (see B3.1.2 Material properties).

B3.5.2 Boundary conditions

See Figure 179 and Figure 180 for the initial boundary conditions of either model.

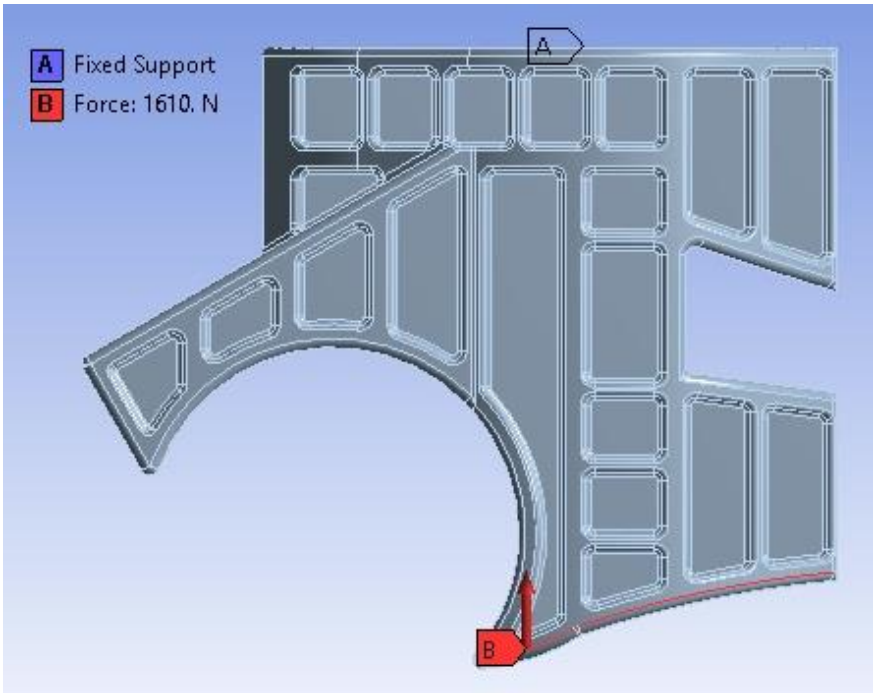

Figure 179 – Boundary conditions of edge loading model for existing Strathclyde foot

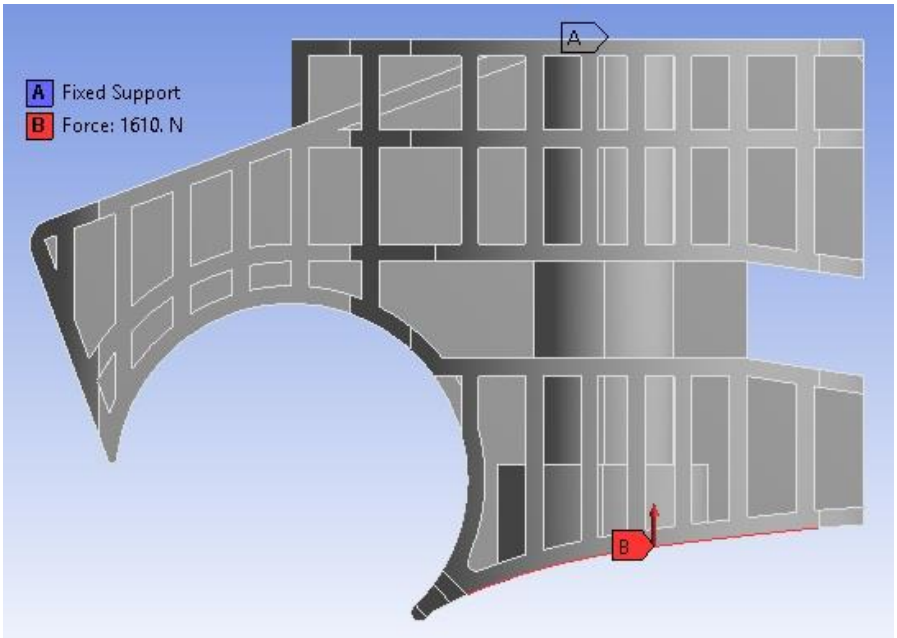

Figure 180 – Boundary conditions of edge loading model for revision design

B3.5.3 Mesh

Each model was meshed using a relevance centre setting of ‘coarse’ with a medium smoothing and fast transition (see Figure 182).

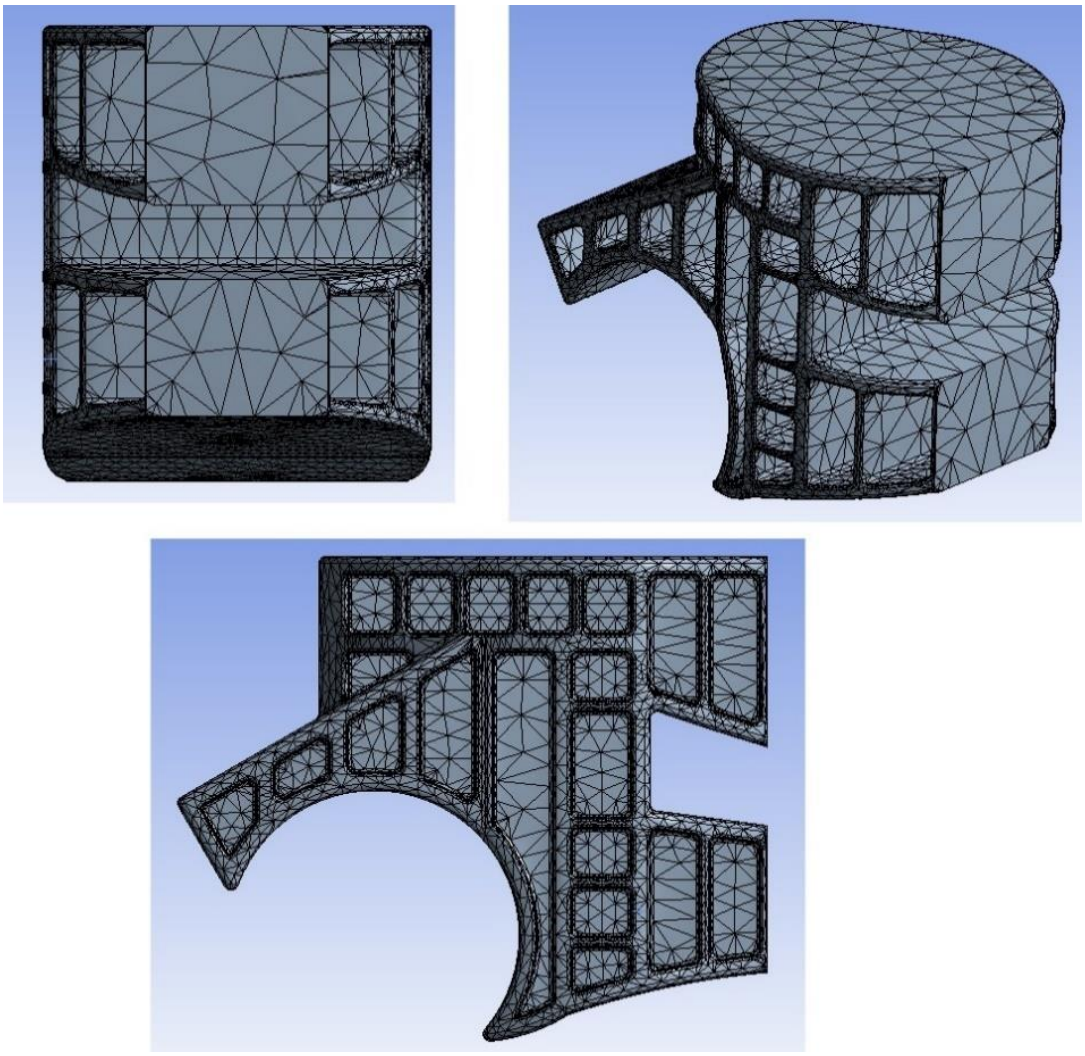

Figure 181 – Mesh used for edge loading model for existing Strathclyde foot

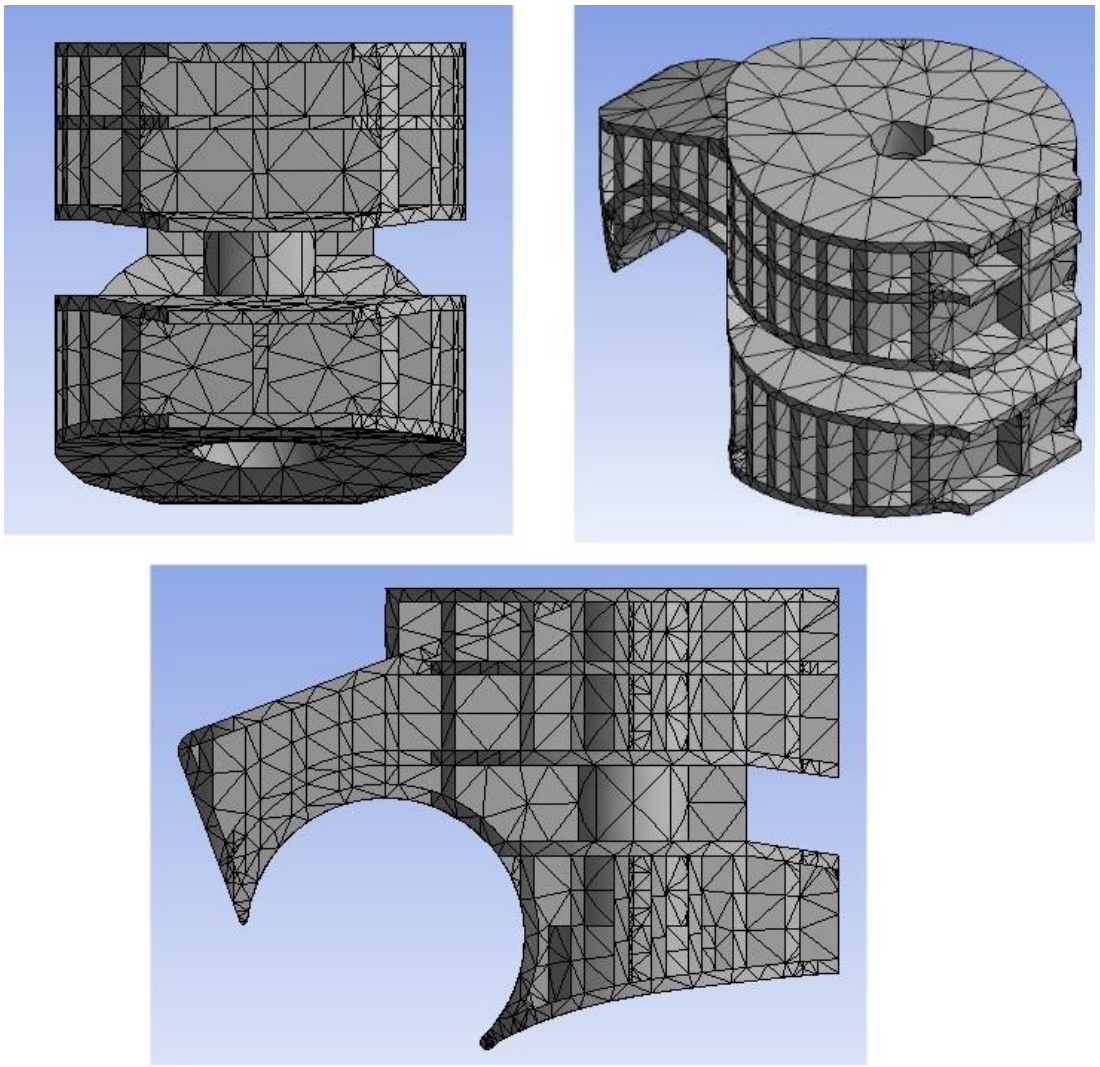

Figure 182 – Mesh used for edge loading model for revision design

B3.5.4 Loading

A load of 1610N (the P3 static load from ISO 10328) was applied to the edges on the side of the mid-section of the keel at the bottom, vertically upwards (see Figure 179 and Figure 180). This loading condition was not specified or required by ISO 10328 but was felt to be useful as a benchmark.

B3.5.5 Analysis settings

Each model was set to run over 9.2 seconds split into 500 sub steps, this would give a loading rate of 175N/s, which is midway in the range of 100N/s to 250N/s

specified in ISO 10328. Weak springs were turned off, large deflection was turned on while inertia relief was off, and the solver type left as program controlled.

The required information from the solution was total deformation, directional deformation, equivalent elastic strain and equivalent stress.

B3.5.6 Results

The existing Strathclyde design reached a maximum deformation of approximately 4mm at 1610N load (see Figure 183). This occurred in a section of the model that was directly loaded and buckled. Flexing of the lower surface where load was applied was observed. No significant deformation of the model was seen in areas away from where the load was applied.

The high stresses found in the model were concentrated around the area where load was applied (see Figure 184). The point marked ‘1’ in Figure 184 was the first to reach yield stress at a load of 235.1N. Other corners between the lower surface and the vertical ribs soon followed in reaching yield stress.

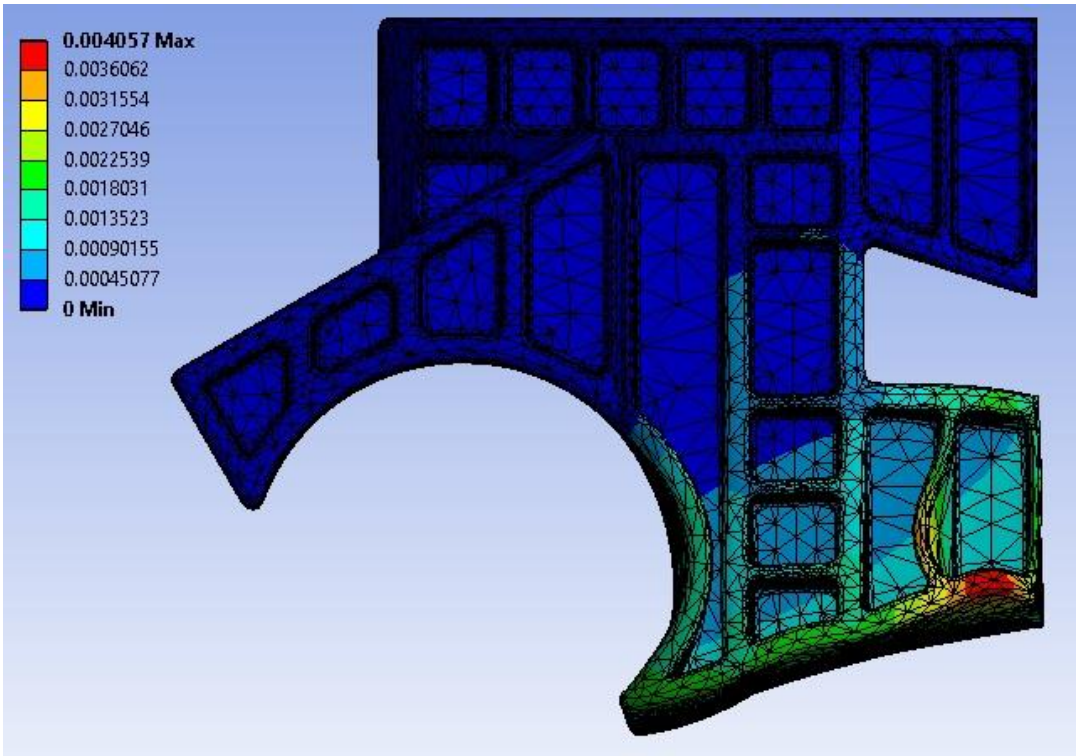

Figure 183 – Maximum deformation of the existing Strathclyde foot design at 1610N edge load

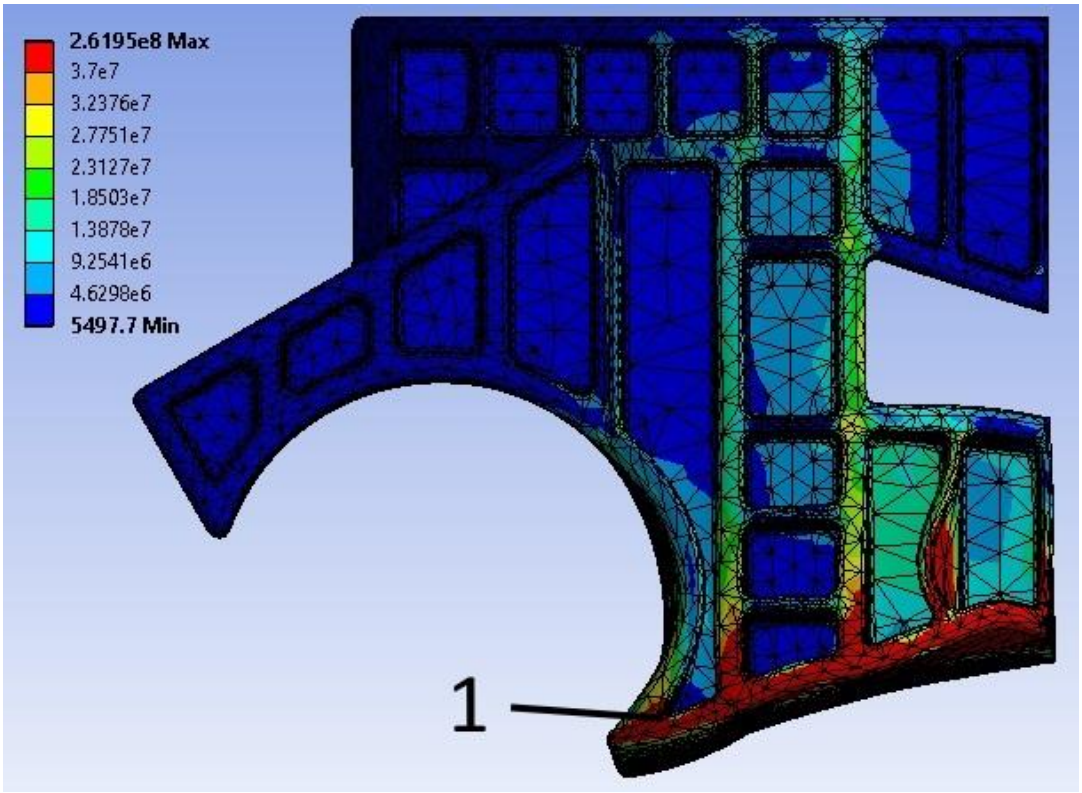

Figure 184 – Stresses on the existing Strathclyde design at 1610N

In the revised design a maximum deformation of 15.5mm was observed on the loaded edge of the foot with the largest deformations occurring because of the rotation caused by the loading. Bending of the central cylindrical section (containing the bolthole) is visible. This may possible to some degree however any bolt that is included would be expected to be steel and relatively stiff so likely to reduce the extent of deflection of this area.

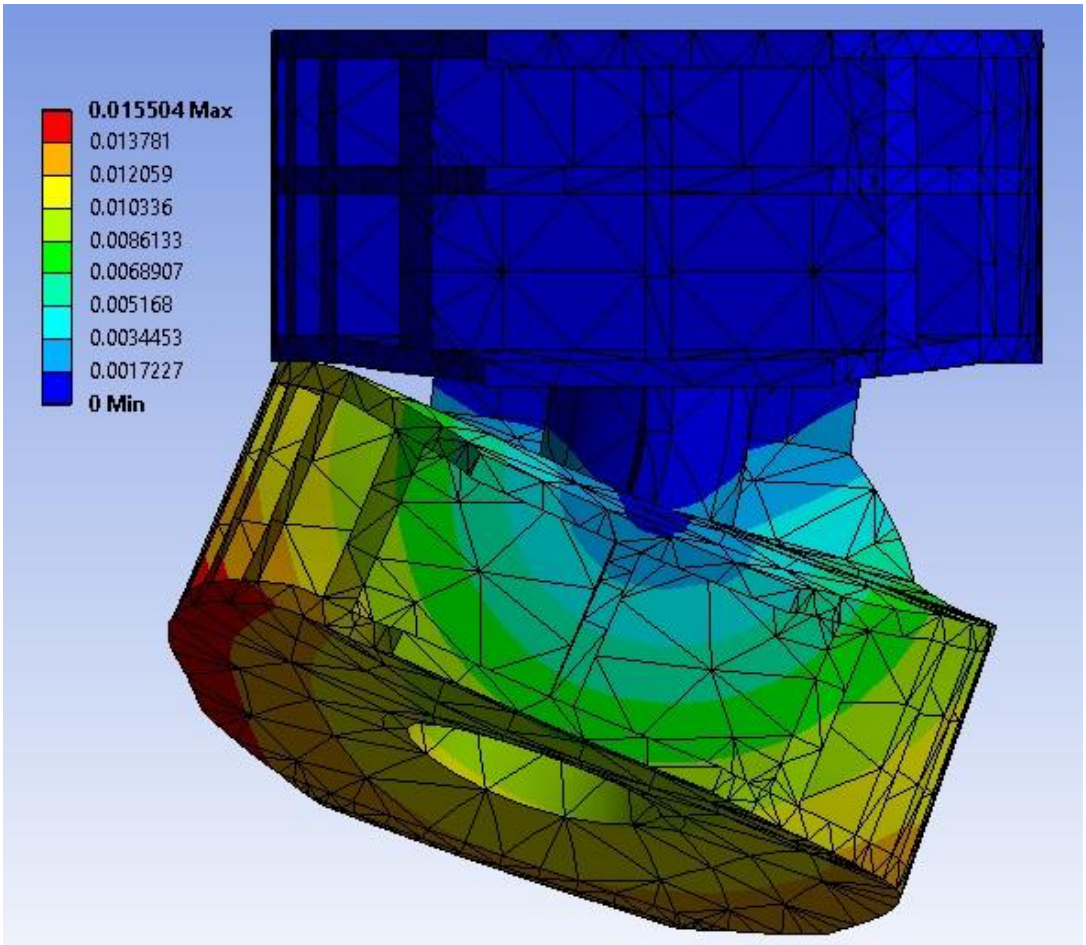

Figure 185 – Deformation at maximum edge load in the revised design

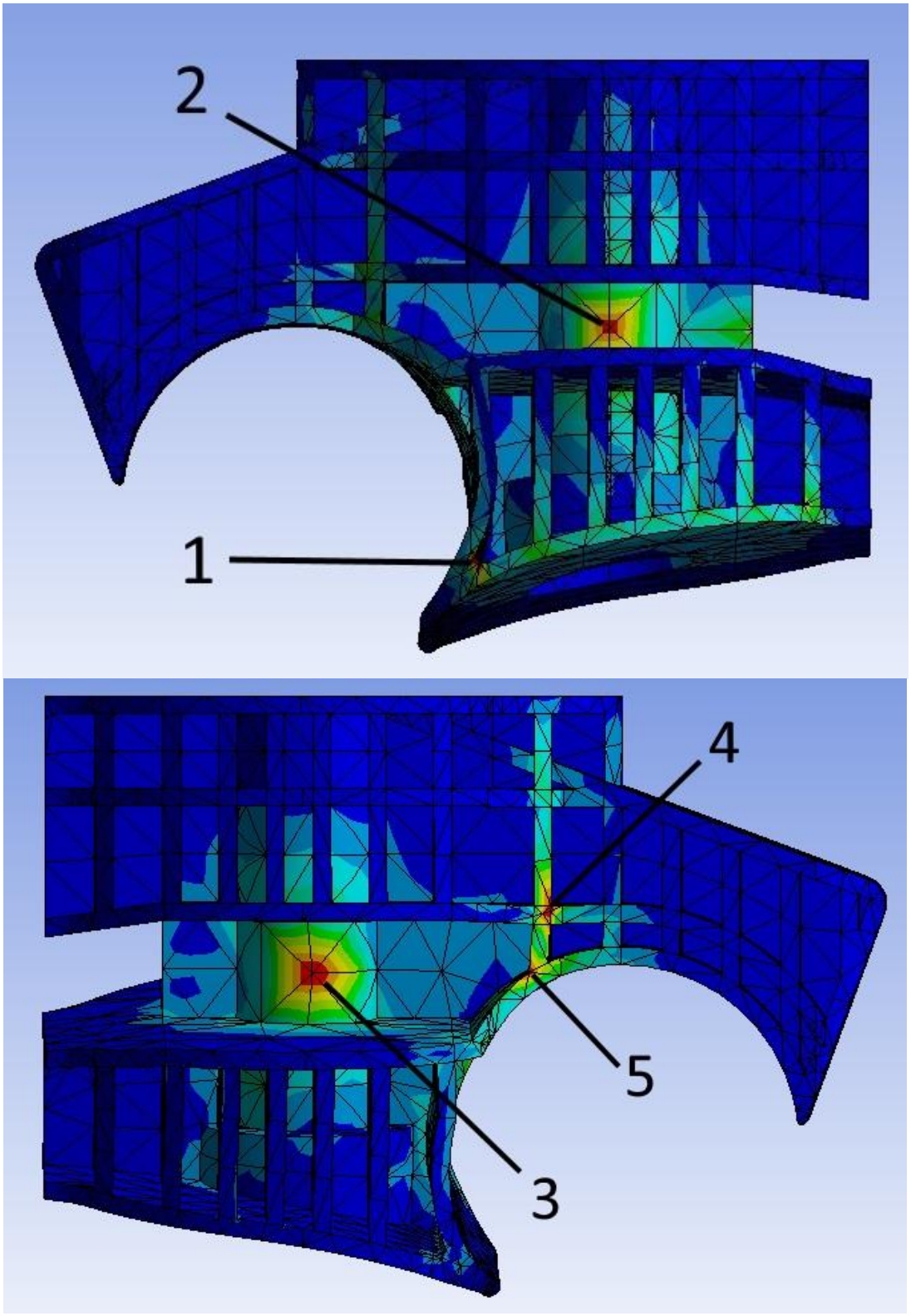

Figure 186 – High stress areas observed in edge loading conditions on the revised design

Five high stress areas became visible during loading of the revised design (see Figure 186 for identification). Point 1 reached yield stress at a load of 351.0N, point 2 reached yield at 531.5N, point 3 at 631.1N, point 4 at 650.4N and point 5 at 673.0N. Other high stress points became apparent as the load continued to increase but as those listed were likely to fail before yield could be met at the other locations they were discounted.

B3.5.7 Discussion

The values of stress observed in the existing Strathclyde design were not considered to be accurate due to the nature of loading applied. The use of a model edge would cause high stress concentrations at the area of loading and was not representative of the real-world conditions that could be applied. With that said the deformation was also unlikely to reflect what could be achieved in a physical test of the design however, for the purposes of comparing the two design this was considered acceptable.

The stress at point 1 in the revised design is also likely to be a product of the loading applied however the relative flexibility of this design means that higher stresses were observed elsewhere. The stress observed at point 2 in the revised design appeared to be compressive and was not matched on the inside of the cylindrical central support, an area that did not reach yield stress by the maximum loading condition. Point 3 was on the opposite side of the cylinder from point 2 and so in tension, but did not reach yield stress until the load had increased by 100N. Points 4 and 5 reached yield stress at similar loads (650.4N and 673.0N respectively) at corners in the vertical rib extending from the cylindrical section at the heel. Point 4 was at an internal corner which was extended by the deformation caused under loading leading to the stresses observed. The stress at point 5

appeared to be caused by the rotation of the lower foot section causing the vertical support to descend and so collapsing the corner.

B3.5.8 Conclusion

The deformation in the revised design was much greater than that of the existing Strathclyde design, which was unsurprising given the reduced support from removing vertical supports to allow for an energy return feature. It is possible that such a feature would provide support and reduce the deformation occurring by partially filling the gap between the upper and lower foot sections. The stresses could not be reasonably compared between models given the role of the model design in the stresses of the existing foot. The stresses in the revised design did suggest that the keel would fail prior to meeting the P3 static load conditions of ISO 10328 if they were applied in this way. The standard did not call for loading in such a manner and this may be considered to be a blind spot in the standard as it is only concerned with toe and heel loading of prosthetic feet. The revised design showed weakness in lateral loading which should be revisited in further design.

B3.6 Whole design evaluation

Having made several changes and evaluated them separately the entire redesign was evaluated per the conditions of ISO 10328 toe loading. For the initial set up the settings used would be identical to those used to evaluate the existing Strathclyde foot (detailed in section B2.2 Model generation).

B3.6.1 Material properties

The same material properties were used as for the previous models (see B3.1.2 Material properties).

B3.6.2 Boundary conditions

The flat top surface of the keel was fixed as a support with the four vertical sides of the metal plate being treated as frictionless supports. The faces along the centreline split in the model had a symmetry condition applied.

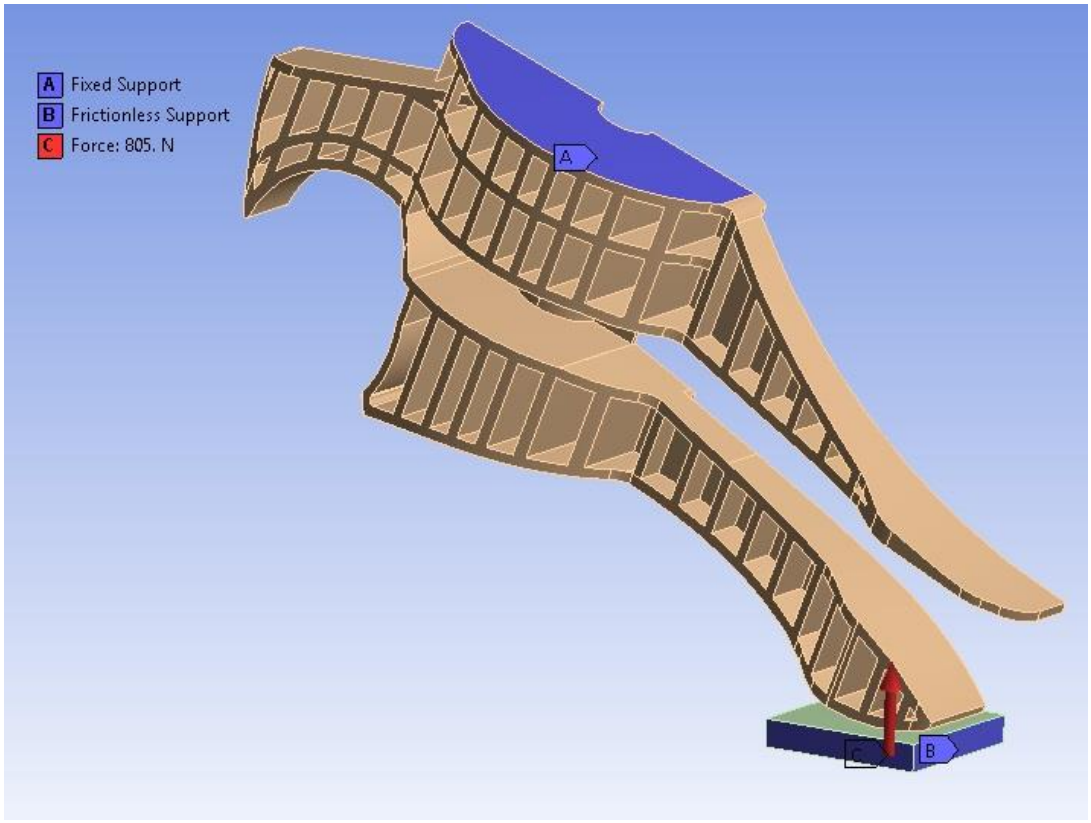

Figure 187 – Boundary conditions on revision design toe loading model

B3.6.3 Mesh

The meshing procedure was the same for both setups. Initially the entire model was meshed using a relevance centre setting of ‘coarse’ with a medium smoothing and fast transition. The contact areas were then further refined by element size, which was set to 0.002m (see Figure 188).

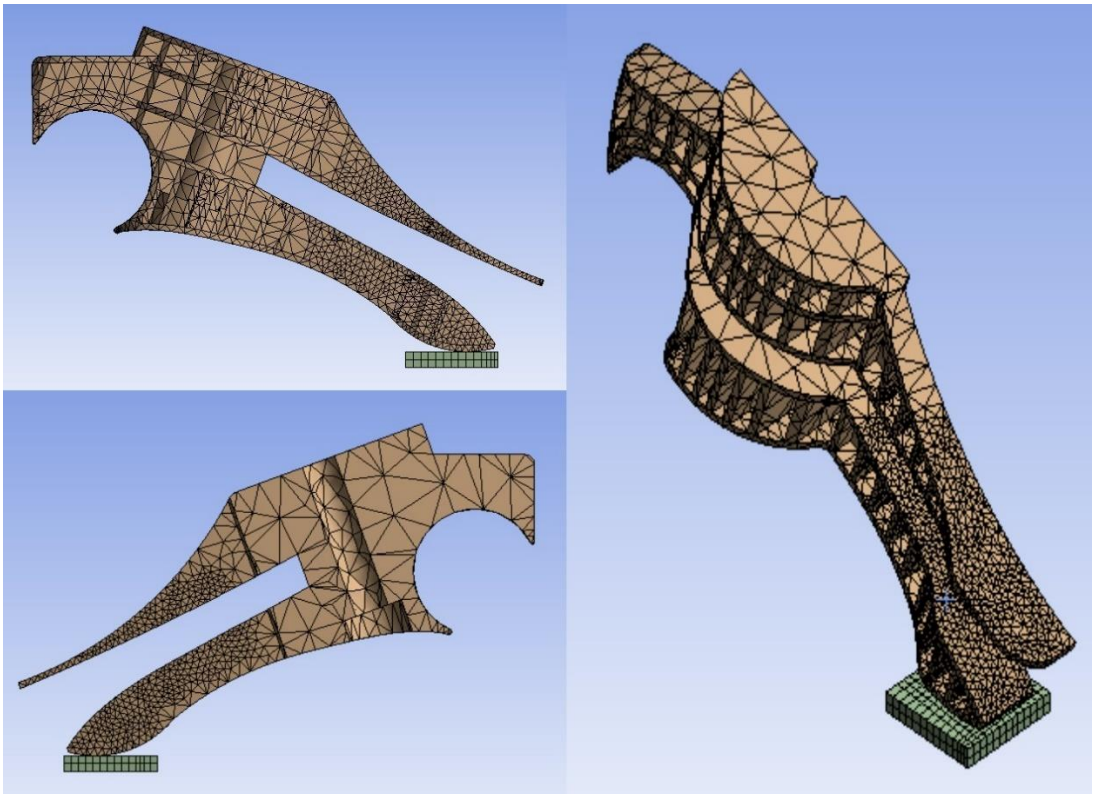

Figure 188 – Mesh of revision design toe loading model

B3.6.4 Loading

A load was applied on the underside of the steel plate, acting vertically upwards and ramped to reach 805N (half the static proof load at the P3 level).

B3.6.5 Analysis settings

The model was set to run over 4.6 seconds split into 250 sub steps, this gave a loading rate of 175N/s, which was midway in the range of 100N/s to 250N/s specified in ISO 10328. Weak springs were turned off, large deflection was turned on while inertia relief was off, and the solver type left as program controlled.

B3.6.6 Results

The bottom section of the toe was observed to have deformed upwards, meeting the upper section of the toe, which then reduced the rate of deformation. The maximum deformation calculated was 3.61×10^{-2}m at the tip of the bottom toe

section. The maximum deflection on the upper toe section was $2.16x10^{-2}$m (see Figure 189).

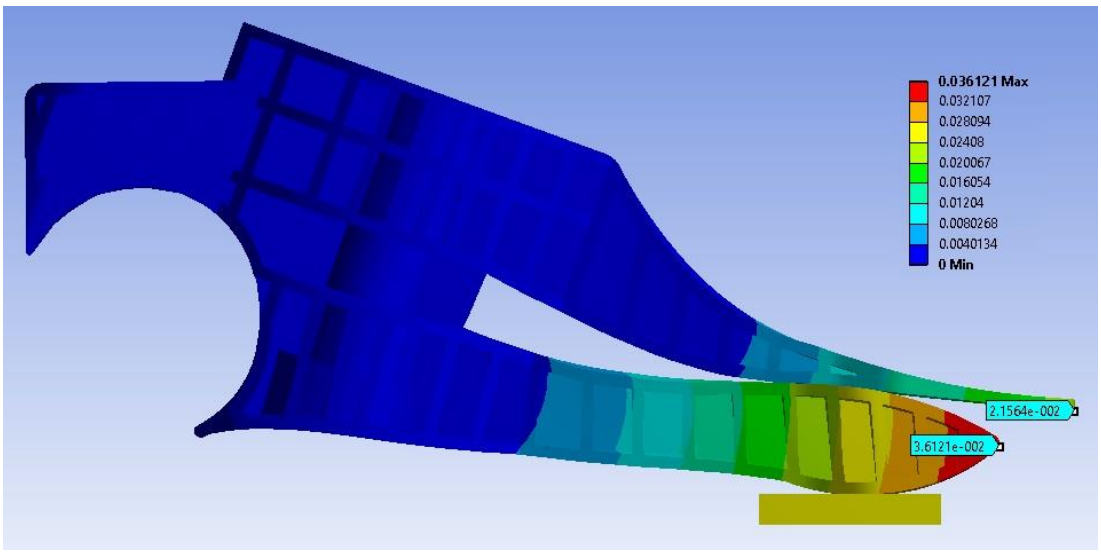

Figure 189 - The deformed condition of the revised design shown at 805N model load. The highest deformations of the upper and lower toe sections are highlighted.

In the analysis five major areas of high stress became apparent and are highlighted in Figure 190. While other high stress areas were visible these are achieved later than the five highlighted areas and as such the foot would be likely to fail due to one of the five highlighted areas before the other areas were able to reach yield stress.

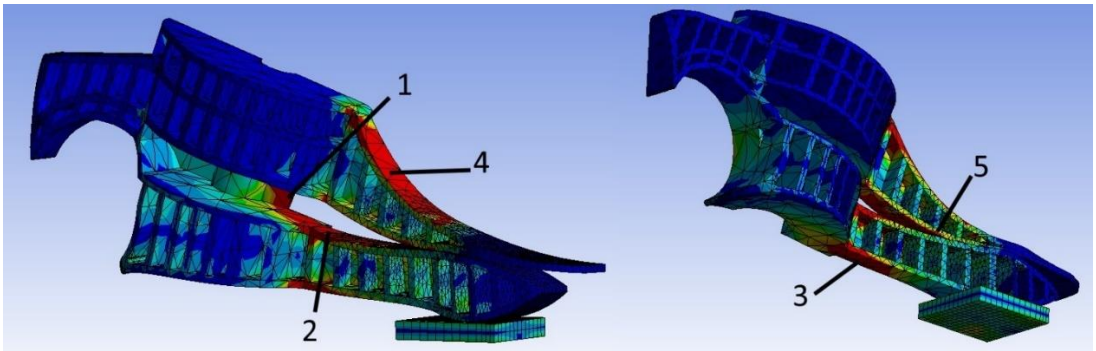

Figure 190 – The high stress areas in the revised design with identifying numbers.

$3.5x10^{7}$Pa (the yield stress of the polypropylene) was first passed at area 1 at a load on the model of 135.2N (270.4N on the full foot).

In area 2 the tensile yield stress of the polypropylene was surpassed at 141.7N loading (283.4N on the full foot).

In area 3 the tensile yield stress was reached at 154.6N (309.1N on the full foot).

In area 4 the tensile yield stress was reached at 541.0N (1081.9N on the full foot).

In area 5 the tensile yield stress was reached at 566.7N (1185.0N on the full foot).

B3.6.7 Discussion

The high stress areas observed were very similar to those present in the existing Strathclyde foot design with points 2-5 occurring in equivalent locations. Point 1 in either case was different due to the changed geometry in the areas in question. The location of point 1 in the existing Strathclyde design was the lower corner of the vertical support at the rear of the lower toe section whereas for the revised design point 1 was identified as the centre of the vertical support (see Figure 191). It should be noted that point 1 was the designation of the locations only and does not imply equivalence.

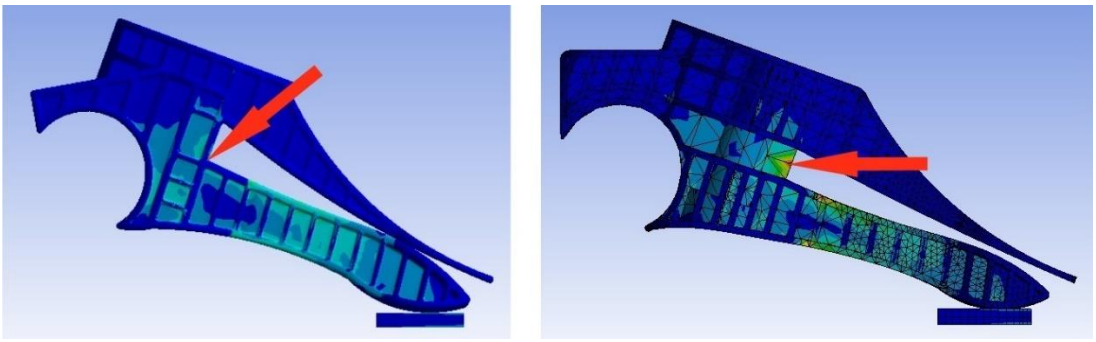

Figure 191 – Comparison of location of ‘point 1’ in the existing Strathclyde design (L) and the revision design (R)

In either case point 1 was the first location to reach yield stress in loading. For the existing Strathclyde foot this occurred at 177.1N while for the revision design it

was at 135.2N. The reduced reinforcement of the keel at the midsection led to the increased stress observed at point 1 in the revised design while in the existing design point 1 was a result of the corner acting as a stress concentrator. When points 2 and 3 were compared in either case, larger differences were observed with yield stress reached at much lower loads in the revision design than in the existing Strathclyde design (see Table 19).

	Existing Strathclyde design	**Revision design**
Point		
1	177.1N	135.2N
2	238.3N	141.7N
3	376.7N	154.6N
4	615.0N	541.0N
5	631.1N	566.7N

Table 19 – Load at which yield stress is reached for each point in existing Strathclyde design and revision design

Point 2 (on the upper side of the lower toe section) reached yield stress at a load slightly less than two-thirds the load observed at yield in the existing Strathclyde design while at point 3 (the lower side of the lower toe section) the load at yield in the revision design was less than half the load at yield observed in the existing Strathclyde design. The gap between upper and lower toe sections increased in the revised design from that of the existing Strathclyde design which resulted in a later contact between upper and lower toes section in the revised design. This led to failure stress being recorded at a lower load as the lower toe section was unsupported by the upper toe section unlike in the existing design. The yield stress was met at lower loads at points 4 and 5 in the revised design than in

the existing design. The webs were reduced in thickness from 2.5mm to 2mm which will have increased the stress by reducing the cross-sectional area available for forces to act on.

The main block of the revised design was examined under vertical loading in section B3.4 Vertical loading of keel, and shows the same high stress area as the model when toe loaded at 20° elevation. This was explained as being a result of loading causing a rotation of the toe section upwards, a greater case of which happens under the loading conditions examined here. It was not a surprise then that a lower load was observed on failure in this testing condition (289.8N compared to 1610N in vertical loading).

B3.6.8 Conclusion

The changes made to the design appeared to have an adverse reaction on performance of the keel under ISO 10328 P3 static loading test conditions with failure expected at 41-90% (point 3-point 5) of the loads seen in the existing design. Some of the features added were unavoidable additions, such as the bolt hole inclusion and the energy return feature allowance. As the inclusion of an energy return feature would be expected to change the behaviour of the system a model was generated to include such a feature. This was combined with a change in material properties to reflect prototype samples for physical testing.

B3.7 Duraform EX models

Prototype models were to be produced via SLS from Duraform EX. As such it was decided to create models of toe loading, with and without a blade, using material properties for Duraform EX to allow comparison to physical test results.

B3.7.1 Bladeless model setup

The model that was used in section B3.6 Whole design evaluation, was used again with the only change being the material of the keel being changed to Duraform EX with the following properties:

Density	1010 kgm^{-3}
Young's Modulus	1.281 x 10^9 Pa
Poisson's ratio	0.4
Bulk Modulus	2.135 x 10^9 Pa
Shear Modulus	4.575 x 10^8 Pa
Tensile Yield Strength	3.7 x 10^7 Pa
Tensile Ultimate Strength	4.28 x 10^7 Pa

Table 20 – Duraform EX material properties used in FEA

Young's modulus, tensile yield strength and tensile ultimate strength were determined from experimental results (see sections 4.3 Material testing and 4.4 Extensometer testing). Poisson's ratio was unavailable so an average value for Nylon (Duraform EX's base material) was used. Bulk modulus and shear modulus were calculated by Ansys using Young's modulus and Poisson's ratio. The data from testing was also used to provide uniaxial stress-strain values up to 0.01 strain.

B3.7.2 Results

The bottom section of the toe was observed to have deformed upwards, contacting the upper section of the toe, which then reduced the rate of deformation. The maximum deformation shown in Workbench was $3.59x10^{-2}$m at the tip of the bottom toe section. The maximum deflection on the upper toe section was $2.12x10^{-3}$m (see Figure 192).

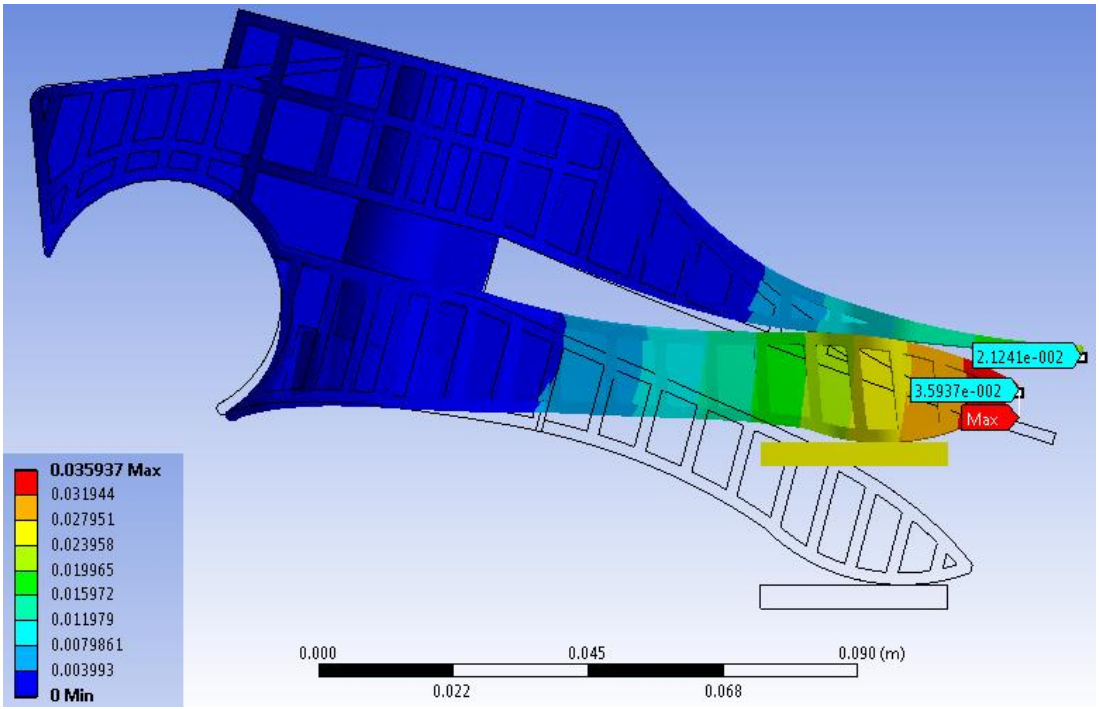

Figure 192 - The deformation of the model shown with the original shape as a wireframe and the highest deformations of the upper and lower toe sections.

The same high stress points were apparent as previously (see Figure 190) with the stresses occurring at values approximately 10-17% higher in the Duraform EX model.

	Revision design (polypropylene)	**Revision design (Duraform EX)**
Point		
1	135.2N	148.1N
2	141.7N	151.3N
3	154.6N	167.4N
4	541.0N	634.3N
5	566.7N	647.2N

Table 21 - Load at which yield stress is reached for each point in the revision design in copolymer polypropylene and Duraform EX

B3.7.3 Discussion

The results here were similar to those observed in polypropylene with the order of yield stress being reached the same for Duraform as for copolymer polypropylene. The load at yield of the points was between 10 and 17% higher in the Duraform EX model, due to the slightly higher yield stress ($3.7x10^7$Pa vs $3.5x10^7$Pa) Similar deflections were observed under maximum load in either model. This model was created to provide a reference to the physical testing that occurred (see section 4.5 P3 toe tests) rather than to serve as a comparison between materials. A model including the energy return blade was generated following this model.

B3.7.4 Duraform EX model including blade setup

A round of FEA was carried out to support the introduction of the energy return feature (blade) to the system. The introduction of the blade was expected to affect the load pattern and so the stresses in the foot design. The material properties for fibreglass had to be added to best represent the blade. These were taken from (Barbero, 2011) as follows:

Density	1370 kgm^{-3}
Young's Modulus	72 x 10^9 Pa
Poisson's ratio	0.22
Bulk Modulus*	42.86 x 10^9 Pa
Shear Modulus*	29.51 x 10^9 Pa
Tensile Ultimate Strength	3.45 x 10^9 Pa

* Bulk modulus and shear modulus were calculated by Ansys using Young's modulus and Poisson's ratio.

Table 22 - Fibreglass material properties used in FEA

The settings used for the previous, bladeless model were again used where applicable (symmetry, loading, fixed support of keel, frictionless support of plate).

The contact conditions between the upper and lower toe sections were removed and instead contact conditions were included for the lower toe section and the blade and for the blade and upper toe section. These were frictional, μ = 0.28, with a pinball region of 0.001m but otherwise the same to previously used contacts. Contact sizing for the mesh was set to 0.002m for both frictional contacts between the blade and keel. The blade was bonded to the foot at the sites visible in Figure 193.

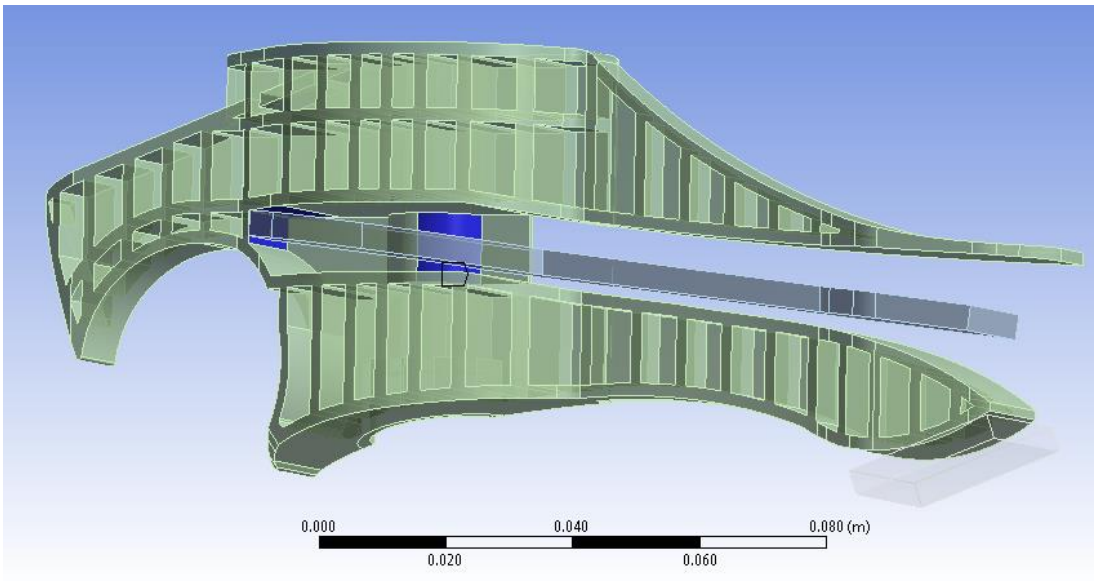

Figure 193 – Image demonstrating bonded sites between the blade and keel

B3.7.5 Results

The lower toe section was observed to deform into contact with the blade. At this point the rate of deformation was reduced, but continued until the blade made contact with the upper toe section at which point the rate of deformation was further reduced. The maximum deformation observed was 2.08×10^{-2}m at the tip of the lower toe section.The upper toe section deformed by 7.89×10^{-3}m at the tip while the tip of the blade deformed by 1.46×10^{-2}m (see Figure 194).

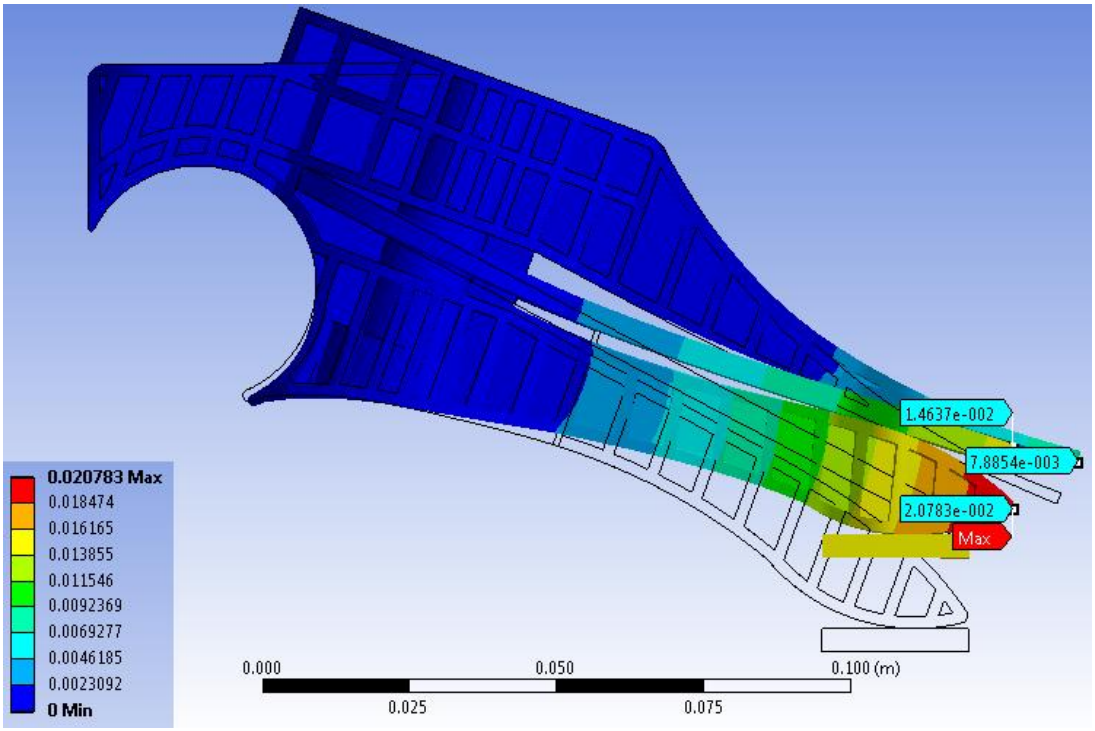

Figure 194 – Image showing the maximum deformation occurring in toe loading with a blade inserted in the keel

The pattern of yield stress being reached in the keel followed a different pattern with a blade included. Points 4 and 5 did not meet yield stress before maximum load was reached. In this case there were three points of high stress in the keel which, while falling near the points identified as 1, 2 and 3 in the previous models were considered to be different in this model (see Figure 195). Other small high stress areas became apparent over the course of loading, but these were related to the bonded surfaces between the blade and keel and as such were considered artefacts of modelling rather than points that would be of concern in a physical model. The three points identified were all found at inside corners in this case, unlike in previous models where they were present at outside corners. Point 1 reached yield stress at 148.1N, point 2 at 209.3N and point 3 at 431.5N.

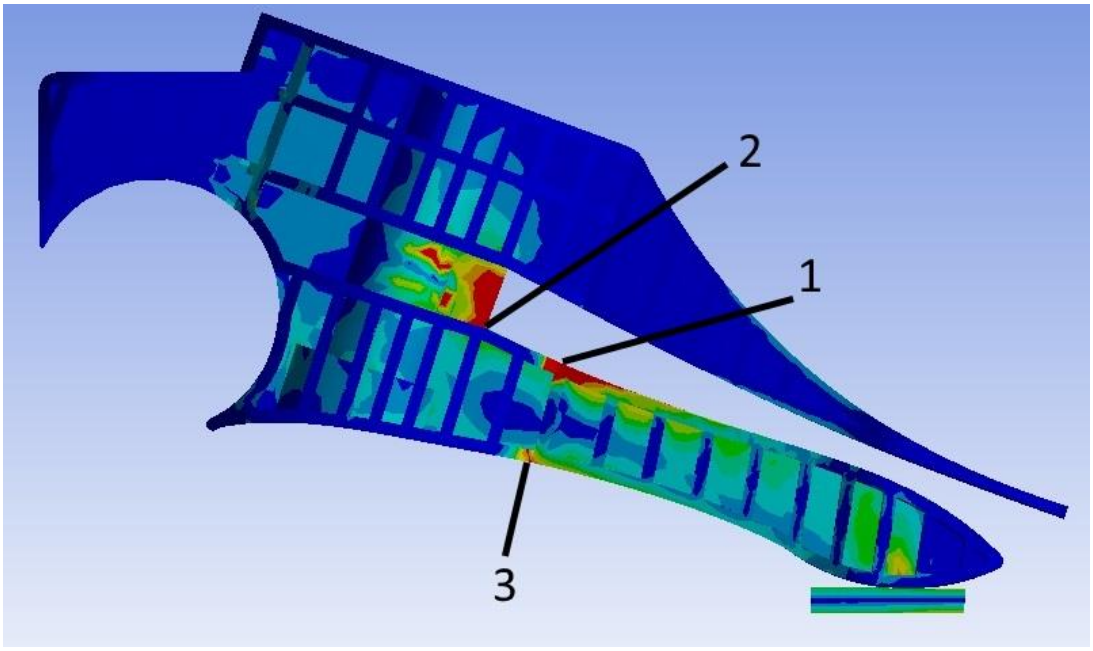

Figure 195 – High stress areas in bladed keel model (blade hidden for clarity)

Fibreglass would be expected to fail in a brittle manner so using the tensile ultimate strength as a failure point for the blade shows that by the maximum load the blade would not expect to fail, reaching a maximum stress of only $6.99x10^8$Pa (see Figure 196). The corners present on the outside of the blade were found to act as stress concentrators.

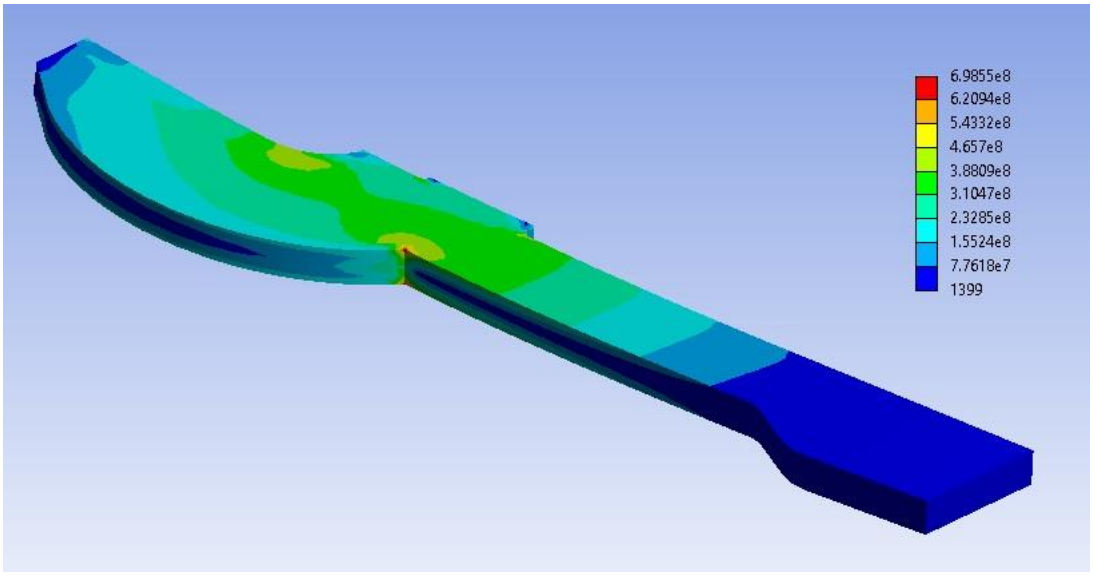

Figure 196 – Stresses on the blade in revision design toe loading model

B3.7.6 Discussion

When comparing the bladed model to the bladeless model of section B3.6 Whole design evaluation, yield stress was first reached at the same load (148.1N) but in two different areas. The central support of the bladeless model was seen to reach yield stress first (point 1 in Figure 190) compared to the top corner where the lower toe section met the main block of the keel in the bladed model (point 1 in Figure 195). This point in the bladed model was in a similar area to point 2 from the bladeless model, which met yield stress at a load of 151.3N. In this case the blade has increased the stress in this area for a given load. Point 2 in the bladed model was closest to the location of point 1 in the bladeless model however for the bladeless model the high stress point was found in the middle of the vertical support whereas in the bladed model the corner where the front edge of the vertical support met the bottom part of the main block was where the high stress in this area was found (see Figure 197).

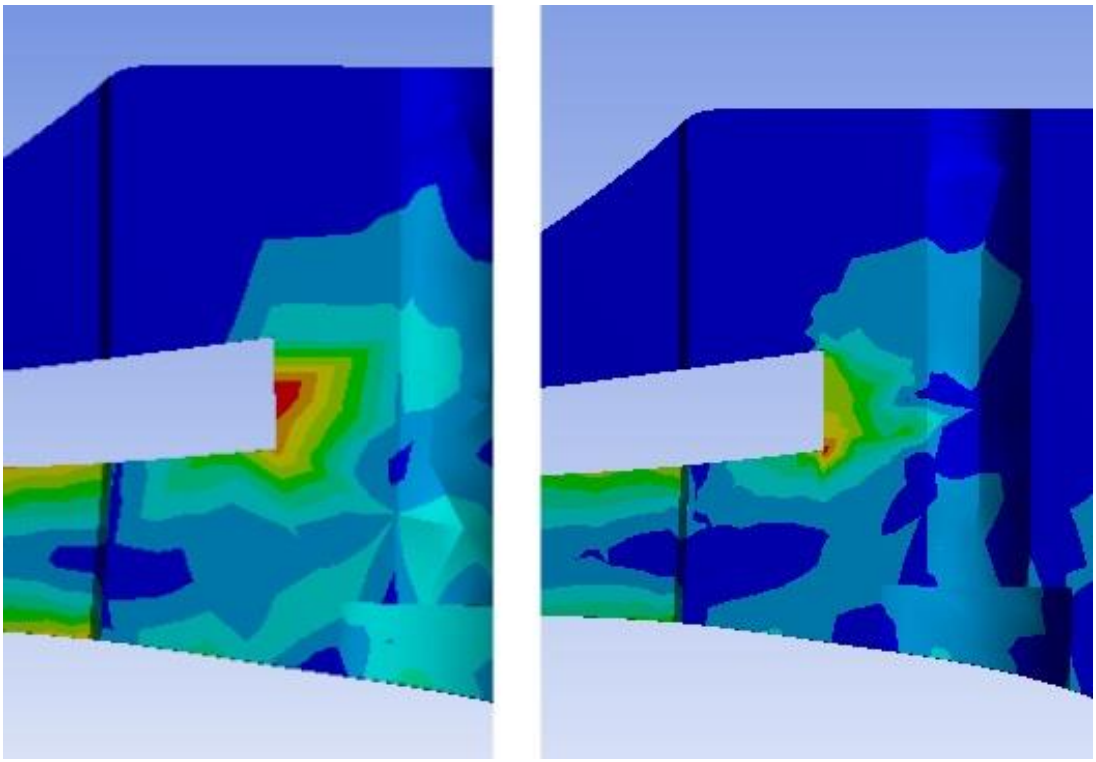

Figure 197 – High stress point (shown in red) in mid-foot for bladeless (L) and bladed (R) models

Point 3 was present at the corner where the underside of the lower toe section meets the main ankle block of the keel, reaching yield at 431.5N. This point was in approximately the area of point 3 in the bladeless model however yield stress was met in the bladeless model at a load of 167.4N compared to the 431.5N of the bladed model.

B3.7.7 Conclusion

The presence of a blade in the keel changes the behaviour of the keel under loading in terms of failure points and the load at which the yield stress is reached. It was decided to carry out testing using prototypes both with and without blades to compare the performance of the model to the physical prototypes.

B4 Second design revision

Following the results of physical testing of prototype samples and the changes proposed to the design a further round of FEA was required to validate these changes. The design was separated into sections which could be compared from the first revision (R1) to the second (R2). The sections were: lower toe section, heel section and ankle block in both main face l loading and edge loading. The upper toe section was only slightly altered and was not deemed a large enough change to justify analysis however a comparison was included in B4.2 Upper toe comparison. The relevant sections from the initial design revision were also run for comparison. Following the individual sections analyses the whole design could be run.

B4.1 Lower toe FEA

The lower toe section of the R1 design failed in three of the four prototype samples tested, partially due to the process used however the work in section B3.6 Whole design evaluation, still predicted failure of the toe section before the maximum load was reached. The changes to the model in this area were intended to increase the second moment of area, thus increasing the stiffness, and to increase the load to yield stress of points 2 and 3 as identified in Figure 190. The section identified as the lower toe was taken forward from the front face of the central support running between the upper and lower sections of the ankle block. Only one section was required, in either case the right toe was used, using the centreline as the cut line. Sections from both the R1 and the R2 design were modelled.

B4.1.1 Material properties

The same material properties were used as for the previous models (see B3.1.2 Material properties).

B4.1.2 Boundary conditions

The toe sections had a fixed support applied on the rearmost face with a frictionless support applied to the face at the centreline (see Figure 198).

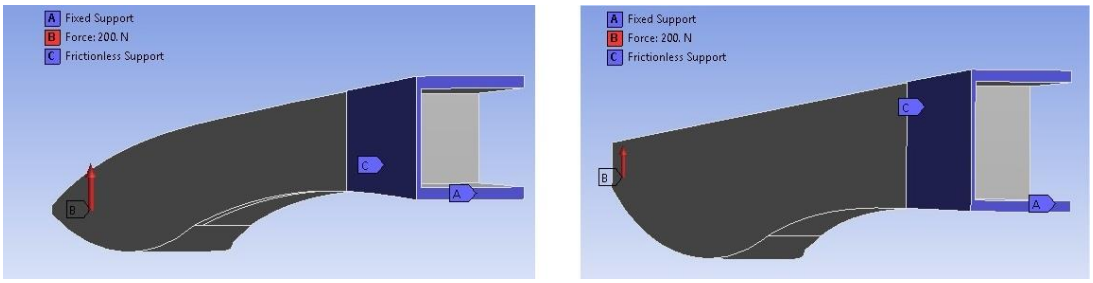

Figure 198 – Boundary conditions used in lower toe section FEA modelling R1 (left), R2 (right)

B4.1.3 Mesh

The meshing procedure was the same for both setups. The model was meshed using a relevance centre setting of ‘coarse’ with a medium smoothing and fast transition (see Figure 199).

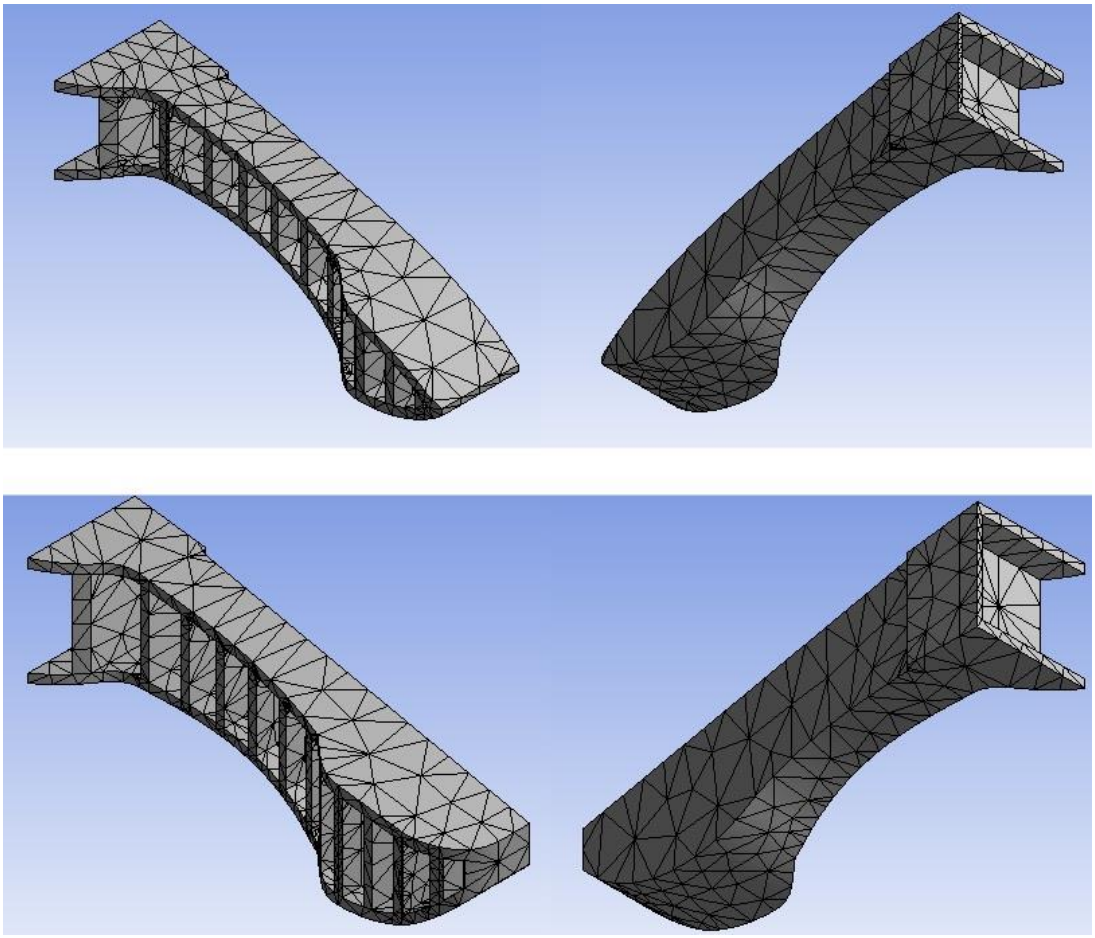

Figure 199 – Mesh of R1 (top) and R2 (bottom) lower toe section model

B4.1.4 Loading

A load was applied vertically upwards to the front most face of the toe section and ramped over 1.15s until 200N was reached. This load was unrelated to any standard however higher loads produced excessive deformation.

B4.1.5 Analysis settings

The model was set to run over 1.15 seconds split into 250 sub steps. Weak springs were turned off, large deflection was turned on while inertia relief was off, and the solver type left as program controlled.

B4.1.6 Results

In the R1 model the points corresponding to points 2 and 3 (from B3.6.6 Results) reached yield stress at 82.4N and 71.2N respectively. An area at approximately halfway down the top surface of the lower toe section also reached yield at a load of 105.6N. This was not observed in the previous models. Figure 200 shows the high stress points present in the R1 model.

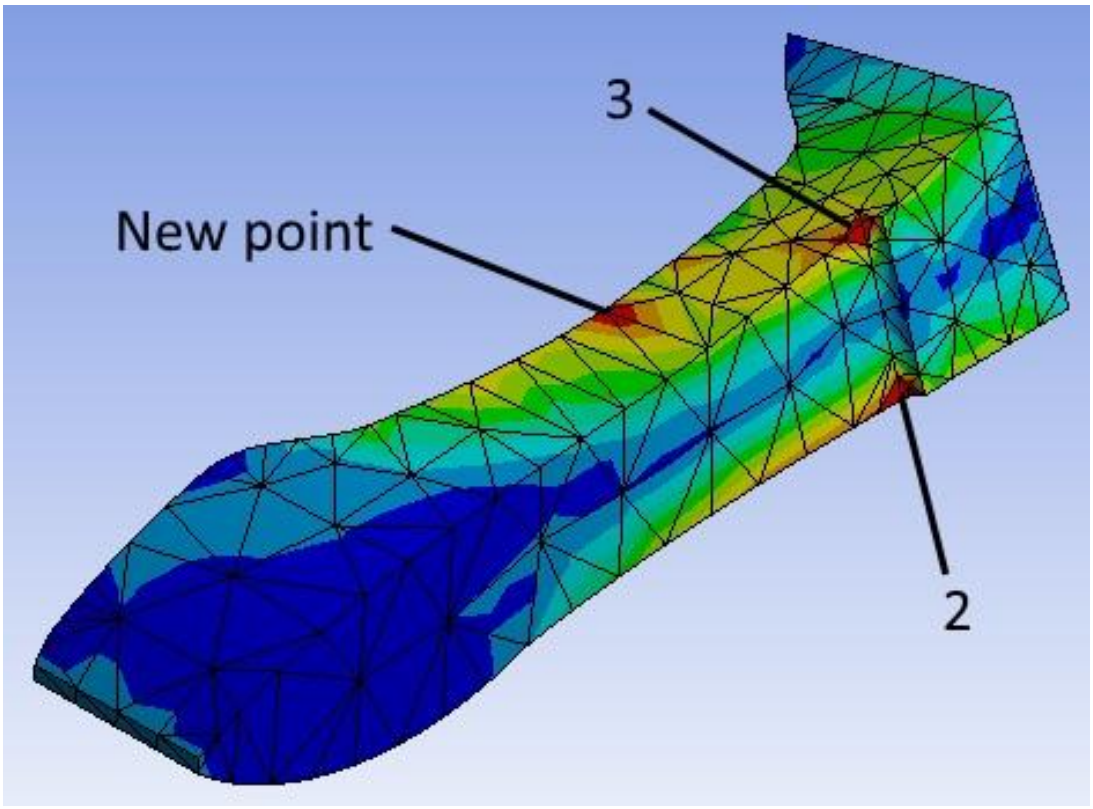

Figure 200 – High stress points in the R1 lower toe model

The maximum deformation at yield of the R1 model was 9.8mm at the outside edge of the front face of the toe (see Figure 201).

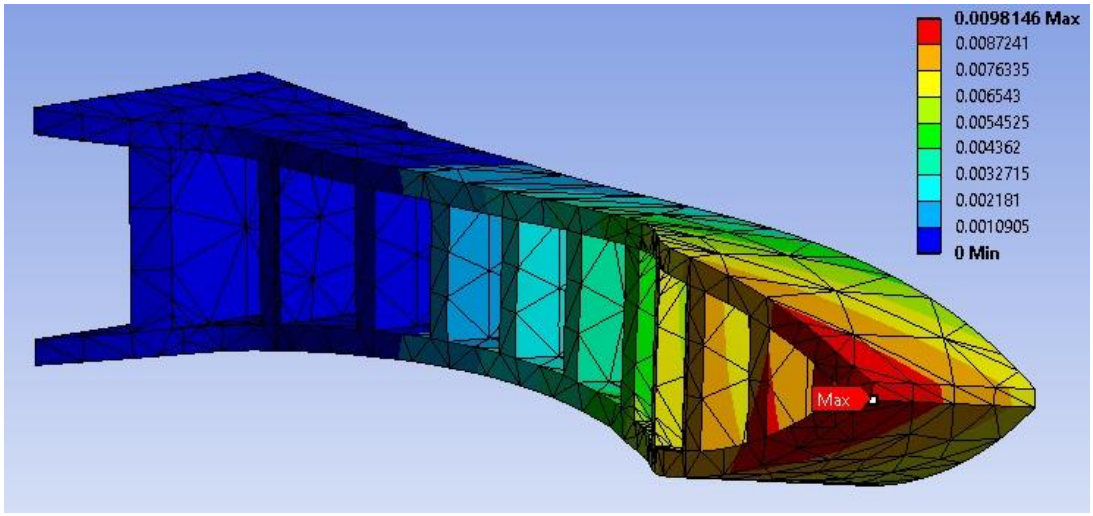

Figure 201 – Maximum deformation at initial yield of R1 model

In the R2 model the points corresponding to points 2 and 3 from B3.6.6 Results reached yield stress at 162.4N and 163.2N respectively (see Figure 202). The front corner of the approximately central rib of the model reached yield stress at 153.6N with the two ribs in front and one behind having reached yield in a similar position by maximum load (see Figure 203).

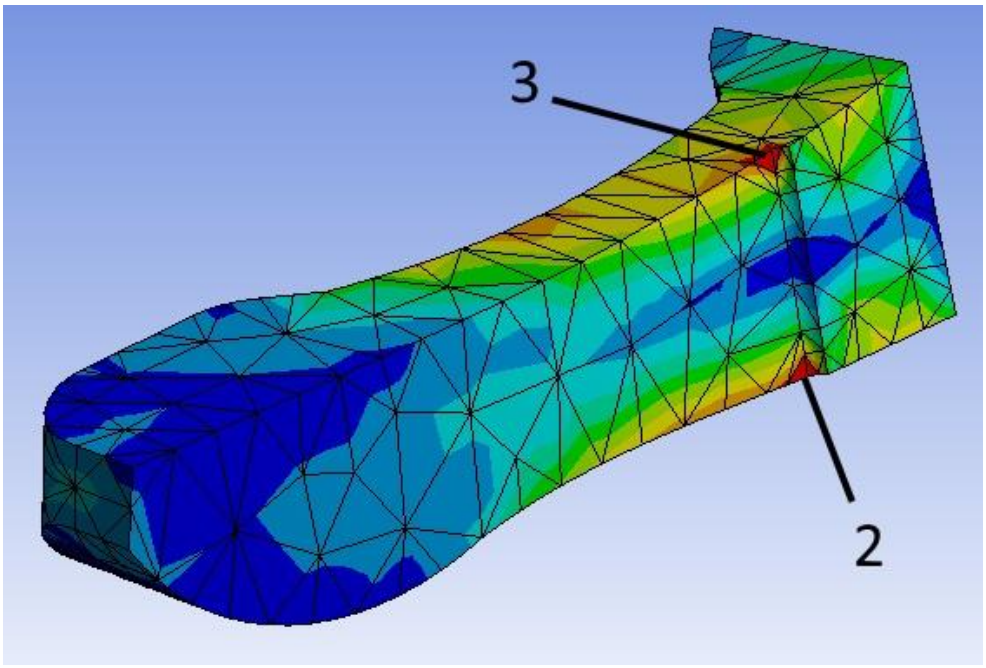

Figure 202 – High stress areas in R2 lower toe model corresponding to points 2 and 3 from B3.6.6 Results

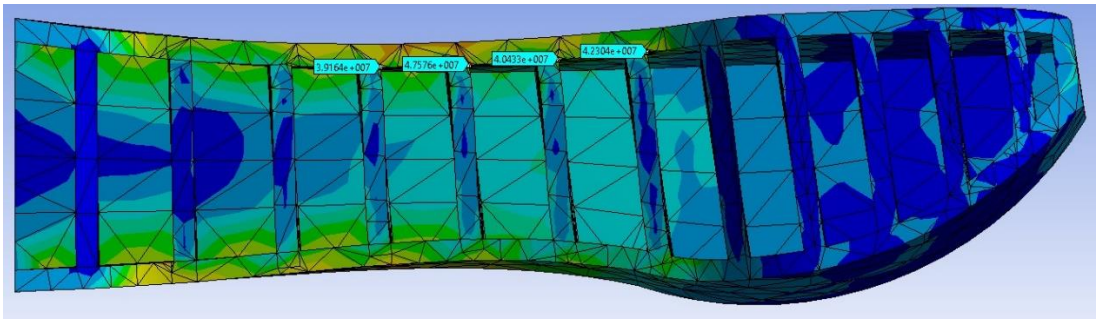

Figure 203 – The high stress points occurring in the corners where ribs meet upper toe surface at maximum load

The maximum deformation at yield of the R2 model was 11.1mm at a point on the lower side of the outside of the lower toe section (see Figure 204).

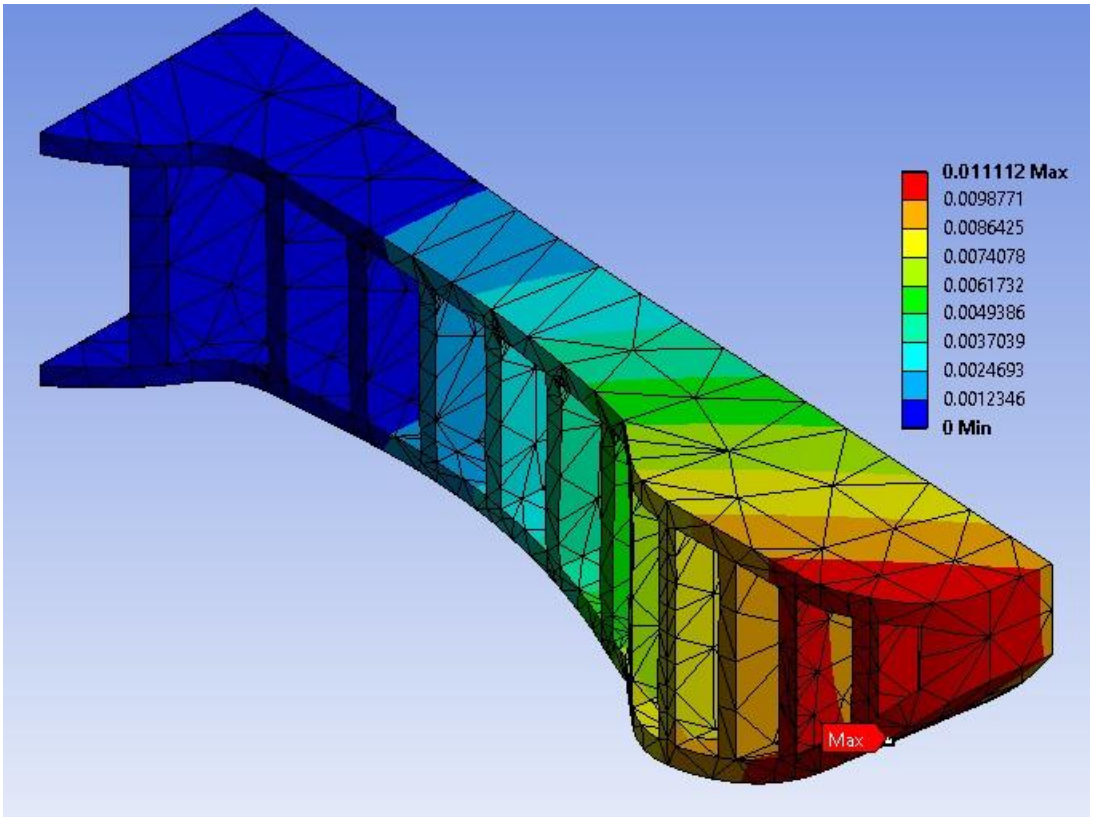

Figure 204 – Deformation at yield of R2 model

B4.1.7 Discussion

The yield points observed in R1 did correspond to those seen in section B3.5.6 Results, however, they did not occur in the same order, in this case point 3 reached

yield prior to point 2. In the previous model point 3 reached yield at 154.6N with point 2 reaching yield at 141.7N compared to 71.2N and 82.4N respectively. The difference in load application was part of the difference with previous loading occuring at 20° offset where in this model the load was appllied vertically only. This means that load applied in the previous model has a vertical component of *load(cos20°)* or approximately 94%. Even allowing for this, yield was reached at a much lower load in the new FEA model. The removal of the structure of the rest of the keel affected the performance, having been replaced with only a fixed support and a frictionless support while the load conditions of the model itself have caused a twisting to occur in the toe which would also contribute to higher stresses, particularly at points 2 and 3. The direct comparison of the two lower toe sections under the same conditions should be reasonable although a full keel model was required. The new high stress point was likely as a result of the twisting that occurred in the model (from the front the toe would be viewed to twist clockwise), which was not present in the model from section B3.5.6 Results due to the loading condition applied. As such this point was not considered to be of concern, having not been observed in the full keel model.

In the R2 model yield stress was reached at the points corresponding to 2 and 3 from section B3.5.6 Results with the load at yield being greatly increased from that seen in the R1 model, 162.4N for point 2 (compared to 82.4N) and 163.2N for point 3 (compared to 71.2N). This was a large improvement, approximately doubling the load at yield compared to the R1 model. High stress points became apparent at the forward corner at the top of some of the vertical ribs in the toe section (see Figure 203). These features occurred partially due to the geometry of the top of the toe section as it had gone from a curved shape to a flat shape and partially due to the introduced torsion of the loading conditions. In comparing the maximum deformation

of the lower toe sections initially deformation at yield was considered however this would give a higher deflection for R2 than R1 (11.1mm compared to 9.8mm), ignoring the higher load that R2 reached at yield (162.4N compared to 71.2N). If the load at yield of R1 is used for both models is used then the deformation for R2 would be only 4.9mm, much stiffer than R1.

B4.1.8 Conclusion

The changes made to the design of the lower toe section did show an improvement in the load to yield of the section. The model setup used introduced torsion not present in the whole keel model and so it was still required that a model of the whole keel be run. The stiffness of the lower toe section was also improved by the changes to design made, reducing from 9.8mm deflection at 71.2N (first yield point) to 4.9mm.

B4.2 Upper toe comparison

The upper toe section of the revised design failed in one of the three failing prototype samples tested, after the lower toe section had failed. This was likely due to shock loading following the failure of the lower section rather than as a result of the standard loading procedure. The upper toe section remained largely the same with only four slight changes from R1 to R2: the overall length increased by 0.32mm, the rear most rib moved 0.32mm backwards, the rear of the section began 1.28mm deeper before ending at the same height and the outside of the end of the toe used a single larger radius instead of two smaller radii with a connecting edge. Figure 205 shows a side view of the sections overlaid, which shows the deeper section and the longer length, and a top view which shows the change in radius of the outside of the end of the toe. Figure 206 shows a detail at the rear of the upper toe sections showing the increased length, section depth and the backward movement of the rearmost rib.

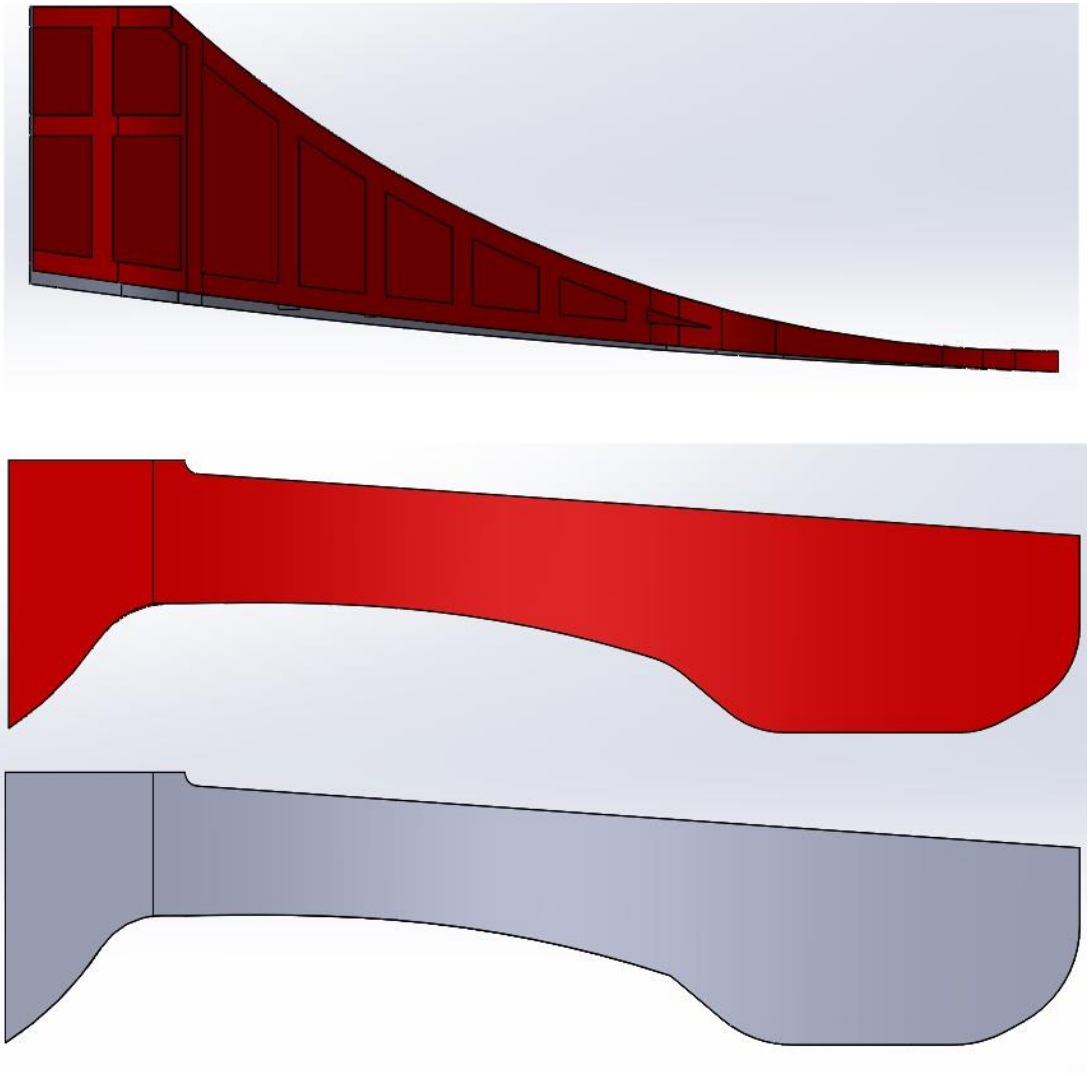

Figure 205 – Comparison of upper toe sections from R1 (red) and R2 (grey); side view (top), top view (bottom)

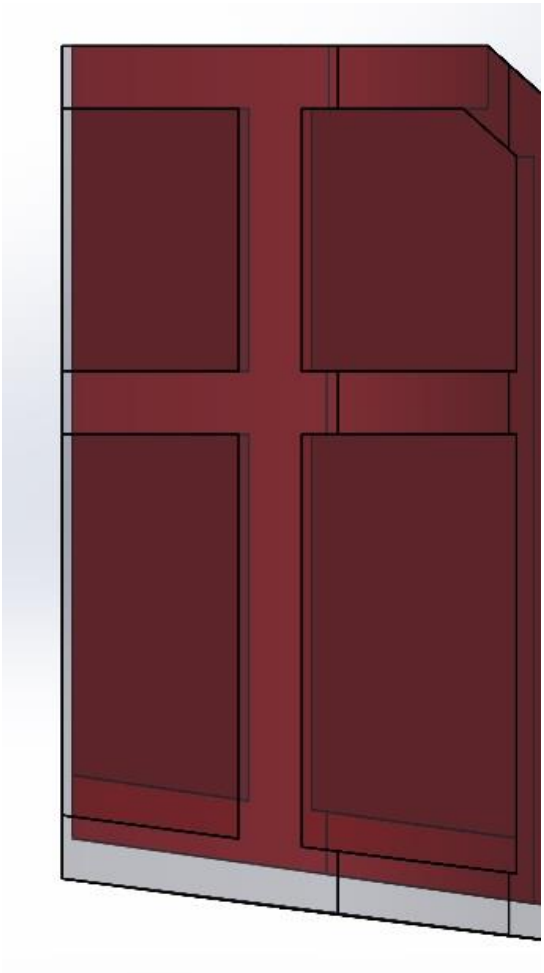

Figure 206 – Comparison of rear of upper toes section of R1 (red) and R2 (transparent grey) showing the increased length, section depth at rear and the backward movement of the rearmost rib

These changes were not considered to be significant enough to have a large effect on the performance of the keel so were not analysed as a separate part but were evaluated instead as part of the whole keel.

B4.3 Heel FEA

With the changes made in the midfoot to improve lateral stability and allow for better energy return feature incorporation the design at the heel was also modified, giving it a different rib pattern (see Figure 207 for comparison).

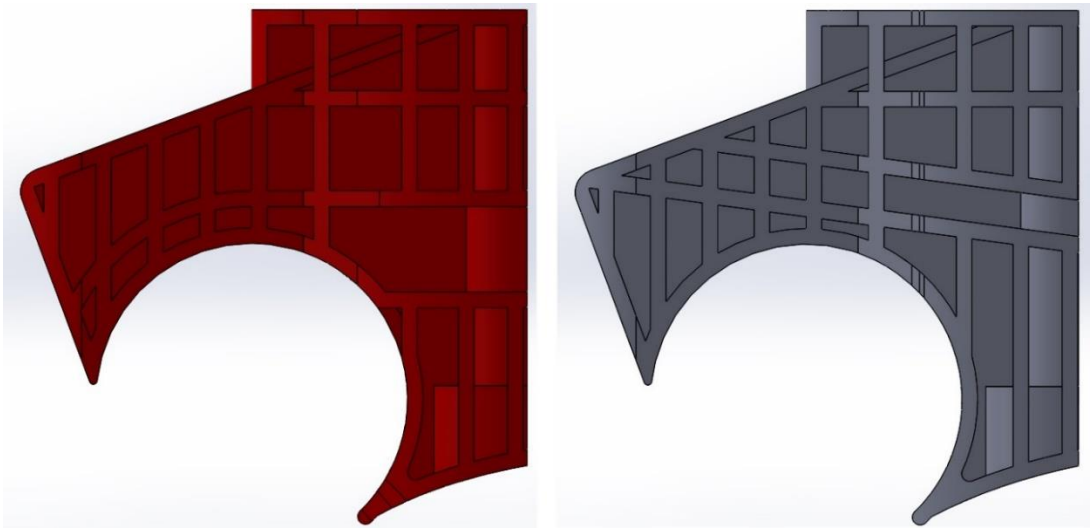

Figure 207 – Comparison of R1 heel design (left, red) to R2 heel design (right, grey)

B4.3.1 Material properties

The same material properties were used as for the previous models (see B3.1.2 Material properties).

B4.3.2 Boundary conditions

The flat top surface of the keel and the bolthole were fixed as supports (see Figure 208).

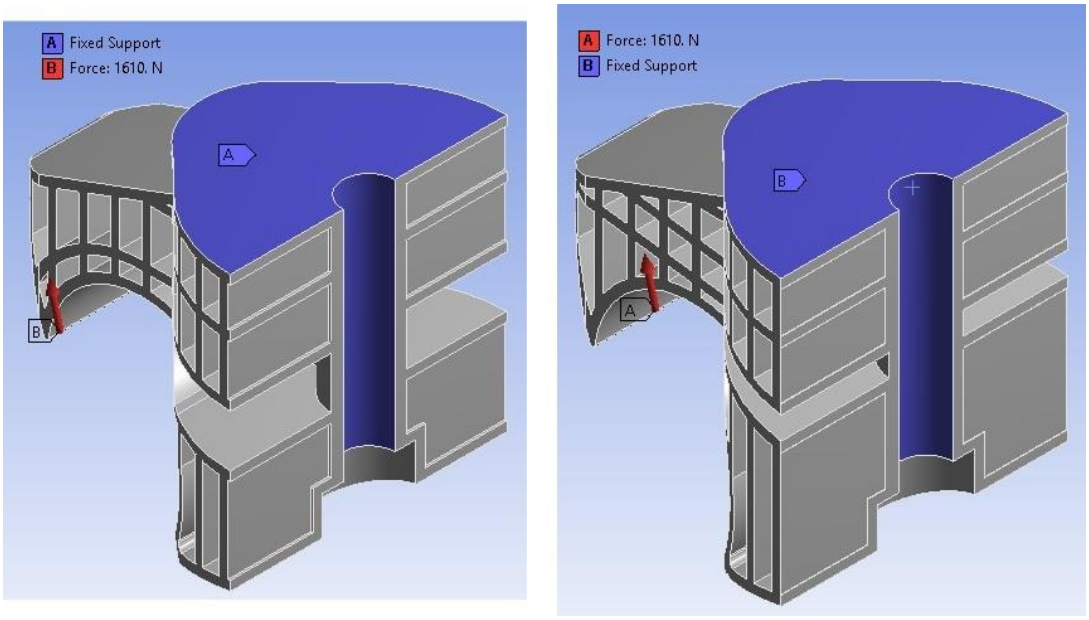

Figure 208 – Boundary conditions of heel models; R1 (left) and R2 (right)

B4.3.3 Mesh

The meshing procedure was the same for both setups. Initially the entire model was meshed using a relevance centre setting of ‘coarse’ with a medium smoothing and fast transition (see Figure 209).

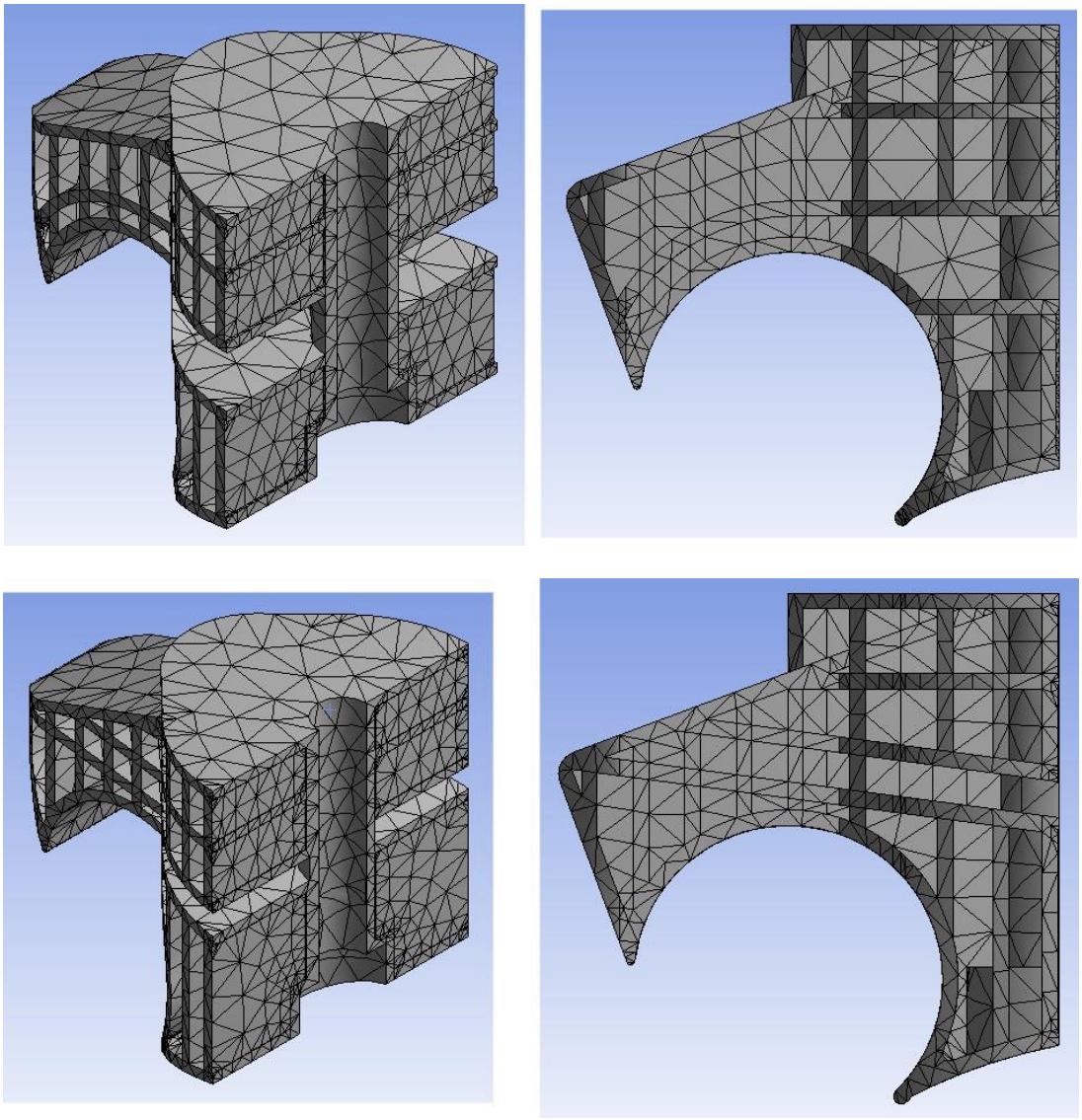

Figure 209 – Mesh of heel models; R1 (top) and R2 (bottom)

B4.3.4 Loading

A distributed load was applied on the filleted lower face of the heel, acting parallel to the rear face of the heel and ramped to reach 1610N (the static proof load at the P3 level) as shown in Figure 208.

B4.3.5 Analysis settings

The model was set to run over 4.6 seconds split into 250 sub steps, this gave a loading rate of 175N/s, which was midway in the range of 100N/s to 250N/s specified in ISO 10328. Weak springs were turned off, large deflection was turned on while inertia relief was off, and the solver type left as program controlled.

B4.3.6 Results

The maximum deformation at first yield of the R1 model was 3.2mm on the tip of the model where the force was applied. For R2 the same location had 2.9mm as the largest deformation at yield. See Figure 210 for images of the deformation at yield.

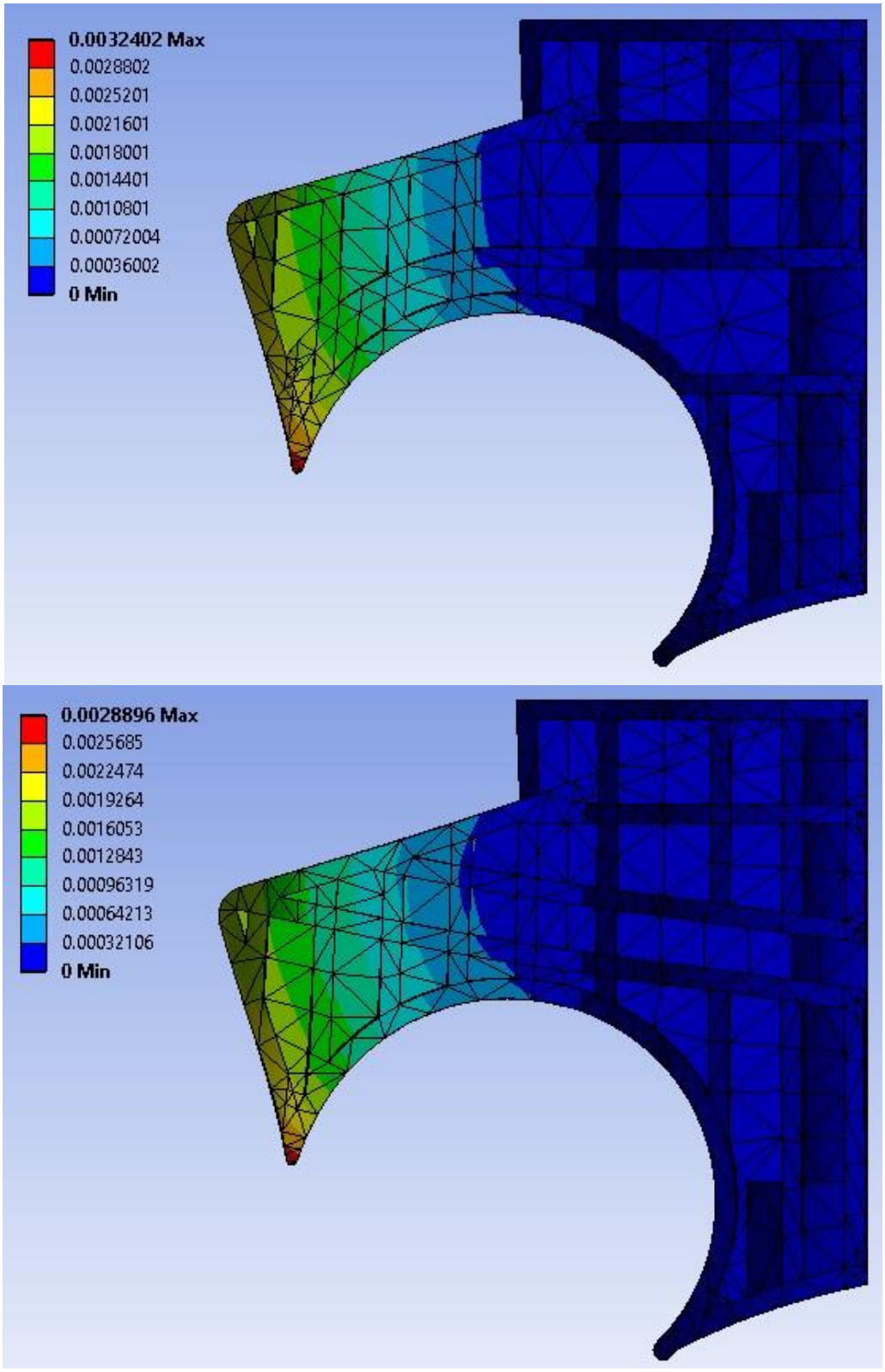

Figure 210 – Maximum deformation at first yield in heel models; R1 (top) and R2 (bottom)

The initial yield point of either model was on the rear face of the heel just above where the load was applied. This was considered to be an artefact of the model construction and not a likely location for failure to occur in testing conditions. In R1 a further three areas of high stress were highlighted, as shown in Figure 211, Figure 212 and Figure 213.

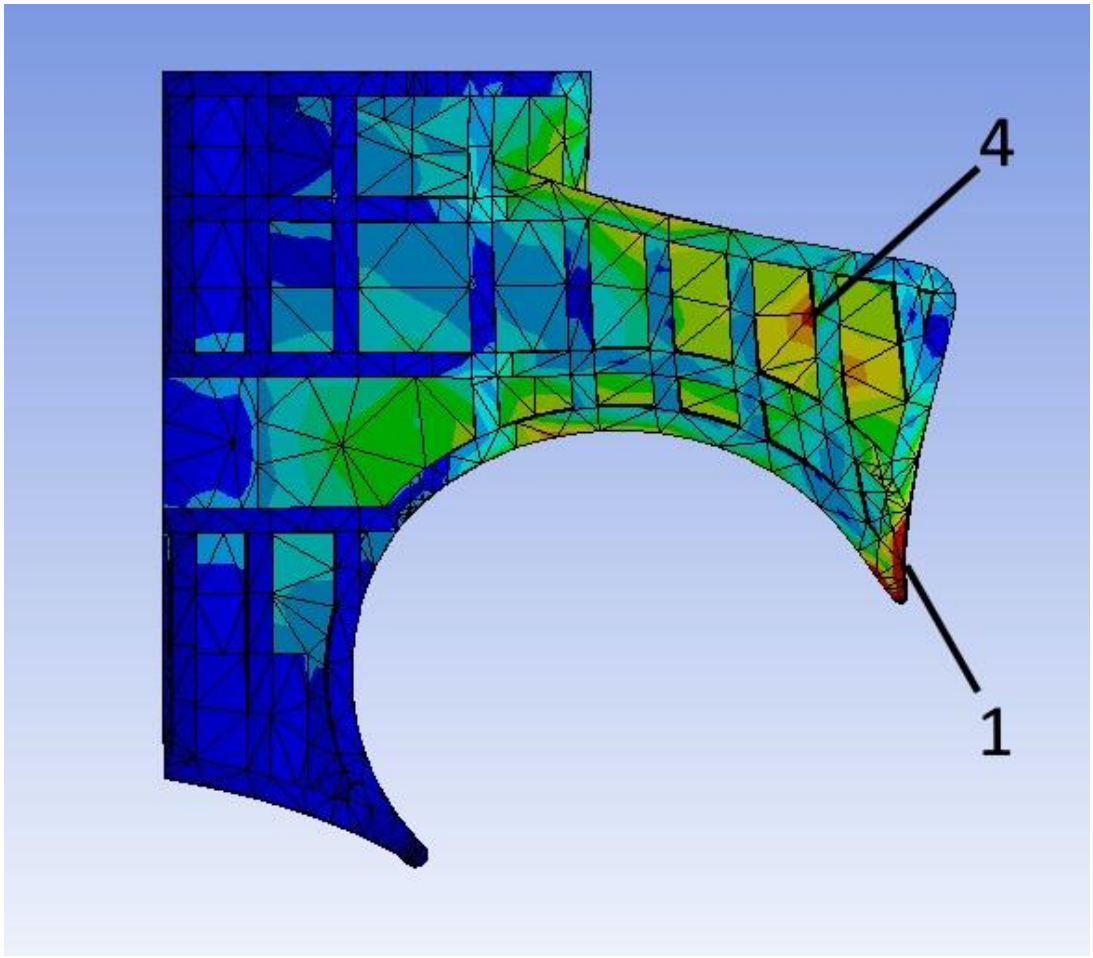

Figure 211 – High stress areas 1 and 4 from R1 heel model

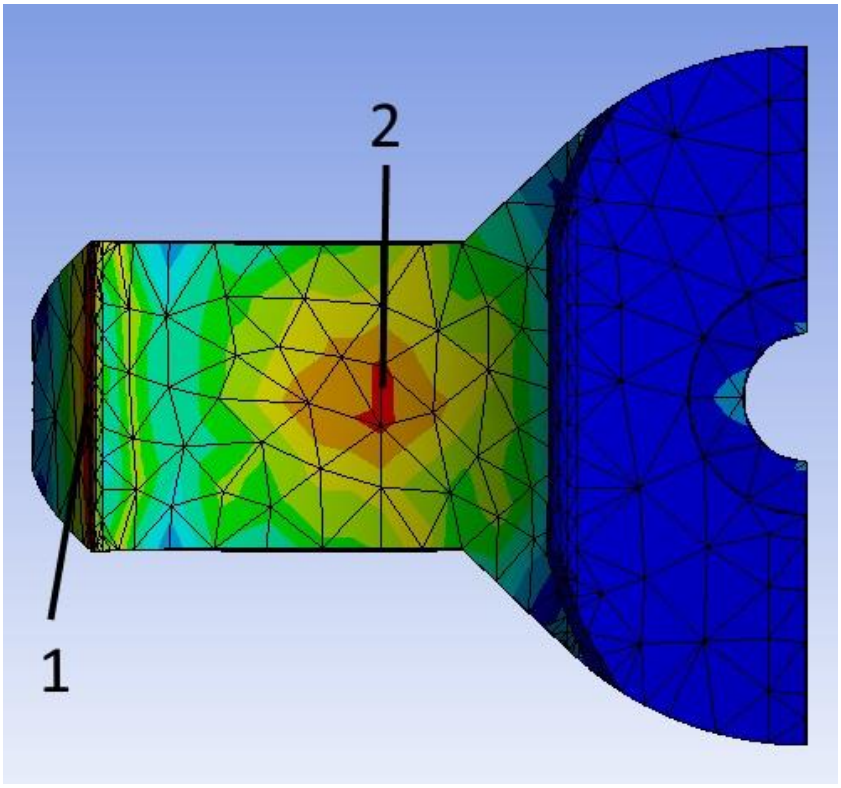

Figure 212 - High stress areas 1 and 2 from R1 heel model (view from below)

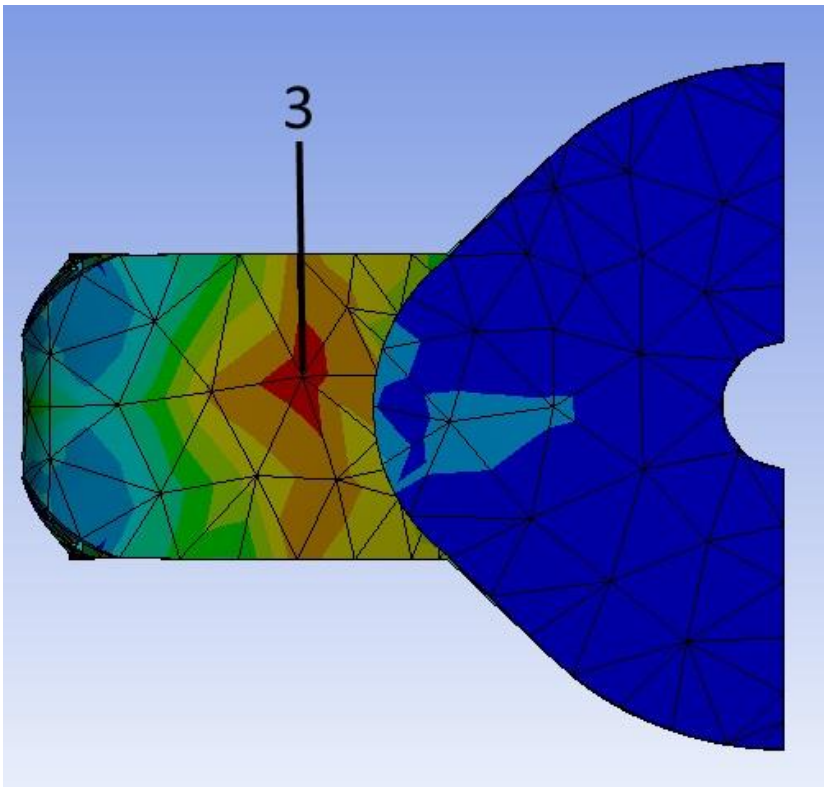

Figure 213 - High stress area 3 from R1 heel model (view from above)

Point 4 seen in the R1 heel loading model was not present in the R2 model. Where high stresses occurred in this area in R2 was due to the increasing stress around point 1. Figure 214, Figure 215 and Figure 216 show the high stress points of interest in the R2 heel loading model.

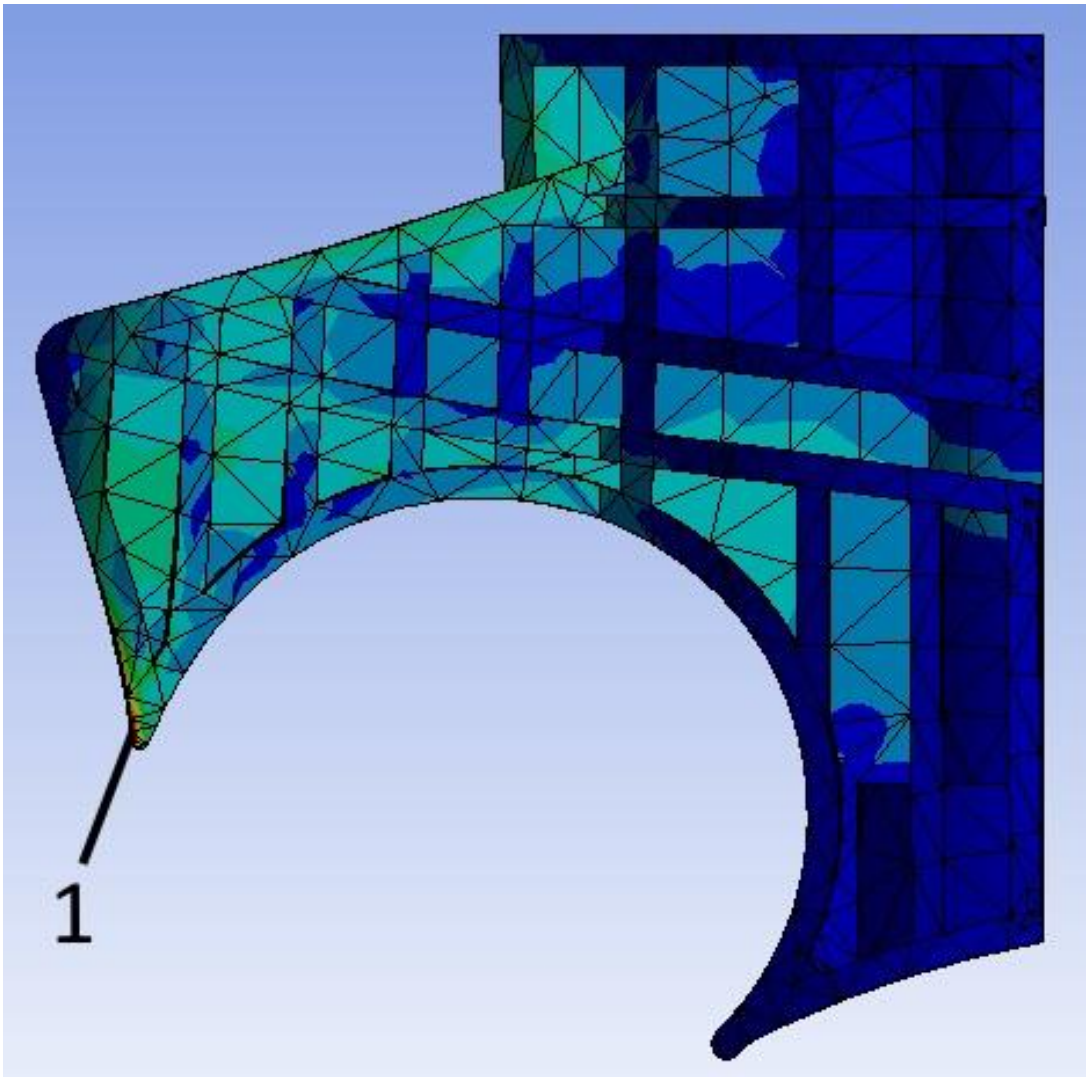

Figure 214 – Stress point 1 in the R2 heel loading model

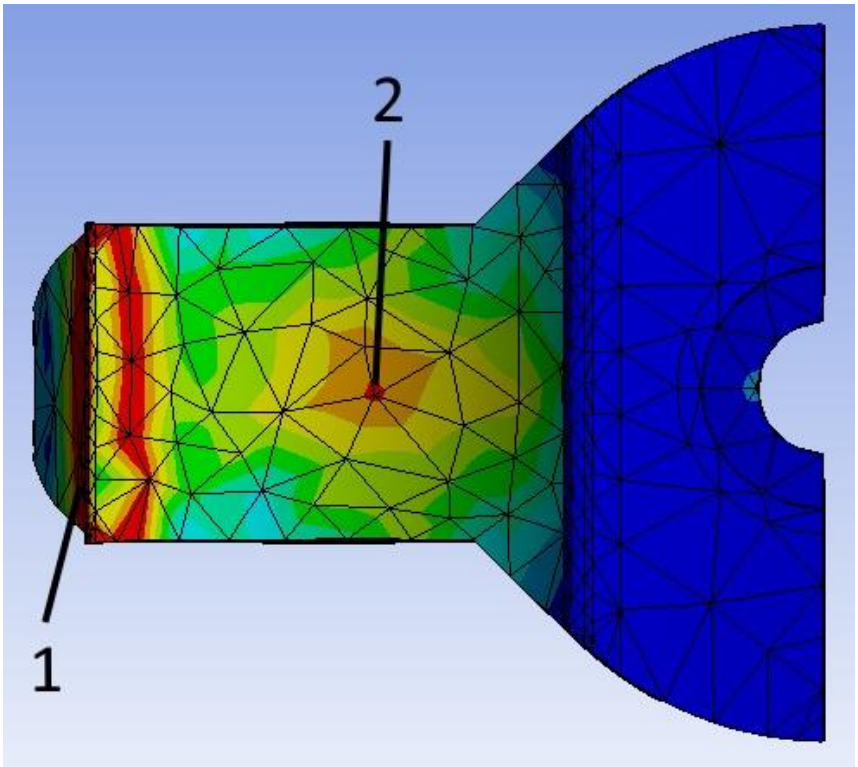

Figure 215 – Stress points 1 and 2 in the R2 heel loading model (view from below)

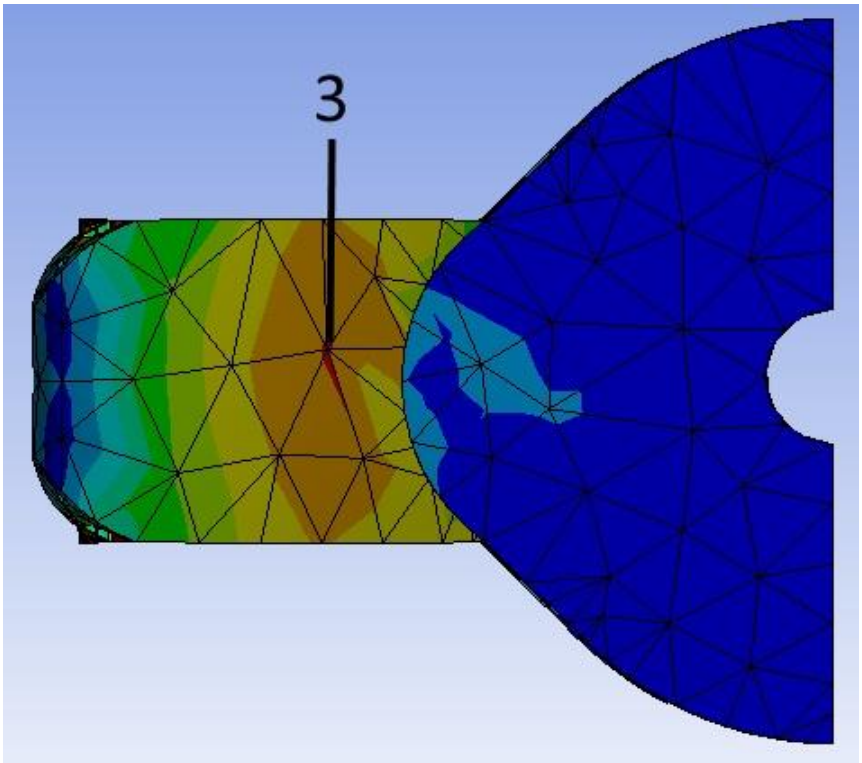

Figure 216 – Stress point 3 in the R2 heel loading model (view from above)

The load at yield for both models at the points indicated was as follows:

	R1	**R2**
Point		
1	534.5N	515.2N
2	827.5N	946.7N
3	949.9N	1030.4N
4	949.9N	N/A

Table 23 – Comparison of load at yield of heel loading model for R1 and R2

B4.3.7 Discussion

The load at yield of point 1 in R2 was lower than that of R1 however, the failure of this point was due to the loading conditions and was not expected to be seen in physical testing of prototypes.

The load at yield of both point 2 and point 3 was increased from R1 to R2 by 119.2N and 80.5N respectively. This suggested that the two transverse (as opposed to vertical) ribs increased the load to yield when compared to the single curved rib present in R1 as there were no other changes in the heel section. Point 4 as identified in R1 (see Figure 211) was not present in R2 due to the changed stress distribution caused by the change to the rib design in the heel.

In previous heel testing “B3.3 Heel modification” the “tall heel, narrow gaps” model is equivalent to the R1 model in this case. Different boundary conditions were applied in comparing R1 to R2 however, the high stress areas observed in both models were similar, with the exception that point 1 in the previous model was found to be in the corner where the vertical support met the angled slope, compared to point 3 in this model which was found to be on the top surface of the heel but away from the vertical support. The order of failure was different between models, with points 3 and 1 swapping positions between models, however the values were within

60N of one another in either case (see Table 24). Points 2 and 4 showed greater difference in load at yield with R1 reaching yield at point 2 at 90N less than the “tall heel, narrow gaps” model but point 4 required 139N more load to reach yield.

	Tall heel, narrow gaps	**R1**
Point **(Tall heel/ R1)**		
1/3	889N	949.9N
2/2	915N	827.5N
3/1	586N	534.5N
4/4	811N	949.9N

Table 24 – Comparison of results from section B3.3 and R1 model

B4.3.8 Conclusion

The changes made to the heel from R1 to R2 were an improvement to the strength of the heel section, although excessive loading on the lower tip of the heel may cause local failure at a lower load than in R1.

B4.4 Ankle block FEA

The changes made to allow for an energy return feature modified the rib pattern of the ankle block and so FEA was carried out to evaluate these changes. The design evaluated in “B3.6 Whole design evaluation” was that of R1 so was not reproduced here but the details of R2 are below.

B4.4.1 Material properties

The same material properties were used as for the previous models (see B3.1.2 Material properties).

B4.4.2 Boundary conditions

The flat top surface of the keel was fixed as a support (see Figure 217). Symmetry was applied to the faces on the centreline.

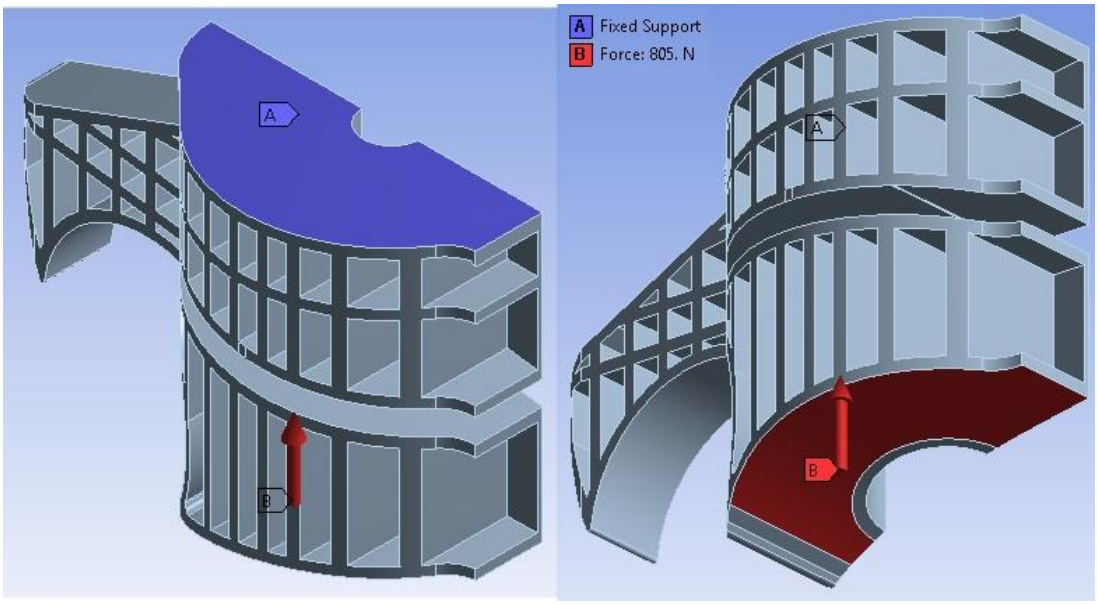

Figure 217 – Boundary condition on main block loading of R2 design

B4.4.3 Mesh

The entire model was meshed using a relevance centre setting of ‘coarse’ with a medium smoothing and fast transition (see Figure 218).

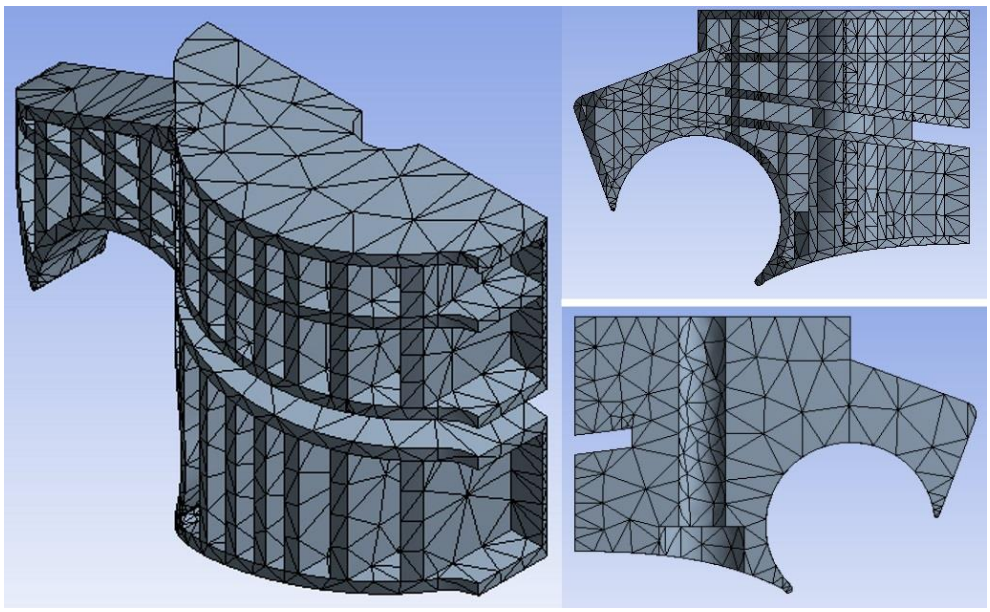

Figure 218 – Mesh of ankle block loading for R2 model

B4.4.4 Loading

A load was applied on the faces of the underside of the keel (see Figure 217), acting vertically upwards and ramped to reach 805N (half the static proof load at the P3 level).

B4.4.5 Analysis settings

The model was set to run over 4.6 seconds split into 250 sub steps, this gave a loading rate of 175N/s, which was midway in the range of 100N/s to 250N/s specified in ISO 10328. Weak springs were turned off, large deflection was turned on while inertia relief was off, and the solver type left as program controlled.

B4.4.6 Results

At maximum load a deflection of the lower half of the keel was viewed, reaching a maximum of 0.9mm at the underside of the front edge (see Figure 219).

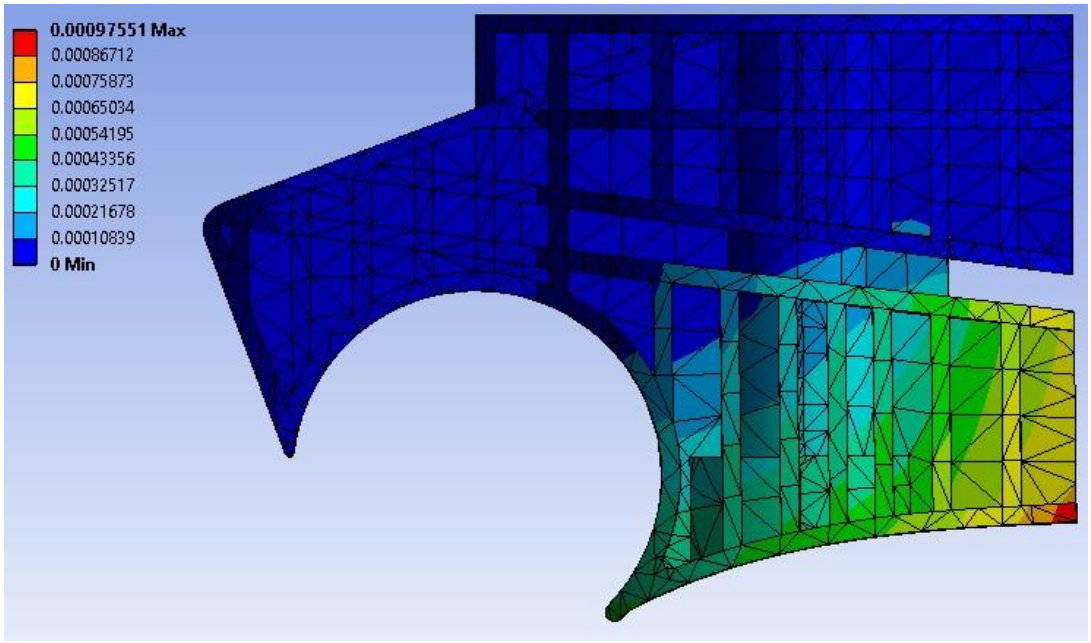

Figure 219 – Deflection at maximum loading of ankle block model of R2 (values in m)

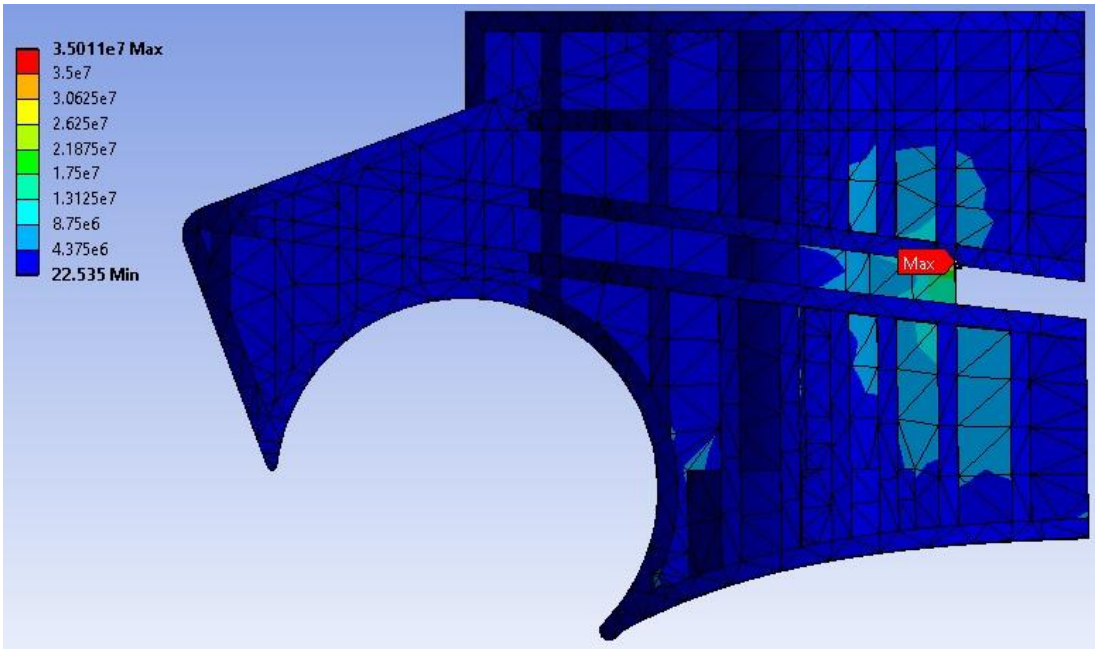

Figure 220 – Stress at maximum load on ankle block model of R2

Yield stress was only reached at the maximum load of 805N in a single location, where the top edge of the vertical support running along the centreline of the keel met the upper section of the keel. No other area showed a high stress under this loading.

B4.4.7 Discussion

A single high stress point was similar to that observed in the R1 design (see Figure 177) however the location had changed slightly. In the R1 design it was observed in the centre of the vertical support however in the R2 design it was in the upper corner of the support. As the load was applied in a similar manner on both models, the same moment generation observed in section B3.4.7 Discussion, also applies to interpretation of this model with the upward deflection of the lower section causing stress to build in the relatively flexible mid section of the foot. The location of the corner in this case.

B4.4.8 Conclusion

The R2 design appeared to be equally capable as the R1 design with both only reaching yield stress at the maximum load per the P3 static condition.

B4.5 Edge loaded ankle block FEA

The R2 design was modelled as being loaded in edge load conditions as the R1 design was previously in B3.5 Vertical edge loading of keel. The same method was to be applied to the R2 model, detailed below.

B4.5.1 Material properties

The same material properties were used as for the previous models (see B3.1.2 Material properties).

B4.5.2 Boundary conditions

The flat top surface of the keel was fixed as a support (see Figure 221).

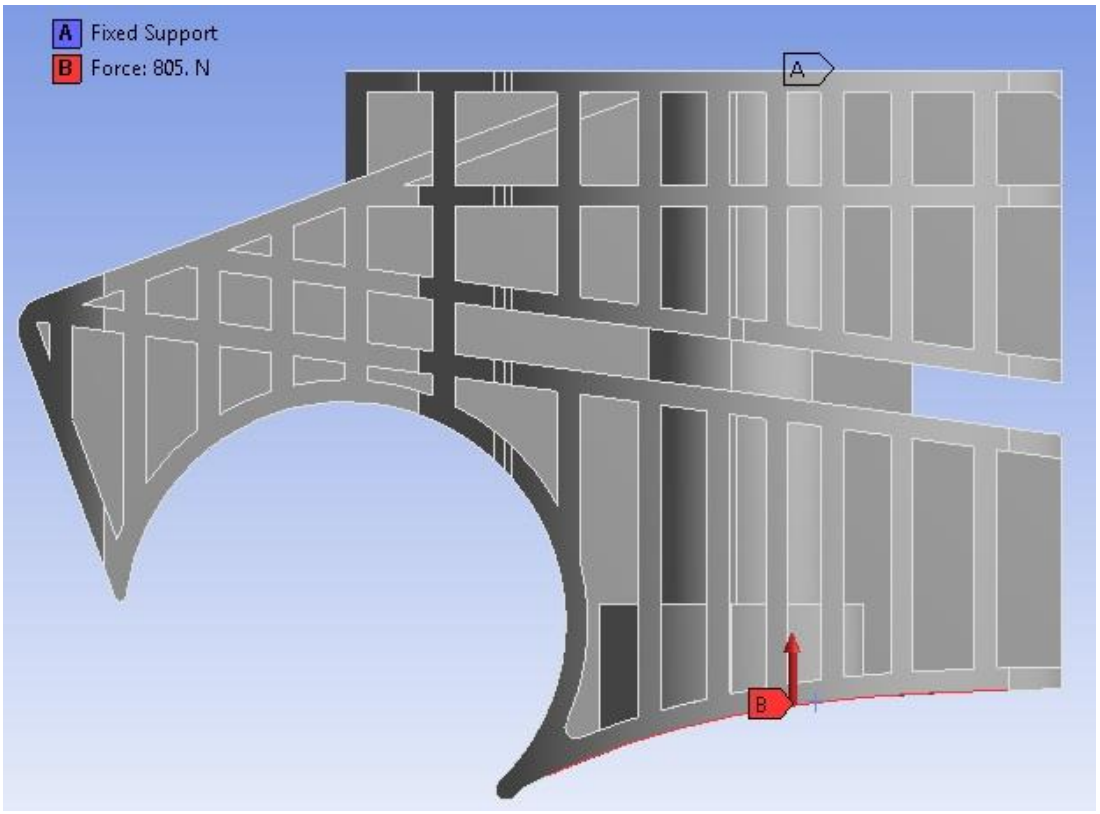

Figure 221 – Boundary conditions of edge loading model for R2 design

B4.5.3 Mesh

The entire model was meshed using a relevance centre setting of ‘coarse’ with a medium smoothing and fast transition. The contact areas were then further refined by element size, which was set to 0.002m (see Figure 222).

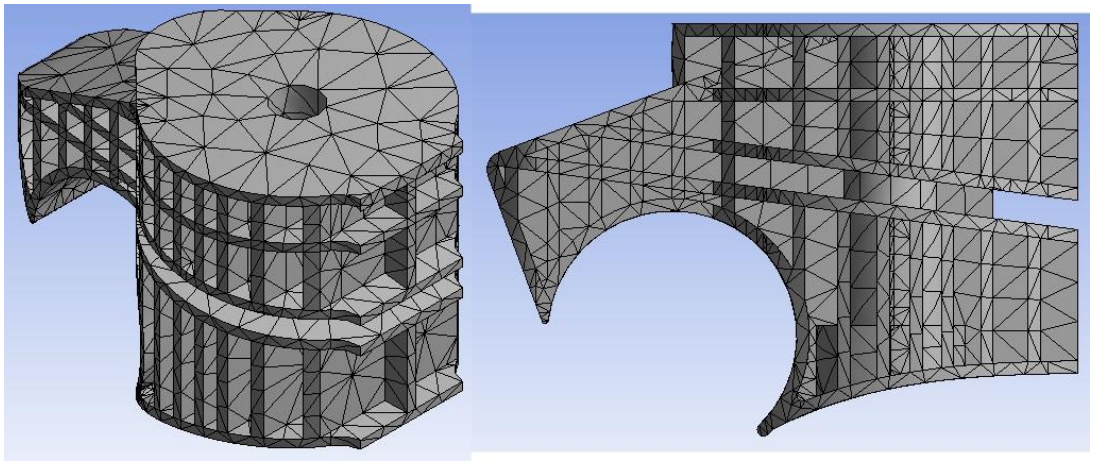

Figure 222 – Mesh used for edge loading model of R2 design

B4.5.4 Loading

A load of 1610N (the P3 static load from ISO 10328) was applied to the edges on the side of the mid-section of the keel at the bottom, vertically upwards (see Figure 221). This loading condition was not specified or required by ISO 10328 but was felt to be useful as a benchmark.

B4.5.5 Analysis settings

The model was set to run over 9.2 seconds split into 500 sub steps, this would give a loading rate of 175N/s, which was midway in the range of 100N/s to 250N/s specified in ISO 10328. Weak springs were turned off, large deflection was turned on while inertia relief was off, and the solver type left as program controlled.

The required information from the solution was total deformation, directional deformation, equivalent elastic strain and equivalent stress.

B4.5.6 Results

During loading a number of high stress points became visible, shown in Figure 223 and Figure 224. These were numbered the same as the high stress points from B3.6 Whole design evaluation. Points 2 and 3 had not reached yield stress by maximum load in the R2 model so were not included here. An additional high stress point occurred which was numbered as point 6.

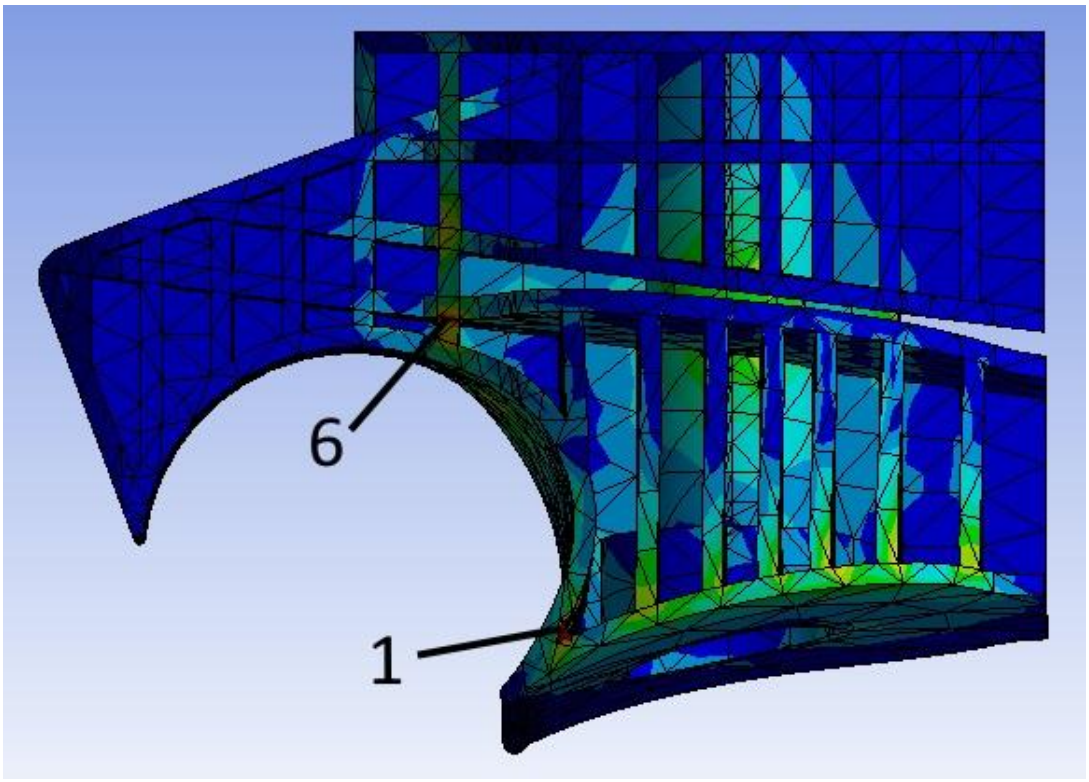

Figure 223 – High stress points 1 and 6 in R2 edge loading model

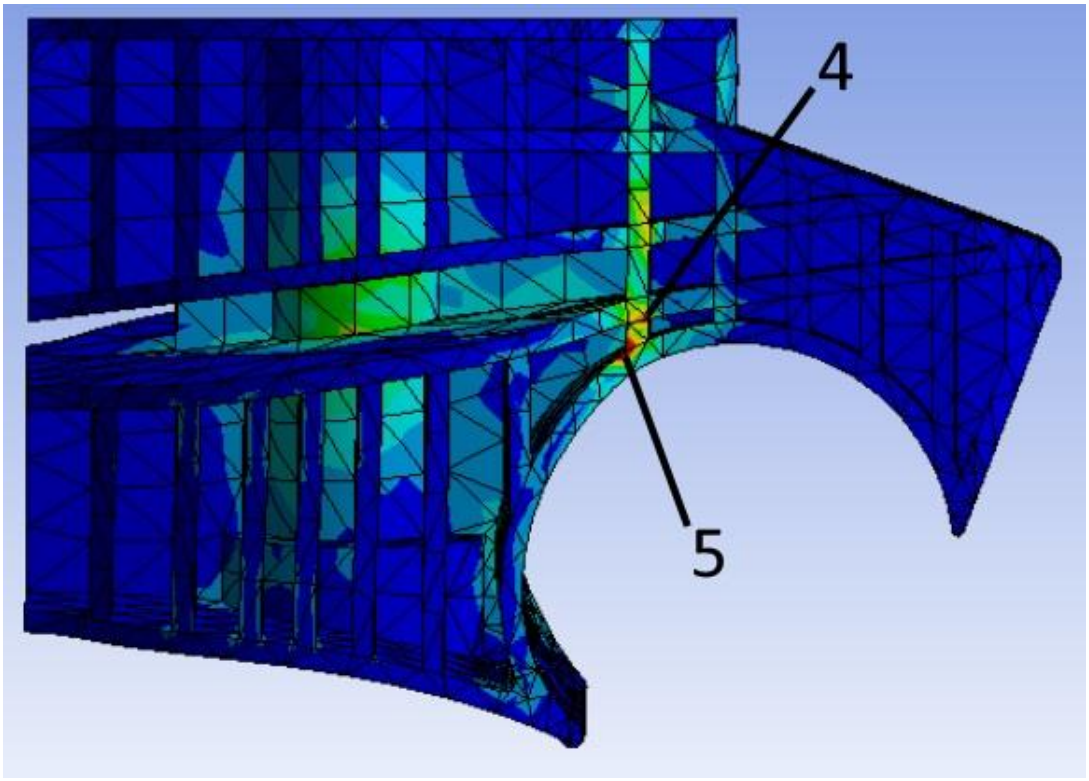

Figure 224 – High stress points 4 and 5 in R2 edge loading model

The results from R2 are listed in Table 25 below as well as the counterparts from R1 described in (section B3.5).

	R1	**R2**
Point		
1	351.0N	669.8N
2	531.5N	N/A
3	631.1N	N/A
4	650.4N	1474.8N
5	673.0N	1230.0N
6	N/A	1423.2N

Table 25 – Load at yield of high stress points in R1 and R2 edge load models

The maximum deformation of R2 was 5.8mm under maximum load compared to 15.5mm in R1 (see Figure 185 in B3.6.6 Results).

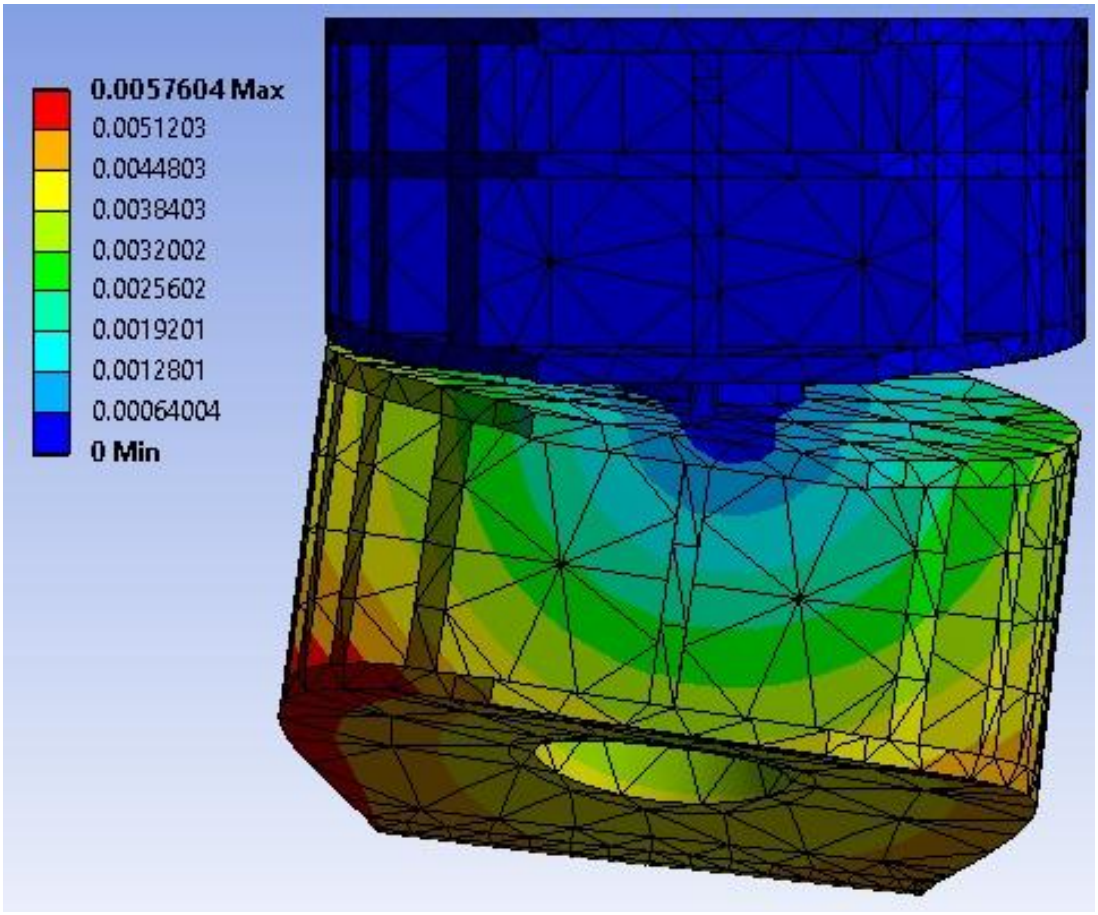

Figure 225 – Deflection of R2 design under maximum edge load

B4.5.7 Discussion

The same caveat regarding loading conditions being unrepresentative of real-world conditions applies as in the models of B3.6 Whole design evaluation. As in the R1 model the high stress point 1 was a result of the loading conditions and not considered relevant Points 2 and 3 from R1 were no longer present in R2, with the reduced gap between upper and lower keel sections serving to reduce the stress occuring in this area. The absence of these points was positive in that the lowest load at yield (excluding point 1) increases from 531.5N to 1230.0N suggesting that the R2 keel would be better able to have increased lateral loading before failure.

Although point 6 was a new point of interest the load at yield was higher than that of point 5 and only 51.6N lower than point 4 so still showed improvement from the R1 model. The increase in stiffness (reduced deflection from 15.5mm to 5.8mm) was positive in providing a stable base to the prosthesis.

B4.5.8 Conclusion

The changes made to the mid-section appeared to provide improvements in terms of stiffness and load to yield in the R2 design over the R1 design although it was still less stiff than the existing Strathclyde design. Models of the R1 and R2 design were to be carried out including the blade feature and a fixed support representing the bolt inserted into the keel.

B4.6 Modified edge loaded ankle block FEA

Both the R1 and R2 design would be used with a bolt in the bolthole, of a relatively high stiffness compared to the material of the keel itself. The boundary conditions of the previous model did not take this into account and so permitted flexing of the central column in either keel. The intention of this model was to include conditions in the model to reflect this central bolt. The blade to be included in the midsection would also limit the deflection possible and so was also included in either case.

B4.6.1 Material properties

The same material properties were used as for the previous models (see B3.1.2 Material properties for polypropylene properties and B3.7.4 Duraform EX model including blade setup for fibreglass properties).

B4.6.2 Boundary conditions

The flat top surface of the keel was fixed as a support (see Figure 226). Additionally, the inside faces of the bolthole were fixed.

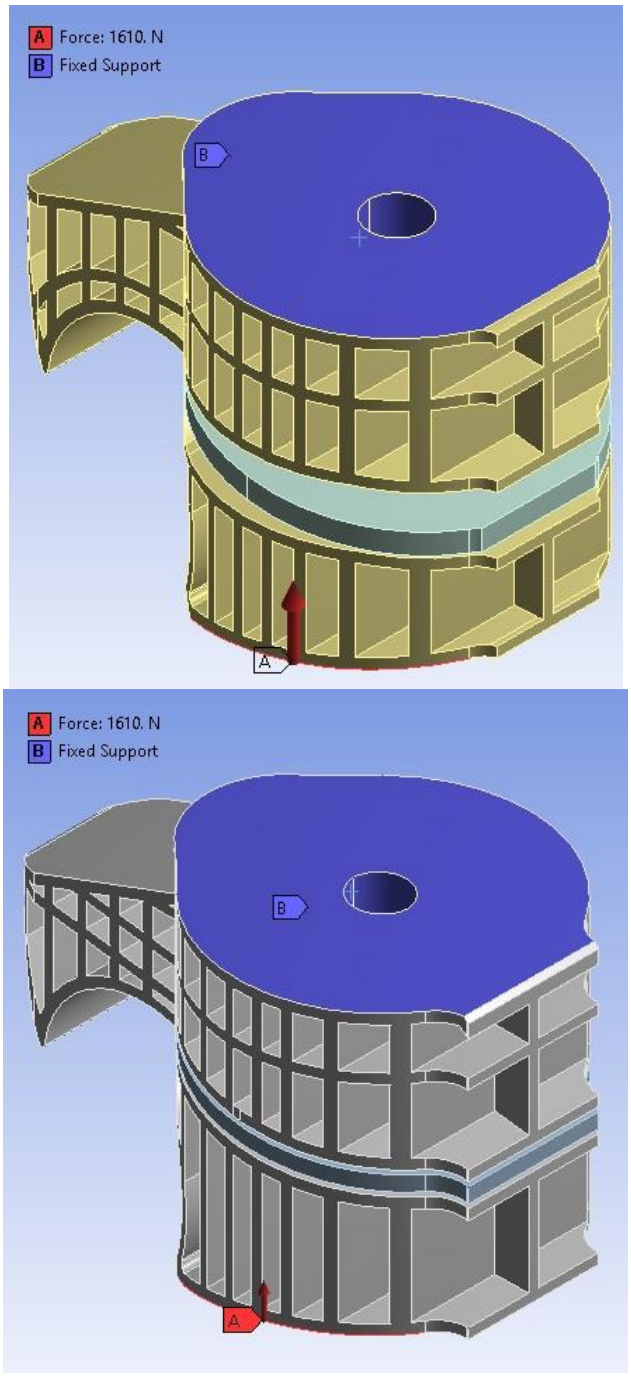

Figure 226 – Boundary condition of R1 (top) and R2 (bottom) in the modified edge loaded ankle block model

The bonded surfaces were different in either case. The R1 model was bonded at the sites shown in Figure 227. Site 1 was between the side wall of the vertical support in the keel and the inside of the cut out in the blade. Site 2 was between the top rear corner of the blade and the underside of the top section of the keel. Site 2 was between the bottom rear corner of the blade and the flat, vertical face at the rear of the blade cut outs in the keel. Each of these sites was mirrored on the opposite half of the model.

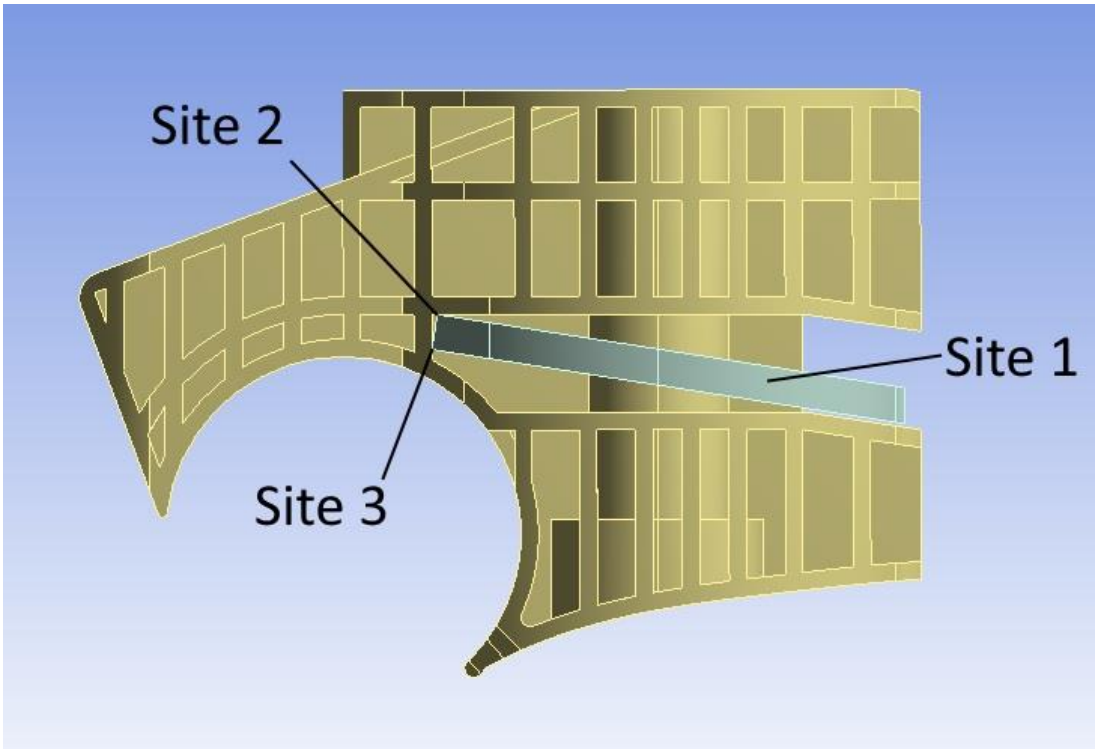

Figure 227 – Bonding sites used in the R1 model for edge loading

In R2 a single bonding site was used to connect the rear face of the blade to the flat, vertical face of the cut out for the blade in the keel (see Figure 228).

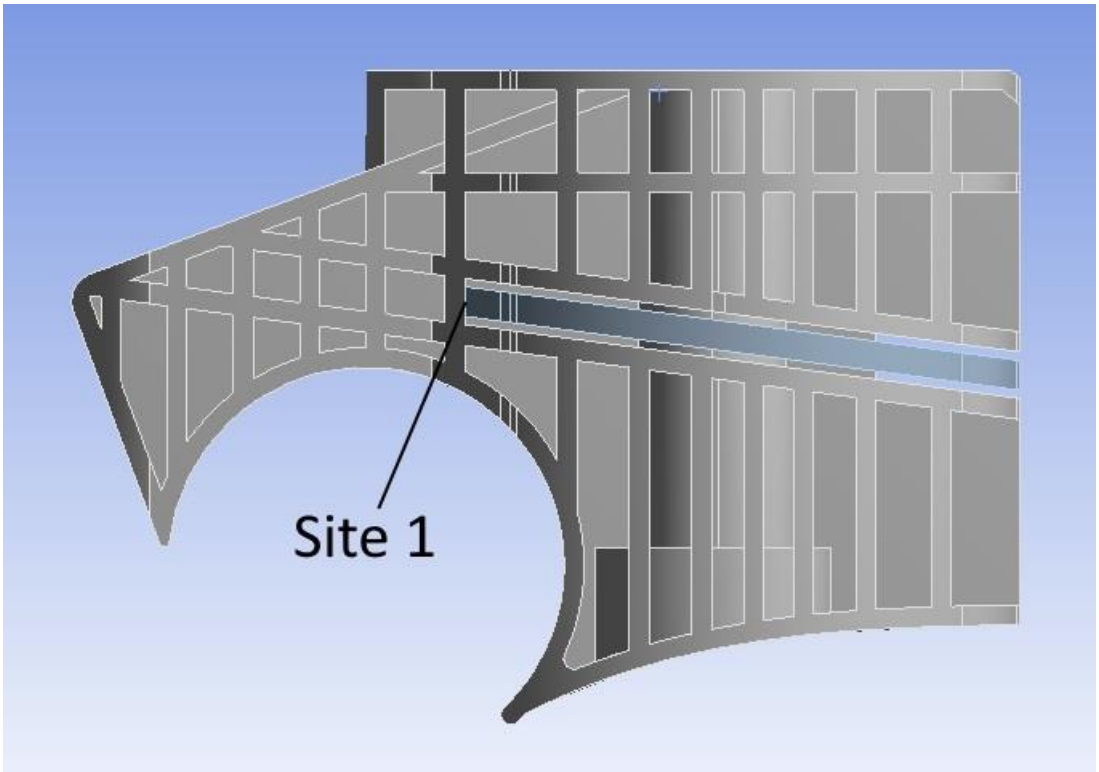

Figure 228 – Bond site used in R2 edge loading model

B4.6.3 Mesh

Both models were meshed using a relevance centre setting of ‘coarse’ with a medium smoothing and fast transition (see Figure 229).

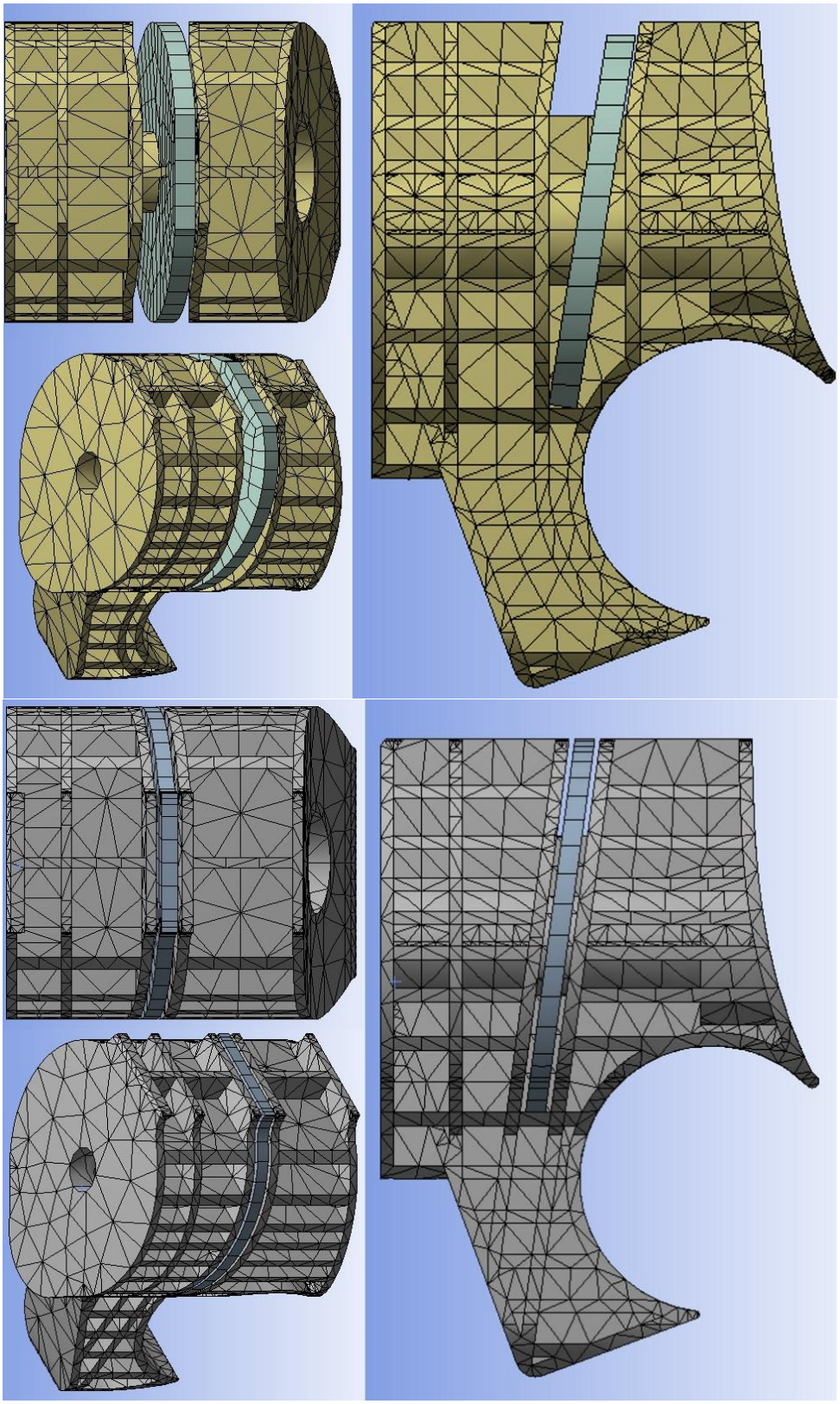

Figure 229 – Mesh used for modified edge loading model of R1 design (top) and R2 design (bottom)

B4.6.4 Loading

A load of 1610N (the P3 static load from ISO 10328) was applied to the edges on the side of the mid-section of the keel at the bottom, vertically upwards (see Figure 226). This loading condition was not specified or required by ISO 10328 but was felt to be useful as a benchmark.

B4.6.5 Analysis settings

The model was set to run over 9.2 seconds split into 1000 sub steps, giving a loading rate of 175N/s, which was midway in the range of 100N/s to 250N/s specified in ISO 10328. Weak springs were turned off, large deflection was turned on while inertia relief was off, and the solver type left as program controlled.

The required information from the solution was total deformation, directional deformation, equivalent elastic strain and equivalent stress.

B4.6.6 Results

In the R1 foot the model showed a maximum deflection of 2.4mm at 1610N load at the forward edge of where loading was applied (see Figure 230). This occurred midway between two vertical ribs and was likely the largest deflection due to deformation of the section in between the supports. Little deformation of the blade occurs, with only 1.3mm recorded as a maximum deformation.

In the R2 foot the model showed a maximum deflection of only 1.5mm (see Figure 231). Two areas of higher deformation were visible on the R2 keel, both in between vertical ribs, on the surface where load was applied, as in the R1 model. In this case the blade deflected by only 0.3mm.

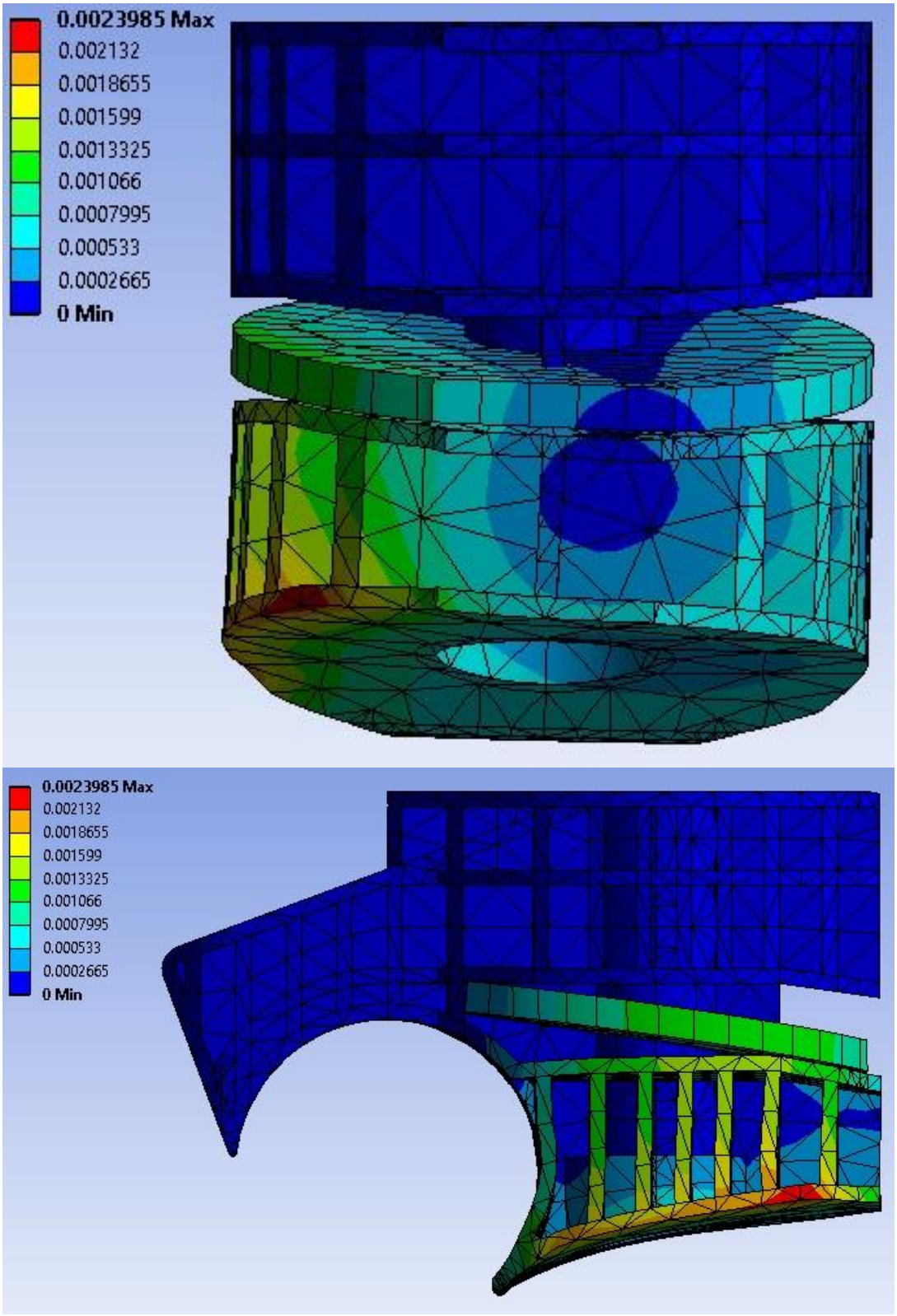

Figure 230 – Deformation of R1 at maximum load, front view (top) and side view (bottom)

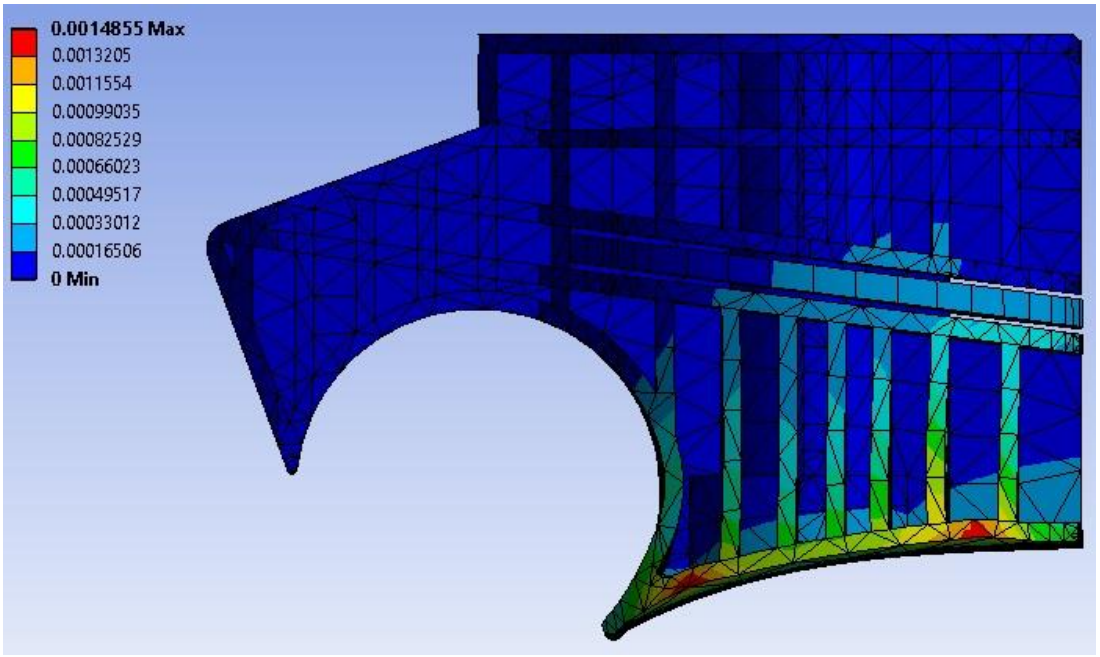

Figure 231 – Deformation of the R2 model at maximum load

Yield stress was reached at several locations on the R1 model before maximum load, with all occurring on the keel. The yield points on the keel all occurred on the forward side of vertical supports where they met the lower face of the keel (see Figure 232). The first yield point reached on the keel was at the rearmost corner of the lower face at 391.2N. The lower edge of the bolthole meeting the recessed area had a higher stress than surrounding areas, but at 2.9×10^7Pa was still below yield at maximum load (see Figure 233).

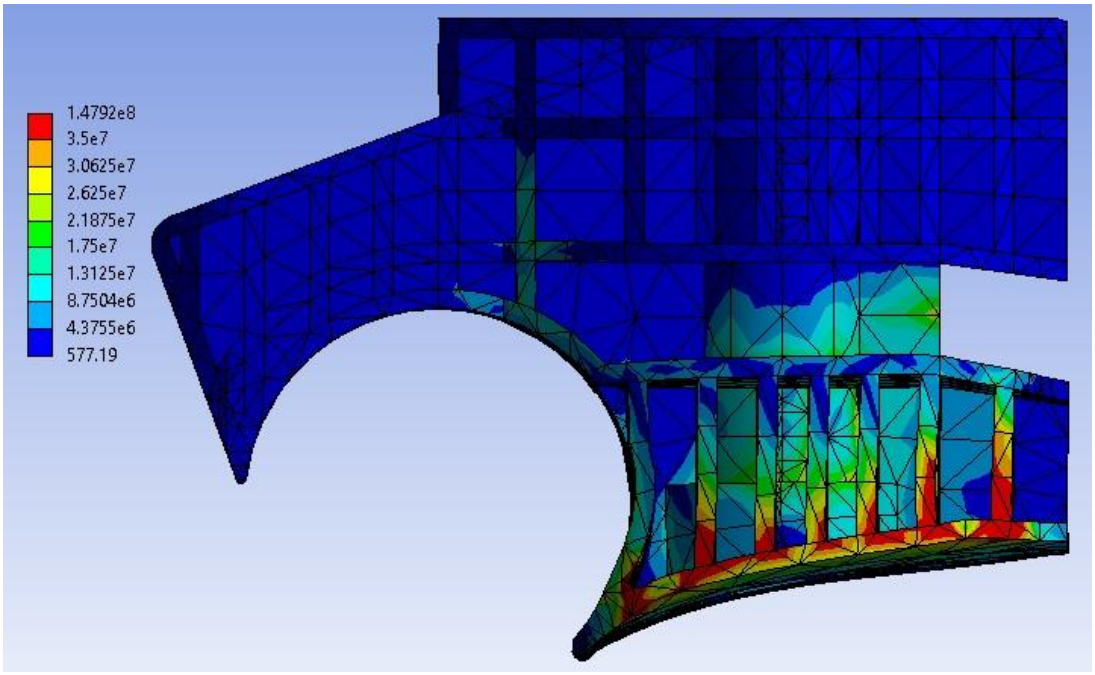

Figure 232 - Stress on the keel of R1 at maximum load (side view)

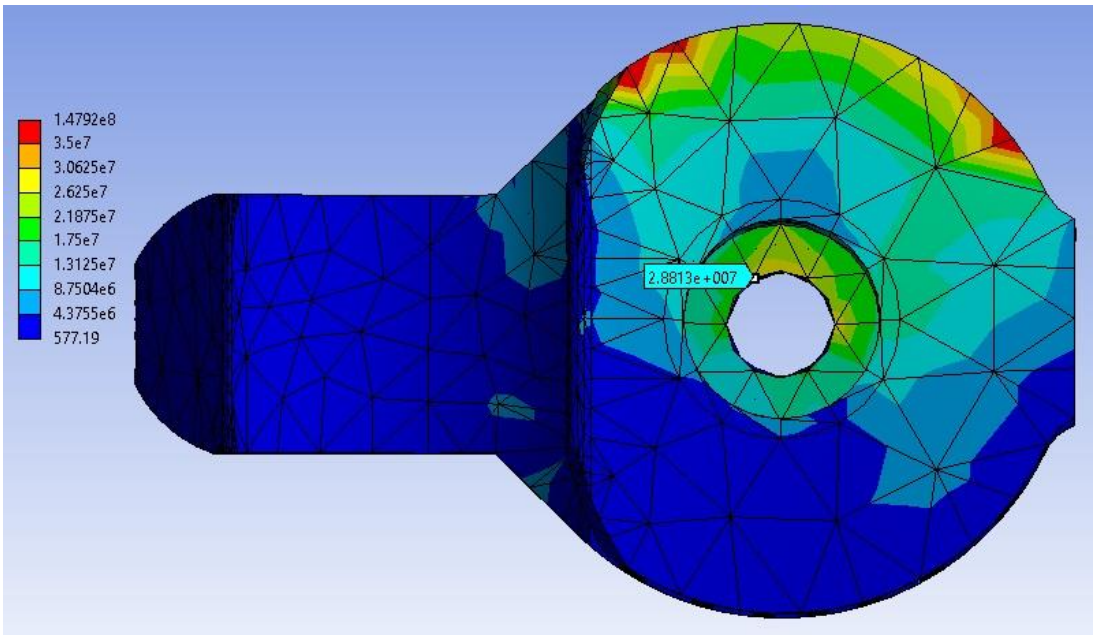

Figure 233 – Stress on the keel of R1 at maximum load (bottom view)

The yield stress of fibreglass was not reached on the blade by maximum load with a maximum stress of 2.1×10^{8}Pa recorded, below the ultimate stress of the fibreglass at 3.45×10^{9}Pa. As the stress was calculated at a sharp corner it was also likely to be higher than what may be expected with a rounded edge in production.

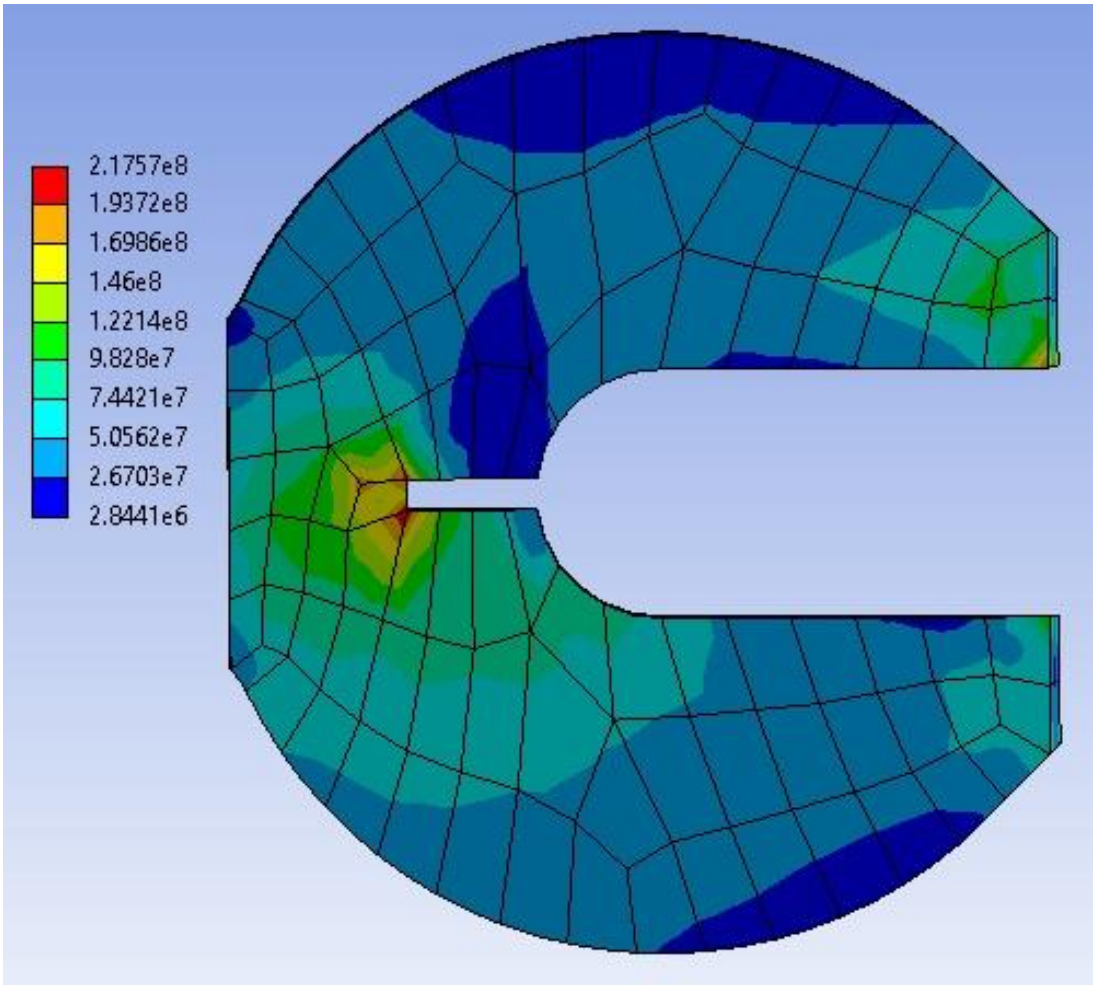

Figure 234 – Stresses on the blade in the R1 model at maximum load (top view)

In the R2 model the first yield point of the keel was observed at 362.3N at the same location as in the R1 model. As load increased the other corners described previously also reached yield stress (see Figure 235). The stresses around the bottom of the bolthole were lower than those observed in the R1 model, peaking at only 1.25×10^{7}Pa.

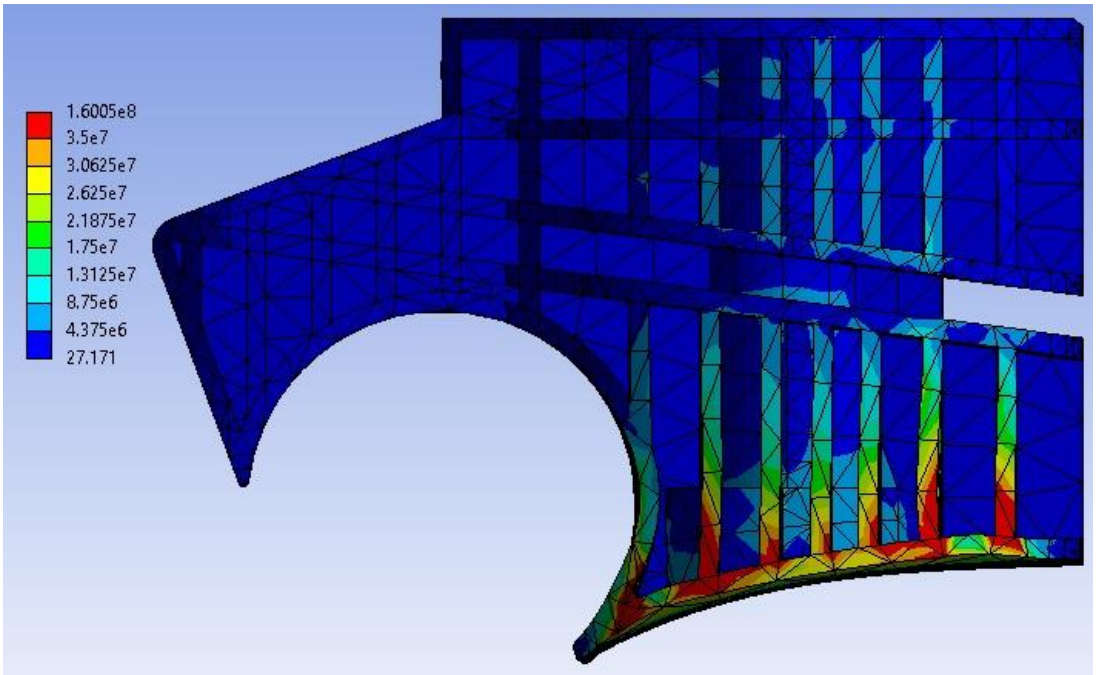

Figure 235 – Stresses on the keel only at maximum load in the R2 model

As in the R1 model the ultimate stress of the fibreglass was not met by the maximum load condition with a peak stress on the blade of 9.45×10^7Pa (see Figure 236). The location of the high stress on the blade was again in the forward corner and so these values were also likely to be higher than with a rounded corner.

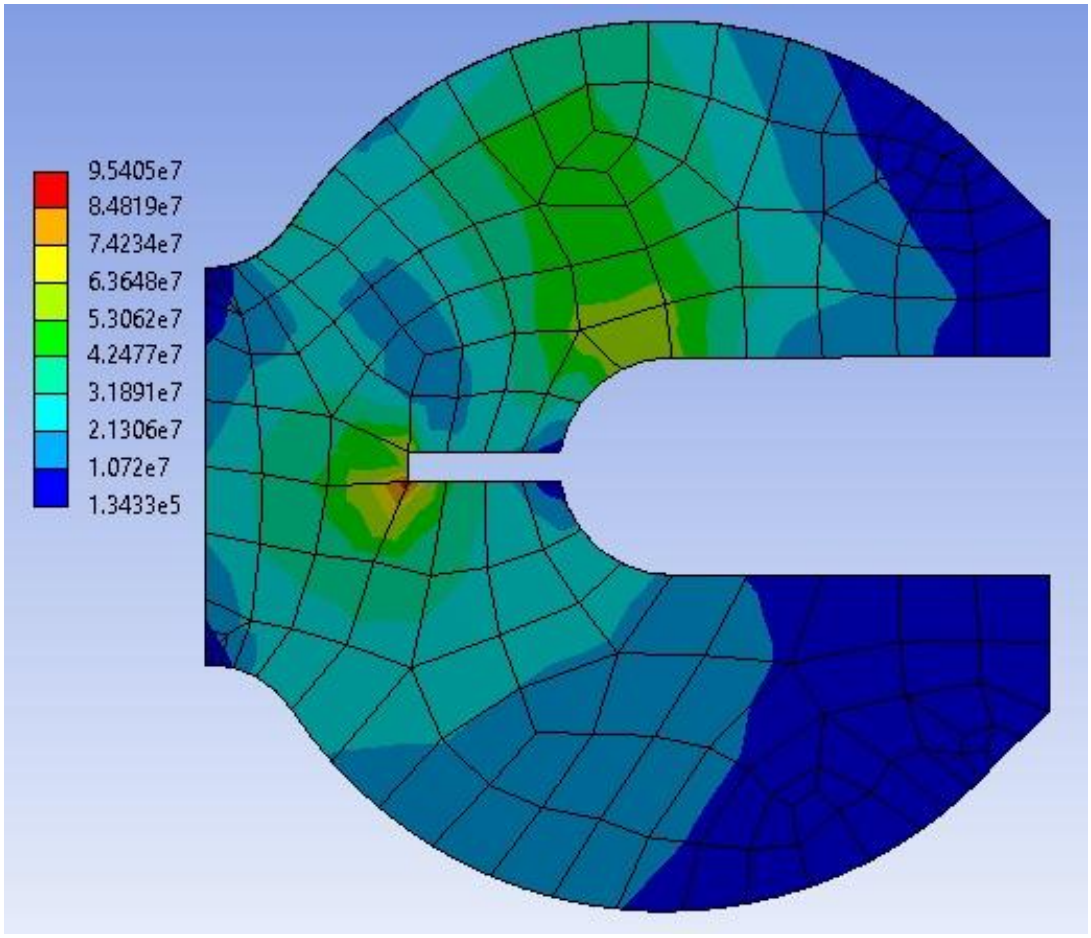

Figure 236 – Stresses on the blade of the R2 model at maximum load

B4.6.7 Discussion

In both cases deformation was reduced under these modelling conditions when compared to the results in (section B3.6 Whole design evaluation and section B4.5 Edge loaded ankle block FEA). By restraining the inside of the bolthole, the central column was unable to flex which then reduced the overall flexibility of the ankle blocks. In doing so the stress on the central areas of either keel design were reduced to the point where at maximum load these areas had not reached yield. The stresses in either case were highest on the side of the foot where load was applied in the corners of the bottom of the keel and the vertical ribs extending from them. This loading condition was unrealistic as it was applied on an edge which would be difficult to achieve as modelled. Without load being as concentrated these areas are

less likely to reach such high stress and were not considered to be a likely failure point for either keel in real-world use. Both blades showed maximum stress at the corner of the central cut out in the front of the blade. This sharp corner led to stress concentration in the model and would be higher than the rounded corner expected in production. In either case the stress was far below the ultimate stress of the fibreglass and so is considered unlikely to fail in loading up to 1610N.

The R2 model was stiffer than the R1 model although it did have higher stresses at maximum load and reach yield stress before the R1 model. The blade in the R2 model did not contact either the upper or lower keel section as it was bonded on the rear face midway. The blade could have been moved to initially be in contact with the lower section which would have likely increased the stiffness of the model however there is no guarantee of the blade initially being in contact with the lower section of the keel. In the R1 case the blade was intended to be installed in such a way as contact would occur between the blade and the lower keel section, so this model setup was deemed appropriate. Without the blades in either case the R2 model would be expected to have a similar performance while the R1 model would be expected to be more flexible. In either case an improvement was seen over the existing Strathclyde design, although that model did not include any energy return feature

The use of a fixed support on the inside of the bolthole in either case constrained the keel model to a greater degree than a bolt would be expected to, as the bolt could flex under loading, unlike the fixed support condition of the model. The performance of the keels would be expected to fall somewhere between the models presented here and those described in B3.5 Vertical edge loading of keel and B4.5 Edge loaded ankle block FEA. The models had a lower load to yield in both cases with the fixed bolthole preventing the central column from flexing and the

deformation remaining localised in the area near the load application, causing the high stresses there.

B4.6.8 Conclusion

The model presented here was a more accurate representation of the performance of the keels, with the R2 keel providing the stiffer response to loading. The model could be made more accurate by including a metal bolt and pyramid adapter with appropriate properties to permit some flexion. The increased stiffness of the bolthole did appear to increase the risk of failure at the loaded edge compared to the previous models however the fixed condition was closer to the conditions of use and so was believed to be better representative.

B4.7 Full foot bladeless polypropylene

Having made several changes and evaluated them separately the entire redesign was evaluated per the conditions of ISO 10328 toe loading. For the initial set up the settings used would be identical to those used to evaluate the existing Strathclyde foot and the R1 design (detailed in section B2.2 Model generation).

B4.7.1 Material properties

The same material properties were used as for the previous models (see B3.1.2 Material properties).

B4.7.2 Boundary conditions

The flat top surface of the keel was fixed as a support with the four vertical sides of the metal plate being treated as frictionless supports. The faces along the centreline split in the model had a symmetry condition applied.

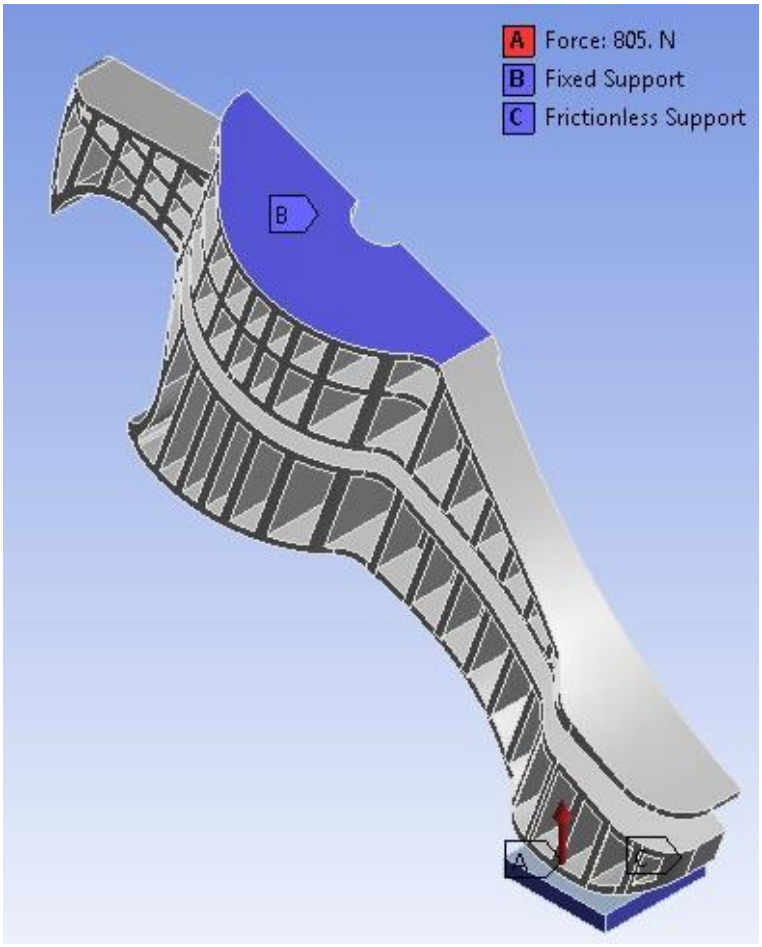

Figure 237 – Boundary conditions on R2 design toe loading model

B4.7.3 Mesh

The entire model was meshed using a relevance centre setting of ‘coarse’ with a medium smoothing and fast transition. The contact areas were then further refined by element size, which was set to 0.002m (see Figure 238).

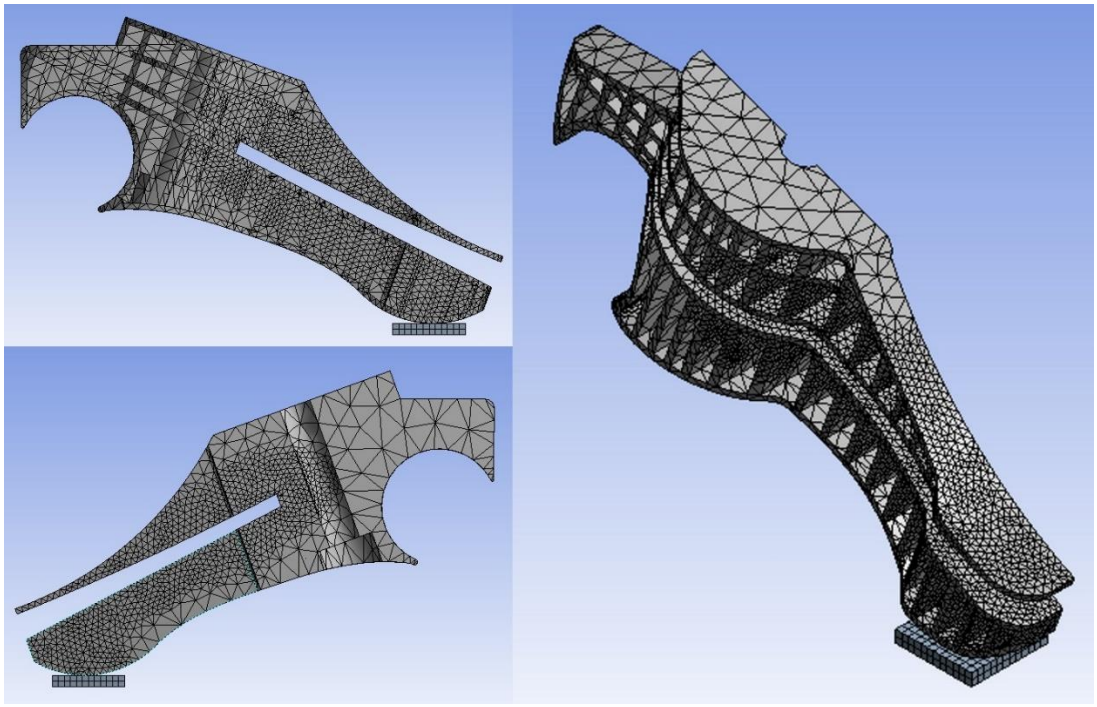

Figure 238 – Mesh of R2 design toe loading model

B4.7.4 Loading

A load was applied on the underside of the steel plate, acting vertically upwards and ramped to reach 805N (see Figure 237).

B4.7.5 Analysis settings

The model was set to run over 4.6 seconds split into 250 sub steps, this gave a loading rate of 175N/s, which was midway in the range of 100N/s to 250N/s specified in ISO 10328. Weak springs were turned off, large deflection was turned on while inertia relief was off, and the solver type left as program controlled.

B4.7.6 Results

The bottom section of the toe was observed to have deformed upwards, meeting the upper section of the toe, which then reduced the rate of deformation. The maximum deformation calculated was 21.0mm at the tip of the bottom toe section. The maximum deflection on the upper toe section was 13.3mm (see Figure 239).

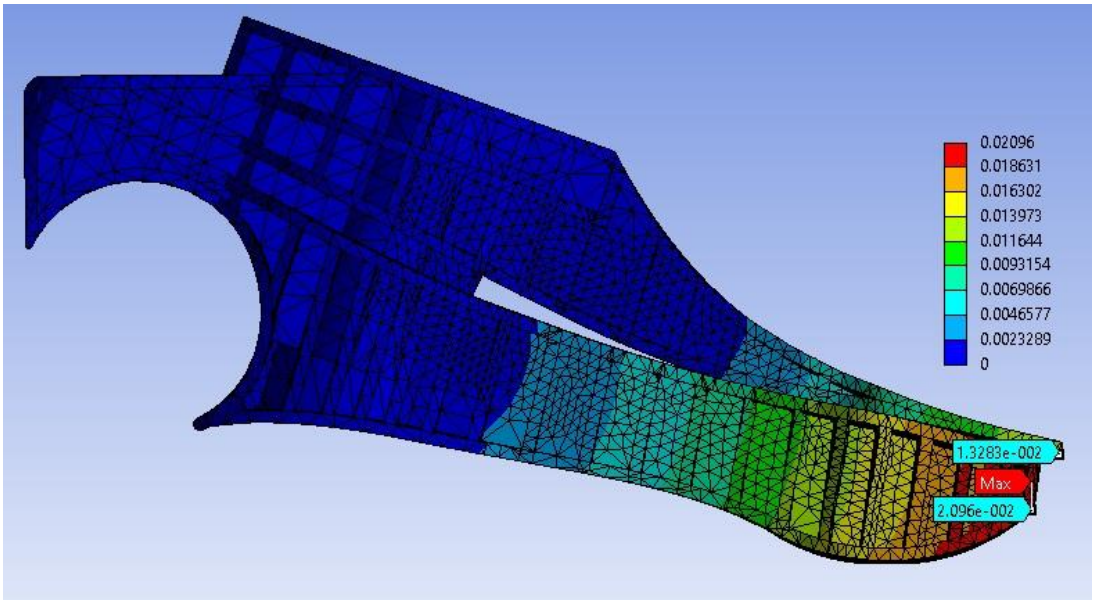

Figure 239 - The deformed condition of the R2 design shown at 805N model load.

In the analysis four major areas of high stress became apparent and were highlighted in Figure 240. The numbers follow those of B3.6 Whole design evaluation however as the equivalents of points 2 and 5 had not met yield stress by maximum load they were not included. A new point of high stress was apparent, and this was included as point 6.

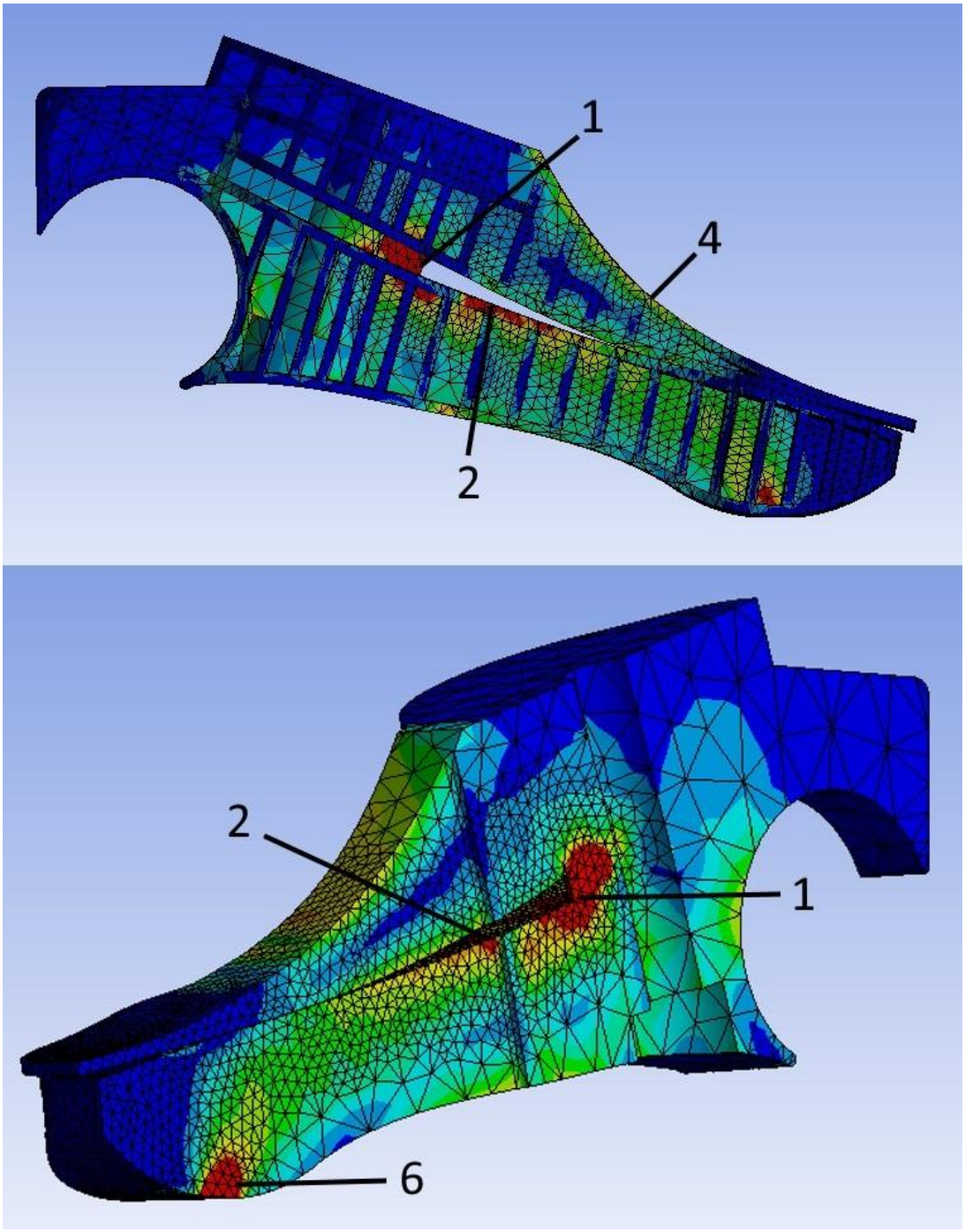

Figure 240 – The high stress areas in the R2 design with identifying numbers.

$3.5x10^7$Pa (the yield stress of the polypropylene) was first passed at area 1 at a load on the model of 122.4N (244.8N on the full foot).

In area 2 the tensile yield stress was reached at 437.9N (875.8N on the full foot).

In area 4 the tensile yield stress was reached at 708.4N (1416.8N on the full foot).

In area 6 the tensile yield stress was reached at 228.6N (457.2N on the full foot).

B4.7.7 Discussion

The highest deflections of the lower and upper toes sections were less than those seen in the R1 model, confirming that the changed lower section of the keel had increased the stiffness of the lower toe.

The new high stress area observed at point 6 was not considered to be relevant to the analysis as it was caused by the unfilleted corner contacting the loading plate, causing high stress to be calculated. In production the corner would be filleted and so would reduce this stress concentrating effect.

Point 1 was the first point to reach yield stress in the R2 model as it was in the R1 model however the load was slightly reduced in the R2 model, from 135.2N to 122.4N. The shorter vertical support upon which point 1 was found was less flexible in the R2 model than the R1 model and so will deflect less and raise stresses.

Point 2 was the second point to reach yield stress in either design (if excluding point 6 from R2) however the load required in the R2 model was approximately three times higher than in the R1 model (see Table 26). This was due to flexion of the toe section being spread across the region and so distributing the stress as the corner present in R1 was removed in favour of a flat top to the lower section of the keel.

Points 3 and 5 did not reach yield stress in R2 by the maximum load. This was a positive development as point 3 appears to be approximately where the failures of the prototype samples occurred during testing in section 4.5 P3 toe tests. Again, the removal of the corner on the top of the lower foot section will have contributed to this

as well as the increased stiffness of the lower section not contacting the upper section leading to the higher load to yield of point 4 and the absence of point 5.

	R1 design	**R2 design**
Point		
1	135.2N	122.4N
2	141.7N	437.9N
3	154.6N	N/A
4	541.0N	708.4N
5	566.7N	N/A
6	N/A	228.6N

Table 26 – Load at which yield stress is reached for each point in the bladeless R1 and R2 designs

B4.7.8 Conclusion

The changes made to the design generally had a positive effect on the behaviour of the keel. Point 1 did show a lower load to yield in the R2 design than in the R1 design but only by a small amount and this was not a failure point observed in prototype testing (see section 4.5 P3 toe tests). The inclusion of fillets into the model would reduce the concentration of stresses around corners and so increase the load to yield, a feature that is highly recommended for production. The model was to be repeated with the properties of Duraform EX used instead of polypropylene to allow comparison to physical prototypes.

B4.8 Duraform EX models

As with the R1 design, prototype models were to be produced via SLS from Duraform EX. Models of toe loading, with and without a blade, were formed using material properties for Duraform EX to allow comparison to physical test results.

B4.8.1 Bladeless model setup

The model that was used in section B4.7 Full foot bladeless polypropylene, was used again with the only change being the material of the keel being changed to Duraform EX with the following properties:

Density	1010 kgm^{-3}
Young's Modulus	1.281 x 10^9 Pa
Poisson's ratio	0.4
Bulk Modulus	2.135 x 10^9 Pa
Shear Modulus	4.575 x 10^8 Pa
Tensile Yield Strength	3.7 x 10^7 Pa
Tensile Ultimate Strength	4.28 x 10^7 Pa

Table 27 Duraform EX material properties used in FEA

Young's modulus, tensile yield strength and tensile ultimate strength were determined from experimental results (see sections 4.3 Material testing and 4.4 Extensometer testing). Poisson's ratio was unavailable so an average value for Nylon (Duraform EX's base material) was used. Bulk modulus and shear modulus were calculated by Ansys using Young's modulus and Poisson's ratio. The data from testing was also used to provide uniaxial stress-strain values up to 0.01 strain.

B4.8.2 Results

The bottom section of the toe was observed to have deformed upwards, contacted the upper section of the toe, which then reduced the rate of deformation. The maximum deformation shown in Ansys was 17.3mm at the tip of the bottom toe section. The maximum deflection on the upper toe section was 9.2mm (see Figure 241).

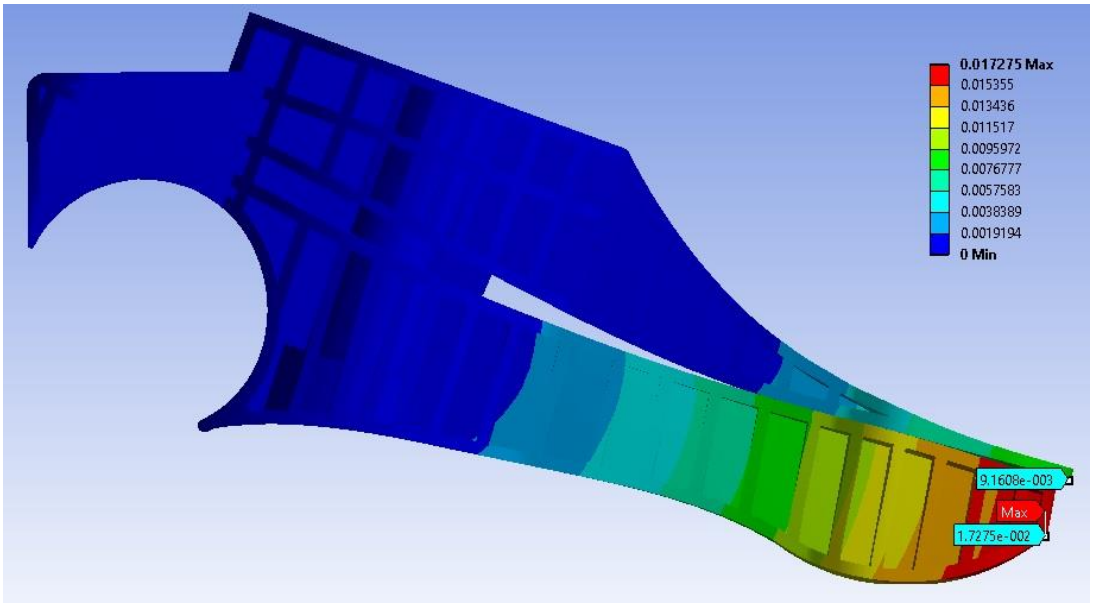

Figure 241 - The deformation of the model shown with the highest deformations of the upper and lower toe sections

High stress points of interest are shown in Figure 242. The numbering system was brought forward from the R1 and R2 polypropylene models however yield stress was not met at point 4 by the time maximum load was applied so no value is recorded in Table 28.

As previously point 6 was not considered to be of significance to a prototype due to the concentration of stress occurring at the corner of the keel where it contacts the loading plate.

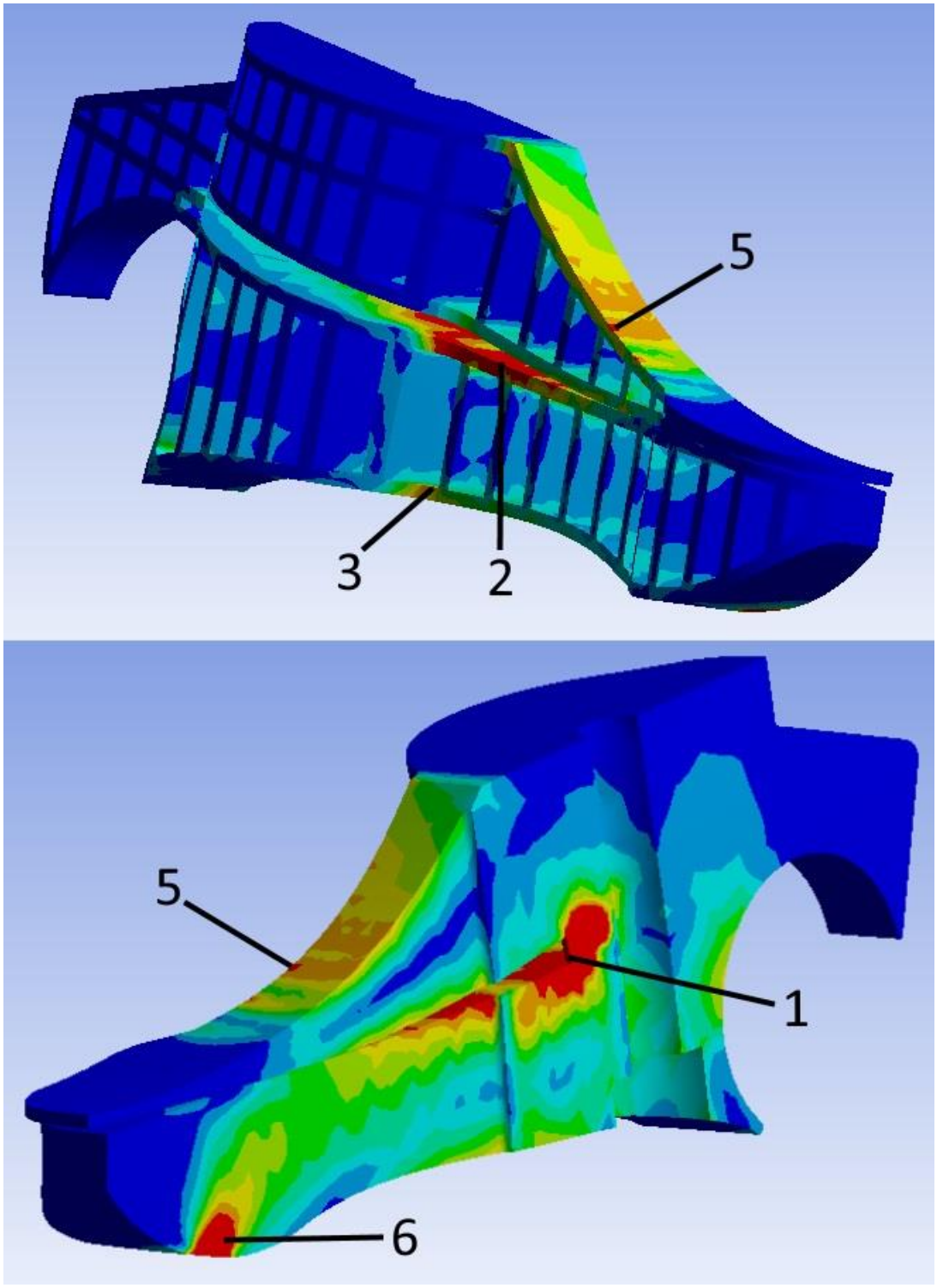

Figure 242 – High stress points observed in the R2 Duraform EX model

	R2 design (Polypropylene)	R2 design (Duraform EX)	R1 design (Duraform EX)
Point			
1	122.4N	132.0N	148.1N
2	437.9N	412.2N	151.3N
3	N/A	727.7N	167.4N
4	N/A	N/A	634.3N
5	708.4N	769.6N	647.2N
6	148.1N	128.1N	N/A

Table 28 - Load at which yield stress is reached for each point in the R2 design in copolymer polypropylene and Duraform EX, with the R1 Duraform EX results

B4.8.3 Discussion

When compared to the polypropylene results for the R2 design the Duraform EX results showed a reduced performance at points 2, 3 and 6 but an improved performance at points 1 and 5. At point 4 neither model reached yield so no comparison is possible. The change in material properties had affected the response to loading of the keel design causing the change in load at yield seen. As discussed previously point 6 was not of concern as it was an artefact from loading conditions. Points 2 and 3 are significant to the strength of the lower toe section, an area viewed to fail during the testing of the R1 design prototypes. Point 2 was only slightly reduced in load at yield (412.2N compared to 437.9N in R2 polypropylene) however point 3 was much reduced in load at yield, at least 77.3N.

In all but point 1 R2 Duraform EX was found to have reached a higher load at yield than the Duraform EX model of R1. At point 1 the R2 Duraform EX model was found to have a load at yield of 16.1N lower than in the R1 Duraform EX, an amount that was considered negligible.

Despite this potential reduction in performance between the polypropylene and Duraform EX model a further model was created to include a blade while still using the Duraform EX material properties.

B4.8.4 Bladed model

A round of FEA was carried out to support the introduction of the energy return feature (blade) to the system. The introduction of the blade was expected to affect the load pattern and so the stresses in the foot design. The same properties used previously were applied here (taken from (Barbero, 2011)) as follows:

Density	1370 kgm^{-3}
Young's Modulus	72 x 10^9 Pa
Poisson's ratio	0.22
Bulk Modulus*	42.86 x 10^9 Pa
Shear Modulus*	29.51 x 10^9 Pa
Tensile Ultimate Strength	3.45 x 10^9 Pa

* Bulk modulus and shear modulus were calculated by Ansys using Young's modulus and Poisson's ratio.

Table 29 Fibreglass material properties used in FEA

The settings used for the previous, bladeless model were again used where applicable (symmetry, loading, fixed support of keel, frictionless support of plate). The contact conditions between the upper and lower toe sections were removed and instead contact conditions were included for the lower toe section and the blade and for the blade and upper toe section. These were frictional, μ = 0.28, with a pinball region of 0.0001m but otherwise the same to previously used contacts. Contact sizing for the mesh was set to 0.002m for both frictional contacts between the blade and keel. The blade was bonded to the foot at the sites visible in Figure 243.

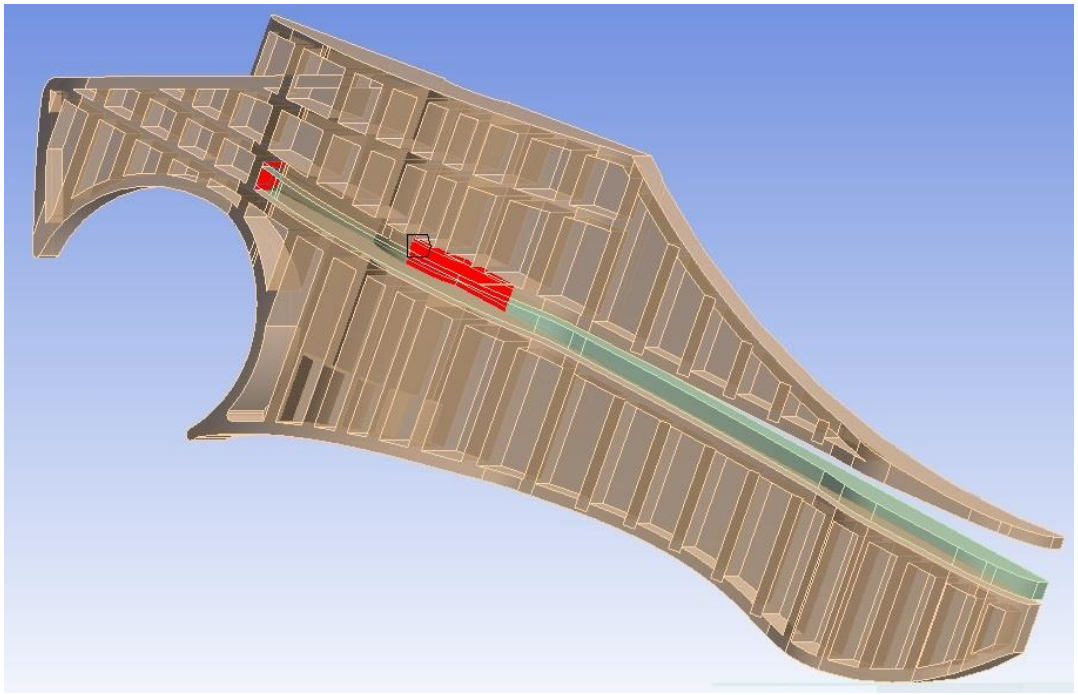

Figure 243 – Image demonstrating bonded sites between the blade and keel (shown in red)

B4.8.5 Results

The lower toe section was observed to deform into contact with the blade. At this point the rate of deformation was reduced, but continued until the blade made contact with the upper toe section at which point the rate of deformation was further reduced. The maximum deformation observed was 1.06×10^{-2}m at the tip of the lower toe section.The upper toe section deformed by 5.25×10^{-3}m at the tip while the tip of the blade deformed by 1.03×10^{-2}m (see Figure 194).

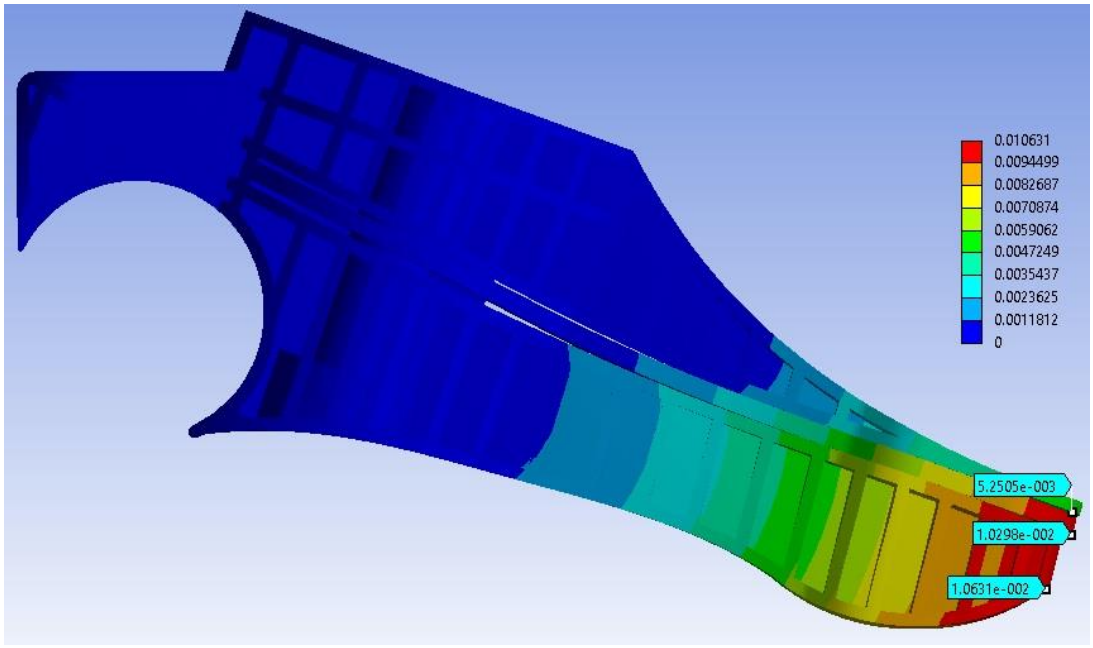

Figure 244 – Image showing the maximum deformation occurring in toe loading with a blade inserted in the R2 keel

Following the numbering convention used in B3.7.5 Results, the points reaching yield stress by maximum load were identified (see Figure 245). Points 1 and 2 both reached yield at 666.5N and 196.4N respectively, the opposite order to the R1 model, while point 3 did not reach yield by the maximum load. A new point was identified, point 4, that reached yield at 309.1N. Point 4 was not considered important as it was a result of the loading conditions of the model, occurring in the same location as point 6 in the bladeless models (see B4.7.6 Results and B4.8.5 Results).

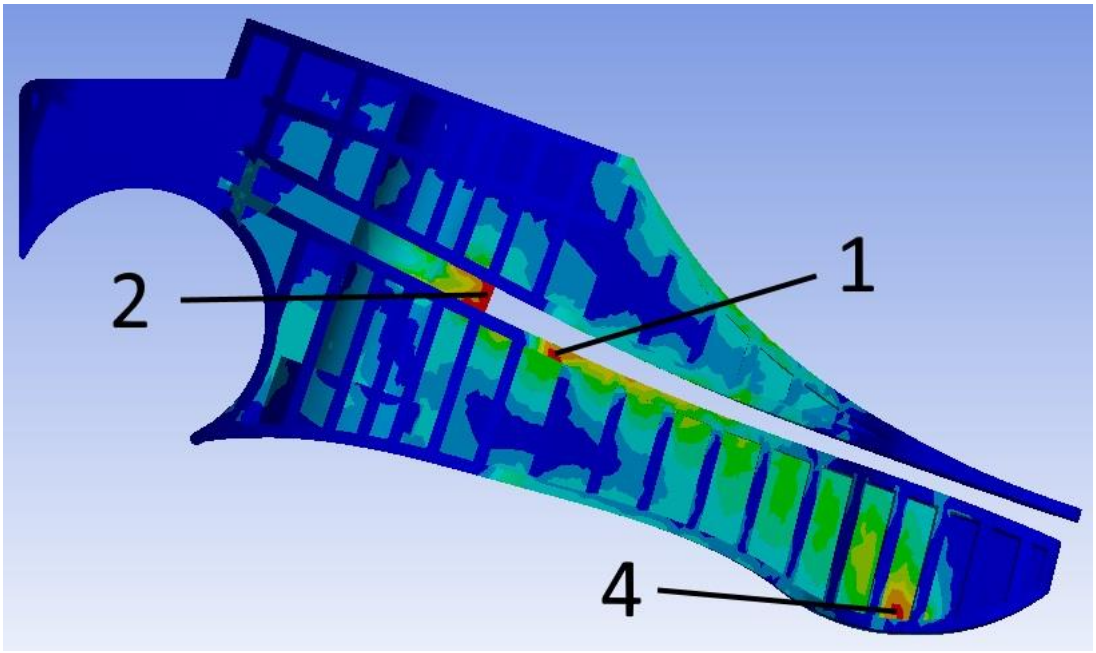

Figure 245 – High stress areas in the R2 bladed keel model (blade hidden for clarity)

As previously the fibreglass blade did not reach ultimate stress value however in this case the highest stress was much greater ($1.4755x10^9$Pa compared to $6.99x10^8$Pa in the R1 case). The outside corners had been removed in the blade and so did not serve to concentrate the stress in the R2 design. The lower front corner of the blade was the point of highest stress in the blade however its nature as an unfilleted corner will have led Ansys to calculate higher stresses than may be expected in real world testing. It was recommended that further models include a fillet on this corner to reduce this effect.

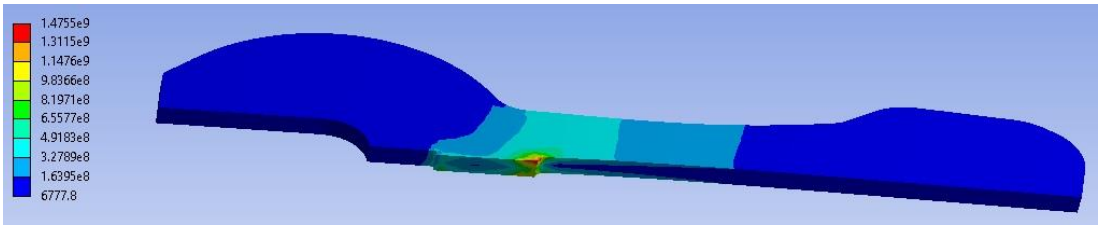

Figure 246 – Stresses on the blade in R2 toe loading model (underside up)

B4.8.6 Discussion

When comparing the bladed model to the bladeless model of section B4.8.2 Results, yield stress was first reached at the same point (identified as 1 in the bladeless model and 2 in the bladed model). The high stress area formed differently in the two models, with the bladeless model having two points simultaneously form in the same area, one midway up the vertical support and the other in the lower corner, while the bladed model only had a single high stress point form in the lower corner of the vertical support (see Figure 247). The bladeless model reached yield at 132.0N compared to 196.4N in the bladed model. At the second point to reach failure (point 2 in the bladeless model, point 1 in the bladed model) the difference had increased with the bladed model reaching yield at a load 228.6N higher than in the bladeless model however the location was the same.

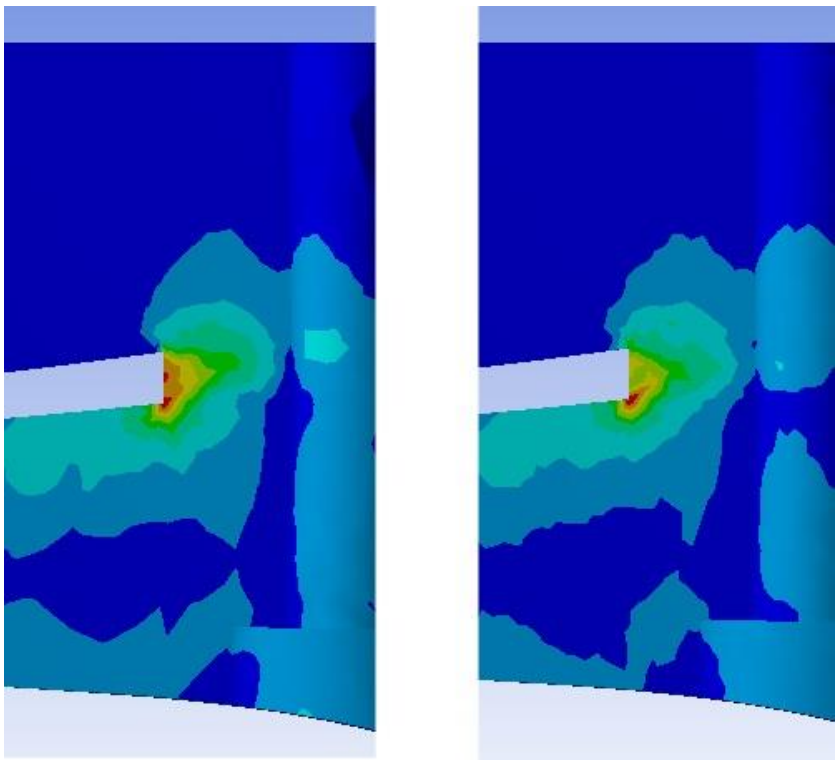

Figure 247 – High stress point (shown in red) in mid-foot for bladeless (L) and bladed (R) R2 models

Point 3 was not present in the R2 model, having not reached yield stress by the time the maximum load was applied.

The deformation observed in the bladed model was less than that of the bladeless model, as would be expected given the inclusion of the stiff blade with a maximum deformation of 17.4mm in the bladeless model compared to 10.6mm in the bladed model.

In the R2 model the load at yield at point 1 was much higher than in R1 (see Table 30) however the load at yield at point 2 was slightly less (by 12.9N) in the R2 model than the R1 model. Point 3 did not reach yield by the maximum load in the R2 model however a new high stress point was observed in R2 that was not present in R1. Point 4 was not considered a realistic representation of real world conditions, which occurred in the same location as point 6 in the bladeless R2 model. The location of point 1 was within a corner in R1 however the design was modified for the R2 design so that no corner was present in this location, leading to the greatly increased load at yield at this point in R2. The slight reduction in load at yield of point 2 in R2 was potentially due to the lower toe section being stiffer and so flexing less and transferring stress to point 2 resulting in a slightly lower load at yield than the R1 model.

	R1	**R2**
Point		
1	148.1N	666.5N
2	209.3N	196.4N
3	425.0N	N/A
4	N/A	309.1N

Table 30 – Load at yield at high stress points identified for R1 and R2 bladed models

The deformation of the R2 bladed model was much reduced from that of the R1 bladed model (10.6mm compared to 20.8mm at maximum load in either case. The deformation of the blades was more similar with 14.6mm in the R1 model and 10.3mm in the R2 model while the deformation of the top toe section was more similar again at 7.9mm in the R1 model and 5.3mm in the R2 model. The increased stiffness of the lower toe section in the R2 design led to a reduced deflection of the lower toe section when compared to the R1 model however, due to the increased height of the lower toe section, contact with the blade and the subsequent contact with the upper toe section occurred relatively quickly despite the reduced deflection of the lower toe section and so the deflection of these sections was closer in magnitude to those observed in the R1 model.

B4.8.7 Conclusion

The changes made to the design from R1 to R2 were predicted to have a largely positive effect, increasing load at yield at certain key locations while reducing the overall deflection. Certain areas were predicted to have a lower load at yield than in R1 however these are small in difference and not at the site of any observed failure in prototype testing (see section 3.3 Strathclyde foot testing).

When changing material from polypropylene to Duraform EX a lower load at yield was expected at two points of interest in the bladeless model, the top side of the lower toe section (point 2) and the lower side of the lower toe section (point 3 – see Figure 242).

The prototypes of R1 were observed to behave differently than the FEA models predicted so it was decided that prototypes should be made and tested to the static loading conditions of ISO 10328 standard.